Lecture Notes in Mathematics 2146

Christophe Besse
Jean-Claude Garreau *Editors*

Nonlinear Optical and Atomic Systems

At the Interface of Physics and Mathematics

CEMPI CENTRE EUROPÉEN POUR LES MATHÉMATIQUES, LA PHYSIQUE ET LEURS INTERACTIONS

Springer

Lecture Notes in Mathematics 2146

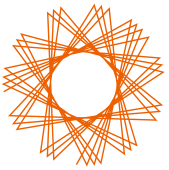

CEMPI is a joint project for research, training and technology transfer of the Laboratoire de Mathématiques Paul Painlevé and the Laboratoire de Physique des Lasers, Atomes et Molécules (PhLAM) of the Université Lille 1 and the CNRS. It was created as a "Laboratoire d'Excellence" in the framework of the "Programme d'Investissements d'Avenir" of the French government in February 2012.

Research at CEMPI covers a wide spectrum of knowledge from pure and applied mathematics to experimental and applied physics. CEMPI organizes every year the Painlevé-CEMPI-PhLAM Thematic Semester that brings together leading scholars from around the world for a series of conferences, workshops and post-graduate courses on CEMPI's main research topics.

For more information, see CEMPI's homepage http://math.univ-lille1.fr/~cempi/.

More information about this series at
http://www.springer.com/series/304

Christophe Besse • Jean-Claude Garreau
Editors

Nonlinear Optical and Atomic Systems

At the Interface of Physics and Mathematics

Springer

CEMPI CENTRE EUROPÉEN POUR LES MATHÉMATIQUES, LA PHYSIQUE ET LEURS INTERACTIONS

Editors
Christophe Besse
Institut de Mathématiques de Toulouse
Université Toulouse 3
Toulouse, France

Jean-Claude Garreau
Sciences et Technologies
PhLAM, Université de Lille 1
Villeneuve d'Ascq Cedex, France

ISSN 0075-8434 ISSN 1617-9692 (electronic)
Lecture Notes in Mathematics
ISBN 978-3-319-19014-3 ISBN 978-3-319-19015-0 (eBook)
DOI 10.1007/978-3-319-19015-0

Library of Congress Control Number: 2015945575

Mathematics Subject Classification (2010): 35-01, 35Q41, 35Q70, 35Bxx, 35Jxx, 35Pxx

Springer Cham Heidelberg New York Dordrecht London

Printed on acid-free paper

Springer International Publishing AG Switzerland is part of Springer Science+Business Media (www.springer.com)

Preface

This is the first volume of the new "CEMPI subseries" common to Lecture Notes in Mathematics and Lecture Notes in Physics. CEMPI, acronym for "Centre Européen pour les Mathématiques, la Physique et leurs Interactions" is a "Laboratoire d'Excellence" based on the campus of the Université Lille 1, presented on p. iii. The material in this volume is based on lectures given during the 2013 Painlevé-CEMPI-PhLAM Thematic Semester. The central theme of this semester—and hence of this volume—was the study of the deterministic and stochastic aspects of the nonlinear complex dynamics of optical and atomic systems, a subject clearly at the interface of mathematics and physics, and one of the core research areas of CEMPI.

More precisely, the contributions of Professor S. Flach, on one hand, and of Professors X. Antoine and R. Duboscq, on the other hand, are based on short post-graduate courses taught during the opening conference of this semester, on "Nonlinear Optical and Atomic Systems: Deterministic and Stochastic Aspects", which took place in January 2013. The contribution by S. De Bièvre, F. Genoud, and S. Simona Rota Nodari (CEMPI postdoc) grew out of discussions during the one-month visit of F. Genoud to CEMPI in the framework of the semester. Finally, F. Macia also spent a month at CEMPI as invited scholar and on that occasion delivered several lectures that form the basis of his contribution to this volume.

The first chapter, entitled "Nonlinear Lattice Waves in Random Potentials", is physics-oriented and is written by Sergej Flach, professor at the New Zealand Institute for Advanced Study, Massey University, Auckland. It deals with the quantum dynamics of disordered systems, a very active research area at the confluence of mathematics and of theoretical and experimental physics. Starting originally from the celebrated Anderson model, introduced more than 50 years ago, the field has recently experimented a new burst of activity with the advent of very clean experiments performed with laser-cooled atoms. In particular, the use of Bose-Einstein condensates in such experiments has introduced a new and theoretically challenging characteristic to these systems, namely the presence of nonlinearities in the mean-field approaches leading to the Nonlinear Schrödinger or Gross-Pitaevskii equation. In his contribution, Professor Flach provides first a broad and accessible review of the subject that will constitute a very useful introduction

for young researchers interested in this field. He then describes some of his many contributions to the field (which can be found in the references of his text).

The second chapter, entitled "Modeling and Computation of Bose-Einstein Condensates: Stationary States, Nucleation, Dynamics, Stochasticity", deals with another aspect of the study of complex nonlinear dynamical systems. It mainly concerns numerical simulations of Bose-Einstein condensates (BECs) via the Gross-Pitaevskii equation. Written by Professors Xavier Antoine, from the Institut Elie Cartan de Lorraine at the Université de Lorraine, and Romain Duboscq, from the Institut de Mathématiques de Toulouse at the Université de Toulouse, this chapter gives a review on the Bose-Einstein condensation, including history, mathematical models, computations of stationary states and dynamics, and some extensions. The authors introduce different numerical methods to compute both stationary states and dynamics of equations. They present the tool GPELab, which allows to compute multi-component BECs and handle stochastic effects. Many examples are provided to show the effectiveness of GPELab.

The third chapter, entitled "Orbital Stability: Analysis Meets Geometry", is written by three authors. Stephan De Bièvre is professor at the Laboratoire Paul Painlevé from the Université Lille 1 and CEMPI Scientific Coordinator, François Genoud is professor at the Faculty of Mathematics from the University of Vienna, and Simona Rota Nodari is a CEMPI Postdoc. This chapter deals with yet another aspect of nonlinear dynamics that continues to receive much attention not only in nonlinear PDE theory, but also in many areas of physics, namely the question of orbital stability of relative equilibria.The chapter gives an introduction to the study of this notion of stability for both finite and infinite dimensional Hamiltonian dynamical systems with symmetry on Banach spaces. Emphasis is put on the important interplay between geometry and analysis in this subject and in particular in the energy-momentum method that is explained in detail here. The text is specifically aimed at young researchers at the Ph.D. or postdoctoral level who wish to familiarize themselves with the subject. Appendices are provided to introduce concepts from Lie group theory, Hamiltonian dynamics, and differential geometry, with the aim of making the text self-contained. Several illustrative examples are treated in detail for the nonlinear Schrödinger equation, the wave equation, and the Manakov system. In addition, recent results of F. Genoud on the orbital stability of solitons for the spatially inhomogeneous nonlinear Schrödinger equation are presented in some detail to further illustrate the general theory.

The fourth and the last chapter, entitled "High-Frequency Dynamics for the Schrödinger Equation, with Applications to Dispersion and Observability", is written by Fabricio Macià, professor at Universidad Politécnica de Madrid. The results presented in this chapter are motivated by the fact that an important part of the study of nonlinear partial differential equations relies on the study of the corresponding linear problem. For instance, when one wants to prove some (local or global) existence property for a nonlinear problem, one often has to understand the "smoothing" properties of the associated linear flow—the most famous example is given by the so-called Strichartz estimates. The objective of this survey is to describe some recent results on the regularity properties of the linear Schrödinger flow via

its Wigner (semiclassical) measures. This survey also covers the introduction to the semiclassical techniques that are used to define and study Wigner measures in connection with solutions to the Schrödinger equation. Fabricio Macià presents recent results on these measures in various geometric settings, with a particular emphasis on the case of completely integrable systems. He also discusses the connection of these results with control theory in partial differential equations.

The reader shall thus find in this volume a thorough introduction to various aspects of the vast domain of nonlinear complex dynamics in infinite dimensional systems, from mathematical, as well as numerical and physical viewpoints.

Toulouse, France — Christophe Besse
Villeneuve d'Ascq Cedex, France — Jean-Claude Garreau
March 2015

Acknowledgements

This work was supported in part by the Labex CEMPI (ANR-11-LABX-0007-01).

Contents

List of Contributors

Xavier Antoine Université de Lorraine, Institut Elie Cartan de Lorraine, UMR 7502, Vandoeuvre-lès-Nancy, France

Inria Nancy Grand-Est/IECL - ALICE, Villers-lès-Nancy, France

Stephan De Bièvre Laboratoire Paul Painlevé, CNRS, UMR 8524 et UFR de Mathématiques, Université Lille 1, Sciences et Technologies Villeneuve d'Ascq Cedex, France

Equipe-Projet MEPHYSTO, Centre de Recherche INRIA Futurs, Parc Scientifique de la Haute Borne, Villeneuve d'Ascq Cedex, France

Romain Duboscq Institut de Mathématiques de Toulouse, UMR 5219, Université de Toulouse, CNRS, INSA, Toulouse, France

Sergej Flach Centre for Theoretical Chemistry and Physics, New Zealand Institute for Advanced Study, Massey University, Auckland, New Zealand

François Genoud Faculty of Mathematics, University of Vienna, Vienna, Austria

Current Address: Delft Institute of Applied Mathematics, Delft University of Technology, Delft, The Netherlands

Fabricio Macià Universidad Politécnica de Madrid, DCAIN, ETSI Navales, Madrid, Spain

Simona Rota Nodari Laboratoire Paul Painlevé, CNRS, UMR 8524 et UFR de Mathématiques, Université Lille 1, Sciences et TechnologiesVilleneuve d'Ascq Cedex, France

Nonlinear Lattice Waves in Random Potentials

Sergej Flach

1 Introduction

In this chapter we will discuss the mechanisms of wave packet spreading in nonlinear disordered lattice systems. More specifically, we will consider cases when the corresponding linear wave equations show Anderson localization, and the localization length is bounded from above by a finite value.

There are several reasons to analyze such situations. Wave propagation in spatially disordered media has been of practical interest since the early times of studies of conductivity in solids. In particular, it became of much practical interest for the conductance properties of electrons in semiconductor devices more than half a century ago. It was probably these issues which motivated P.W. Anderson to perform his groundbreaking lattice wave studies on what is now called Anderson localization [1]. With evolving modern technology, wave propagation became of importance also in photonic and acoustic devices in structured materials [2, 3]. Finally, recent advances in the control of ultracold atoms in optical potentials made it possible to observe Anderson localization there as well [4].

In many if not all cases wave-wave interactions can be of importance, or can even be controlled experimentally. Short range interactions hold for s-wave scattering of atoms. When many quantum particles interact, mean field approximations often lead to effective nonlinear wave equations. Electron-electron interactions in solids and mesoscopic devices are also interesting candidates with the twist of a new statistics of fermions. As a result, nonlinear wave equations in disordered media become

S. Flach (✉)
Centre for Theoretical Chemistry and Physics, New Zealand Institute for Advanced Study, Massey University, 0745 Auckland, New Zealand

Center for Theoretical Physics of Complex Systems, Institute for Basic Science, Daejeon, Korea
e-mail: s.flach@massey.ac.nz; sflach@ibs.re.kr

C. Besse, J.-C. Garreau (eds.), *Nonlinear Optical and Atomic Systems*,
Lecture Notes in Mathematics 2146, DOI 10.1007/978-3-319-19015-0_1

of practical importance. High intensity light beams propagating through structured optical devices induce a nonlinear response of the medium and subsequent nonlinear contributions to the light wave equations. While electronic excitations often suffer from dephasing due to interactions with other degrees of freedom (e.g. phonons), the level of phase coherence can be controlled in a much stronger way for ultracold atomic gases and light.

There is moreover a fundamental mathematical interest in the understanding, how Anderson localization is modified in the presence of nonlinear terms in the wave equations. All of the above motivates the choice of corresponding linear wave equations with finite upper bounds on the localization length. Then, the linear equations admit no transport. Analyzing transport properties of nonlinear disordered wave equations allows to observe and characterize the influence of wave-wave interactions on Anderson localization in a straightforward way. Finite upper bounds on the localization length for the corresponding linear wave equations are obtained for few band problems, which are essentially emulating waves on lattices. Finite upper bounds on the localization length also allow to exclude overlap of initial states with eigenstates of the linear equation which have a localization length larger than the considered system size, or which even have a diverging localization length.

No matter how tempting the general research theme of this chapter is, one has to break it down to a list of more specific questions to be addressed. Let us attempt to file such a list, without pretending completeness:

- I. In his pioneering work Anderson addressed the fate of an initially localized wave packet during the subsequent evolution within the Schrödinger equation for a single particle [1]. In particular, he showed that the return probability stays finite for infinite times, which essentially proves localization for the whole wave packet for all times. What is the outcome for the case with nonlinear terms?
- II. Anderson localization is equivalent to the statement that all eigenstates of the corresponding time-independent Schrödinger equation are spatially localized. Can these stationary states be continued into the nonlinear wave equation? What are the properties of such stationary states in the nonlinear wave equation?
- III. The linear wave equation which enjoys Anderson localization yields zero conductivity, i.e. the system is an insulator, which is particularly true even for finite densities of an infinitely extended wave state. Will the conductivity stay zero for nonlinear wave equations, or become finite?
- IV. If qualitatively new physics is found in the presence of nonlinear terms in any of the above cases, how does it reconnect back to the linear equation which enjoys Anderson localization?
- V. Quantizing the field equations leads to many-body interactions. What is the outcome for the above cases?
- VI. Wave localization for linear wave equations can be obtained also with quasiperiodic potentials (or in general correlated random potentials), even for potentials with nonzero dc bias, but also for kicked systems (dynamical localization in momentum space). What is the outcome for all above cases (where applicable) then?

We will mainly focus on the first item. A number of studies was devoted to that subject (see e.g. [5–10] as entree appetizers). It goes beyond the capabilities of this chapter to give a full account on all publications for the listed items. Some of them will be briefly discussed. Nevertheless we list also a number of key publications as entree appetizers for the items II–VI: II [11, 12], III [13, 14], IV [15–18], V [19–21], VI [22–25].

The chapter is structured in the following way. In Sect. 2 we introduce the models, and briefly discuss Anderson localization in Sect. 3. In Sect. 4 we then proceed with adding nonlinear terms to the wave equations. Using a secular normal form approach we demonstrate that a number of approximate treatments of the nonlinear terms keep localization intact, in contrast to a large number of numerical observations. We identify omitted resonances, their occurrence probabilities, and formulate expected dynamical regimes on that basis. Section 4 is closed with a technical discussion of different ways to characterize the evolution of wave packets. A number of numerical results on wave packet spreading are discussed in Sect. 5. Section 6 is devoted to the formulation of an effective noise theory which is capable of describing the numerical observations. The various additional predictions of the effective noise theory, along with their numerical tests, are presented in Sect. 7. A short discussion of wave packet dynamics in related models with correlated potentials is given in Sect. 8. Section 9 closes this chapter with a discussion the probalistici restoring of Anderson localization for weak nonlinearity, and issues open for future research.

2 Lattice Wave Equations

For the sake of simplicity we will first discuss one-dimensional lattice models, and subsequently generalize. We will use the Hamiltonian of the disordered discrete nonlinear Schrödinger equation (DNLS)

$$\mathscr{H}_D = \sum_l \epsilon_l |\psi_l|^2 + \frac{\beta}{2}|\psi_l|^4 - (\psi_{l+1}\psi_l^* + \psi_{l+1}^*\psi_l) \tag{1}$$

with complex variables ψ_l, lattice site indices l and nonlinearity strength $\beta \geq 0$. The uncorrelated random on-site energies ϵ_l are distributed with the probability density distribution (PDF) $\mathscr{P}_\epsilon(|x| \leq W/2) = 1/W$ and $\mathscr{P}_\epsilon(|x| > W/2) = 0$. where W denotes the disorder strength. The equations of motion are generated by $\dot{\psi}_l = \partial\mathscr{H}_D/\partial(i\psi_l^\star)$:

$$i\dot{\psi}_l = \epsilon_l\psi_l + \beta|\psi_l|^2\psi_l - \psi_{l+1} - \psi_{l-1} \ . \tag{2}$$

Equation (2) conserve the energy (1) and the norm $S = \sum_l |\psi_l|^2$. Note that varying the norm of an initial wave packet is strictly equivalent to varying β. Note also

that the transformation $\psi_l \to (-1)^l \psi_l^*$, $\beta \to -\beta$, $\epsilon_l \to -\epsilon_l$ leaves the equations of motion invariant. Therefore the sign of the nonlinear coefficient β can be fixed without loss of generality. Equations (1) and (2) are derived e.g. when describing two-body interactions in ultracold atomic gases on an optical lattice within a mean field approximation [26], but also when describing the propagation of light through networks of coupled optical waveguides in Kerr media [27].

Alternatively we also refer to results for the Hamiltonian of the quartic Klein-Gordon lattice (KG)

$$\mathscr{H}_K = \sum_l \frac{p_l^2}{2} + \frac{\tilde{\epsilon}_l}{2} u_l^2 + \frac{1}{4} u_l^4 + \frac{1}{2W}(u_{l+1} - u_l)^2, \tag{3}$$

where u_l and p_l are respectively the generalized coordinates and momenta, and $\tilde{\epsilon}_l$ are chosen uniformly from the interval $\left[\frac{1}{2}, \frac{3}{2}\right]$. The equations of motion are $\ddot{u}_l = -\partial \mathscr{H}_K / \partial u_l$ and yield

$$\ddot{u}_l = -\tilde{\epsilon}_l u_l - u_l^3 + \frac{1}{W}(u_{l+1} + u_{l-1} - 2u_l) \; . \tag{4}$$

Equation (4) conserve the energy (3). They serve e.g. as simple models for the dissipationless dynamics of anharmonic optical lattice vibrations in molecular crystals [28]. The energy of an initial state $E \geq 0$ serves as a control parameter of nonlinearity similar to β for the DNLS case. For small amplitudes the equations of motion of the KG chain can be approximately mapped onto a DNLS model [29, 30]. For the KG model with given parameters W and E, the corresponding DNLS model (1) with norm $S = 1$, has a nonlinearity parameter $\beta \approx 3WE$. The norm density of the DNLS model corresponds to the normalized energy density of the KG model [30].

The theoretical considerations will be performed within the DNLS framework. It is straightforward to adapt them to the KG case.

3 Anderson Localization

For $\beta = 0$ with $\psi_l = A_l \exp(-i\lambda t)$ Eq. (1) is reduced to the linear eigenvalue problem

$$\lambda A_l = \epsilon_l A_l - A_{l-1} - A_{l+1} \; . \tag{5}$$

The normal modes (NM) are characterized by the normalized eigenvectors $A_{\nu,l}$ ($\sum_l A_{\nu,l}^2 = 1$). The eigenvalues λ_ν are the frequencies of the NMs. The width of the eigenfrequency spectrum λ_ν of (5) is $\Delta = W + 4$ with $\lambda_\nu \in \left[-2 - \frac{W}{2}, 2 + \frac{W}{2}\right]$. While the usual ordering principle of NMs is with their increasing eigenvalues, here

we adopt a spatial ordering with increasing value of the center-of-norm coordinate $X_\nu = \sum_l l A_{\nu,l}^2$.

The asymptotic spatial decay of an eigenvector is given by $A_{\nu,l} \sim \mathrm{e}^{-|l|/\xi(\lambda_\nu)}$ where $\xi(\lambda_\nu)$ is the localization length and $\xi(\lambda_\nu) \approx 24(4-\lambda_\nu^2)/W^2$ for weak disorder $W \leq 4$ [31].

The NM participation number $p_\nu = 1/\sum_l A_{\nu,l}^4$ measures the number of strongly excited lattice sites in a given wave density distribution. It is one possible way to quantize the spatial extend V_ν (localization volume) of a NM. However fluctuations of the density distribution inside a given NM lead to an underestimate of V_ν when using p_ν. A better way to estimate the distance between the two exponential tails of an eigenvector is to use the second moment of its density distribution $m_2^{(\nu)} = \sum_l (X_\nu - l)^2 A_{\nu,l}^2$. It follows that the estimate $V_\nu = \sqrt{12 m_2^{(\nu)}}$ is highly precise and sufficient for most purposes [32]. The localization volume V is on average of the order of 3ξ for weak disorder, and tends to $V = 1$ in the limit of strong disorder.

Consider an eigenstate $A_{\nu,l}$ for a given disorder realization. How many of the neighboring eigenstates will have non-exponentially small amplitudes inside its localization volume V_ν? Note that there is a one-to-one correspondence between the number of lattice sites, and the number of eigenstates. Therefore, on average the number of neighboring eigenstates will be simply V_ν. Let us consider sets of neighboring eigenstates. Their eigenvalues will be in general different, but confined to the interval Δ of the spectrum. Therefore the average spacing d of eigenvalues of neighboring NMs within the range of a localization volume is of the order of $d \approx \Delta/V$, which becomes $d \approx \Delta W^2/300$ for weak disorder. The two scales $d \leq \Delta$ are expected to determine the packet evolution details in the presence of nonlinearity.

Due to the localized character of the NMs, any localized wave packet with size L which is launched into the system for $\beta = 0$, will stay localized for all times. If $L \ll V$, then the wave packet will expand into the localization volume. This expansion will take a time of the order of $\tau_{lin} = 2\pi/d$. If instead $L \geq V$, no substantial expansion will be observed in real space. We remind that Anderson localization is relying on the phase coherence of waves. Wave packets which are trapped due to Anderson localization correspond to trajectories in phase space evolving on tori, i.e. they evolve quasi-periodically in time.

Finally, the linear wave equations constitute an integrable system with conserved actions where the dynamics happens to be on quasiperiodic tori in phase space. This can be safely stated for any finite, whatever large, system.

4 Adding Nonlinearity

The equations of motion of (2) in normal mode space read

$$i\dot{\phi}_\nu = \lambda_\nu \phi_\nu + \beta \sum_{\nu_1,\nu_2,\nu_3} I_{\nu,\nu_1,\nu_2,\nu_3} \phi_{\nu_1}^* \phi_{\nu_2} \phi_{\nu_3} \tag{6}$$

with the overlap integral

$$I_{\nu,\nu_1,\nu_2,\nu_3} = \sum_l A_{\nu,l} A_{\nu_1,l} A_{\nu_2,l} A_{\nu_3,l} \ . \tag{7}$$

The variables ϕ_ν determine the complex time-dependent amplitudes of the NMs.

The frequency shift of a single site oscillator induced by the nonlinearity is $\delta_l = \beta|\psi_l|^2$. If instead a single mode is excited, its frequency shift can be estimated by $\delta_\nu = \beta|\phi_\nu|^2/p_\nu$.

As it follows from (6), nonlinearity induces an interaction between NMs. Since all NMs are exponentially localized in space, each normal mode is effectively coupled to a finite number of neighboring NMs, i.e. the interaction range is finite. However the strength of the coupling is proportional to the norm density $n = |\phi|^2$. Let us assume that a wave packet spreads. In the course of spreading its norm density will become smaller. Therefore the effective coupling strength between NMs decreases as well. At the same time the number of excited NMs grows. One possible outcome would be: (I) that after some time the coupling will be weak enough to be neglected. If neglected, the nonlinear terms are removed, the problem is reduced to an integrable linear wave equation, and we obtain again Anderson localization. That implies that the trajectory happens to be on a quasiperiodic torus—on which it must have been in fact from the beginning. It also implies that the actions of the linear wave equations are not strongly varying in the nonlinear case, and we are observing a kind of Anderson localization in action subspace. Another possibility is: (II) that spreading continues for all times. That would imply that the trajectory does not evolve on a quasiperiodic torus, but instead evolves in some chaotic part of phase space. This second possibility (II) can be subdivided further, e.g. assuming that the wave packet will exit, or enter, a Kolmogorov-Arnold-Moser (KAM) regime of mixed phase space, or stay all the time outside such a perturbative KAM regime. In particular if the wave packet dynamics will enter a KAM regime for large times, one might speculate that the trajectory will get trapped between denser and denser torus structures in phase space after some spreading, leading again to localization as an asymptotic outcome, or at least to some very strong slowing down of the spreading process. We will not go into details of such possible scenaria, but want the reader to be aware of the fact that the rather innocent set of questions at stake can quickly lead into highly sophisticated mathematical fields.

Consider a wave packet with size L and norm density n. Replace it by a *finite* system of size L and norm density n. Such a finite system will be in general nonintegrable. Therefore the only possibility to generically obtain a quasiperiodic evolution is to be in the regime where the KAM theorem holds. Then there is a finite fraction of the available phase space volume which is filled with KAM tori. For a given L it is expected that there is a critical density $n_{KAM}(L)$ below which the KAM regime will hold. We do not know this L-dependence. Computational studies may not be very conclusive here, since it is hard to distinguish a regime of very weak chaos from a strict quasiperiodic one on finite time scales.

The above first possible outcome (I) (localization) will be realized if the packet is launched in a KAM regime. Whether that is possible at all for an infinite system is an open issue. The second outcome (II) (spreading) implies that we start in a chaotic regime and remain there. Since the packet density is reduced and is proportional to its inverse size L at later times, this option implies that the critical density $n_{KAM}(L)$ decays faster than $1/L$, possibly faster than any power of $1/L$.

Let us discuss briefly one example of an integrable system, for which Anderson localization will not be destroyed. Consider a Hamiltonian in NM representation using actions J_ν and angles θ_ν as coordinates:

$$\mathscr{H}_{int} = \sum_\nu \lambda_\nu J_\nu + \beta \sum_{\nu_1,\nu_2,\nu_3,\nu_4} I_{\nu_1,\nu_2,\nu_3,\nu_4} \sqrt{J_{\nu_1} J_{\nu_2} J_{\nu_3} J_{\nu_4}} \; . \tag{8}$$

We assume that the set of eigenfrequencies $\{\lambda_\nu\}$ and the overlap integrals $I_{\nu_1,\nu_2,\nu_3,\nu_4}$ are identical with those describing the DNLS model (6), (7). The equations of motion $\dot{J}_\nu = -\partial \mathscr{H}_{int}/\partial\theta_\nu$ and $\dot{\theta}_\nu = \partial \mathscr{H}_{int}/\partial J_\nu$ yield $\dot{J}_\nu = 0$ since the integrable Hamiltonian (8) depends only on the actions. Therefore, any localized initial condition (e.g. $J_\nu(t=0) \propto \delta_{\nu,\nu_0}$) will stay localized, since actions of modes which are at large distances will never get excited. Thus, any observed spreading of wave packets, which we will study in detail in the present work, is presumably entirely due to the nonintegrability of the considered models, at variance to (8).

4.1 The Secular Normal Form

Let us perform a further transformation $\phi_\nu = \mathrm{e}^{-i\lambda_\nu t}\chi_\nu$ and insert it into Eq. (6):

$$i\dot{\chi}_\nu = \beta \sum_{\nu_1,\nu_2,\nu_3} I_{\nu,\nu_1,\nu_2,\nu_3} \chi^*_{\nu_1} \chi_{\nu_2} \chi_{\nu_3} \mathrm{e}^{i(\lambda_\nu + \lambda_{\nu_1} - \lambda_{\nu_2} - \lambda_{\nu_3})t} \; . \tag{9}$$

The right hand side contains oscillating functions with frequencies

$$\lambda_{\nu,\mathbf{n}} \equiv \lambda_\nu + \lambda_{\nu_1} - \lambda_{\nu_2} - \lambda_{\nu_3} \; , \; \mathbf{n} \equiv (\nu_1, \nu_2, \nu_3) \; . \tag{10}$$

For certain values of $\nu, \mathbf{n}$ the value $\lambda_{\nu,\mathbf{n}}$ becomes exactly zero. These secular terms define some slow evolution of (9). Let us perform an averaging over time of all terms in the rhs of (9), leaving therefore only the secular terms. The resulting secular normal form equations (SNFE) take the form

$$i\dot{\chi}_\nu = \beta \sum_{\nu_1} I_{\nu,\nu,\nu_1,\nu_1} |\chi_{\nu_1}|^2 \chi_\nu \; . \tag{11}$$

Note that possible missing factors due to index permutations can be absorbed into the overlap integrals, and are not of importance for what is following. The SNFE

can be now solved for any initial condition $\chi_\nu(t=0)=\eta_\nu$ and yields

$$\chi_\nu(t)=\eta_\nu e^{-i\Omega_\nu t}\ ,\ \Omega_\nu=\beta\sum_{\nu_1} I_{\nu,\nu,\nu_1,\nu_1}|\eta_{\nu_1}|^2\ . \tag{12}$$

Since the norm of every NM is preserved in time for the SNFE, it follows that Anderson localization is preserved within the SNFE. The only change one obtains is the renormalization of the eigenfrequencies λ_ν into $\tilde{\lambda}_\nu=\lambda_\nu+\Omega_\nu$. Moreover, the phase coherence of NMs is preserved as well. Any different outcome will be therefore due to the nonsecular terms, neglected within the SNFE. We note that $I_{\nu,\nu,\nu,\nu}\equiv p_\nu^{-1}$. Then the sum in (7) contains only nonnegative terms. By normalization $A_{\nu,l}\sim 1/\sqrt{V}$ inside its localization volume, and therefore $I_{\nu,\nu,\nu,\nu}\sim 1/V$. Similar argumentation leads to $I_{\nu,\nu,\nu_1,\nu_1}\sim 1/V$ if both modes reside in the same localization volume.

Let us discuss several different initial states. (a) If only one normal mode is initially excited to norm n, then it follows from (12) that its frequency renormalization $\Omega_\nu=\beta n p_\nu^{-1}\sim\beta n/V$ where V is a typical localization volume of a normal mode. Comparing this value to the spacing $d\sim\Delta/V$ we conclude that a perturbation approach (and therefore Anderson localization) might survive up to finite values of $\beta n\sim\Delta$. (b) If however a large group of normal modes is excited inside a wave packet such that all normal modes have norm n, then the sum in (12) will change the frequency renormalization to $\Omega_\nu\sim\beta n$ for each of the participating modes. Comparing that to the spacing d we now find that perturbation approaches might break down at sufficiently weaker nonlinearities $\beta n\sim\Delta/V$. (c) Finally assume that only one lattice site is initially excited with norm n. That means that V normal modes are excited each with norm n/V. And that is also what we will see in a dynamical evolution of the linear wave equation—after some short transient time the wave packet will occupy a localization volume region and stay in there. Then the frequency normalization for each participating mode becomes $\Omega_\nu\sim\beta n/V$ as in (a), and perturbation theory is expected to break down again at $\beta n\sim\Delta$.

All of the considered lattices allow for selftrapped states in the regime of strong nonlinearity. These are well known as discrete breathers, intrinsic localized modes, and discrete solitons [33] which are time-periodic but spatially localized exact solutions of the equations of motion. They exist for any sign of nonlinearity due to the underlying lattice, which generates finite bounds on the spectrum of the linear wave equation. Discrete breathers appear because the nonlinear terms renormalize (shift) frequencies completely out of the linear wave spectrum. In the limit of strong nonlinearity these states are essentially single site excitations, with very little amplitudes present on neighboring sites. Therefore, the natural basis for the physics of selftrapping is the original lattice itself, rather than the normal modes of the linear wave equation. This becomes evident when considering a lattice without any disorder, for which the normal modes of the linear wave equation are extended states, yet selftrapping and discrete breathers are perfectly present as well within the nonlinear wave equation. Selftrapping and discrete breathers are examples of a *nonperturbative* physics of strong nonlinearity. For the above cases of initial conditions, selftrapping can be effectively predicted whenever a single oscillator

on one site renormalizes its frequency $\epsilon_l + \beta|\psi_l|^2$ such that it exits the linear wave spectrum. For the above initial state case (a) this happens when $\beta n \sim V(\Delta/2 - \lambda_\nu)$, about V times larger than the perturbation threshold. For case (b) the norm n per normal mode is also the norm n per lattice site. Therefore selftrapping is expected at $\beta n \sim \Delta/2$, again about V times larger than the corresponding perturbation threshold. However, case (c) is different. Here we place a norm n *initially* on one site. If the selftrapping condition for that site holds, the dynamics will stay from scratch in the nonperturbative discrete breather regime, without any chance to spread into a localization volume region set by the linear wave equation. Therefore the selftrapping threshold reads $\beta n \sim \Delta/2 - \epsilon_l$ and becomes of the same order as the perturbation threshold. Single site excitations will be thus launched either in a perturbative regime, or in a self trapped one. The other initial states allow for a third regime—outside the perturbative regime, but well below the selftrapping one. For reasons to come, we coin this additional regime *strong chaos regime*, and the perturbative regime *weak chaos regime*. We recapitulate again, that single site excitations are expected to be either in the regime of weak chaos, or selftrapping. Other initial states allow for another intermediate regime of strong chaos.

4.2 Expected Dynamical Regimes

Consider a wave packet at $t = 0$ which has norm density n and size L. Let us wrap the above discussion into expected dynamical regimes [34]. Note that due to the above ambiguities, the following estimates are at the best semi-quantitative.

SINGLE SITE EXCITATIONS with norm n and $\epsilon_l = 0$ at the excitation site:

$$\begin{aligned} \beta n < \Delta/2 \ &: \ \text{weak chaos} \\ \text{strong chaos not present} \\ \beta n > \Delta/2 \ &: \ \text{selftrapping} \end{aligned} \tag{13}$$

SINGLE MODE EXCITATIONS with norm n and $\lambda_\nu = 0$ for the excited mode:

$$\begin{aligned} \beta n < \Delta \ &: \ \text{weak chaos} \\ \Delta < \beta n < V\Delta/2 \ &: \ \text{strong chaos} \\ V\Delta/2 < \beta n \ &: \ \text{selftrapping} \end{aligned} \tag{14}$$

MULTI SITE/MODE WAVE PACKET with norm density n per site/mode and size V:

$$\begin{aligned} \beta n < \Delta/V \ &: \ \text{weak chaos} \\ \Delta/V < \beta n < \Delta/2 \ &: \ \text{strong chaos} \\ \Delta/2 < \beta n \ &: \ \text{selftrapping} \end{aligned} \tag{15}$$

4.3 Beyond the Secular Normal Form

The time-averaged secular norm form (11) keeps the integrability of the nonlinear wave equation, and therefore also keeps Anderson localization. Any deviation from Anderson localization is therefore due to the omitted time-dependent oscillating terms in (9). Let us isolate one of the many terms in the rhs sum in (9)

$$\dot{\chi}_\nu = \beta I_{\nu,\mathbf{n}} \chi^*_{\nu_1} \chi_{\nu_2} \chi_{\nu_3} e^{i\lambda_{\nu,\mathbf{n}} t} \ . \tag{16}$$

Assume a solution of the secular normal form equations (11) in the limit of weak nonlinearity which we coined weak chaos. Consider the solution of (16) as a first order correction. This correction has an amplitude

$$|\chi^{(1)}_\nu| = |\beta \eta_{\nu_1} \eta_{\nu_2} \eta_{\nu_3}| R^{-1}_{\nu,\mathbf{n}} \ , \ R_{\nu,\mathbf{n}} \sim \left| \frac{\lambda_{\nu,\mathbf{n}}}{I_{\nu,\mathbf{n}}} \right| \ . \tag{17}$$

The perturbation approach breaks down, and resonances set in, when $|\eta_\nu| < |\chi^{(1)}_\nu|$ for at least one triplet $\mathbf{n}$, and for at least one excited reference mode ν:

$$|\eta_\nu| < |\eta_{\nu_1} \eta_{\nu_2} \eta_{\nu_3}| \frac{\beta}{R_{\nu,\mathbf{n}}} \ . \tag{18}$$

Let us discuss this result. The eigenfrequencies contribute through the quadruplet $\lambda_{\nu,\mathbf{n}}$ (10). This quantity can be also interpreted as the difference of two eigenvalue differences. Resonances will be triggered for small quadruplets. However, for this to hold we do not need to request that two of the participating eigenvalues are close. In fact, since we consider only participating states from one localization volume, level repulsion between neighboring eigenvalues will be present anyway, such that the level spacing of nearest neighbor eigenvalues shows signatures of Wigner-Dyson distributions characteristic for random matrices (Fig. 4 in [32]). This means in particular, that the probability density function (PDF) and therefore the probability of finding weakly separated (well beyond d) eigenvalues tends to zero for vanishing separation. However, the above quadruplet can become small for eigenvalues which are separated way beyond d. An extreme example is an equidistant spectrum which allows for exact zeros of quadruplets. In the disordered case with $V \gg 1$, for one reference mode ν we consider V states in its localization volume, which allow for about V^3 quadruplet combinations. It is reasonable to assume that the set of V eigenvalues will show correlations on energy separations of the order of d (level spacing), but a decay of these correlations at larger energy distances. Therefore, for most of the V^3 combinations, the participating eigenvalues can be considered to be uncorrelated. With that assumption, the PDF $\mathscr{W}_\lambda(\lambda_{\nu,\mathbf{n}})$, which is a sum of four random numbers, can be expected to be close to a normal distribution due to the

central limit theorem, i.e.

$$\mathscr{W}_\lambda(x) \approx \frac{1}{\sqrt{2\pi}\sigma} \mathrm{e}^{-\frac{x^2}{2\sigma^2}} \ , \ \sigma^2 = \frac{\Delta^2}{12} \ . \tag{19}$$

In a recent study of a one-dimensional ladder geometry [35] the closeness of the normal distribution to $\mathscr{W}_\lambda$ was numerically confirmed. Since we are interested in small quadruplet values, we stress that the normal distribution has a finite value at zero argument, i.e.

$$\mathscr{W}_\lambda(0) \approx \frac{\sqrt{3}}{\sqrt{2\pi}\Delta} \ . \tag{20}$$

Again the predicted value is only a factor of two off the actual numbers computed in [35].

The second important quantity which enters (18) through the definition of $R_{\nu,\mathbf{n}}$ in (17) are the overlap integrals $I_{\nu,\mathbf{n}}$. Much less is known about these matrix elements (however see [32]). It is instructive to mention that the same overlap integrals play a crucial role when estimating the localization length of two interacting particles (e.g. within a Bose-Hubbard chain) with onsite disorder [20, 36, 37] and are the main reason for the absence of any consensus on the scaling properties of this localization length. This is mainly due to the strong correlations between eigenvectors of states residing in the same localization volume but having sufficiently well separated eigenvalues. Let us ignore those difficulties for the moment, and assume that we can operate with one characteristic (average) overlap integral $\langle I \rangle$. Then the PDF $\mathscr{W}_R$ of R becomes

$$\mathscr{W}_R(x) = \langle I \rangle \mathscr{W}_\lambda(\langle I \rangle x) \ , \ \mathscr{W}_R(0) = \frac{\sqrt{3}\langle I \rangle}{\sqrt{2\pi}\Delta} \ . \tag{21}$$

With the additional assumption that all amplitudes $\eta \sim \sqrt{n}$ (note that this excludes a systematic consideration of a single normal mode excitation) we arrive at the resonance condition

$$\beta n < R_{\nu,\mathbf{n}} \ . \tag{22}$$

For a given set $\{\nu, \mathbf{n}\}$ the probability of meeting such a resonance is given by

$$\mathscr{P}_{\nu,\mathbf{n}} = \int_0^{\beta n} \mathscr{W}_R(x) dx \ , \ \mathscr{P}_{\nu,\mathbf{n}}|_{\beta n \to 0} \to \frac{\sqrt{3}\langle I \rangle}{\sqrt{2\pi}\Delta} \beta n \ . \tag{23}$$

For a given reference mode ν there are V^3 combinations of quadruplets. The probability that at least one of these quadruplets satisfies the resonance condition

is equivalent to the probability that the given mode violates perturbation theory:

$$\mathscr{P}_\nu = 1 - \left(1 - \int_0^{\beta n} \mathscr{W}_R(x)dx\right)^{V^3} \ , \ \mathscr{P}_\nu|_{\beta n \to 0} \to \frac{\sqrt{3}V^3\langle I\rangle}{\sqrt{2\pi}\Delta}\beta n \ . \tag{24}$$

The main outcome is that the probability of resonance is proportional to βn for weak nonlinearity. Moreover, within the disorder interval $1 \le W \le 6$ a numerical evaluation of the average overlap integral $\langle I\rangle \approx 0.6\ V^{-1.7}$ [32]. This yields $\mathscr{P}_\nu|_{\beta n\to 0} \approx 0.43\ V^{0.3}(\beta n/d)$. The uncertainty of the correct estimate of the overlap integral average, and the restricted studied disorder range may well address the weak dependence $V^{0.3}$. What remains however is evidence that the resonance probability for weak nonlinearity is proportional to the ratio $(\beta n)/d$. Therefore a practical outcome is that the average spacing d sets the energy scale—for $\beta n \ll d$ the resonance probability $\mathscr{P} \sim (\beta n)/d$, while for $\beta n \gg d$ the resonance probability $P \approx 1$. As already anticipated at the end of the previous subsection, two regimes of weak and strong chaos can be defined depending on the ratio $(\beta n)/d$. In the regime of strong chaos, any normal mode within an excited wave packet will be resonant and not obeying perturbation theory. In the regime of weak chaos, this will be true for a fraction of modes.

A straightforward numerical computation of the above probability can be performed avoiding a number of the above assumptions. For a given NM ν we define $R_{\nu,\mathbf{n}_0} = \min_{\mathbf{n}} R_{\nu,\mathbf{n}}$. Collecting $R_{\nu,\mathbf{n}_0}$ for many ν and many disorder realizations, we can obtain the probability density distribution $\mathscr{W}(R_{\nu,\mathbf{n}_0})$. The probability $\mathscr{P}$ for a mode, which is excited to a norm n (the average norm density in a packet of modes), to be resonant with at least one triplet of other modes at a given value of the interaction parameter β is again given by Krimer and Flach [32] and Skokos et al. [10]

$$\mathscr{P} = \int_0^{\beta n} \mathscr{W}(x)\mathrm{d}x \ . \tag{25}$$

Therefore again $\mathscr{W}(R_{\nu,\mathbf{n}_0} \to 0) \to C(W) \neq 0$ [10]. For the cases studied, the constant C drops with increasing disorder strength W, in agreement with (24), which suggests $C = \frac{\sqrt{3}V^3\langle I\rangle}{\sqrt{2\pi}\Delta}$.

The large power V^3 in (24) allows to make a simple exponential approximation

$$\mathscr{W}(R) \approx C\mathrm{e}^{-CR} \ , \ C = \frac{\sqrt{3}V^3\langle I\rangle}{\sqrt{2\pi}\Delta} \ . \tag{26}$$

which in turn can be expected to hold also for the case of weak disorder. It leads to the approximative result

$$\mathscr{P} = 1 - \mathrm{e}^{-C\beta n} \ . \tag{27}$$

Therefore the probability for a mode in the packet to be resonant is proportional to $C\beta n$ in the limit of small n [9, 10].

We stress again that the discussed uncertainty in the definition of an average overlap integral, and the fact that the distribution of quadruplets is expected to be controlled by the *stiffness* of the set of eigenvalues of the normal mode set $\{\nu, \mathbf{n}\}$ rather than its spacing d, might be related. This does become evident if assuming an equidistant set. But then again, for a disordered system discussed here, the only scale on which the quadruplets can fluctuate close to zero, is the spacing d.

4.4 Measuring Properties of Spreading Wave Packets

We remind that the ordering of NMs is chosen to be by increasing value of the center-of-norm coordinate X_ν. We will analyze normalized distributions $n_\nu \geq 0$ using the second moment $m_2 = \sum_\nu (\nu - \bar{\nu})^2 n_\nu$, which quantifies the wave packet's degree of spreading and the participation number $P = 1/\sum_\nu n_\nu^2$, which measures the number of the strongest excited sites in n_ν. Here $\bar{\nu} = \sum_\nu \nu n_\nu$. We follow norm density distributions $n_\nu \equiv |\phi_\nu|^2/\sum_\mu |\phi_\mu|^2$. The second moment m_2 is sensitive to the distance of the tails of a distribution from the center, while the participation number P is a measure of the inhomogeneity of the distribution, being insensitive to spatial correlations. Thus, P and m_2 can be used to quantify the sparseness of a wave packet through the compactness index

$$\zeta = \frac{P^{2/D}}{m_2} \tag{28}$$

where D is the dimension of the lattice.

In order to have a scale for ζ, we can consider a system of harmonic oscillators (normal modes) which are weakly interacting through nonlinear couplings. The contribution of the nonlinear interaction to the overall energy E of the system is assumed to be small and negligible. However it is essential in order to assume that the considered system is ergodic, i.e. we can replace time averages by suitable ensemble distribution averages. We also assume for simplicity that the distribution is of Boltzmann type. Therefore with good accuracy each oscillator is characterized by its own distribution $\rho(E_\nu) = \mathrm{e}^{-\beta_B E_\nu}/\beta_B$ where β_B is the inverse temperature, and E_ν is the energy of an oscillator with average $1/\beta_B$. We consider a lattice bounded by a D-dimensional sphere with radius $R \gg 1$ which contains N lattice sites, and therefore N oscillators. For $D = 1$ we have $N = 2R$, for $D = 2$ it follows $N = \pi R^2$ and for $D = 3$ we have $N = 4\pi R^3/3$. We now evaluate the normalized energy distribution $\beta_B E_\nu/N$. Due to ergodicity the inverse of the participation number $1/P = (\beta_B/N)^2 \sum_\nu E_\nu^2 = \beta_B^2/N \int \rho(E) E^2 = 2/N$. The second moment can be estimated at any time to be $m_2 = R^2/2$ (for $D = 2$) and $m_2 = 3R^2/5$ (for $D = 3$) since enough oscillators at large but constant distance from the center allow for an ensemble average. In the one-dimensional case such an estimate can be

performed only after a time average over times larger than the equipartition times (equivalently the correlation decay times) and yields $m_2 = L^2/3$ (for $D = 1$). Finally we neglect correlations between P and m_2 and find with the definition of (28) that the compactness index of a thermal cloud of weakly interacting oscillators $\zeta = 3$ (for $D = 1$), $\zeta = 2\pi \approx 6.28$ (for $D = 2$) and $\zeta = (4\pi/3)^{2/3}5/3 \approx 4.33$ (for $D = 3$). Such a result can be straightforwardly used for the KG lattice. For norm density distributions of the DNLS model a W-dependent correction can be expected, however the numerical data show that this is not of central importance. If we assume that density distributions experience large gaps between isolated fragments of the wave packet, then the compactness index will be lowered down from its equipartition value. In particular, for the above discussed case of selftrapping, we expect that at least a part of the initial state stays localized, while another part might spread. Then the second moment m_2 is expected to grow, the participation number P will stay approximately constant, and consequently the compactness index ζ will drop substantially down from its equipartition value.

In order to probe the spreading, we can also compute higher order moments $m_\eta = \sum_\nu (\nu - \bar{\nu})^\eta n_\nu$. In particular the kurtosis $\gamma = m_4/m_2^2 - 3$ is useful as an indicator of the overall shape of the probability distribution profile. Large values correspond to profiles with sharp peaks and long extending tails. Low values are obtained for profiles with rounded/flattened peaks and steeper tails. For example, the Laplace distribution has $\gamma = 3$, while a compact uniform distribution has $\gamma = -1.2$ [38].

5 Computing Spreading Wave Packets: Collecting Evidence

We will present results on long time numerical simulations. We therefore first discuss the methods and particularities of our computations (see [10] for more details). For both models, symplectic integrators were used. These integration schemes replace the original Hamiltonian by a slightly different (and time-dependent) one, which is integrated exactly. The smaller the time steps, the closer both Hamiltonians. Therefore, the computed energy (or norm) of the original Hamiltonian function will fluctuate in time, but not grow. The fluctuations are bounded, and are due to the fact, that the actual Hamiltonian which is integrated, has slightly different energy.

Another possible source of errors is the roundoff procedure of the actual processor, when performing operations with numbers. Sometimes it is referred to as 'computational noise' although it is exactly the opposite, i.e. purely deterministic and reproducible. The influence of roundoff errors on the results was discussed in [10].

The KG chain was integrated with the help of a symplectic integrator of order $\mathcal{O}(\tau^4)$ with respect to the integration time step τ, namely the SABA_2 integrator with corrector ($\mathrm{SABA}_2\mathrm{C}$), introduced in [39]. A brief presentation of the integration scheme, as well as its implementation for the particular case of the KG lattice (3) is given in Appendix [10]. The $\mathrm{SABA}_2\mathrm{C}$ integration scheme proved to be very

efficient for long integrations (e.g. up to 10^{10} time units) of lattices having typically $N = 1000$ sites, since it kept the required computational time to feasible levels, preserving at the same time quite well the energy of the system. For example, an integration time step $\tau = 0.2$ usually kept the relative error of the energy smaller than 10^{-4}.

The DNLS chain was integrated with the help of the $SBAB_2$ integrator [39] which introduces an error in energy conservation of the order $\mathcal{O}(\tau^2)$. The number of sites used in computations varied from $N = 500$ to $N = 2000$, in order to exclude finite size effects in the evolution of the wave packets. For $\tau = 0.1$ the relative error of energy was usually kept smaller than 10^{-3}. It is worth mentioning that, although the $SBAB_2$ integrator and the commonly used leap-frog integrator introduce errors of the same order, the $SBAB_2$ scheme exhibits a better performance since it requires less CPU time, keeping at the same time the relative energy error to smaller values than the leap-frog scheme.

We remind that we order the NMs in space by increasing value of the center-of-norm coordinate $X_\nu = \sum_l l A_{\nu,l}^2$. We analyze normalized distributions $z_\nu \geq 0$ using the second moment $m_2 = \sum_\nu (\nu - \bar{\nu})^2 z_\nu$, which quantifies the wave packet's degree of spreading and the participation number $P = 1/\sum_\nu z_\nu^2$, which measures the number of the strongest excited sites in z_ν. Here $\bar{\nu} = \sum_\nu \nu z_\nu$. For DNLS we follow norm density distributions $z_\nu \equiv |\phi_\nu|^2 / \sum_\mu |\phi_\mu|^2$. For KG we follow normalized energy density distributions $z_\nu \equiv E_\nu / \sum_\mu E_\mu$ with $E_\nu = \dot{A}_\nu^2/2 + \omega_\nu^2 A_\nu^2/2$, where A_ν is the amplitude of the νth NM and $\omega_\nu^2 = 1 + (\lambda_\nu + 2)/W$.

5.1 Single Site Excitations

We first show results for single site excitations from [10] in Fig. 1 with $W = 4$, $n = 1$ and $\epsilon_l = 0$ at the excitation site. We plot the time dependence of the second moment m_2, the participation number P and the compactness index ζ. Let us discuss the DNLS model (left plots in Fig. 1). The outcome for the KG model (right plots in Fig. 1) is impressively similar. For $\beta = 0$ both m_2 and P are constant in time respecting Anderson localization. For $\beta = 0.1$ the quantities fluctuate around their $\beta = 0$ values up to $t \approx 10^6$ and start to grow for larger times, signaling a spreading of the wave packet and a departure from Anderson localization. For $\beta = 1$ the spreading is observable already at shorter times. Note that the compactness index ζ tends to its equipartition value $\zeta \approx 3$. Finally, deep in the selftrapping regime $\beta = 4.5$ the participation number P stays finite, since a significant part of the wave packet stays localized. Nevertheless, a part of the wave packet spreads with the second moment m_2 again growing in time. This growth appears to follow a subdiffusive law $m_2 \sim t^{1/3}$. For single site excitations strong chaos is not expected to be observed (13). Note that the observed crossover from weak chaos to selftrapping happens for $1 < \beta < 4.5$ which compares well with the expected value $\beta \approx 4$ using (13). Repeating the simulations for 20 different disorder realizations in the regime of

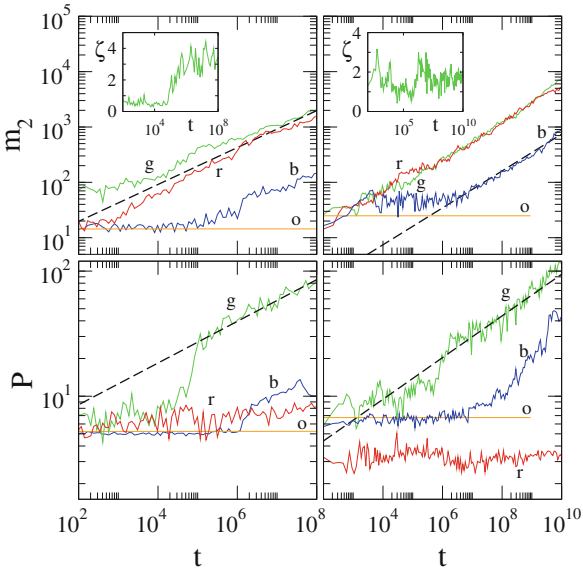

Fig. 1 Single site excitations. m_2 and P versus time in log–log plots. *Left plots*: DNLS with $W = 4$, $\beta = 0, 0.1, 1, 4.5$ [(o), orange; (b), blue; (g) green; (r) red]. *Right plots*: KG with $W = 4$ and initial energy $E = 0.05, 0.4, 1.5$ [(b) blue; (g) green; (r) red]. (o) Orange curves for the linear equations of motion, where the term u_l^3 in (4) was absent. The disorder realization is kept unchanged for each of the models. *Dashed straight lines* guide the eye for exponents 1/3 (m_2) and 1/6 (P) respectively. *Insets*: the compactness index ζ as a function of time in linear-log plots for $\beta = 1$ (DNLS) and $E = 0.4$ (KG). Adapted from [10]

weak chaos, with subdiffusive growth of $m_2 \sim t^\alpha$ starting around $t = 10^2$, an average $\langle \log_{10} m_2 \rangle$ is obtained. Its time dependence over 6 (DNLS) up to 8 (KG) decades in time was fitted with a power law, yielding $\alpha = 0.33 \pm 0.02$ for DNLS and $\alpha = 0.33 \pm 0.05$ for KG [10].

5.2 Single Mode Excitations

For single mode excitations we find a similar outcome, but with rescaled critical values for the nonlinearity strength which separate the different regimes. Examples are shown in Fig. 2 for $W = 4$, $n = 1$ and $\lambda_\nu \approx 0$ for the initially excited mode. As in the case of single site excitations presented in Fig. 1, the compactness index ζ plotted in the insets in Fig. 2 remains practically constant for excitations avoiding selftrapping, attaining the values $\zeta = 1.5$ at $t = 10^8$ for the DNLS model and $\zeta = 3.3$ at $t = 10^9$ for the KG chain. According to (14) weak chaos is realized for $\beta < 8$, and selftrapping should set in for $\beta \approx 80$. The order of magnitude of these thresholds are well captured by the computations. Moreover, pay attention that the

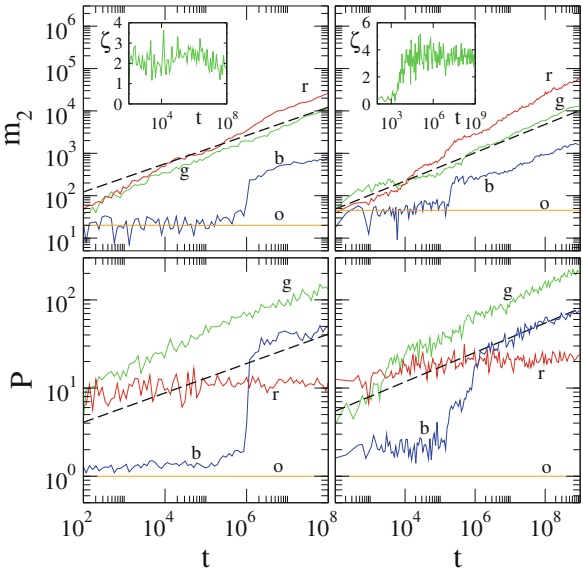

Fig. 2 Single mode excitations. m_2 and P versus time in log–log plots. *Left plots*: DNLS with $W = 4$, $\beta = 0, 0.6, 5, 30$ [(o) orange; (b) blue; (g) green; (r) red]. *Right plots*: KG with $W = 4$ and initial energy $E = 0.17, 1.1, 13.4$ [(b) blue; (g) green; (r) red]. (o) Orange curves for the linear equations of motion, where the term u_l^3 in (4) was absent. The disorder realization is kept unchanged for each of the models. *Dashed straight lines* guide the eye for exponents 1/3 (m_2) and 1/6 (P) respectively. *Insets*: the compactness index ζ as a function of time in linear-log plots for $\beta = 5$ (DNLS) and $E = 1.1$ (KG). Adapted from [10]

second moment growth in the strong chaos and selftrapping regimes appears to be subdiffusive $m_2 \sim t^\alpha$ but with an exponent $\alpha > 1/3$. It is hard to make quantitative conclusions about the observed subdiffusive growth laws. For that to be achieved, we need to perform averaging over disorder realizations.

The final norm density distribution for the DNLS model is plotted in Fig. 3 for both single site and single mode excitations. The wave packets grow substantially beyond the maximum size dictated by Anderson localization. The wave packets show thermal fluctuations, which are barely seen on logarithmic scales (bottom plots). On these logarithmic scales the remnants of Anderson localization are nicely observed—these are the exponential tails at the edges of the wave packet. As time increases, the wave packet spreads further, and the exponential tails are pushed into outer space. The average value $\overline{\zeta}$ of the compactness index over 20 realizations at $t = 10^8$ for the DNLS model with $W = 4$ and $\beta = 5$ was found to be $\overline{\zeta} = 2.95 \pm 0.39$ [10]. The slow subdiffusive spreading is apparently sufficient for a rough thermalization of the wave packet and the formation of exponential Anderson-localized tails.

The observed start of the growth of m_2 for weak nonlinearity at times $t \sim 10^6$ in Figs. 1 and 2 can, but must not signal a qualitative change in the dynamics.

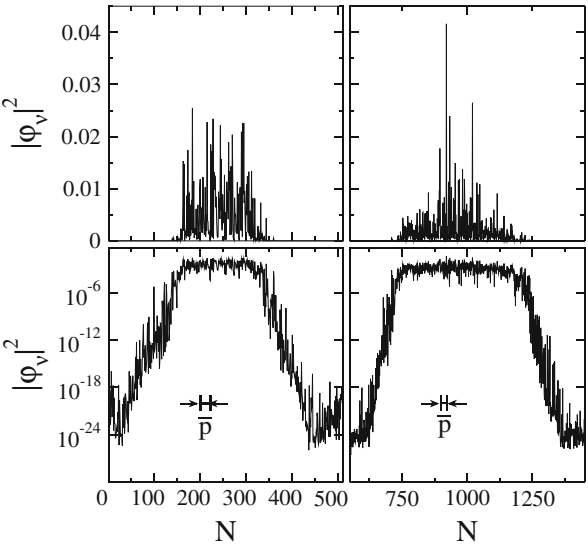

Fig. 3 Norm density distributions in the NM space at time $t = 10^8$ for the initial excitations of the DNLS model shown in the *left plots* of Figs. 1 and 2. *Left plots*: single site excitation for $W = 4$ and $\beta = 1$. *Right plots*: single mode excitation for $W = 4$ and $\beta = 5$. $|\phi_\nu|^2$ is plotted in linear (logarithmic) scale in the *upper (lower) plots*. The maximal mean value of the localization volume of the NMs $\overline{p} \approx 22$ (shown schematically in the *lower plots*) is much smaller than the length over which the wave packets have spread. Adapted from [10]

Indeed, relaunching wave packets which have spread already substantially (at somewhat stronger nonlinearity) will yield similar transient curves from a constant to a growing function [10]. Therefore an alternative explanation for the observed transients is a large characteristic diffusion time scale for a given initial state, which will be observable in the time-dependence of the second moment only beyond a corresponding, potentially large, time.

5.3 Normal Mode Dephasing

For single site excitations the exponent $\alpha \approx 1/3$ does not appear to depend on β in the case of the DNLS model or on the value of E in the case of KG, as shown in Fig. 4. What is the origin of the observed slow subdiffusive process? If the dynamics is accompanied by an enforced randomization of phases of the variables ψ_l in real space (respectively the phases of the oscillators of the KG model) then even for the linear wave equation Anderson localization is destroyed, and instead a process of normal diffusion with $m_2 \sim t$ is observed [40], which is much faster than the observed subdiffusion. The above tests of the linear wave equation in Figs. 1 and 2 also show that the numerical scheme is correctly reproducing Anderson localization.

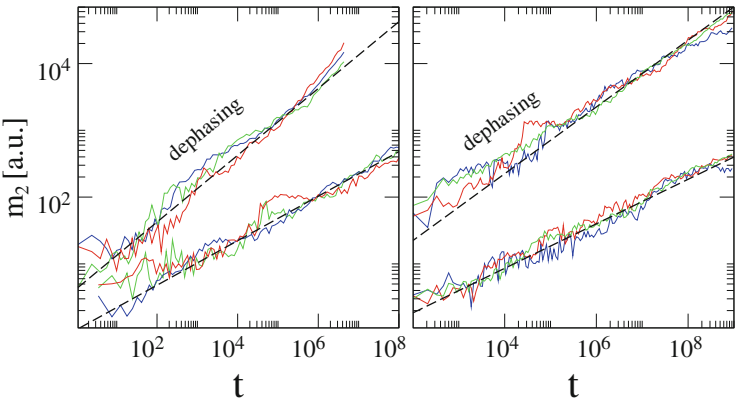

Fig. 4 Single site excitations. m_2 (in arbitrary units) versus time in log–log plots for different values of W. *Lower set of curves*: plain integration (without dephasing); *upper set of curves*: integration with dephasing of NMs. *Dashed straight lines* with exponents 1/3 (no dephasing) and 1/2 (dephasing) guide the eye. *Left plot*: DNLS, $W = 4$, $\beta = 3$ (*blue*); $W = 7$, $\beta = 4$ (*green*); $W = 10$, $\beta = 6$ (*red*). *Right plot*: KG, $W = 10$, $E = 0.25$ (*blue*), $W = 7$, $E = 0.3$ (*red*), $W = 4$, $E = 0.4$ (*green*). The *curves* are shifted vertically in order to give maximum overlap within each group. Adapted from [10]

Could it then be that the relative phases of the participating normal modes are randomized leading to the observed slow spreading? We test this by enforcing decoherence of NM phases. Each 100 time units on average 50 % of the NMs were randomly chosen, and their phases were shifted by π (DNLS). For the KG case we change the signs of the corresponding NM momenta. We obtain $m_2 \sim t^{1/2}$ [10] (see Fig. 4). This is also a subdiffusive process, yet faster than the observed one with $\alpha = 1/3$. Therefore, we can expect that the numerical integration is rather accurate. When the NMs dephase completely, the exponent $\tilde{\alpha} = 1/2$, *contradicting* numerical observations *without dephasing*. Thus, not all NMs in the packet are randomizing their phases quickly, and dephasing is at best a partial outcome.

6 Nonlinear Diffusion

The integrable equations of the secular normal form preserve Anderson localization. It is therefore tempting to assume that the observed departure from Anderson localization is due to nonintegrability and chaos. Indeed, assume that a wave packet with $V \gg 1$ NMs is excited. Trap it and replace the exponential edges (see Fig. 3) by fixed walls (boundaries). Then continue to evolve the equations. We are dealing for sure with a nonintegrable system with many degrees of freedom (DOF). Will the dynamics be chaotic or regular? That depends on the number of DOF, and on the energy/norm density of the system. The question touches the range

of validity of the Kolmogorov-Arnold-Moser regime for persisting invariant tori with finite measure of a weakly perturbed integrable system. To the best of our knowledge, no results are known which can help and guide our search. Yet in a huge body of molecular dynamical simulations of various systems, a large enough number of degrees of freedom usually ensures equipartition down to extremely small temperatures (energy densities), with the only consequence that decoherence time scales increase with lowering the temperature. Let us therefore take the point that the dynamics inside the trapped wave packet is chaotic. Then, as we will show below, a removing of the trap (the fixed walls) will inevitably lead to a spreading and increase of the wave packet size. Therefore the participating number of DOF increases—linearly with the wave packet size. At the same time the densities drop—inversely proportional to the wave packet size. The nonlinear terms in the equations of motion (2), (4) become small compared to the linear ones. It is therefore tempting to skip the nonlinear terms at some point. But if we skip them, we return to the linear wave equation, restore integrability, and recover Anderson localization. So then, for that enlarged wave packet, we can again add trapping hard walls, but keep the nonlinear terms, and ask the question whether the dynamics inside the wave packet remains regular, or will be chaotic at large enough times. Again the experience of molecular dynamics tells that the dynamics will stay chaotic with high probability, but the decoherence times increase. Therefore the possible flaw in the argument when dropping the nonlinear terms is the time scale. For sure, at weak enough nonlinearity, and up to some finite time, the nonlinear terms can be neglected. But how will that time scale with weak nonlinearity? If it stays finite, then the dropping of nonlinear terms will be incorrect for large enough times. Which might be just the times at which we observe the slow subdiffusive wave packet spreading.

6.1 Measuring Chaos

Michaeli and Fishman studied the evolution of single site excitations for the DNLS model [41]. They considered the rhs of Eq. (9) as a function of time $i\dot{\chi}_\nu = F_\nu(t)$ for a mode $\nu = 0$ which was strongly excited at time $t = 0$. The statistical analysis of the time dependence of $F_0(t)$ shows a quick decay of its temporal correlations for spreading wave packets. Therefore the force $F_0(t)$ can be considered as a random noise function on time scales relevant for the spreading process. This is a clear signature of chaos inside the wave packet.

Vermersch and Garreau (VG) [42] followed a similar approach for the DNLS model. They measured the time dependence of the participation number $P(t)$ of a spreading wave packet (see e.g. the curves in Figs. 1 and 2). VG then extracted a spectral entropy, i.e. a measure of the number of participating frequencies which characterize this time dependence. Spectral entropies are convenient measure to discriminate between regular and chaotic dynamics. VG concluded that the dynamics of spreading wave packets *is* chaotic. They also measured short time Lyapunov exponents to support their conclusion.

The long-time dependence of the largest Lyapunov exponent Λ as chaos strength indicators inside spreading wave packets for KG models was recently tested in [43]. The crucial point is that during spreading the energy density *is* decreasing, and therefore a weakening of the momentary chaos indicator is expected. Therefore $\Lambda(t)$ will be not constant in time, but decrease its value with increasing time. Moreover, the calculation of Lyapunov exponents for integrable systems will also yield nonzero numbers when integrating the system over any finite time. This is due to the method used—one evolves the original trajectory in phase space, and in parallel runs the linearized perturbation dynamics of small deviations from the original trajectory in tangent space. Since this deviation is nonzero, any computer code will produce nonzero estimates for the Lyapunov exponent at short times. The crucial point is that for integrable systems the long-time dependence of Λ follows $\Lambda \sim 1/t$. This is also the result found in [43] for the *linear* wave equation which obeys Anderson localization. However the nonlinear case of wave packet spreading yields a dependence

$$\Lambda(t) \sim \frac{1}{t^{1/4}} \gg \frac{1}{t} \,. \tag{29}$$

In Fig. 5a we first show the result for a trajectory of a single site excitation with total energy $E = 0.4$ and $W = 4$ (Case I). We show the time dependence of the second moment (red curve) and observe the expected subdiffusive growth $m_2 \sim t^{1/3}$. The simulation of a single site excitation in the absence of nonlinear terms (orange curve) corresponds to regular motion and Anderson localization is observed. In Fig. 5b we plot the time dependence of $\Lambda(t)$ for the two cases of Fig. 5a. At variance to the t^{-1}

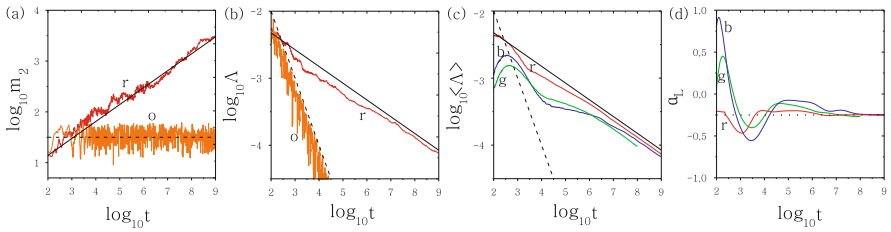

Fig. 5 (**a**) Time evolution of the second moment m_2 for one disorder realization of an initially single site excitation with $E = 0.4$, $W = 4$ (Case I), in log–log scale (*red (r) curve*). The *orange (o) curve* corresponds to the solution of the linear equations of motion, where the term u_l^4 in Eq. (3) is absent. *Straight lines* guide the eye for slopes 1/3 (*solid line*) and 0 (*dashed line*). (**b**) Time evolution of the finite time maximum Lyapunov exponent Λ (multiplied by 10 for the *orange (o) curve*) for the trajectories of panel (**a**) in log–log scale. The *straight lines* guide the eye for slope -1 (*dashed line*), and $-1/4$ (*solid line*). (**c**) Time evolution of the averaged Λ over 50 disorder realizations for the "weak chaos" cases I, II and III [(*r*) red; (*b*) blue; (*g*) green] (see text for more details). *Straight lines* guide the eye for slopes -1 and $-1/4$ as in panel (**b**). (**d**) Numerically computed slopes α_L of the *three curves* of panel (**c**). The *horizontal dotted line* denotes the value $-1/4$. Adapted from [43]

decay for the regular nonchaotic trajectory (orange curve), the observed decay for the weak chaos orbit is much weaker and well fitted with $\Lambda \sim t^{-1/4}$ (red curve).

These findings are further substantiated by averaging $\log_{10} \Lambda$ over 50 realizations of disorder and extending to two more weak chaos parameter cases with initial energy density $\epsilon = 0.01$ distributed evenly among a block of 21 central sites for $W = 4$ (case II) and 37 central sites for $W = 3$ (case III). All cases show convergence towards $\Lambda \sim t^{-1/4}$ (Fig. 5c). The curves are further analyzed by estimating their slope $\alpha_L = \frac{d(\log_{10} \Lambda(t))}{d \log_{10} t}$. The results in Fig. 5d underpin the above findings.

The authors of [43] further compare the obtained chaoticity time scales $1/\Lambda$ with the time scales governing the slow subdiffusive spreading and conclude, that the assumption about persistent and fast enough chaoticity needed for thermalization and inside the wave packet is correct. The dynamics inside the spreading wave packet is chaotic, and remains chaotic up to the largest simulation times, without any signature of a violation of this assumption for larger times (no visible slowing down).

A further very important result concerns the seeds of deterministic chaos and their *meandering* through the packet in the course of evolution. Indeed, assume that their spatial position is fixed. Then such seeds will act as spatially pinned random force sources on their surrounding. The noise intensity of these centers will decay in time. At any given time the exterior of the wave packet is then assumed to be approximated by the linear wave equation part which enjoys Anderson localization. However, even for constant intensity it was shown [44] that the noise will not propagate into the system due to the dense discrete spectrum of the linear wave equation. Therefore the wave packet can only spread if the nonlinear resonance locations meander in space and time.

The motion of these chaotic seeds was visualized by following the spatial evolution of the deviation vector distribution (DVD) used for the computation of the largest Lyapunov exponent [43]. This vector tends to align with the most unstable direction in the system's phase space. Thus, monitoring how its components on the lattice sites evolve allow to identify the most chaotic spots. Large DVD values tell at which sites the sensitivity on initial conditions (which is a basic ingredient of chaos) is larger.

In Fig. 6a we plot the energy density distribution for an individual trajectory of case I (cf. Fig. 5) at three different times $t \approx 10^6, 10^7, 10^8$ and in Fig. 6b the corresponding DVD. We observe that the energy densities spread more evenly over the lattice the more the wave packet grows. At the same time the DVD stays localized, but the peak positions clearly meander in time, covering distances of the order of the wave packet width. The full time evolution of the energy density and the DVD is shown in Fig. 6c, d together with the track of the distribution's mean position (central white curve). While the energy density distribution shows a modest time dependence of the position of its mean, the DVD mean position is observed to perform fluctuations whose amplitude increases with time.

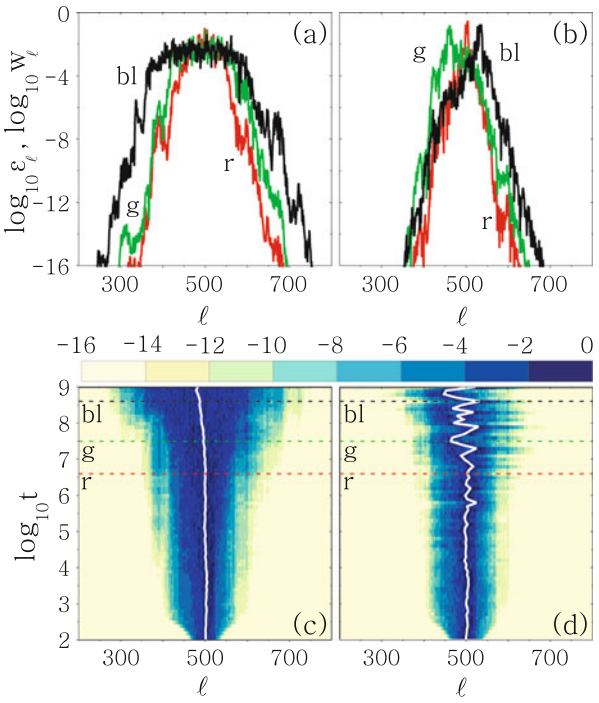

Fig. 6 The dynamics of an individual trajectory of case I. Normalized (**a**) energy (ϵ_l) and (**b**) deviation vector (w_l) distributions at $t = 4 \times 10^6$, $t = 3 \times 10^7$, $t = 4 \times 10^8$ [(r) red; (g) green; (bl) black]. Time evolution of (**c**) the energy distribution and (**d**) the DVD for the realization of panel (**a**) in $\log_{10}$ scale. The position of the distribution's mean position is traced by a *thick white curve*. The times at which the distributions of panels (**a**) and (**b**) are taken are denoted by *straight horizontal lines* in (**c**) and (**d**). Adapted from [43]

6.2 *Effective Noise Theory*

Having established that the dynamics inside a spreading wave packet is chaotic, let us proceed to construct an effective noise theory for spreading. For that we replace the time dependence on the rhs of Eq. (9) by a random function in time:

$$i\dot{\chi}_\nu = F(t)\ ,\ \langle F\rangle = 0\ ,\ \langle F^2(t)\rangle = f^2;\ . \tag{30}$$

Assume that the norm density (norm per site/mode) inside the wave packet is n. What are the consequences? Consider a normal mode μ which is outside the wave packet, but in a boundary layer of one of its edges. For obvious reasons the boundary layer thickness is of the order of V. The equation of motion for this mode is given by (30). At some initial time t_0 assume that the norm of the considered mode is close to zero $|\chi_\mu(t_0)|^2 = n_\mu(t_0) \ll n$. Then the solution of the stochastic differential equation (30) is yielding a diffusion process in norm/energy space of the considered NM:

$$n_\mu(t) \sim f^2 t\ . \tag{31}$$

The considered mode will reach the packet norm n after a time T whose inverse will be proportional to the momentary diffusion rate of the wave packet $D \sim 1/T$:

$$D \sim \frac{f^2}{n} \ . \tag{32}$$

Let us estimate the variance f for the nonlinear wave equation. It follows from estimating the absolute value of the rhs of (9) which corresponds to the absolute value of the stochastic force $F(t)$ in (30). We find that $f \sim \beta n^{3/2}\langle I\rangle$. With that, we arrive at $D \sim (\beta n\langle I\rangle)^2$. The main point here is that the diffusion coefficient is proportional to n^2, therefore the more the packet spreads, the lower its density, and the smaller D. We obtain a time-dependent diffusion coefficient, and a tendency to spread slower than within a normal diffusion process. What are the consequences? A quick first argumentation line is to observe that the second moment m_2 of a wave packet is inverse proportional to its squared norm density $m^2 \sim 1/n^2$. At the same time it should obey $m_2 \sim Dt$. Since $D \sim 1/m_2$ it follows $m_2 \sim t^{1/2}$.

The second way is to write down a nonlinear diffusion equation [45] for the norm density distribution (replacing the lattice by a continuum for simplicity, see also [46]):

$$\partial_t n = \partial_\nu (D\partial_\nu n) \ , \ D \sim n^\kappa \ . \tag{33}$$

The solution $n(\nu, t)$ obeys the scaling $n(\nu, t/a) = bn(c\nu, t)$ with $b = c = a^{1/(\kappa+2)}$ if $n(\nu \pm \infty, t) \to 0$. Therefore the second moment

$$m_2 \sim t^\alpha \ , \ \alpha = \frac{2}{\kappa + 2} \ . \tag{34}$$

Notably an explicit self-similar solution was calculated by Tuck in 1976 [47] which has the following spatial profile:

$$n(\nu) = \left(B - \frac{\kappa \nu^2}{2(\kappa + 2)} \right)^{1/\kappa} \ . \tag{35}$$

Here B is an integration constant (see also [48]).

With $\kappa = 2$ we obtain the subdiffusive law $m_2 \sim t^{1/2}$ again. We do arrive at a subdiffusive spreading. Note that the above nonlinear diffusion equation can be derived through a master equation and a Fokker-Planck equation for both norm and energy densities [49], or Boltzmann equations [50]. However the exponent is $1/2$ *and not* $1/3$. Furthermore, recall that an enforcing of the randomization of NM phases during the spreading *does yield the exponent* $1/2$. Therefore, we are on the right track—enforcing the assumption of random NM phases, both numerics and effective noise theory approaches coincide. What is then the reason for the even slower subdiffusion with $\alpha = 1/3$? We recall that perturbation theory in Sect. 4.2 leads to a probability $\mathscr{P}$ of a given NM being resonant which is small for small

densities (24): $\mathscr{P}_\nu|_{\beta n\to 0} \to \frac{\sqrt{3}V^3\langle I\rangle}{\sqrt{2\pi}\Delta}\beta n$. In case when this probability is equal to one, the above diffusion constant assumption should make sense, since in that case every degree of freedom participating in the wave packet evolves chaotically, i.e. randomly in time. In the case when the resonance probability is zero, perturbation theory should be applicable, the resonance normal form from Sect. 4.1 yields Anderson localization, and spreading should stop. In that case $f = 0$ and then $D = 0$. In best traditions of phenomenology we assume that another factor is missing in the expression of f. This factor shall be a function of $\mathscr{P}$ such that the factor becomes one when $\mathscr{P} = 1$ and zero when $\mathscr{P} = 0$. The simplest prefactor is $\mathscr{P}$ itself. Let us test whether this works (recalling $d = \Delta/V$):

$$f \sim \mathscr{P}\beta n^{3/2}\langle I\rangle\ ,\ D \sim (\mathscr{P}\beta n\langle I\rangle)^2\ ,\ \mathscr{P} = 1 - \mathrm{e}^{-C\beta n}\ ,\ C = \frac{\sqrt{3}V^2\langle I\rangle}{\sqrt{2\pi}d}\ . \tag{36}$$

Then the solution of the nonlinear diffusion equation (33) reads

$$m_2 \sim (\beta\langle I\rangle V)^{4/3}d^{-2/3}t^{1/3}\ ,\ C\beta n \ll 1\ :\ \text{weak chaos}\ , \tag{37}$$

$$m_2 \sim \beta\langle I\rangle t^{1/2}\qquad\quad ,\ C\beta n \gg 1\ :\ \text{strong chaos}\ . \tag{38}$$

We arrived at a construction which results in the correct weak chaos exponent $\alpha = 1/3$ [9]. We also predict that there must be an intermediate regime of strong chaos for which $\alpha = 1/2$—*without any enforcing of the randomization of NM phases* [34]. It has to be intermediate, since with an assumed further spreading of the wave packet, the density n will decrease, and at some point satisfy the weak chaos condition (37) instead of the strong chaos condition (38). Therefore, a potentially long lasting regime of strong chaos has to cross over into the asymptotic regime of weak chaos [34]. That crossover is not a sharp one in the time evolution of the wave packet. It might take several orders of magnitude in time to observe the crossover. Therefore, instead of fitting the numerically obtained time dependence $m_2(t)$ with power laws, it is much more conclusive to compute derivatives $d\langle\log_{10} m_2\rangle/d\log_{10} t$ in order to identify a potentially long lasting regime of strong chaos, crossovers, or the asymptotic regime of weak chaos.

The conditions for weak and strong chaos in (37), (38) match those in Eqs. (13)–(15) if the constant C is replaced by $1/d$. Although this is not strictly correct according to Eq. (36), numerical data [9] suggest that both estimates yield the same order of magnitude in a wide range of weak and intermediate disorder strength.

6.3 Generalizations

Let us consider **D**-dimensional lattices with nonlinearity order $\sigma > 0$:

$$i\dot{\psi}_{\mathbf{l}} = \epsilon_{\mathbf{l}}\psi_{\mathbf{l}} - \beta|\psi_{\mathbf{l}}|^\sigma\psi_{\mathbf{l}} - \sum_{\mathbf{m}\in D(\mathbf{l})}\psi_{\mathbf{m}}\ . \tag{39}$$

Here $\mathbf{l}$ denotes a $\mathbf{D}$-dimensional lattice vector with integer components, and $\mathbf{m} \in D(\mathbf{l})$ defines its set of nearest neighbor lattice sites. We assume that (a) all NMs are spatially localized (which can be obtained for strong enough disorder W), (b) the property $\mathscr{W}(x \to 0) \to const \neq 0$ holds, and (c) the probability of resonances on the edge surface of a wave packet is tending to zero during the spreading process. A wavepacket with average norm n per excited mode has a second moment $m_2 \sim 1/n^{2/\mathbf{D}}$. The nonlinear frequency shift is proportional to $\beta n^{\sigma/2}$. The typical localization volume of a NM is still denoted by V, and the average spacing by d.

Consider a wave packet with norm density n and volume $L < V$. A straightforward generalization of the expected regimes of spreading leads to the following:

$$\beta n^{\sigma/2} \left(\frac{L}{V}\right)^{\sigma/2} V < \Delta \ : \ \text{weak chaos} \ ,$$

$$\beta n^{\sigma/2} \left(\frac{L}{V}\right)^{\sigma/2} V > \Delta \ : \ \text{strong chaos} \ ,$$

$$\beta n^{\sigma/2} > \Delta \ : \ \text{selftrapping} \ .$$

The regime of strong chaos, which is located between selftrapping and weak chaos, can be observed only if

$$L > L_c = V^{1-2/\sigma} \ , \ n > n_c = \frac{V}{L}\left(\frac{d}{\beta}\right)^{2/\sigma} \ . \tag{40}$$

For $\sigma = 2$ we need $L > 1$, for $\sigma \to \infty$ we need $L > V$, and for $\sigma < 2$ we need $L \geq 1$. Thus the regime of strong chaos can be observed e.g. in a one-dimensional system with a single site excitation and $\sigma < 2$.

If the wave packet size $L > V$ then the conditions for observing different regimes simplify to

$$\beta n^{\sigma/2} < d \ : \ \text{weak chaos} \ ,$$

$$\beta n^{\sigma/2} > d \ : \ \text{strong chaos} \ ,$$

$$\beta n^{\sigma/2} > \Delta \ : \ \text{selftrapping} \ .$$

The regime of strong chaos can be observed if

$$n > n_c = \left(\frac{d}{\beta}\right)^{2/\sigma} \ . \tag{41}$$

Similar to the above we obtain a diffusion coefficient

$$D \sim \beta^2 n^{\sigma} (\mathscr{P}(\beta n^{\sigma/2}))^2 \ . \tag{42}$$

In both regimes of strong and weak chaos the spreading is subdiffusive [9, 34]:

$$m_2 \sim (\beta^2 t)^{\frac{2}{2+\sigma \mathbf{D}}} \ , \ \text{strong chaos} \ , \tag{43}$$

$$m_2 \sim (\beta^4 t)^{\frac{1}{1+\sigma \mathbf{D}}} \ , \ \text{weak chaos} \ . \tag{44}$$

Note that the strong chaos result was also obtained within a Boltzmann theory approach [50].

Let us calculate the number of resonances in the wave packet volume (N_{RV}) and on its surface (N_{RS}) in the regime of weak chaos:

$$N_{RV} \sim \beta n^{\sigma/2-1} \ , \ N_{RS} \sim \beta n^{\frac{\mathbf{D}(\sigma-2)+2}{2\mathbf{D}}} \ . \tag{45}$$

We find that there is a critical value of nonlinearity power $\sigma_c = 2$ such that the number of volume resonances grows for $\sigma < \sigma_c$ with time, drops for $\sigma > \sigma_c$ and stays constant for $\sigma = \sigma_c$. Therefore subdiffusive spreading is expected to be more effective for $\sigma < \sigma_c$.

We also find that the number of surface resonances will grow with time for

$$\mathbf{D} > \mathbf{D_c} = \frac{1}{1-\sigma/2} \ , \ \sigma < 2 \ . \tag{46}$$

Therefore, for these cases, the wave packet surface might not stay compact. Instead surface resonances may lead to a resonant leakage of excitations into the exterior. This process can increase the surface area, and therefore lead to even more surface resonances, which again increase the surface area, and so on. The wave packet could even fragmentize, perhaps get a fractal-like structure, and lower its compactness index. The spreading of the wave packet would speed up, but not anymore be due to pure incoherent transfer, instead it might even become a complicated mixture of incoherent and coherent transfer processes.

7 Testing the Predictions

In this chapter we will review numerical results which test the above predictions. We will in particular discuss the crossover from strong to weak chaos, the scaling of the density profiles, the impact of different powers of nonlinearity and different lattice dimensions, and the temperature dependence of heat conductivity. We will also extend the discussion to quasiperiodic Aubry-Andre localization, dynamical localization with kicked rotors, Wannier-Stark localization, and time-dependent ramping protocols of the nonlinearity strength which speed up the slow subdiffusive spreading process up to normal diffusion.

7.1 The Crossover from Strong to Weak Chaos

The first prediction concerns the possibility to observe subdiffusive spreading of wave packets in the intermediate regime of strong chaos (15), and the crossover to the asymptotic regime of weak chaos. The discussed results were obtained by Laptyeva et al. [51]. We consider compact wave packets at $t = 0$ spanning a width V centered in the lattice, such that within V there is a constant initial norm density of n and a random phase at each site (outside the volume V the norm density is zero). In the KG case, this equates to exciting each site in the width V with the same energy density, $\mathscr{E} = E/V$, i.e. initial momenta of $p_l = \pm\sqrt{2\mathscr{E}}$ with randomly assigned signs. Figure 7 (left plot—DNLS, inset right plot—KG) summarizes the predicted regimes, in which lines represent the regime boundaries. It should be noted that the regime boundaries are NOT sharp, rather there is some transitional width between the regimes. The weaker the strength of disorder, the larger the window of strong chaos. Inversely, for $W \geq 8$ the strong chaos window closes almost completely. Ideally, one should utilize the smallest possible value of W. Computational limits restrict this, so a reference of $W = 4$ was chosen. It is important to note that δ will be reduced in time, since a spreading wave packet increases in size and drops its norm (energy) density. This gives the following interpretation of Fig. 7: given an initial norm density, the packet is in one of the three regimes (for example, the three circles in Fig. 7). A packet launched in the weak chaos regime stays in this regime, while one launched in the strong chaos regime spreads to the point that it eventually crosses over into the asymptotic regime of weak chaos at later times.

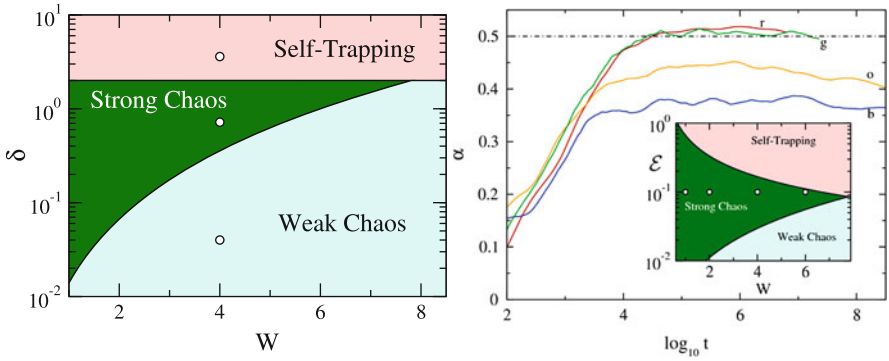

Fig. 7 *Left plot:* parametric space of disorder, W, vs. the frequency shift induced by nonlinearity, δ, for the DNLS model. Three spreading regimes are shown for dynamics dictated by: (1) weak chaos (*pale blue*), (2) strong chaos (*green*), and (3) the onset of self-trapping (*pale red*). The *three circles* show the initial numerical values used in Fig. 8. *Right plot:* spreading behavior in the strong chaos regime for the KG model, with an initial energy density of $\mathscr{E} = 0.1$. The *four curves* are for the disorder strengths of: $W = 1$—(*r*)ed, $W = 2$—(*g*)reen, $W = 4$—(*o*)range, $W = 6$—(*b*)lue. *Inset*: the KG analog of the DNLS parametric space. It is obtained by the small amplitude mapping $\mathscr{E} \to 3W\delta$. The four points correspond to the disorder strengths used in the main portion of the figure. Adapted from [51]

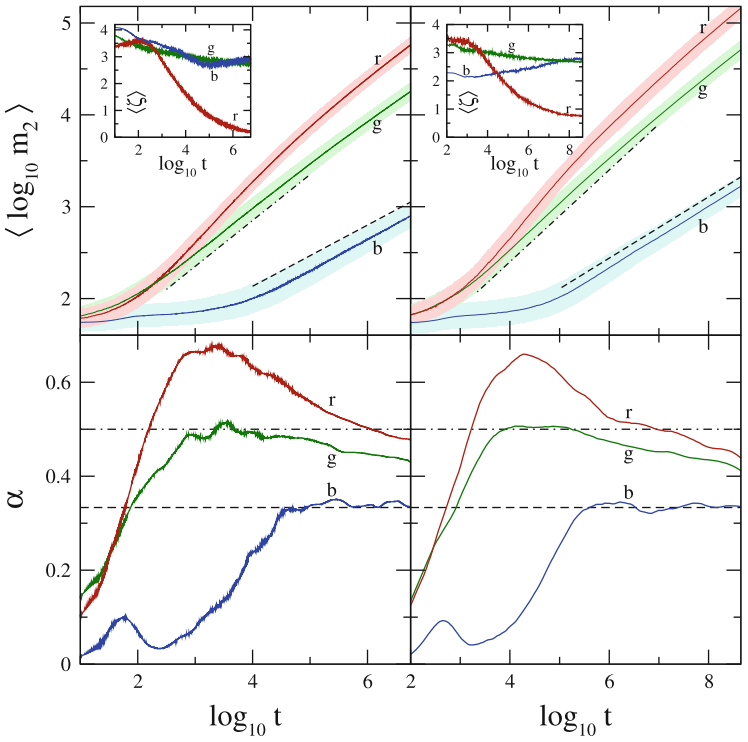

Fig. 8 *Upper row*: Average log of second moments (*inset*: average compactness index) vs. log time for the DNLS (KG) on the *left* (*right*), for $W = 4, L = 21$. *Colors/letters* correspond the three different regimes: (1) weak chaos—(*b*)lue, $\beta = 0.04$ ($\mathscr{E} = 0.01$), (2) strong chaos—(*g*)reen, $\beta = 0.72$ ($\mathscr{E} = 0.2$), (3) self-trapping—(*r*)ed, $\beta = 3.6$ ($\mathscr{E} = 0.75$). The respective lighter surrounding areas show one standard deviation error. *Dashed lines* are to guide the eye to $\sim t^{1/3}$, while *dotted-dashed* guides for $\sim t^{1/2}$. *Lower row*: finite difference derivatives for the smoothed m_2 data respectively from above curves. Adapted from [51]

For DNLS, an initial norm density of $n = 1$ was used, so that initially $\delta \sim \beta$. Nonlinearities ($\mathscr{E}$ for KG) were chosen within the three spreading regimes (see Fig. 7), respectively $\beta \in \{0.04, 0.72, 3.6\}$ and $\mathscr{E} \in \{0.01, 0.2, 0.75\}$.

Ensemble averages over disorder were calculated for 1000 realizations and are shown in Fig. 8 (upper row). In the regime of weak chaos we find a subdiffusive growth of m_2 at large times according to $m_2 \sim t^{\alpha}$, $\alpha \leq 1$, with a compactness index $\zeta \approx 3$. Note that the subdiffusive growth is difficult to see initially in Fig. 8 for two reasons. Firstly, the logarithmic scaling hides any small initial growth, and secondly, there is a characteristic time scale for the packet to spread from its initial preparation. In the regime of strong chaos we observe a faster subdiffusive growth of m_2, with an additional slowing down at larger times, as expected from the predicted crossover. The compactness index is also $\zeta \approx 3$, as in the weak chaos regime. Finally, in the regime of partial self-trapping m_2 grows, but the compactness index ζ decreases

in time substantially. This indicates that a part of the wave packet is arrested, and another part is spreading.

In order to quantify these findings, smoothed data $\langle \log m_2 \rangle$ were produced [51], with a locally weighted regression algorithm [52], and a subsequently applied central finite difference to calculate the local derivative

$$\alpha(\log t) = \frac{\mathrm{d}\langle \log m_2 \rangle}{\mathrm{d} \log t} \ . \tag{47}$$

The outcome is plotted in the lower row in Fig. 8. In the weak chaos regime the exponent $\alpha(t)$ increases up to $1/3$ and stays at this value for later times. In the strong chaos regime $\alpha(t)$ first rises up to $1/2$, keeps this value for one decade, and then drops down, as predicted. Finally, in the self-trapping regime we observe an even larger rise of $\alpha(t)$. Additionally, we also mention numerics for $W \in \{1, 2, 6\}$ with respective initial packet widths of $L = V \in \{361, 91, 11\}$ [51]. Results are qualitatively similar to those shown in Fig. 8, and thus omitted for graphical clarity.

The duration of the strong chaos regime with $\alpha = 1/2$ (and thus the location of the crossover) is largely dependent on how deep in the strong chaos regime the state is initially. Since the boundaries between different regimes are NOT sharp, but rather have some characteristic width, ideally one should utilize the smallest possible value of W. This is shown in Fig. 7 (right plot) for the KG model. For $W \in \{1, 2\}$, a long plateau at $\alpha = 1/2$ is clearly observed. For $W \in \{4, 6\}$, the initial energy density approaches one of the boundary lines and likely crosses into a boundary window, in which $\alpha < 1/2$.

7.2 *Density Profile Scaling*

If the effective noise theory (Sect. 6.2) applies, then the density distribution (energy for KG, norm for DNLS) should obey the nonlinear diffusion equation (33). In the weak chaos regime we have $\kappa = 4$. A numerical study was performed by Laptyeva et al. [53] to test whether the scaling properties of the solutions (see Sect. 6.2) hold. The main results are shown in Fig. 9 (for details we refer to [53]). The evolution of the averaged energy density profiles (KG) $\langle E \rangle$ in the course of spreading is illustrated in the left plot in Fig. 9. The peaked initial distribution profiles transform into more flat ones as time evolves. The most striking result is obtained by rescaling the profiles in Fig. 9 according to the scaling laws of the nonlinear diffusion equation (33). The rescaled densities are plotted in the inset of the left plot of Fig. 4. We observe very good scaling behavior. For the DNLS with $\beta = 0.04$ similar data are shown in the right plot in Fig. 9 for the times $t \approx to^5$, $t \approx 10^6$, $t \approx 10^7$. The data are rescaled similar to the KG case. The result is shown in the inset of the right plot of Fig. 9 and shows again very good agreement. Together with the proper scaling of the edge of the wave packets, which was tested in [54], this is the strongest argument to support the applicability of NDE and MNDE to the spreading of wave packets

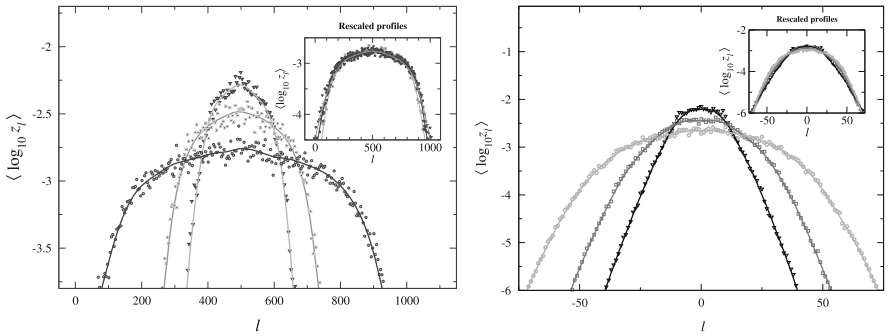

Fig. 9 *Left plot:* KG. The log of the normalized energy density distribution $\langle \log_{10} z_l \rangle$ at three different times (from *top* to *bottom* $t \approx 10^4$, $t \approx 10^7$, $t \approx 10^8$). The initial parameters are $E = 0.2$, $W = 4$ and $V = 21$. *Symbols* correspond to the average over 10^3 disorder realizations, and *solid lines* correspond to an additional smoothing. *Inset*: rescaled distributions (see text). *Right plot:* DNLS. The log of the normalized norm density distribution $\langle \log_{10} z_l \rangle$ at three different times (from *top* to *bottom* $t \approx to^5$, $t \approx 10^6$, $t \approx 10^7$). The initial parameters are $\beta = 0.04$, $W = 4$, and $V = 21$. *Symbols* correspond to the average over 10^3 disorder realizations, and *solid lines* correspond to an additional smoothing. *Inset*: rescaled distributions (see text). Adapted from [53]

in nonlinear disordered systems. It also strongly supports that the spreading process follows the predicted asymptotics and does not slow down or even halt.

7.3 Tuning the Power of Nonlinearity and the Lattice Dimension

Let us consider a generalization of DNLS model (gDNLS) by tuning the power of nonlinearity, which corresponds to the case $\mathbf{D} = 1$ in (39)

$$i\dot{\psi}_l = \epsilon_l \psi_l + \beta |\psi_l|^\sigma \psi_l - \psi_{l+1} - \psi_{l-1}, \tag{48}$$

where σ is a positive real number. We want to test the predictions presented in Sect. 6.3. Note that the previous DNLS and KG models had $\sigma = 2$ which correspond to cubic nonlinearities in the equations of motion, quartic anharmonicities in the Hamiltonian, and are related to two-body interactions in quantum many-body systems. Some other integer values of σ might well have physical relevance, e.g. $n = \sigma/2 + 1$ corresponds to n-body interactions, and $\sigma = 1$ relates to quadratic Kerr media in nonlinear optics.

Mulansky [55] presented numerical simulations of the gDNLS model for a few integer values of σ and single site excitations, and fitted the dependence $m_2(t) \sim t^\alpha$ with exponents α which depend on σ (see open circle data in left plot in Fig. 10). In [57] numerical simulations of the gDNLS model were performed for non integer

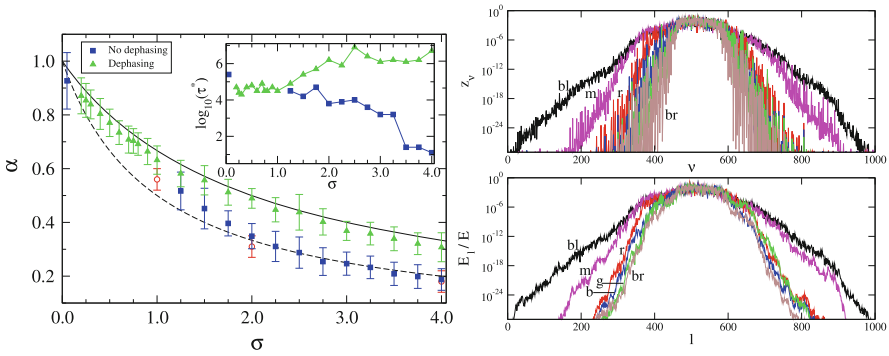

Fig. 10 *Left plot:* exponent α ($m_2 \sim t^\alpha$) versus the nonlinearity order σ for plain integration without dephasing (*filled squares*) and for integration with dephasing of NMs (*filled triangles*). Results without dephasing obtained in [55] are plotted with *empty circle symbols*. The theoretically predicted functions $\alpha = 1/(1+\sigma)$ (weak chaos) and $\alpha = 2/(2+\sigma)$ (strong chaos) are plotted by *dashed and solid lines* respectively. *Inset*: the logarithm of the minimum time τ^* for which the evolution of m_2 can be numerically fitted by a function of the form t^α versus σ for integration with (*filled triangles*) and without (*filled squares*) dephasing. *Right plot:* normalized energy distributions in NM (*upper plot*) and real (*lower plot*) space for $\sigma = 0.05, 0.2, 0.8, 1.25, 2.0, 3.0$ [(*bl*) black; (*m*) magenta; (*r*) red; (*b*) blue; (*g*) green; (*br*) brown] at times $t = 3.6 \times 10^5, 1.3 \times 10^5, 2.5 \times 10^5, 1.4 \times 10^6, 3 \times 10^7, 10^9$ respectively. The second moment of each distribution is $m_2 \approx 10^3$. In the *upper plot* the distributions for $\sigma = 1.25, 2.0$ are not clearly visible as they are overlapped by the distribution for $\sigma = 3.0$. Adapted from [56]

values of σ on rather short time scales, leaving the characteristics of the asymptotic ($t \to \infty$) evolution of wave packets aside.

The corresponding generalized KG model (gKG) follows the equations of motion

$$\ddot{u}_l = -\tilde{\epsilon}_l u_l - |u_l|^\sigma u_l + \frac{1}{W}(u_{l+1} + u_{l-1} - 2u_l) \; . \tag{49}$$

and was studied by Skokos et al. [56], again for single site excitations, and a whole range of different values of $0.02 \leq \sigma \leq 4$. The dependence $m_2(t) \sim t^\alpha$ was again fitted with exponents α which depend on σ. In order to emulate strong chaos from scratch, an additional normal mode dephasing (see Sect. 5.3 and Fig. 4) was performed, and again the data were fitted with σ-dependent values of α. The outcome is shown in the left plot in Fig. 10. The data with dephasing (filled triangles) are nicely following the prediction from strong chaos (43) $\alpha = 2/(2+\sigma)$ in the range $0.2 \leq \sigma \leq 4$. The data without dephasing (filled squares) show very good agreement with the prediction from weak chaos (44) $\alpha = 1/(1+\sigma)$ in the range $2 \leq \sigma \leq 4$. However for $1 \leq \sigma \leq 1.8$ the numerical results overestimate the weak chaos prediction, and tend towards the strong chaos ones. The reason for that is simply, that for $\sigma < 2$ a single site excitation *can* be launched in the strong chaos regime [34]. Therefore fitting procedures will average over the strong chaos region, crossover region, and weak chaos region, and result in a number which is located

somewhere between the two theoretical lines. Instead of fitting the numerically obtained time dependence $m_2(t)$ with power laws, one should compute derivatives $d\langle \log_{10} m_2 \rangle / d \log_{10} t$ in order to identify a potentially long lasting regime of strong chaos, crossovers, or the asymptotic regime of weak chaos. This is a task yet to be accomplished for the above cases.

The order of nonlinearity σ influences not only the spreading rate of wave packets, but also the morphology of their profiles. In the right plot in Fig. 10 we plot the normalized energy distributions of initial single site excitations, for different σ values in NM (upper plot) and real (lower plot) space. Starting from the outer, most extended wave packet we plot distributions for $\sigma = 0.05$ (black curves), $\sigma = 0.2$ (magenta curves), $\sigma = 0.8$ (red curves), $\sigma = 1.25$ (blue curves), $\sigma = 2$ (green curves) and $\sigma = 3$ (brown curves). All wave packets were considered for the same disorder realization but at different times of their evolution when they have the same value of second moment $m_2 \approx 10^3$. These times are $t = 3.6 \times 10^5$ for $\sigma = 0.05$, $t = 1.3 \times 10^5$ for $\sigma = 0.2$, $t = 2.5 \times 10^5$ for $\sigma = 0.8$, $t = 1.4 \times 10^6$ for $\sigma = 1.25$, $t = 3 \times 10^7$ for $\sigma = 2$ and $t = 10^9$ for $\sigma = 3$ and increase for $\sigma \geq 0.2$ since the spreading becomes slower for larger σ. When $\sigma \to 0$ wave packets remain localized for very large time intervals before they start to spread [56]. This is why for $\sigma = 0.05$ the second moment becomes $m_2 \approx 10^3$ at a larger time than in cases with $\sigma = 0.2$ and $\sigma = 0.8$. From the results of Fig. 10 we see that for large enough values of σ ($0.8 \leq \sigma \leq 3$), the distributions on a logarithmic scale have a chapeau-like shape consisting of a highly excited central part and exponential tails having practically the same slope. Contrarily, the distributions for $\sigma = 0.2$ and $\sigma = 0.05$ become more extended having different slopes in the tails.

A characteristic of the NM space distributions in the right plot in Fig. 10 for $\sigma \geq 0.8$ is that they exhibit very large value fluctuations (up to 5–10 orders of magnitude) in their tails, contrarily to the corresponding distributions in real space. Tail NMs are driven by the core of the wave packet, but may also interact with neighboring tail NMs. The presence of large tail amplitude fluctuations signals that neighboring tail NMs do not interact significantly (otherwise we would expect a tendency towards equipartition). Tail NMs are then excited only by the core. The further away they are, the weaker the excitation. But within a small tail volume, NMs with larger localization length will be more strongly excited than those with smaller localization length, hence the large observed fluctuations, which on a logarithmic scale are of the order of the relative variation of the localization length. Therefore Anderson localization is preserved in the tails of the distributions over very long times (essentially until the given tail volume becomes a part of the core). But the NM space distributions for $\sigma = 0.05$ and $\sigma = 0.2$ exhibit less fluctuations in their tail values with respect to the other distributions in the upper right plot of Fig. 10, implying that tail NMs are now interacting with each other on comparatively short time scales and reach a visible level of local equipartition. Therefore we observe for these cases a destruction of Anderson localization even in the tails of the spreading wave packets.

How is Anderson localization restored in the limit $\sigma \to 0$, since we obtain a linear wave equation for $\sigma = 0$? Both weak and strong chaos exponents yield $\alpha(\sigma \to 0) \to 1$ in this case, i.e. normal diffusion. The answer is in the prefactor of the subdiffusive law $m_2 = Ct^\alpha$. The only possibility is to assume $C(\sigma \to 0) \to 0$. The diverging waiting times for single site excitations in this limit, which have to pass before spreading is observed, are a good confirmation of the above assumption [56].

Let us move on to two-dimensional cases. The two-dimensional DNLS case yields the equations of motion

$$i\dot{\psi}_{\mathbf{b}} = \epsilon_{\mathbf{b}}\psi_{\mathbf{b}} + \beta\,|\psi_{\mathbf{b}}|^\sigma\,\psi_{\mathbf{b}} - \sum_{\mathbf{n}} \psi_{\mathbf{n}}. \tag{50}$$

Here $\mathbf{b} = (l, m)$ denotes a two-dimensional lattice vector with integer components, and $\mathbf{n}$ runs over nearest neighbors. Garcia-Mata et al. [7] studied (50) with $\sigma = 2$. Single site excitations were launched and the numerically obtained time dependence of $m_2(t)$ was fitted with power laws. With the largest integration time $t = 10^6$ and 10 disorder realizations the fitting result was $\alpha \approx 0.23$. Note that the effective noise theory predicts $\alpha = 1/3$ for the strong chaos case (43), and $\alpha = 0.2$ for the asymptotic weak chaos case (44). Therefore the result from [7] is again located between both predictions, which might be due to crossover effects, and insufficient averaging and integration time (see above discussion).

A further work by Laptyeva et al. [58] studies the two-dimensional KG case for various values of σ:

$$\ddot{u}_{\mathbf{b}} = -\tilde{\epsilon}_{\mathbf{b}}u_{\mathbf{b}} - |u_{\mathbf{b}}|^\sigma\,u_{\mathbf{b}} + \frac{1}{W}\sum_{\mathbf{n}}(u_{\mathbf{n}} - u_{\mathbf{b}})\,. \tag{51}$$

Rather than fitting the numerically obtained time dependence $m_2(t)$ with power laws as in [7], Laptyeva et al. [58] computed derivatives $d\langle\log_{10} m_2\rangle/d\log_{10} t$ in order to identify a potentially long lasting regime of strong chaos, crossovers, and the asymptotic regime of weak chaos. The number of disorder realizations was as large as 400, and integration times extended up to $t = 10^8$. Initial states were wave packets occupying a typical localization volume $V \sim 30$ of the linear wave equation. In Fig. 11 the results for $\sigma = 2$ are shown. The weak chaos exponent measures as $\alpha \approx 0.21$ which is very close to the theoretical prediction $\alpha = 0.2$. Extensions to $\sigma = 1.5, 1.3$ in the weak chaos regime and to $\sigma = 0.7, 0.5$ in the strong chaos regime show very good agreement between the numerically observed exponents, and the theoretical predictions in Fig. 12.

We can conclude, that the predictions from effective noise theory and the nonlinear diffusion approach have been impressively confirmed in various numerical studies.

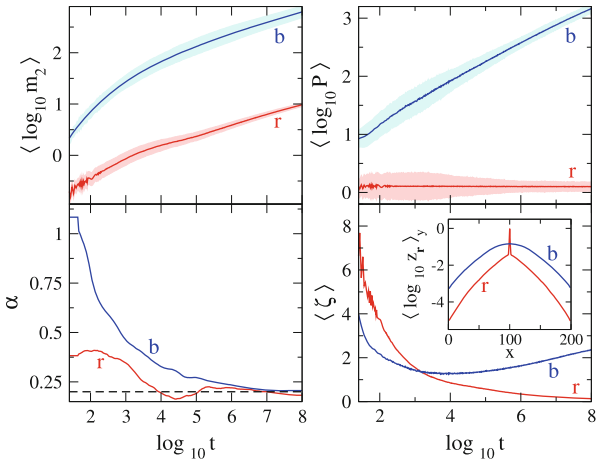

Fig. 11 The parameters $(\sigma, \mathscr{E}) = (2, 0.3), (2, 2.0)$ correspond to the weak chaos [(*b*)lue] and self-trapping [(*r*)ed]. *Left column*: average log of second moment (*upper*) and its power-law exponent (*lower*) vs. log time. The *dashed line* is the theoretical expectation for the weak chaos $\alpha = 0.20$. *Right column*: average log of participation number (*upper*) and average compactness index (*lower*) vs. log time. In both columns of the *upper row* the lighter clouds correspond to a standard deviation. *Inset:* normalized radial density distributions at $t = 10^8$. Adapted from [58]

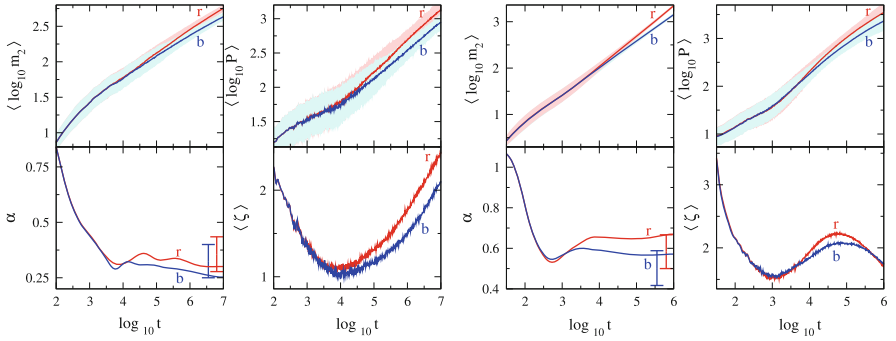

Fig. 12 *Left plot:* The parameters $(\sigma, \mathscr{E}) = (1.3, 0.025), (1.5, 0.04)$ are colored respectively as (*r*)ed and (*b*)lue. *Left column*: average log of second moment (*upper*) and its power-law exponent (*lower*) vs. log time. *Right column*: average log of participation number (*upper*) and average compactness index (*lower*) vs. log time. *Right plot:* the parameters $(\sigma, \mathscr{E}) = (0.5, 0.005), (0.7, 0.03)$ are colored respectively as (*r*)ed and (*b*)lue. *Left column*: average log of second moment (*upper*) and its power-law exponent (*lower*) vs. log time. *Right column*: average log of participation number (*upper*) and average compactness index (*lower*) vs. log time. In both columns of the *upper row*, the lighter clouds correspond to a standard deviation. The I-bar bounds denote the theoretical expectations from Eqs. (43), (44) for weak chaos (*lower bound*) and strong chaos (*upper bound*). Adapted from [58]

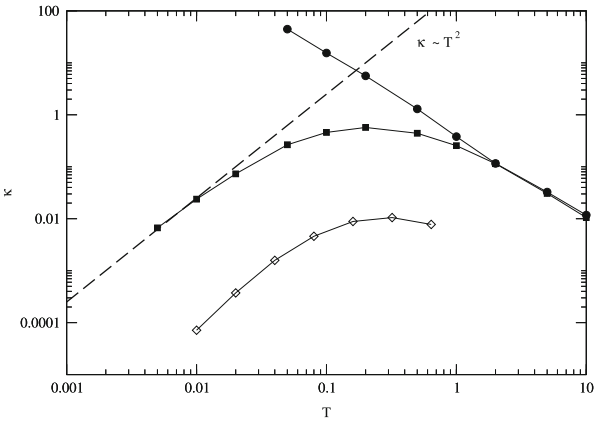

Fig. 13 KG chain: heat conductivity $\kappa(T)$ for $W = 2$ (*filled squares*). For comparison we also show the data for the ordered case $\tilde{\epsilon}_l \equiv 1$ (*filled circles*). *Thin solid lines* guide the eye. The *dashed line* corresponds to the power law T^2. The stronger disorder case $W = 6$ corresponds to the open diamond data points. Adapted from [59]

7.4 Heat Conductivity

Assuming the validity of effective noise theory, we arrive at the next prediction that the heat conductivity of a thermalized system at small temperature (density) must be proportional to the diffusion coefficient (36) where the density n is replaced by the temperature T. While one has to be careful in the DNLS case, where two conserved quantities (energy, norm) enforce Gibbs, or non-Gibbs distributions [49], the KG case might be again a better testing ground, where one conserved quantity (energy) can be expected to enforce a Boltzmann distribution. The calculation of the heat conductivity for (4) was performed in [59]. Its dependence on the temperature is shown in Fig. 13. The strong chaos scaling $\kappa(T) \sim T^2$ is observed nicely. The expected weak chaos regime was not reachable by the heavily extensive numerical efforts. Note that the decay of the heat conductivity for large temperatures is due to selftrapping, and observed even for the ordered chain at $W = 0$ (solid circles in Fig. 13).

7.5 Ramping Nonlinearity

Subdiffusion is notoriously slow. This poses problems for numerical studies, especially in two and even more in three space dimensions. The situation is even more severe with experimental studies of ultracold interacting K atomic clouds, where the conversion of the maximum time of keeping the coherence of the macroscopic quantum cloud is about 10 s [61], which turns into $t \approx 10^4 \ldots 10^5$ dimensionless time units used throughout this chapter. Consequently the probing of subdiffusion in [61] allowed to conclude qualitatively that the onset of a subdiffusive spreading of the interacting cloud does take place, but was not sufficient to reliably measure the exponent. In order to fit a power law, we need at least two decades of

variation in both variables. With a weak chaos exponent $1/3$ and two decades in the second moment we arrive at six decades in time—added to $t \approx 10^2$ which is the time the linear wave equation spreads into the localization volume. Therefore times $\sim 10^8$ are desirable, which turn into experimental times of the order of 10^5 s—clearly not reachable with nowadays techniques. On the other side, the reader is welcome to reread the above presented numerical data and analysis and welcome to observe that restricting to maximum integration time 10^5 will not allow for an accurate estimate of the exponents. At the same time, numerical studies also suffer from the computational time restriction. While this appears to be no serious issue for most one-dimensional system studies, already two dimensional systems can easily raise the problem of insufficient computational times.

Gligoric et al. [60] suggested a possible way out. Instead of trying to substantially increase available time scales, they propose to speed up the subdiffusive process itself. This is done by a temporal ramping of the two-body interaction strength, which can be varied e.g. for K atoms by three orders of magnitude close to the Feshbach resonance [62]. Why should that help? The momentary diffusion rate D of a spreading packet in one spatial dimension is proportional to the fourth power of the product of interaction strength β and particle density n: $D \sim (\beta n)^4$ for the asymptotic case of weak chaos (36). In the course of cloud spreading the density n decreases, and therefore also D. This is the reason for the predicted subdiffusion process, which is substantially slower than normal diffusion. The proposal is to compensate the decrease of the density n with an increase in the interaction strength β. Depending on the concrete ramping protocol $\beta(\tau)$ one can expect different faster subdiffusion processes, and possibly even normal diffusion. The condition for that outcome to be realized is, that the internal chaos time scales (basically the inverse Lyapunov coefficients) will be still short enough so that the atomic cloud can first decohere, and then spread. With that achieved, the cloud spreading will be faster, and one can expect that the available experimental time will suffice for the precise observation and analysis of the process.

Let us get into numbers for one spatial dimension. The second moment is $m_2 \sim 1/n^2$ and the momentary diffusion constant $D \sim (\beta n)^4$. For a constant β the solution of $m_2 = Dt$ yields $m_2 \sim 1/n^2 \sim t^{1/3}$, and therefore $n \sim t^{-1/6}$. Thus we choose now a time dependence $\beta \sim t^\nu$. Then the resulting spreading is characterized by

$$m_2 \sim t^{(1+4\nu)/3} \ , \ d = 1 \ . \tag{52}$$

For $\nu = 1/2$ we already obtain normal diffusion $m_2 \sim t$.

Similar for two spatial dimensions, where $m_2 \sim 1/n$, for a constant β the cloud spreading is even slower with $m_2 \sim t^{1/5}$. With a time dependent ramping $\beta \sim t^\nu$ the resulting speedup is

$$m_2 \sim t^{(1+4\nu)/5} \ , \ d = 2 \ . \tag{53}$$

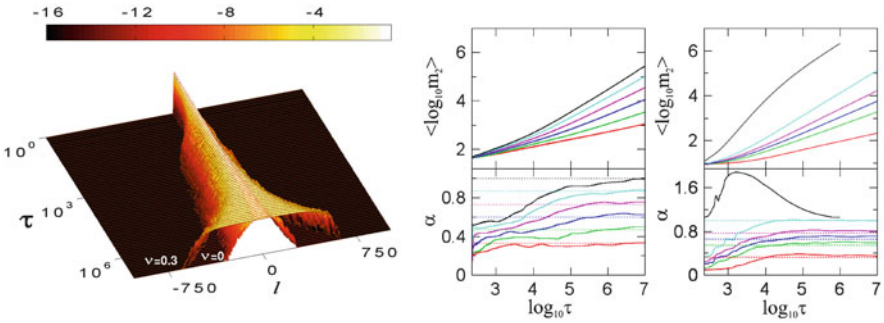

Fig. 14 *Left plot:* evolution of the averaged norm density $< n_l(\tau) >$ in the case without ($\nu = 0$) and with ramping ($\nu = 0.3$) in log scale for the DNLS model. *Right plot: left column:* the second moments (*upper*) and their power-law exponents α (*lower*) for the DNLS model for $\nu = 0$ (*red*), $\nu = 0.1$ (*green*), $\nu = 0.2$ (*blue*), $\nu = 0.3$ (*magenta*), $\nu = 0.4$ (*cyan*), and $\nu = 0.5$ (*black*). *Right column:* the second moments (*upper*) and their power-law exponents α (*lower*) for the NQKR model for $\nu = 0$ (*red*), $\nu = 0.17$ (*green*), $\nu = 0.25$ (*blue*), $\nu = 0.33$ (*magenta*), $\nu = 0.5$ (*cyan*), and $\nu = 1.5$ (*black*). *Dashed colored lines* correspond to expected values for exponents in both cases. Adapted from [60]

For $\nu = 1$ we again obtain normal diffusion. Note that if numerics confirm the above predictions then also the above conditions for the chaoticity time scales are met with good probability.

Once ramping is too fast, one can expect to see several different scenaria. Either fragmenting atomic clouds appear since some parts of the cloud get self-trapped and some other parts do not. If self-trapping is avoided, one may also see ramping-induced diffusion: while the internal cloud dynamics does not suffice to decohere phases, initial fluctuations in the density distribution can lead to considerably different temporal energy renormalizations in different cloud spots, and therefore to an effective dephasing similar to a random noise process in real time and space.

The spreading of wave packets in the DNLS model, without and with ramping of the nonlinearity are shown in the left plot in Fig. 14 (note that time t is coined τ in the plots). Clearly packets spread faster when the nonlinearity is ramped in time. To quantify the spreading exponent, the authors of [60] averaged the logs (base 10) of m_2 over 1000 different realizations and smoothened additionally with locally weighted regression [52]. The (time-dependent) spreading exponents are obtained through central finite difference method [52], $\alpha = \frac{d<\log_{10}(m_2)>}{d(\log_{10}(t))}$. The results for the DNLS model are shown in the right plot in Fig. 14. The exponents of subdiffusive spreading reach the theoretically predicted values. Note that the first assumption of the asymptotic exponent occurs after similar waiting times for all ν. Monitoring of the participation number P for the DNLS model indicates that self-trapping starts to occur already for $\nu = 0.4$. Results for the nonlinear quantum kicked rotor (NQKR) model (see Sect. 8.3), are also shown in the right plot in Fig. 14. Since self-trapping is avoided in the NQKR model, a normal diffusion process for $\nu = 0.5$ can be reached, as predicted.

8 Correlated Potentials

The effective noise and nonlinear diffusion theories need only a few assumptions on input, in particular that (1) the linear wave equation has a regime of localization with finite upper bound on the localization length, and (2) the nonlinear dynamical system should be nonintegrable to allow for deterministic chaos (and therefore normal mode dephasing). The predicted subdiffusive exponents are controlled only by the lattice dimension, and the power of nonlinearity.

So far we discussed the resulting nonlinear diffusion for uncorrelated random potentials ϵ_l. For linear wave equations, a number of other *correlated* potentials are known to result in wave localization for a corresponding linear wave equation.

8.1 Subdiffusive Destruction of Aubry-Andre Localization

Let us replace the uncorrelated disorder potential in Sect. 2 by

$$\epsilon_l = \lambda \cos(2\pi \alpha_{AA} l + \theta) \; . \tag{54}$$

For the linear wave equation $\beta = 0$ and any irrational choice of α_{AA} this results in the well-known Aubry-Andre localization [64]. Note that the irrationality of α_{AA} implies that the spatial period of (54) is incommensurate with the lattice spacing $\Delta l = 1$, and therefore the lattice potential becomes a quasiperiodic one. For shallow potentials $\lambda < 2$ all eigenstates are extended. At the critical value $\lambda = 2$ a metal-insulator transition takes place, and for $\lambda > 2$ all eigenstates are localized with localization length $\xi = 1/\ln(\lambda/2)$, independent of α_{AA} and the eigenenergy of the state [64]. One peculiarity of the linear wave equation is that its eigenvalue spectrum is fractal, has a self-similar Cantor set structure and fractal dimension 1 for all $\lambda \neq 0 \; , \; 2$. In particular it displays a self-similar hierarchy of gaps and subgaps, which implies that self-trapped states can be generated at any weak nonlinearity.

Spreading wave packets were studied by Larcher et al. [63] in the presence of nonlinearity (see Fig. 15). Again a clear regime of weak chaos $m_2 \sim t^{\gamma}$ was observed, with the exponent $\gamma \approx 1/3$. Signatures of strong chaos are also observed, which however might be affected by the presence of selftrapping even at weak nonlinearities.

8.2 Subdiffusive Destruction of Wannier-Stark Localization

An even simpler choice of a dc bias potential

$$\epsilon_l = El \tag{55}$$

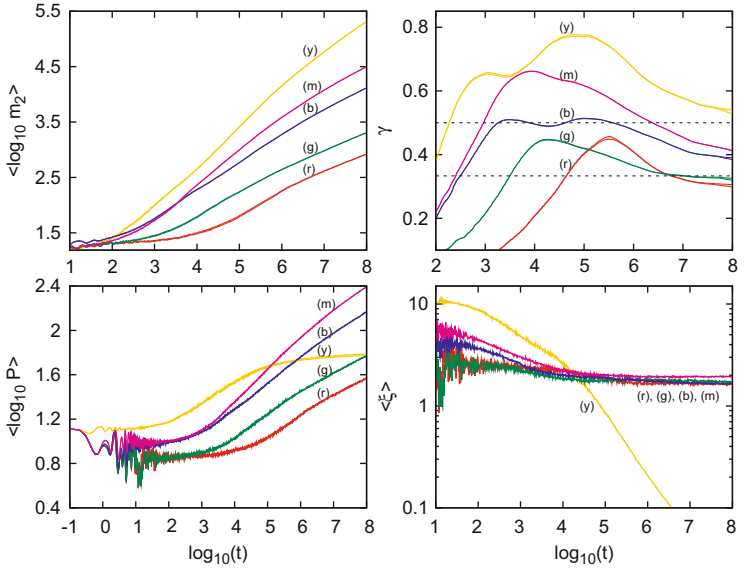

Fig. 15 *Top left panel*: time evolution of $\langle \log_{10} m_2 \rangle$; *top right panel*: $\langle \log_{10} P \rangle$; *bottom left panel*: spreading exponent γ; *bottom right panel*: average compactness index $\langle \xi \rangle$. The nonlinear parameter $\beta = 0.1, 1, 5, 10, 100$ (red (*r*), green (*g*), blue (*b*), magenta (*m*) and yellow (*y*) *curves* respectively). The initial wave packet has $V = 13$ sites excited, and $\lambda = 2.5$. The *two dashed lines* in the *top right panel* correspond to the values $\gamma = 1/3$ and $\gamma = 1/2$. Adapted from [63]

with a constant dc field value E is generating localized states as well. The spectrum of the linear wave equation is an equidistant Wannier-Stark ladder with $\lambda_\nu = E\nu$. All states are localized with localization volume $V \sim |1/(E \ln E)|$ for weak field strength $E < 1$, and $V(E \to \infty) \to 1$. These Wannier-Stark states are superexponentially localized $|A^{(0)}_{\nu,l\to\infty}| \to (1/E)^l/l!$ and therefore very compact in the tails, even for weak dc fields.

Spreading wave packets were studied by Krimer et al. [24] in the presence of nonlinearity (see Fig. 16). While subdiffusion is observed for a wide range of parameters, there are distinct differences to the cases discussed so far. Namely, initial states may be trapped for very long times, but then explosively start to spread. Further, the subdiffusive growth $m_2 \sim t^\alpha$ shows a field dependence of the exponent $\alpha(E)$. Krimer et al. [24] report $\alpha(E = 2) \approx 0.38$, while Kolovsky et al. [65] report $\alpha(E = 0.25) \approx 0.5$. The reason for this dependence might be routed in the fact, that a spreading wave packet has to excite exterior modes close to its boundary, whose eigenenergies are *outside* of the energy spectrum excited inside the wave packet (due to the Wannier-Stark ladder spectrum). The larger E, the larger is this frequency mismatch. Another interesting feature of this model is, that exact quadruplet resonances exist, which seem to leave no room for perturbation approaches.

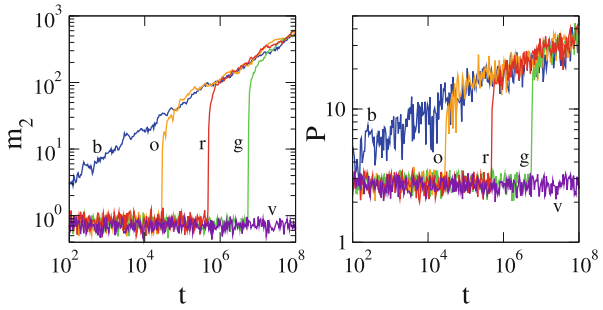

Fig. 16 Single site excitation for $E = 2$. Second moment m_2 and participation number P versus time in log–log plots for different values of β inside the interval where an explosive delocalization of the trapped regime occurs: $\beta = 8.15, 8.25, 8.5$ [(o) orange; (g) green; (r) red]. $\beta = 8$ [(b), blue]: intermediate regime. $\beta = 8.9$ [(v), violet]: trapped regime. Adapted from [24]

8.3 *Subdiffusive Destruction of Dynamical Localization*

Experiments of quantum kicked rotor systems [66, 67] within Bose-Einstein condensates [68], where many-body interactions play a significant role, focus theoretical attention on dynamical localization in the presence of nonlinear interactions. In the mean-field approximation, the dynamics of the kicked rotor can be modeled by the following form of the Gross-Pitaevskii equation (Fig. 17)

$$i\hbar\frac{\partial\psi}{\partial t} = -\frac{\hbar^2}{2M}\frac{\partial^2\psi}{\partial\theta^2} + \tilde{\beta}|\psi|^2\psi + \bar{k}\cos(\theta)\cdot\psi\sum_m \delta(t - mT). \tag{56}$$

Here $\tilde{\beta}$ is the nonlinear strength, which is proportional to the tunable scattering length of atoms in a BEC. M is the mass of the atoms, $\bar{k}$ is the perturbative kick strength, and T is the period of applied kicks. Note that the analogy between an abstract rotor and the atomic wavefunctions is obtained when the atoms are loaded into a momentum eigenstate of the lattice with Bloch wavenumber zero, Spatially homogeneous kicks will keep the Bloch wavenumber invariant, but allow to change the momentum. The solution $\psi(\theta, t)$ can be expanded in an angular momentum basis

$$\psi(\theta, t) = \frac{1}{\sqrt{2\pi}}\sum_{n=-\infty}^{\infty} A_n(t)e^{in\theta} \tag{57}$$

where the coefficients $A_n(t)$ are Fourier coefficients of the time-dependent wave function $\psi(\theta, t)$. The dynamics between two successive kicks is described by following equation

$$i\frac{\partial A_n}{\partial t} = -\frac{1}{2}\tau n^2 A_n + \beta\sum_{n_1}\sum_{n_2} A^*_{n_1}A_{n_2}A_{n-(n_2-n_1)}, \tag{58}$$

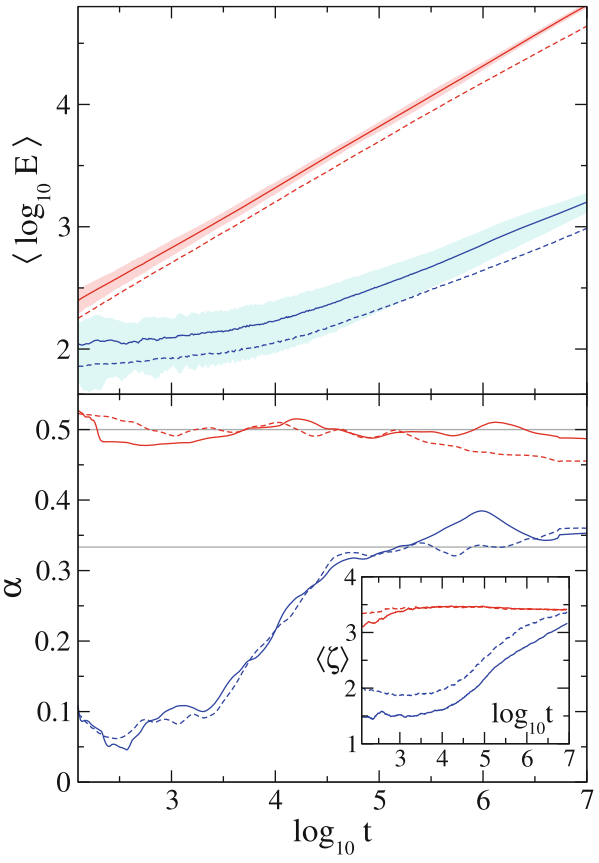

Fig. 17 Under a kick strength of $k = 5$, measures for $\beta = 0.3$ (*blue*) and $\beta = 10$ (*red*), for both quasiperiodic sequences set by $\tau = 1$ (*solid line*), and for random sequences (*dashed line*, see [23] for details). *Upper row*: Mean logarithms for energy $< \log_{10} E >$. The clouds around the quasiperiodic sequences correspond to one standard deviation error. *Lower row*: finite-difference derivative of the above. *Grey horizontal lines* correspond to exponents for weak and strong chaos regimes. *Inset*: average compactness index $\langle \zeta \rangle$ as a function of time. Adapted from [23]

where $\beta = \tilde{\beta} T / 2\pi\hbar$. Keeping only the diagonal terms in Eq. (58) and integrating over the free motion between two delta kicks, $A_n(t)$ evolves according to

$$A_n(t+1) = A_n(t) e^{-i\frac{\tau}{2}n^2 + i\beta|A_n|^2}, \tag{59}$$

After additional integration over the infinitesimal interval over one kick, the map—which now describes the evolution over one whole period—becomes

$$A_n(t+1) = \sum_m (-i)^{n-m} J_{n-m}(k) A_m(t) e^{-i\frac{\tau}{2}m^2 + i\beta|A_m|^2}. \tag{60}$$

This map was first introduced by Shepelyansky in [69]. Comparison of the results of this map with direct numerical simulation of the corresponding model, Eq. (56), has shown differences on a short time scale, but the same asymptotic behavior in the rotor energy [70]. At the same time, this model allows for more efficient and faster numerical computation.

For $\beta = 0$ all eigenstates are exponentially localized [67]. The eigenvalues are located on the unit circle, and therefore embedded in a compact space. This implies, that nonlinear frequency shifts, i.e. shifts of eigenvalues along the unit circle, may shift points out of a cloud, but with increasing nonlinearity the shifted point will return after making one revolution. Therefore the nonlinear quantum kicked rotor (NQKR) serves as a model which lacks selftrapping. It should thus be an ideal testing ground not only of weak chaos, but also of strong chaos.

Shepelyansky performed the first pioneering study on subdiffusive spreading and destruction of dynamical localization for $\beta \neq 0$ in [69]. Due to the possible presence of strong chaos, the method to extract exponents from fitting power laws to $m_2(t)$ lead to inconclusive results. Gligoric et al. [23] repeated the calculations with more averaging over initial conditions, and computing derivatives $\alpha = \frac{d<\log_{10} E>}{d(\log_{10} t)}$ instead (note here that the second moment m_2 is equivalent to the rotor energy E). The results impressively obtain a regime of weak chaos with $\alpha \approx 1/3$, and also strong chaos with $\alpha \approx 1/2$. The original simulations of Shepelyansky [69] were performed in the crossover region between strong and weak chaos, leading to incorrect fitting results—which are however between the two weak and strong chaos limits, as expected.

9 Discussion

If a linear wave equation generates localization with upper bounds on the localization length (degree of localization), then the corresponding nonlinear wave equation shows destruction of this localization in a broad range of control parameters, and a subdiffusive spreading of initially localized wave packets. This observation holds for a broad range of wave equations, e.g. with uncorrelated random potentials (Anderson localization), quasiperiodic potentials (Aubry-Andre localization), dc fields (Wannier-Stark localization), kicked systems (dynamical localization in momentum space). What is the cause for the observed subdiffusion? Firstly it is the nonintegrability of the systems, which leads to generic intrinsic deterministic chaos in the dynamics of the nonlinear system. Second, wave localization is inherently based on keeping the phases of participating waves coherent. Chaos is destroying phase coherence, and therefore destroying localization. Wave packets can spread, but the densities will drop as spreading goes on. Therefore the effective nonlinearity and strength of chaos decreases, and spreading is slowing down, becoming subdiffusive. The subdiffusive exponents are controlled by very few parameters and therefore rather universal. Typically we only need to know the dimensionality of the system, and the power of nonlinearity (Anderson, Aubry-Andre, and dynamical localization). For Wannier-Stark localization the dc field strength is also becoming a control parameter, probably because the wave packet not only expands in space, but also in the frequency (energy) domain. A typical evolution outcome for the DNLS chain discussed at length here (see Sect. 2) is shown in Fig. 18 with all three

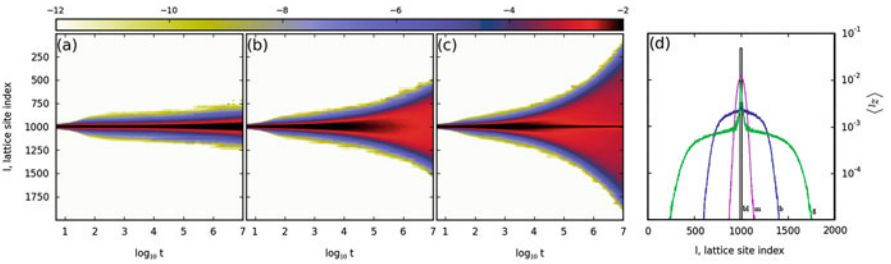

Fig. 18 DNLS, $W = 4$: time evolution of average norm density distributions $\langle z_l \rangle$ in real space for (**a**) $\beta = 0.04$, (**b**) $\beta = 0.72$ and (**c**) $\beta = 3.6$. The *color scales* shown on *top* of panels (**a**)–(**c**) are used for coloring each lattice site according to its $\log_{10}\langle z_l \rangle$ value. (**d**) The values $\langle z_l \rangle$ (in logarithmic scale) at the end time $t = 10^7$ of numerical simulations for $\beta = 0.04, 0.72, 3.6$ [(*m*) magenta; (*b*) blue; (*g*) green]. For comparison the initial norm distribution is also plotted [(*bl*) black]. Adapted from [71]

regimes of weak chaos, strong chaos, and selftrapping. The effective noise theory (which contains a phenomenological twist) and the nonlinear diffusion theory yield a rather coherent and consistent explanation. Many predictions of this approach were tested, and verified to the extend of current computational possibilities. A number of construction places are left unfinished and call for more work. This includes e.g. (a) the explanation of the dc-field dependent subdiffusive exponents for Wannier-Stark localization, (b) the testing of the prefactor (37), (38), (c) its complete derivation for higher dimensions and different powers of nonlinearity, and also (d) for other localization potentials (quasiperiodic, dc field, kicked, etc.). A rather unexplored direction concerns the breaking of time-reversal symmetry, which should lead to an increase of the stiffness of the spectrum of interacting modes, and therefore affect the statistics of interactions. A first work has been recently finished [35], but certainly more is needed.

One of the hotly debated questions in the community is whether the subdiffusive spreading will continue forever or eventually slow down, or even stop (see e.g. [72] and references therein). This is an interesting and perhaps mathematically deep question, despite the absence of rigorous results which would fuel the above doubts. From the perspective of current computational studies, efforts to observe any slowing down directly were not successful [71].

Another question concerns the restoring of Anderson localization in the limit of weak nonlinearity. The answer appears to depend strongly on the considered initial states. For instance, in an infinite lattice, we have to discuss the temperature dependence of the conductivities. One possibility is that the conductivities vanish in the zero temperature limit (see Sect. 7.4), which restores the linear wave equation, and Anderson localization. Then, Anderson localization will be destroyed at the smallest amount of nonlinearity. But may be there is a small but finite nonzero critical temperature/density/nonlinearity threshold at which the conductivity vanishes, similar to the quantum many body localization case [19]? Another type of initial states are the ones mostly considered in this chapter—compact localized

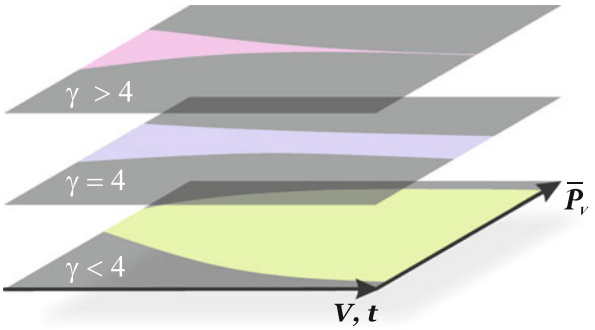

Fig. 19 Schematic dependence of the probability $\mathscr{P}_V$ for wave packets to stay localized (*dark area*) together with the complementary *light area* of spreading wave packets versus the wave packet volume V (either initial or attained at some time t) for three different orders of nonlinearity $\gamma < 4$, $\gamma = 4$ and $\gamma > 4$. Adapted from [17]

wave packets in a zero density surrounding. Then, if nonlinearity is lowered, several papers study the fate of these states [15–17]. The main outcome appears to be, that for a *given and fixed* initial state, at small enough nonlinearity, the dynamics will be in a KAM regime, i.e. there will be a finite probability P_R that the state is launched on a torus in phase space, dynamics is regular, phase coherence is conserved, and no spreading will occur. But then, there is the complementary probability $P_{Ch} = 1 - P_R$ to miss the torus, and instead to be launched on a chaotic trajectory, where dynamics is irregular, phase coherence is lost, and spreading may occur. Here probability is meant with respect to the disorder realization (or the space location of the initial state). The probability P_R increases to one for vanishing nonlinearity, and therefore Anderson localization is restored in this probabilistic sense. A consequence of the considerations in [17] is shown in Fig. 19, where $\gamma = \sigma + 2$ measures the power of nonlinearity [see (39)]. Namely, we assume that the dynamics starts on a chaotic trajectory. Then by assumption, we will continue to be on a chaotic trajectory, and spread. For the typical size of the wave packet at a later stage, we may recalculate the probability to keep chaoticity if we suddenly change the disorder realization. The answer is, that for $\sigma = 2$ (cubic nonlinearity), even in the limit of an infinitely spread wave packet (with infinitesimally small densities) the probability of chaos stays finite (and can be anything between zero and one). For $\sigma < 2$ this chaos probability tends to one in the infinite time/spreading limit—despite the fact that the densities drop to zero. In this case chaos always wins. Finally, for $\sigma > 2$ the chaos probability shrinks to zero. Therefore, even if our chaotic trajectory will spread forever, it will enter a phase space region which is predominantly regular. What kind of regime is that? Is there place for Arnold diffusion? Will subdiffusive spreading slow down in that case (apparently numerical studies do not report on anything suspicious in that case)?

The above studies were restricted to lattice wave equations, which introduce upper bounds for the localization length. Spatially continuous wave equations may

lack these upper bounds. Therefore an initially compact localized wave packet may overlap with normal modes whose localization length is unbounded in principle. While this may become an intricate matter of counting overlap weights, it is instructive to see that numerical studies of such cases also indicate the appearance of the universal subdiffusive spreading as observed for lattices [73].

The more models are accumulated for the above studies, the more qualitative differences are becoming visible. For instance, models can be classified according to the number of integrals of motion (KG—one, DNLS—two). Other models differ in the connectivity in normal mode space—while cubic DNLS and KG equations have connectivity $K = 4$ (four modes are coupled), other models discussed e.g. in [17, 74] have connectivity $K = 2$. Again the strong disorder limit of $K = 4$ models yields $K = 2$ in leading order, which is one of the cases where analytical methods are applied (see references in [72]). Time might be ripe to perform comparative studies.

Acknowledgements I thank all cited authors with whom I had the pleasure to jointly work and publish. In addition I thank I. Aleiner, B.L. Altshuler, P. Anghel-Vasilescu, D. Basko, S. Fishman, J.C. Garreau, A.R. Kolovsky, Y. Krivolapov, Y. Lahini, G. Modugno, M. Mulansky, R. Schilling, D. Shepelyansky, A. Pikovsky, W.-M. Wang and H. Veksler for stimulating and useful discussions.

References

1. P.W. Anderson, Phys. Rev. **109**, 1492 (1958)
2. T. Schwartz, G. Bartal, S. Fishman, M. Segev, Nature **446**, 52 (2007)
3. Y. Lahini, A. Avidan, F. Pozzi, M. Sorel, R. Morandotti, D.N. Christodoulides, Y. Silberberg, Phys. Rev. Lett. **100**, 013906 (2008)
4. D. Clement, A.F. Varon, J.A. Retter, L. Sanchez-Palencia, A. Aspect, P. Bouyer, New J. Phys. **8**, 165 (2006); L. Sanches-Palencia, D. Clement, P. Lugan, P. Bouyer, G.V. Shlyapnikov, A. Aspect, Phys. Rev. Lett. **98**, 210401 (2007); J. Billy, V. Josse, Z. Zuo, A. Bernard, B. Hambrecht, P. Lugan, D. Clement, L. Sanchez-Palencia, P. Bouyer, A. Aspect, Nature **453**, 891 (2008); G. Roati, C. D'Errico, L. Fallani, M. Fattori, C. Fort, M. Zaccanti, G. Modugno, M. Modugno, M. Inguscio, Nature **453**, 895 (2008)
5. M.I. Molina, Phys. Rev. B **58**, 12547 (1998)
6. A.S. Pikovsky, D.L. Shepelyansky, Phys. Rev. Lett. **100**, 094101 (2008)
7. I. García-Mata, D.L. Shepelyansky, Phys. Rev. E **79**, 026205 (2009)
8. G. Kopidakis, S. Komineas, S. Flach, S. Aubry, Phys. Rev. Lett. **100**, 084103 (2008)
9. S. Flach, D. Krimer, Ch. Skokos, Phys. Rev. Lett. **102**, 024101 (2009)
10. Ch. Skokos, D.O. Krimer, S. Komineas, S. Flach, Phys. Rev. E **79**, 056211 (2009)
11. G. Kopidakis, S. Aubry, Phys. Rev. Lett. **84**, 3236 (2000); G. Kopidakis, S. Aubry, Phys. D **139**, 247 (2000)
12. A. Iomin, S. Fishman, Phys. Rev. E **76**, 056607 (2007)
13. D.M. Basko, Ann. Phys. **326**, 1577 (2011)
14. S. Flach, M.V. Ivanchenko, N. Li, PRAMANA J. Phys. **77**, 1007 (2011)
15. M. Johansson, G. Kopidakis, S. Aubry, Europhys. Lett. **91**, 50001 (2010)
16. S. Aubry, Int. J. Bifurcation Chaos Appl. Sci. Eng. **21**, 2125 (2011)
17. M.V. Ivanchenko, T.V. Laptyeva, S. Flach, Phys. Rev. Lett. **107**, 240602 (2011)
18. D.M. Basko, Phys. Rev. E **86**, 036202 (2012)
19. D.M. Basko, I.L. Aleiner, B.L. Altshuler, Ann. Phys. **321**, 1126 (2006)

20. D.O. Krimer, R. Khomeriki, S. Flach, JETP Lett. **94**, 406 (2011)
21. M.V. Ivanchenko, T.V. Laptyeva, S. Flach, Phys. Rev. B **89**, 060301R (2014)
22. D.L. Shepelyansky, Phys. Rev. Lett. **73**, 2607 (1994)
23. G. Gligoric, J.D. Bodyfelt, S. Flach, Europhys. Lett. **96**, 30004 (2011)
24. D.O. Krimer, R. Khomeriki, S. Flach, Phys. Rev. E **80**, 036201 (2009)
25. M. Larcher, T.V. Laptyeva, J.D. Bodyfelt, F. Dalfovo, M. Modugno, S. Flach, New J. Phys. **14**, 103036 (2012)
26. O. Morsch, M. Oberthaler, Rep. Prog. Phys. **78**, 176 (2006)
27. Yu.S. Kivshar, G.P. Agrawal, *Optical Solitons: From Fibers to Photonic Crystals* (Academic, Amsterdam, 2003)
28. A.A. Ovchinnikov, N.S. Erikhman, K.A. Pronin, *Vibrational-Rotational Excitations in Nonlinear Molecular Systems* (Kluwer, New York, 2001)
29. Yu.S. Kivshar, M. Peyrard, Phys. Rev. A **46**, 3198 (1992); Yu.S. Kivshar, Phys. Lett. A **173**, 172 (1993); M. Johansson, Phys. D **216**, 62 (2006)
30. J. Bodyfelt, T.V. Laptyeva, Ch. Skokos. D. Krimer, S. Flach, Phys. Rev. E **84**, 016205 (2011)
31. B. Kramer, A. MacKinnon, Rep. Prog. Phys. **56**, 1469 (1993)
32. D.O. Krimer, S. Flach, Phys. Rev. E **82**, 046221 (2010)
33. S. Flach, C.R. Willis, Phys. Rep. **295**, 181 (1998); D.K. Campbell, S. Flach, Yu.S. Kivshar, Phys. Today **57**(1), 43 (2004); S. Flach, A.V. Gorbach, ibid. **467**, 1 (2008)
34. S. Flach, Chem. Phys. **375**, 548 (2010)
35. X. Yu, S. Flach, Phys. Rev. E 90, 032910 (2014)
36. D.L. Shepelyansky, Phys. Rev. Lett. **73**, 2607 (1994); Y. Imry, Europhys. Lett. **30**, 405 (1995); K. Frahm, A. Müller-Groeling, J.-L. Pichard, D. Weinmann, Europhys. Lett. **31**, 169 (1995); R.A. Römer, M. Schreiber, T. Vojta, Phys. Status Solidi **211**, 681 (1999)
37. M.V. Ivanchenko, T.V. Laptyeva, S. Flach, Phys. Rev. B **89**, 060301(R) (2014)
38. Y. Dodge, *The Oxford Dictionary of Statistical Terms* (Oxford University Press, New York, 2003)
39. J. Laskar, P. Robutel, Celest. Mech. Dyn. Astron. **80**, 39 (2001); H. Yoshida, Phys. Lett. A **150**, 262 (1990); H. Yoshida, Celest. Mech. Dyn. Astron. **56**, 27 (1993)
40. K. Rayanov, G. Radons, S. Flach, Phys. Rev. E **88**, 012901 (2013)
41. E. Michaeli, S. Fishman, Phys. Rev. E **85**, 046218 (2012)
42. B. Vermersch, J.C. Garreau, New J. Phys. **15**, 045030 (2013)
43. Ch. Skokos, I. Gkolias, S. Flach, Phys. Rev. Lett. **111**, 064101 (2013)
44. S. Aubry, R. Schilling, Phys. D **238**, 2045 (2009)
45. Y.B. Zeldovich, Y.P. Raizer, *Physics of Shock Waves and High-Temperature Hydrodynamic Phenomena* (Academic, New York, 1966); Y.B. Zeldovich, A. Kompaneets, *Collected Papers of the 70th Anniversary of the Birth of Academician A.F. Ioffe*, Moscow (1950); G.I. Barenblatt, Prikl. Mat. Mekh. **16**, 67 (1952)
46. A.R. Kolovsky, E.A. Gomez, H.J. Korsch, Phys. Rev. A **81**, 025603 (2010)
47. B. Tuck, J. Phys. D **9**, 1559 (1976)
48. W.F. Ames, *Non-linear Partial Differential Equations in Engineering*, vol. 1 (Academic, New York, 1965); F.A. Cunnell, C.H. Gooch, J. Phys. Chem. Solids **15**, 127 (1960); H. Ikezi, Y. Kiwamoto, K.E. Lonngren, C.M. Burde, H.C.S. Hsuan, Plasma Phys. **15**, 1141 (1973); M.A.H. Kadhim, B. Tuck, J. Mater. Sci. **7**, 68 (1972); K.E. Lonngren, W.F. Ames, A. Hirose, J. Thomas, Phys. Fluids **17**, 1919 (1974)
49. D.M. Basko, Phys. Rev. E **89**, 022921 (2014)
50. G. Schwiete, A.M. Finkelstein, Phys. Rev. A **88**, 053611 (2013)
51. T.V. Laptyeva, J.D. Bodyfelt, D.O. Krimer, Ch. Skokos, S. Flach, Europhys. Lett. **91**, 30001 (2010)
52. W.S. Cleveland, S.J. Devlin, J. Am. Stat. Assoc. **83**, 596 (1988)
53. T.V. Laptyeva, J.D. Bodyfelt, S. Flach, Phys. D **256–257**, 1 (2013)
54. M. Mulansky, A. Pikovsky, Europhys. Lett. **90**, 10015 (2010)
55. M. Mulansky, *Localization Properties of Nonlinear Disordered Lattices*, Diplomarbeit Universität Potsdam (2009), http://opus.kobv.de/ubp/volltexte/2009/3146/

56. Ch. Skokos, S. Flach, Phys. Rev. E **82**, 016208 (2010)
57. H. Veksler, Y. Krivolapov, S. Fishman, Phys. Rev. E **80**, 037201 (2009)
58. T.V. Laptyeva, J.D. Bodyfelt, S. Flach, Europhys. Lett. **98**, 60002 (2012)
59. S. Flach, M. Ivanchenko, N. Li, PRAMANA J. Phys. **77**, 1007 (2011)
60. G. Gligoric, K. Rayanov, S. Flach, Europhys. Lett. **101**, 10011 (2013)
61. E. Lucioni, B. Deissler, L. Tanzi, G. Roati, M. Zaccanti, M. Modugno, M. Larcher, F. Dalfovo, M. Ignuscio, G. Modugno, Phys. Rev. Lett. **106**, 230403 (2011)
62. G. Roati, C. D'Errico, J. Catani, M. Modugno, A. Simoni, M. Ignuscio, G. Modugno, Phys. Rev. Lett. **99**, 010403 (2007)
63. M. Larcher, T.V. Laptyeva, J.D. Bodyfelt, F. Dalfovo, M. Modugno, S. Flach, New J. Phys. **14**, 103036 (2012)
64. S. Aubry, G. Andrè, Ann. Isr. Phys. Soc. **3**, 133 (1980)
65. A.R. Kolovsky, E.A. Gomez, H.J. Korsch, Phys. Rev. A **81**, 025603 (2010)
66. B. Chirikov, Phys. Rep. **52**, 263 (1979)
67. S. Fishman, D. Grempel, R. Prange, Phys. Rev. Lett. **49**, 509 (1982); D. Grempel, R. Prange, S. Fishman, Phys. Rev. A **29**, 1639 (1984)
68. C. Ryu, M. Andersen, A. Vaziri, M. d' Arcy, J. Grossman, K. Helmerson, W. Phillips, Phys. Rev. Lett. **96**, 160403 (2006); G. Behinaein, V. Ramareddy, P. Ahmadi, G. Summy, Phys. Rev. Lett. **97**, 244101 (2006); J. Kanem, S. Maneshi, M. Partlow, M. Spanner, A. Steinberg, Phys. Rev. Lett. **98**, 083004 (2007)
69. D. Shepelyansky, Phys. Rev. Lett. **70**, 1787 (1993)
70. L. Rebuzzini, S. Wimberger, R. Artuso, Phys. Rev. E **71**, 036220 (2005)
71. J.D. Bodyfelt, T.V. Laptyeva, Ch. Skokos, D.O. Krimer, S. Flach, Phys. Rev. E **84**, 016205 (2011)
72. S. Fishman, Y. Krivolapov, A. Soffer, Nonlinearity **25**, R53 (2012)
73. I. Brezinova, J. Burgdörfer, A.U.J. Lode, A.I. Streltsov, L.S. Cederbaum, O.E. Alon, L.A. Collins, B.I. Schneider, J. Phys. Conf. Ser. **488**, 012032 (2014)
74. M. Mulansky, A. Pikovsky, Phys. Rev. E **86**, 056214 (2012); M. Mulansky, A. Pikovsky, New J. Phys. **15**, 053015 (2013); M. Mulansky, Chaos **24**, 024401 (2014)

Modeling and Computation of Bose-Einstein Condensates: Stationary States, Nucleation, Dynamics, Stochasticity

Xavier Antoine and Romain Duboscq

1 Modeling: Bose, Einstein, Gross, and Pitaevskii

1.1 From the Theory to the Realization of Bose-Einstein Condensates

The discovery of Bose-Einstein Condensates (BECs), from their theoretical prediction by Bose and Einstein in 1925 to their first experimental realization in 1995 by Cornell and Wiemann, results from extraordinary scientific achievements that led to the birth of condensed matter physics. The origin of the theory of BECs comes from an Indian physicist, Satyendra Nath Bose, who proposed in 1924 a statistics for the photons that is different from the classical Maxwell-Boltzmann statistics. This latter allows to know the distribution of the particles velocity in an ideal gas with elastic shocks, corresponding to a classical description of matter. However, such statistics cannot be applied to microscopic particles where quantum effects must be included. An example is the Heisenberg uncertainty principle which states that both the position and velocity of a massive particle cannot be known simultaneously. Therefore, the introduction of a new statistical distribution of the particles in the phase space is required. In his works, Bose considers the photons which are particles

X. Antoine (✉)
Université de Lorraine, Institut Elie Cartan de Lorraine, UMR 7502, Vandoeuvre-lès-Nancy, 54506, France

Inria Nancy Grand-Est/IECL - ALICE, Villers-lès-Nancy, France
e-mail: xavier.antoine@univ-lorraine.fr

R. Duboscq
Institut de Mathématiques de Toulouse, UMR 5219, Université de Toulouse, CNRS, INSA, 31077 Toulouse, France
e-mail: Romain.Duboscq@math.univ-toulouse.fr

C. Besse, J.-C. Garreau (eds.), *Nonlinear Optical and Atomic Systems*,
Lecture Notes in Mathematics 2146, DOI 10.1007/978-3-319-19015-0_2

that belong to the class of bosons (particles with an integer spin). Photons can occupy the same quantum state, implying that two photons with the same energy and position cannot be distinguished. Based on this property, Bose developed the foundations of the theory of quantum statistical mechanics. He sent his paper to Albert Einstein who submitted it for him to *Zeitschrift für Physik* [39] and who generalized this result to atoms [59]. In this work, Einstein predicts the existence of a new state of matter which is now better known as Bose-Einstein condensates. When a gas of dilute atoms is at a very low temperature (close to the absolute zero), there is a phase transition where a part of the gas condensates, which means that a large fraction of the atoms simultaneously occupy the lowest level quantum energy state, also called fundamental state. The critical temperature to observe the condensation phenomena is related to the property that the distance between the atoms is about one de Broglie wavelength $\lambda_{\text{de Broglie}}$ [53]

$$\lambda_{\text{de Broglie}} = \frac{h}{(2\pi m k_B T)^{1/2}},$$

where h is the Planck constant, m is the atomic mass, k_B is the Boltzmann constant and T is the temperature. When the characteristic distances of the system are about the same, quantum phenomena arise in the gas. A dimensional analysis argument [98] provides the formula

$$T_c = 3.3\frac{\hbar^2 n^{2/3}}{m k_B}$$

to determine the critical temperature T_c, where n is the number of particles per unit volume in the gas and $\hbar$ is the reduced Planck constant ($\hbar = \frac{h}{2\pi}$). At the time of these first predictions, experimentalists where not able to maintain the atoms in a gaseous state when cooling them, resulting in a transition to the solid state. In addition to the fact that extremely low temperatures had to be obtained, well-chosen candidates were required to experimentally observe the condensates.

In 1937, Kapitsa discovers the superfluidity phenomena that occurs in the helium gas [79]. Helium ^{4}He has the property to not solidify when it is cooled but to be in the liquid state even at very low temperatures. Kapitsa shows that a transition phase occurs in the helium fluid under 2.17 K. Moreover, this new phase possesses amazing properties. For instance, there is almost no viscosity in the fluid. In 1938, London suggests that there is a connection between superfluidity in helium ^{4}He and BECs [89], the difference being that, in the case of the helium superfluid, only a small part of the atoms is at the fundamental state. The main reason is that strong interactions exist in the helium which is in a fluid state while BECs creation arises in ideal gazes with weak interactions. Nevertheless, the helium superfluid plays a key role in the development of some physical concepts that have next been applied to BECs. In 1949, Onsager predicts the existence of quantum vortices in superfluids. His ideas have been further developed by Feynman [62, 63] in 1955. Quantum vortices are not an extension of classical vortices observed in a classical

rotating fluid (like for example in water). For a superfluid, the velocity is given by the gradient of the phase function. Indeed, it is possible to describe a superfluid through a wavefunction

$$\psi(t,\mathbf{x}) = \sqrt{\rho(t,\mathbf{x})}e^{iS(t,\mathbf{x})},$$

where $\rho(t,\mathbf{x})$ is the superfluid density and $S := S(t,\mathbf{x})$ its phase, $\mathbf{x} := (x,y,z) \in \mathbb{R}^3$ is a spatial point in the system $(\mathbf{O},\mathbf{e}_x,\mathbf{e}_y,\mathbf{e}_z)$ and $t > 0$ is the time variable. The velocity of a superfluid is given by $\mathbf{v}(t,\mathbf{x}) = \nabla S(t,\mathbf{x})$. Hence, a direct calculation shows that $\nabla \times \mathbf{v}(t,\mathbf{x}) = \nabla \times \nabla S(t,\mathbf{x}) = \mathbf{0}$, where S is smooth ($\mathbf{a} \times \mathbf{b}$ is the exterior product of two complex-valued vectors/operators $\mathbf{a}$ and $\mathbf{b}$). We can then deduce that the superfluid is irrotational where there is no singularity point, e.g. when the superfluid density is zero. These singularities create "holes" in the condensate that are called *quantum vortices*.

In 1959, Hecht suggests that the hydrogen atom with a polarized spin could be a suitable candidate to observe a condensate in the framework of weak interactions [73]. The interaction between two atoms of hydrogen with an aligned spin being weak, a cooling of the gas would not create a molecule nor a liquefaction. Hecht's idea is validated in practice in 1976 by Stwalley and Nosanow [114] who confirmed the hypothesis of the weak interaction of hydrogen and hence started the race to the experimental realization of a hydrogen condensate. The first experiments used a magnetic field to cool the atoms. However, this technique was not robust enough since only a small part of the atoms was practically cooled. New cooling techniques were therefore necessary for confining the atoms. In 1987, a physics group from the Massachusetts Institute of Technology (MIT), supervised by Greytak and Kleppner, published [75] a method where they first confined the hydrogen atoms by a magnetic trap and next cooled the gas to about 10^{-3} K by evaporation. Starting from a gas made of trapped atoms, the evaporation process consists in progressively letting the hottest atoms going out by diminishing the trap strength as illustrated on Fig. 1. We represent the trapping potential by a parabol and the atoms by small colored disks according to their temperature. During the cooling of the gas, a significant part of

Fig. 1 Cooling of atoms by evaporation in a magnetic trap

the atoms is lost. Therefore, it is necessary to start the process with a large enough quantity of atoms.

The realization of a condensate made of hydrogen atoms has been obtained in 1998 [64]. Meanwhile, the advances in terms of cooling by a laser, in particular for alkaline atoms, have finally led in 1995 the Boulder University group headed by Cornell and Wieman to create the first Bose-Einstein condensate [9]. This BEC, made of rubidium atoms ^{87}Rb, has been directly followed by a second realization by Ketterle's team at the MIT by using sodium atoms ^{23}Na [52]. Cornell, Wieman, and Ketterle have been awarded the Nobel prize in Physics in 2001 for their contributions on BECs. In parallel, a group from Rice University, supervised by Hulet, created a BEC with lithium atoms ^{7}Li [104]. Since the lithium atoms are characterized by strong interactions, the condensate collapsed but Hulet was able to stabilize it through a quantum pressure technique. After these developments, other kinds of atoms were used to produce new BECs.

1.2 Modeling Bose-Einstein Condensates

Various mathematical models can be used to describe BECs [16, 84, 105]. In this section, we are most particularly interested in one of the most important models found in the Physics literature: the Gross-Pitaevskii Equation (GPE).

1.2.1 From Classical to Quantum Mechanics

In quantum mechanics, the state of a system is described by a fundamental time-dependent equation: the Schrödinger equation. This equation plays the role of the Euler-Lagrange or Hamilton equations used in classical mechanics. Let us assume that we have a physical system driven by the classical mechanics rules, for example a solid ball. The Lagrangian of a classical physical system [42] is given by

$$\mathscr{L} = T_{\text{kin}} - V,$$

where T_{kin} is the kinetic energy and V is the potential energy of the system. For an object with mass m which is assimilated to a point and subject to an exterior conservative force $\mathbf{F}(\mathbf{x}) = -\nabla V(\mathbf{x})$ (∇ is the usual gradient operator) at point $\mathbf{x}$, the kinetic and potential energies are respectively given by

$$T_{\text{kin}} = \frac{1}{2} m |\dot{\mathbf{x}}(t)|^2 \quad \text{and} \quad V = V(\mathbf{x}(t)),$$

where $\dot{\mathbf{x}}(t)$ is the object velocity obtained by deriving its position $\mathbf{x}(t)$ with respect to the time variable t. Therefore, at a given time t, the Lagrangian depends on two variables that describe the configuration of the physical system: the speed and the

position of the object. For a punctual object, one gets

$$\mathscr{L}(\mathbf{x}, \dot{\mathbf{x}}, t) = \frac{1}{2} m |\dot{\mathbf{x}}(t)|^2 - V(\mathbf{x}(t)). \tag{1}$$

The Euler-Lagrange equations characterize the dynamics of a classical system from its Lagrangian. They can be written as

$$\frac{\partial \mathscr{L}}{\partial \mathbf{x}}(\mathbf{x}, \dot{\mathbf{x}}, t) - \frac{d}{dt} \frac{\partial \mathscr{L}}{\partial \dot{\mathbf{x}}}(\mathbf{x}, \dot{\mathbf{x}}, t) = 0.$$

By applying this equation to the previous Lagrangian, we derive the fundamental equation of dynamics: $m\ddot{\mathbf{x}}(t) + \nabla V(\mathbf{x}(t)) = 0$, which provides the trajectory of the object.

The Hamilton's equations are a second approach to deduce the dynamics of a classical system [15]. We have already seen that the Lagrangian of a punctual object depends on both its position and velocity. It is possible to extend the expression of the Lagrangian by considering some generalized coordinates $\mathbf{q}$ and the associated generalized velocity $\dot{\mathbf{q}}$. The generalized coordinates must be chosen to uniquely define the configuration of the physical system. The Hamiltonian of the system is obtained by the following formula which corresponds to a Legendre transformation of the Lagrangian

$$\mathscr{H}(\mathbf{q}, \mathbf{p}, t) = \mathbf{p} \cdot \mathbf{q} - \mathscr{L}(\mathbf{q}, \dot{\mathbf{q}}, t), \tag{2}$$

$\mathbf{a} \cdot \mathbf{b}$ being the hermitian product between two complex-valued vector fields $\mathbf{a}$ and $\mathbf{b}$, the associated norm is $|\mathbf{a}| := \sqrt{\mathbf{a} \cdot \mathbf{a}}$. In the previous equation, $\mathbf{p}$ denotes the generalized momentum such that

$$\mathbf{p} = \frac{\partial \mathscr{L}}{\partial \dot{\mathbf{q}}}(\mathbf{q}, \dot{\mathbf{q}}, t). \tag{3}$$

The Hamilton's equations are given by

$$\dot{\mathbf{q}} = \frac{\partial \mathscr{H}}{\partial \mathbf{p}}(\mathbf{q}, \mathbf{p}, t), \quad \dot{\mathbf{p}} = -\frac{\partial \mathscr{H}}{\partial \mathbf{q}}(\mathbf{q}, \mathbf{p}, t).$$

By considering a particle subject to an exterior conservative force, we have seen that we obtain the Lagrangian (1). We determine the associated Hamiltonian by using the relations (2) and (3). Relation (3) allows us to identify the generalized impulsion of the particle: $\mathbf{p} = m\dot{\mathbf{q}}$. By using (2), we obtain the Hamiltonian of the particle

$$\mathscr{H}(\mathbf{q}, \mathbf{p}, t) = \frac{1}{2m} |\mathbf{p}|^2 + V(\mathbf{q}) = T_{\text{kin}} + V,$$

where $\mathscr{H}$ is the sum of the kinetic energy T_{kin} and the potential energy V of the particle. The total energy $\mathscr{E}$ of the particle is given *via* the Hamiltonian

$$\mathscr{E} := T_{\text{kin}} + V = \mathscr{H}(\mathbf{q}, \mathbf{p}, t). \tag{4}$$

This second approach is the one adopted to describe quantum particles. The main difference is related to the way the massive particles are considered. Indeed, the modeling of microscopic particles is realized through a wave function. The idea behind the oscillating nature of matter comes from some physical experiments where the duality wave-particles was observed [53, 74]. This duality is associated to the probabilistic character of quantum mechanics: this is not possible to know in a deterministic way the state of a quantum system. Following this point of view, a wave function ψ is associated to a particle and leads to the probability to determine a particle at a given point of the space. The probability to find a particle in a volume M at time t is

$$\mathbb{P}(\text{particle} \in M) = \int_M |\psi(t, \mathbf{x})|^2 d\mathbf{x} \in [0, 1],$$

implying the so-called "mass conservation" property

$$\mathbb{P}(\text{particle} \in \mathbb{R}^3) = \int_{\mathbb{R}^3} |\psi(t, \mathbf{x})|^2 d\mathbf{x} = 1. \tag{5}$$

This description of the particles is given by the de Broglie's relations [53] $\hat{\mathbf{p}} = \hbar \mathbf{k}$ and $\hat{\mathscr{E}} = \hbar\omega$, where $\hat{\mathbf{p}}$ is the impulsion of a particle and $\mathbf{k}$ its wave number. The total energy $\hat{\mathscr{E}}$ of a particle is the sum of its kinetic and potential energies, and ω its angular frequency. The relation expresses both the impulsion and the energy of the particle (assimilated to a wave function) under an operator form. Considering that a particle is given as the sum of monochromatic plane waves (by Fourier superposition)

$$\psi(t, \mathbf{x}) = \frac{1}{(2\pi)^4} \int_{\mathbb{R}\times\mathbb{R}^3} \hat{\psi}(\omega, \mathbf{k}) e^{i(\mathbf{x}\cdot\mathbf{k} - \omega t)} d\mathbf{k} d\omega,$$

the de Broglie's relations formally lead to

$$-i\hbar\nabla\psi(t, \mathbf{x}) = \frac{1}{(2\pi)^4} \int_{\mathbb{R}\times\mathbb{R}^3} \hat{\mathbf{p}}\hat{\psi}(\omega, \mathbf{k}) e^{i(\mathbf{x}\cdot\mathbf{k} - \omega t)} d\mathbf{k} d\omega,$$

$$i\hbar\partial_t\psi(t, \mathbf{x}) = \frac{1}{(2\pi)^4} \int_{\mathbb{R}\times\mathbb{R}^3} \hat{\mathscr{E}}\hat{\psi}(\omega, \mathbf{k}) e^{i(\mathbf{x}\cdot\mathbf{k} - \omega t)} d\mathbf{k} d\omega.$$

This makes a parallel between the momentum operator $\hat{\mathbf{p}}$ and the operator ∇: $\hat{\mathbf{p}} \sim -i\hbar\nabla$, and between the energy operator $\hat{\mathscr{E}}$ and the partial derivative ∂_t: $\hat{\mathscr{E}} \sim i\hbar\partial_t$. By using relation (4) and the previous ones, we deduce the following evolution equation

for the wave function with Hamiltonian $\mathscr{H}$

$$i\hbar\partial_t\psi(t,\mathbf{x}) = \mathscr{H}(\mathbf{x}, -i\hbar\nabla, t)\psi(t,\mathbf{x}).$$

Hence, $\mathscr{H}$ is now considered as an operator. This famous equation has been derived by Schrödinger [107]. It provides the dynamics of the wave function associated to the particles. In the case of a particle subject to an exterior potential V, we have the following Hamiltonian

$$\mathscr{H} = \frac{1}{2m}|\hat{\mathbf{p}}|^2 + V(\mathbf{x}),$$

which leads to the Schrödinger equation

$$i\hbar\partial_t\psi(t,\mathbf{x}) = -\frac{\hbar^2}{2m}\Delta\psi(t,\mathbf{x}) + V(\mathbf{x})\psi(t,\mathbf{x}).$$

Let us now introduce a new energy $\mathscr{E}$ corresponding to the mean-value of the Hamiltonian

$$\mathscr{E}(\psi)(t) := \int_{\mathbb{R}^3} \psi(t,\mathbf{x})^* \mathscr{H}(\mathbf{x}, -i\hbar\nabla, t)\psi(t,\mathbf{x})d\mathbf{x}, \tag{6}$$

where ψ^* designates the complex conjugate function of ψ. We can also write this energy as

$$\mathscr{E} = \langle \psi(t,\mathbf{x}), \mathscr{H}(\mathbf{x}, -i\hbar\nabla, t)\psi(t,\mathbf{x})\rangle_{L^2_{\mathbf{x}}},$$

where $\langle .,. \rangle_{L^2_{\mathbf{x}}}$ is the hermitian inner product

$$\forall(\psi,\phi) \in L^2_{\mathbf{x}} \times L^2_{\mathbf{x}}, \langle \phi, \psi\rangle_{L^2_{\mathbf{x}}} := \int_{\mathbb{R}^3} \phi(\mathbf{x})^*\psi(\mathbf{x})d\mathbf{x},$$

for square-integrable functions on $\mathbb{R}^3$

$$L^2_{\mathbf{x}} = L^2(\mathbb{R}^3) := \left\{ \phi : \mathbb{R}^3 \to \mathbb{C} / \int_{\mathbb{R}^3} |\phi(\mathbf{x})|^2 d\mathbf{x} < \infty \right\}.$$

The associated norm in $L^2_{\mathbf{x}}$ is

$$\forall\phi \in L^2_{\mathbf{x}}, \|\phi\|_{L^2_{\mathbf{x}}} := \langle \phi, \phi\rangle^{1/2}_{L^2_{\mathbf{x}}}.$$

When the Hamiltonian is self-adjoint, i.e.,

$$\forall\phi_1,\phi_2 \in \mathscr{C}^\infty_0(\mathbb{R}^3), \langle \mathscr{H}(\mathbf{x}, -i\hbar\nabla, t)\phi_1, \phi_2\rangle_{L^2_{\mathbf{x}}} = \langle \phi_1, \mathscr{H}(\mathbf{x}, -i\hbar\nabla, t)\phi_2\rangle_{L^2_{\mathbf{x}}},$$

and time homogeneous, i.e.

$$\mathscr{H}(\mathbf{x}, -i\hbar\nabla, t) = \mathscr{H}(\mathbf{x}, -i\hbar\nabla),$$

the energy $\mathscr{E}$ is conserved with respect to the time variable. Indeed, we have

$$\begin{aligned}\partial_t \mathscr{E}(\psi) = &\int_{\mathbb{R}^3} [\partial_t \psi(t,\mathbf{x})]^* \mathscr{H}(\mathbf{x}, -i\hbar\nabla)\psi(t,\mathbf{x})d\mathbf{x} \\ &+ \int_{\mathbb{R}^3} \psi(t,\mathbf{x})^* \mathscr{H}(\mathbf{x}, -i\hbar\nabla)[\partial_t \psi(t,\mathbf{x})]d\mathbf{x}.\end{aligned}$$

Since ψ satisfies the Schrödinger equation associated with $\mathscr{H}$, we deduce that

$$\begin{aligned}\partial_t \mathscr{E}(\psi) = &\int_{\mathbb{R}^3} \left[-\frac{i}{\hbar}\mathscr{H}(\mathbf{x}, -i\hbar\nabla)\psi(t,\mathbf{x})\right]^* \mathscr{H}(\mathbf{x}, -i\hbar\nabla)\psi(t,\mathbf{x})d\mathbf{x} \\ &+ \int_{\mathbb{R}^3} \psi(t,\mathbf{x})^* \mathscr{H}(\mathbf{x}, -i\hbar\nabla)\left[-\frac{i}{\hbar}\mathscr{H}(\mathbf{x}, -i\hbar\nabla)\psi(t,\mathbf{x})\right] d\mathbf{x}.\end{aligned}$$

By using the property that the Schrödinger operator is self-adjoint, one gets

$$\begin{aligned}\partial_t \mathscr{E}(\psi) = &\frac{i}{\hbar}\int_{\mathbb{R}^3} [\mathscr{H}(\mathbf{x}, -i\hbar\nabla)\psi(t,\mathbf{x})]^* \mathscr{H}(\mathbf{x}, -i\hbar\nabla)\psi(t,\mathbf{x})d\mathbf{x} \\ &- \frac{i}{\hbar}\int_{\mathbb{R}^3} [\mathscr{H}(\mathbf{x}, -i\hbar\nabla)\psi(t,\mathbf{x})]^* \mathscr{H}(\mathbf{x}, -i\hbar\nabla)\psi(t,\mathbf{x})d\mathbf{x} = 0.\end{aligned}$$

In addition, we remark that

$$\mathscr{H}(\mathbf{x}, -i\hbar\nabla, t)\psi(t,\mathbf{x}) = D_{\psi^*}\mathscr{E}(\psi)(t,\mathbf{x}), \tag{7}$$

where the derivative of the energy is defined as a functional derivative in $L^2_{\mathbf{x}}$ equipped with the hermitian inner product $\langle ., . \rangle_{L^2_{\mathbf{x}}}$. More precisely, in Eq. (7), we differentiate $\mathscr{E}(\psi)$ with respect to ψ^* by considering that ψ and ψ^* are independent: we identify $D_{\psi^*}\mathscr{E}(\psi)$ as satisfying

$$\int_{\mathbb{R}^3} \phi^* D_{\psi^*}\mathscr{E}(\psi)d\mathbf{x} = \lim_{\eta\to 0}\frac{1}{\eta}\left(\int_{\mathbb{R}^3}(\psi+\eta\phi)^*\mathscr{H}\psi d\mathbf{x} - \int_{\mathbb{R}^3}\psi^*\mathscr{H}\psi d\mathbf{x}\right). \tag{8}$$

This energy allows us to come back to the Schrödinger equation associated with a system by an equation like (7).

The notion of wave function can be generalized to a system of N_{part} particles by using the Hamiltonian: $\mathscr{H} = \mathscr{H}(\mathbf{x}_1, \ldots, \mathbf{x}_{N_{\text{part}}}, \mathbf{p}_1, \ldots, \mathbf{p}_{N_{\text{part}}}, t)$. For example,for N_{part} noninteracting distinct particles under the action of an exterior potential V, the Hamiltonian is

$$\mathscr{H} = \sum_{j=1}^{N_{\text{part}}} -\frac{\hbar^2}{2m}\Delta_{\mathbf{x}_j} + V(\mathbf{x}_j), \tag{9}$$

where $\mathbf{x}_j$ designates the position of the j-th particle, $j = 1, \ldots, N_{\text{part}}$. We can then deduce the wave function $\psi = \psi(t, \mathbf{x}_1, \ldots, \mathbf{x}_{N_{\text{part}}})$ for system (9) through a Schrödinger equation. One then gets

$$\begin{aligned}&\mathbb{P}(\text{particle } 1 \in M_1, \ldots, \text{particle } N_{\text{part}} \in M_{N_{\text{part}}})\\ &= \int_{M_1 \times \ldots \times M_{N_{\text{part}}}} |\psi(t, \mathbf{x}_1, \ldots, \mathbf{x}_{N_{\text{part}}})|^2 d\mathbf{x}_1 \ldots d\mathbf{x}_{N_{\text{part}}},\end{aligned}$$

where M_j is the j-th volume associated with the j-th particle, $1 \leq j \leq N_{\text{part}}$.

1.2.2 Application to Bose-Einstein Condensates

We propose here a construction that can be found in [98]. For a BEC, the set of condensed particles occupies the same quantum state, that is the ground state. The condensate is considered as a system of indistinguishable particles with the same wave function ψ. The condensate wave function writes down as

$$\tilde{\psi}(t, \mathbf{x}_1, \mathbf{x}_2, \ldots, \mathbf{x}_{N_{\text{part}}}) = \prod_{j=1}^{N_{\text{part}}} \psi(t, \mathbf{x}_j). \tag{10}$$

Furthermore, the condensate corresponds to a set of particles subject to an exterior potential V and an interaction force U_{int} between the particles that depends on the distance between two given particles. The Hamiltonian of the system is

$$\mathscr{H} = \sum_{j=1}^{N_{\text{part}}} -\frac{\hbar^2}{2m}\Delta_{\mathbf{x}_j} + V(\mathbf{x}_j) + \sum_{1 \leq k < j \leq N_{\text{part}}} U_{\text{int}}(\mathbf{x}_j - \mathbf{x}_k).$$

We obtain the energy $\mathscr{E}_{\text{sys}}$ of the system of particles at time t by using formulation (10) and the mass conservation (5)

$$\begin{aligned}\mathscr{E}_{\text{sys}} &:= \int_{(\mathbb{R}^3)^{N_{\text{part}}}} \tilde{\psi}^*(t,\mathbf{x}_1,\ldots,\mathbf{x}_{N_{\text{part}}})\mathscr{H}\tilde{\psi}(t,\mathbf{x}_1,\ldots,\mathbf{x}_{N_{\text{part}}})d\mathbf{x}_1\ldots d\mathbf{x}_{N_{\text{part}}}\\ &= N_{\text{part}}\int_{\mathbb{R}^3}\left[\frac{\hbar^2}{2m}|\nabla\psi(t,\mathbf{x})|^2 + V(\mathbf{x})|\psi(t,\mathbf{x})|^2\right]d\mathbf{x}\\ &+ N_{\text{part}}\frac{N_{\text{part}}-1}{2}\int_{\mathbb{R}^3}\int_{\mathbb{R}^3} U_{\text{int}}(\mathbf{x}'-\mathbf{x})|\psi(t,\mathbf{x}')|^2 d\mathbf{x}'|\psi(t,\mathbf{x})|^2 d\mathbf{x}.\end{aligned}$$

Let us consider the variable change $\psi \to 1/\sqrt{N_{\text{part}}}\psi$ and let us assume that the number of atoms is sufficiently large so that $(N_{\text{part}}-1)/N_{\text{part}} \approx 1$. This yields the normalized energy

$$\begin{aligned}&\mathscr{E}(\psi)\\ &= \int_{\mathbb{R}^3}\left[\frac{\hbar^2}{2m}|\nabla\psi(t,\mathbf{x})|^2 + (V(\mathbf{x}) + \frac{1}{2}\int_{\mathbb{R}^3} U_{\text{int}}(\mathbf{x}'-\mathbf{x})|\psi(t,\mathbf{x}')|^2 d\mathbf{x}')|\psi(t,\mathbf{x})|^2\right]d\mathbf{x}.\end{aligned}$$

To derive the Schrödinger equation that describes the evolution of the wave function ψ, we compute the functional derivative of the energy

$$\begin{aligned}\int_{\mathbb{R}^3}\phi^* D_{\psi^*}\mathscr{E}(\psi)d\mathbf{x} &= \int_{\mathbb{R}^3}\phi(\mathbf{x})^*\left(-\frac{\hbar^2}{2m}\Delta + V(\mathbf{x})\right)\psi(t,\mathbf{x})d\mathbf{x}\\ &+ \frac{1}{2}\int_{\mathbb{R}^3}\phi(\mathbf{x})^*\left(\int_{\mathbb{R}^3} U_{\text{int}}(\mathbf{x}'-\mathbf{x})|\psi(t,\mathbf{x}')|^2 d\mathbf{x}'\right)\psi(t,\mathbf{x})d\mathbf{x}\\ &+ \frac{1}{2}\int_{\mathbb{R}^3}\left(\int_{\mathbb{R}^3} U_{\text{int}}(\mathbf{x}'-\mathbf{x})\psi(t,\mathbf{x}')\phi(\mathbf{x}')^* d\mathbf{x}'\right)|\psi(t,\mathbf{x})|^2 d\mathbf{x}.\end{aligned}$$

From the Fubini theorem and by assuming that the interaction potential U_{int} is even $U_{\text{int}}(\mathbf{x}'-\mathbf{x}) = U_{\text{int}}(\mathbf{x}-\mathbf{x}')$ for any points $\mathbf{x}$ and $\mathbf{x}'$, we remark that

$$\begin{aligned}&\int_{\mathbb{R}^3}\left(\int_{\mathbb{R}^3} U_{\text{int}}(\mathbf{x}'-\mathbf{x})\psi(t,\mathbf{x}')\phi(\mathbf{x}')^* d\mathbf{x}'\right)|\psi(t,\mathbf{x})|^2 d\mathbf{x}\\ &= \int_{\mathbb{R}^3}\left(\int_{\mathbb{R}^3} U_{\text{int}}(\mathbf{x}-\mathbf{x}')\phi(\mathbf{x})^*\psi(t,\mathbf{x})d\mathbf{x}\right)|\psi(t,\mathbf{x}')|^2 d\mathbf{x}'.\end{aligned}$$

Hence, one gets

$$\begin{aligned}\int_{\mathbb{R}^3}\phi^* D_{\psi^*}\mathscr{E}(\psi)d\mathbf{x} &= \int_{\mathbb{R}^3}\phi(\mathbf{x})^*(-\frac{\hbar^2}{2m}\Delta + V(\mathbf{x}))\psi(t,\mathbf{x})d\mathbf{x}\\ &+ \int_{\mathbb{R}^3}\phi(\mathbf{x})^*(\int_{\mathbb{R}^3} U_{\text{int}}(\mathbf{x}'-\mathbf{x})|\psi(t,\mathbf{x}')|^2 d\mathbf{x}')\psi(t,\mathbf{x})d\mathbf{x}.\end{aligned}$$

This leads to the Schrödinger equation satisfied by ψ

$$i\hbar\partial_t\psi = D_{\psi^*}\mathscr{E}(\psi) = (-\frac{\hbar^2}{2m}\Delta + V(\mathbf{x}) + \int_{\mathbb{R}^3} U_{\text{int}}(\mathbf{x}' - \mathbf{x})|\psi(t,\mathbf{x}')|^2 d\mathbf{x}')\psi.$$

Let us remark that the parity assumption of U_{int} is not restrictive in practice because the interatomic interactions are symmetrical. Furthermore, this type of potential can describe a wide variety of interactions between the atoms. For instance, the Van der Waals interaction created by a dipole-dipole electric interaction between the atoms writes [98]

$$U_{\text{vdW}}(|\mathbf{x} - \mathbf{x}'|) = -\frac{C_6}{|\mathbf{x} - \mathbf{x}'|^6}.$$

From a mathematical point of view, we remark that the nonlocal interaction term is given by an integral operator. To avoid the problem of evaluating this class of interactions, physicists introduced the concept of effective interaction. By considering a system of two interacting particles with low energy, the interaction between the particles can be quantified by a constant a that is usually called the "scattering length". This simplification leads to the computation of an effective interaction U_{eff} between two particles that formally satisfies

$$U_0 := \int_{\mathbb{R}^d} U_{\text{eff}}(\mathbf{x}_0 - \mathbf{x})d\mathbf{x} = \frac{4\pi\hbar^2 a}{m},$$

where m is the mass of the particles, $\mathbf{x}_0$ is the reference particle position and $\mathbf{x}$ corresponds to the position of the other particle. Therefore, if we assume that the interatomic distance inside the condensate is sufficiently large compared to the scattering length a, the interaction between the particles can be replaced by a localized interaction which is proportional to U_0, that is: $U(\mathbf{x}_0 - \mathbf{x}) = U_0\delta_0(\mathbf{x}_0 - \mathbf{x})$. We deduce a Schrödinger equation for the wave function ψ as

$$i\hbar\partial_t\psi(t,\mathbf{x}) = (-\frac{\hbar^2}{2m}\Delta + V(\mathbf{x}) + \frac{4\pi\hbar^2 a}{m}|\psi(t,\mathbf{x})|^2)\psi(t,\mathbf{x}). \tag{11}$$

This equation has been obtained independently by Gross [72] and Pitaevskii [99] in 1961 and is called the Gross-Pitaevskii Equation (GPE). More recently, the equation was derived in more general frameworks [86, 87]. In the sequel, we consider this equation for modeling a BEC.

1.3 Enrichment of the GPE: Quantum Vorticity, Dipole-Dipole Interaction, Multi-components, Stochasticity

1.3.1 Rotating Bose-Einstein Condensates and Quantum Vortices

One of the most interesting characteristics of superfluids is their response to rotation. In a superfluid, the velocity of the fluid is given by the gradient of its wave function. As mentioned before, the fluid is irrotational everywhere except at the singularities called quantum vortices. Furthermore, another feature of superfluids is that there exists a characteristic velocity given by the spectrum of the excited states of the quantum system. Above this critical velocity, the system is excited. For example, an impurity moving in a superfluid will not cause any perturbation in the fluid unless its speed is above the critical velocity.

Since Bose-Einstein condensates are supposed to behave like superfluids, a lot of experiments were proposed to investigate properties like the existence of critical velocity or the nucleation of quantum vortices when a rotation is applied to the condensate. Two teams, one from the ENS Paris led by Dalibard [92–94] and a second one from the MIT and headed by Ketterle, have developed a method involving anisotropic harmonic potentials to stir the condensate and rotate it. They observed that there is no nucleation of vortices in the condensate under a certain rotation speed. The process of nucleation only begins when a certain rotational speed is obtained. In addition, the number of vortices is directly proportional to the rotation speed (see Fig. 2).

For modeling a rotating BEC, we need to change from the reference frame of the laboratory to the rotating frame of the condensate. If the rotation axis is the z-direction (i.e. $\boldsymbol{\Omega} = (0, 0, \Omega)$, where Ω is the rotation speed), this change of frame leads to the following transformation of variables

$$\begin{cases} x' = \cos(\Omega t)x + \sin(\Omega t)y, \\ y' = -\sin(\Omega t)x + \cos(\Omega t)y. \end{cases}$$

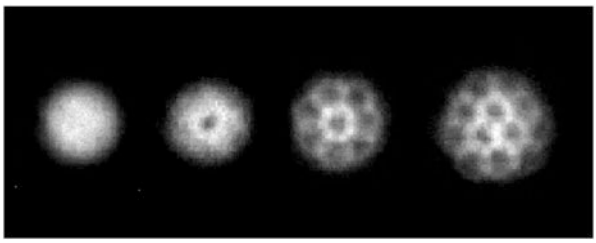

Fig. 2 Nucleation of quantized vortices for an increasing rotation speed (from *left to right*). The experiments were done by a group led by Jean Dalibard in 2001 at the Kastler Brossel laboratory (ENS Paris, France)

Therefore, to any vector $\mathbf{x}$ in the reference frame is associated a time dependent vector $\mathbf{x}'(t)$ in the rotating frame. We remark that: $\dot{\mathbf{x}}(t) = \dot{\mathbf{x}}'(t) + \boldsymbol{\Omega} \times \mathbf{x}'(t)$. We now consider a particle in rotation and subject to a potential V. The Lagrangian associated to this particle is

$$\mathscr{L}(\mathbf{x}, \dot{\mathbf{x}}, t) = \frac{1}{2} m \dot{\mathbf{x}}(t)^2 - V(\mathbf{x}(t)).$$

By using the change of variables, we deduce the Lagrangian in the rotating frame

$$\mathscr{L}(\mathbf{x}', \dot{\mathbf{x}}', t) = \frac{1}{2} m (\dot{\mathbf{x}}'(t) + \boldsymbol{\Omega} \times \mathbf{x}'(t))^2 - V(\mathbf{x}'(t))$$

and the generalized momentum operator

$$\mathbf{p}' = \frac{\partial \mathscr{L}}{\partial \dot{\mathbf{x}}'} = m(\dot{\mathbf{x}}' + \boldsymbol{\Omega} \times \mathbf{x}').$$

The Hamiltonian of a particle in the rotating frame is then

$$\mathscr{H}(\mathbf{x}', \mathbf{p}', t) = \mathbf{p}' \cdot \mathbf{x}' - \mathscr{L}(\dot{\mathbf{x}}', \mathbf{x}', t) = \frac{\mathbf{p}'^2}{2m} - (\boldsymbol{\Omega} \times \mathbf{x}') \cdot \mathbf{p}' + V(\mathbf{x}').$$

Applying the same procedure for the Hamiltonian of a system of N_{part} interacting particles under the action of a potential V, we obtain

$$\mathscr{H} = \sum_{j=1}^{N_{\text{part}}} -\frac{\hbar^2}{2m} \Delta_{\mathbf{x}_j} + i\hbar(\boldsymbol{\Omega} \times \mathbf{x}_j) \cdot \nabla_{\mathbf{x}_j} + V(\mathbf{x}_j) + \sum_{1 \le k < j \le N_{\text{part}}} U_{\text{int}}(\mathbf{x}_j - \mathbf{x}_k).$$

Similarly, we deduce the GPE for a rotating BEC

$$i\hbar \partial_t \psi(t, \mathbf{x}) = (-\frac{\hbar^2}{2m} \Delta - i\hbar \boldsymbol{\Omega} \cdot (\mathbf{x} \times \nabla) + V(\mathbf{x}) + \frac{4\pi\hbar^2 a}{m} |\psi(t, \mathbf{x})|^2) \psi(t, \mathbf{x}),$$

since $(\boldsymbol{\Omega} \times \mathbf{x}) \cdot \nabla = -\boldsymbol{\Omega} \cdot (\mathbf{x} \times \nabla)$.

1.3.2 BECs Including Dipolar Interactions

BECs were first obtained for alkali and hydrogen atoms. Since these two families of atoms have a weak magnetic moment, the magnetic dipole-dipole interaction can be neglected in the associated GPE. Latter, BECs made of chromium atoms ^{52}Cr were created, leading to a GPE where the dipole-dipole interactions must be included [70, 71]. As a consequence, an additional interaction term modeling the magnetic

forces between the atoms has to be added to the Hamiltonian

$$\mathscr{H} = \sum_{j=1}^{N_{\text{part}}} -\frac{\hbar^2}{2m}\Delta_{\mathbf{x}_j} + V(\mathbf{x}_j) + \sum_{1\le k<j\le N_{\text{part}}} U_0\delta_0(\mathbf{x}_j-\mathbf{x}_k) + U_{\text{dipole}}(\mathbf{x}_j-\mathbf{x}_k). \quad (12)$$

The notation U_{dipole} corresponds to the magnetic dipole-dipole interaction given by

$$U_{\text{dipole}}(\mathbf{x}_j-\mathbf{x}_k) = \frac{\mu_0}{4\pi}\frac{\boldsymbol{\mu}_{\text{mag},j}(\mathbf{x}_j)\cdot\boldsymbol{\mu}_{\text{mag},k}(\mathbf{x}_k) - 3(\boldsymbol{\mu}_{\text{mag},j}(\mathbf{x}_j)\cdot\mathbf{u}_{j,k})(\boldsymbol{\mu}_{\text{mag},k}(\mathbf{x}_k)\cdot\mathbf{u}_{j,k})}{|\mathbf{x}_j-\mathbf{x}_k|^3},$$

where $\boldsymbol{\mu}_{\text{mag},j}$ (respectively $\boldsymbol{\mu}_{\text{mag},k}$) is the magnetic momentum of the j-th atom (respectively k-th atom),

$$\mathbf{u}_{j,k} = \frac{\mathbf{x}_j-\mathbf{x}_k}{|\mathbf{x}_j-\mathbf{x}_k|},$$

and μ_0 is the permeability of vacuum. We now assume that all the atoms are polarized by an external magnetic field in the z-direction, implying that $\boldsymbol{\mu}_{\text{mag},j} = \boldsymbol{\mu}_{\text{mag},k} = \mu_{\text{mag}}\,\mathbf{e}_z$, where μ_{mag} is the amplitude of the magnetic momentum of chromium atoms. Thus, the magnetic dipole-dipole interaction is

$$U_{\text{dipole}}(\mathbf{x}_j-\mathbf{x}_k) = \frac{\mu_0\mu_{\text{mag}}^2}{4\pi}\frac{1-3\cos(\text{angle}(\mathbf{x}_j-\mathbf{x}_k,\mathbf{e}_z))}{|\mathbf{x}_j-\mathbf{x}_k|^3},$$

where $\text{angle}(\mathbf{x}_j-\mathbf{x}_k,\mathbf{e}_z)$ is the angle between $\mathbf{x}_j-\mathbf{x}_k$ and $\mathbf{e}_z$. By using the Hamiltonian (12), we obtain the following GPE with a nonlocal interaction term

$$\begin{aligned} i\hbar\partial_t\psi(t,\mathbf{x}) &= (-\frac{\hbar^2}{2m}\Delta + V(\mathbf{x}) + [\frac{4\pi\hbar^2 a}{m}|\psi(t,\mathbf{x})|^2 \\ &\quad + \frac{\mu_0\mu_{\text{mag}}^2}{2\pi}\int_{\mathbb{R}^3} U(\mathbf{x}-\mathbf{x}')|\psi(t,\mathbf{x}')|^2 d\mathbf{x}'])\psi(t,\mathbf{x}), \end{aligned}$$

where

$$U(\mathbf{x}) = \frac{1-3\cos(\text{angle}(\mathbf{x},\mathbf{e}_z))}{|\mathbf{x}|^3}.$$

1.3.3 Origin of Stochastic Effects in BECs

Some classes of GPEs include some random terms to describe the stochastic effects that may arise in BECs. For example, let us cite the modeling of random fluctuations in an optical trap [1–3, 68, 69, 106] or the consideration of the interactions between a cloud of non condensed atoms and the BEC [40, 66, 67, 111, 112]. This latter model involves a space and time stochastic process that describes the fluctuations of the phase and density of the condensate. Here, we focus on the first model and derive the associated stochastic GPE.

In [106], the authors model randomness in the intensity of the optical trapping device used to confine the BEC. In the case of a magneto-optical trap, the laser beam used is slightly detuned to a frequency less than the resonant frequency of the atoms. When the laser beam is coupled to a spatially varying magnetic field which changes the resonant frequency of the atoms, a potential force is induced, then creating an atomic trapping device [95]. Using multiple laser beams leads to the potential

$$V(t,\mathbf{x}) = -\frac{1}{4}\alpha|E(t,\mathbf{x})|^2,$$

where α is the atomic polarizability and E is the amplitude of the electric field generated by the laser beam. For a small detuning effect of the laser (less than 10 %), the atomic polarizability is given by the approximation: $\alpha = -\frac{\tau^2}{\hbar\Delta\omega}$, where τ is the transition dipole momentum and $\Delta\omega = \omega - \omega_0$ is the detuning parameter between the laser pulsation ω and the electronic transition pulsation ω_0 of the atoms. For a gaussian laser beam, the intensity of the electric field created by the laser is

$$|E(t,\mathbf{x})|^2 = E_0(t)^2 e^{-\frac{|\mathbf{x}|^2}{\ell^2}},$$

where ℓ is the gaussian beam radius. If the size of the condensate is small compared to ℓ ($|\mathbf{x}| \ll \ell$), a Taylor's expansion gives the following approximation of the potential

$$V(t,\mathbf{x}) = -\frac{\alpha}{4}|E_0(t)|^2 + \frac{\alpha}{4\ell^2}|E_0(t)|^2|\mathbf{x}|^2.$$

By a gauge transformation

$$\psi(t,\mathbf{x}) \to \psi(t,\mathbf{x})e^{\frac{i\alpha}{4\hbar}\int_0^t |E_0(s)|^2 ds},$$

we eliminate in the GPE (11) the constant term that appears in the previous potential and obtain

$$i\hbar\partial_t\psi(t,\mathbf{x}) = (-\frac{\hbar^2}{2m}\Delta + \frac{\alpha}{4\ell^2}|E_0(t)|^2|\mathbf{x}|^2 + \frac{4\pi\hbar^2 a}{m}|\psi(t,\mathbf{x})|^2)\psi(t,\mathbf{x}).$$

Finally, the fluctuations in the laser intensity are modeled by a random process $\dot{\xi}$ which determines the difference between the mean intensity $|E_0|^2$ and the intensity $|E_0(t)|^2$ at time t. If we set

$$\dot{\xi}(t) = \frac{|E_0(t)|^2 - |E_0|^2}{|E_0|^2},$$

we deduce the following stochastic GPE

$$i\hbar\partial_t\psi(t,\mathbf{x}) = (-\frac{\hbar^2}{2m}\Delta + \frac{\alpha}{4\ell^2}|E_0|^2(1+\dot{\xi}(t))|\mathbf{x}|^2 + \frac{4\pi\hbar^2 a}{m}|\psi(t,\mathbf{x})|^2)\psi(t,\mathbf{x}).$$

A process which is widely used by physicists is the brownian motion $(w_t)_{t\in\mathbb{R}+}$. The associated noise (e.g. the time derivative of the process) is the so-called white noise $(\dot{w}_t)_{t\in\mathbb{R}+}$, a real-valued centered gaussian process with covariance $\mathbb{E}[\dot{w}_t\dot{w}_s] = \delta(t-s)$.

1.3.4 Multi-components BECs

In the derivation of the Gross-Pitaevskii model for BECs, we omitted the effect of the spin of the atoms. For each species of particles, there exists a principal quantum spin number s that is either an half-integer for the fermions ($s = 1/2, 3/2, \ldots$) or an integer for the bosons ($s = 0, 1, 2, \ldots$). The quantum spin number S of a particle corresponds to a new degree of freedom $S \in \{-s, -(s-1), \ldots, (s-1), s\}$. For example, a fermion with principal quantum spin number $s = 1/2$ can only have two possible spin numbers: $S = 1/2$ or $S = -1/2$. Each value of S corresponds to a quantum state of the particle. To describe the quantum system, we introduce a vector-valued wave function, where each component is associated to a value of S. This requires the extension of the GPE to a system of GPEs when $s \neq 0$. This situation corresponds to multi-components BECs.

Let us consider a mixture between two different species of atoms (denoted by type 1 and type 2), the extension to more components being direct. We suppose that each type of quantum system occupies the ground state. The first (respectively second) gas has $N_{\text{part},1}$ (respectively $N_{\text{part},2}$) atoms. Each component is described by a wave function, ψ_1 or ψ_2, according to the gas, that satisfies the mass conservation

$$\int_{\mathbb{R}^3} |\psi_\ell(t,\mathbf{x})|^2 d\mathbf{x} = N_{\text{part},\ell}, \text{ for } \ell = 1, 2. \tag{13}$$

The wave function of the BEC is

$$\tilde{\psi}(t, \mathbf{x}_1^1, \ldots, \mathbf{x}_{N_{\text{part},1}}^1, \mathbf{x}_1^2, \ldots, \mathbf{x}_{N_{\text{part},2}}^2) = \prod_{j=1}^{N_{\text{part},1}} \psi_1(t, \mathbf{x}_j^1) \prod_{k=1}^{N_{\text{part},2}} \psi_2(t, \mathbf{x}_k^2),$$

where $\mathbf{x}_j^1$ is the position of the j-th atom of type 1 and $\mathbf{x}_k^2$ is the position of the k-th atom of species 2. If we assume that the ℓ-th component is subject to an external potential V_ℓ, has a mass m_ℓ and that the components interact, we obtain the following Hamiltonian

$$\begin{aligned}\mathscr{H} = &\sum_{j=1}^{N_{\text{part},1}} -\frac{\hbar^2}{2m_1}\Delta_{\mathbf{x}_j^1} + V_1(\mathbf{x}_j^1) + \sum_{1\le j<l\le N_{\text{part},1}} U_{\text{int},1}(\mathbf{x}_j^1 - \mathbf{x}_l^1)\\ &+ \sum_{k=1}^{N_{\text{part},2}} -\frac{\hbar^2}{2m_2}\Delta_{\mathbf{x}_k^2} + V_2(\mathbf{x}_j^2) + \sum_{1\le k<m\le N_{\text{part},2}} U_{\text{int},2}(\mathbf{x}_k^2 - \mathbf{x}_m^2)\\ &+ \sum_{j=1}^{N_{\text{part},1}}\sum_{k=1}^{N_{\text{part},2}} U_{\text{int},1,2}(\mathbf{x}_j^1 - \mathbf{x}_k^2),\end{aligned}$$

where $U_{\text{int},\ell}$ corresponds to the interactions between the atoms of the type $\ell(=1,2)$ and $U_{\text{int},1,2}$ describes the interatomic interaction. By symmetry, the interaction term $U_{\text{int},1,2}$ is even. We deduce the energy $\mathscr{E}_{\text{sys}}$ of the system by using (13)

$$\begin{aligned}&\mathscr{E}_{\text{sys}}(\psi_1,\psi_2)\\ &= N_{\text{part},1}\int_{\mathbb{R}^3}\left[\frac{\hbar^2}{2m_1}|\nabla\psi_1(t,\mathbf{x})|^2 + V_1(\mathbf{x})|\psi_1(t,\mathbf{x})|^2\right]d\mathbf{x}\\ &\quad + N_{\text{part},1}(N_{\text{part},1}-1)/2\int_{\mathbb{R}^3}\int_{\mathbb{R}^3} U_{\text{int},1}(\mathbf{x}-\mathbf{x}')|\psi_1(t,\mathbf{x}')|^2 d\mathbf{x}'|\psi_1(t,\mathbf{x})|^2 d\mathbf{x}\\ &\quad + N_{\text{part},2}\int_{\mathbb{R}^3}\left[\frac{\hbar^2}{2m_2}|\nabla\psi_2(t,\mathbf{x})|^2 + V_2(\mathbf{x})|\psi_2(t,\mathbf{x})|^2\right]d\mathbf{x}\\ &\quad + N_{\text{part},2}(N_{\text{part},2}-1)/2\int_{\mathbb{R}^3}\int_{\mathbb{R}^3} U_{\text{int},2}(\mathbf{x}-\mathbf{x}')|\psi_2(t,\mathbf{x}')|^2 d\mathbf{x}'|\psi_2(t,\mathbf{x})|^2 d\mathbf{x}\\ &\quad + N_{\text{part},1}N_{\text{part},2}\int_{\mathbb{R}^3}\int_{\mathbb{R}^3} U_{\text{int},1,2}(\mathbf{x}-\mathbf{x}')|\psi_1(t,\mathbf{x}')|^2|\psi_2(t,\mathbf{x})|^2 d\mathbf{x}' d\mathbf{x}.\end{aligned}$$

Let us consider the following changes of variables: $\psi_\ell \to 1/\sqrt{N_{\text{part},\ell}}\psi_\ell$, $\ell = 1,2$. Moreover, we assume that $N_{\text{part},\ell}$ is large enough to satisfy: $(N_{\text{part},\ell}-1)/N_{\text{part},\ell} \approx 1$, $\ell = 1,2$. This leads to the normalized energy of the system

$$\begin{aligned}&\mathscr{E}(\psi_1,\psi_2)\\ &= \int_{\mathbb{R}^3}\left[\frac{\hbar^2}{2m_1}|\nabla\psi_1(t,\mathbf{x})|^2 + (V_1(\mathbf{x})\right.\\ &\quad \left. + \frac{1}{2}\int_{\mathbb{R}^3} U_{\text{int},1}(\mathbf{x}-\mathbf{x}')|\psi_1(t,\mathbf{x}')|^2 d\mathbf{x}')|\psi_1(t,\mathbf{x})\,|^2\right]d\mathbf{x}\end{aligned}$$

$$+\int_{\mathbb{R}^3}\Big[\frac{\hbar^2}{2m_2}|\nabla\psi_2(t,\mathbf{x})|^2+ (V_2(\mathbf{x})$$
$$+\frac{1}{2}\int_{\mathbb{R}^3} U_{\text{int},2}(\mathbf{x}-\mathbf{x}')|\psi_2(t,\mathbf{x}')|^2 d\mathbf{x}')|\psi_2(t,\mathbf{x})\ |^2\Big]\, d\mathbf{x}$$
$$+\int_{\mathbb{R}^3}\int_{\mathbb{R}^3} U_{\text{int},1,2}(\mathbf{x}-\mathbf{x}')|\psi_1(t,\mathbf{x}')|^2|\psi_2(t,\mathbf{x})|^2 d\mathbf{x}' d\mathbf{x}. \tag{14}$$

We obtain the Schrödinger equations that govern the evolution of ψ_ℓ, $\ell = 1, 2$, by using the derivative of the energy with respect to ψ_1 and ψ_2. We have

$$i\hbar\partial_t\psi_\ell(t,\mathbf{x}) = D_{\psi_\ell^*}\mathscr{E}(\psi_1,\psi_2),$$

for $\ell = 1, 2$, which is equivalent to the following system of equations

$$\begin{cases} i\hbar\partial_t\psi_1(t,\mathbf{x}) = (-\dfrac{\hbar^2}{2m_1}\Delta + V_1(\mathbf{x}) + \displaystyle\int_{\mathbb{R}^3} U_{\text{int},1}(\mathbf{x}-\mathbf{x}')|\psi_1(t,\mathbf{x}')|^2 d\mathbf{x}')\psi_1(t,\mathbf{x}) \\ \qquad\qquad + \displaystyle\int_{\mathbb{R}^3} U_{\text{int},1,2}(\mathbf{x}-\mathbf{x}')|\psi_2(t,\mathbf{x}')|^2 d\mathbf{x}'\psi_1(t,\mathbf{x}), \\ i\hbar\partial_t\psi_2(t,\mathbf{x}) = (-\dfrac{\hbar^2}{2m_2}\Delta + V_2(\mathbf{x}) + \displaystyle\int_{\mathbb{R}^3} U_{\text{int},1}(\mathbf{x}-\mathbf{x}')|\psi_2(t,\mathbf{x}')|^2 d\mathbf{x}')\psi_2(t,\mathbf{x}) \\ \qquad\qquad + \displaystyle\int_{\mathbb{R}^3} U_{\text{int},1,2}(\mathbf{x}-\mathbf{x}')|\psi_1(t,\mathbf{x}')|^2 d\mathbf{x}'\psi_2(t,\mathbf{x}). \end{cases}$$

Like for the one-component case, the interaction between the particles can be simplified by introducing an effective interaction

$$U_{\text{int},\ell}(\mathbf{x}-\mathbf{x}') = \frac{4\pi\hbar^2 a_\ell}{m_\ell}\delta_0(\mathbf{x}-\mathbf{x}'),$$

where a_ℓ is the scattering length of the atoms of species $\ell(= 1, 2)$. The effective interatomic interaction is given by

$$U_{\text{int},1,2}(\mathbf{x}-\mathbf{x}') = \frac{4\pi\hbar^2 a_{1,2}}{m_{1,2}}\delta_0(\mathbf{x}-\mathbf{x}'),$$

where $a_{1,2}$ is the scattering length between an atom of type 1 and an atom of type 2. The quantity $m_{1,2}$ is the reduced mass of a pair of atoms of types 1 and 2, i.e.

$$m_{1,2} = \frac{m_1 m_2}{m_1 + m_2}.$$

Finally, the evolution of a two-components BEC is modeled by the following system of GPEs

$$\begin{cases} i\hbar\partial_t\psi_1(t,\mathbf{x}) = (-\dfrac{\hbar^2}{2m_1}\Delta + V_1(\mathbf{x}) + \dfrac{4\pi\hbar^2 a_1}{m_1}|\psi_1(t,\mathbf{x})|^2 \\ \qquad\qquad + \dfrac{4\pi\hbar^2 a_{1,2}}{m_{1,2}}|\psi_2(t,\mathbf{x})|^2)\psi_1(t,\mathbf{x}), \\ i\hbar\partial_t\psi_2(t,\mathbf{x}) = (-\dfrac{\hbar^2}{2m_2}\Delta + V_2(\mathbf{x}) + \dfrac{4\pi\hbar^2 a_2}{m_2}|\psi_2(t,\mathbf{x})|^2 \\ \qquad\qquad + \dfrac{4\pi\hbar^2 a_{1,2}}{m_{1,2}}|\psi_1(t,\mathbf{x})|^2)\psi_2(t,\mathbf{x}). \end{cases}$$

1.4 Stationary States

In quantum mechanics, an excited state of a quantum system is a quantum state with an energy higher than the energy of the ground state (i.e. the quantum state with the lowest energy). Furthermore, the stationary states of a quantum system are the eigenfunctions of the Hamiltonian operator associated to the system. The eigenvalues for each stationary state are quantified energies related to the spectrum of the Hamiltonian operator. For a stationary state ψ, we have

$$i\partial_t\psi = \mathscr{H}\psi = \mu\psi,$$

where μ is the eigenvalue linked to ψ. Therefore, the stationary state is searched as: $\psi(t,\mathbf{x}) = \phi(\mathbf{x})e^{-i\mu t}$, where ϕ is a time independent square-integrable function such that: $\|\phi\|^2_{L^2_{\mathbf{x}}} = 1$. We directly compute an eigenvalue μ, also called the chemical potential, by using the associated eigenfunction ϕ since

$$\mu = \mu\int_{\mathbb{R}^d}|\phi|^2 d\mathbf{x} = \int_{\mathbb{R}^d}\phi^*\mathscr{H}\phi d\mathbf{x}.$$

1.4.1 Critical Points of the Energy Functional $\mathscr{E}$

Stationary states are critical points of the energy functional. To prove this statement, we follow a proof similar to [98]. Let us consider a GPE for a rotating condensate

$$i\hbar\partial_t\psi(t,\mathbf{x}) = (-\frac{\hbar^2}{2m}\Delta - i\hbar\boldsymbol{\Omega}\cdot(\mathbf{x}\times\nabla) + V(\mathbf{x}) + (N_{\text{part}}-1)\frac{4\pi\hbar^2 a}{m}|\psi(t,\mathbf{x})|^2)\psi(t,\mathbf{x}).$$

We have seen that the energy associated to a given system, defined by (6), can be directly written through the Hamiltonian. For a nonlinear Hamiltonian, a corrective

term must be added to fulfill (7)

$$\begin{aligned}\mathscr{E}(\psi) &= \langle \psi(t,\mathbf{x}), \mathscr{H}(\mathbf{x}, -i\hbar\nabla)\psi(t,\mathbf{x})\rangle_{L^2} \\ &\quad - \int_{\mathbb{R}^3} \frac{1}{2}\frac{4\pi\hbar^2 a}{m}|\psi(t,\mathbf{x})|^4 d\mathbf{x} \\ &= \int_{\mathbb{R}^3} \left[\frac{\hbar^2}{2m}|\nabla\psi(t,\mathbf{x})|^2 + V(\mathbf{x})|\psi(t,\mathbf{x})|^2\right. \\ &\quad \left. -\psi(t,\mathbf{x})^* i\hbar\boldsymbol{\Omega}\cdot(\mathbf{x}\times\nabla)\psi(t,\mathbf{x})\right] d\mathbf{x} \\ &\quad + \int_{\mathbb{R}^3} \frac{1}{2}\frac{4\pi\hbar^2 a}{m}|\psi(t,\mathbf{x})|^4 d\mathbf{x}. \end{aligned} \tag{15}$$

Let us set

$$\mathscr{H}_0(\mathbf{x}, -i\hbar\nabla) = -\frac{\hbar^2}{2m}\Delta + V(\mathbf{x}) - i\hbar\boldsymbol{\Omega}\cdot(\mathbf{x}\times\nabla).$$

We remark that the Hamiltonian operator $\mathscr{H}_0$ is an hermitian operator in $L^2_{\mathbf{x}}$. Let us now compute the critical points of the energy functional (15) under the mass conservation constraint. To this end, we introduce a Lagrange multiplier λ and solve

$$D_{\psi^*}\mathscr{E}(\phi) + D_{\psi}\mathscr{E}(\phi) - \lambda\left[D_{\psi^*}\left(\|\psi\|_{L^2}\right)(\phi) + D_{\psi}\left(\|\psi\|_{L^2}\right)(\phi)\right] = 0. \tag{16}$$

Since $\mathscr{H}_0$ is an hermitian operator, the functional derivatives are given by

$$\begin{aligned} D_{\psi^*}\mathscr{E}(\phi) = D_{\psi}\mathscr{E}(\phi) &= \mathscr{H}_0\phi + \frac{4\pi\hbar^2 a}{m}|\phi|^2\phi, \\ D_{\psi^*}\left(\|\psi\|_{L^2}\right)(\phi) = D_{\psi}\left(\|\psi\|_{L^2}\right)(\phi) &= \phi(\mathbf{x}), \end{aligned}$$

leading a more explicit formulation of (16)

$$\mathscr{H}_0\psi + \frac{4\pi\hbar^2 a}{m}|\psi|^2\psi - \lambda\psi = 0.$$

This finally means that the stationary states are the critical points of $\mathscr{E}$.

1.4.2 Ansatz of the Stationary States

For a magneto-optical trap, the potential is

$$V(t,\mathbf{x}) = -\frac{1}{4}\alpha|E(t,\mathbf{x})|^2.$$

If we assume that the laser is gaussian, then it generates an electric field such that

$$|E(t,\mathbf{x})|^2 = E_0^2 e^{-\frac{x^2}{\ell_x^2}-\frac{y^2}{\ell_y^2}-\frac{z^2}{\ell_z^2}},$$

where ℓ_x, ℓ_y and ℓ_z are the intensity radii of the beam in the x-, y-, and z-directions, respectively. Hence, if the characteristic length of the condensate is small compared to the lengths $\ell_{x,y,z}$ and if we use a gauge transformation, one gets the following GPE with harmonic trap

$$i\hbar\partial_t\psi(t,\mathbf{x}) = (-\frac{\hbar^2}{2m}\Delta + \frac{\alpha}{4}|E_0|^2(\frac{x^2}{\ell_x^2}+\frac{y^2}{\ell_y^2}+\frac{z^2}{\ell_z^2}) + \frac{4\pi\hbar^2 a}{m}|\psi(t,\mathbf{x})|^2)\psi(t,\mathbf{x}).$$

For a noninteracting BEC (e.g. $a = 0$), this system is a linear quantum harmonic oscillator. The ground state is then [98]

$$\phi_{\text{ho}}(\mathbf{x}) = \frac{1}{\pi^{3/4}(a_x a_y a_z)^{1/2}} e^{-\frac{x^2}{2a_x^2}-\frac{y^2}{2a_y^2}-\frac{z^2}{2a_z^2}}, \tag{17}$$

where

$$a_{\{x,y,z\}} = \sqrt{\frac{\sqrt{2}\hbar l_{\{x,y,z\}}}{|E_0|\sqrt{\alpha m}}},$$

with $a_{\{x,y,z\}}$ equal to a_x, a_y or a_z according to the subscript x, y or z, respectively. The associated energy is

$$\mathscr{E}_{\text{osc}} := \mathscr{E}(\phi_{\text{ho}}) = \hbar|E_0|\sqrt{\frac{\alpha}{2m}}(\frac{1}{\ell_x}+\frac{1}{\ell_y}+\frac{1}{\ell_z}).$$

If there are interactions inside the BEC (e.g. $a \neq 0$), we have

$$\mathscr{E}(\phi_{\text{ho}}) = \mathscr{E}_{\text{osc}} + \frac{1}{2(2\pi)^{3/2}a_x a_y a_z}\frac{4\pi\hbar^2 a}{m}.$$

The gaussian function can still be considered as a suitable approximation of the exact ground state if the energy associated to the interaction term is small compared to the energy associated to the quantum harmonic oscillator. Thus, if $\ell_x = \ell_y = \ell_z$, the approximation of the ground state by a gaussian function is correct when $a_x \gg a$.

If the interaction energy is strong (e.g. $a \gg a_x$), this approximation is no longer valid. In this case, we consider the so-called Thomas-Fermi approximation [98, 100] which consists in neglecting the kinetic energy and keeping the potential and interaction energies, e.g.

$$\begin{aligned}\mathscr{E}_{\Delta}(\psi) &:= \int_{\mathbb{R}^3} |\nabla\psi|^2 d\mathbf{x} \ll \mathscr{E}_{\mathrm{TF}}(\psi) \\ &:= \int_{\mathbb{R}^3} \left[V(\mathbf{x})|\psi(t,\mathbf{x})|^2 + \frac{1}{2}\frac{4\pi\hbar^2 a}{m}|\psi(t,\mathbf{x})|^4 \right] d\mathbf{x}.\end{aligned}$$

The total energy is approximated by $\mathscr{E}(\psi) \approx \mathscr{E}_{\mathrm{TF}}(\psi)$. Let us set $U_0 = \frac{4\pi\hbar^2 a}{m}$. The minimizer of $\mathscr{E}_{\mathrm{TF}}$ under the mass conservation constraint is computed by introducing a Lagrange multiplier μ_{TF} and by solving

$$(V + U_0|\phi_{\mathrm{TF}}|^2)\phi_{\mathrm{TF}} = \mu_{\mathrm{TF}}\phi_{\mathrm{TF}}.$$

Multiplying the previous equation by ϕ_{TF}^* leads to

$$\forall \mathbf{x} \in \mathrm{supp}(\phi_{\mathrm{TF}}), \quad |\phi_{\mathrm{TF}}(\mathbf{x})|^2 = \frac{\mu_{\mathrm{TF}} - V(\mathbf{x})}{U_0}.$$

Since $|\phi_{\mathrm{TF}}|^2 > 0$, it follows that

$$\phi_{\mathrm{TF}}(\mathbf{x}) = \begin{cases} \sqrt{\frac{\mu_{\mathrm{TF}} - V(\mathbf{x})}{U_0}}, & \text{for } \mu_{\mathrm{TF}} - V(\mathbf{x}) > 0, \\ 0 \qquad\qquad\quad , & \text{for } \mu_{\mathrm{TF}} - V(\mathbf{x}) \leq 0. \end{cases}$$

The mass conservation gives the chemical potential μ_{TF}. For example, for a quadratic potential (with $\ell_x = \ell_y = \ell_z$), we have

$$\mu_{\mathrm{TF}} = \frac{15^{2/5}\hbar^2}{2ma_x}\left(\frac{a}{a_x}\right)^{2/5}.$$

1.5 The Rotating GPE with a Quadratic Potential: Dimensionless Form in 3d, 2d and 1d

Let us consider the 3d rotating GPE with a quadratic potential

$$i\hbar\partial_t\psi = \left(-\frac{\hbar^2}{2m}\Delta + \frac{\alpha}{4}|E_0|^2\left(\frac{x^2}{\ell_x^2} + \frac{y^2}{\ell_y^2} + \frac{z^2}{\ell_z^2}\right) - i\hbar\boldsymbol{\Omega}\cdot(\mathbf{x}\times\nabla) + \frac{4\pi\hbar^2 a}{m}|\psi|^2\right)\psi,$$

where $\mathbf{x} = (x, y, z) \in \mathbb{R}^3$.

1.5.1 Dimensionless Form of the GPE

Let us set

$$\omega_x = \sqrt{\frac{\alpha}{2m}}\frac{|E_0|}{\ell_x},\ \ \omega_y = \sqrt{\frac{\alpha}{2m}}\frac{|E_0|}{\ell_y},\ \ \omega_z = \sqrt{\frac{\alpha}{2m}}\frac{|E_0|}{\ell_z},\ \ U_0 = \frac{4\pi\hbar^2 a}{m}.$$

By using these new variables, the GPE writes down

$$i\hbar\partial_t\psi = (-\frac{\hbar^2}{2m}\Delta + \frac{m}{2}\left(\omega_x^2x^2 + \omega_y^2y^2 + \omega_z^2z^2\right) - i\hbar\boldsymbol{\Omega}\cdot(\mathbf{x}\times\nabla) + U_0|\psi|^2)\psi.$$

Let us introduce the following changes of variables

$$t \to \frac{t}{\omega_m},\quad \omega_m = \min(\omega_x,\omega_y,\omega_z),\quad \mathbf{x}\to\mathbf{x}a_0,$$
$$a_0 = \sqrt{\frac{\hbar}{m\omega_m}},\quad \psi\to\frac{\psi}{a_0^{3/2}},\quad \Omega\to\Omega\omega_m. \tag{18}$$

Then, we obtain the dimensionless GPE

$$i\partial_t\psi = (-\frac{1}{2}\Delta + \frac{1}{2}\left(\gamma_x^2x^2 + \gamma_y^2y^2 + \gamma_z^2z^2\right) - i\boldsymbol{\Omega}\cdot(\mathbf{x}\times\nabla) + \beta|\psi|^2)\psi,$$

where $\gamma_x = \omega_x/\omega_m$, $\gamma_y = \omega_y/\omega_m$, $\gamma_z = \omega_z/\omega_m$ and $\beta = \frac{U_0}{a_0^3\hbar\omega_m}$.

1.5.2 Dimension Reductions

Let us consider the dimensionless GPE

$$i\partial_t\psi(t,\mathbf{x}) = (-\frac{1}{2}\Delta + V(\mathbf{x}) - i\boldsymbol{\Omega}\cdot(\mathbf{x}\times\nabla) + \beta|\psi(t,\mathbf{x})|^2)\psi(t,\mathbf{x}), \tag{19}$$

where $\boldsymbol{\Omega} = (0,0,\Omega)$. We already know that a stationary state is a critical point of

$$\mathscr{E}(\phi) = \int_{\mathbb{R}^3}(\frac{1}{2}|\nabla\phi(\mathbf{x})|^2 + V(\mathbf{x})|\phi(\mathbf{x})|^2 - \phi^*(\mathbf{x})\Omega L_z\phi(t,\mathbf{x}) + \frac{\beta}{2}|\phi(\mathbf{x})|^4)d\mathbf{x},$$

with $L_z = -i(x\partial_y - y\partial_x)$. We assume that

$$V(\mathbf{x}) = \frac{1}{2}\left(\gamma_x^2x^2 + \gamma_y^2y^2 + \gamma_z^2z^2\right).$$

If $\gamma_x \approx \gamma_y$ and $\gamma_z \gg \gamma_x$, the condensate has a stationary state that expands in the x- and y-directions but is confined along the z-axis (disc-shaped condensate). Indeed, the energy associated to the potential operator in the z-direction is large compared to the energies in the x- and y-directions. Most particularly, an excitation of the condensate generates less dynamics in the z- than in the x- and y-directions [25]. Therefore, the dynamical solution is written as [77, 85]: $\psi(t, \mathbf{x}) = \psi_2(t, x, y)\psi_3(z)$, where

$$\psi_3(z) = (\int_{\mathbb{R}^2} |\psi_0(x, y, z)|^2 dxdy)^{1/2},$$

setting ψ_0 as the 3d stationary state. Since ψ_0 is normalized, we have

$$\int_{\mathbb{R}} |\psi_3(z)|^2 dz = 1.$$

Injecting ψ in (19), we obtain

$$\begin{aligned} i\psi_3(z)\partial_t\psi_2(t, x, y) = &-\frac{1}{2}\psi_3(z)\Delta\psi_2(t, x, y) - \frac{1}{2}\psi_2(t, x, y)\partial_z^2\psi_3(z) \\ &+ \frac{1}{2}\left(\gamma_x^2x^2 + \gamma_y^2y^2\right)\psi_2(t, x, y)\psi_3(z) \\ &+ \frac{1}{2}\gamma_z^2z^2\psi_2(t, x, y)\psi_3(z) - \psi_3(z)\Omega L_z\psi_2(t, x, y) \\ &+ \beta|\psi_2(t, x, y)|^2|\psi_3(z)|^2\psi_2(t, x, y)\psi_3(z). \end{aligned}$$

Multiplying by ψ_3^* and integrating on the whole space with respect to z leads to

$$\begin{aligned} i\partial_t\psi_2(t, x, y) = &(-\frac{1}{2}\Delta + \frac{1}{2}\left(\gamma_x^2x^2 + \gamma_y^2y^2\right) - \Omega L_z \\ &+ \frac{1}{2}\sigma + \kappa_2|\psi_2(t, x, y)|^2)\psi_2(t, x, y), \end{aligned}$$

where

$$\sigma = \int_{\mathbb{R}} \left(\gamma_z^2z^2|\psi_3(z)|^2 + |\partial_z\psi_3(z)|^2\right) dz, \quad \kappa_2 = \int_{\mathbb{R}} \beta|\psi_3(z)|^4 dz.$$

By using the gauge transformation $\psi_2(t, x, y) \to \psi(t, x, y)e^{-\frac{i\sigma}{2}t}$, one gets the two-dimensional rotating GPE

$$i\partial_t\psi(t, x, y) = (-\frac{1}{2}\Delta + \frac{1}{2}(\gamma_x^2x^2 + \gamma_y^2y^2) - \Omega L_z + \kappa_2|\psi(t, x, y)|^2)\psi(t, x, y).$$

Let us now assume that the BEC is nonrotating and that $\gamma_{y,z} \gg \gamma_x$. Similar arguments to the previous ones [25, 77, 85] show that $\psi(t, \mathbf{x}) = \psi_1(t, x)\psi_{2,3}(y, z)$, where

$$\psi_{2,3}(y, z) = (\int_{\mathbb{R}} |\psi_0(x, y, z)|^2 dx)^{1/2}.$$

Here, we assume that the condensate is cigar-shaped. Similarly to the 2d reduction, we obtain the following one-dimensional GPE

$$i\partial_t \psi(t, x) = (-\frac{1}{2}\partial_x^2 + \frac{1}{2}\gamma_x^2 x^2 + \kappa_1 |\psi(t, x)|^2)\psi(t, x),$$

where

$$\kappa_1 = \int_{\mathbb{R}^2} \beta |\psi_{2,3}(y, z)|^4 dydz.$$

Finally, a general form of the rotating GPE in dimension d $(= 1, 2, 3)$ is

$$i\partial_t \psi(t, \mathbf{x}) = (-\frac{1}{2}\Delta + V_d(\mathbf{x}) - \Omega_d L_z + \kappa_d |\psi(t, \mathbf{x})|^2)\psi(t, \mathbf{x}),$$

where $\Omega_{2,3} = \Omega$, $\Omega_1 = 0$ (no rotation),

$$\kappa_d = \begin{cases} \int_{\mathbb{R}^2} \beta |\psi_{2,3}(y, z)|^4 dydz, & \text{for } d = 1, \\ \int_{\mathbb{R}} \beta |\psi_3(z)|^4 dz, & \text{for } d = 2, \\ \beta, & \text{for } d = 3, \end{cases}$$

and

$$V_d(\mathbf{x}) = \begin{cases} 1/2\gamma_x^2 x^2, & \text{for } d = 1, \\ 1/2\left(\gamma_x^2 x^2 + \gamma_y^2 y^2\right), & \text{for } d = 2, \\ 1/2\left(\gamma_x^2 x^2 + \gamma_y^2 y^2 + \gamma_z^2 z^2\right), & \text{for } d = 3. \end{cases}$$

2 Stationary States and Nucleation of Quantized Vortices

2.1 *Stationary States Formulation: Solving a Minimization Problem for the Energy Functional or a Nonlinear Eigenvalue Problem (Under Constraint)?*

The critical points of the energy functional associated to a GPE-like system are in fact the stationary states (see Sect. 1.4, page 67). An impressive number of publications has been devoted to this topic over the last years in the condensed matter physics literature (see for example [43, 49, 83, 110]). Indeed, stationary states correspond to (meta)stable states of the condensate. As seen in the first section, the practical realization of a BEC requires a sophisticated experimental system that is only owned by a few laboratories worldwide. More generally, reaching a temperature to condensate the atomic gas is very challenging. In addition, imaging a condensate is a difficult task due to its small size. A widely used technique consists in letting the condensate expands during a short time scale and then imaging it when its size is large enough [60]. Let us remark that imaging a condensate destroys it immediately. As a consequence, some physical phenomenae are extremely difficult to observe in a BEC on a larger time scale [41, 61, 101]. Therefore, numerical simulations are helpful [34, 80, 109] to provide a complete visualization of a BEC and to compute some of its features (e.g. phase structure) in some various and complex situations (e.g. multi-components, different potentials, nonlinear long-range interactions). The limitations are essentially due to the model that is chosen.

Let us consider the model problem of a GPE with a nonlinearity defined by a function f and with a rotation term

$$\begin{cases} i\partial_t \psi(t,\mathbf{x}) = -\dfrac{1}{2}\Delta\psi(t,\mathbf{x}) - \Omega L_z \psi(t,\mathbf{x}) + V(\mathbf{x})\psi(t,\mathbf{x}) \\ \qquad\qquad +f(|\psi|^2)\psi(t,\mathbf{x}),\ \forall t>0,\ \forall \mathbf{x}\in\mathbb{R}^d, \\ \psi(0,\mathbf{x}) = \psi_0(\mathbf{x}) \text{ in } L^2_{\mathbf{x}}. \end{cases} \tag{20}$$

Function V which acts from $\mathbb{R}^d_{\mathbf{x}}$ onto $\mathbb{R}^+$ corresponds to a (confining) potential. Function f can be a real-valued smooth function like for the standard case $f(|\psi|^2) = \beta|\psi|^{2\sigma}$, with $\beta \in \mathbb{R}$ and $\sigma > 0$. In practice, many other situations exist. As seen before (Sect. 1.3.2, page 61), f is not necessarily a function but can also be an integro-differential operator like for dipole-dipole magnetic interactions. The parameter $\Omega \in \mathbb{R}$ is the rotation speed. The rotation operator L_z is given by: $L_z = -i(x\partial_y - y\partial_x)$. To fix the ideas, let us remark that we may choose a transverse rotation which is written *via* the operator L_z. For $d = 1$, there is no rotation ($\Omega = 0$).

The computation of the stationary states can be done *via* the minimization of the energy under constraint. For (20), the energy is given by

$$\mathscr{E}_{\Omega,F}(\psi) := \int_{\mathbb{R}^d} \left(\frac{1}{2}|\nabla\psi|^2 + V(\mathbf{x})|\psi|^2 - \Omega\psi^* L_z\psi + F(|\psi|^2)\right) d\mathbf{x}, \tag{21}$$

where F is the primitive function of f

$$\forall r \in [0, \infty[, \quad F(r) := \int_0^r f(q)dq.$$

Hence, the minimization problem consists in computing a function $\phi \in L^2_{\mathbf{x}}$ such that

$$\mathscr{E}_{\Omega,F}(\phi) = \min_{\|\psi\|_{L^2_{\mathbf{x}}}=1} \mathscr{E}_{\Omega,F}(\psi). \tag{22}$$

From a numerical point of view, this implies that a strategy based on numerical nonlinear optimization techniques under constraints can be used to obtain the stationary states. A second approach is related to the property (see Sect. 1.4.1, page 67) that the problem can also be formulated as the nonlinear eigenvalue problem: find an eigenfunction $\phi \in L^2_{\mathbf{x}}$ and an eigenvalue $\mu \in \mathbb{R}$ such that

$$\mu\phi = -\frac{1}{2}\Delta\phi - \Omega L_z\phi + V(\mathbf{x})\phi + f(|\phi|^2)\phi, \tag{23}$$

under the $L^2_{\mathbf{x}}$-normalization constraint for ϕ. Concerning the nonlinear eigenvalue solvers, we refer for example to [56] for an application in the framework of GPEs.

Here, we essentially develop a method that is embedded in the class of the minimization methods. This approach is called *Conjugate Normalized Gradient Flow* (CNGF) and corresponds to the well-known *imaginary time* method in physics [4, 22, 35, 47, 48, 58, 65]. Let us however remark that other minimization methods can be used [25, 46, 51, 56]. The CNGF method consists in building a minimizing sequence of the energy functional $\mathscr{E}_{\Omega,F}$ given by (21). To this end, we consider a time discretization $(t_n)_{n\in\mathbb{N}}$, with $t_0 = 0$, and we define the local time step: $\delta t_n = t_{n+1} - t_n$, $\forall n \in \mathbb{N}$. The CNGF method is given by the algorithm: compute the sequence of iterates $(\phi(\mathbf{x}, t_n))_{n\in\mathbb{N}}$ defined by

$$\begin{cases} \partial_t\phi(\mathbf{x},t) = -D_{\phi^*}\mathscr{E}_{\Omega,F}(\phi) = \dfrac{1}{2}\Delta\phi(\mathbf{x},t) + \Omega L_z\phi(\mathbf{x},t) - V(\mathbf{x})\phi(\mathbf{x},t) \\ \qquad\qquad -f(|\phi|^2)\phi(\mathbf{x},t), \quad \forall t \in [t_n, t_{n+1}[, \ \forall \mathbf{x} \in \mathbb{R}^d, \\ \phi(\mathbf{x}, t_{n+1}) := \phi(\mathbf{x}, t^+_{n+1}) = \dfrac{\phi(\mathbf{x}, t^-_{n+1})}{||\phi(\mathbf{x}, t^-_{n+1})||_{L^2_{\mathbf{x}}}}, \\ \phi(\mathbf{x}, 0) = \phi_0(\mathbf{x}) \in L^2_{\mathbf{x}}, \text{ with } ||\phi_0||_{L^2_{\mathbf{x}}} = 1. \end{cases} \tag{24}$$

In the above equations, we designate by $g(t^+_{n+1})$ (respectively $g(t^-_{n+1})$) the limit from the right (respectively from the left) of a function g. The discrete times t_n parametrize the sequence. This explains why we use the "inverse" notation $\phi(\mathbf{x}, t)$ instead of $\phi(t, \mathbf{x})$. Correctly choosing the initial data ϕ_0 in the iterative algorithm is important to ensure the convergence. In practice, as we will see later in Sect. 2.3

(page 88), a suitable choice consists in considering initial data built as Ansatz of the underlying equation (GPE) with respect to a given asymptotic regime.

The CNGF method conserves the $L^2_{\mathbf{x}}$-norm of the solution [22]. Moreover, Bao and Du [22] proved that the algorithm (24) produces a sequence that minimizes the energy in the linear case (i.e. $f(|\phi|^2) = 0$) for a positive potential (i.e. $V(\mathbf{x}) \geq 0$). Hence, under these assumptions, we prove that

$$\lim_{t\to\infty} \phi(\mathbf{x}, t) = \phi_g(\mathbf{x}), \tag{25}$$

where ϕ_g is a stationary state. Practically, the long time computation (25) is fixed according to a stopping criterion that we will precise later.

2.2 Time and Space Discretizations of System (24)

In this section, we consider several time and space discretization schemes for the system (24). The Partial Differential Equation that we want to solve is similar to a heat equation (and not a Schrödinger equation) in imaginary time. At first glance, one may think that using a standard method adapted to this class of equations would lead to an admissible scheme. Nevertheless, an important point to keep in mind is that a normalization constraint must be fulfilled and, more importantly, that we want to build a minimizing sequence of the energy functional. Therefore, as precise before, the imaginary time parametrizes the optimization algorithm at the continuous level. As a consequence, a suitable scheme must produce a minimizing sequence, at least in some situations (e.g. for $f := 0$). In [22], Bao and Du analyze a few a priori standard schemes for (24). The conclusion is the following. The time splitting scheme (see Sect. 4.2, page 109, for the real time-domain GPE) which is generally an efficient and accurate method in computational dynamics must not be used here since the time step required to get a decaying energy is too small. This property can be observed even in simple situations, for example for the non rotating case ($\Omega = 0$). Another solution consists in applying the unconditionally stable Crank-Nicolson (CN) scheme that has the a priori advantage of being second-order accurate both in space and time. The difficulty is that this scheme is extremely time consuming since it requires the accurate solution to a nonlinear PDE at each time step. A possibility consists in writing in an explicit way the nonlinear term (semi-implicit scheme) resulting in the solution of a linear (and not nonlinear) system at each time step. Even if this solution seems attractive, the associated sequence is minimizing if a strong restrictive CFL (Courant-Friedrichs-Lewy) condition between the time and spatial steps holds. Concerning the backward Euler scheme (and similarly to the CN scheme), a nonlinear system must also be solved at each time step. However, the very nice result obtained by Bao and Du [22] is that the semi-implicit backward Euler scheme (see Sect. 2.2.1) produces

a minimizing sequence without any CFL condition, unlike the CN scheme. This property holds when the potential V is positive.

Concerning the spatial discretization, we consider two approaches (Sect. 2.2.2). The first one consists in simply choosing a standard second-order finite difference scheme. An alternative discretization is the pseudo-spectral scheme based on Fast Fourier Transforms (FFTs). The reason why this last choice is seducing is that the resulting CNGF method is very robust while also being simple. Indeed, it leads to the accurate computation of the stationary states even for GPEs with large rotation speeds Ω. These states cannot be reached when considering low-order spatial discretization schemes (second-order for example). Finally, the efficiency of the FFT algorithms on large clusters of HPC can lead to the possibility of computing extremely complex 3d BECs configurations, based on CPU, GPU or hybrid computers.

2.2.1 Semi-implicit Backward Euler Scheme in Time

Let us introduce the semi-implicit Euler scheme [22] (which is a reference scheme in the sequel). We consider a uniform time discretization: $\delta t_n = \delta t = t_{n+1} - t_n$, $\forall n \in \mathbb{N}$, and obtain the semi-discrete time scheme for CNGF

$$\begin{cases} \dfrac{\tilde{\phi}(\mathbf{x}) - \phi(\mathbf{x}, t_n)}{\delta t} = \dfrac{1}{2}\Delta\tilde{\phi}(\mathbf{x}) + \Omega L_z\tilde{\phi}(\mathbf{x}) - V(\mathbf{x})\tilde{\phi}(\mathbf{x}) \\ \qquad\qquad -f(|\phi(\mathbf{x}, t_n)|^2)\tilde{\phi}(\mathbf{x}), \quad \forall \mathbf{x} \in \mathbb{R}^d, \\ \phi(\mathbf{x}, t_{n+1}) = \dfrac{\tilde{\phi}(\mathbf{x})}{||\tilde{\phi}||_{L^2_{\mathbf{x}}}}, \\ \phi(\mathbf{x}, 0) = \phi_0(\mathbf{x}), \text{ with } ||\phi_0||_{L^2_{\mathbf{x}}} = 1. \end{cases} \tag{26}$$

The reason why this scheme is considered as a "good" discretization scheme for CNGF is a consequence of the following theorem (Bao and Du [22]).

Theorem 1 *Let us assume that $V(\mathbf{x}) \geq 0$, $\forall \mathbf{x} \in \mathbb{R}^d$, $\Omega = 0$ and $f(|\phi|^2) = \beta|\phi|^2$. Then, for any $\beta \geq 0$, the following results hold: $\forall n \in \mathbb{N}$,*

$$\|\phi(\mathbf{x}, t_n)\|_{L^2_{\mathbf{x}}} = \|\phi_0\|_{L^2_{\mathbf{x}}} = 1,$$

and

$$\mathscr{E}_{\Omega,f}(\tilde{\phi}(\cdot)) \leq \mathscr{E}_{\Omega,f}(\phi(\cdot, t_n)).$$

Theorem 1 confirms that the semi-implicit Euler discretization scheme leads to a decaying modified energy $\mathscr{E}_{\Omega,f}$ at each step of the projected steepest descent algorithm.

To numerically check that the numerical solution converged to the stationary state, we consider in the sequel the following (strong) criterion

$$||\phi(\cdot, t_{n+1}) - \phi(\cdot, t_n)||_\infty < \varepsilon \delta t, \tag{27}$$

where $\|\cdot\|_\infty$ is the infinity norm. We need to fix ε small enough to obtain a good accuracy of the stationary state, most particularly when considering highly accurate solutions based on pseudo-spectral approximation techniques. Let us remark that we may also choose another (weak) stopping criterion that is associated with the evolution of the energy

$$|\mathscr{E}_{\Omega,F}(\phi(\cdot, t_{n+1})) - \mathscr{E}_{\Omega,F}(\phi(\cdot, t_n))| < \varepsilon \delta t. \tag{28}$$

This second criterion is defined in GPELab.

2.2.2 Spatial Discretizations

We now focus on the spatial discretization of system (26). We consider the case of the dimension $d = 2$, the generalization to $d = 1$ and $d = 3$ being direct by adapting the notations. Since problem (26) is set in the whole space, the computational domain has to be truncated. Because there is no physical boundary, it is natural to choose a rectangular computational domain $\mathscr{O} :=]-a_x, a_x[\times]-a_y, a_y[$. We consider a uniform discretization grid for $\mathscr{O}$: for any indices $J(\geq 3)$ and $K(\geq 3)$ in $\mathbb{N}$, we define

$$\mathscr{O}_{J,K} = \left\{\mathbf{x}_{j,k} = (x_j, y_k) \in \mathscr{O}, \quad \forall j \in \{0, \ldots, J\} \text{ and } \forall k \in \{0, \ldots, K\}\right\}, \tag{29}$$

with $h_x = x_{j+1} - x_j$, $\forall j \in \{0, \ldots, J-1\}$, and $h_y = y_{k+1} - y_k$, $\forall k \in \{0, \ldots, K-1\}$. We introduce: $x_0 = -a_x$, $x_J = a_x$, $y_0 = -a_y$ and $y_K = a_y$. Furthermore, we define the set of indices: $\mathscr{F}_{J,K} = \left\{(j,k) \in \mathbb{N}^2; 1 \leq j \leq J-1 \text{ and } 1 \leq k \leq K-1\right\}$, for finite difference schemes with a Dirichlet boundary condition, and $\mathscr{P}_{J,K} = \left\{(j,k) \in \mathbb{N}^2; 1 \leq j \leq J \text{ and } 1 \leq k \leq K\right\}$, for the pseudo-spectral approximation with periodic boundary condition.

Finite difference discretization. We give the discretization of the operators appearing in problem (26) when using finite differences. We assume that the potential V confines the stationary states in $\mathscr{O}$ (which is physically realistic) and that we can choose a Dirichlet boundary condition, i.e. $\tilde{\phi}(\mathbf{x}) = 0$, for $\mathbf{x} \in \partial\mathscr{O}$. For any function φ defined on the grid $\mathscr{O}_{J,K}$, we set: $\varphi(\mathbf{x}_{j,k}) = \varphi(x_j, y_k) = \varphi_{j,k}$, for points $\mathbf{x}_{j,k}$ in the computational grid, $j \in \{1, \ldots, J-1\}$, $k \in \{1, \ldots, K-1\}$, considering the Dirichlet boundary condition. Concerning the directional derivatives along x or y, we use the second-order approximations

$$\forall (j,k) \in \mathscr{F}_{J,K}, \quad \delta_x \phi_{j,k} = \frac{\phi_{j+1,k} - \phi_{j-1,k}}{2h_x}, \quad \delta_y \phi_{j,k} = \frac{\phi_{j,k+1} - \phi_{j,k-1}}{2h_y}. \tag{30}$$

Since we impose a Dirichlet boundary condition, we have: $\forall (j,k) \in \mathscr{F}_{J,K}$

$$\delta_x \phi_{1,k} = \frac{\phi_{2,k}}{2h_x}, \quad \delta_y \phi_{j,1} = \frac{\phi_{j,2}}{2h_y}, \quad \delta_x \phi_{J-1,k} = -\frac{\phi_{J-2,k}}{2h_x}, \quad \delta_y \phi_{j,K-1} = -\frac{\phi_{j,K-2}}{2h_y}.$$

Consequently, the second-order discretization of the rotation operator L_z is

$$\forall (j,k) \in \mathscr{F}_{J,K}, ([L_z]\boldsymbol{\phi})_{j,k} := -i(x_j \delta_y \phi_{j,k} - y_k \delta_x \phi_{j,k}). \tag{31}$$

If $L = (J-1)(K-1)$, we associate the matrix $[L_z] \in \mathscr{M}_L(\mathbb{C})$ to this discrete operator and we denote by $\boldsymbol{\phi} := (\phi_{I(j,k)})_{(j,k)\in\mathscr{F}_{J,K}}$ the unknown vector in $\mathbb{C}^L$, where we assume that the indices ordering is such that: $I(j,k) = j + (J-1)(k-1)$, and $\phi_{I(j,k)} = \phi_{j,k}$.

Concerning the derivatives of order two, we use the second-order centered three-points formulae in the directions x and y: $\forall (j,k) \in \mathscr{F}_{J,K}$

$$\delta_x^2 \phi_{j,k} = \frac{\phi_{j+1,k} - 2\phi_{j,k} + \phi_{j-1,k}}{h_x^2}, \qquad \delta_y^2 \phi_{j,k} = \frac{\phi_{j,k+1} - 2\phi_{j,k} + \phi_{j,k-1}}{h_y^2}. \tag{32}$$

Since we consider a Dirichlet boundary condition, we have: $\forall (j,k) \in \mathscr{F}_{J,K}$

$$\delta_x^2 \phi_{1,k} = \frac{\phi_{2,k} - 2\phi_{1,k}}{h_x^2}, \quad \delta_y^2 \phi_{j,1} = \frac{\phi_{j,2} - 2\phi_{j,1}}{h_y^2},$$

$$\delta_x^2 \phi_{J-1,k} = \frac{-2\phi_{J-1,k} + \phi_{J-2,k}}{h_x^2}, \quad \delta_y \phi_{j,K-1} = \frac{-2\phi_{j,K-1} + \phi_{j,K-2}}{h_y^2}.$$

The Laplacian operator Δ is then classically discretized by the five-points finite difference scheme

$$\forall (j,k) \in \mathscr{F}_{J,K}, \quad ([\Delta]\boldsymbol{\phi})_{j,k} = \delta_x^2 \phi_{j,k} + \delta_y^2 \phi_{j,k}. \tag{33}$$

We associate the matrix $[\Delta] \in \mathscr{M}_L(\mathbb{C})$ to this discrete operator.

The potential and nonlinear operators are pointwise evaluated: $\forall (j,k) \in \mathscr{F}_{J,K}$

$$([V]\boldsymbol{\phi})_{j,k} = V(\mathbf{x}_{j,k})\phi_{j,k} \text{ and } ([f(|\boldsymbol{\phi}^n|^2)]\boldsymbol{\phi})_{j,k} = f(|\phi_{j,k}^n|^2)\phi_{j,k}. \tag{34}$$

The matrices $[V] \in \mathscr{M}_L(\mathbb{C})$ and $[f(|\boldsymbol{\phi}^n|^2)] \in \mathscr{M}_L(\mathbb{C})$ are diagonal after the indices reordering.

Finally, the finite difference discretization of problem (26) leads to the finite dimensional approximation: compute the sequence of vector fields $(\boldsymbol{\phi}^n)_{n\in\mathbb{N}}$ in $\mathbb{C}^L$ through

$$\begin{cases} \mathbb{A}_{\mathrm{FD}}^{\mathrm{BE},n}\tilde{\boldsymbol{\phi}} = \mathbf{b}^n, \\ \boldsymbol{\phi}^{n+1} = \dfrac{\tilde{\boldsymbol{\phi}}}{||\tilde{\boldsymbol{\phi}}||_{\ell_0^2}}, \\ \boldsymbol{\phi}^0 = \boldsymbol{\phi}_0, \end{cases} \tag{35}$$

with

$$\begin{cases} \mathbb{A}_{\mathrm{FD}}^{\mathrm{BE},n} := \dfrac{1}{\delta t}[I] - \dfrac{1}{2}[\Delta] - \Omega[L_z] + [V] + [f(|\boldsymbol{\phi}^n|^2)], \\ \mathbf{b}^n := \dfrac{\boldsymbol{\phi}^n}{\delta t}. \end{cases}$$

In the above system, $[I]$ is the identity matrix in $\mathscr{M}_L(\mathbb{C})$. The initial data $\boldsymbol{\phi}^0$ is fixed by the values of ϕ_0 at the grid points. In the framework of Dirichlet boundary conditions, we define the two-norm $||\cdot||_{\ell_0^2}$ of a complex-valued vector $\boldsymbol{\phi} \in \mathbb{C}^L$ by

$$||\boldsymbol{\phi}||_{\ell_0^2} := h_x^{1/2} h_y^{1/2} \Big(\sum_{(j,k)\in\mathscr{F}_{J,K}} |\phi_{I(j,k)}|^2 \Big)^{1/2}. \tag{36}$$

Furthermore, we define the discrete (strong) stopping criterion as

$$||\boldsymbol{\phi}^{n+1} - \boldsymbol{\phi}^n||_\infty < \varepsilon \delta t, \tag{37}$$

with the discrete uniform norm defined by: $\forall \boldsymbol{\phi} \in \mathbb{C}^L$, $\|\boldsymbol{\phi}\|_\infty = \max_{(j,k)\in\mathscr{F}_{J,K}} |\phi_{I(j,k)}|$, and the discrete (weak) stopping criterion as

$$|\mathscr{E}_{\Omega,F}(\boldsymbol{\phi}^{n+1}) - \mathscr{E}_{\Omega,F}(\boldsymbol{\phi}^n)| < \varepsilon \delta t, \tag{38}$$

with the discrete energy

$$\mathscr{E}_{\Omega,F}(\boldsymbol{\phi}) = (h_x h_y)^{1/2} \sum_{(j,k)\in\mathscr{F}_{J,K}} \Re \left\{ \boldsymbol{\phi}_{I(j,k)}^* \left(-\frac{1}{2}[\Delta]\boldsymbol{\phi} - \Omega[L_z]\boldsymbol{\phi} + [V]\boldsymbol{\phi} + [F(|\boldsymbol{\phi}|^2)]\boldsymbol{\phi} \right)_{j,k} \right\}.$$

In the sequel, the discretization scheme (35) is called BEFD (for *Backward Euler Finite Difference*). This scheme produces a minimizing sequence $(\boldsymbol{\phi}^n)_{n\in\mathbb{N}}$ of the modified energy under the assumptions of Theorem 1, without CFL condition, and with second-order accuracy in space.

Pseudo-spectral discretization. Let us now consider the pseudo-spectral approximation scheme based on FFTs. We still assume that the state is localized in

the box $\mathscr{O}$. Unlike finite differences, we consider a periodic boundary condition which is satisfied since the function a priori vanishes on the boundary. If one chooses a Dirichlet boundary condition, then Fast Sine Transforms must be used. For a Neumann boundary condition, Fast Cosine Transforms must be applied. Nevertheless, these two last transforms require to be correctly coded through FFTs to be efficient. For example, these two methods are not included in the basic version of Matlab (but are defined in the signal processing toolbox) contrary to the FFT (which is a compiled version of FFT3W). Since GPELab is developed under the basic Matlab version, we restrict our study to the FFT-based algorithm.

In this framework, a function φ [that can be considered as an approximation of the solution $\tilde{\phi}$ of problem (26)] is defined on the uniform grid $\mathscr{O}_{J,K}$ by $\varphi_{j,k}$, for any indices $(j,k) \in \mathscr{P}_{J,K}$, i.e. excluding $j = 0$ and $k = 0$. Let $M := JK$ be the number of degrees of freedom for the periodic boundary-value problem. Let us introduce $\boldsymbol{\varphi} := (\varphi_{j,k})_{(j,k)\in\mathscr{P}_{J,K}}$, that is, $\boldsymbol{\varphi} \in \mathbb{C}^M$ by a lexicographic reordering (that we do not precise for conciseness). The approximate pseudo-spectral approximations of a function ϕ in the x- and y-directions (which is represented on $\mathscr{O}_{J,K}$) are respectively based on truncated partial inverse Fourier series representations: $\forall (j,k) \in \mathscr{P}_{J,K}$,

$$\begin{aligned}
\phi(t,x_j,y_k) &\approx \varphi(x_j,y_k,t) = \tfrac{1}{J}\textstyle\sum_{p=-J/2}^{J/2-1} \widehat{\varphi_p}(y_k,t)e^{i\mu_p(x_j+a_x)},\\
\phi(t,x_j,y_k) &\approx \varphi(x_j,y_k,t) = \tfrac{1}{K}\textstyle\sum_{q=-K/2}^{K/2-1} \widehat{\varphi_q}(x_k,t)e^{i\lambda_q(y_k+a_y)},
\end{aligned} \tag{39}$$

where $\widehat{\varphi_p}$ and $\widehat{\varphi_q}$ are respectively the Fourier coefficients of the function φ in the directions x and y, the Fourier multipliers being: $\mu_p = \frac{\pi p}{a_x}$ and $\lambda_q = \frac{\pi q}{a_y}$. The functions $\widehat{\varphi_p}$ and $\widehat{\varphi_q}$ can be expressed as

$$\begin{aligned}
\widehat{\varphi_p}(y_k,t) &= \sum_{j=0}^{J-1} \varphi(x_j,y_k,t)e^{-i\mu_p(x_j+a_x)},\\
\widehat{\varphi_q}(x_j,t) &= \sum_{k=0}^{K-1} \varphi(x_j,y_k,t)e^{-i\lambda_q(y_k+a_y)}.
\end{aligned} \tag{40}$$

Consequently, the effect of a directional derivative along x or y, respectively, is written under the form, $\forall (j,k) \in \mathscr{P}_{J,K}$,

$$\begin{aligned}
([[\partial_x]]\boldsymbol{\varphi})_{j,k} &= \frac{1}{J}\sum_{p=-J/2}^{J/2-1} i\mu_p\widehat{\varphi_p}(y_k,t)e^{i\mu_p(x_j+a_x)},\\
([[\partial_y]]\boldsymbol{\varphi})_{j,k} &= \frac{1}{K}\sum_{q=-K/2}^{K/2-1} i\lambda_q\widehat{\varphi_q}(x_k,t)e^{i\lambda_q(y_k+a_y)}.
\end{aligned}$$

Hence, we deduce the following approximation of the rotational operator L_z on $\mathscr{O}_{J,K}$

$$([[L_z]]\boldsymbol{\varphi})_{j,k} = -i\left(x_j([[\partial_y]]\boldsymbol{\varphi})_{j,k} - y_k([[\partial_x]]\boldsymbol{\varphi})_{j,k}\right). \tag{41}$$

The formal applications of derivatives to the previous representations yield the approximations of the second-order derivatives: $\forall (j,k) \in \mathscr{P}_{J,K}$,

$$\begin{aligned}([[\partial_x^2]]\boldsymbol{\varphi})_{j,k} &= \frac{1}{J}\sum_{p=-J/2}^{J/2-1} -\mu_p^2 \widehat{\varphi_p}(y_k,t)e^{i\mu_p(x_j+a_x)},\\ ([[\partial_y^2]]\boldsymbol{\varphi})_{j,k} &= \frac{1}{K}\sum_{q=-K/2}^{K/2-1} -\lambda_q^2 \widehat{\varphi_q}(x_k,t)e^{i\lambda_q(y_k+a_y)},\end{aligned}$$

leading to the approximation of the Laplacian operator Δ

$$([[\Delta]]\boldsymbol{\varphi})_{j,k} = \left([[\partial_x^2]]\boldsymbol{\varphi} + [[\partial_y^2]]\boldsymbol{\varphi}\right)_{j,k}. \tag{42}$$

The potential and nonlinear operators are given pointwise, $\forall (j,k) \in \mathscr{P}_{J,K}$,

$$([[V]]\boldsymbol{\varphi})_{j,k} = V(\mathbf{x}_{j,k})\varphi_{j,k} \quad \text{and} \quad ([[f(|\boldsymbol{\phi}^n|^2)]]\boldsymbol{\varphi})_{j,k} = f(|\phi_{j,k}^n|^2)\varphi_{j,k}. \tag{43}$$

The pseudo-spectral approximation of (26) then produces a sequence of vectors $(\boldsymbol{\phi}^n)_{n\in\mathbb{N}}$ solution to

$$\begin{cases} \mathbb{A}_{\mathrm{SP}}^{\mathrm{BE},n}\tilde{\boldsymbol{\phi}} = \mathbf{b}^{\mathrm{BE},n},\\ \boldsymbol{\phi}^{n+1} = \dfrac{\tilde{\boldsymbol{\phi}}}{||\tilde{\boldsymbol{\phi}}||_{\ell^2_\pi}},\\ \boldsymbol{\phi}^0 := \boldsymbol{\phi}_0, \end{cases} \tag{44}$$

where $\tilde{\boldsymbol{\phi}} \in \mathbb{C}^M$. The right-hand side is

$$\mathbf{b}^{\mathrm{BE},n} := \frac{\boldsymbol{\phi}^n}{\delta t},$$

with $\boldsymbol{\phi}^n \in \mathbb{C}^M$. The map $\|\cdot\|_{\ell^2_\pi}$ corresponds to the discrete $L^2_{\mathbf{x}}$-norm on the grid $\mathscr{O}_{J,K}$ for a vector $\boldsymbol{\phi} \in \mathbb{C}^M$

$$||\boldsymbol{\phi}||_{\ell^2_\pi} := h_x^{1/2}h_y^{1/2}\Big(\sum_{(j,k)\in\mathscr{P}_{J,K}} |\phi_{j,k}|^2\Big)^{1/2}. \tag{45}$$

Furthermore, we define the discrete (strong) stopping criterion as

$$||\boldsymbol{\phi}^{n+1} - \boldsymbol{\phi}^{n}||_{\infty} < \varepsilon \delta t, \tag{46}$$

with the discrete uniform norm defined by: $\forall \boldsymbol{\phi} \in \mathbb{C}^M$, $\|\boldsymbol{\phi}\|_{\infty} = \max_{(j,k)\in\mathscr{P}_{J,K}} |\phi_{j,k}|$, and the discrete (weak) stopping criterion as

$$|\mathscr{E}_{\Omega,F}(\boldsymbol{\phi}^{n+1}) - \mathscr{E}_{\Omega,F}(\boldsymbol{\phi}^{n})| < \varepsilon \delta t, \tag{47}$$

with the discrete energy

$$\mathscr{E}_{\Omega,F}(\boldsymbol{\phi}) = (h_x h_y)^{1/2} \sum_{(j,k)\in\mathscr{P}_{J,K}} \Re\left\{ \phi_{j,k}^{*} \left(-\frac{1}{2}[[\Delta]]\boldsymbol{\phi} - \Omega[[L_z]]\boldsymbol{\phi} + [[V]]\boldsymbol{\phi} + [[F(|\phi|^2)]]\boldsymbol{\phi} \right)_{j,k} \right\}.$$

In (44), the operator $\mathbb{A}_{\mathrm{SP}}^{\mathrm{BE},n}$ is a map which, for any vector $\boldsymbol{\phi} \in \mathbb{C}^M$, associates a vector $\boldsymbol{\psi} \in \mathbb{C}^M$ such that

$$\begin{aligned} \boldsymbol{\psi} &:= \mathbb{A}_{\mathrm{SP}}^{\mathrm{BE},n}\boldsymbol{\phi} = \mathbb{A}_{\mathrm{TF}}^{\mathrm{BE},n}\boldsymbol{\psi} + \mathbb{A}_{\Delta,\Omega}^{\mathrm{BE}}\boldsymbol{\phi}, \\ \mathbb{A}_{\mathrm{TF}}^{\mathrm{BE},n}\boldsymbol{\phi} &:= \left(\frac{[[I]]}{\delta t} + [[V]] + [[f(|\boldsymbol{\phi}^{n}|^2)]]\right)\boldsymbol{\phi}, \\ \mathbb{A}_{\Delta,\Omega}^{\mathrm{BE}}\boldsymbol{\phi} &:= \left(-\frac{1}{2}[[\Delta]] - \Omega[[L_z]]\right)\boldsymbol{\phi}, \end{aligned} \tag{48}$$

where $[[I]]$ is the identity matrix of $\mathscr{M}_M(\mathbb{C})$.

To evaluate the operator $\mathbb{A}_{\mathrm{TF}}^{\mathrm{BE},n}$, we use (43). We remark that the operator is diagonal in the physical space. For $\mathbb{A}_{\Delta,\Omega}^{\mathrm{BE}}$, we consider (41) and (42) for $[[L_z]]$ and $[[\Delta]]$, respectively. Let us note that $\mathbb{A}_{\Delta,\Omega}^{\mathrm{BE}}$ is not diagonal in the physical space but $[[\Delta]]$, defined by (42), is diagonal in the Fourier space. The semi-implicit backward Euler scheme with a pseudo-spectral approximation is now designated by BESP (for *Backward Euler pseudo-SPectral*).

2.2.3 Fully Discretized Semi-implicit Crank-Nicolson Scheme

The discretization of (24) by using the semi-implicit Crank-Nicolson scheme is

$$\begin{cases} \dfrac{\tilde{\phi}(\mathbf{x}) - \phi(\mathbf{x}, t_n)}{\delta t} = \dfrac{1}{2}\Delta\left(\dfrac{\tilde{\phi}(\mathbf{x}) + \phi(\mathbf{x}, t_n)}{2}\right) \\ \qquad\qquad + \Omega L_z\left(\dfrac{\tilde{\phi}(\mathbf{x}) + \phi(\mathbf{x}, t_n)}{2}\right) - V(\mathbf{x})\left(\dfrac{\tilde{\phi}(\mathbf{x}) + \phi(\mathbf{x}, t_n)}{2}\right) \\ \qquad\qquad - f(|\phi(\mathbf{x}, t_n)|^2)\left(\dfrac{\tilde{\phi}(\mathbf{x}) + \phi(\mathbf{x}, t_n)}{2}\right), \ \forall \mathbf{x} \in \mathbb{R}^d, \\ \phi(\mathbf{x}, t_{n+1}) = \dfrac{\tilde{\phi}(\mathbf{x})}{||\tilde{\phi}(\mathbf{x})||_{L^2_{\mathbf{x}}}}, \\ \phi^0 = \phi_0, \ \text{with } ||\phi_0||_{L^2_{\mathbf{x}}} = 1. \end{cases} \tag{49}$$

In [22], Bao and Du proved that the scheme (49) for the one-dimensional case generates a minimizing sequence of the energy functional under some assumptions similar to Theorem 1, with $\beta = 0$, *but* with the following strong CFL constraint

$$\delta t \leq \frac{2h_x^2}{2 + h_x^2 \max\limits_{j \in \{1,\dots,J-1\}} V(x_j)}, \tag{50}$$

for a uniform finite difference discretization $(x_j)_{j\in\{1,\dots,J-1\}}$, with spatial step h_x, on an interval $]-a_x, a_x[$. In a practical computation, this CFL is very restrictive.

Concerning the spatial discretization, the previous approaches (FD and SP) directly extend. For example, for the finite difference scheme at the iteration n, we obtain the CNFD scheme

$$\begin{cases} \mathbb{A}_{\mathrm{FD}}^{\mathrm{CN},n} \tilde{\boldsymbol{\phi}} = \mathbf{b}^n, \\ \boldsymbol{\phi}^{n+1} = \dfrac{\tilde{\boldsymbol{\phi}}}{||\tilde{\boldsymbol{\phi}}||_{\ell_0^2}}, \end{cases} \tag{51}$$

with

$$\mathbb{A}_{\mathrm{FD}}^{\mathrm{CN},n} := \frac{1}{\delta t}[I] + \frac{1}{2}\left(-\frac{1}{2}[\Delta] - \Omega[L_z] + [V] + [f(|\boldsymbol{\phi}^n|^2)]\right),$$

$$\mathbf{b}^n := \frac{\boldsymbol{\phi}^n}{\delta t} + \frac{1}{2}\left(\frac{1}{2}[\Delta] + \Omega[L_z] - [\mathbb{V}] - [f(|\boldsymbol{\phi}^n|^2)]\right)\boldsymbol{\phi}^n,$$

and the initial data $\boldsymbol{\phi}^0 = \boldsymbol{\phi}_0 \in \mathbb{C}^L$.

For the pseudo-spectral approximation at iteration n, the CNSP scheme is

$$\begin{cases} \mathbb{A}_{\mathrm{SP}}^{\mathrm{CN},n}\tilde{\boldsymbol{\phi}} = \mathbf{b}^{\mathrm{CN},n}, \\ \boldsymbol{\phi}^{n+1} = \dfrac{\tilde{\boldsymbol{\phi}}}{||\tilde{\boldsymbol{\phi}}||_{\ell^2_\pi}}, \end{cases} \tag{52}$$

where $\mathbb{A}_{\mathrm{SP}}^{\mathrm{CN},n}$ is the operator which maps any vector $\boldsymbol{\phi} \in \mathbb{C}^M$ to $\boldsymbol{\psi} \in \mathbb{C}^M$ through the relations

$$\begin{aligned} \boldsymbol{\psi} &:= \mathbb{A}_{\mathrm{SP}}^{\mathrm{CN},n}\boldsymbol{\phi} = \mathbb{A}_{\mathrm{TF}}^{\mathrm{CN},n}\boldsymbol{\phi} + \mathbb{A}_{\Delta,\Omega}^{\mathrm{CN},n}\boldsymbol{\phi}, \\ \mathbb{A}_{\mathrm{TF}}^{\mathrm{CN},n}\boldsymbol{\phi} &:= (\frac{[[I]]}{\delta t} + \frac{1}{2}[[V]] + \frac{1}{2}[[f(|\boldsymbol{\phi}^n|^2)]])\boldsymbol{\phi}, \\ \mathbb{A}_{\Delta,\Omega}^{\mathrm{CN}}\boldsymbol{\phi} &:= (-\frac{1}{4}[[\Delta]] - \frac{1}{2}\Omega[[L_z]])\boldsymbol{\phi}. \end{aligned} \tag{53}$$

The right-hand side is

$$\mathbf{b}^{\mathrm{CN},n} := (\frac{[[I]]}{\delta t} + \frac{1}{2}(\frac{1}{2}[[\Delta]] + \Omega[[L_z]] - [[V]] - [[f(|\boldsymbol{\phi}^n|^2)]]))\boldsymbol{\phi}^n. \tag{54}$$

Like for the semi-implicit Euler scheme, we remark that $\mathbb{A}_{\mathrm{TF}}^{\mathrm{CN},n}$ is diagonal in the physical space and $\mathbb{A}_{\Delta,0}$ is also diagonal but in the Fourier space.

2.2.4 BESP or CNSP? That Is the Question

In Sects. 2.2.1–2.2.3, we introduced the BESP and CNSP schemes that correspond to the semi-implicit Euler and Crank-Nicolson schemes for a pseudo-spectral spatial discretization. We have seen that BESP diminishes the energy without any CFL condition between the time and spatial steps while the CNSP scheme is constrained. We illustrate here through a numerical example that the constraint related to CNSP makes it useless for computing a stationary state while BESP is robust. A similar conclusion applies to BEFD and CNFD.

Let us consider the two-dimensional problem

$$\begin{cases} i\partial_t\psi(t,\mathbf{x}) = -\dfrac{1}{2}\Delta\psi(t,\mathbf{x}) - \Omega L_z\psi(t,\mathbf{x}) + V(\mathbf{x})\psi(t,\mathbf{x}) + \beta|\psi|^2\psi(t,\mathbf{x}), \\ \psi(0,\mathbf{x}) = \psi_0(\mathbf{x}) \in L^2_{\mathbf{x}}, \end{cases} \tag{55}$$

for $t > 0$ and $\mathbf{x} \in \mathbb{R}^2$. The potential is harmonic: $V(\mathbf{x}) = \frac{1}{2}(\gamma_x^2x^2 + \gamma_y^2y^2)$, with $\gamma_x = \gamma_y = 1$. Moreover, we assume that: $\beta \in \mathbb{R}^+$ and $\Omega \in \mathbb{R}$. We consider BESP and CNSP for $\delta t = 10^{-1}$ to show the behavior of the associated energy. When using BESP and CNSP, each iteration n requires the solution to a linear system

by a Krylov subspace iterative solver (see Sect. 2.4). The computational domain is: $\mathscr{O} =]-10, 10[^2$, for a uniform grid $\mathscr{O}_{J,K}$, with $J = K = 2^9$. The initial data is chosen as the Thomas-Fermi approximation (65) when $\beta \neq 0$ and the centered gaussian

$$\phi_{\text{osc}}(\mathbf{x}) = \frac{(\gamma_x \gamma_y)^{1/4}}{\sqrt{\pi}} e^{-(\gamma_x x^2 + \gamma_y y^2)/2}, \tag{56}$$

for $\beta = 0$.

We report on Fig. 3a, b the evolution of the energy $\Delta \mathscr{E}_{\Omega,F} = \mathscr{E}_{\Omega,F}(\boldsymbol{\phi}^1) - \mathscr{E}_{\Omega,F}(\boldsymbol{\phi}^0)$ for BESP and CNSP for the first time step with respect to β and Ω. We observe that the energy decays for BESP in all cases. However, the energy increases for CNSP, leading to the divergence of the scheme almost immediately (this is worst for large values of β). To illustrate the difference between these two schemes, we draw on Fig. 4a, b the evolution of the energy for BESP and CNSP, respectively, until $T = 1$

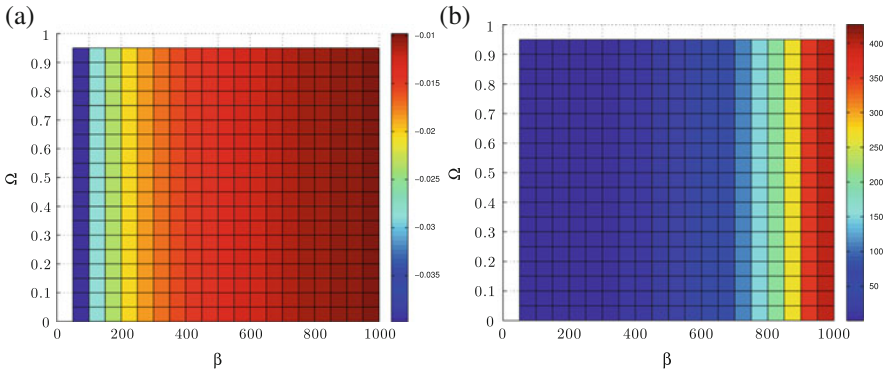

Fig. 3 Evolution of the energy for the first time step for BESP and CNSP. (**a**) Evolution of the energy for BESP. (**b**) Evolution of the energy for CNSP

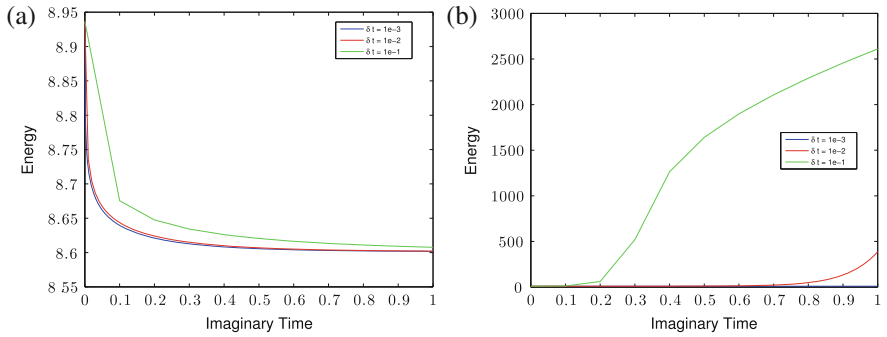

Fig. 4 Evolution of the energy until $T = 1$ for BESP and CNSP with $\beta = 500$ and $\Omega = 0.5$. (**a**) Evolution of the energy for BESP and different δt. (**b**) Evolution of the energy for CNSP and different δt

for the time steps $\delta t = 10^{-1}, 10^{-2}$ and 10^{-3}, with $\beta = 500$ and $\Omega = 0.5$. For BESP, the energy decays for the three time steps. We can also see that the energy decays faster as the time step is smaller. Concerning CNSP, we observe that the method diverges for $\delta t = 10^{-1}$ since the energy increases. For the time steps $\delta t = 10^{-2}$ and 10^{-3}, the energy decays smoothly all along the simulation similarly to BESP. To have a diminishing energy, a significantly smaller time step must be chosen, limiting hence the application range of CNSP most particularly in terms of convergence rate towards the minimum. For this reason, BESP is a robust scheme. Other simulations support this conclusion for $\Omega > 0$. Finally, only BESP and BEFD are considered in the sequel.

2.2.5 BESP or BEFD? This Is Another Question

We analyze now the spatial accuracy of BESP and BEFD. In particular, we show that there is a great interest in considering the pseudo-spectral approximation rather than the finite difference scheme. A similar study has been conducted by Bao et al. [31], for $\Omega = 0$, where the authors show that BESP provides a spectral precision compared with BEFD.

We first consider a numerical test similar to [31]. The problem is

$$\begin{cases} i\partial_t \psi(t,x) = -\dfrac{1}{2}\partial_x^2 \psi(t,\mathbf{x}) + V(x)\psi(t,x) + \beta|\psi|^2\psi(t,x), \\ \psi(0,x) = \psi_0(x) \in L_x^2, \end{cases} \tag{57}$$

where $V(x) = \frac{1}{2}x^2$, $\beta = 300$ and ψ_0 is the centered normalized gaussian, i.e.

$$\forall x \in \mathbb{R}, \quad \psi_0(x) = \frac{1}{\pi^{1/4}} e^{-\frac{x^2}{2}}.$$

We choose the computational domain $\mathscr{O} =]-10, 10[$ and the associated uniform grid $\mathscr{O}_J$, with $6 \leq J \leq 12$. We use BESP and BEFD for computing a stationary state of (57) on various grids. The time step is $\delta t = 10^{-1}$ and the linear systems are solved by BiCGStab with a stopping criterion $\varepsilon^{\text{Krylov}} = 10^{-12}$. Let $\boldsymbol{\phi}_J^{\text{SP}}$ (respectively, $\boldsymbol{\phi}_J^{\text{FD}}$) be the stationary state computed on $\mathscr{O}_J$, $6 \leq J \leq 12$, with BESP (respectively, BEFD), and $\boldsymbol{\phi}_{\text{ref}}^{\text{SP}} = \boldsymbol{\phi}_{2^{12}}^{\text{SP}}$ (respectively, $\boldsymbol{\phi}_{\text{ref}}^{\text{FD}} = \boldsymbol{\phi}_{2^{12}}^{\text{FD}}$) the reference stationary state. We report in Table 1 the quadratic error, the infinity norm error and finally the energy norm error between the reference and computed stationary states for BESP and BEFD. We observe the spectral accuracy of the stationary states obtained with BESP and the quadratic precision of BEFD with respect to the different grids.

Let us now consider the two-dimensional example given by system (55) for the harmonic potential: $V(\mathbf{x}) = \frac{1}{2}(\gamma_x^2 x^2 + \gamma_y^2 y^2)$, with $\gamma_x = \gamma_y = 1$. We fix $\beta = 300$ and $\Omega = 0.6$. The computational domain is $\mathscr{O} =]-10, 10[^2$, for a uniform spatial grid $\mathscr{O}_{J,K}$, with: $5 \leq J, K \leq 9$. The time step is $\delta t = 10^{-1}$. The linear systems are solved by BiCGStab for a stopping criterion on the residual equal to $\varepsilon^{\text{Krylov}} = 10^{-12}$. For

Table 1 Numerical accuracy for BESP/BEFD for computing the ground state associated to (57)

	$J = 2^6$	$J = 2^7$	$J = 2^8$	$J = 2^9$	$J = 2^{10}$	$J = 2^{11}$
$\|\boldsymbol{\phi}_{\text{ref}}^{\text{SP}} - \boldsymbol{\phi}_J^{\text{SP}}\|_\infty$	5.00e−5	8.30e−9	<1e−12	<1e−12	<1e−12	<1e−12
$\|\boldsymbol{\phi}_{\text{ref}}^{\text{FD}} - \boldsymbol{\phi}_J^{\text{FD}}\|_\infty$	3.21e−5	2.12e−6	1.33e−7	8.32e−9	6.03e−10	1.94e−10
$\|\boldsymbol{\phi}_{\text{ref}}^{\text{SP}} - \boldsymbol{\phi}_J^{\text{SP}}\|_{\ell_\pi^2}$	4.51e−5	1.00 e−8	<1e−12	<1e−12	<1e−12	<1e−12
$\|\boldsymbol{\phi}_{\text{ref}}^{\text{FD}} - \boldsymbol{\phi}_J^{\text{FD}}\|_{\ell_0^2}$	2.99e−5	1.96e−6	1.23e−7	7.83e−9	7.15e−10	1.74e−10
$\|\mathscr{E}_{\Omega,F}(\boldsymbol{\phi}_{\text{ref}}^{\text{SP}}) - \mathscr{E}_{\Omega,F}(\boldsymbol{\phi}_J^{\text{SP}})\|$	9.19e−5	3.65e−10	2.22e−12	2.66e−12	<1e−12	1.91e−12
$\|\mathscr{E}_{\Omega,F}(\boldsymbol{\phi}_{\text{ref}}^{\text{FD}}) - \mathscr{E}_{\Omega,F}(\boldsymbol{\phi}_J^{\text{FD}})\|$	8.30e−6	5.54e−7	3.51e−8	2.23e−9	1.52e−10	1.25e−11

J and K varying, we can compare the different computed stationary states with a reference numerical solution $\boldsymbol{\phi}_{\text{ref}}$ obtained with BESP on a fine uniform grid (here $\mathscr{O}_{J,K}$, with $J = K = 2^9$). Let $\boldsymbol{\phi}_J$ be the state calculated on a grid $\mathscr{O}_{J,K}$ ($J = K$). We report on Fig. 5a–f the different densities obtained for BESP and BEFD. We remark that, for coarse grids, the solutions are very different and the finite difference discretization seems to lead to the most accurate results in this case. In Table 2, we can see that there is an improved accuracy of BESP when going from a grid with $J = 2^6$ to a grid with $J = 2^7$. We observe a convergence towards a different stationary state for the grids with $J \leq 2^6$ and the grids for $J > 6$ as seen on Fig. 5a–f. We see that BESP provides a high resolution calculation and the accuracy is far better than for BEFD for discretization grids with $J \geq 2^7$.

To conclude, BESP is far more accurate than BEFD when fine enough grids are considered. As seen in the examples, this precision directly impacts the accuracy of the associated physical quantities. In the sequel, we focus on BESP.

2.3 Which Initial Guess for CNGF?

As we discussed above, our goal is to compute a (global) minimizer of the optimization problem (22). Before any numerical computation by BESP (or another iterative scheme), it is quite natural to prospect if some explicit exact or approximate solutions to the GPE are available. This is important for two reasons. Indeed, having such a solution allows to better understand the physical properties of the GPEs and BECs from the mathematical point of view. Many developments can be found in the Physics literature [98, 100]. We give below the example of the Thomas-Fermi approximation. In addition, since the optimization problem is extremely complex, it is unexpected to get an analytical solution for the problem, valid for any interesting situation (weak or strong nonlinearity, various potentials, inclusion of a rotation term, ...). Since the optimization problem is nonlinear, there is no other alternative than developing some iterative numerical methods. To this end, we need to determine a suitable initial guess that is injected into the algorithm.

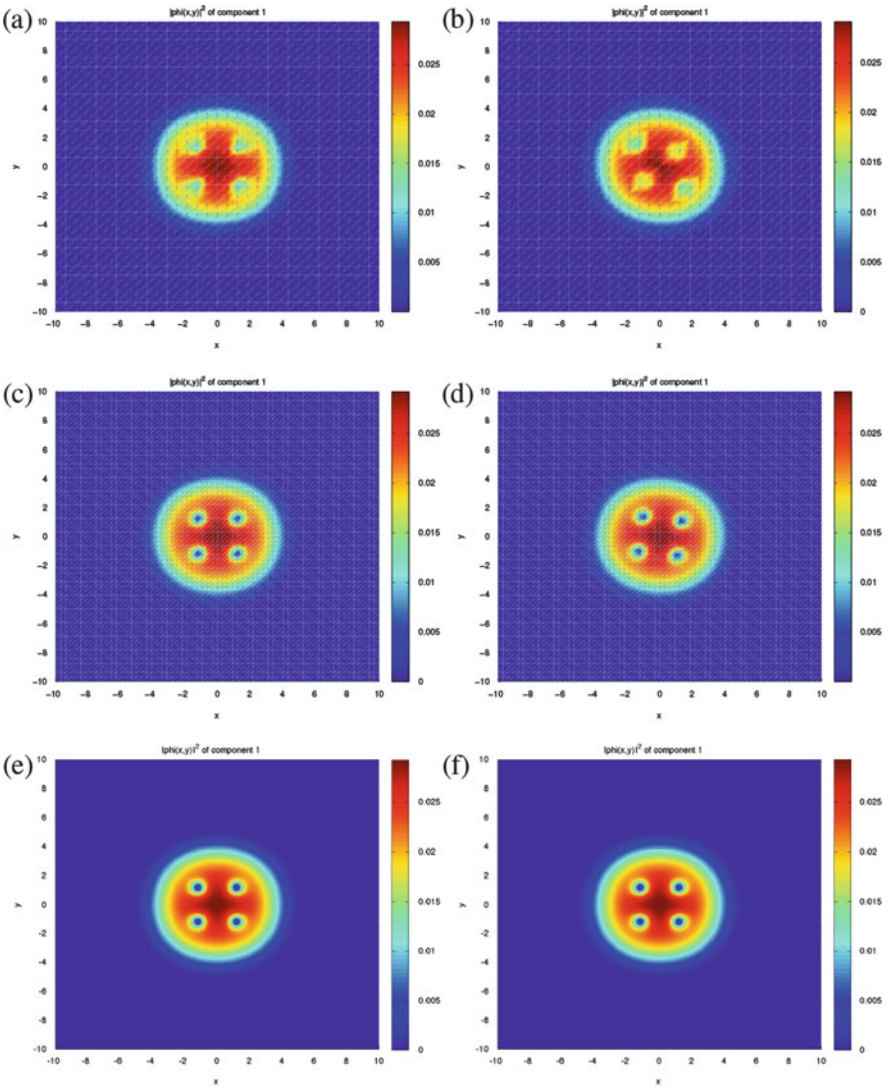

Fig. 5 Representation of $|\boldsymbol{\phi}_J|^2$ obtained by BEFD (*left*) and BESP (*right*) for different spatial discretizations. (**a**) BEFD: $J = 2^5$; (**b**) BESP: $J = 2^5$; (**c**) BEFD: $J = 2^6$; (**d**) BESP: $J = 2^6$; (**e**) BEFD: $J = 2^7$; (**f**) BESP: $J = 2^7$

In particular, a well-chosen approximate analytical solution can play this role. In Sect. 1.4 (page 67), we distinguished two cases where it is possible to build an approximate solution. Let us precise these approximations for different situations.

Table 2 Numerical accuracy of BESP and BEFD for computing the stationary state associated with problem (55)

	$J = 2^5$	$J = 2^6$	$J = 2^7$	$J = 2^8$
$\|\boldsymbol{\phi}_{\text{ref}}^{\text{SP}} - \boldsymbol{\phi}_J^{\text{SP}}\|_\infty$	1.47e−1	6.95e−2	5.41e−7	1.78e−9
$\|\boldsymbol{\phi}_{\text{ref}}^{\text{FD}} - \boldsymbol{\phi}_J^{\text{FD}}\|_\infty$	1.29e−1	5.02e−3	6.71e−5	4.39e−6
$\|\boldsymbol{\phi}_{\text{ref}}^{\text{SP}} - \boldsymbol{\phi}_J^{\text{SP}}\|_{\ell_\pi^2}$	1.82e−1	4.23e−2	<1e−12	<1e−12
$\|\boldsymbol{\phi}_{\text{ref}}^{\text{FD}} - \boldsymbol{\phi}_J^{\text{FD}}\|_{\ell_0^2}$	4.77e−2	6.46e−5	3.79e−8	1.44e−10
$\|\mathscr{E}_{\Omega,F}(\boldsymbol{\phi}_{\text{ref}}^{\text{SP}}) - \mathscr{E}_{\Omega,F}(\boldsymbol{\phi}_J^{\text{SP}})\|$	7.55e−3	5.29e−5	2.54e−8	<1e−12
$\|\mathscr{E}_{\Omega,F}(\boldsymbol{\phi}_{\text{ref}}^{\text{FD}}) - \mathscr{E}_{\Omega,F}(\boldsymbol{\phi}_J^{\text{FD}})\|$	5.274e−2	3.054e−3	1.871e−4	1.12e−5

When there is no rotation (i.e. $\Omega = 0$) and the potential is confining, the minimization problem (22) admits a unique global solution ϕ_g up to a phase factor [88]. For a potential V such that: $\forall \mathbf{x} \in \mathbb{R}^d$, $V(\mathbf{x}) = V_0(\mathbf{x}) + W(\mathbf{x})$, where

$$V_0(\mathbf{x}) = \frac{1}{2}\sum_{j=1}^{d} \gamma_{x_j}^2 x_j^2 \text{ and } \lim_{|\mathbf{x}|\to\infty} \frac{W(\mathbf{x})}{V(\mathbf{x})} = 0, \tag{58}$$

and for a weak nonlinear interaction (for example $|f(1)| \leq 10$), a suitable approximation [31] of the fundamental state of problem (20) is given by

$$\forall \mathbf{x} \in \mathbb{R}^d, \quad \phi_{\text{osc}}(\mathbf{x}) = \frac{(\prod_{j=1}^{d} \gamma_{x_j})^{1/4}}{\pi^{d/4}} e^{-\frac{1}{2}\sum_{j=1}^{d} \gamma_{x_j} x_j^2}, \tag{59}$$

which corresponds to the fundamental state of the quantum harmonic oscillator [88]

$$\begin{cases} i\partial_t \psi(t,\mathbf{x}) = -\dfrac{1}{2}\Delta\psi(t,\mathbf{x}) + V_0(\mathbf{x})\psi(t,\mathbf{x}), \ \forall t \in \mathbb{R}^+, \ \forall \mathbf{x} \in \mathbb{R}^d, \\ \psi(0,\mathbf{x}) = \psi_0(\mathbf{x}) \in L^2_{\mathbf{x}}. \end{cases} \tag{60}$$

If one considers now a rotation term (i.e. $\Omega \neq 0$), finding a good approximation is much more problematic. In particular, the solution to the minimization problem is not necessarily unique, local minimizers possibly exist (22) and there is sometimes not even existence of a solution if the rotation is too large [108]. In the case of a harmonic potential (58), the critical velocity above which there is no existence of a fundamental state is given by $\Omega_c = \min\{\gamma_x, \gamma_y\}$. In [102], the author shows that some phase transition phenomenae occur with respect to the rotation velocity when a quadratic-plus-quartic potential is considered. In particular, it is proved that a second critical velocity exists above which a giant vortex is created. For more details about the theory of quantum vortices, we refer to Rougerie et al. [38, 50, 103], Aftalion et al. [5–8] and Tsubota et al. [81, 82, 120]. An initial data allowing to converge

towards the correct fundamental state has been proposed by Bao et al. [30] and consists in choosing the following approximation

$$\phi(\mathbf{x}) = \frac{(1-\Omega)\phi_{\text{osc}}(\mathbf{x}) + \Omega\phi^v_{\text{osc}}(\mathbf{x})}{||(1-\Omega)\phi_{\text{osc}}(\mathbf{x}) + \Omega\phi^v_{\text{osc}}(\mathbf{x})||_{L^2_{\mathbf{x}}}}, \tag{61}$$

with

$$\phi_{\text{osc}}(\mathbf{x}) = e^{-\frac{1}{2}(\gamma_x x^2+\gamma_y y^2)} \quad \text{and} \quad \phi^v_{\text{osc}}(\mathbf{x}) = (\gamma_x x + i\gamma_y y)e^{-\frac{1}{2}(\gamma_x x^2+\gamma_y y^2)}. \tag{62}$$

This approximation is in fact an interpolation of the gaussian (59) and the same gaussian with an added centered vortex (singularity). In the case of a confining potential in the x-direction, we can simplify the equation as a two-dimensional GPE (see Sect. 1.5.2, page 71). Moreover, by using the polar coordinates and for an isotropic potential $\gamma_x = \gamma_y$, we obtain [30]

$$\phi^v_{\text{osc}}(\mathbf{x}) = \frac{\gamma_x^2 e^{im\theta}}{\sqrt{\pi}} e^{-\gamma_x r^2/2}, \tag{63}$$

where $m = 1$ is the "winding number" of the central vortex and corresponds to the first vortex mode. By using these initial data, it is possible to converge to the fundamental state in the case of a subcritical velocity $\Omega < \Omega_c$. We present on Fig. 6a, b the initial data (61) in 2d for two rotation speeds. For completeness, we report the three- and one-dimensional cases [respectively, on Figs. 7 (for two rotation velocities) and [8].

In the case of a strong interaction, we consider the Thomas-Fermi approximation (cf. Sect. 1.4, page 67) which consists in neglecting the kinetic energy related to the

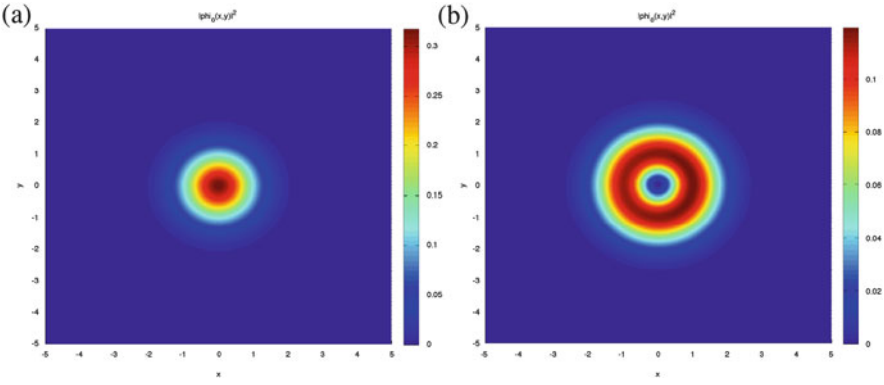

Fig. 6 Representation of $|\phi_0|^2$ for the two-dimensional harmonic potential problem ($\gamma_x = \gamma_y = 1$) with a weak nonlinear interaction, without and with a rotation term, by using formula (61). (**a**) $\Omega = 0$; (**b**) $\Omega = 0.99$

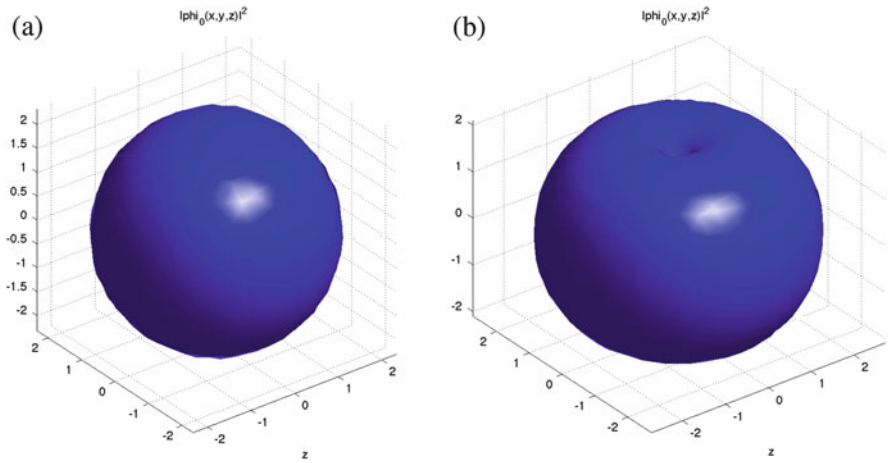

Fig. 7 Isovalues $|\phi_0|^2 = 10^{-3}$ for a three-dimensional harmonic problem ($\gamma_x = \gamma_y = \gamma_z = 1$) with a weak interaction, without and with a rotation term, by using formula (61). (**a**) $\Omega = 0$; (**b**) $\Omega = 0.99$

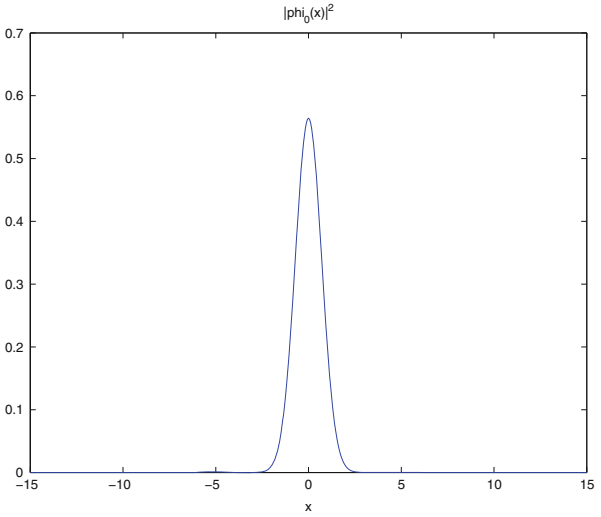

Fig. 8 Representation of $|\phi_0|^2$ for a one-dimensional harmonic problem ($\gamma_x = 1$) with a weak interaction

Laplacian and rotation operators. One then gets a simplified minimization problem where the energy is given by

$$\mathscr{E}_{\Omega,F}(\psi) \approx \mathscr{E}_{\mathrm{TF}}(\psi) := \int_{\mathbb{R}^d} \left[V(\mathbf{x})|\psi(t,\mathbf{x})|^2 + F(|\psi(t,\mathbf{x})|^2) \right] d\mathbf{x}.$$

More precisely, coming back to an eigenvalue problem similarly to the general case (23), we are looking for the eigenfunction $\phi_{\mathrm{TF}} \in L^2_{\mathbf{x}}$ and the eigenvalue $\mu_{\mathrm{TF}} \in \mathbb{R}$ of the problem

$$\mu_{\mathrm{TF}}\phi_{\mathrm{TF}} = f(|\phi_{\mathrm{TF}}|^2)\phi_{\mathrm{TF}} + V\phi_{\mathrm{TF}},$$

under the normalization constraint $\mathcal{N}(\phi_{\mathrm{TF}}) = \|\phi_{\mathrm{TF}}\|_{L^2_{\mathbf{x}}} = 1$. We obtain

$$\forall \mathbf{x} \in \mathrm{supp}(\phi_{\mathrm{TF}}), \quad \mu_{\mathrm{TF}} = f(|\phi_{\mathrm{TF}}|^2) + V(\mathbf{x}). \tag{64}$$

By assuming that it is possible to inverse the function f on $\mathbb{R}$, we can then deduce an explicit form of ϕ_{TF} which is assumed to be real-valued,

$$\forall \mathbf{x} \in \mathbb{R}^d, \quad \phi_{\mathrm{TF}}(\mathbf{x}) = \begin{cases} \sqrt{f^{-1}\left(\mu_{\mathrm{TF}} - V(\mathbf{x})\right)}, & \text{for } f^{-1}\left(\mu_{\mathrm{TF}} - V(\mathbf{x})\right) > 0, \\ 0 \qquad\qquad\qquad\quad , & \text{for } f^{-1}\left(\mu_{\mathrm{TF}} - V(\mathbf{x})\right) \leq 0. \end{cases}$$

To get μ, we use the mass conservation. For a cubic nonlinearity $f(|\phi|^2) = \beta|\phi|^2$, with $\beta \in \mathbb{R}^+$, we can choose the following approximation of the fundamental state

$$\phi_{\mathrm{TF}}(\mathbf{x}) = \begin{cases} \sqrt{\frac{\mu_{\mathrm{TF}} - V(\mathbf{x})}{\beta}}, & \text{for } \mu_{\mathrm{TF}} - V(\mathbf{x}) > 0, \\ 0 \qquad\qquad , & \text{for } \mu_{\mathrm{TF}} - V(\mathbf{x}) \leq 0, \end{cases} \tag{65}$$

where μ_{TF} is given by the expression [31]

$$\mu_{\mathrm{TF}} = \frac{1}{2} \begin{cases} (3\beta\gamma_x)^{2/3} & \text{for } d = 1, \\ (4\beta\gamma_x\gamma_y)^{1/2} & \text{for } d = 2, \\ \left(\frac{15\beta\gamma_x\gamma_y\gamma_z}{4\pi}\right)^{2/5} & \text{for } d = 3. \end{cases} \tag{66}$$

We represent on Fig. 9 the moduli of the Thomas-Fermi approximations (65) for a quadratic potential ($\gamma_x = \gamma_y = \gamma_z = 1$) and a cubic nonlinearity in 1d, 2d and 3d.

The Thomas-Fermi approximation has the advantage of being less restrictive than the weak interaction approximation concerning the classes of potentials and nonlinearities that are eligible. In particular, the following potentials can be considered ($d = 2$)

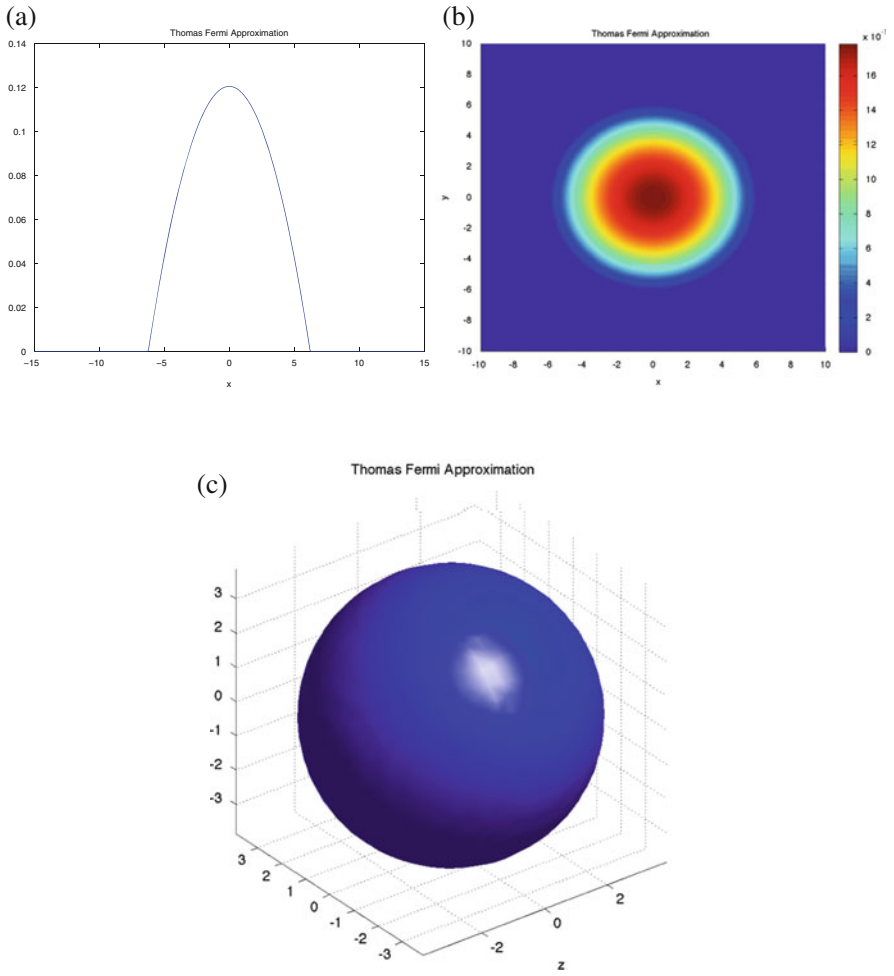

Fig. 9 Representation of $|\phi_0|^2$ for the Thomas-Fermi approximation and a quadratic potential, $\beta = 1000$ (strong interaction) for the 1d, 2d and 3d cases. (**a**) Dimension $d = 1$; (**b**) dimension $d = 2$; (**c**) dimension $d = 3$

- Quadratic-plus-quartic potential [125]

$$V(\mathbf{x}) = (1-\alpha)\frac{1}{2}(\gamma_x^2 x^2 + \gamma_y^2 y^2) + \frac{\kappa}{4}(\gamma_x^2 x^2 + \gamma_y^2 y^2)^2. \tag{67}$$

- Quadratic-plus-gaussian potential [78]

$$V(\mathbf{x}) = \frac{1}{2}(\gamma_x^2 x^2 + \gamma_y^2 y^2) + w_0 e^{-\frac{(x-x_0)^2+(y-y_0)^2}{d^2}}. \tag{68}$$

- Quadratic-plus-sine potential (also called optical potential) [125]

$$V(\mathbf{x}) = \frac{1}{2}(\gamma_x^2 x^2 + \gamma_y^2 y^2) + \frac{a_1}{2}\sin(\frac{\pi x}{d_1})^2 + \frac{a_2}{2}\sin(\frac{\pi y}{d_2})^2. \tag{69}$$

- Double-well potential [123]

$$V(\mathbf{x}) = \frac{1}{2}(\gamma_x^2 x^2 + \gamma_y^2 y^2) + V_0 e^{-x^2/2d^2}. \tag{70}$$

Examples of Thomas-Fermi approximations for these potentials are given on Figs. 10 and 11.

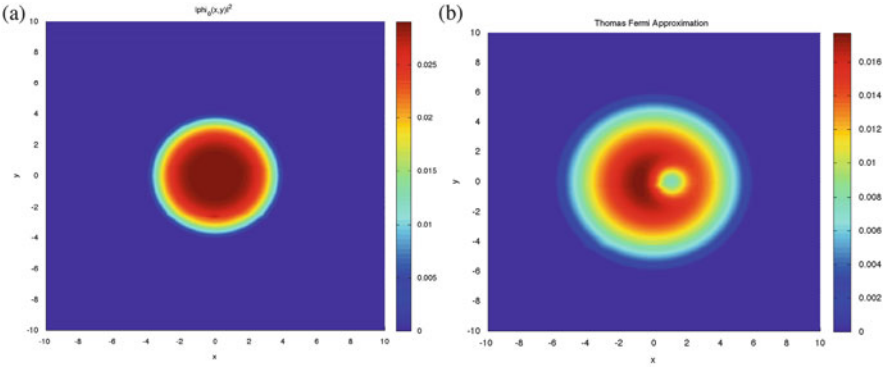

Fig. 10 Examples of Thomas-Fermi approximations for potentials (67) (*left*) and (68) (*right*). (**a**) $\gamma_x = \gamma_y = 1$; (**b**) $\gamma_x = \gamma_y = 1; \mathbf{x}_0 = (1, 0); d = 1; w_0 = 10$

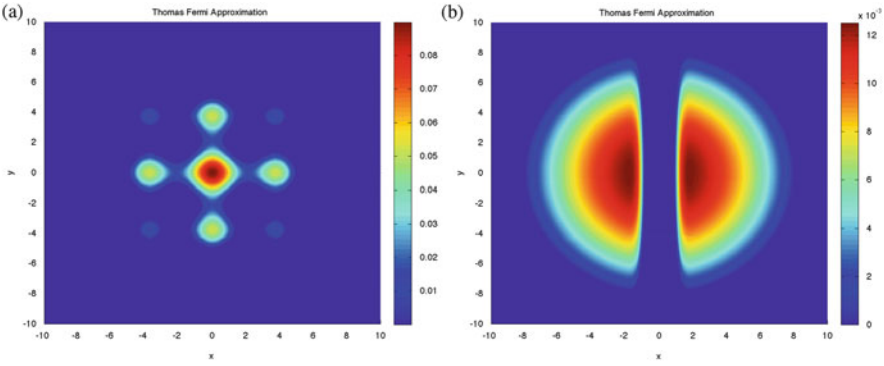

Fig. 11 Examples of Thomas-Fermi approximations for potentials (69) (*left*) and (70) (*right*). (**a**) $\gamma_x = \gamma_y = 1; a_1 = a_2 = 25; d_1 = d_2 = 4$; (**b**) $\gamma_x = \gamma_y = 1/2; V_0 = 40; d = 0.5$

2.4 Solving BESP Linear Systems: The Fixed Point Method, Its Limitations and Krylov Subspace Iterative Solvers

We consider now the BESP scheme

$$\begin{cases} \mathbb{A}^{\mathrm{BE},n}\tilde{\boldsymbol{\phi}} = \mathbf{b}^{\mathrm{BE},n}, \\ \boldsymbol{\phi}^{n+1} = \dfrac{\tilde{\boldsymbol{\phi}}}{||\tilde{\boldsymbol{\phi}}||_{\ell^2_\pi}}, \\ \boldsymbol{\phi}^0 := \boldsymbol{\phi}_0, \end{cases} \tag{71}$$

where, for the sake of conciseness, we set: $\mathbb{A}^{\mathrm{BE},n} := \mathbb{A}^{\mathrm{BE},n}_{\mathrm{SP}}$. At each iteration n, it is clear that the minimization method requires the solution of a linear system: $\mathbb{A}^{\mathrm{BE},n}\tilde{\boldsymbol{\phi}} = \mathbf{b}^{\mathrm{BE},n}$. Since we use pseudo-spectral approximation methods, the operator $\mathbb{A}^{\mathrm{BE},n}$ is given implicitly through a FFT, meaning that the matrix $\mathbb{A}^{\mathrm{BE},n}$ is not explicitly known by its coefficients. As a consequence, using a direct matrix solver is not permitted. An alternative solution consists in considering a matrix-free iterative method. A first approach, introduced by Bao et al. [31] for non rotating GPEs, is based on stationary (fixed-point) methods. It has been next extended to rotating BEC by Zeng and Zhang [125]. Nevertheless, in [12], some examples show that the method does not converge when the rotation speed Ω is too large. In [12], the introduction of Krylov subspace iterative solvers (GMRES, BiCGStab) accelerated by simple operator-based preconditioners provides robust and fast iterative methods that can be easily extended to the multi-components case.

2.5 Extension to Multi-components BECs

In this section, we present the extension of BESP to BECs with $N_c \in \mathbb{N}$ components. The GPEs system that describes this situation is

$$\begin{cases} i\partial_t \Psi(t,\mathbf{x}) = -\dfrac{1}{2}\Delta\Psi(t,\mathbf{x}) - \Omega L_z \Psi(t,\mathbf{x}) + \mathbf{V}(\mathbf{x})\Psi(t,\mathbf{x}) \\ \qquad\qquad +\mathbf{f}(\Psi)\Psi(t,\mathbf{x}),\ \forall t \in \mathbb{R}^+,\ \forall \mathbf{x} \in \mathbb{R}^d, \\ \Psi(0,\mathbf{x}) = \Psi_0(\mathbf{x}) \in L^{2,N_c}_{\mathbf{x}},\ \forall \mathbf{x} \in \mathbb{R}^d, \end{cases} \tag{72}$$

where we set $\Psi(t,\mathbf{x}) = (\Psi_\ell(t,\mathbf{x}))_{\ell\in\{1,\dots,N_c\}}$ and $|\Psi(t,\mathbf{x})|^2 = \sum_{\ell=1}^{N_c} |\Psi_\ell(t,\mathbf{x})|^2$. The non diagonal operators involved in this system are: $\mathbf{V}(\mathbf{x}) = (\mathbf{V}_{\ell,m}(\mathbf{x}))_{\ell,m\in\{1,\dots,N_c\}}$, and

$$\mathbf{f}(\Psi) = \left(\mathbf{f}_{\ell,m}(\Psi_1,\dots,\Psi_{N_c},\Psi_1^*,\dots,\Psi_{N_c}^*)\right)_{\ell,m\in\{1,\dots,N_c\}}.$$

For the partial differential operators, we have

$$\Delta\Psi(t,\mathbf{x}) = (\Delta\Psi_\ell(t,\mathbf{x}))_{\ell\in\{1,\dots,N_c\}}, \quad L_z\Psi(t,\mathbf{x}) = (L_z\Psi_\ell(t,\mathbf{x}))_{\ell\in\{1,\dots,N_c\}}.$$

We furthermore assume that $\mathbf{f}_{\ell,m}$, $1 \le \ell, m \le N_c$, are smooth real-valued polynomial functions and that the operators $\mathbf{V}$ and $\mathbf{f}$ are symmetrical, i.e. $\mathbf{V}_{\ell,m} = \mathbf{V}_{m,\ell}$ and $\mathbf{f}_{\ell,m} = \mathbf{f}_{m,\ell}$, $1 \le \ell, m \le N_c$, in such a way that we have the mass conservation. For the multi-components case, let us recall that the mass is given by

$$\mathscr{N}(\Psi) := \|\Psi\|_{L^2_{\mathbf{x}}}^2 = \sum_{\ell=1}^{N_c} \|\Psi_\ell(t,\mathbf{x})\|_{L^2_{\mathbf{x}}}^2 = \sum_{\ell=1}^{N_c} \int_{\mathbb{R}^d} |\Psi_\ell(t,\mathbf{x})|^2 d\mathbf{x},$$

and the energy by

$$\begin{aligned}\mathscr{E}_{\Omega,\mathbf{F}}(\Psi) := &\sum_{\ell=1}^{N_c} \int_{\mathbb{R}^d} \left(\frac{1}{2}|\nabla\Psi_\ell(t,\mathbf{x})|^2 - \Omega\Psi_\ell^*(t,\mathbf{x})L_z\Psi_\ell(t,\mathbf{x})\right) d\mathbf{x} \\ &+ \sum_{\ell,m=1}^{N_c} \int_{\mathbb{R}^d} \mathbf{V}_{\ell,m}(t,\mathbf{x})\Psi_\ell^*(t,\mathbf{x})\Psi_m(t,\mathbf{x}) + \mathbf{F}_{\ell,m}(\Psi) d\mathbf{x},\end{aligned}$$

where

$$\mathbf{F}_{\ell,m}(\Psi) := \int_0^1 \mathbf{f}_{\ell,m}(\Psi_1,\dots,\Psi_{N_c},\Psi_1^*,\dots,\iota\Psi_\ell^*,\dots,\Psi_{N_c}^*)\Psi_\ell^*\Psi_m d\iota.$$

2.5.1 CNGF for Multi-components BECs

Similarly to the proof detailed in Sect. 1.4 (page 67), we show that a stationary state is a critical point of the energy functional, i.e. it is solution to the minimization problem: find a function $\Phi \in L^{2,N_c}_{\mathbf{x}}$ such that

$$\mathscr{E}_{\Omega,\mathbf{F}}(\Phi) = \min_{\mathscr{N}(\Psi)=1} \mathscr{E}_{\Omega,\mathbf{F}}(\Psi). \tag{73}$$

The CNGF method directly applies to the multi-components case

$$\begin{cases} \partial_t \Phi(t,\mathbf{x}) = -D_{\Phi^*}\mathscr{E}_{\Omega,\mathbf{F}}(\Phi) = \dfrac{1}{2}\Delta\Phi(\mathbf{x},t) + \Omega L_z\Phi(\mathbf{x},t) + \mathbf{V}(\mathbf{x})\Phi(\mathbf{x},t) \\ \qquad\qquad +\mathbf{f}(\Phi)\Phi(\mathbf{x},t),\ \forall t \in [t_n, t_{n+1}[,\ \forall \mathbf{x} \in \mathbb{R}^d, \\ \Phi(\mathbf{x}, t_{n+1}) = \dfrac{\Phi(\mathbf{x}, t_{n+1}^-)}{\|\Phi(\mathbf{x}, t_{n+1}^-)\|_{L^2_{\mathbf{x}}}}, \\ \Phi(0,\mathbf{x}) = \Phi_0(\mathbf{x}) \in L^{2,N_c}_{\mathbf{x}}. \end{cases} \tag{74}$$

This problem has been studied for example in [17, 18]. Let us recall the following result which proves that the energy associated with the solution to (74) is decaying under suitable assumptions.

Theorem 2 *Let us assume that the potential operator is diagonal, i.e.* $\mathbf{V}(\mathbf{x}) = (\mathbf{V}_\ell(\mathbf{x}))_{\ell\in\{1,\dots,N_c\}}$, *and is such that* $\mathbf{V}_\ell(\mathbf{x}) \geq 0$, $\forall \mathbf{x} \in \mathbb{R}^d$, $\forall \ell \in \{1,\dots,N_c\}$. *Furthermore, we suppose that the nonlinearity is diagonal:* $\mathbf{f}(\Phi) = (\mathbf{f}_\ell(\Psi))_{\ell\in\{1,\dots,N_c\}}$, *and such that* $\mathbf{f}_\ell(\Psi) = \sum_{m=1}^{N_c} \beta_{\ell,m}|\phi_m|^2|\phi_\ell|^2$, *with* $\beta_{\ell,m} \geq 0$, $\forall \ell, m \in \{1,\dots,N_c\}$. *Finally, we consider that there is no rotation, i.e.* $\Omega = 0$. *Then, the solution* Φ *to (74) satisfies,* $\forall n \in \mathbb{N}$,

$$\forall t \in [t_n, t_{n+1}[, \quad \mathscr{E}_{0,\mathbf{F}}(\Phi(\mathbf{x},t)) \leq \mathscr{E}_{0,\mathbf{F}}(\Phi(\mathbf{x},t_n)).$$

2.5.2 BESP for Multi-components BECs

We now essentially focus on the semi-implicit backward Euler time discretization of (74)

$$\begin{cases} \dfrac{\tilde{\Phi}(\mathbf{x}) - \Phi(\mathbf{x},t_n)}{\delta t} = \dfrac{1}{2}\Delta\tilde{\Phi}(\mathbf{x}) + \Omega L_z\tilde{\Phi}(\mathbf{x}) + \mathbf{V}(\mathbf{x})\tilde{\Phi}(\mathbf{x}) \\ \qquad\qquad +\mathbf{f}(\Phi(\mathbf{x},t_n))\tilde{\Phi}(\mathbf{x}),\ \forall t \in [t_n, t_{n+1}[,\ \forall \mathbf{x} \in \mathbb{R}^d, \\ \Phi(\mathbf{x}, t_{n+1}) = \dfrac{\tilde{\Phi}(\mathbf{x})}{\|\tilde{\Phi}\|_{L^2_{\mathbf{x}}}}, \\ \Phi(0,\mathbf{x}) = \Phi_0(\mathbf{x}) \in L^{2,N_c}_{\mathbf{x}}. \end{cases} \tag{75}$$

Let us precise the spatial discretization of (75) leading to BESP. We consider that $d = 2$, the extension to $d = 1$ and $d = 3$ being straightforward. The computational box is $\mathscr{O} :=]-a_x, a_x[\times]-a_y, a_y[$. The associated discrete grid $\mathscr{O}_{J,K}$ is given by (29). Let: $\mathscr{P}_{N_c,J,K} = \left\{(\ell,j,k) \in \mathbb{N}^3; 1 \leq \ell \leq N_c,\ 1 \leq j \leq J \text{ and } 1 \leq k \leq K\right\}$. For the pseudo-spectral approximation, the multi-components Laplacian is discretized by

$$\forall (\ell,j,k) \in \mathscr{P}_{N_c,J,K}, \quad ([[\Delta]]\boldsymbol{\Phi})_{\ell,j,k} = ([[\Delta]]\Phi_\ell)_{(j,k)},$$

where $[[\Delta]]$ that appears in the right-hand side is given by the expression (42). Similarly, the multi-components rotation operator is discretized by

$$\forall(\ell,j,k)\in\mathscr{P}_{N_c,J,K},\quad ([[L_z]]\boldsymbol{\Phi})_{\ell,j,k}=([[L_z]]\Phi_\ell)_{(j,k)},$$

where $[[L_z]]$ is fixed by (41). For the potential and nonlinear operators, the discretization is direct on the grid $\mathscr{O}_{J,K}$

$$[[\mathbf{V}]]:=\begin{pmatrix}[[\mathbf{V}_{1,1}]] & [[\mathbf{V}_{1,2}]] & \cdots & [[\mathbf{V}_{1,N_c}]]\\ [[\mathbf{V}_{2,1}]] & [[\mathbf{V}_{2,2}]] & \cdots & [[\mathbf{V}_{2,N_c}]]\\ \vdots & \vdots & \ddots & \vdots\\ [[\mathbf{V}_{N_c,1}]] & [[\mathbf{V}_{2,N_c}]] & \cdots & [\mathbf{V}_{N_c,N_c}]]\end{pmatrix}\in\mathscr{M}_{MN_c}(\mathbb{C}),\tag{76}$$

where $[[\mathbf{V}_{m,\ell}]]$ is given by (43), and

$$[[\mathbf{f}(\Phi^n)]]:=\begin{pmatrix}[[\mathbf{f}_{1,1}(\Phi^n)]] & [[\mathbf{f}_{1,2}(\Phi^n)]] & \cdots & [[\mathbf{f}_{1,N_c}(\Phi^n)]]\\ [[\mathbf{f}_{2,1}(\Phi^n)]] & [[\mathbf{f}_{2,2}(\Phi^n)]] & \cdots & [[\mathbf{f}_{2,N_c}(\Phi^n)]]\\ \vdots & \vdots & \ddots & \vdots\\ [[\mathbf{f}_{N_c,1}(\Phi^n)]] & [[\mathbf{f}_{2,N_c}(\Phi^n)]] & \cdots & [[\mathbf{f}_{N_c,N_c}(\Phi^n)]]\end{pmatrix}\in\mathscr{M}_{MN_c}(\mathbb{C}),\tag{77}$$

where $[[\mathbf{f}_{m,\ell}(\Phi^n)]]$, $\forall\ell,m\in\{1,\ldots,N_c\}$, is defined, for any vector field $\boldsymbol{\varphi}\in\mathbb{C}^M$, $\forall(j,k)\in\mathscr{P}_{J,K}$, by

$$([\mathbf{f}_{m,\ell}(\Phi^n)]\boldsymbol{\varphi})_{j,k}=\mathbf{f}_{m,\ell}(\Phi^n(\mathbf{x}_{j,k}))\varphi_{j,k},\tag{78}$$

with $\Phi^n(\mathbf{x})=\Phi(\mathbf{x},t_n)$ for (75). Setting $\tilde{\boldsymbol{\Phi}}\in\mathbb{C}^{MN_c}$ as the solution to (75), one obtains the BESP scheme, $\forall n\in\mathbb{N}$,

$$\begin{cases}\mathbb{A}^{\mathrm{BE},n}\tilde{\boldsymbol{\Phi}}=\mathbf{b}^{\mathrm{BE},n},\\ \boldsymbol{\Phi}^{n+1}=\dfrac{\tilde{\boldsymbol{\Phi}}}{||\tilde{\boldsymbol{\Phi}}||_{\ell^2_\pi}},\end{cases}\tag{79}$$

where the operator $\mathbb{A}^{\mathrm{BE},n}$ maps a given vector $\boldsymbol{\Phi}\in\mathbb{C}^{MN_c}$ to $\boldsymbol{\Psi}\in\mathbb{C}^{MN_c}$ through

$$\begin{aligned}\boldsymbol{\Psi}:=\mathbb{A}^{\mathrm{BE},n}\boldsymbol{\Phi}&=\mathbb{A}^{\mathrm{BE},n}_{\mathrm{TF}}\boldsymbol{\Phi}+\mathbb{A}^{\mathrm{BE},n}_{\Delta,\Omega}\boldsymbol{\Phi},\\ \mathbb{A}^{\mathrm{BE},n}_{\mathrm{TF}}\boldsymbol{\Phi}&:=(\frac{[[\mathbf{I}]]}{\delta t}+[[\mathbf{V}]]+[[\mathbf{f}(\boldsymbol{\Phi}^n)]])\boldsymbol{\Phi},\\ \mathbb{A}^{\mathrm{BE}}_{\Delta,\Omega}\boldsymbol{\Phi}&:=(-\frac{1}{2}[[\Delta]]-\Omega[[L_z]])\boldsymbol{\Phi}.\end{aligned}\tag{80}$$

The right-hand side is

$$\mathbf{b}^{\mathrm{BE},n} := \frac{\boldsymbol{\Phi}^n}{\delta t}. \tag{81}$$

The matrix $[[\mathbf{I}]]$ is the identity matrix of $\mathscr{M}_{MN_c}(\mathbb{C})$. Finally, the discrete $L^{2,N_c}_{\mathbf{x}}$-norm of a vector $\boldsymbol{\Phi} \in \mathbb{C}^{MN_c}$ is defined by

$$||\boldsymbol{\Phi}||_{\ell^2_\pi} := (\sum_{\ell=1}^{N_c} \|\Phi_\ell\|^2_{\ell^2_\pi})^{1/2}. \tag{82}$$

Furthermore, we define the discrete (strong) stopping criterion as

$$||\boldsymbol{\Phi}^{n+1} - \boldsymbol{\Phi}^n||_\infty < \varepsilon \delta t, \tag{83}$$

with the discrete uniform norm defined by: $\forall \boldsymbol{\Phi} \in \mathbb{C}^{MN_c}$, $\|\boldsymbol{\Phi}\|_\infty = \sum_{\ell=1}^{N_c} \max_{(j,k)\in\mathscr{P}_{J,K}} |\Phi_{\ell,j,k}|$, and the discrete (weak) stopping criterion as

$$|\mathscr{E}_{\Omega,\mathbf{F}}(\boldsymbol{\Phi}^{n+1}) - \mathscr{E}_{\Omega,\mathbf{F}}(\boldsymbol{\Phi}^n)| < \varepsilon \delta t, \tag{84}$$

with the discrete energy

$$\mathscr{E}_{\Omega,\mathbf{F}}(\boldsymbol{\Phi}) = (h_x h_y)^{1/2} \sum_{\substack{(j,k)\in\mathscr{P}_{J,K} \\ 1\le\ell\le N_C}} \Re\left\{ \Phi^*_{\ell,j,k} \left(-\frac{1}{2}[[\Delta]]\boldsymbol{\Phi} - \Omega[[L_z]]\boldsymbol{\Phi} \right.\right.$$
$$\left.\left. +[[V]]\boldsymbol{\Phi} + [[F(|\Phi|^2)]]\boldsymbol{\Phi}\right)_{\ell,j,k} \right\}.$$

As in the one-component case, preconditioned Krylov subspace solvers can be used to iteratively solve the associated linear systems (see [12]).

3 The Gross-Pitaevskii Equation Laboratory

3.1 GPELab: A Short Presentation

As seen in Sect. 2 for the stationary state computation and as it will be explained in Sect. 4 for the dynamics, the numerical methods that we present are robust and efficient. Furthermore, they can be quite directly extended to different kinds of Gross-Pitaevskii Equations and systems. The aim of this section is to present a freely

available Matlab toolbox called GPELab[1] (Gross-Pitaevskii Equation Laboratory) which is based on these advanced numerical schemes. The computational tools are developed in such a way that they can be easily used by physicists working on BECs. GPELab allows the user to make various computations in 1d-2d-3d, for multi-components GPEs with general potentials and nonlinearities. In addition, the stochastic effects that are described for the dynamics can be numerically simulated according to efficient and accurate schemes. Even if GPELab is dedicated to Gross-Pitaevskii Equations, it is more generally useful when one wants to solve problems related to nonlinear Schrödinger equations. Let us remark that at the time of writing this contribution, other interesting computational codes for solving GPEs (with a cubic nonlinearity) are proposed by different authors. In [119], a Fortran 90 solver based on the imaginary time method can solve the stationary state problem for the one-component GPE with a quadratic potential and without rotation term. In [96, 121], the authors distribute finite difference Fortran 90 codes for one-component problems with radial and spherical potentials, and no rotation. Improvements, in particular the parallelization of the code with OpenMP, are provided in [121]. Other codes (developed with Fortran or Matlab) for GPEs are available [44, 76, 91]. Nevertheless, it seems that none of these solvers propose the flexibility that GPELab offers where many physical situations of interest can be considered: any potential and nonlinearity, inclusion of gradient-like terms for fast rotations, multi-components cases, stationary states and dynamics of BECs, stochastic effects. To show how GEPLab is powerful, we now consider a few numerical examples. Other interesting situations (with downloadable source files) are given in the GPELab user guide and the associated papers [10, 11, 13].

3.2 *Experiment I: Stationary State of a 1d BEC with Josephson Junction*

In this example, we want to reproduce the numerical simulations obtained in [18] where the following one-dimensional ($d = 1$) system of GPEs with a Josephson junction is considered

$$\begin{cases} i\partial_t \psi_1 = \left[-\frac{1}{2}\Delta + V(\mathbf{x}) + \delta + (\beta_{11}|\psi_1|^2 + \beta_{12}|\psi_2|^2)\right]\psi_1 + \lambda\psi_2, \\ i\partial_t \psi_2 = \left[-\frac{1}{2}\Delta + V(\mathbf{x}) + (\beta_{22}|\psi_2|^2 + \beta_{12}|\psi_1|^2)\right]\psi_2 + \lambda\psi_1. \end{cases} \tag{85}$$

In the above system, δ is the detuning constant of the Raman transition, β_{jk} are the interaction constants between the gazes and λ is the effective Rabi frequency. We use BESP for a time step $\delta t = 10^{-1}$ and a uniform spatial grid with $2^{10} + 1$ points on $]-16, 16[$. In addition, the (strong) stopping criterion for computing the

[1] http://gpelab.math.cnrs.fr/.

stationary states is 10^{-6}. Following [18], the values of the physical parameters are: $\lambda = -1, \delta = 0, \beta = 500, \beta_{11} = \beta, \beta_{12} = 0.94\beta, \beta_{22} = 0.97\beta$. The initial data is a centered gaussian for each component. At the end of the computation, we obtain each component of the stationary state and some interesting physical outputs (see Table 3). We can also simultaneously print out the moduli of the components and conclude that they are the same as the ones reported in [18] (see Fig. 12).

Table 3 Stationary states outputs for the two-components GPEs system with Josephson junction

```
----------------------------
Iteration 164 on 1000000
--Outputs of component 1----------
Square at the origin: 0.03512761887793
x-radius mean square: 2.67309309073190
Energy: 9.97806793424214
Chemical potential: 32.84198217411518
Energy evolution: 0.00000000000000
--Outputs of component 2----------
Square at the origin: 0.04853615539806
x-radius mean square: 2.99189318517412
Energy: 13.16187704973455
Chemical potential: 38.16552799804442
Energy evolution: 0.00000000000000
----------------------------
CPU time: 8.28
»
```

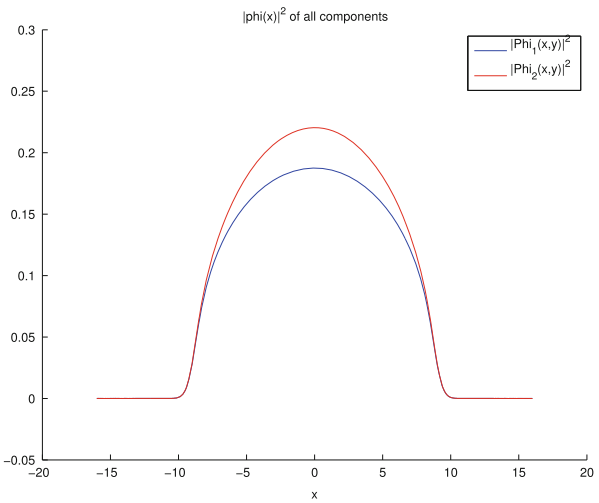

Fig. 12 Moduli of the two-components BEC

3.3 Experiment II: Stationary State of a Fast Rotating 2d BEC in a Strongly Confining Trap

We consider the stationary state computation for a two-dimensional ($d = 2$) GPE with a quadratic-plus-quartic potential, a cubic nonlinearity and a rotation operator

$$i\partial_t \psi = \frac{1}{2}\Delta\psi + \left[\frac{1-\alpha}{2}\left(\gamma_x|x|^2 + \gamma_y|y|^2\right) + \frac{\kappa}{4}\left(\gamma_x|x|^2 + \gamma_y|y|^2\right)^2\right]\psi + \beta|\psi|^2\psi + i\Omega\left(y\partial_x - x\partial_y\right)\psi,$$

with the parameters values $\alpha = 1.2, \kappa = 0.3, \gamma_x = \gamma_y = 1, \beta = 1000$ and $\Omega = 3.5$. This is a typical example of a fast rotating BEC. We consider BESP with $\delta t = 10^{-3}$. The computational domain is $]-10, 10[^2$, discretized by a uniform grid with $2^8 + 1$ points in each direction x and y. The (strong) stopping criterion of BESP is 10^{-5} and the initial data is the Thomas-Fermi approximation associated with the physical problem. In Table 4, we report the outputs at the end of the simulation. We represent the modulus of the ground state on Fig. 13 obtained by GPELab. In particular, we can see the existence of many uniformly distributed vortices in the annulus.

3.4 Experiment III: Stationary State of a 3d Dipole-Dipole BEC

We show here a last numerical experiment for the three-dimensional ($d = 3$) GPE with a quadratic potential, a cubic nonlinearity to which a dipole-dipole nonlocal

Table 4 Outputs at the end of the computation

```
---------------------------
Iteration 46766 on 1000000
--Outputs of component 1----------
Square at the origin: 0.00000000000000
x-radius mean square: 4.57951169686043
y-radius mean square: 4.57951071463754
Energy: 115.52164061561449
Chemical potential: 122.58168418655728
Angular momentum: 146.32747911959200
Energy evolution: -0.00000000141087
»
```

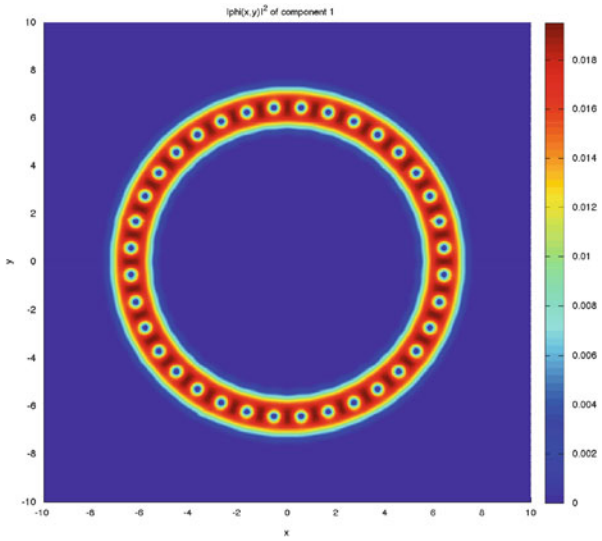

Fig. 13 Modulus of the converged stationary state

nonlinear interaction is added

$$i\partial_t\psi = -\frac{1}{2}\Delta\psi + \frac{1}{2}\left(\gamma_x|x|^2 + \gamma_y|y|^2 + \gamma_z|z|^2\right)\Psi$$
$$+\beta|\psi|^2\psi + d^2\Big(\int_{\mathbb{R}^3}\frac{1-3\cos^2(\widehat{\mathbf{a},\tilde{\mathbf{x}}})}{||(x,y,z)-\tilde{\mathbf{x}}||^3}|\psi(t,\tilde{\mathbf{x}})|^2 d\tilde{\mathbf{x}}\Big)\psi, \tag{86}$$

with $\gamma_x = \gamma_y = \gamma_z = 1$, $\beta = 2000$ and $\mathbf{a} = (0,0,1)$. The discretization for BESP uses $\delta t = 10^{-2}$ and a uniform grid with $2^6 + 1$ points in each direction x, y and z for the computational domain $]-15,15[^3$. The (strong) stopping criterion is fixed to 10^{-6}. In GEPLab, the nonlinearity which is defined by the dipole-dipole interaction can be efficiently computed by using FFTs *via*

$$d^2\int_{\mathbb{R}^3}\frac{1-3\cos^2(\widehat{\mathbf{a},\tilde{\mathbf{x}}})}{||\mathbf{x}-\tilde{\mathbf{x}}||^3}|\psi(t,\tilde{\mathbf{x}})|^2 d\tilde{\mathbf{x}}$$
$$= \mathscr{F}^{-1}\left(\frac{4\pi}{3}d^2(3\cos^2(\widehat{\mathbf{a},\boldsymbol{\omega}})-1)\mathscr{F}\left(|\psi(t,\mathbf{x})|^2\right)(\boldsymbol{\omega})\right)(\mathbf{x}).$$

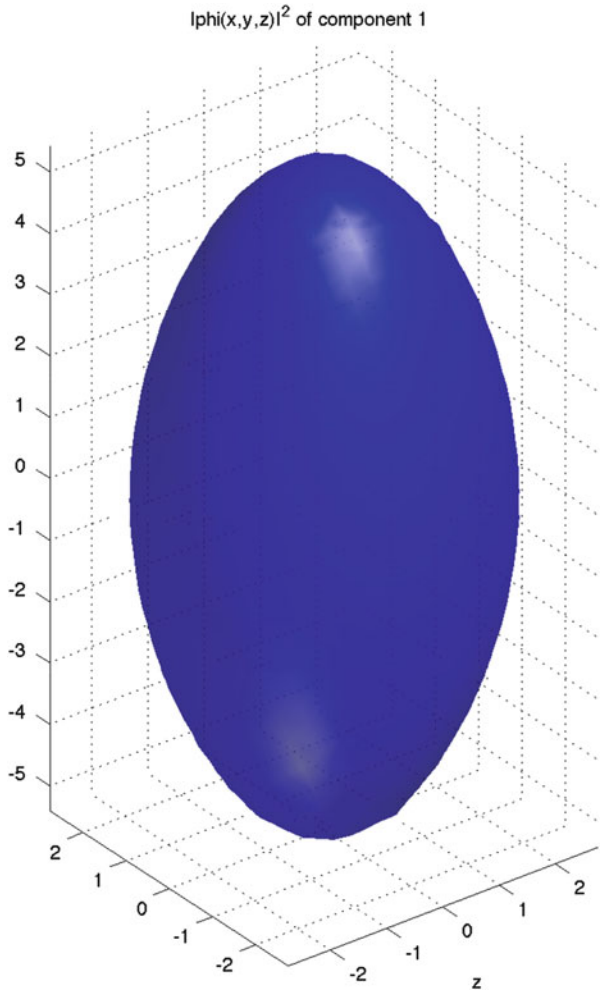

Fig. 14 10^{-3}-isovalues of the modulus for the converged stationary state

The initial data is the Thomas-Fermi approximation. The converged stationary state is given on Fig. 14 where we report the isovalues of the solution. We remark that the stationary state has the property of being elongated along the dipolar direction.

4 Computation of the Dynamics

We develop now the numerical simulation of the dynamics of deterministic (Sect. 4) or stochastic (Sect. 5) GPEs (or systems of GPEs) with a rotational term. Let us consider the model equation

$$\begin{cases} i\partial_t \psi(t,\mathbf{x}) = -\dfrac{1}{2}\Delta\psi(t,\mathbf{x}) - \Omega L_z \psi(t,\mathbf{x}) + V(t,\mathbf{x})\psi(t,\mathbf{x}) \\ \qquad\qquad +f(|\psi|^2)\psi(t,\mathbf{x}),\ \forall t \in \mathbb{R}^+,\ \forall \mathbf{x} \in \mathbb{R}^d, \\ \psi(0,\mathbf{x}) = \psi_0(\mathbf{x}) \in L^2_{\mathbf{x}}. \end{cases} \tag{87}$$

Our aim is to propose some efficient, robust and accurate discretization schemes that reproduce at the discrete level some continuous physical properties (see Sect. 4.1). Like for the stationary states computation, we use high-precision pseudo-spectral FFT-based discretization schemes. Essentially, we analyze the time-splitting (Sect. 4.2) and relaxation (Sect. 4.3) schemes. We discuss some other schemes that we do not recommend (Sect. 4.4). We also present a recent idea [33] based on a change of frame for a rotational BEC that should be further investigated in the future since it simplifies the implementation of the standard schemes. We extend the time-splitting and relaxation schemes to multi-components GPEs (Sect. 4.5). We detail three examples of numerical simulations for a rotating BEC (Sect. 4.6). The orders of all these schemes are computed and we check the mass and energy conservation properties. The examples are based on GPELab.

Section 5 concerns the extension and study of these numerical schemes for solving the stochastic GPE

$$\begin{cases} i\partial_t \psi(t,\mathbf{x}) = -\dfrac{1}{2}\Delta\psi(t,\mathbf{x}) - \Omega L_z \psi(t,\mathbf{x}) + V(\dot{w}_t,\mathbf{x})\psi(t,\mathbf{x}) \\ \qquad\qquad +f(|\psi|^2)\psi(t,\mathbf{x}),\ \forall t \in \mathbb{R}^+,\ \forall \mathbf{x} \in \mathbb{R}^d, \\ \psi(0,\mathbf{x}) = \psi_0(\mathbf{x}) \in L^2_{\mathbf{x}}, \end{cases} \tag{88}$$

introduced in Sect. 1.3.3 (page 63).

4.1 Dynamics of the GPE and Continuous/Discrete Properties

The dynamics of a BEC is driven by the GPE ($d = 1, 2, 3$)

$$\begin{cases} i\partial_t \psi(t,\mathbf{x}) = -\dfrac{1}{2}\Delta\psi(t,\mathbf{x}) - \Omega L_z \psi(t,\mathbf{x}) + V(t,\mathbf{x})\psi(t,\mathbf{x}) \\ \qquad\qquad +f(|\psi|^2)\psi(t,\mathbf{x}),\ \forall t \in \mathbb{R}^+,\ \forall \mathbf{x} \in \mathbb{R}^d, \\ \psi(0,\mathbf{x}) = \psi_0(\mathbf{x}) \in L^2_{\mathbf{x}}. \end{cases} \tag{89}$$

We use the notations introduced in Sect. 2.1. We assume that the initial data is localized in a rectangular domain $\mathscr{O} =]-a_x, a_x[\times]-a_y, a_y[\times]-a_z, a_z[$, with a_x, a_y, $a_z \in \mathbb{R}^+$ (depending on the dimension). Let $\Omega = 0$ and $V(t, \mathbf{x}) = V(\mathbf{x})$. The solution ψ of (87) fulfills some important mathematical/physical properties that the approximation schemes should preserve at the discrete level. In the positive case, the scheme is considered as a "good" scheme. These continuous properties are the following

- *Time reversibility*: the solution ψ is still the solution of Eq. (87) after changing the time variable $t \to -t$ and applying a complex conjugation.
- *Dispersion relation*: if $V \equiv 0$, the plane wave solution $\psi(t, \mathbf{x}) = \rho e^{i(\mathbf{k}\cdot\mathbf{x}-\omega t)}$ satisfies the following *dispersion relation*

$$\omega = \frac{|\mathbf{k}|^2}{2} + f(|\rho|).$$

- *Gauge transformation*: the translation of the potential

$$\forall \rho \in \mathbb{R}, \forall \mathbf{x} \in \mathbb{R}^d, \quad V(\mathbf{x}) \longrightarrow V(\mathbf{x}) + \rho,$$

  creates the following change of phase in the solution

$$\forall t \in \mathbb{R}^+, \ \forall \mathbf{x} \in \mathbb{R}^d, \quad \psi(t, \mathbf{x}) \longrightarrow \psi(t, \mathbf{x}) e^{-i\rho t}.$$

  We remark that the modulus of the solution remains unchanged.
- *Mass conservation*: the total mass is conserved over the time

$$\mathscr{N}(\psi)(t) := \|\psi(t, \cdot)\|^2_{L^2_{\mathbf{x}}} = \int_{\mathbb{R}^d} |\psi(t, \mathbf{x})|^2 d\mathbf{x} = \mathscr{N}(\psi_0), \forall t > 0. \tag{90}$$

- *Energy conservation*: if $f(|\psi|^2) = \beta|\psi|^2$, the energy is preserved [20]

$$\begin{aligned} \mathscr{E}_{0,\beta}(\psi)(t) &:= \int_{\mathbb{R}^d} \left(\frac{1}{2}|\nabla\psi(t, \mathbf{x})|^2 + V(\mathbf{x})|\psi(t, \mathbf{x})|^2 + \frac{\beta}{2}|\psi(t, \mathbf{x})|^4\right) d\mathbf{x} \\ &= \mathscr{E}_{0,\beta}(\psi_0), \end{aligned}$$

  for any $t > 0$.

We consider the two-dimensional case, the extensions to the dimensions $d = 1$ and $d = 3$ are direct. Let δt be the uniform time step and

$$(\psi^n_{(j,k)})_{(j,k)\in\mathscr{T}_{j,k}}$$

the approximate solution at time $t_n = n\delta t$ on a uniform grid $\mathscr{O}_{J,K}$. At the discrete level, the previous properties read

- *Time reversibility*: changing the indices $(n, n+1) \leftrightarrow (n+1, n)$ lets the solution unchanged: $\psi^{n+1} \leftrightarrow \psi^n$.
- *Dispersion relation*: if $V \equiv 0$ and the initial data is given by

$$\psi^0_{(j,k)} = \rho e^{i\mathbf{k}\cdot\mathbf{x}_{j,k}},$$

the discrete solution is

$$\psi^n_{(j,k)} = \rho e^{i(\mathbf{k}\cdot\mathbf{x}_{j,k} - \omega t_n)},$$

where we have the *dispersion relation*

$$\omega = \frac{|\mathbf{k}|^2}{2} + f(|\rho|).$$

This property characterizes the fact that the numerical and exact velocities are the same or not.

- *Gauge transformation*: the change of potential

$$\forall \rho \in \mathbb{R}, \forall \mathbf{x} \in \mathbb{R}^d, \quad V(\mathbf{x}) \longrightarrow V(\mathbf{x}) + \rho,$$

implies that the solution is modified as follows

$$\forall n \in \mathbb{N},\ \forall (j,k) \in \mathscr{P}_{J,K}, \quad \psi^n_{(j,k)} \longrightarrow \psi^n_{(j,k)} e^{-i\rho t_n},$$

letting the modulus of the solution unchanged. This characterizes the property that the scheme may induce a phase error in the numerical solution.

- *Mass conservation*: the discrete mass conservation writes

$$\forall n \in \mathbb{N}^*, \quad \mathscr{N}(\boldsymbol{\psi}^n) := \|\boldsymbol{\psi}^n\|^2_{\ell^2_\pi} = \mathscr{N}(\boldsymbol{\psi}^0), \tag{91}$$

also stating the ℓ^2_π-stability of the scheme.

- *Energy conservation*: if $\Omega = 0$ and $f(|\psi|^2) = \beta|\psi|^2$, the energy conservation [20] is given by: $\forall n \in \mathbb{N}^*$, $\mathscr{E}_{0,\beta}(\boldsymbol{\psi}^n) = \mathscr{E}_{0,\beta}(\boldsymbol{\psi}^0)$, where

$$\mathscr{E}_{0,\beta}(\boldsymbol{\psi}^n) := (h_x h_y)^{1/2} \sum_{(j,k)\in\mathscr{P}_{J,K}} \Re\left\{ \psi^{n,*}_{j,k} \left(-\frac{1}{2}[[\Delta]]\boldsymbol{\psi}^n + [[V]]\boldsymbol{\psi}^n + \frac{\beta}{2}[[|\psi^n|^4]]\boldsymbol{\psi}^n \right)_{j,k} \right\}.$$

4.2 Time-Splitting Pseudo-spectral Schemes for the Rotating GPE

4.2.1 General Principle of Time-Splitting Techniques

The first schemes that we present is the class of time-splitting schemes for (87). This scheme, which is known since a long time, has been studied in particular by Strang [113] in a general framework. It has next been applied to the nonlinear Schrödinger equation in [57, 97, 116, 122]. The numerical analysis of the *Lie* and *Strang* time-splitting schemes for the Schrödinger equation can be found in particular in [37, 90].

To present the time-splitting schemes (also called fractional step methods), we consider a general dynamical problem. Let A and B be two self-adjoint operators such that: $\mathscr{D}(A) \subset L^2_{\mathbf{x}}$, $\mathscr{D}(B) \subset L^2_{\mathbf{x}}$ and $A+B$ a self-adjoint operator on $\mathscr{D}(A) \cap \mathscr{D}(B)$. We denote by $\mathscr{D}(A)$ and $\mathscr{D}(B)$ the domains of the operators A and B, respectively. Let us consider the system

$$\begin{cases} \partial_t \psi(t,\mathbf{x}) = A\psi(t,\mathbf{x}) + B\psi(t,\mathbf{x}), \ t \in \mathbb{R}^+, \ \mathbf{x} \in \mathbb{R}^d, \\ \psi(0,\mathbf{x}) = \psi_0(\mathbf{x}) \in L^2_{\mathbf{x}}. \end{cases}$$

Let $\psi(t,\mathbf{x}) = e^{(A+B)t}\psi_0(\mathbf{x})$ be the solution of this system, for $t > 0$ and $\mathbf{x} \in \mathbb{R}^d$. The time-splitting scheme consists in approximating the solution ψ of this problem *via* an approximation of the operator $e^{(A+B)\cdot}$ through the operators $e^{A\cdot}$ and $e^{B\cdot}$. This leads to solve successively two simpler systems. We seek an approximation of the form

$$\psi(t+\delta t,\mathbf{x}) = e^{(A+B)\delta t}\psi(t,\mathbf{x}) \approx e^{a_1 A\delta t}e^{b_1 B\delta t}e^{a_2 A\delta t}e^{b_2 B\delta t}\dots e^{a_p A\delta t}e^{b_p B\delta t}\psi(t,\mathbf{x}),$$

where $\{a_k, b_k\}_{1\le k\le p} \subset \mathbb{R}$ are some computed weights such that the approximation of $e^{(A+B)\delta t}$ has a given order for a local time step $\delta t (\ll 1)$. The two most well-known time-splitting methods are the Lie (corresponding to $a_1 = b_1 = 1$) and the Strang (for $a_1 = a_2 = 1/2$, $b_1 = 1$ and $b_2 = 0$) schemes. They are respectively of order one and two in time. It is possible to get higher-order schemes by suitably choosing the weights [45, 117, 118]. We now focus on the Lie and Strang schemes.

In the case of the GPE with a rotation term, we make the following choice [26, 28]

- we set

$$A = \frac{i}{2}\Delta + i\Omega L_z, \tag{92}$$

  which leads to the solution of a linear Schrödinger equation, without potential operator but with a rotational term,

- and

$$B = -iV(t,\mathbf{x}) - if(|\psi(t,\mathbf{x})|^2), \tag{93}$$

  which gives a nonlinear differential equation that can be solved explicitly in some cases.

The previous decomposition is motivated by the fact that, by using an *Alternating Direction Implicit* (ADI) method [26], the equation associated to the operator (92) can be solved spectrally by using FFTs. Furthermore, as already mentioned, the equation associated to the operator (93) is solved explicitly. This leads to highly accurate methods. Other choice of operators A and B (e.g. including a part of the potential V in A) lead to different spectral basis that diagonalize the operators (see [23, 24, 32] for Hermite or Laguerre polynomials).

4.2.2 Lie Time-Splitting Scheme for (87)

Application of the Lie time-splitting scheme and ADI method. The Lie scheme leads to the following approximation of the solution

$$\psi(t+\delta t,\mathbf{x}) \approx e^{i(\frac{1}{2}\Delta+\Omega L_z)\delta t} e^{-i(V(t,\mathbf{x})+f(|\psi(t,\mathbf{x})|^2))\delta t}\psi(t,\mathbf{x}).$$

Let us assume that we want to compute the solution ψ on $[0;T]$ that is uniformly discretized into N intervals (a non uniform grid can also be used): $T = N\delta t$, $N \in \mathbb{N}$. Let us set: $t_n := n\delta t$, $0 \le n \le N$. For an initial condition $\psi^0 = \psi_0$, the scheme writes: for $0 \le n \le N-1$,

1. Compute ψ_1 such that

$$\begin{cases} i\partial_t\psi_1(t,\mathbf{x}) = -\dfrac{1}{2}\Delta\psi_1(t,\mathbf{x}) - \Omega L_z\psi_1(t,\mathbf{x}),\ n\delta t < t \le (n+1)\delta t,\ \forall \mathbf{x}\in\mathbb{R}^d, \\ \psi_1(t_n,\mathbf{x}) = \psi^n(\mathbf{x}),\ \forall \mathbf{x}\in\mathbb{R}^d. \end{cases} \tag{94}$$

2. Determine ψ_2 satisfying

$$\begin{cases} i\partial_t\psi_2(t,\mathbf{x}) = V(t,\mathbf{x})\psi_2(t,\mathbf{x}) + f(|\psi_2(t,\mathbf{x})|^2)\psi_2(t,\mathbf{x}), \\ \qquad\qquad n\delta t < t \le (n+1)\delta t,\ \forall \mathbf{x}\in\mathbb{R}^d, \\ \psi_2(t_n,\mathbf{x}) = \psi_1(t_{n+1},\mathbf{x}),\ \forall \mathbf{x}\in\mathbb{R}^d. \end{cases} \tag{95}$$

If $\psi^{n+1}(\mathbf{x}) := \psi_2(t_{n+1},\mathbf{x})$, we have $\psi^{n+1}(\mathbf{x}) \approx \psi(t_{n+1},\mathbf{x})$.

We consider the two-dimensional case to simplify the presentation (but the one- and three-dimensional cases can be easily deduced). The first step (94) of the splitting scheme can be spectrally resolved for $\Omega = 0$ since the Laplacian operator is diagonal in the Fourier space. However, when $\Omega > 0$, the situation is more

complex since the operator $L_z = -i(x\partial_y - y\partial_x)$ cannot be directly inverted by using FFTs. Indeed, variable coefficients are present in its expression. A solution to this problem has been proposed by Bao et al. [26]. It consists in applying the ADI method to split the derivations with respect to x and y in two successive steps, allowing to use one-directional FFTs. More precisely, the resulting scheme for solving (94) is given by

1(a) Compute $\psi^{(1)}$ solution to

$$\begin{cases} i\partial_t \psi^{(1)}(t,\mathbf{x}) = -\dfrac{1}{2}\partial_x^2 \psi^{(1)}(t,\mathbf{x}) \\ \qquad\qquad -i\Omega y \partial_x \psi^{(1)}(t,\mathbf{x}),\ \forall t \in]t_n, t_{n+1}],\ \forall \mathbf{x} \in \mathbb{R}^2, \\ \psi^{(1)}(t_n,\mathbf{x}) = \psi^n(\mathbf{x}),\ \forall \mathbf{x} \in \mathbb{R}^2. \end{cases} \tag{96}$$

1(b) Determine $\psi^{(2)}$ such that

$$\begin{cases} i\partial_t \psi^{(2)}(t,\mathbf{x}) = -\dfrac{1}{2}\partial_y^2 \psi^{(2)}(t,\mathbf{x}) \\ \qquad\qquad +i\Omega x \partial_y \psi^{(2)}(t,\mathbf{x}),\ \forall t \in]t_n, t_{n+1}],\ \forall \mathbf{x} \in \mathbb{R}^2, \\ \psi^{(2)}(t_n,\mathbf{x}) = \psi^{(1)}(t_{n+1},\mathbf{x}),\ \forall \mathbf{x} \in \mathbb{R}^2. \end{cases} \tag{97}$$

We remark that each partial differential operator appearing in the above equations can be diagonalized by FFTs. After this process, one gets an approximation: $\psi_1(t_{n+1},\mathbf{x}) \approx \psi^{(2)}(t_{n+1},\mathbf{x})$ for the first step (94), the second step leading to resolve the ODE (95) which is written as: $\forall \mathbf{x} \in \mathbb{R}^2$

$$\begin{cases} i\partial_t \psi^{(3)}(t,\mathbf{x}) = V(t,\mathbf{x})\psi^{(3)}(t,\mathbf{x}) \\ \qquad\qquad +f(|\psi^{(3)}(t,\mathbf{x})|^2)\psi^{(3)}(t,\mathbf{x}),\ \forall t \in]t_n, t_{n+1}], \\ \psi^{(3)}(t_n,\mathbf{x}) = \psi^{(2)}(t_{n+1},\mathbf{x}). \end{cases} \tag{98}$$

This ordinary differential equation is explicitly integrable thanks to the following result [28].

Lemma 1 *Let $\psi^{(3)}$ be the solution to (98). Then, we have*

$$\forall t \in]t_n, t_{n+1}],\ \forall \mathbf{x} \in \mathbb{R}^2, \quad |\psi^{(3)}(t,\mathbf{x})| = |\psi^{(2)}(t_{n+1},\mathbf{x})|.$$

Proof The proof is direct since we have: $\forall t \in]t_n, t_{n+1}]$,

$$\begin{aligned} \partial_t |\psi^{(3)}(t,\mathbf{x})|^2 &= 2\Re(\psi^{(3)^*}(t,\mathbf{x})\partial_t \psi^{(3)}(t,\mathbf{x})) \\ &= -2\Im(V(t,\mathbf{x})|\psi^{(3)}(t,\mathbf{x})|^2) - 2\Im(f(|\psi^{(3)}|^2)|\psi^{(3)}(t,\mathbf{x})|^2) = 0. \end{aligned}$$

We then get the solution to (98)

$$\forall t \in [t_n, t_{n+1}], \quad \psi^{(3)}(t, \mathbf{x}) = e^{-if(|\psi^{(2)}(t_{n+1},\mathbf{x})|^2)(t-t_n)-i\int_{t_n}^{t} V(s,\mathbf{x})ds}\psi^{(2)}(t_{n+1}, \mathbf{x}). \tag{99}$$

Finally, the Lie scheme with ADI leads to the approximation $\psi^{n+1}(\mathbf{x}) \approx \psi^{(3)}(t_{n+1}, \mathbf{x})$.

Let us remark that the above ADI method implies a loss of symmetry of the global scheme. Indeed, we first solve the equation in the x-direction *via* (96) and then in the y-direction by using (97). The symmetry can be obtained easily by alternating the directions at each step. For problem (94), we first solve (96) and (97) at time t_n and next (97) and (96) at time t_{n+1}.

Pseudo-spectral discretization in space. Let us now consider the problem of the spatial discretization. We again assume that the solution remains confined within the computational box: $\mathscr{O} =]-a_x, a_x[\times]-a_y, a_y[$, with $a_x, a_y > 0$. We impose some periodic boundary conditions on $\partial\mathscr{O}$ and consider a uniform discretization grid $\mathscr{O}_{J,K}$ associated with $\mathscr{O}$. Let us recall that $\mathscr{P}_{J,K}$ designates the set of grid points indices used for the pseudo-spectral discretization

$$\mathscr{P}_{J,K} = \left\{(j,k) \in \mathbb{N}^2; 1 \le j \le J \text{ and } 1 \le k \le K\right\}.$$

We consider an approximation of $\psi^{(m)}$ on this grid that we designate by $\varphi^{(m)}$, $m = 1$, 2, 3. Moreover, the approximation of ψ^n is denoted by φ^n. As for the stationary case, we use the following pseudo-spectral discretization of a function ψ in the x- and y-directions on $\mathscr{O}_{J,K}$ and based on the truncated inverse partial Fourier series, $\forall (j,k) \in \mathscr{P}_{J,K}$, $\forall t \in \mathbb{R}^+$, respectively,

$$\begin{aligned}
\psi(t, x_j, y_k) \approx \varphi(t, x_j, y_k) &= \frac{1}{J}\sum_{p=-J/2}^{J/2-1} \widehat{\varphi_p}(t, y_k) e^{i\mu_p(x_j+a_x)}, \\
\psi(t, x_j, y_k) \approx \varphi(t, x_j, y_k) &= \frac{1}{K}\sum_{q=-K/2}^{K/2-1} \widehat{\varphi_q}(t, x_k) e^{i\lambda_q(y_k+a_y)},
\end{aligned} \tag{100}$$

where $\widehat{\varphi_p}$ and $\widehat{\varphi_q}$ are respectively the Fourier coefficients of the function φ in the x- and y-directions, the Fourier multipliers being: $\mu_p = \frac{\pi p}{a_x}$ and $\lambda_q = \frac{\pi q}{a_y}$. The functions $\widehat{\varphi_p}$ and $\widehat{\varphi_q}$ are written as

$$\begin{aligned}
\widehat{\varphi_p}(t, y_k) &= \sum_{j=0}^{J-1} \varphi(t, x_j, y_k) e^{-i\mu_p(x_j+a_x)}, \\
\widehat{\varphi_q}(t, x_j) &= \sum_{k=0}^{K-1} \varphi(t, x_j, y_k) e^{-i\lambda_q(y_k+a_y)}.
\end{aligned} \tag{101}$$

In the x-direction of the Fourier space, we have, $1 - J/2 \le p \le J/2$,

$$\forall t \in [t_n, t_{n+1}],\ \forall 1 \le k \le K, \quad i\partial_t \hat{\varphi}_p^{(1)}(t, y_k) = (\frac{1}{2}\mu_p^2 + \Omega y \mu_p)\hat{\varphi}_p^{(1)}(t, y_k).$$

Integrating this equation yields

$$\forall t \in [t_n, t_{n+1}],\ \forall 1 \le k \le K, \quad \hat{\varphi}_p^{(1)}(t, y_k) = e^{-i\left(\frac{1}{2}\mu_p^2 + \Omega y \mu_p\right)(t-t_n)}\hat{\varphi}_p^{(1)}(t_n, y_k).$$

Similarly, (97) leads to: $1 - K/2 \le q \le K/2$,

$$\forall t \in [t_n, t_{n+1}],\ \forall 1 \le j \le J, \quad \hat{\varphi}_q^{(2)}(t, x_j) = e^{-i\left(\frac{1}{2}\lambda_q^2 - \Omega x \lambda_q\right)(t-t_n)}\hat{\varphi}_q^{(2)}(t_n, x_j).$$

Therefore, the first part of the Lie time-splitting scheme, where we first solve (96) and next (97) on $[t_n, t_{n+1}]$, is implemented as: $\forall (j,k) \in \mathscr{P}_{J,K}$,

$$\begin{aligned}
\varphi^{(1)}(t_{n+1}, x_j, y_k) &= \frac{1}{J}\sum_{p=-J/2}^{J/2-1} e^{-i\left(\frac{1}{2}\mu_p^2 + \Omega y_k \mu_p\right)(t_{n+1}-t_n)}\widehat{\varphi_p^n}(y_k)e^{i\mu_p(x_j+L_x)}, \\
\varphi^{(2)}(t_{n+1}, x_j, y_k) &= \frac{1}{K}\sum_{q=-K/2}^{K/2-1} e^{-i\left(\frac{1}{2}\lambda_q^2 - \Omega x_j \lambda_q\right)(t_{n+1}-t_n)}\hat{\varphi}_q^{(1)}(t_{n+1}, x_j)e^{i\lambda_q(y_k+L_y)}.
\end{aligned} \tag{102}$$

For solving (99) and for a time-dependent potential V, we use the Simpson's quadrature rule

$$\begin{aligned}
\int_{t_n}^{t_{n+1}} V(s, x_j, y_k)ds \approx \frac{1}{6}\big(&V(t_n, x_j, y_k) + 6V(t_{n+1/2}, x_j, y_k) \\
&+ V(t_{n+1}, x_j, y_k)\big)\,(t_{n+1} - t_n) := \tilde{V}_n(x_j, y_k)\delta t,
\end{aligned}$$

where $t_{n+\frac{1}{2}} = (t_n + t_{n+1})/2$ and $(j,k) \in \mathscr{P}_{J,K}$. This leads to

$$\varphi^{(3)}(t_{n+1}, x_j, y_k) = \varphi^{(2)}(t_{n+1}, x_j, y_k)e^{-i\delta t\left(f(|\varphi^{(2)}(t_{n+1}, x_j, y_k)|^2) + \tilde{V}_n(x_j, y_k)\right)}. \tag{103}$$

The complete scheme (102) and (103) is first-order accurate in time and spectral in space. In the sequel, the *Time-Splitting SPectral scheme of order 1-ADI* is denoted by TSSP1-ADI.

4.2.3 Strang Time-Splitting Scheme for (87)

To improve the time accuracy of the Lie scheme, we now discuss the second-order Strang TSSP scheme. Since the derivation is quite similar to the previous scheme, we do not detail too much its construction. The Strang time-splitting scheme requires three fractional steps while only one is needed for the Lie scheme. We first resolve the operator A on a time step $\delta t/2$, next B for δt and finally A for $\delta t/2$. This leads to the following approximation

$$\psi(t+\delta t,\mathbf{x}) \approx e^{i(\frac{1}{2}\Delta+\Omega L_z)\frac{\delta t}{2}} e^{-i(V(t,\mathbf{x})+f(|\psi(t,\mathbf{x})|^2))\delta t} e^{i(\frac{1}{2}\Delta+i\Omega L_z)\frac{\delta t}{2}} \psi(t,\mathbf{x}),$$

for $t > 0$. An alternative solution consists in changing the roles of A and B. The Strang time-splitting scheme with ADI is then

1. Compute $\psi^{(1)}$ solution to

$$\begin{cases} i\partial_t \psi^{(1)}(t,\mathbf{x}) = -\dfrac{1}{2}\partial_x^2 \psi^{(1)}(t,\mathbf{x}) \\ \qquad\qquad -i\Omega y \partial_x \psi^{(1)}(t,\mathbf{x}),\ \forall t \in]t_n, t_{n+\frac{1}{2}}], \forall \mathbf{x} \in \mathbb{R}^2, \\ \psi^{(1)}(t_n,\mathbf{x}) = \psi_n(\mathbf{x}), \forall \mathbf{x} \in \mathbb{R}^2. \end{cases} \tag{104}$$

2. Determine $\psi^{(2)}$ solution of the equation

$$\begin{cases} i\partial_t \psi^{(2)}(t,\mathbf{x}) = -\dfrac{1}{2}\partial_y^2 \psi^{(2)}(t,\mathbf{x}) \\ \qquad\qquad +i\Omega x \partial_y \psi^{(2)}(t,\mathbf{x}),\ \forall t \in]t_n, t_{n+\frac{1}{2}}], \forall \mathbf{x} \in \mathbb{R}^2, \\ \psi^{(2)}(t_n,\mathbf{x}) = \psi^{(1)}(t_{n+\frac{1}{2}},\mathbf{x}), \forall \mathbf{x} \in \mathbb{R}^2. \end{cases} \tag{105}$$

3. Compute $\psi^{(3)}$ such that

$$\begin{cases} i\partial_t \psi^{(3)}(t,\mathbf{x}) = V(t,\mathbf{x})\psi^{(3)}(t,\mathbf{x}) \\ \qquad\qquad +f(|\psi^{(3)}(t,\mathbf{x})|^2)\psi^{(3)}(t,\mathbf{x}),\ \forall t \in]t_n, t_{n+1}], \forall \mathbf{x} \in \mathbb{R}^2, \\ \psi^{(3)}(t_n,\mathbf{x}) = \psi^{(2)}(t_{n+\frac{1}{2}},\mathbf{x}), \forall \mathbf{x} \in \mathbb{R}^2. \end{cases} \tag{106}$$

4. Obtain $\psi^{(4)}$ solution to

$$\begin{cases} i\partial_t \psi^{(4)}(t,\mathbf{x}) = -\dfrac{1}{2}\partial_y^2 \psi^{(4)}(t,\mathbf{x}) \\ \qquad\qquad +i\Omega x \partial_y \psi^{(4)}(t,\mathbf{x}),\ \forall t \in]t_n, t_{n+1}/2], \forall \mathbf{x} \in \mathbb{R}^2, \\ \psi^{(4)}(t_n,\mathbf{x}) = \psi^{(3)}(t_{n+1},\mathbf{x}), \forall \mathbf{x} \in \mathbb{R}^2. \end{cases} \tag{107}$$

5. Determine $\psi^{(5)}$ such that

$$\begin{cases} i\partial_t \psi^{(5)}(t,\mathbf{x}) = -\dfrac{1}{2}\partial_x^2 \psi^{(5)}(t,\mathbf{x}) \\ \qquad\qquad -i\Omega y \partial_x \psi^{(5)}(t,\mathbf{x}), \ \forall t \in]t_n, t_{n+1}/2], \forall \mathbf{x} \in \mathbb{R}^2, \\ \psi^{(5)}(t_n,\mathbf{x}) = \psi^{(4)}(t_{n+\frac{1}{2}},\mathbf{x}), \forall \mathbf{x} \in \mathbb{R}^2. \end{cases} \tag{108}$$

The last step gives $\psi^{n+1}(\mathbf{x}) \approx \psi^{(5)}(t_{n+\frac{1}{2}},\mathbf{x})$. Like the Lie scheme, we solve (104), (105), (107) and (108) by using one-directional FFTs. Equation (106) is explicitly integrated. The Strang scheme is second-order in time and spectral in space which makes it very attractive for the deterministic simulations. Extensions to the one- and three-dimensional cases are direct. The total computational cost of both schemes is $O(M \log M)$, with $M := J, JK, JKL$, in dimensions $d = 1, 2, 3$, respectively, since we use FFTs. The Strang scheme is *time reversible*, *mass preserving*, *invariant under gauge transformation* and the *dispersive relation* holds. However, it is not energy conserving but the scheme is unconditionally stable for the two-norm [26]. More details can be found in [14, 27, 29]. In the sequel, the scheme (104)–(108) (with FFTs) is called TSSP2-ADI for *Time Splitting SPectral scheme of order 2-ADI*.

4.3 The Relaxation Scheme for the Rotating GPE

Introduced by Besse [36] for nonlinear Schrödinger equations, the relaxation scheme has some analogies with the standard Crank-Nicolson scheme (Sect. 4.4) but the nonlinearity is relaxed to avoid a fixed point or a Newton-Raphson method. Therefore, the computational cost is strongly reduced while the scheme is simple to implement. For problem (87), the relaxation scheme is

$$\begin{cases} \dfrac{\phi^{n+1/2} + \phi^{n-1/2}}{2} = f(|\psi^n|^2), \\ i\dfrac{\psi^{n+1} - \psi^n}{\delta t} = (-\dfrac{1}{2}\Delta - \Omega L_z)(\dfrac{\psi^{n+1} + \psi^n}{2}) + \dfrac{V^{n+1}\psi^{n+1} + V^n\psi^n}{2} \\ \qquad\qquad +\phi^{n+1/2}(\dfrac{\psi^{n+1} + \psi^n}{2}), \end{cases} \tag{109}$$

where $\psi^n = \psi(t_n,\mathbf{x})$ and $V^n = V(t_n,\mathbf{x})$, $0 \le n \le N-1$. The initial conditions are: $\psi^0(\mathbf{x}) = \psi_0(\mathbf{x})$ and $\phi^{-1/2}(\mathbf{x}) = f(|\psi^0(\mathbf{x})|^2)$. The operator $(-\Delta - \Omega L_z)$ is discretized by the highly accurate pseudo-spectral scheme [see page 81 and Eqs. (100) and (101)]. Under the same notations, the discrete system is

$$\begin{cases} \boldsymbol{\phi}^{n+1/2} = \mathbf{c}^{\mathrm{Re},n}, \\ \mathbb{A}^{\mathrm{Re},n+1}\boldsymbol{\psi}^{n+1} = \mathbf{b}^{\mathrm{Re},n}, \end{cases} \tag{110}$$

where $\mathbb{A}^{\mathrm{Re},n+1}$, $\mathbf{b}^{\mathrm{Re},n}$ and $\mathbf{c}^{\mathrm{Re},n}$ are such that

$$\begin{aligned}\mathbb{A}^{\mathrm{Re},n+1} &:= i\frac{[[I]]}{\delta t} + \frac{1}{4}[[\Delta]] + \frac{1}{2}\Omega[[L_z]] - \frac{1}{2}[[V^{n+1}]] - \frac{1}{2}[[\boldsymbol{\phi}^{n+1/2}]],\\ \mathbf{b}^{\mathrm{Re},n} &:= (i\frac{[[I]]}{\delta t} - \frac{1}{4}[[\Delta]] - \frac{1}{2}\Omega[[L_z]] + \frac{1}{2}[[V^n]] + \frac{1}{2}[[\boldsymbol{\phi}^{n+1/2}]])\boldsymbol{\psi}^n,\\ \mathbf{c}^{\mathrm{Re},n} &:= 2f(|\boldsymbol{\psi}^n|^2) - \boldsymbol{\phi}^{n-1/2}.\end{aligned} \tag{111}$$

The linear system appearing in (110) and depending on n is solved by a Krylov subspace iterative solver (CGS, BiCGStab, GMRES) [12]. The method is called Relaxation SPectral (ReSP) scheme. The discretization is second-order in time and spectrally accurate in space like for the TSSP2-ADI scheme. Moreover, it is *time reversible*, *mass preserving*, unconditionally stable and *energy preserving* (for a cubic nonlinearity, i.e. $f(|\psi|^2) = \beta|\psi|^2$). However, it is not invariant under *gauge transformation* and the *dispersive relation* does not hold [14, 36]. The computational cost is $O(M \log M)$ since we again use FFTs.

4.4 Other Schemes: Euler, Crank-Nicolson, Leap-Frog, Rotating Frame System

In this section, we give a brief description of other schemes that could be applied to Eq. (87). These schemes are not recommended because of some problems that we detail now. We end by presenting a nice idea that can be found in [33] and which considers a change of frame to simplify the implementation of well-adapted schemes.

The forward or backward Euler schemes are simple schemes in the framework of evolution problems. For (87), the forward Euler scheme is given by

$$i\frac{\psi^{n+1} - \psi^n}{\delta t} = (-\frac{1}{2}\Delta - \Omega L_z + V^n + f(|\psi^n|^2))\psi^n, \tag{112}$$

where $\psi^n = \psi(t_n, \mathbf{x})$ and $V^n = V(t_n, \mathbf{x})$, $\forall n \in \mathbb{N}$. The spatial discretization can be obtained, for instance, by using the pseudo-spectral FFT-based approximation leading to

$$\boldsymbol{\psi}^{n+1} = -i\delta t\mathbf{b}_{\mathrm{Exp}}^{\mathrm{Euler},n}, \tag{113}$$

where $\mathbf{b}_{\mathrm{Exp}}^{\mathrm{Euler},n}$ is such that

$$\mathbf{b}_{\mathrm{Exp}}^{\mathrm{Euler},n} := (i\frac{[[I]]}{\delta t} - \frac{1}{2}[[\Delta]] - \Omega[[L_z] + [[V^n]] + [[f(|\boldsymbol{\psi}^n|^2)]])\boldsymbol{\psi}^n.$$

Since there is no linear system to solve, the computational effort is low. However, this first-order scheme is well-known to be conditionally stable under a CFL condition and is therefore useless. The backward Euler scheme is

$$i\frac{\psi^{n+1}-\psi^n}{\delta t} = (-\frac{1}{2}\Delta - \Omega L_z + V^{n+1} + f(|\psi^{n+1}|^2))\psi^{n+1}, \tag{114}$$

leading to the linear system

$$\mathbb{A}_{\text{Imp}}^{\text{Euler},n}\boldsymbol{\psi} = \mathbf{b}_{\text{Imp}}^{\text{Euler},n}, \tag{115}$$

where $\mathbb{A}_{\text{Imp}}^{\text{Euler},n}$ and $\mathbf{b}_{\text{Imp}}^{\text{Euler},n}$ are such that

$$\mathbb{A}_{\text{Imp}}^{\text{Euler},n} := i\frac{[[I]]}{\delta t} + \frac{1}{2}[[\Delta]] + \Omega[[L_z]] - [[V^{n+1}]] - [[f(|\boldsymbol{\psi}^{n+1}|^2)]],$$
$$\mathbf{b}_{\text{Imp}}^{\text{Euler},n} := i\frac{[[I]]}{\delta t}\boldsymbol{\psi}^n.$$

The system (115) cannot be directly inverted since the nonlinearity is implicit. At each iteration, a fixed point or a Newton-Raphson method is required to resolve the nonlinearity leading to a computationally expensive scheme. Finally, the scheme is only first-order accurate in time.

The implicit Crank-Nicolson scheme [14, 19, 20] is

$$i\frac{\psi^{n+1}-\psi^n}{\delta t} = (-\frac{1}{2}\Delta - \Omega L_z + g(\psi^{n+1},\psi^n))\frac{\psi^{n+1}+\psi^n}{2} + \frac{1}{2}(V^{n+1}\psi^{n+1} + V^n\psi^n), \tag{116}$$

with

$$g(\psi^{n+1},\psi^n) := \int_0^1 f(\iota|\psi^{n+1}|^2 + (1-\iota)|\psi^n|^2)d\iota.$$

Even if this scheme is second-order accurate in time, the presence of the nonlinearity makes it computationally expensive.

The semi-implicit Leap-Frog scheme [14, 19–21] is

$$i\frac{\psi^{n+1}-\psi^{n-1}}{\delta t} = (-\frac{1}{2}\Delta - \Omega L_z)\frac{\psi^{n+1}+\psi^{n-1}}{2} + (V^n + f(|\psi^n|^2))\psi^n. \tag{117}$$

For the initialization, we use

$$i\frac{\psi^1-\psi^0}{\delta t} = (-\frac{1}{2}\Delta - \Omega L_z + V^0 + f(|\psi^0|^2))\psi^0.$$

The major disadvantages of this scheme are that it is conditionally stable and it does not satisfy most of the properties from Sect. 4.1 (see [14]).

In Sect. 1.3 (page 60), we have seen that a change of variables is used for modeling a rotating condensate. This change of frame, with respect to the reference frame in dimensions $d = 2$ and 3, is based on: for $\mathbf{x} = (x, y) \in \mathbb{R}^2$ or $\mathbf{x} = (x, y, z) \in \mathbb{R}^3$,

$$\begin{cases} x' = \cos(\Omega t)x + \sin(\Omega t)y, \\ y' = -\sin(\Omega t)x + \cos(\Omega t)y, \end{cases}$$

where $\Omega \in \mathbb{R}$ is the rotational speed of the condensate. This gives the relation: $\mathbf{x}' = \boldsymbol{\Omega}(t)\mathbf{x}$, where, for $d = 2$,

$$\boldsymbol{\Omega}(t) = \begin{pmatrix} \cos(\Omega t) & \sin(\Omega t) \\ -\sin(\Omega t) & \cos(\Omega t) \end{pmatrix},$$

and, for $d = 3$,

$$\boldsymbol{\Omega}(t) = \begin{pmatrix} \cos(\Omega t) & \sin(\Omega t) & 0 \\ -\sin(\Omega t) & \cos(\Omega t) & 0 \\ 0 & 0 & 1 \end{pmatrix}.$$

This change of variables makes the rotation operator L_z appear. In [33], the authors propose to compute the dynamics of a rotating condensate by considering the coordinates $\boldsymbol{\Omega}(t)\mathbf{x}$ instead of $\mathbf{x}'$. By setting $\psi_\Omega(t, \mathbf{x}) := \psi(t, \boldsymbol{\Omega}(t)\mathbf{x})$, where ψ satisfies (87), we obtain that ψ_Ω is solution to

$$\begin{cases} i\partial_t\psi_\Omega(t, \mathbf{x}) = -\frac{1}{2}\Delta\psi_\Omega(t, \mathbf{x}) + V(t, \boldsymbol{\Omega}(t)\mathbf{x})\psi_\Omega(t, \mathbf{x}) \\ \qquad\qquad +f(|\psi_\Omega|^2)\psi_\Omega(t, \mathbf{x}), \ \forall t \in \mathbb{R}^+, \ \forall \mathbf{x} \in \mathbb{R}^d, \\ \psi_\Omega(0, \mathbf{x}) = \psi_0(\mathbf{x}) \in L^2_{\mathbf{x}}. \end{cases} \tag{118}$$

By simply modifying the potential: $V_\Omega(t, \mathbf{x}) := V(t, \boldsymbol{\Omega}(t)\mathbf{x})$, we do not need to discretize the rotation operator which greatly simplifies the resolution of the initial-value problem. For example, ADI is no longer necessary for the time-splitting scheme. This recent approach is very promising for both the dynamics and stationary states computation and should be further studied.

4.5 The Multi-components Case

We now extend the splitting and relaxation schemes to the case of a system of GPEs with N_c components

$$\begin{cases} i\partial_t \Psi(t,\mathbf{x}) = -\dfrac{1}{2}\Delta\Psi(t,\mathbf{x}) - \Omega L_z \Psi(t,\mathbf{x}) + \mathbf{V}(t,\mathbf{x})\Psi(t,\mathbf{x}) \\ \qquad\qquad +\mathbf{f}(\Psi)\Psi(t,\mathbf{x}),\ \forall t \in \mathbb{R}^+,\ \forall \mathbf{x} \in \mathbb{R}^d, \\ \Psi(0,\mathbf{x}) = \Psi_0(\mathbf{x}) \in L^{2,N_c}_{\mathbf{x}},\ \forall \mathbf{x} \in \mathbb{R}^d, \end{cases} \tag{119}$$

where $L^{2,N_c}_{\mathbf{x}} := (L^2_{\mathbf{x}})^{N_c}$. We refer to Sect. 2.5 (page 96) for the notations.

4.5.1 Time-Splitting Schemes for a System with N_c Components

The strategy adopted here is closely related to the one developed for the one-component case. We will see that the explicit formula is only valid for a specific form of the nonlinearity, which explains why the method has some limitations. For the sake of simplicity, we only present the Lie TSSP scheme, the extension to the Strang TSSP scheme being direct. The scheme is given by the two following steps

1. Solve the following system with respect to $\Psi^{(1)}$

$$\begin{cases} i\partial_t \Psi^{(1)}(t,\mathbf{x}) = -\dfrac{1}{2}\Delta\Psi^{(1)}(t,\mathbf{x}) - \Omega L_z \Psi^{(1)}(t,\mathbf{x}), \\ \qquad\qquad \forall t \in]t_n, t_{n+1}], \forall \mathbf{x} \in \mathbb{R}^d, \\ \Psi^{(1)}(t_n,\mathbf{x}) = \Psi^n(\mathbf{x}),\ \forall \mathbf{x} \in \mathbb{R}^d. \end{cases} \tag{120}$$

2. Compute $\Psi^{(2)}$ such that

$$\begin{cases} i\partial_t \Psi^{(2)}(t,\mathbf{x}) = \mathbf{V}(t,\mathbf{x})\Psi^{(2)}(t,\mathbf{x}) + \mathbf{f}(\Psi^{(2)}(t,\mathbf{x}))\Psi^{(2)}(t,\mathbf{x}), \\ \qquad\qquad \forall t \in]t_n, t_{n+1}],\ \forall \mathbf{x} \in \mathbb{R}^d, \\ \Psi^{(2)}(t_n,\mathbf{x}) = \Psi^{(1)}(t_{n+1},\mathbf{x}),\ \forall \mathbf{x} \in \mathbb{R}^d. \end{cases} \tag{121}$$

Since the operators are diagonal in (120), the unknowns are uncoupled. Therefore, we can apply the ADI method to effectively solve the system of equations by using FFTs. For example, Eq. (120) is solved in the two-dimensional case through the two following successive steps

$$\begin{cases} i\partial_t \Psi^{(1,1)}(t,\mathbf{x}) = -\dfrac{1}{2}\partial_{xx}\Psi^{(1,1)}(t,\mathbf{x}) - i\Omega y\partial_x \Psi^{(1,1)}(t,\mathbf{x}), \\ \qquad\qquad \forall t \in]t_n, t_{n+1}],\ \forall \mathbf{x} \in \mathbb{R}^2, \\ \Psi^{(1,1)}(t_n,\mathbf{x}) = \Psi^n(\mathbf{x}),\ \forall \mathbf{x} \in \mathbb{R}^2, \end{cases} \tag{122}$$

and

$$\begin{cases} i\partial_t \Psi^{(1,2)}(t,\mathbf{x}) = -\dfrac{1}{2}\partial_{yy}\Psi^{(1,2)}(t,\mathbf{x}) + i\Omega x \partial_y \Psi^{(1,2)}(t,\mathbf{x}), \\ \qquad\qquad\qquad\qquad\qquad\qquad \forall t \in]t_n, t_{n+1}],\ \forall \mathbf{x} \in \mathbb{R}^2, \\ \Psi^{(1,2)}(t_n,\mathbf{x}) = \Psi^{(1,1)}(t_{n+1},\mathbf{x}),\ \forall \mathbf{x} \in \mathbb{R}^2. \end{cases} \tag{123}$$

For the system of equations (121), we have the following result.

Lemma 2 *Let $\Psi^{(2)}$ be the solution of (121). Then, we have*

$$\forall t \in [t_n, t_{n+1}], \quad |\Psi^{(2)}(t,\mathbf{x})| = |\Psi^{(2)}(t_n,\mathbf{x})|.$$

Proof First, we have, $\forall t \in]t_n, t_{n+1}]$, $\forall \mathbf{x} \in \mathbb{R}^2$,

$$\begin{aligned} \sum_{m=1}^{N_c} \partial_t |\Psi_m^{(2)}(t,\mathbf{x})|^2 &= 2\sum_{m=1}^{N_c} \Re(\Psi_m^{(2)}(t,\mathbf{x})^* \partial_t \Psi_m^{(2)}(t,\mathbf{x})) \\ &= -2\sum_{m,o=1}^{N_c} \Im(\Psi_m^{(2)}(t,\mathbf{x})^* (\mathbf{V}_{mo}(t,\mathbf{x}) + \mathbf{f}_{mo}(\Psi^{(2)}))\Psi_o^{(2)}(t,\mathbf{x})). \end{aligned}$$

By using: $\mathbf{V}_{mo}(t,\mathbf{x}) = \mathbf{V}_{om}(t,\mathbf{x})$ and $\mathbf{f}_{mo}(\Psi^{(2)}(t,\mathbf{x})) = \mathbf{f}_{om}(\Psi^{(2)}(t,\mathbf{x}))$, it follows that

$$\begin{aligned} &\sum_{m=1}^{N_c} \partial_t |\Psi_m^{(2)}(t,\mathbf{x})|^2 \\ &= -2\sum_{N_c \geq o > m \geq 1} \Im\Big((\mathbf{V}_{mo}(t,\mathbf{x}) + \mathbf{f}_{mo}(\Psi^{(2)}(t,\mathbf{x}))) \\ &\qquad (\Psi_m^{(2)}(t,\mathbf{x})^* \Psi_o^{(2)}(t,\mathbf{x}) + \Psi_o^{(2)}(t,\mathbf{x})^* \Psi_m^{(2)}(t,\mathbf{x}))\Big) \\ &\quad -2\sum_{N_c \geq m \geq 1} \Im\Big((\mathbf{V}_{mm}(t,\mathbf{x}) + \mathbf{f}_{mm}(\Psi^{(2)}(t,\mathbf{x})))|\Psi_m^{(2)}(t,\mathbf{x})|^2\Big) \\ &= -4\sum_{N_c \geq o > m \geq 1} \Im\Big((\mathbf{V}_{mo}(t,\mathbf{x}) + \mathbf{f}_{mo}(\Psi^{(2)}(t,\mathbf{x})))\Re(\Psi_m^{(2)}(t,\mathbf{x})^* \Psi_o^{(2)}(t,\mathbf{x}))\Big) = 0. \end{aligned}$$

Thus, we conclude that $|\Psi^{(2)}(t,\mathbf{x})| = |\Psi^{(2)}(t_n,\mathbf{x})|$, $\forall t \in [t_n, t_{n+1}]$.

According to the above result, the modulus of the solution is time preserved. This implies that we can obtain an explicit formulation of the solution by using an exponential operator assuming that $\mathbf{f}$ is such that: $\mathbf{f}(\Psi) = \mathbf{f}(|\Psi|) = (\mathbf{f}_{m,\ell}(|\Psi|))_{m,\ell \in \{1,\ldots,N_c\}}$, and that the potential is time-independent: $\mathbf{V}(t,\mathbf{x}) := \mathbf{V}(\mathbf{x})$.

Under these assumptions, the system of equations (121) admits the following solution

$$\Psi^{(2)}(t,\mathbf{x}) = e^{-i\mathbf{f}(|\Psi^{(1,2)}(t_{n+1},\mathbf{x})|)(t-t_n)-i\mathbf{V}(\mathbf{x})(t-t_n)}\Psi^{(1,2)}(t_{n+1},\mathbf{x}). \tag{124}$$

This finally leads to the approximation: $\Psi^{n+1}(\mathbf{x}) \approx \Psi^{(2)}(t_{n+1},\mathbf{x})$.

The form (124) of the solution requires the evaluation of an exponential matrix. Moreover, the Lie and Strang splitting schemes need to be symmetrized as for the one-component case because of the ADI method. In the sequel, we call again these methods TSSP1-ADI and TSSP2-ADI, respectively. The computational cost $O(M \log M)$ is essentially related to the FFTs.

4.5.2 Relaxation Scheme for a System with N_c Components

For a system of equations, the relaxation scheme is given by

$$\begin{cases} \dfrac{\Phi^{n+1/2}+\Phi^{n-1/2}}{2} = \mathbf{f}(\Psi^n) + \mathbf{V}^n,\ \mathbf{x}\in\mathbb{R}^d, \\ \dfrac{\Psi^{n+1}-\Psi^n}{\delta t} = -i(-\dfrac{1}{2}\Delta - \Omega L_z + \Phi^{n+1/2})\dfrac{\Psi^{n+1}+\Psi^n}{2},\ \mathbf{x}\in\mathbb{R}^d, \end{cases}$$

where $\Psi^n = \Psi(t_n,\mathbf{x})$ and $\mathbf{V}^n = \mathbf{V}(t_n,\mathbf{x})$. The initial data are given by $\Psi^0(\mathbf{x}) = \Psi_0(\mathbf{x})$ and $\Phi^{-1/2}(\mathbf{x}) = \mathbf{f}(\Psi^0(\mathbf{x}))$. By using the pseudo-spectral scheme, we are led to solve

$$\begin{cases} \mathbb{M}^{\mathrm{Re},n+1/2} = 2[[\mathbf{f}(\boldsymbol{\Psi}^n)]] - \mathbb{M}^{\mathrm{Re},n-1/2}, \\ \mathbb{A}^{\mathrm{Re},n+1}\boldsymbol{\Psi}^{n+1} = \mathbb{B}^{\mathrm{Re},n}\boldsymbol{\Psi}^n, \end{cases} \tag{125}$$

where $\boldsymbol{\Psi}^n = (\psi_1^n,\ldots,\psi_{N_c}^n)$ is the unknown in $\mathbb{C}^{MN_c}$, with $M := JK$. The nonlinear operator $\mathbb{M}^{\mathrm{Re},n+1/2} \in \mathscr{M}_{MN_c}(\mathbb{C})$ corresponding to the relaxation is computed by using the nonlinear operator

$$[[\mathbf{f}(\boldsymbol{\Psi}^n)]] := \begin{pmatrix} [[\mathbf{f}_{1,1}(\boldsymbol{\Psi}^n)]] & [[\mathbf{f}_{1,2}(\boldsymbol{\Psi}^n)]] & \cdots & [[\mathbf{f}_{1,N_c}(\boldsymbol{\Psi}^n)]] \\ [[\mathbf{f}_{2,1}(\boldsymbol{\Psi}^n)]] & [[\mathbf{f}_{2,2}(\boldsymbol{\Psi}^n)]] & \cdots & [[\mathbf{f}_{2,N_c}(\boldsymbol{\Psi}^n)]] \\ \vdots & \vdots & \ddots & \vdots \\ [[\mathbf{f}_{N_c,1}(\boldsymbol{\Psi}^n)]] & [[\mathbf{f}_{N_c,2}(\boldsymbol{\Psi}^n)]] & \cdots & [[\mathbf{f}_{N_c,N_c}(\boldsymbol{\Psi}^n)]] \end{pmatrix} \in \mathscr{M}_{MN_c}(\mathbb{R}),$$

where we set $[[\mathbf{f}_{\ell,m}(\boldsymbol{\Psi}^n)]] = \left(\mathbf{f}_{\ell,m}(\boldsymbol{\Psi}^n(\mathbf{x}_{j,k})\right)_{(j,k)\in\mathscr{P}_{J,K}}$, $1 \le \ell, m \le N_c$. Furthermore, we choose $\mathbb{M}^{\mathrm{Re},-1/2} = \mathbf{f}(\Psi_0(\mathbf{x}))$. The operator $\mathbb{A}^{\mathrm{Re},n} \in \mathscr{M}_{MN_c}(\mathbb{C})$ is such that

$$\mathbb{A}^{\mathrm{Re},n+1}\boldsymbol{\Psi} = \mathbb{A}_{\mathrm{TF}}^{\mathrm{Re},n+1}\boldsymbol{\Psi} + \mathbb{A}_{\Delta,\Omega}^{\mathrm{Re}}\boldsymbol{\Psi},$$

$$\mathbb{A}_{\mathrm{TF}}^{\mathrm{Re},n+1}\boldsymbol{\Psi} := i\frac{[[\mathbf{I}]]}{\delta t}\boldsymbol{\Psi} - \frac{1}{2}([[\mathbf{V}^{n+1}]] + \mathbb{M}^{\mathrm{Re},n+1/2})\boldsymbol{\Psi},$$

$$\mathbb{A}_{\Delta,\Omega}^{\mathrm{Re}}\boldsymbol{\Psi} := \frac{1}{2}(\frac{1}{2}[[\Delta]] + \Omega[[L_z]])\boldsymbol{\Psi}. \tag{126}$$

The operator $\mathbb{A}_{\mathrm{TF}}^{\mathrm{Re},n+1} \in \mathscr{M}_{MN_c}(\mathbb{C})$ is defined through the block-matrices

$$[[\mathbf{I}]] := \begin{pmatrix} [[I]] & 0 & \cdots & 0 \\ 0 & [[I]] & \cdots & 0 \\ \vdots & \vdots & \ddots & \vdots \\ 0 & 0 & \cdots & [[I]] \end{pmatrix} \in \mathscr{M}_{MN_c}(\mathbb{R}),$$

$$[[\mathbf{V}^n]] := \begin{pmatrix} [[\mathbf{V}_{1,1}^n]] & [[\mathbf{V}_{1,2}^n]] & \cdots & [[\mathbf{V}_{1,N_c}^n]] \\ [[\mathbf{V}_{2,1}^n]] & [[\mathbf{V}_{2,2}^n]] & \cdots & [[\mathbf{V}_{2,N_c}^n]] \\ \vdots & \vdots & \ddots & \vdots \\ [[\mathbf{V}_{N_c,1}^n]] & [[\mathbf{V}_{N_c,2}^n]] & \cdots & [[\mathbf{V}_{N_c,N_c}^n]] \end{pmatrix} \in \mathscr{M}_{MN_c}(\mathbb{R}),$$

where: $[[\mathbf{V}_{\ell,m}^n]] = (\mathbf{V}_{\ell,m}^n(\mathbf{x}_{j,k}))_{(j,k)\in\mathscr{P}_{J,K}} \in \mathscr{M}_M(\mathbb{R})$. The diagonal operator $\mathbb{A}_{\Delta,\Omega}^{\mathrm{Re}}$ in (126) is implicitly given by

$$[[\Delta]]\boldsymbol{\Psi} := ([[\Delta\Psi_\ell]])_{\ell=1,\dots,N_c} \in \mathbb{C}^{MN_c} \quad \text{and}$$
$$[[L_z]]\boldsymbol{\Psi} := ([[L_z\Psi_\ell]])_{\ell=1,\dots,N_c} \in \mathbb{C}^{MN_c}.$$

Finally, the right-hand side is defined by the operator $\mathbb{B}^{\mathrm{Re},n} : \mathbb{C}^{MN_c} \to \mathbb{C}^{MN_c}$

$$\mathbb{B}^{\mathrm{Re},n}\boldsymbol{\Psi} = \mathbb{B}_{\mathrm{TF}}^{\mathrm{Re},n}\boldsymbol{\Psi} + \mathbb{B}_{\Delta,\Omega}^{\mathrm{Re}}\boldsymbol{\Psi},$$

$$\mathbb{B}_{\mathrm{TF}}^{\mathrm{Re},n}\boldsymbol{\Psi} := i\frac{[[\mathbf{I}]]}{\delta t}\boldsymbol{\Psi} + \frac{1}{2}\mathbb{M}^{\mathrm{Re},n+1/2}\boldsymbol{\Psi},$$

$$\mathbb{B}_{\Delta,\Omega}^{\mathrm{Re}}\boldsymbol{\Psi} := \frac{1}{2}(-\frac{1}{2}[[\Delta]] - \Omega[[L_z]])\boldsymbol{\Psi}. \tag{127}$$

The linear system in (125) is solved by a preconditioned Krylov subspace iterative solver [12] at a computational cost $O(M \log M)$. Unlike the splitting

schemes, no assumption is required for the relaxation scheme concerning the nonlinear or potential operators.

4.6 Numerical Study of the TSSP1-ADI, TSSP2-ADI and ReSP Schemes for the Dynamics of Rotating GPEs

4.6.1 Experiment I: Dynamics of a Rotating BEC in a Harmonic Trap

The first numerical experiment consists in solving

$$\begin{cases} i\partial_t \psi(t,\mathbf{x}) = -\dfrac{1}{2}\Delta\psi(t,\mathbf{x}) - \Omega L_z \psi(t,\mathbf{x}) + V(\mathbf{x})\psi(t,\mathbf{x}) \\ \qquad\qquad +\beta|\psi|^2\psi(t,\mathbf{x}),\ \ \forall t \in [0,T],\ \ \forall \mathbf{x} \in \mathbb{R}^2, \\ \psi(0,\mathbf{x}) = \psi_0(\mathbf{x}) \in L^2_{\mathbf{x}}, \end{cases} \tag{128}$$

where $\Omega = 0.4$ and $\beta = 1000$. We fix the quadratic potential

$$V(\mathbf{x}) = \frac{1}{2}(\gamma_x x^2 + \gamma_y y^2),$$

with $\gamma_x = \gamma_y = 1$. The initial data ψ_0 is computed (by using BESP) as the stationary state (see Fig. 15) associated with the problem (128) for the quadratic potential with $\gamma_x = \gamma_y = 2$. The modification of the coefficients increases the confinement of the BEC. This creates a contraction without changing its global shape.

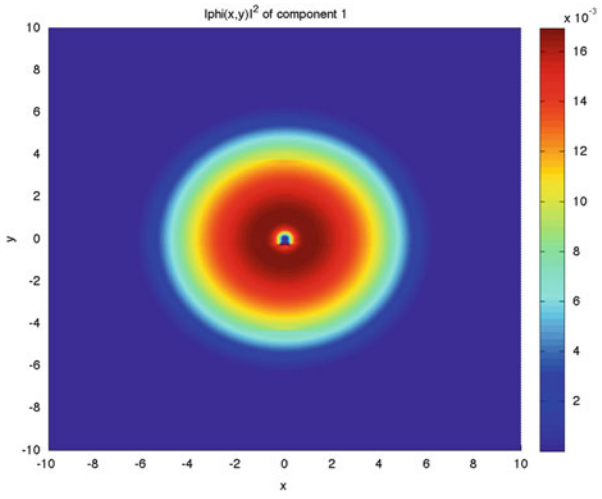

Fig. 15 Initial data $|\psi_0|^2$ (on the domain $\mathscr{O} =]-10, 10[^2$, $J = K = 2^9$ for BESP)

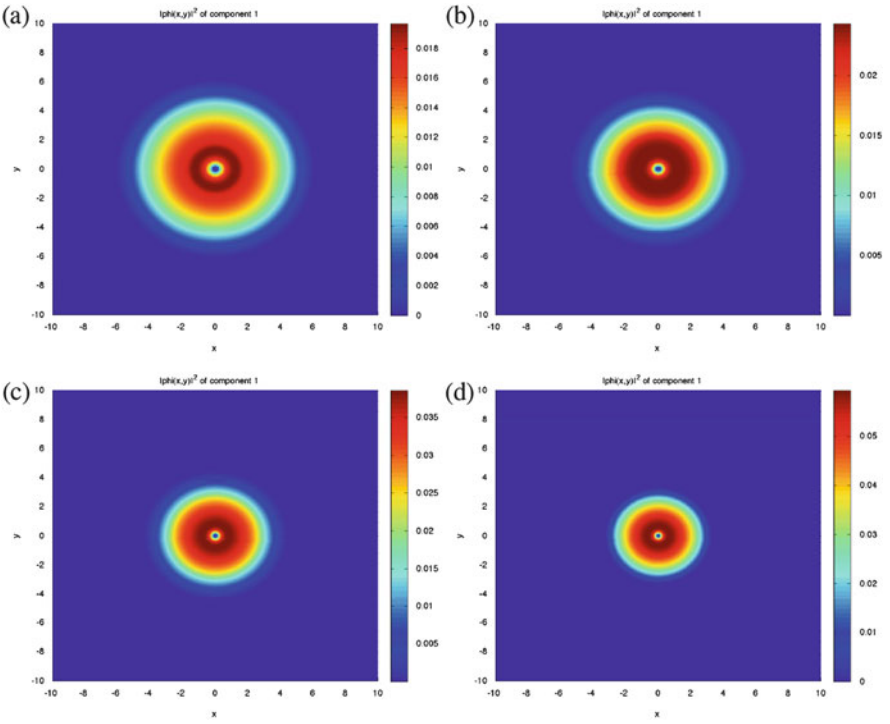

Fig. 16 Evolution of the density $|\psi|^2$ for problem (128) computed by the ReSP scheme. (**a**) $t = 0.13$; (**b**) $t = 0.26$; (**c**) $t = 0.39$; (**d**) $t = 0.52$

For TSSP1-ADI, TSSP2-ADI and ReSP, we use a time step equal to $\delta t = 10^{-3}$ for a final computational time $T = 1$ ($T := N\delta t$). The pseudo-spectral discretization scheme considers $J = K = 2^9$ points for the computational domain $\mathscr{O} =]-10, 10[^2$. For ReSP, we solve the linear system by using BiCGStab with a stopping criterion set to $\varepsilon^{\text{Krylov}} = 10^{-12}$. We report on Fig. 16 the solution $\boldsymbol{\psi}^{n,\text{ref}}$ obtained by the ReSP scheme at different times. We remark that the potential confines the condensate. Visualizing the solutions computed by TSSP1-ADI, TSSP2-ADI and ReSP does not allow to make the difference between them.

Let us analyze the spatial accuracy of the schemes. The previous simulation is repeated on different uniform grids $\mathscr{O}_{J,K}$, with $5 \leq J, K \leq 9$, where the reference grid is considered for $J = K = 9$. For each grid, the initial data is computed by using the BESP scheme with the parameters of problem (128) for the finest grid. We represent on Fig. 17 the maximum error $\text{Err}_{J,K}^{n,\infty}$ between the solution $\boldsymbol{\psi}_{J,K}^n$ on the grid $\mathscr{O}_{J,K}$ and the solution $\boldsymbol{\psi}^{n,\text{ref}}$ computed on the grid $\mathscr{O}_{9,9}$ and then extrapolated on the coarser grid $\mathscr{O}_{J,K}$, i.e.: $\text{Err}_{J,K}^{n,\infty} := ||\boldsymbol{\psi}_{J,K}^n - \boldsymbol{\psi}^{n,\text{ref}}||_\infty$. We also report the error between the energy (without the rotational term) $\mathscr{E}_{0,\beta}(\boldsymbol{\psi}_{J,K}^n)$ on the grid $\mathscr{O}_{J,K}$ and the reference energy $\mathscr{E}_{0,\beta}(\boldsymbol{\psi}^{n,\text{ref}})$: $\mathscr{E}_{J,K}^{n,\infty} := |\mathscr{E}_{0,\beta}(\boldsymbol{\psi}_{J,K}^n) - \mathscr{E}_{0,\beta}(\boldsymbol{\psi}^{n,\text{ref}})|$. We remark

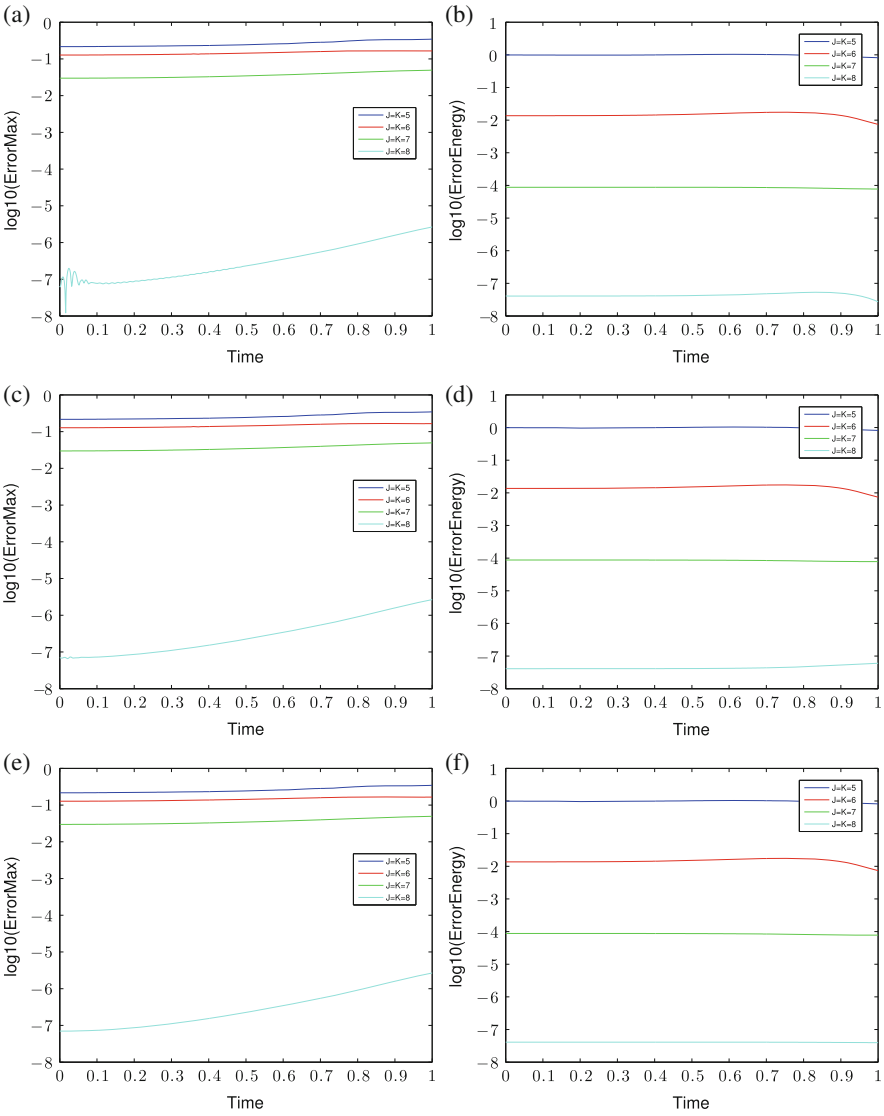

Fig. 17 Evolution of $\mathrm{Err}_{J,K}^{n,\infty}$ and $\mathscr{E}_{J,K}^{n,\infty}$ for the TSSP1-ADI, TSSP2-ADI and ReSP schemes and different spatial grids. (**a**) $\mathrm{Err}_{J,K}^{n,\infty}$ for TSSP1-ADI; (**b**) $\mathscr{E}_{J,K}^{n,\infty}$ for TSSP1-ADI; (**c**) $\mathrm{Err}_{J,K}^{n,\infty}$ for TSSP2-ADI; (**d**) $\mathscr{E}_{J,K}^{n,\infty}$ for TSSP2-ADI; (**e**) $\mathrm{Err}_{J,K}^{n,\infty}$ for ReSP; (**f**) $\mathscr{E}_{J,K}^{n,\infty}$ for ReSP

that the high accuracy of the TSSP1-ADI, TSSP2-ADI and ReSP is obtained for a sufficiently fine grid, i.e. $J, K \geq 8$. Concerning the coarser grids, the error is relatively important and localized near the central vortex. For this example, the

spatial accuracy of the three schemes is about the same. Finally, the energy which is a global quantity is quite accurately computed even for coarse grids.

We are now interested in computing the order of accuracy in time of the three schemes. We also want to analyze the mass and energy (without the rotational term) conservation properties. To numerically obtain the order, we use the Richardson method. Let us denote by $\boldsymbol{\psi}_{\delta t}^k \in \mathbb{C}^M$, $k \in \mathbb{N}$, the numerical approximation of a solution ψ^k of the problem (130) at time $t_k > 0$ by a numerical scheme for a time step δt. Then, the Richardson method consists in computing the numerical order of accuracy by the expression

$$p_{k,\text{num}} := \log_2 \left(\frac{\|\boldsymbol{\psi}_{\delta t}^k - \boldsymbol{\psi}_{\delta t/2}^k\|_{\ell_\pi^2}}{\|\boldsymbol{\psi}_{\delta t/2}^k - \boldsymbol{\psi}_{\delta t/4}^k\|_{\ell_\pi^2}} \right), 1 \leq k \leq N_{\delta t}. \tag{129}$$

Indeed, if we assume that the order is p, we have

$$\|\boldsymbol{\psi}_{\delta t}^k - \boldsymbol{\psi}_{\delta t/2}^k\|_{\ell_\pi^2} \approx C\delta t^p,$$

and

$$\|\boldsymbol{\psi}_{\delta t/2}^k - \boldsymbol{\psi}_{\delta t/4}^k\|_{\ell_\pi^2} \approx C\frac{\delta t^p}{2^p},$$

leading to (129). Let us consider $J = K = 2^9$ grid points. We take: $t_k N_{\delta t} = k$, with $1 \leq k \leq N_{\delta t}$. We report two cases: $\delta t = 10^{-2}$ (Table 5) and $\delta t = 10^{-3}$ (Table 6). Here, we introduce the different quantities

$$\max p_{N_{\delta t},\text{num}} := \max_{1\leq k\leq N_{\delta t}} p_{k,\text{num}}, \qquad \min p_{N_{\delta t},\text{num}} := \min_{1\leq k\leq N_{\delta t}} p_{k,\text{num}},$$

and

$$\text{mean } p_{N_{\delta t},\text{num}} := \frac{1}{N_{\delta t}} \sum_{k=1}^{N_{\delta t}} p_{k,\text{num}}.$$

Table 5 Numerical orders of the TSSP1-ADI, TSSP2-ADI and ReSP schemes for $\delta t = 10^{-2}$

	TSSP1-ADI	TSSP2-ADI	ReSP
$\max p_{N_{\delta t},\text{num}}$	5.45	6.01	2.04
$\min p_{N_{\delta t},\text{num}}$	1.00	2.02	1.84
$\text{mean } p_{N_{\delta t},\text{num}}$	2.54	3.97	1.91

Table 6 Numerical orders of the TSSP1-ADI, TSSP2-ADI and ReSP schemes for $\delta t = 10^{-3}$

	TSSP1-ADI	TSSP2-ADI	ReSP
$\max p_{N_{\delta t},\text{num}}$	1.00	2.00	1.99
$\min p_{N_{\delta t},\text{num}}$	0.99	2.00	1.99
$\text{mean } p_{N_{\delta t},\text{num}}$	1.00	2.00	1.99

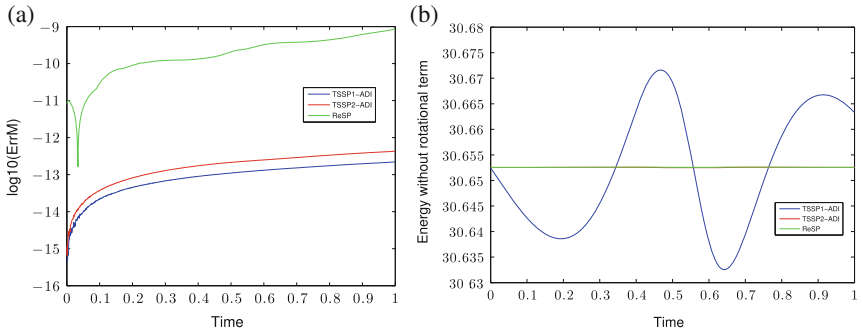

Fig. 18 Mass and energy (without rotational term) conservation properties for the three schemes, for $\delta t = 10^{-3}$ and problem (130). (**a**) Mass conservation; (**b**) energy (without rotational term) conservation

For $\delta t = 10^{-2}$, the numerical orders of TSSP1-ADI and TSSP2-ADI are in average higher than those expected. This can be explained by the fact that the time step is too large to get a stable scheme and that instabilities arise most particularly because of the rotational term. The ReSP scheme seems to provide a better accuracy. For $\delta t = 10^{-3}$, we recover the expected orders for the three schemes.

We now report (see Fig. 18a) the error on the mass of the solution: $\text{ErrM}^n := ||1 - \mathcal{N}(\boldsymbol{\psi}^n)||_\infty$ and the error (Fig. 18b) on the non rotating energy of the solution: $\mathscr{E}_{0,\beta}(\boldsymbol{\psi}^n)$, for a time step $\delta t = 10^{-3}$. We can see that the mass is not exactly conserved but the error is relatively small, even if it increases in time. The ReSP scheme is the scheme that presents the best mass conservation property for this example. In addition, the non rotational energy is well conserved for both the TSSP2-ADI and ReSP schemes while TSSP1-ADI exhibits large fluctuations.

We end the analysis by showing the evolution of the error on the mass (Fig. 19a) and energy without the rotational term $\mathscr{E}_{0,\beta}(\boldsymbol{\psi}^n)$ (Fig. 19b) for $\delta t = 10^{-2}$. For the three schemes, we observe that the error on the mass is smaller than when considering the time step $\delta t = 10^{-3}$. Nevertheless, the energy also grows substantially in the middle of the simulation for both TSSP1-ADI and TSSP2-ADI. The ReSP scheme conserves correctly the non rotating energy. This example shows that ReSP is a robust and accurate scheme.

4.6.2 Experiment II: Dynamics of a BEC in Quadratic-Plus-Quartic Trap

The second example consists in solving the following two-dimensional GPE

$$\begin{cases} i\partial_t \psi(t,\mathbf{x}) = -\dfrac{1}{2}\Delta\psi(t,\mathbf{x}) - \Omega L_z \psi(t,\mathbf{x}) + V(\mathbf{x})\psi(t,\mathbf{x}) \\ \qquad\qquad +\beta|\psi|^2\psi(t,\mathbf{x}),\ \forall t \in [0,T],\ \forall \mathbf{x} \in \mathbb{R}^2, \\ \psi(0,\mathbf{x}) = \psi_0(\mathbf{x}) \in L^2_{\mathbf{x}}, \end{cases} \tag{130}$$

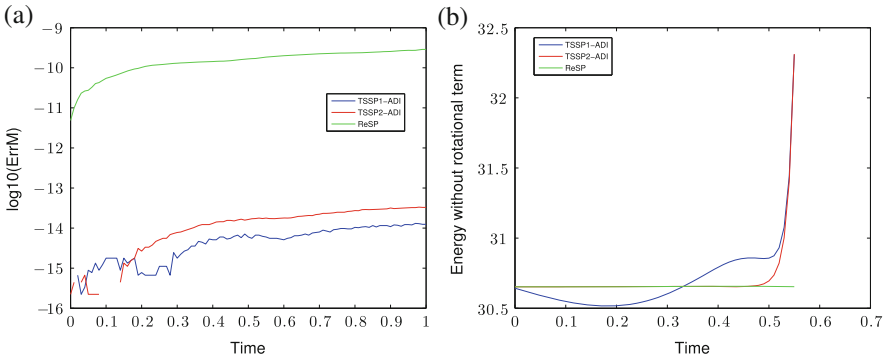

Fig. 19 Mass and energy conservation (without rotational term) properties for the three schemes, for $\delta t = 10^{-2}$ and problem (130). (**a**) Mass conservation; (**b**) energy conservation (without rotational term)

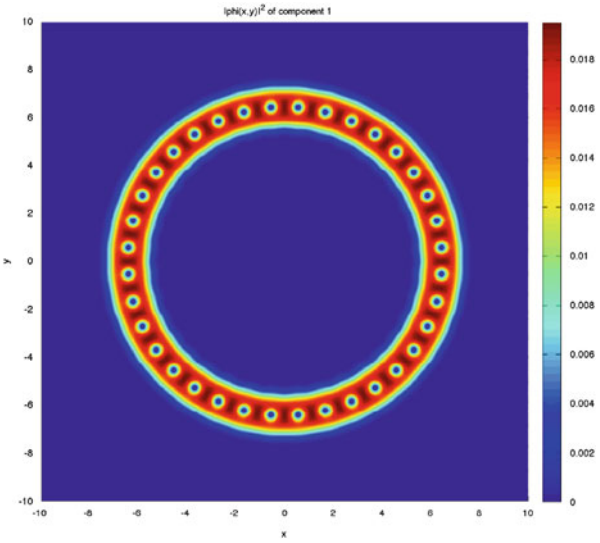

Fig. 20 Density $|\psi_0|^2$ of the stationary state (with a domain $\mathscr{O} =]-10, 10[^2$, $J = K = 2^8$ for BESP)

where $\Omega = 3.5$ and $\beta = 1000$. The potential is the quadratic-plus-quartic potential

$$V(\mathbf{x}) = \frac{1-\alpha}{2}(\gamma_x x^2 + \gamma_y y^2) + \frac{\kappa}{4}(\gamma_x x^2 + \gamma_y y^2)^2,$$

where $\gamma_x = \gamma_y = 1$, $\alpha = 1.2$ and $\kappa = 0.7$. To obtain the initial data ψ_0, we compute the stationary state of (130) for the trapping parameters $\gamma_x = \gamma_y = 1$, $\alpha = 1.2$ and $\kappa = 0.3$ (see Fig. 20). The stationary state is a circular ring with 36 uniformly distributed vortices.

The parameters for the simulation of the dynamics with TSSP1-ADI, TSSP2-ADI and ReSP are: $\delta t = 10^{-3}$ for a maximal time of computation $T = 1$ ($T := N\delta t$), a spatial discretization with $J = K = 2^8$ points in $\mathscr{O} =]-10, 10[^2$. Concerning the ReSP scheme, the linear system is again solved by BiCGStab for a stopping criterion on the residual equal to $\varepsilon^{\text{Krylov}} = 10^{-12}$. We report on Fig. 21 some snapshots of the solution obtained with TSSP2-ADI. We observe a complex dynamics in the ring

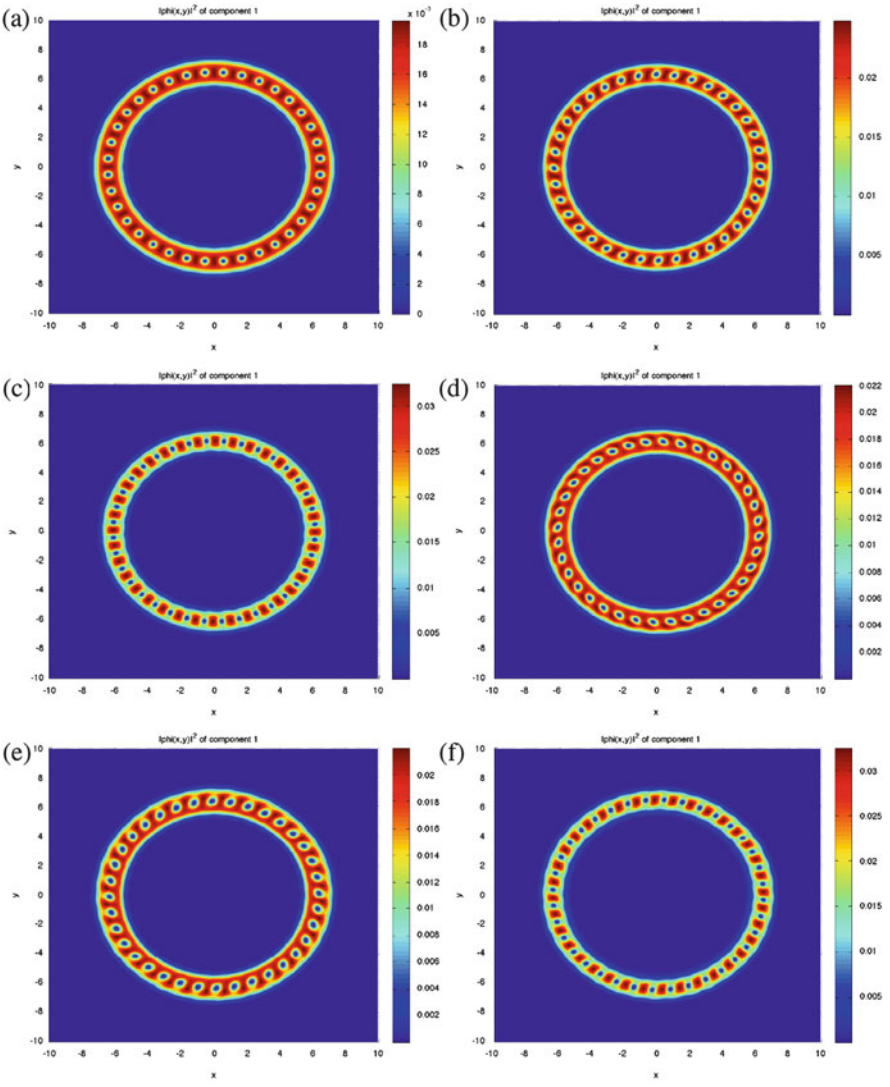

Fig. 21 Snapshots of the density $|\psi|^2$ computed with TSSP2-ADI for problem (130). (**a**) $t = 0$; (**b**) $t = 0.07$; (**c**) $t = 0.14$; (**d**) $t = 0.21$; (**e**) $t = 0.28$; (**f**) $t = 0.35$

Table 7 Numerical orders of the TSSP1-ADI, TSSP2-ADI and ReSP schemes for $\delta t = 10^{-2}$

	TSSP1-ADI	TSSP2-ADI	ReSP
max $p_{N_{\delta t},\text{num}}$	1.15	1.97	1.55
min $p_{N_{\delta t},\text{num}}$	0.89	0.85	0.08
mean $p_{N_{\delta t},\text{num}}$	0.95	1.08	0.92

Table 8 Numerical orders of the TSSP1-ADI, TSSP2-ADI and ReSP schemes for $\delta t = 10^{-3}$

	TSSP1-ADI	TSSP2-ADI	ReSP
max $p_{N_{\delta t},\text{num}}$	1.01	2.30	1.99
min $p_{N_{\delta t},\text{num}}$	0.99	2.00	1.98
mean $p_{N_{\delta t},\text{num}}$	1.00	2.02	1.99

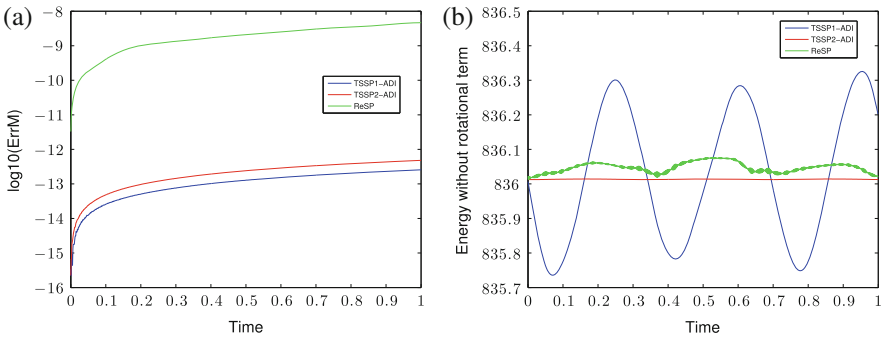

Fig. 22 Mass and energy conservation properties for the three schemes, for $\delta t = 10^{-3}$ and problem (130). (**a**) Mass conservation; (**b**) conservation of the energy without rotational term

BEC. The solutions computed by TSSP2-ADI and ReSP looks the same. Unlike the first experiment, it is not possible here to analyze the spatial accuracy of the schemes since the extrapolated stationary state is not accurate enough on a coarse grid with $J = K = 2^7$ points. If one considers more grid points ($J = K \geq 2^9$ points), the computational time is too large for GPELab.

We now focus on the numerical order of the TSSP1-ADI, TSSP2-ADI and ReSP schemes and on the discrete mass and energy conservation properties. For $\delta t = 10^{-2}$, the orders are not recovered because the time step is too large (Table 7). For $\delta t = 10^{-3}$ (Table 8), the numerical orders are consistent with their respective theoretical values, meaning that the time step is sufficiently small.

We consider now the evolution of the error ErrM^n on the mass of the solution (Fig. 22a) and the non rotational energy $\mathscr{E}_{0,\beta}(\boldsymbol{\psi}^n)$ (Fig. 22b) for $\delta t = 10^{-3}$. The mass is not exactly preserved for the three schemes but is numerically acceptable. The energy (without the rotational term) $\mathscr{E}_{0,\beta}(\boldsymbol{\psi}^n)$ is well conserved for the TSSP2-ADI scheme. Concerning the ReSP scheme, the energy fluctuates a little. For the TSSP1-ADI scheme, the energy is not conserved. For $\delta t = 10^{-2}$, we have no energy conservation for the three schemes. Globally, TSSP2-ADI is the best scheme for this specific problem.

4.6.3 Experiment III: Dynamics of a 2d Dark Soliton

The last example consists in the simulation of a black soliton inside a BEC. We consider the two-dimensional GPE

$$i\partial_t \psi(t,\mathbf{x}) = -\frac{1}{2}\Delta\psi(t,\mathbf{x}) + \frac{1}{2}\left(|x|^2 + |y|^2\right)\psi(t,\mathbf{x}) + \beta|\psi(t,\mathbf{x})|^2\psi(t,\mathbf{x}), \qquad (131)$$

with $\beta = 10000$. To get a physically admissible initial data, we first compute a stationary state of (131) by using the BESP scheme for $\delta t = 10^{-1}$ and the stopping criterion $\varepsilon = 10^{-8}$. The computational domain $\mathscr{O} =]-10, 10[^2$ is discretized by a uniform grid with $2^9 + 1$ points in the x- and y-directions. We choose the Thomas-Fermi approximation to initialize the computation. The converged solution is given on Fig. 23.

We now phase-imprint the black soliton in the condensate and simulate its dynamics. We use ReSP with a time step δt equal to 10^{-3}. The final time of computation is $T = 1.5$. A phase-imprinting method [54] is used to initiate the

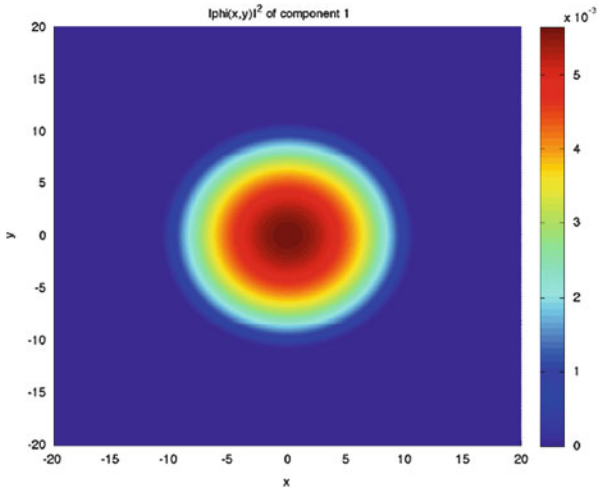

Fig. 23 Modulus of the stationary state computed by BESP with the parameters of Sect. 4.6.3

propagation of a black soliton in the condensate. More precisely, the initial data is multiplied by

$$\xi(\mathbf{x}) = e^{i\frac{\Delta\theta_0}{2}(1+\tanh(\frac{x-x_0}{s}))},$$

where $\Delta\theta_0 = \pi/3$, $x_0 = 5$ and $s = 0.2$. We represent a few snapshots of the computed solution on Fig. 24 with the new initial data.

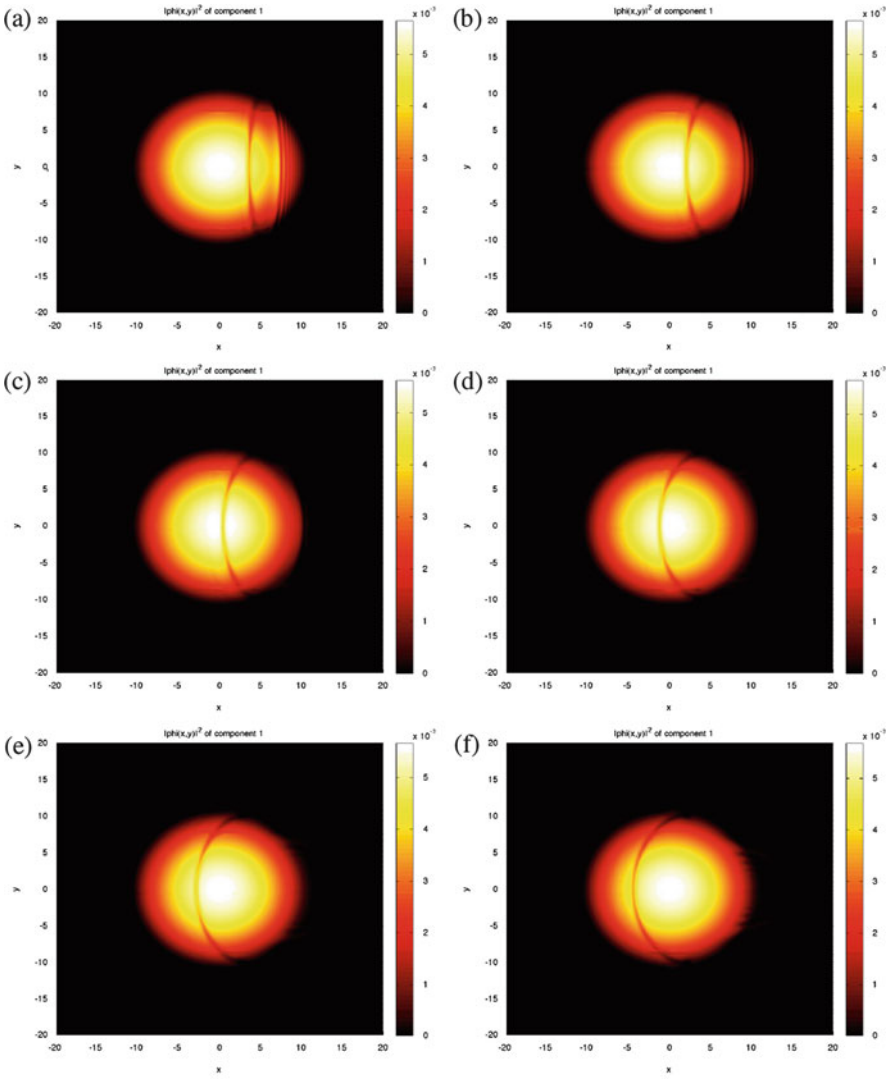

Fig. 24 Dynamics of a phase-imprinted black soliton in a BEC by using the ReSP scheme. (**a**) Soliton at time $t = 0.25$; (**b**) soliton at time $t = 0.5$; (**c**) soliton at time $t = 0.75$; (**d**) soliton at time $t = 1$; (**e**) soliton at time $t = 1.25$; (**f**) soliton at time $t = 1.5$

5 Computation of the Dynamics with Stochastic Terms

The aim of this last section is to provide a few ideas concerning the extension of the previous schemes when a random term is included into the GPE. Let us consider the stochastic GPE (see Sect. 1.3.3)

$$\begin{cases} i\partial_t\psi(t,\mathbf{x}) = -\dfrac{1}{2}\Delta\psi(t,\mathbf{x}) - \Omega L_z\psi(t,\mathbf{x}) + \dfrac{1}{2}|\mathbf{x}|^2\psi(t,\mathbf{x})(1+\dot{w}_t) \\ \qquad\qquad +\beta|\psi|^{2\sigma}\psi(t,\mathbf{x}),\ \forall t\in\mathbb{R}^+,\ \forall\mathbf{x}\in\mathbb{R}^d, \\ \psi(0,\mathbf{x}) = \psi_0(\mathbf{x}) \in L^2_{\mathbf{x}}, \end{cases} \tag{132}$$

where $\beta\in\mathbb{R}$, $\sigma>0$ and $(w_t)_{t\in\mathbb{R}+}\in\mathscr{C}^\gamma_t(\mathbb{R}^+)$ is a Hölder continuous function, with $\gamma\in]0,1[$. More generally, we consider the following stochastic GPE ($d=1,2,3$) for the potential $V(\dot{w}_t,\mathbf{x}) := V(\mathbf{x})\dot{w}_t$

$$\begin{cases} i\partial_t\psi(t,\mathbf{x}) = -\dfrac{1}{2}\Delta\psi(t,\mathbf{x}) - \Omega L_z\psi(t,\mathbf{x}) + V(\dot{w}_t,\mathbf{x})\psi(t,\mathbf{x}) \\ \qquad\qquad +f(|\psi|^2)\psi(t,\mathbf{x}),\ \forall t\in\mathbb{R}^+,\ \forall\mathbf{x}\in\mathbb{R}^d, \\ \psi(0,\mathbf{x}) = \psi_0(\mathbf{x}) \in L^2_{\mathbf{x}}, \end{cases} \tag{133}$$

where f is a real-valued polynomial function.

5.1 Numerical Schemes for the Stochastic GPE

We discuss the way the stochastic potential has to be discretized in the (Lie and Strang) time-splitting and relaxation schemes. For the time-splitting schemes (Sect. 5.1.1), the integration is similar to the deterministic case. Concerning the meaning of the time-derivative of a continuous process, we use the definition given by Sussmann [115]. For the relaxation scheme (Sect. 5.1.2), we introduce the Stratonovich product to precise the formal time-derivative of a continuous process that will have to be discretized.

5.1.1 The Time-Splitting Schemes

Following Sussmann's approach, we first assume that the process $(w_t)_{t\in\mathbb{R}+}$ is in $\mathscr{C}^1_t(\mathbb{R}^+)$. For the Lie time-splitting scheme, we use the following decomposition of the problem (133): let $\delta t>0$, $n\in\mathbb{N}$,

1. Solve the system

$$\begin{cases} i\partial_t \psi_1(t,\mathbf{x}) = -\dfrac{1}{2}\Delta\psi_1(t,\mathbf{x}) - \Omega L_z \psi_1(t,\mathbf{x}),\ t \in]t_n, t_{n+1}], \\ \psi_1(t_n,\mathbf{x}) = \psi^n(\mathbf{x}). \end{cases} \tag{134}$$

2. Compute ψ_2 solution to

$$\begin{cases} i\partial_t \psi_2(t,\mathbf{x}) = V(\dot{w}_t,\mathbf{x})\psi_2(t,\mathbf{x}) + \beta|\psi_2(t,\mathbf{x})|^2\psi_2(t,\mathbf{x}),\ t \in]t_n, t_{n+1}], \\ \psi_2(t_n,\mathbf{x}) = \psi_1(t_{n+1},\mathbf{x}). \end{cases} \tag{135}$$

The Eq. (134) is solved by the ADI method and one-directional FFTs like for the deterministic case (see Sect. 4.2.2). For (135), we have seen in Sect. 4.2.2 that it is possible to exactly integrate the equation for the nonlinearity and potential, and then to obtain an explicit formula. It follows that, for all $t \in [t_n, t_{n+1}]$,

$$\psi_2(t,\mathbf{x}) = \psi_1(t_{n+1},\mathbf{x}) e^{-if(|\psi_1(t_{n+1},\mathbf{x})|^2)(t-t_n) - i\int_{t_n}^t V(\dot{w}_s,\mathbf{x})ds}.$$

The time integration of the stochastic potential is direct

$$\int_{t_n}^t V(\dot{w}_s,\mathbf{x})ds = \int_{t_n}^t V(\mathbf{x})\dot{w}_s ds = V(\mathbf{x})(w_t - w_{t_n}) = V(w_t - w_{t_n},\mathbf{x}),$$

leading to the exact formula for (135)

$$\psi_2(t,\mathbf{x}) = \psi_1(t_{n+1},\mathbf{x}) e^{-if(|\psi_1(t_{n+1},\mathbf{x})|^2)(t-t_n) - iV(w_t - w_{t_n},\mathbf{x})}.$$

This means that the implementation in the Lie time-splitting scheme is straightforward. Moreover, it is easy to see that this solution is continuous with respect to $(w_t)_{t\in\mathbb{R}^+} \in \mathscr{C}_t(\mathbb{R}^+)$. Following a similar approach to Sussmann, we can extend the solution to the case of a continuous process by using a density argument. The extension to the Strang time-splitting scheme is trivial. The stochastic schemes are still called TSSP1-ADI and TSSP2-ADI.

5.1.2 The Relaxation Scheme

In Sect. 4.3, we derived the relaxation scheme for the deterministic GPE. Concerning the extension to the stochastic case, the main difference is related to the way the noise is discretized. To have a better understanding of how to discretize the derivative of the stochastic process, it is necessary to define the meaning of the

following stochastic integral

$$\int_{t_n}^{t_{n+1}} V(\dot{w}_s, \mathbf{x})\psi(s, \mathbf{x})ds = V(\mathbf{x}) \int_{t_n}^{t_{n+1}} \dot{w}_s \psi(s, \mathbf{x})ds.$$

Here, we consider this integral as the Stratonovich integral, i.e.

$$\begin{aligned}\int_{t_n}^{t_{n+1}} \dot{w}_s \psi(s, \mathbf{x})ds &= \int_{t_n}^{t_{n+1}} \psi(s, \mathbf{x}) \circ dw_s \\ &:= \lim_{\ell \to \infty} \sum_{(s_k)_{0 \le k \le \ell}} \frac{\psi(s_{k+1}, \mathbf{x}) + \psi(s_k, \mathbf{x})}{2} \left(w_{s_{k+1}} - w_{s_k}\right),\end{aligned}$$

where, $\forall \ell \in \mathbb{N}$, $(s_k)_{0 \le k \le \ell}$ is a partition of the interval $[t_n, t_{n+1}]$. This type of integral takes its meaning for a Wiener process $(W_t)_{t \in \mathbb{R}+}$ (also called the brownian motion) through

$$\int_{t_n}^{t_{n+1}} V(\dot{w}_s, \mathbf{x})\psi(s, \mathbf{x}) \approx V(\mathbf{x}) \frac{\psi(t_{n+1}, \mathbf{x}) + \psi(t_n, \mathbf{x})}{2} \left(w_{t_{n+1}} - w_{t_n}\right). \tag{136}$$

The associated ReSP scheme related to the discretization (136) for the problem (133) is then

$$\begin{cases} \dfrac{\phi^{n+1/2} + \phi^{n-1/2}}{2} = f(|\psi^n|^2), \\ i\dfrac{\psi^{n+1} - \psi^n}{\delta t} = (-\dfrac{1}{2}\Delta - \Omega L_z + V^n + \phi^{n+1/2})(\dfrac{\psi^{n+1} + \psi^n}{2}), \end{cases} \tag{137}$$

where $\phi^{n+1/2} = \phi(t_{n+1/2}, \mathbf{x})$, $\psi^n = \psi(t_n, \mathbf{x})$ and $V^n = V((w_{t_{n+1}} - w_{t_n})/\delta t, \mathbf{x})$. The initial data are

$$\psi^0(\mathbf{x}) = \psi_0(\mathbf{x}), \quad \text{and} \quad \phi^{-1/2}(\mathbf{x}) = \beta|\psi_0(\mathbf{x})|^2.$$

5.2 *Numerical Examples*

We present here a few numerical simulations. First, we explain how to correctly and efficiently simulate a fractional brownian motion (Sect. 5.2.1). Next, examples of computations are given for a one-dimensional example. Most particularly, we numerically explore the order of the schemes of the stochastic GPE under consideration (see Sect. 5.2.2).

5.2.1 Simulation of Fractional Brownian Motions

The simulation of stochastic gaussian processes with stationary increments can be efficiently and accurately realized by using FFTs [124]. Let us recall that a fractional brownian motion (fbm) $(W_t^H)_{t\in\mathbb{R}+}$, with Hurst index $H \in]0,1[$, is a gaussian process with the following properties

- $(W_t^H)_{t\in\mathbb{R}+}$ is continuous and self-similar, i.e.

$$\forall t \in \mathbb{R}^+,\ \forall a \in \mathbb{R}^+, \quad \frac{1}{a^H} W_{at}^H = W_t^H \text{ in law}, \tag{138}$$

- $W_0^H = 0$ almost surely,
- the increments $W_t^H - W_s^H$, for all $t, s \in \mathbb{R}^+$, such that $t \geq s$, are stationary and follow a normal distribution law with zero mean and $(t-s)^{2H}$ as variance,
- for all $t, s \in \mathbb{R}^+$, such that $t \geq s$, we have

$$\mathbb{E}[W_t^H W_s^H] = \frac{1}{2}(t^{2H} + s^{2H} - |t-s|^{2H}). \tag{139}$$

Let $(t_j)_{j\in\mathbb{N}}$ be a uniform time discretization of $[0,1]$. Then, we remark that, being given the increments $(\delta W_{t_{j+1}}^H)_{j\in\mathbb{N}} = (W_{t_{j+1}}^H - W_{t_j}^H)_{j\in\mathbb{N}}$, the fbm can be built through the telescoping sum

$$W_{t_j}^H = \sum_{k=1}^{j} \delta W_{t_k}^H.$$

Therefore, we have to simulate the fbm increments to construct the process. Moreover, thanks to the self-similarity of the process (138), we remark that the simulation of a fbm for $(t_j)_{j\in\mathbb{N}}$ boils down to the simulation of a fbm for the time discretization $(t_j = j)_{j\in\mathbb{N}}$. In this case, for all $k \in \mathbb{Z}$, the autocovariance function $c_{W^H}(k)$ of the process $(\delta W_j^H)_{j\in\mathbb{N}}$ is given by

$$c_{W^H}(k) = \mathbb{E}[\delta W_{j+k}^H \delta W_j^H] = \frac{1}{2}(|k+1|^{2H} + |k-1|^{2H} - 2|k|^{2H}).$$

If we assume that we want to construct a process of length $N \in \mathbb{N}$ and being given the stationary process $(\delta W_j^H)_{j\in\{1,\ldots,N\}}$, its spectral density [55, 124] is such that

$$\forall j \in \{-N/2, \ldots, N/2-1\}, \quad s_{W^H}(j) = \sum_{k=-N/2}^{N/2-1} c_{W^H}(k) e^{-2\pi i \frac{jk}{N}}.$$

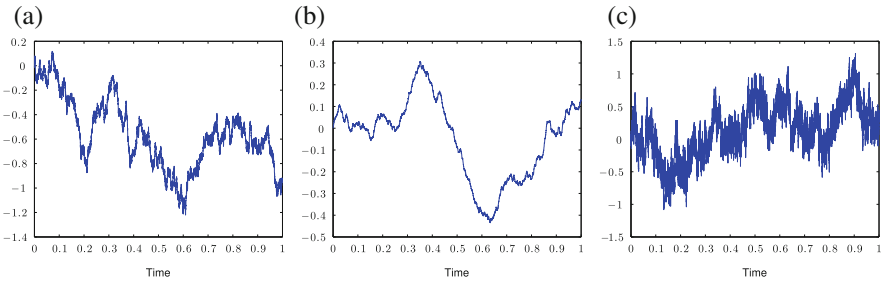

Fig. 25 Trajectories of the fbm for various Hurst indices H on the time interval $[0, 1]$. (**a**) Fractional brownian motion for $H = 1/2$. (**b**) Fractional brownian motion for $H = 3/4$. (**c**) Fractional brownian motion for $H = 1/4$

By using this expression, the following spectral representation of the process [124] can be obtained

$$\delta W_k^H = \Re\Big(\sqrt{\frac{2}{N}} \sum_{j=-N/2}^{N/2-1} \sqrt{s_{W^H}(j)}\, \widehat{W^{1/2}}_j e^{2\pi i \frac{jk}{N}}\Big),$$

where $(\widehat{W^{1/2}}_j)_{j\in\{-N/2,\ldots,N/2-1\}}$ is the discrete Fourier transform of the brownian motion. Therefore, the increments of a fbm can be efficiently computed with high precision. We report on Fig. 25 the simulation of fbm trajectories for various values of H, on a uniformly discretized time interval $[0, 1]$ (with $\delta t = 10^{-4}$).

5.2.2 Order in Time of the Schemes for the Stochastic GPE

We now numerically study the order in time of the Lie and Strang time-splitting and relaxation schemes for a stochastic potential. The order in time can be understood as the largest real number p such that

$$\mathbb{E}\Big[\|\psi_{\delta t}(t_n, \mathbf{x}) - \psi(t_n, \mathbf{x})\|_{L^2_{\mathbf{x}}}^2\Big]^{1/2} \leq C(\delta t)^p,$$

where $C > 0$ is a real-valued positive constant, ψ is the exact solution of the dynamical system and $\psi_{\delta t}$ is the approximation of ψ by using a numerical scheme for a time step δt. Numerically computing such an order requires the simulation of a large number of trajectories of the process $(w_t)_{t\in\mathbb{R}+}$ for the problem (132) since the mean error is approximated by a Monte-Carlo method. For $N(\in \mathbb{N})$ trajectories $(w_t^j)_{t\in\mathbb{R}+}$, $1 \leq j \leq N$, we compute the numerical approximation of the solution $\psi_{\delta t}^j$ of (132) by using one of the numerical schemes. For a sufficiently large value N,

one gets

$$\mathbb{E}\left[\|\psi_{\delta t}(t_n,\mathbf{x})-\psi(t_n,\mathbf{x})\|_{L^2_{\mathbf{x}}}^2\right]^{1/2} \approx \sum_{j=1}^{N}\left(\|\psi^j_{\delta t}(t_n,\mathbf{x})-\psi(t_n,\mathbf{x})\|_{L^2_{\mathbf{x}}}^2\right)^{1/2}.$$

Therefore, p can be estimated by a numerical order p_{num} that is computed thanks to a formula similar to (129)

$$p(t_k) \approx p_{\text{num}}(t_k) := \log_2\left(\frac{\mathbb{E}[\|\psi_{\delta t}(t_k,\mathbf{x})-\psi_{\delta t/2}(t_k,\mathbf{x})\|_{L^2_{\mathbf{x}}}^2]^{1/2}}{\mathbb{E}[\|\psi_{\delta t/2}(t_k,\mathbf{x})-\psi_{\delta t/4}(t_k,\mathbf{x})\|_{L^2_{\mathbf{x}}}^2]^{1/2}}\right). \tag{140}$$

In the following study, we are interested in the fbm of Hurst index H that we denote by $(W_t^H)_{t\in\mathbb{R}+}$, $H\in]0,1[$. As previously mentioned, the fbm are gaussian processes with zero mean that are generalizations of the brownian motion. Moreover, their trajectories are $(H-\eta)$-Hölder continuous, for all $\eta>0$. This means that we can analyze the schemes for processes with various smoothness.

Let us now consider the following one-dimensional stochastic GPE

$$\begin{cases} i\partial_t\psi(t,x) = -\dfrac{1}{2}\partial_x^2\psi(t,x)+\dfrac{1}{2}x^2\psi(t,x)(1+\dot{W}_t^H) \\ \qquad\qquad +\beta|\psi|^2\psi(t,x),\ \forall t\in\mathbb{R}^+,\ \forall x\in\mathbb{R}, \\ \psi(0,x)=\psi_0(x)\in L^2_x, \end{cases} \tag{141}$$

where $\beta=300$ and $(W_t^H)_{t\in\mathbb{R}+}$ is a fbm with Hurst index $H\in]0,1[$. The initial data ψ_0 is a stationary state computed by the BESP scheme. The computational domain $\mathscr{O}=]-15,15[$ is discretized by a uniform grid $\mathscr{O}_J$, where $J=2^9$. We fix the time step to $\delta t=10^{-3}$ and the final time of computation to $T=1$. The numerical results of the Monte-Carlo method are based on $N=1000$ trajectories.

We report in Table 9 the numerical orders resulting from formula (140) for the Lie splitting scheme. We remark that the order is linked to the Hurst index H. For $H\geq 1/2$, the order saturates to 1 while for $H<1/2$ it is less than 1. For $H=1/4$, we observe that N is not large enough to yield a good approximation of the order and the scheme seems unstable.

We consider now the Strang time-splitting scheme (TSSP2-ADI). The numerical orders are given in Table 10. We observe that the order can be larger than 1 like for $H=3/4$. There is no saturation in the numerical order. Furthermore, we notice that the numerical order for a fbm of Hurst index $H=1/4$ significantly fluctuates.

Table 9 Numerical orders of the TSSP1-ADI scheme for the stochastic GPE (141), with various Hurst indices H of the fbm

	$H=1/4$	$H=1/2$	$H=3/4$
$\max_{t_k} p_{\text{num}}(t_k)$	0.87	1.10	1.06
$\min_{t_k} p_{\text{num}}(t_k)$	0.67	0.91	0.97
$\text{mean}_{t_k} p_{\text{num}}(t_k)$	0.76	1.01	1.01

Table 10 Numerical orders of the TSSP2-ADI scheme for the stochastic GPE (141), with various Hurst indices H for the fbm

	$H = 1/4$	$H = 1/2$	$H = 3/4$
$\max_{t_k} p_{\text{num}}(t_k)$	1.59	1.14	1.59
$\min_{t_k} p_{\text{num}}(t_k)$	−0.04	0.90	0.97
$\text{mean}_{t_k} p_{\text{num}}(t_k)$	0.89	1.01	1.33

Table 11 Numerical orders of the ReSP scheme for the stochastic GPE (141), with various Hurst indices H for the fbm and $\beta = 300$

	$H = 1/4$	$H = 1/2$	$H = 3/4$
$\max_{t_k} p_{\text{num}}(t_k)$	1.10	0.80	1.58
$\min_{t_k} p_{\text{num}}(t_k)$	0.27	0.43	1.31
$\text{mean}_{t_k} p_{\text{num}}(t_k)$	0.84	0.58	1.49

Table 12 Numerical orders of the ReSP scheme for the stochastic GPE (141), with various Hurst indices H for the fbm and $\beta = 100$

	$H = 1/4$	$H = 1/2$	$H = 3/4$
$\max_{t_k} p_{\text{num}}(t_k)$	0.02	0.99	1.60
$\min_{t_k} p_{\text{num}}(t_k)$	−0.12	0.43	1.42
$\text{mean}_{t_k} p_{\text{num}}(t_k)$	0.00	0.76	1.51

This is probably due to the fact that N is not large enough to obtain a correct approximation of the order of TSSP2-ADI. The numerical order of the standard brownian motion ($H = 1/2$) is not improved in comparison with the TSSP1-ADI scheme.

Table 11 shows the results obtained for the ReSP scheme. For a standard brownian motion ($H = 1/2$), the order of the ReSP scheme is lower order than for the time-splitting schemes. In the case of a fbm of Hurst index $H = 3/4$, the numerical order is larger than 1 and higher than for TSSP2-ADI. The numerical order for the fbm with $H = 1/4$ is fluctuating. Therefore, it is not possible to conclude on the effective order of the scheme. This is probably due to the fact that the discretization used for the noise [see Eq. (136)] is not adapted to a process with a smoothness lower than the brownian motion.

To complete the numerical simulation for ReSP, we run the same tests as before but with a smaller nonlinearity β ($\beta = 100$ here) to show its influence on the order of the scheme. We report the numerical orders on Table 12. For the brownian motion, we observe an improved order of accuracy which is closer to the value 1 obtained for the time-splitting schemes. For the fbm with Hurst index $3/4$, the order is practically unchanged. Finally, for $H = 1/4$, the problem of the discretization remains.

As seen before, TSSP2-ADI and ReSP are some suitable schemes for the stochastic GPE (accordingly to H). When a rotation term is further added, then they should be privileged for a practical computation. Since the related computations are too heavy for GPELab, we do not analyze this problem here. Furthermore, it would be interesting to develop a complete numerical analysis of these schemes to understand the rigorous mathematical properties that can be expected. However, these points are beyond the scope of this paper and can be considered as some open questions.

6 Conclusion

In this paper, we have developed some elements related to the modeling and computation of Bose-Einstein Condensates when the Gross-Pitaevskii Equation is used. We have introduced a few GPE systems in various physical situations of interest: dynamics, stationary states, multi-components BECs, inclusion of rotation and stochastic terms. Next, we have developed in details some stable pseudo-spectral numerical methods for computing the stationary states of GPEs. A few numerical examples have been produced by using the dedicated Matlab toolbox GPELab. Then, we have explained how to correctly reproduce the dynamics of BECs by using adapted computational schemes (time-splitting and relaxation methods). Again, various numerical examples have been presented to have a better understanding of the schemes. Finally, the extensions of the schemes to a stochastic GPE are explained and numerical simulations based on GPELab show what are the expected properties of the schemes, in particular concerning the accuracy in time.

Acknowledgements This work was partially supported by the French ANR grant ANR-12-MONU-0007-02 BECASIM ("Modèles Numériques" call).

References

1. F.K. Abdullaev, J.C. Bronski, G. Papanicolaou, Soliton perturbations and the random Kepler problem. Phys. D Nonlinear Phenomena **135**(3–4), 369–386 (2000)
2. F.K. Abdullaev, B.B. Baizakov, V.V. Konotop, Dynamics of a Bose-Einstein condensate in optical trap, in *Nonlinearity and Disorder: Theory and Applications*, ed. by F.K. Abdullaev, O. Bang, M.P. Sørensen. NATO Science Series, vol. 45 (Springer, Netherlands, 2001), pp. 69–78
3. F.K. Abdullaev, J.C. Bronski, R.M. Galimzyanov, Dynamics of a trapped 2d Bose-Einstein condensate with periodically and randomly varying atomic scattering length. Phys. D Nonlinear Phenomena **184**(1–4), 319–332 (2003)
4. S.K. Adhikari, Numerical solution of the two-dimensional Gross-Pitaevskii equation for trapped interacting atoms. Phys. Lett. A **265**(1), 91–96 (2000)
5. A. Aftalion, Q. Du, Vortices in a rotating Bose-Einstein condensate: critical angular velocities and energy diagrams in the Thomas-Fermi regime. Phys. Rev. A **64**(6), 063603 (2001)
6. A. Aftalion, T. Riviere, Vortex energy and vortex bending for a rotating Bose-Einstein condensate. Phys. Rev. A **64**(4), 043611 (2001)
7. A. Aftalion, X. Blanc, J. Dalibard, Vortex patterns in a fast rotating Bose-Einstein condensate. Phys. Rev. A **71**(2), 023611 (2005)
8. A. Aftalion, X. Blanc, F. Nier, Vortex distribution in the lowest Landau level. Phys. Rev. A **73**(1), 011601 (2006)
9. M.H. Anderson, J.R. Ensher, M.R. Matthews, C.E. Wieman, E.A. Cornell, Observation of Bose-Einstein condensation in a dilute atomic vapor. Science **269**(5221), 198–201 (1995)
10. X. Antoine, R. Duboscq, GPELab, a matlab toolbox for computing stationary solutions and dynamics of Gross-Pitaevskii equations (2014), http://www.gpelab.math.cnrs.fr
11. X. Antoine, R. Duboscq, GPELab, a Matlab toolbox to solve Gross-Pitaevskii equations I: computation of stationary solutions. Comput. Phys. Commun. **185**(11), 2969–2991 (2014)

12. X. Antoine, R. Duboscq, Robust and efficient preconditioned Krylov spectral solvers for computing the ground states of fast rotating and strongly interacting Bose-Einstein condensates. J. Comput. Phys. **258C**, 509–523 (2014)
13. X. Antoine, R. Duboscq, GPELab, a Matlab toolbox to solve Gross-Pitaevskii equations II: dynamics and stochastic simulations. Comput. Phys. Commun. **193**, 95–117 (2015)
14. X. Antoine, W. Bao, C. Besse, Computational methods for the dynamics of the nonlinear Schrödinger/Gross-Pitaevskii equations. Comput. Phys. Commun. **184**(12), 2621–2633 (2013)
15. V.I. Arnol'd, *Mathematical Methods of Classical Mechanics*. Graduate Texts in Mathematics (Springer, Berlin, 1989)
16. A.V. Avdeenkov, K.G. Zloshchastiev, Quantum Bose liquids with logarithmic nonlinearity: Self-sustainability and emergence of spatial extent. J. Phys. B Atomic Mol. Opt. Phys. **44**(19), 195303 (2011)
17. W. Bao, Ground states and dynamics of multicomponent Bose-Einstein condensates. Multiscale Model. Simul. **2**(2), 210–236 (2004)
18. W. Bao, Y. Cai, Ground states of two-component Bose-Einstein condensates with an internal atomic Josephson junction. East Asian J. Appl. Math. **1**, 49–81 (2011)
19. W. Bao, Y. Cai, Uniform error estimates of finite difference methods for the nonlinear Schrödinger equation with wave operator. SIAM J. Numer. Anal. **50**(2), 492–521 (2012)
20. W. Bao, Y. Cai, Mathematical theory and numerical methods for Bose-Einstein condensation. Kinet. Relat. Models **6**(1), 1–135 (2013)
21. W. Bao, Y. Cai, Optimal error estimates of finite difference methods for the Gross-Pitaevskii equation with angular momentum rotation. Math. Comput. **82**(281), 99–128 (2013)
22. W. Bao, Q. Du, Computing the ground state solution of Bose-Einstein condensates by a normalized gradient flow. SIAM J. Sci. Comput. **25**(5), 1674–1697 (2004)
23. W. Bao, J. Shen, A fourth-order time-splitting Laguerre-Hermite pseudospectral method for Bose-Einstein condensates. SIAM J. Sci. Comput. **26**(6), 2010–2028 (2005)
24. W. Bao, J. Shen, A generalized-Laguerre-Hermite pseudospectral method for computing symmetric and central vortex states in Bose-Einstein condensates. J. Comput. Phys. **227**(23), 9778–9793 (2008)
25. W. Bao, W. Tang, Ground-state solution of Bose-Einstein condensate by directly minimizing the energy functional. J. Comput. Phys. **187**(1), 230–254 (2003)
26. W. Bao, H. Wang, An efficient and spectrally accurate numerical method for computing dynamics of rotating Bose-Einstein condensates. J. Comput. Phys. **217**(2), 612–626 (2006)
27. W. Bao, S. Jin, P.A. Markowich, On time-splitting spectral approximations for the Schrödinger equation in the semiclassical regime. J. Comput. Phys. **175**(2), 487–524 (2002)
28. W. Bao, D. Jaksch, P.A. Markowich, Numerical solution of the Gross-Pitaevskii equation for Bose-Einstein condensation. J. Comput. Phys. **187**(1), 318–342 (2003)
29. W. Bao, S. Jin, P.A. Markowich, Numerical study of time-splitting spectral discretizations of nonlinear Schrödinger equations in the semiclassical regimes. SIAM J. Sci. Comput. **25**(1), 27–64 (2003)
30. W. Bao, H. Wang, P.A. Markowich, Ground, symmetric and central vortex states in rotating Bose-Einstein condensates. Commun. Math. Sci. **3**(1), 57–88 (2005)
31. W. Bao, I. Chern, F.Y. Lim et al., Efficient and spectrally accurate numerical methods for computing ground and first excited states in Bose-Einstein condensates. J. Comput. Phys. **219**(2), 836–854 (2006)
32. W. Bao, H. Li, J. Shen, A generalized-Laguerre-Fourier-Hermite pseudospectral method for computing the dynamics of rotating Bose-Einstein condensates. SIAM J. Sci. Comput. **31**(5), 3685–3711 (2009)
33. W. Bao, D. Marahrens, Q. Tang, Y. Zhang, A simple and efficient numerical method for computing the dynamics of rotating Bose-Einstein condensates via rotating lagrangian coordinates. SIAM J. Sci. Comput. **35**(6), A2671–A2695 (2013)
34. R.A. Battye, N.R. Cooper, P.M. Sutcliffe, Stable skyrmions in two-component Bose-Einstein condensates. Phys. Rev. Lett. **88**, 080401 (2002)

35. D. Baye, J-M. Sparenberg, Resolution of the Gross-Pitaevskii equation with the imaginary-time method on a Lagrange mesh. Phys. Rev. E **82**(5), 056701 (2010)
36. C. Besse, A relaxation scheme for the nonlinear Schrödinger equation. SIAM J. Numer. Anal. **42**(3), 934–952 (2004)
37. C. Besse, B. Bidégaray, S. Descombes, Order estimates in time of splitting methods for the nonlinear Schrödinger equation. SIAM J. Numer. Anal. **40**(1), 26–40 (2002)
38. X. Blanc, N. Rougerie, Lowest-Landau-level vortex structure of a Bose-Einstein condensate rotating in a harmonic plus quartic trap. Phys. Rev. A **77**(5), 053615 (2008)
39. S. Bose, Planck's law and the light quantum hypothesis. J. Astrophys. Astron. **15**(1), 3–7 (1994)
40. A.S. Bradley, C.W. Gardiner, The stochastic Gross-Pitaevskii equation: III (2006) [arXiv preprint cond-mat/0602162]
41. V. Bretin, S. Stock, Y. Seurin, J. Dalibard, Fast rotation of a Bose-Einstein condensate. Phys. Rev. Lett. **92**(5), 050403 (2004)
42. A.J. Brizard, *An Introduction to Lagrangian Mechanics* (World Scientific, Singapore, 2008)
43. D.A. Butts, D.S. Rokhsar, Predicted signatures of rotating Bose-Einstein condensates. Nature **397**(6717), 327–329 (1999)
44. M. Caliari, S. Rainer, GSGPEs: a matlab code for computing the ground state of systems of Gross-Pitaevskii equations. Comput. Phys. Commun. **184**(3), 812–823 (2013)
45. M. Caliari, C. Neuhauser, M. Thalhammer, High-order time-splitting Hermite and Fourier spectral methods for the Gross-Pitaevskii equation. J. Comput. Phys. **228**(3), 822–832 (2009)
46. E. Cancès, SCF algorithms for HF electronic calculations, in *Mathematical Models and Methods for Ab Initio Quantum Chemistry*, ed. by M. Defranceschi, C. Le Bris. Lecture Notes in Chemistry, vol. 74 (Springer, Berlin, 2000), pp. 17–43
47. M.M. Cerimele, M.L. Chiofalo, F. Pistella, S. Succi, M.P. Tosi, Numerical solution of the Gross-Pitaevskii equation using an explicit finite-difference scheme: an application to trapped Bose-Einstein condensates. Phys. Rev. E **62**(1), 1382 (2000)
48. M.L. Chiofalo, S. Succi, M.P. Tosi, Ground state of trapped interacting Bose-Einstein condensates by an explicit imaginary-time algorithm. Phys. Rev. E **62**(5), 7438 (2000)
49. N.R. Cooper, N.K. Wilkin, J.M.F. Gunn, Quantum phases of vortices in rotating Bose-Einstein condensates. Phys. Rev. Lett. **87**, 120405 (2001)
50. M. Correggi, N. Rougerie, J. Yngvason, The transition to a giant vortex phase in a fast rotating Bose-Einstein condensate. Commun. Math. Phys. **303**(2), 451–508 (2011)
51. I. Danaila, P. Kazemi, A new Sobolev gradient method for direct minimization of the Gross-Pitaevskii energy with rotation. SIAM J. Sci. Comput. **32**(5), 2447–2467 (2010)
52. K.B. Davis, M.-O. Mewes, M.R. van Andrews, N.J. Van Druten, D.S. Durfee, D.M. Kurn, W. Ketterle, Bose-Einstein condensation in a gas of sodium atoms. Phys. Rev. Lett. **75**(22), 3969–3973 (1995)
53. L. de Broglie, Ann. Phys. **3**, 22 (1925)
54. J. Denschlag, J.E. Simsarian, D.L. Feder, C.W. Clark, L.A. Collins, J. Cubizolles, L. Deng, E.W. Hagley, K. Helmerson, W.P. Reinhardt et al., Generating solitons by phase engineering of a Bose-Einstein condensate. Science **287**(5450), 97–101 (2000)
55. A.B. Dieker, M. Mandjes, On spectral simulation of fractional brownian motion. Probab. Eng. Inf. Sci. **17**(03), 417–434 (2003)
56. C.M. Dion, E. Cancès, Ground state of the time-independent Gross-Pitaevskii equation. Comput. Phys. Commun. **177**(10), 787–798 (2007)
57. P. Donnat, Quelques contributions mathématiques en optique non linéaire. Ph.D. thesis, 1994
58. M. Edwards, K. Burnett, Numerical solution of the nonlinear Schrödinger equation for small samples of trapped neutral atoms. Phys. Rev. A **51**, 1382–1386 (1995)
59. A. Einstein, Sitzber. Kgl. Preuss. Akad. Wiss. **23**, 3 (1925)
60. P. Engels, I. Coddington, P.C. Haljan, E.A. Cornell, Nonequilibrium effects of anisotropic compression applied to vortex lattices in Bose-Einstein condensates. Phys. Rev. Lett. **89**(10), 100403 (2002)

61. P. Engels, I. Coddington, P.C. Haljan, V. Schweikhard, E.A. Cornell, Observation of long-lived vortex aggregates in rapidly rotating Bose-Einstein condensates. Phys. Rev. Lett. **90**(17), 170405 (2003)
62. R.P. Feynman, Phys. Rev. **94**, 262 (1954)
63. R.P. Feynman, Application of quantum mechanics to liquid helium. *Progress in Low Temperature Physics*, vol. 1, ed. by C.J. Gorter (Elsevier, Amsterdam, 1955), pp. 17–53
64. D.G. Fried, T.C. Killian, L. Willmann, D. Landhuis, S.C. Moss, D. Kleppner, T.J. Greytak, Bose-Einstein condensation of atomic hydrogen. Phys. Rev. Lett. **81**, 3811–3814 (1998)
65. A. Gammal, T. Frederico, L. Tomio, Improved numerical approach for the time-independent Gross-Pitaevskii nonlinear Schrödinger equation. Phys. Rev. E **60**(2), 2421 (1999)
66. C.W. Gardiner, M.J. Davis, The stochastic Gross-Pitaevskii equation: II. J. Phys. B Atomic Mol. Opt. Phys. **36**(23), 4731 (2003)
67. C.W. Gardiner, J.R. Anglin, T.I.A. Fudge, The stochastic Gross-Pitaevskii equation. J. Phys. B Atomic Mol. Opt. Phys. **35**(6), 1555 (2002)
68. J. Garnier, F.K. Abdullaev, B.B. Baizakov, Collapse of a Bose-Einstein condensate induced by fluctuations of the laser intensity. Phys. Rev. A **69**, 053607 (2004)
69. M.E. Gehm, K.M. O'Hara, T.A. Savard, J.E. Thomas, Dynamics of noise-induced heating in atom traps. Phys. Rev. A **58**, 3914–3921 (1998)
70. K. Góral, K. Rzążewski, T. Pfau, Bose-Einstein condensation with magnetic dipole-dipole forces. Phys. Rev. A **61**, 051601 (2000)
71. A. Griesmaier, J. Werner, S. Hensler, J. Stuhler, T. Pfau, Bose-Einstein condensation of chromium. Phys. Rev. Lett. **94**, 160401 (2005)
72. E.P. Gross, Structure of a quantized vortex in boson systems. Il Nuovo Cimento Ser. 10 **20**(3), 454–477 (1961)
73. C.E. Hecht, Physica **25**, 262 (1959)
74. W. Heisenberg, The actual content of quantum theoretical kinematics and mechanics. Zhurnal Physik **43**, 172–198 (1983)
75. H.F. Hess, G.P. Kochanski, J.M. Doyle, N. Masuhara, D. Kleppner, T.J. Greytak, Magnetic trapping of spin-polarized atomic hydrogen. Phys. Rev. Lett. **59**, 672–675 (1987)
76. U. Hohenester, OCTBEC: a Matlab toolbox for optimal quantum control of Bose-Einstein condensates. Comput. Phys. Commun. **185**, 194–216 (2013)
77. A.D. Jackson, G.M. Kavoulakis, C.J. Pethick, Solitary waves in clouds of Bose-Einstein condensed atoms. Phys. Rev. A **58**, 2417–2422 (1998)
78. B. Jackson, J.F. McCann, C.S. Adams, Vortex formation in dilute inhomogeneous Bose-Einstein condensates. Phys. Rev. Lett. **80**, 3903–3906 (1998)
79. P.L. Kapitza, Nature **141**, 913 (1938)
80. K. Kasamatsu, M. Tsubota, M. Ueda, Giant hole and circular superflow in a fast rotating Bose-Einstein condensate. Phys. Rev. A **66**, 053606 (2002)
81. K. Kasamatsu, M. Tsubota, M. Ueda, Nonlinear dynamics of vortex lattice formation in a rotating Bose-Einstein condensate. Phys. Rev. A **67**(3), 033610 (2003)
82. K. Kasamatsu, M. Tsubota, M. Ueda, Vortices in multicomponent Bose-Einstein condensates. Int. J. Mod. Phys. B **19**(11), 1835–1904 (2005)
83. M. Koashi, M. Ueda, Exact eigenstates and magnetic response of spin-1 and spin-2 Bose-Einstein condensates. Phys. Rev. Lett. **84**, 1066–1069 (2000)
84. E.B. Kolomeisky, T.J. Newman, J.P. Straley, X. Qi, Low-dimensional Bose liquids: beyond the Gross-Pitaevskii approximation. Phys. Rev. Lett. **85**(6), 1146 (2000)
85. P. Leboeuf, N. Pavloff, Bose-Einstein beams: Coherent propagation through a guide. Phys. Rev. A **64**, 033602 (2001)
86. M. Lewin, P.T. Nam, N. Rougerie, Derivation of Hartree's theory for generic mean-field Bose systems. Adv. Math. **254**(0), 570 –621 (2014)

87. E.H. Lieb, R. Seiringer, Derivation of the Gross-Pitaevskii equation for rotating Bose gases. Commun. Math. Phys. **264**(2), 505–537 (2006)
88. E.H. Lieb, R. Seiringer, J. Yngvason, Bosons in a trap: a rigorous derivation of the Gross-Pitaevskii energy functional, in *The Stability of Matter: From Atoms to Stars*, ed. by W. Thirring (Springer, Berlin, 2005), pp. 759–771
89. F. London, Nature **141**, 643 (1938)
90. C. Lubich, On splitting methods for Schrödinger-Poisson and cubic nonlinear Schrödinger equations. Math. Comput. **77**(264), 2141–2153 (2008)
91. E.J.M. Madarassy, V.T. Toth, Numerical simulation code for self-gravitating Bose-Einstein condensates. Comput. Phys. Commun. **184**(4), 1339–1343 (2013)
92. K.W. Madison, F. Chevy, W. Wohlleben, J. Dalibard, Vortex formation in a stirred Bose-Einstein condensate. Phys. Rev. Lett. **84**(5), 806–809 (2000)
93. K.W. Madison, F. Chevy, W. Wohlleben, J. Dalibard, Vortices in a stirred Bose-Einstein condensate. J. Mod. Opt. **47**(14–15), 2715–2723 (2000)
94. K.W. Madison, F. Chevy, V. Bretin, J. Dalibard, Stationary states of a rotating Bose-Einstein condensate: routes to vortex nucleation. Phys. Rev. Lett. **86**(20), 4443–4446 (2001)
95. H.J. Metcalf, P. Van der Straten, *Laser Cooling and Trapping* (Springer, Berlin, 1999)
96. P. Muruganandam, S.K. Adhikari, Fortran programs for the time-dependent Gross-Pitaevskii equation in a fully anisotropic trap. Comput. Phys. Commun. **180**(10), 1888–1912 (2009)
97. D. Pathria, J.L.l. Morris, Pseudo-spectral solution of nonlinear Schrödinger equations. J. Comput. Phys. **87**(1), 108–125 (1990)
98. C.J. Pethick, H. Smith, *Bose-Einstein Condensation in Dilute Gases* (Cambridge University Press, Cambridge, 2002)
99. L.P. Pitaevskii, Vortex lines in an imperfect Bose gas. Sov. Phys. JETP USSR **13**(2), (1961)
100. L.P. Pitaevskii, S. Stringari, *Bose-Einstein Condensation*, vol. 116 (Clarendon Press, Oxford, 2003)
101. S.P. Rath, T. Yefsah, K.J. Günter, M. Cheneau, R. Desbuquois, M. Holzmann, W. Krauth, J. Dalibard, Equilibrium state of a trapped two-dimensional Bose gas. Phys. Rev. A **82**(1), 013609 (2010)
102. N. Rougerie, La théorie de Gross-Pitaevskii pour un condensat de Bose-Einstein en rotation: vortex et transitions de phase. Ph.D. thesis, Université Pierre et Marie Curie-Paris VI, 2010
103. N. Rougerie, Vortex rings in fast rotating Bose-Einstein condensates. Arch. Ration. Mech. Anal. **203**(1), 69–135 (2012)
104. C.A. Sackett, C.C. Bradley, M. Welling, R.G. Hulet, Bose-Einstein condensation of lithium. Appl. Phys. B **65**(4–5), 433–440 (1997)
105. L. Salasnich, A. Parola, L. Reatto, Effective wave equations for the dynamics of cigar-shaped and disk-shaped Bose condensates. Phys. Rev. A **65**(4), 043614 (2002)
106. T.A. Savard, K.M. O'Hara, J.E. Thomas, Laser-noise-induced heating in far-off resonance optical traps. Phys. Rev. A **56**, R1095–R1098 (1997)
107. E. Schrödinger, An undulatory theory of the mechanics of atoms and molecules. Phys. Rev. **28**, 1049–1070 (1926)
108. R. Seiringer, Gross-Pitaevskii theory of the rotating Bose gas. Commun. Math. Phys. **229**(3), 491–509 (2002)
109. T.P. Simula, A.A. Penckwitt, R.J. Ballagh, Giant vortex lattice deformations in rapidly rotating Bose-Einstein condensates. Phys. Rev. Lett. **92**(6), 060401 (2004)
110. J. Stenger, S. Inouye, D.M. Stamper-Kurn, H.-J. Miesner, A.P. Chikkatur, W. Ketterle, Spin domains in ground-state Bose-Einstein condensates. Nature **396**(6709), 345–348 (1998)
111. H.T.C. Stoof, Coherent versus incoherent dynamics during Bose-Einstein condensation in atomic gases. J. Low Temp. Phys. **114**(1–2), 11–108 (1999)
112. H.T.C. Stoof, M.J. Bijlsma, Dynamics of fluctuating Bose-Einstein condensates. J. Low Temp. Phys. **124**(3–4), 431–442 (2001)
113. G. Strang, On the construction and comparison of difference schemes. SIAM J. Numer. Anal. **5**(3), 506–517 (1968)
114. W.C. Stwalley, L.H. Nosanov, Phy. Rev. Lett. **36**, 910 (1976)

115. H.J. Sussmann, On the gap between deterministic and stochastic ordinary differential equations. Ann. Probab. **6**(1), 19–41 (1978)
116. T.R. Taha, M.I. Ablowitz, Analytical and numerical aspects of certain nonlinear evolution equations. ii. numerical, nonlinear Schrödinger equation. J. Comput. Phys. **55**(2), 203–230 (1984)
117. M. Thalhammer, High-order exponential operator splitting methods for time-dependent Schrödinger equations. SIAM J. Numer. Anal. **46**(4), 2022–2038 (2008)
118. M. Thalhammer, M. Caliari, C. Neuhauser, High-order time-splitting Hermite and Fourier spectral methods. J. Comput. Phys. **228**(3), 822–832 (2009)
119. R.P. Tiwari, A. Shukla, A basis-set based fortran program to solve the Gross-Pitaevskii equation for dilute Bose gases in harmonic and anharmonic traps. Comput. Phys. Commun. **174**(12), 966–982 (2006)
120. M. Tsubota, K. Kasamatsu, M. Ueda, Vortex lattice formation in a rotating Bose-Einstein condensate. Phys. Rev. A **65**(2), 023603 (2002)
121. D. Vudragović, I. Vidanović, A. Balaž P. Muruganandam, S.K. Adhikari, C programs for solving the time-dependent Gross-Pitaevskii equation in a fully anisotropic trap. Comput. Phys. Commun. **183**(9), 2021–2025 (2012)
122. J.A.C. Weideman, B.M. Herbst, Split-step methods for the solution of the nonlinear Schrödinger equation. SIAM J. Numer. Anal. **23**(3), 485–507 (1986)
123. L. Wen, H. Xiong, B. Wu, Hidden vortices in a Bose-Einstein condensate in a rotating double-well potential. Phys. Rev. A **82**(5), 053627 (2010)
124. Z.-M. Yin, New methods for simulation of fractional brownian motion. J. Comput. Phys. **127**(1), 66–72 (1996)
125. R. Zeng, Y. Zhang, Efficiently computing vortex lattices in rapid rotating Bose-Einstein condensates. Comput. Phys. Commun. **180**(6), 854–860 (2009)

Orbital Stability: Analysis Meets Geometry

Stephan De Bièvre, François Genoud, and Simona Rota Nodari

1 Introduction

The purpose of these notes is to provide an introduction to the theory of orbital stability of relative equilibria, a notion from the theory of (mostly Hamiltonian) dynamical systems with symmetry that finds its origins in the study of planetary motions [2]. In more recent times it has proven important in two new ways at least. It has on the one hand found an elegant reformulation in the modern framework of Hamiltonian mechanics of finite dimensional systems with symmetry in terms of symplectic geometry. It can indeed be phrased and studied in terms of the theory of momentum maps and of symplectic reduction [2, 66, 67, 80, 81, 83–85, 88]. On the other hand, it also underlies the stability analysis of plane waves, of travelling wave solutions and of solitons in infinite dimensional nonlinear Hamiltonian PDE's, which has received considerable attention over the last 40 years or so, and continues

S. De Bièvre (✉)
Laboratoire Paul Painlevé, CNRS, UMR 8524 et UFR de Mathématiques, Université Lille 1, Sciences et Technologies, 59655 Villeneuve d'Ascq Cedex, France

Equipe-Projet MEPHYSTO, Centre de Recherche INRIA Futurs, Parc Scientifique de la Haute Borne, 40, avenue Halley B.P. 70478, 59658 Villeneuve d'Ascq Cedex, France
e-mail: Stephan.De-Bievre@math.univ-lille1.fr

F. Genoud
Faculty of Mathematics, University of Vienna, Oskar-Morgenstern-Platz 1, 1090 Vienna, Austria

Current address: Delft Institute of Applied Mathematics, Delft University of Technology, Mekelweg 4, 2628 CD, Delft, The Netherlands
e-mail: francois.genoud@univie.ac.at; S.F.Genoud@tudelft.nl

S. Rota Nodari
Laboratoire Paul Painlevé, CNRS, UMR 8524 et UFR de Mathématiques, Université Lille 1, Sciences et Technologies, 59655 Villeneuve d'Ascq Cedex, France
e-mail: Simona.Rota-Nodari@math.univ-lille1.fr

C. Besse, J.-C. Garreau (eds.), *Nonlinear Optical and Atomic Systems*,
Lecture Notes in Mathematics 2146, DOI 10.1007/978-3-319-19015-0_3

to be a very active area of research. We will give a brief historical account of the notion of orbital stability in the context of nonlinear PDE's in Sect. 11.

It is clear that in this field nonlinear analysis can be expected to meet geometry in interesting and beautiful ways. It nevertheless appears that in the literature on Hamiltonian PDE's, the simple and elegant geometric ideas underlying the proofs of orbital stability aren't emphasized. The goal of these notes is to provide a unified formulation of the theory in a sufficiently general but not too abstract framework that allows one to treat finite and infinite dimensional systems on the same footing. In this manner, one may hope to harness the geometric intuition readily gained from treating finite dimensional systems and use it as a guide when dealing with the infinite dimensional ones that are the main focus of our interest, but that demand more sophisticated technical tools from functional analysis and PDE theory. The text is of an introductory nature and suitable for young researchers wishing to familiarize themselves with the field. It is aimed at analysts not allergic to geometry and at geometers with a taste for analysis, and written in the hope such people exist.

1.1 Notions of Stability

There are many notions of stability for dynamical systems. One may in particular consider stability with respect to perturbations in the vector field generating the dynamics, or stability with respect to a variation in the initial conditions. It is the latter one we shall be considering here. For a sampling of possible definitions in this context, one can consult Sect. 6.3 of Abraham and Marsden [2], who give nine different ones and mention there exist others still... We start by introducing the ones of interest to us in these notes.

The simplest possible one is presumably the following. Let E be a normed vector space, d the corresponding metric on E, and X a vector field on E. Let $u \in E$ and $t \in \mathbb{R} \to u(t) \in E$ a flow line of X [i.e. $\dot{u}(t) = X(u(t))$, with $u(0) = u$]. Let us assume the flow is well-defined globally, with $u(t) = \Phi_t^X(u)$. Then one says that the initial condition u is stable if for all $\epsilon > 0$, there exists a $\delta > 0$ so that, for all $v \in E$,

$$\mathrm{d}(v,u) \leq \delta \Rightarrow \sup_{t\in\mathbb{R}} \mathrm{d}(v(t),u(t)) \leq \epsilon. \tag{1}$$

Here $v(t) = \Phi_t^X(v)$. This can be paraphrased as follows: once close, forever not too far. Note that, if u is stable in this sense, then so is $u(t)$ for all $t \in \mathbb{R}$. There exists one situation where proving stability is straightforward. It is the case where $u = u_*$ is a fixed point of the dynamics, meaning $u(t) = u_*$, for all $t \in \mathbb{R}$, and where u_* is a local non-degenerate minimum of a constant of the motion, that is a function $\mathscr{L} : E \to \mathbb{R}$, referred to as a *Lyapunov function*, satisfying $\mathscr{L}(v(t)) = \mathscr{L}(v)$ for all $t \in \mathbb{R}$, and for all v in a neighbourhood of u_*. Let us sketch the argument, which is classic. Supposing $\mathscr{L} \in C^2(E,E)$ and that $D^2_{u_*}\mathscr{L}$ is positive definite, one obtains

from a Taylor expansion of $\mathscr{L}$ about u_* an estimate of the type

$$c\mathrm{d}(v,u_*)^2 \leq \mathscr{L}(v) - \mathscr{L}(u_*) \leq C\mathrm{d}(v,u_*)^2, \tag{2}$$

for all v in a neighbourhood of u_*. Then, for v sufficiently close to u_*, one can easily show, using an argument by contradiction, that $v(t)$ stays in this neighbourhood and hence, for all t,

$$c\mathrm{d}(v(t),u_*)^2 \leq \mathscr{L}(v(t)) - \mathscr{L}(u_*) = \mathscr{L}(v) - \mathscr{L}(u_*) \leq C\mathrm{d}(v,u_*)^2, \tag{3}$$

from which (1) follows immediately. This approach is known as the Lyapunov method for proving stability.[1]

In Hamiltonian systems, at least one constant of the motion always exists, namely the Hamiltonian itself. The above argument leads therefore to the perfectly standard result that local minima of the Hamiltonian are stable fixed points of the dynamics. All orbital stability results that we shall discuss below are, *in fine*, based on this single argument, appropriately applied and combined with additional geometric properties of (Hamiltonian) systems with symmetry, and, of course, with an appropriate dose of (functional) analysis. Let us finally point out that when this approach does not work, and this is very often the case, one is condemned to resort to considerably more sophisticated techniques, involving the KAM theorem or Nekhoroshev estimates, for example.

A stronger version of stability than (1) is an asymptotic one, and goes as follows: there exists a $\delta > 0$ so that, for all $v \in E$,

$$\mathrm{d}(v,u) \leq \delta \Rightarrow \lim_{t\to+\infty} \mathrm{d}(v(t),u(t)) = 0.$$

This phenomenon can only occur in dissipative systems. When u is a fixed point of the dynamics, it corresponds to requiring it is attractive. If the flow line issued from u is periodic, one obtains a limit cycle. So in this second definition, the idea is that, if two points start close enough, they end up together. Since our focus here is on Hamiltonian systems, where such behaviour cannot occur (because volumes are preserved), we shall not discuss it further. Note, however, that another notion of "asymptotic stability" has been introduced and studied in the context of Hamiltonian nonlinear dispersive PDE's. We shall briefly comment on this in Sect. 11.

There are several cases when definition (1) is too strong, and a weaker notion is needed, referred to as *orbital stability*. The simplest definition of this notion goes as follows. Suppose $t \in \mathbb{R} \to u(t) \in E$ is a flow line of the dynamics and consider the dynamical orbit

$$\gamma = \{u(t) \mid t \in \mathbb{R}\}.$$

[1] Remark that $\mathscr{L}(v(t)) \leq \mathscr{L}(v)$ would suffice in (3). But in these notes we will exclusively work with constants of the motion.

We say $u = u(0)$ is orbitally stable if the following holds. For all $\epsilon > 0$, there exists $\delta > 0$, so that

$$\mathrm{d}(v, u) < \delta \Rightarrow \forall t \in \mathbb{R}, \mathrm{d}(v(t), \gamma) \leq \epsilon. \tag{4}$$

The point here is that the new dynamical orbit $\tilde{\gamma} = \{v(t) \mid t \in \mathbb{R}\}$ stays close to the initial one, while possibly $v(t)$ can drift away from $u(t)$, for the same value of the time t. As we will see, this can be expected to be the rule since the nearby orbit may no longer be periodic even if the original one was, or have a different period. A simple example that can be understood without computation is this. Think of two satellites on circular orbits around the earth. Imagine the radii are very close. Then the periods of both motions will be close but different. Both satellites will eternally move on their respective circles, which are close, but they will find themselves on opposite sides of the earth after a long enough time, due to the difference in their angular speeds. In addition, a slight perturbation in the initial condition of one of the satellites will change its orbit, which will become elliptical, and again have a different period. But the new orbit will stay close to the original circle. So here the idea is this: if an initial condition v is chosen close to u, then at all later times t, $v(t)$ is close to *some* point on γ, but not necessarily close to $u(t)$, for the same value of t. We will treat this illustrative example in detail in Sect. 5.2.

1.2 Symmetries and Relative Equilibria

The definition of orbital stability in (4) turns out to be too strong still for many applications, in particular in the presence of symmetries of the dynamics. This is notably the case in the study of solitons and standing or travelling wave solutions of nonlinear Hamiltonian differential or partial differential equations. We will therefore present an appropriate generalization of the notion of orbital stability in the presence of symmetries in Sect. 4. For that purpose, we introduce in Sect. 2 dynamical systems Φ_t^X, $t \in \mathbb{R}$, on Banach spaces E, which admit an invariance group G with an action $\Phi_g, g \in G$, on E, i.e. $\Phi_g \Phi_t^X = \Phi_t^X \Phi_g$. We then say $u \in E$ is a *relative equilibrium* if, for all $t \in \mathbb{R}$, $\Phi_t^X(u) \in \mathcal{O}_u$, where $\mathcal{O}_u = \Phi_G(u)$ is the group orbit of u under the action of G. As we will see, solitons, travelling waves and plane waves are relative equilibria. We say a relative equilibrium u is *orbitally stable* if initial conditions $v \in E$ close to u have the property that for all $t \in \mathbb{R}$, $\Phi_t^X(v)$ remains close to $\mathcal{O}_u$. Note that the larger the symmetry group G is, the weaker is the corresponding notion of stability.

The main goal of these notes is to present a general framework allowing to establish orbital stability of such *relative equilibria* of (both finite and infinite) dynamical systems with symmetry, using an appropriate generalization of the Lyapunov method sketched above. This approach to stability is often referred to as the "energy-momentum" method. In the process, we wish to clearly separate the part of the argument which is abstract and very general, from the part that

is model-dependent. We will also indicate for which arguments one needs the dynamics to be Hamiltonian and which ones go through more generally.

In Sect. 5, we treat the illustrative example of the relative equilibria of the motion in a spherical potential, allowing us to present four variations of the proof of orbital stability, which are later extended to a very general setting in Sect. 8. The main hypothesis of the proofs, which work for general dynamical systems on Banach spaces, is the existence of a *coercive Lyapunov function* $\mathscr{L}$, which is a group-invariant constant of the motion satisfying an appropriately generalized coercive estimate of the type (2) [see (111)]. In applications, the proof of orbital stability is thus reduced to the construction of such a function.

It is in this step that the geometry of Hamiltonian dynamical systems with symmetry plays a crucial role. Indeed, the construction of an appropriate Lyapunov function for such systems exploits the special link that exists between their constants of the motion F and their symmetries, as embodied in Noether's theorem and the theory of the momentum map. This is explained in Sects. 6 and 7. The crucial observation is then that in Hamiltonian systems, relative equilibria tend to come in families $u_\mu \in E$, indexed by the value μ of the constants of the motion at u_μ. In fact, it turns out that $u_\mu \in E$ is a relative equilibrium of a Hamiltonian system if (and only if) u_μ is a critical point of the restriction of the Hamiltonian to the level surface $\Sigma_\mu = \{u \in E \mid F(u) = \mu\}$ of these constants of the motion (Theorem 7). This observation at once yields the candidate Lyapunov function $\mathscr{L}_\mu$ [see (110)].

We finally explain (Proposition 5) how the proof of the coercivity of the Lyapunov function can be obtained from a suitable lower bound on its second derivatives $D^2\mathscr{L}_\mu(w,w)$, with w restricted to an appropriate subspace of E, using familiar arguments from the theory of Lagrange multipliers (Sect. 8). This ends the very general, geometric and abstract part of the theory. To control $D^2\mathscr{L}_\mu(w,w)$ finally requires an often difficult, problem-dependent, and detailed spectral analysis of the Hessian of the Lyapunov function, as we will show in the remaining sections.

1.3 Examples

We illustrate the theory in Sect. 9 on a first simple example. We consider the plane waves $u_{\alpha,k}(t,x) = \alpha e^{-ikx} e^{i\xi t}$, $\xi \in \mathbb{R}$, $k \in 2\pi\mathbb{Z}$ and $\alpha \in \mathbb{R}$, which are solutions of the cubic nonlinear Schrödinger equation on the one-dimensional torus $\mathbb{T}$,

$$i\partial_t u(t,x) + \beta\partial_{xx}^2 u(t,x) + \lambda|u(t,x)|^2 u(t,x) = 0,$$

provided $\xi + \beta k^2 = \lambda|\alpha|^2$. This equation is (globally) well-posed on $E = H^1(\mathbb{T},\mathbb{C})$ and its dynamical flow is invariant under the globally Hamiltonian action Φ of the group $G = \mathbb{R}\times\mathbb{R}$ defined by $\big(\Phi_{a,\gamma}(u)\big)(x) = e^{i\gamma}u(x-a)$ (see Sect. 6.5). The plane waves $u_{\alpha,k}(t,x)$ are G-relative equilibria. We establish (Theorem 12) their orbital stability when $\beta(2\pi)^2 > 2\lambda|\alpha|^2$. Although the linear stability analysis for this model is sketched in many places, and the nonlinear (in)stability results seem to be

known to many, we did not find a complete proof of nonlinear orbital stability in the literature. A brief comparison between our analysis and related results [40, 41, 106] ends Sect. 9. Note that the analysis of orbital stability of plane waves of the cubic nonlinear Schrödinger equation on a torus of dimension $d > 1$ is much more involved (see for example [34]).

In Sect. 10 we will present orbital stability results pertaining to curves (i.e. one-dimensional families) of standing waves of nonlinear Schrödinger equations on $\mathbb{R}^d$ with a space-dependent coefficient f:

$$i\partial_t u(t,x) + \Delta u(t,x) + f(x,|u|^2(t,x))u(t,x) = 0. \tag{5}$$

Imposing a non-trivial spatial dependence has two major consequences. First, the space-translation symmetry of the equation is destroyed, and one is left with the reduced one-parameter symmetry group $G = \mathbb{R}$, acting on the Sobolev space $E = H^1(\mathbb{R}^d)$ via $\Phi_\gamma(u) = e^{i\gamma}u$. Note that the associated group orbits are of the simple form $\mathcal{O}_u = \{e^{i\gamma}u : \gamma \in \mathbb{R}\} \subset H^1(\mathbb{R}^d)$. Now, standing waves are, by definition, solutions of (5) of the form $u(x,t) = e^{i\xi t}w(x)$, which are therefore clearly relative equilibria. Such standing waves are sometimes referred to as "solitons" due to the spatial localization of the profile $w(x)$, and to their stability.

Second, constructing curves of standing wave solutions of (5) is now a hard problem, and we will outline the bifurcation theory developed in [44, 45, 48, 49] to solve it. This powerful approach allows one to deal with power-type nonlinearities $f(x,|u|^2) = V(x)|u|^{\sigma-1}$ (under an appropriate decay assumption on the coefficient $V : \mathbb{R}^d \to \mathbb{R}$) but also with more general nonlinearities, for instance the asymptotically linear $f(x,|u|^2) = V(x)\frac{|u|^{\sigma-1}}{1+|u|^{\sigma-1}}$. This will give a good illustration of how involved the detailed analysis of $D^2\mathscr{L}(w,w)$ required by the model can be. As we shall see, this analysis turns out to be deeply connected with the bifurcation behaviour of the standing waves.

In the pure power (space-independent) case $f(x,|u|^2) = |u|^{\sigma-1}$, the appropriate notion of stability is that associated with the action of the full group $G = \mathbb{R}^d \times \mathbb{R}$, $\left(\Phi_{a,\gamma}(u)\right)(x) = e^{i\gamma}u(x-a)$. The stability of standing waves in this context was proved in the seminal paper of Cazenave and Lions [18] for $1 < \sigma < 1 + \frac{4}{d}$, and this result is sharp (i.e. stability does not hold at $\sigma = 1 + \frac{4}{d}$). The contribution [18] is one of the first rigorous results on orbital stability for nonlinear dispersive equations, and is based on variational arguments using the concentration-compactness principle (see for instance [55, 106] for more recent results in this direction). This line of argument is conceptually very different from the energy-momentum approach developed here, so we shall not say more about it.

The modern treatment of Hamiltonian dynamical systems with symmetries uses the language of symplectic geometry, as for example in [2, 6, 67, 95]. But we don't need the full power of this theory, since we will work exclusively with linear symplectic structures on (infinite dimensional) symplectic vector spaces. For the reader not familiar with Hamiltonian mechanics, Lie group theory and symplectic

group actions, elementary self-contained introductions to these subjects sufficient for our purposes are provided in the Appendix.

Acknowledgments This work was supported in part by the Labex CEMPI (ANR-11-LABX-0007-01). F.G. thanks CEMPI and the Lab. Paul Painlevé for their hospitality during his 1-month visit to the Université Lille 1 in September 2013. He also acknowledges the support of the ERC Advanced Grant "Nonlinear studies of water flows with vorticity". The authors are grateful to V. Combet, A. De Laire, S. Keraani, G. Rivière, B. Tumpach and G. Tuynman for stimulating discussions on the subject matter of these notes.

2 Dynamical Systems, Symmetries and Relative Equilibria

2.1 Dynamical Systems on Banach Spaces

Let E be a Banach space. A domain $\mathscr{D}$ is a dense subset of E; in the examples presented in these notes, it will be a dense linear subspace of E.

Definition 1 A *dynamical system* on E is a separately continuous map

$$\Phi^X : (t,u) \in \mathbb{R} \times E \to \Phi_t^X(u) := \Phi^X(t,u) \in E, \tag{6}$$

with the following properties:

(i) For all $t, s \in \mathbb{R}$,

$$\Phi_t^X \circ \Phi_s^X = \Phi_{t+s}^X, \quad \Phi_0^X(u) = \mathrm{Id}_E. \tag{7}$$

(ii) For all $t \in \mathbb{R}$, $\Phi_t^X(\mathscr{D}) = \mathscr{D}$.

(iii) $X : \mathscr{D} \subset E \to E$ is a vector field that generates the dynamics in the sense that, when $u \in \mathscr{D}$, $\Phi_t^X(u) := u(t) \in \mathscr{D}$ is a solution of the differential equation

$$\dot{u}(t) = X(u(t)), \quad u(0) = u. \tag{8}$$

By this we mean that the curve $t \in \mathbb{R} \to u(t) \in E$ is differentiable as a map from $\mathbb{R}$ to E.

In infinite dimensional problems, the vector fields are often only defined on a domain $\mathscr{D}$, where they may not even be continuous. But note that we always assume that the flows themselves are defined on all of E (or on an open subset of E). For examples illustrating these subtleties, see Sect. 3.2. Local flows can be defined in the usual manner. In that case the domains are dense in some open subset of E, but we shall not deal with such situations in these notes since we will always assume the flows to be globally defined.

Suppose there exists a function $F : E \to \mathbb{R}^m$ so that

$$F \circ \Phi_t^X = F, \quad \forall t \in \mathbb{R}. \tag{9}$$

We then say that the vector field X or its associated flow Φ_t^X admits *m constants of the motion*, which are the components F_i of F. In that case, one may consider the restriction of the flow Φ_t^X to the level sets of F: for $\mu \in \mathbb{R}^m$, we define

$$\Sigma_\mu = \{u \in E \mid F(u) = \mu\}, \tag{10}$$

and one has that $\Phi_t^X \Sigma_\mu = \Sigma_\mu$, for all $\mu \in \mathbb{R}^m$.

Remark 1 The role of and the need for a domain $\mathscr{D}$ with the properties (ii) and (iii) in the definition of a dynamical system above will become clear in Sects. 6 and 7. They are in particular needed to prove (9) for suitable F. Some of the stability results that are our main focus can be obtained without those conditions, as we will further explain in Sect. 8. Similarly, global existence is not strictly needed: it can for example be replaced by a weaker "blow-up alternative." We will not further deal with these issues here.

2.2 Symmetries, Reduced Dynamics and Relative Equilibria

We now define the notion of an invariance group for a dynamical system. For that purpose, we need to say a few words about group actions. Let G be a topological group acting on E. By this we mean there exists a separately continuous map

$$\Phi : (g, u) \in G \times E \to \Phi_g(u) \in E,$$

satisfying $\Phi_e = \mathrm{Id}$, $\Phi_{g_1 g_2} = \Phi_{g_1} \circ \Phi_{g_2}$. We will call

$$\mathscr{O}_u = \{\Phi_g(u) \mid g \in G\} \tag{11}$$

the orbit of G through $u \in E$. For later reference, we define the isotropy group of u, G_u, as follows

$$G_u = \{g \in G \mid \Phi_g(u) = u\}. \tag{12}$$

We can then introduce the notion of an invariance group for Φ_t^X.

Definition 2 We say G is an invariance group (or symmetry group) for the dynamical system Φ_t^X if, for all $g \in G$, and for all $t \in \mathbb{R}$,

$$\Phi_g \circ \Phi_t^X = \Phi_t^X \circ \Phi_g. \tag{13}$$

Remark that $G = \mathbb{R}$ is always an invariance group of the dynamical system, with action Φ_t^X on E. While this is correct, this is not of any particular use, as one can suspect from the start. Indeed, the flow Φ_t^X is in applications obtained by integrating a nonlinear differential or partial differential equation, and is not explicitly known. In fact, it is the object of study. "Useful" symmetries are those that help to simplify this study; they need to have a simple and explicit action on E. They are often of a clearcut geometric origin: translations, rotations, gauge transformations, etc. Several examples are provided in the following sections.

Finally, it should be noted we did not define "the" symmetry group for Φ_t^X, but "a" symmetry group. Depending on the problem at hand and the questions addressed, different symmetry groups may prove useful for the same dynamical system, as we shall also illustrate. In particular, any subgroup of an invariance group is also an invariance group, trivially.

It follows immediately from (11) and (13) that, for all $x \in E$,

$$\Phi_t^X \mathcal{O}_u = \mathcal{O}_{\Phi_t^X(u)}. \tag{14}$$

In other words, if G is an invariance group, then the dynamical system maps G-orbits into G-orbits. This observation lies at the origin of the following construction which is crucial for the definitions of relative equilibrium and orbital stability that we shall introduce. We give the general definitions here, and refer to the coming sections for examples. Defining an equivalence relation on E through

$$u \sim u' \Leftrightarrow \mathcal{O}_u = \mathcal{O}_{u'},$$

we consider the corresponding quotient space that we denote by $E_G = E/\sim$ and that we refer to as the reduced phase space. We will occasionally use the notation

$$\pi : u \in E \to \mathcal{O}_u \in E_G \tag{15}$$

for the associated projection. So the elements of E_G are just the G-orbits in E. It is then clear from (14) that the dynamical system Φ_t^X on E naturally induces reduced dynamics on the orbit space E_G: it "passes to the quotient" in the usual jargon. We will use the same notation for these reduced dynamics and write $\Phi_t^X \mathcal{O} = \mathcal{O}(t)$ for any $\mathcal{O} \in E_G$. Note that $\Phi_t^X \mathcal{O}_u = \mathcal{O}_{u(t)}$ (see Fig. 1).

As a general rule of thumb, one may hope that the reduced dynamics are simpler than the original ones, since they take place on a lower dimensional (or in some sense smaller) quotient space. This idea can sometimes provide a useful guideline, notably in the study of stability properties of fixed points or periodic orbits of the original dynamical system, as will be illustrated in the coming sections. Implementing it concretely can nevertheless be complicated, in particular because the quotient itself may be an unpleasant object to do analysis on, even in finite dimensions, as its topology or differential structure may be pathological and difficult

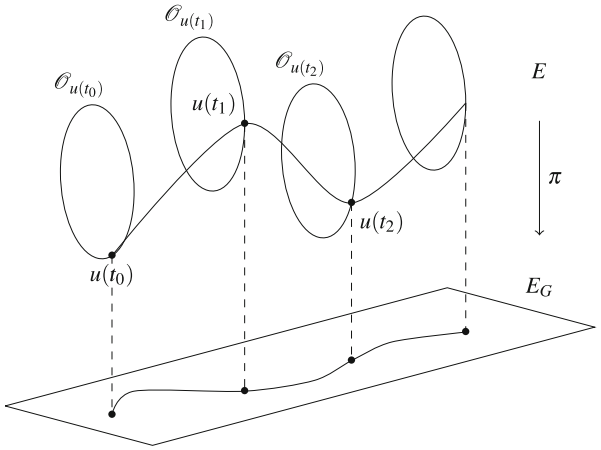

Fig. 1 A dynamical orbit $t \to u(t)$ and its "attached" G-orbits, with the projection into E_G

to deal with. Conditions on G and on the action Φ are needed, for example, to ensure the quotient topology on E_G is Hausdorff, or that it has a differentiable structure [2, 67, 85]. In addition, concrete computations on models are more readily done on E directly, than in the abstract quotient space, particularly in infinite dimensional problems. We will avoid these difficulties, in particular because we will work almost exclusively with *isometric* group actions. Their orbits have simplifying features that we will repeatedly use: see Proposition 1 below.

We are now in a position to introduce the notion of *relative equilibrium*, as follows.

Definition 3 Let $u \in E$. Let Φ_t^X be a dynamical system on E and let G be a symmetry group for Φ_t^X. We say u is a *G-relative equilibrium*[2] for Φ_t^X if, for all $t \in \mathbb{R}$, $u(t) \in \mathcal{O}_u$. Or, equivalently, if for all $t \in \mathbb{R}$, $\Phi_t^X \mathcal{O}_u = \mathcal{O}_u$. When there is no ambiguity about the dynamical system Φ_t^X and the group G considered, we will simply say u is a *relative equilibrium*.

With the language introduced, u is a relative equilibrium if $\mathcal{O}_u$ is a fixed point of the reduced dynamics on E_G. Again, we refer to the following sections for examples. We are interested in these notes in the stability of such relative equilibria. Roughly speaking, we will say a relative equilibrium is orbitally stable if it is stable as a fixed point of the reduced dynamics; we give a precise definition in Sect. 4.

We end this section with two comments. First, the above terminology comes from the literature on Hamiltonian dynamical systems in finite dimensions. We will see in the following sections what the many specificities are of that situation. We refer

[2] In [67], the term *stationary motion* is used for this concept.

to [2, 6, 67] for textbook treatments and historical background and to [66, 80, 81, 84, 85, 88] for more recent developments. Second, we will often need to deal with the restriction of the dynamical systems under consideration to the level sets $\Sigma_\mu \subset E$ of a family of constants of the motion F, as defined in (10). Note that Σ_μ is a metric space. We define

$$G_{\Sigma_\mu} = \{g \in G \mid \forall u \in \Sigma_\mu, \Phi_g(u) \in \Sigma_\mu\}. \tag{16}$$

This is clearly a subgroup of G, which is a symmetry group of the dynamical system restricted to Σ_μ. We will often deal with isometric group actions on such Σ_μ, or on the full Banach space E. The following simple proposition collects some of the essential properties of their orbits that we shall repeatedly need and use. We first recall the definition of the Hausdorff metric. Let (Σ, d) be a metric space and let $S, S' \subset (\Sigma, \mathrm{d})$. Then

$$\Delta(S, S') = \max\{\sup_{u \in S} \mathrm{d}(u, S'), \sup_{u' \in S'} \mathrm{d}(S, u')\}. \tag{17}$$

Notice that this is only a pseudometric[3] and that $\Delta(S, S') = +\infty$ is possible.

Proposition 1 *Let G be a group, (Σ, d) a metric space and $\Phi : G \times \Sigma \to \Sigma$ an action of G on Σ. Suppose that for each $g \in G$, Φ_g is an isometry: $\forall u, u' \in \Sigma, \mathrm{d}(\Phi_g(u), \Phi_g(u')) = \mathrm{d}(u, u')$. Let $\mathscr{O}, \mathscr{O}'$ be two G-orbits in Σ. Then*

(i) $\forall u_1, u_2 \in \mathscr{O}, \forall u_1', u_2' \in \mathscr{O}', \ \mathrm{d}(u_1, \mathscr{O}') = \mathrm{d}(u_2, \mathscr{O}'), \quad \mathrm{d}(u_1', \mathscr{O}) = \mathrm{d}(u_2', \mathscr{O}),$
(ii) $\forall u \in \mathscr{O}, u' \in \mathscr{O}', \quad \mathrm{d}(u, \mathscr{O}') = \Delta(\mathscr{O}, \mathscr{O}') = \mathrm{d}(u', \mathscr{O}),$
(iii) $\forall u \in \mathscr{O}, u' \in \mathscr{O}', \quad \Delta(\mathscr{O}, \mathscr{O}') \leq \mathrm{d}(u, u').$

Proof The first statement follows from the existence of $g \in G$ so that $\Phi_g(u_1) = u_2$. For the second, we proceed by contradiction. Suppose first that, $\forall u \in \mathscr{O}, u' \in \mathscr{O}'$, $\mathrm{d}(u, \mathscr{O}') < \mathrm{d}(u', \mathscr{O})$. Let $u \in \mathscr{O}, u' \in \mathscr{O}'$. Then we know there exists $v \in \mathscr{O}'$ (depending on u, u') so that $\mathrm{d}(u, \mathscr{O}') \leq \mathrm{d}(u, v) < \mathrm{d}(u', \mathscr{O})$. But since, by the first part of the proposition, $\mathrm{d}(v, \mathscr{O}) = \mathrm{d}(u', \mathscr{O})$, this implies $\mathrm{d}(u, v) < \mathrm{d}(v, \mathscr{O})$, which is a contradiction. So we conclude, using the first part again, that $\forall u \in \mathscr{O}, u' \in \mathscr{O}'$, $\mathrm{d}(u, \mathscr{O}') \geq \mathrm{d}(u', \mathscr{O})$. Repeating the argument with the roles of $\mathscr{O}, \mathscr{O}'$ inverted, the result follows.

If the action is not isometric, it is quite possible for all the statements of the theorem to fail. For example, consider on $E = \mathbb{R}^2$ the action $\Phi_a(q, p) = (\exp(a)q, \exp(-a)p)$, $a \in \mathbb{R}$.

[3] $\Delta(S, S') = 0$ does not imply $S = S'$. In particular, $\Delta(S, \overline{S}) = 0$.

3 Examples

3.1 Motion in a Spherical Potential

In this section, we illustrate the preceding notions on a simple Hamiltonian mechanical system: a particle in a spherical potential. We will make free use of the concepts and notation of Appendices "Lie Algebras, Lie Groups and Their Actions" and "Hamiltonian Dynamical System with Symmetry in Finite Dimension" that we invite the reader unfamiliar with Hamiltonian mechanics or Lie group theory to peruse.

By a spherical potential we mean a function $V : \mathbb{R}^3 \to \mathbb{R}$, satisfying $V(Rq) = V(q)$, for all $R \in \mathrm{SO}(3)$. With a slight abuse of notation, we write $V(q) = V(\|q\|)$, for a smooth function $V : \mathbb{R}^+ \to \mathbb{R}$. We consider on $E = \mathbb{R}^6$ the Hamiltonian

$$H(u) = H(q,p) = \frac{1}{2}p^2 + V(\|q\|) \tag{18}$$

and the corresponding Hamiltonian equations of motion

$$\dot{q} = p, \quad \dot{p} = -V'(\|q\|)\hat{q}, \tag{19}$$

where we introduce the notation $\hat{b} = \frac{b}{\|b\|}$ for any $b \in \mathbb{R}^3$. Integrating those, we obtain the Hamiltonian flow $\Phi_t^H(u) = u(t)$, where $u = (q,p) \in \mathbb{R}^6$. Introducing the angular momentum

$$L(q,p) = q \wedge p, \tag{20}$$

one checks immediately that, for any solution $t \in \mathbb{R} \to (q(t), p(t)) \in \mathbb{R}^6$, one has

$$\frac{\mathrm{d}}{\mathrm{d}t} L(q(t), p(t)) = 0. \tag{21}$$

In other words, angular momentum is conserved during the motion in a central potential: its three components are constants of the motion. This implies the familiar result that the motion takes place in the plane perpendicular to L and passing through 0.

We will now use Noether's Theorem (Theorem 19) to show this system is SO(3)-invariant. We start with the following observations. First, the action of the group $G = \mathrm{SO}(3)$ on $E = \mathbb{R}^6$ given by

$$\Phi_R(u) = (Rq, Rp) \tag{22}$$

is easily checked to be globally Hamiltonian.[4] Indeed, for each $\xi \in \mathrm{so}(3)$,

$$\Phi_{\exp(t\xi)} = \Phi_t^{F_\xi},$$

where

$$F_\xi(q,p) = \xi \cdot L(q,p) \tag{23}$$

[recall that we can identify so(3) with $\mathbb{R}^3$ via (197)]. In other words,"angular momentum generates rotations." Next, it is clear that the Hamiltonian satisfies $H \circ \Phi_R = H$. As a result, it follows from Theorem 19(iii) that the dynamical flow is rotationally invariant:

$$\Phi_t^H \circ \Phi_R = \Phi_R \circ \Phi_t^H, \qquad \forall t \in \mathbb{R},\ R \in \mathrm{SO}(3).$$

Note that, here and in what follows, we are using, apart from the symplectic, also the standard Euclidean structure on $\mathbb{R}^6$.

We now wish to identify the relative equilibria of these systems. For that purpose, consider first $u \in \mathbb{R}^6$ with $L(u) = \mu \neq 0$. Then the ensuing dynamical trajectory $u(t)$ lies in the surface

$$\Sigma_\mu = \{u \in \mathbb{R}^6 \mid L(u) = \mu\}. \tag{24}$$

Now, if u is a relative equilibrium, then, for each t, there exists $R(t) \in \mathrm{SO}(3)$ so that $\Phi_{R(t)}u = u(t)$. Hence $\mu = L(u(t)) = L(\Phi_{R(t)}u) = R(t)L(u) = R(t)\mu$. In other words, $R(t)$ belongs to

$$G_\mu = \{R \in \mathrm{SO}(3) \mid R\mu = \mu\} \simeq \mathrm{SO}(2),$$

which is the subgroup of rotations about the μ-axis. It follows that $\|q(t)\| = \|q\|$, for all t. Since $q(t)$ is perpendicular to μ, this means that $q(t)$ lies on the circle of radius $\|q\|$ centered at 0 and perpendicular to μ. The orbit is therefore circular and, in particular, for all t, $q(t) \cdot p(t) = 0$. Conversely, it is clear that all circular dynamical orbits are relative equilibria. The initial conditions corresponding to such circular orbits are easily seen to be of the form

$$q = \rho_* \hat{q}, \quad p = \sigma_* \hat{p}, \quad \sigma_*^2 = \rho_* V'(\rho_*), \quad \hat{q} \cdot \hat{p} = 0, \tag{25}$$

with $\rho_*, \sigma_* > 0$ and hence $V'(\rho_*) > 0$. We will discuss in Sect. 5 under what conditions they are orbitally stable in the sense of (4).

Now, let $u = (q,p) \in \mathbb{R}^6$ be such that $L(u) = 0$. In this case q and p are parallel and this remains true at all times. But if $p(t) \neq 0$ at any time t, u cannot be a relative equilibrium. Indeed, the motion is then along a straight line passing through the

[4] See Definition 14.

origin and such a straight line cannot lie in an SO(3) orbit since the SO(3) action preserves norms. If on the other hand $u = (\rho_* \hat{q}, 0) = u(t)$ is a fixed point of the dynamics, it is a fortiori a relative equilibrium. This occurs if and only if $V'(\rho_*) = 0$ as is clear from the equations of motion. Note that these fixed points fill the sphere of radius ρ_*.

It is clear these fixed points cannot be stable in the sense of definition (1) or (4). Indeed, any initial condition u' close to such fixed point u, but with $p' \neq 0$ gives rise to a trajectory in the plane spanned by q' and p': when q' and p' are not parallel, the trajectory will wind around the origin in this plane, moving away from the initial condition. What we will prove in Sect. 5 is that, provided $V''(\rho_*) > 0$, these trajectories all stay close to

$$\mathcal{O}_{\rho_*,0,0} = \{u \in \mathbb{R}^6 \mid q \cdot q = \rho_*^2,\ p \cdot p = 0,\ q \cdot p = 0\}, \tag{26}$$

which is the SO(3) orbit through the fixed point $u = (\rho_* \hat{q}, 0)$. Those fixed points are therefore SO(3)-orbitally stable, in the sense of Definition 5(i) below.

To end this section, we list, for later purposes, all SO(3)-orbits in $E = \mathbb{R}^6$. Those are easily seen to be the hypersurfaces $\mathcal{O}_{\rho,\sigma,\alpha}$ of the form

$$\mathcal{O}_{\rho,\sigma,\alpha} = \{(q,p) \in \mathbb{R}^6 \mid q \cdot q = \rho^2,\ p \cdot p = \sigma^2,\ q \cdot p = \alpha\}, \tag{27}$$

with $\rho, \sigma \geq 0, \alpha \in \mathbb{R}$. Note that $|\alpha| \leq \rho\sigma$. Those orbits are three-dimensional smooth submanifolds of $\mathbb{R}^6$, except on the set where the angular momentum L vanishes, i.e. on

$$\Sigma_0 = \{(q,p) \in \mathbb{R}^6 \mid L(q,p) = 0\}.$$

This surface (which is not a submanifold of E) is itself SO(3)-invariant and foliated by group orbits as follows:

$$\Sigma_0 = \bigcup_{\rho\sigma = |\alpha|} \mathcal{O}_{\rho,\sigma,\alpha} = \{(0,0)\} \cup \bigcup_{\substack{\rho\sigma = |\alpha| \\ (\rho,\sigma) \neq (0,0)}} \mathcal{O}_{\rho,\sigma,\alpha}.$$

On the latter orbits, q and p are parallel, but do not both vanish, so that these orbits can be identified with two-dimensional spheres.

3.2 The Nonlinear Schrödinger Equation

An important example of an infinite dimensional dynamical system is the nonlinear Schrödinger equation

$$\begin{cases} i\partial_t u(t,x) + \Delta u(t,x) + f(x, u(t,x)) = 0, \\ u(0,x) = u_0(x), \end{cases} \tag{28}$$

with $u(t,x) : \mathbb{R} \times \mathbb{R}^d \to \mathbb{C}$. Here Δ denotes the usual Laplace operator and f is a local nonlinearity. More precisely, consider $f : (x,u) \in \mathbb{R}^d \times \mathbb{R}^+ \to f(x,u) \in \mathbb{R}$ such that f is measurable in x and continuous in u. Assume that

$$f(x,0) = 0 \text{ a.e. in } \mathbb{R}^d \tag{29}$$

and that for every $K > 0$ there exists $L(K) < +\infty$ such that

$$|f(x,u) - f(x,v)| \leq L(K)|u - v| \tag{30}$$

a.e. in $\mathbb{R}^d$ and for all $0 \leq u, v \leq K$. Assume further that

$$\begin{cases} L(\cdot) \in C^0([0,+\infty)) & \text{if } d = 1, \\ L(K) \leq C(1 + K^\alpha) \text{ with } 0 \leq \alpha < \dfrac{4}{d-2} & \text{if } d \geq 2, \end{cases} \tag{31}$$

and extend f to the complex plane by setting

$$f(x,u) = \frac{u}{|u|} f(x,|u|), \tag{32}$$

for all $u \in \mathbb{C}$, $u \neq 0$.

Finally, let H be the Hamiltonian of the system defined by

$$H(u) = \frac{1}{2} \int_{\mathbb{R}^d} |\nabla u|^2(x)\, \mathrm{d}x - \int_{\mathbb{R}^d} \int_0^{|u|(x)} f(x,s)\, \mathrm{d}s\, \mathrm{d}x. \tag{33}$$

We now explain how the Schrödinger equation defines an infinite dimensional dynamical system with symmetries, within the framework of Sects. 2.1 and 2.2. The sense in which the Schrödinger equation defines a Hamiltonian dynamical system will be explained in Sect. 6.

For that purpose, we need the following results on local and global existence of solutions to (28). First, concerning local existence, we have:

Theorem 1 ([17]) *If f is as above, then for every $u_0 \in H^1(\mathbb{R}^d, \mathbb{C})$ there exist numbers $T_{\min}, T_{\max} > 0$ and a unique maximal solution $u : t \in (-T_{\min}, T_{\max}) \to u(t) \in H^1(\mathbb{R}^d, \mathbb{C})$ of (28) satisfying*

$$u \in C^0((-T_{\min}, T_{\max}), H^1(\mathbb{R}^d)) \cap C^1((-T_{\min}, T_{\max}), H^{-1}(\mathbb{R}^d)).$$

Moreover, u depends continuously on u_0 in the following sense: if $u_0^k \to u_0$ in $H^1(\mathbb{R}^d, \mathbb{C})$ and if u_k is the maximal solution of (28) with the initial value u_0^k, then $u_k \to u$ in $C^0([-S,T], H^1(\mathbb{R}^d))$ for every interval $[-S,T] \subset (-T_{\min}, T_{\max})$. In

addition, there is conservation of charge and energy, that is

$$\|u(t)\|_{L^2} = \|u_0\|_{L^2}, \quad H(u(t)) = H(u_0) \tag{34}$$

for all $t \in (-T_{\min}, T_{\max})$.

For global existence of solutions, one needs a growth condition on f in its second variable.

Theorem 2 ([17]) *Let f be as in Theorem 1. Suppose in addition that there exist $A \geq 0$ and $0 \leq \nu < \frac{4}{d}$ such that*

$$\int_0^{|u|} f(x,s)\,\mathrm{d}s \leq A|u|^2(1+|u|^\nu), \quad x \in \mathbb{R}^d,\ u \in \mathbb{C}. \tag{35}$$

It follows that for every $u_0 \in H^1(\mathbb{R}^d, \mathbb{C})$, the maximal strong H^1-solution u of (28) given by Theorem 1 is global and $\sup_{t\in\mathbb{R}} \|u(t)\|_{H^1} < +\infty$.

Note that the condition on f is always satisfied when f is negative. This result implies that one can define Φ_t^X on $E = H^1(\mathbb{R}^d, \mathbb{C})$ by $\Phi_t^X(u) = u(t) \in E$ and that Φ_t^X satisfies (6)–(7). Note however that, whereas the flow lines $t \to u(t) \in E$ are guaranteed to be continuous by the above theorems, they are C^1 only when viewed as taking values in $E^* = H^{-1}(\mathbb{R}^d, \mathbb{C})$. The following "propagation of regularity" theorem allows one to identify the appropriate domain $\mathscr{D}$ on which the stronger condition (8) holds.

Theorem 3 ([17]) *Let f be as in Theorem 1, and consider $u_0 \in H^1(\mathbb{R}^d, \mathbb{C})$ and $u \in C^0((-T_{\min}, T_{\max}), H^1(\mathbb{R}^d))$ the solution of the problem (28) given by Theorem 1. Then the following statements hold.*

(i) If $u_0 \in H^2(\mathbb{R}^d, \mathbb{C})$, then $u \in C^0((-T_{\min}, T_{\max}), H^2(\mathbb{R}^d))$. If, in addition, $f(x,\cdot) \in C^1(\mathbb{C}, \mathbb{C})$, then u depends continuously on u_0 in the following sense: if $u_0^k \to u_0$ in $H^2(\mathbb{R}^d, \mathbb{C})$ and if u_k is the maximal solution of (28) with the initial value u_0^k, then $u_k \to u$ in $C^0([-S,T], H^2(\mathbb{R}^d))$ for every interval $[-S,T] \subset (-T_{\min}, T_{\max})$.

(ii) If $u_0 \in H^m(\mathbb{R}^d, \mathbb{C})$ for some integer $m > \max\left\{\frac{d}{2}, 2\right\}$ and if $f(x,\cdot) \in C^m(\mathbb{C}, \mathbb{C})$, then $u \in C^0((-T_{\min}, T_{\max}), H^m(\mathbb{R}^d))$. In addition, u depends continuously on u_0 in the following sense: if $u_0^k \to u_0$ in $H^m(\mathbb{R}^d, \mathbb{C})$ and if u_k is the maximal solution of (28) with the initial value u_0^k, then $u_k \to u$ in $L^\infty([-S,T], H^m(\mathbb{R}^d))$ for every interval $[-S,T] \subset (-T_{\min}, T_{\max})$.

Note that the derivatives of f should be understood in the real sense here.

Remark 2 It follows from Theorem 3 that, if we take $\mathscr{D} = H^m(\mathbb{R}^d, \mathbb{C})$, with $m \geq 3$, then (8) is satisfied, and so the flow is differentiable as a map from $\mathbb{R}$ to $E = H^1(\mathbb{R}^d, \mathbb{C})$.

Example 1 A typical example of local nonlinearity which satisfies (29), (30), (31) and (32) is the pure power nonlinearity

$$f(u) = \lambda |u|^{\sigma-1} u \tag{36}$$

with

$$\begin{aligned} &1 \leq \sigma < +\infty && \text{for } d = 1, \\ &1 \leq \sigma < 1 + \frac{4}{d-2} && \text{for } d \geq 2, \end{aligned} \tag{37}$$

and $\lambda \in \mathbb{R}$. The standard "cubic" Schrödinger equation corresponds to $\sigma = 3$, which is an allowed value of σ only if $1 \leq d \leq 3$. The Hamiltonian is then given by

$$H(u) = \frac{1}{2} \int_{\mathbb{R}^d} |\nabla u|^2(x)\, \mathrm{d}x - \frac{\lambda}{\sigma+1} \int_{\mathbb{R}^d} |u|^{\sigma+1}(x)\, \mathrm{d}x. \tag{38}$$

In this case, the nonlinear Schrödinger equation reads

$$\begin{cases} i\partial_t u(t,x) + \Delta u(t,x) + \lambda |u|^{\sigma-1}(t,x) u(t,x) = 0, \\ u(0,x) = u_0(x). \end{cases} \tag{39}$$

Theorem 1 then ensures the existence of a local solution

$$u \in C^0((-T_{\min}, T_{\max}), H^1(\mathbb{R}^d)) \cap C^1((-T_{\min}, T_{\max}), H^{-1}(\mathbb{R}^d)) \tag{40}$$

and the conservation of the Hamiltonian energy H. To guarantee the existence of a global flow, we have to distinguish the focusing ($\lambda > 0$) and the defocusing case ($\lambda < 0$). More precisely, Theorem 2 implies the flow is globally defined on $H^1(\mathbb{R}^d, \mathbb{C})$, i.e.

$$\Phi^X : \mathbb{R} \times H^1(\mathbb{R}^d, \mathbb{C}) \to H^1(\mathbb{R}^d, \mathbb{C}), \tag{41}$$

if σ satisfies (37) in the defocusing case or if $1 \leq \sigma < 1 + \frac{4}{d}$ in the focusing case. Note that, in the latter situation, $\sigma = 3$ is allowed only if $d = 1$.

Next, we recall that

$$\begin{aligned} \sigma \in \mathbb{N},\ \sigma \text{ odd } &\Rightarrow f \in C^\infty(\mathbb{C}, \mathbb{C}), \\ \sigma \in \mathbb{N},\ \sigma \text{ even } &\Rightarrow (f \in C^m(\mathbb{C}, \mathbb{C}) \Leftrightarrow m \leq \sigma - 1), \\ \sigma \notin \mathbb{N} &\Rightarrow (f \in C^m(\mathbb{C}, \mathbb{C}) \Leftrightarrow m \leq [\sigma - 1] + 1), \end{aligned}$$

and, in particular, $f \in C^1(\mathbb{C},\mathbb{C})$ for all $\sigma \geq 1$. Hence Theorem 3 applies and the flow can be restricted to $H^2(\mathbb{R}^d,\mathbb{C})$

$$\Phi^X : \mathbb{R} \times H^2(\mathbb{R}^d,\mathbb{C}) \to H^2(\mathbb{R}^d,\mathbb{C}),$$

whenever σ satisfies (37) in the defocusing case or $1 \leq \sigma < 1 + \frac{4}{d}$ in the focusing case. This, however, is not enough for our purposes, since it only guarantees the existence of the derivative of $t \to u(t)$ as a function in $L^2(\mathbb{R}^d,\mathbb{C})$, and not as a function in $E = H^1(\mathbb{R}^d,\mathbb{C})$. In other words, we cannot take $\mathscr{D} = H^2(\mathbb{R}^d,\mathbb{C})$ if we wish to satisfy (8). To obtain sufficient propagation of regularity, having in mind Remark 2, we state the following results.

In dimension $d = 1$ both in the defocusing case, for $3 \leq \sigma < +\infty$, and in the focusing case, for $3 \leq \sigma < 5$,

$$\Phi^X : \mathbb{R} \times H^3(\mathbb{R},\mathbb{C}) \to H^3(\mathbb{R},\mathbb{C}).$$

Hence, in these cases, using the notation introduced in Sect. 2.1, $E = H^1(\mathbb{R},\mathbb{C})$ and the domain $\mathscr{D}$ of the vector field X can be chosen to be the Sobolev space $H^3(\mathbb{R},\mathbb{C})$.

In dimension $d = 2, 3$ and in the defocusing case, the global flow Φ^X can be defined on $E = H^1(\mathbb{R}^d,\mathbb{C})$ for all $3 \leq \sigma < 1 + \frac{4}{d-2}$. As before, the domain $\mathscr{D}$ of the vector field X can be chosen to be the Sobolev space $H^3(\mathbb{R}^d,\mathbb{C})$.

It follows in particular from what precedes that the cubic Schrödinger equation ($\sigma = 3$) fits in the framework of the previous section provided either $d = 1$ (with λ arbitrary) or $\lambda < 0$ and $d = 2, 3$.

We now turn to the study of the symmetries of the nonlinear Schrödinger equation (39). Let $G = \mathrm{SO}(d) \times \mathbb{R}^d \times \mathbb{R}$ and define its action on $E = H^1(\mathbb{R}^d,\mathbb{C})$ via

$$\forall u \in H^1(\mathbb{R}^d), \quad \left(\Phi_{R,a,\gamma}(u)\right)(x) = e^{i\gamma} u(R^{-1}(x-a)). \tag{42}$$

Here the group law of G is

$$(R_1, a_1, \gamma_1)(R_2, a_2, \gamma_2) = (R_1R_2, a_1 + R_1a_2, \gamma_1 + \gamma_2)$$

for all $R_1, R_2 \in \mathrm{SO}(d)$, $a_1, a_2 \in \mathbb{R}^d$ and $\gamma_1, \gamma_2 \in \mathbb{R}$. We claim that G is an invariance group (see Definition 2) for the dynamics Φ_t^X. Indeed, let $u(t,x) = (\Phi_t^X(u))(x)$ a solution to the nonlinear Schrödinger equation (39) and consider $\left((\Phi_{R,a,\gamma} \circ \Phi_t^X)(u)\right)(x) = e^{i\gamma} u(t, Rx - a)$. A straightforward calculation shows that $e^{i\gamma} u(t, R^{-1}(x-a))$ is again a solution to Eq. (39). More precisely,

$$\begin{aligned}
&i\partial_t(e^{i\gamma} u(t, R^{-1}(x-a))) + \Delta(e^{i\gamma} u(t, R^{-1}(x-a))) \\
&\quad + \lambda |e^{i\gamma} u(t, R^{-1}(x-a))|^{\sigma-1}(e^{i\gamma} u(t, R^{-1}(x-a))) \\
&\qquad = e^{i\gamma}\left(i(\partial_t u)(t, R^{-1}(x-a)) + (\Delta u)(t, R^{-1}(x-a)) + (\lambda |u|^{\sigma-1} u)(t, R^{-1}(x-a))\right) \\
&\qquad = 0
\end{aligned}$$

where we use the fact that the Laplace operator is invariant under space rotations, space translations and phase rotations. As a consequence,

$$\left((\Phi_{R,a,\gamma} \circ \Phi_t^X)(u)\right)(x) = \left((\Phi_t^X \circ \Phi_{R,a,\gamma})(u)\right)(x)$$

and G is an invariance group for the dynamics Φ_t^X. Moreover, we can easily prove that $H \circ \Phi_{R,a,\gamma} = H$. Indeed, using the definition of H given in (38), we have

$$\begin{aligned} H \circ \Phi_{R,a,\gamma}(u) &= \frac{1}{2}\int_{\mathbb{R}^d} |\nabla u|^2 (R^{-1}(x-a))\,\mathrm{d}x - \frac{\lambda}{\sigma+1}\int_{\mathbb{R}^d} |u|^{\sigma+1}(R^{-1}(x-a))\,\mathrm{d}x \\ &= H(u). \end{aligned}$$

We will see later (in Sect. 6.3) why this is important.

Now, let us give some examples of G-relative equilibria of the nonlinear Schrödinger equation (39). First, consider the simplest case where $d = 1$ and $\sigma = 3$. The invariance group G reduces to $\mathbb{R} \times \mathbb{R}$ and the nonlinear Schrödinger equation becomes

$$i\partial_t u(t,x) + \partial_{xx}^2 u(t,x) + \lambda |u(t,x)|^2 u(t,x) = 0. \tag{43}$$

In the focusing case ($\lambda > 0$), there exists a two-parameters family of functions, the so-called *bright solitons*,

$$u_{\alpha,c}(t,x) = \alpha\sqrt{\frac{2}{\lambda}}\,\mathrm{sech}(\alpha(x-ct))e^{i\left(\frac{c}{2}x + \left(\alpha^2 - \frac{c^2}{4}\right)t\right)}$$

that are solutions to (43) for all $(\alpha, c) \in \mathbb{R} \times \mathbb{R}$, with initial conditions

$$u_{\alpha,c}(x) = u_{\alpha,c}(0,x) = \alpha\sqrt{\frac{2}{\lambda}}\,\mathrm{sech}(\alpha x)e^{i\left(\frac{c}{2}x\right)} \in E = H^1(\mathbb{R}). \tag{44}$$

For each $(\alpha, c) \in \mathbb{R} \times \mathbb{R}$, $u_{\alpha,c}(x)$ is a G-relative equilibrium of (43). Indeed, the G-orbit of $u_{\alpha,c}(x)$ is given by

$$\mathcal{O}_{u_{\alpha,c}} = \left\{e^{i\gamma}u_{\alpha,c}(x-a), (a,\gamma) \in \mathbb{R} \times \mathbb{R}\right\}. \tag{45}$$

Hence, it is clear that for all $t \in \mathbb{R}$, $u_{\alpha,c}(t,x) \in \mathcal{O}_{u_{\alpha,c}}$ and, by Definition 3, we can conclude that $u_{\alpha,c}(x)$ is a G-relative equilibrium of (43).

More generally, standing and travelling waves are examples of G-relative equilibria of the nonlinear Schrödinger equation (39). More precisely, standing waves are solutions to (39) of the form

$$u_S(t,x) = e^{i\xi t}w_S(x) \tag{46}$$

with $\xi \in \mathbb{R}$. For this to be the case, the profile w_S has to be a solution of the *stationary equation*

$$\Delta w + \lambda |w|^{\sigma-1} w = \xi w.$$

Bright solitons with $c = 0$ are examples of such standing waves, with $d = 1, \sigma = 3$. Standing waves of the one-dimensional Schrödinger equation with a spatially inhomogeneous nonlinearity, as well as their orbital stability, will be studied in Sect. 10. Travelling waves are solutions to (39) of the form

$$u_{TW}(t,x) = e^{i\xi t} w_{TW}(x - ct) \tag{47}$$

with $\xi \in \mathbb{R}$ and $c \in \mathbb{R}^d$. Now, the profile w_{TW} has to be a solution of

$$\Delta w + \lambda |w|^{\sigma-1} w = \xi w + ic \cdot \nabla w.$$

Bright solitons with $c \neq 0$ are examples of such travelling waves, with $d = 1$ and $\sigma = 3$.

The G-orbit of the initial condition $w_S(x)$ is given by

$$\mathcal{O}_{w_S} = \left\{ e^{i\gamma} w_S(R^{-1}(x-a)), (R,a,\gamma) \in G \right\} \tag{48}$$

and it is clear that $u_S(t,x) \in \mathcal{O}_{w_S}$ for all $t \in \mathbb{R}$. The same holds true for u_{TW} with w_S replaced by w_{TW}.

Another, closely related example of an infinite dimensional dynamical system is the cubic Schrödinger equation

$$\begin{cases} i\partial_t u(t,x) + \partial_{xx}^2 u(t,x) \pm |u(t,x)|^2 u(t,x) = 0 \\ u(0,x) = u_0(x) \end{cases} \tag{49}$$

in the space periodic setting $\mathbb{T} = \mathbb{R}/(2\pi\mathbb{Z})$ (the one dimensional torus). In [12], the following theorem is proven.

Theorem 4 ([12]) *The Cauchy problem (49) is globally well-posed for data $u_0 \in H^s(\mathbb{T}, \mathbb{C})$, $s \geq 0$ and the solution $u \in C^0(\mathbb{R}, H^s(\mathbb{T}))$. Moreover, if u, v are the solutions corresponding to data $u_0, v_0 \in H^s(\mathbb{T}, \mathbb{C})$, there is the regularity estimate*

$$\|u(t) - v(t)\|_{H^s} \leq C^{|t|} \|u_0 - v_0\|_{H^s} \tag{50}$$

where C depends on the L^2-size of the data, i.e. $C = C(\|u_0\|_{L^2}, \|v_0\|_{L^2})$.

This ensures the existence of a global flow

$$\Phi^X : \mathbb{R} \times H^s(\mathbb{T}, \mathbb{C}) \to H^s(\mathbb{T}, \mathbb{C}).$$

for all $s \geq 1$. Hence, we can choose $E = H^1(\mathbb{T}, \mathbb{C})$ and $\mathscr{D} = H^3(\mathbb{T}, \mathbb{C})$ to ensure the conditions of Sect. 2.1 are satisfied.

As before, by using the invariance of Eq. (49) under space translations and phase rotations, we can show that the dynamics defined by Φ_t^X are invariant under the action of the group $G = \mathbb{R} \times \mathbb{R}$ given by

$$(\Phi_{a,\gamma}(u))(x) = e^{i\gamma} u(x - a). \tag{51}$$

As an example of G-relative equilibria, we can consider the two-parameter family of plane waves

$$u_{\alpha,k}(t, x) = \alpha e^{-ikx} e^{i\xi t} \tag{52}$$

with $\alpha \in \mathbb{R}$ and $k \in \mathbb{Z}$ and $\xi = -k^2 \pm |\alpha|^2$. The G-orbit of the initial condition $u_{\alpha,k}(x) = \alpha e^{-ikx}$ is given by

$$\mathscr{O}_{u_{\alpha,k}} = \left\{ \alpha e^{i\gamma} e^{-ik(x-a)}, (a, \gamma) \in G \right\}.$$

As before, it is clear that $u_{\alpha,k}(t, x) \in \mathscr{O}_{u_{\alpha,k}}$ for all $t \in \mathbb{R}$. We will study the orbital stability of these relative equilibria in Sect. 9.

Remark that plane waves are the simplest elements of a family of solutions of the NLS equation of the form

$$u_{p,c}(t, x) = e^{i\xi t} e^{-ipx} U(x - ct), \ (t, x) \in \mathbb{R} \times \mathbb{R}$$

with $\xi, p, c \in \mathbb{R}$ and $U : \mathbb{R} \to \mathbb{C}$ a periodic function. This kind of solutions are called *quasi-periodic travelling waves* and their orbital stability has been studied in [40, 41].

3.3 The Manakov Equation

The Manakov equation [43, 73] is a system of two coupled nonlinear Schrödinger equations which describe the evolution of nonlinear electric fields in optical fibers with birefringence, defined by

$$\begin{cases} i\partial_t u(t, x) + \Delta u(t, x) + \lambda |u(t, x)|^2 u(t, x) = 0 \\ u(0, x) = u_0(x) \end{cases} \tag{53}$$

with $u(t, x) = \begin{pmatrix} u_1(t, x) \\ u_2(t, x) \end{pmatrix} : \mathbb{R} \times \mathbb{R} \to \mathbb{C}^2$, $|u(t, x)|^2 = (|u_1(t, x)|^2 + |u_2(t, x)|^2)$ and $\lambda \in \mathbb{R}$.

With the same arguments as those used for the nonlinear Schrödinger equation (39), one can easily show that the flow is globally defined in $H^1(\mathbb{R}, \mathbb{C}^2)$, i.e.

$$\Phi^X : \mathbb{R} \times H^1(\mathbb{R}, \mathbb{C}^2) \to H^1(\mathbb{R}, \mathbb{C}^2) \tag{54}$$

both in the focusing ($\lambda > 0$) and in the defocusing case ($\lambda < 0$). Moreover, thanks to the propagation of regularity, the flow preserves $H^3(\mathbb{R}, \mathbb{C}^2)$ i.e.

$$\Phi^X : \mathbb{R} \times H^3(\mathbb{R}, \mathbb{C}^2) \to H^3(\mathbb{R}, \mathbb{C}^2) \tag{55}$$

as before. Hence, using the notation of Sect. 2.1, one can choose $E = H^1(\mathbb{R}, \mathbb{C}^2)$ and the domain $\mathscr{D} = H^3(\mathbb{R}, \mathbb{C}^2)$.

Now, let $(a, S) \in G = \mathbb{R} \times \mathrm{U}(2)$ act on $E = H^1(\mathbb{R}, \mathbb{C}^2)$ via

$$\Phi_{a,S}(u) = Su(x - a). \tag{56}$$

Here the group law of G is $(a_1, S_1)(a_2, S_2) = (a_1 + a_2, S_1 S_2)$ for all $a_1, a_2 \in \mathbb{R}^d$ and $S_1, S_2 \in \mathrm{U}(2)$. A straightforward calculation proves that G is an invariance group for the dynamics Φ_t^X.

In the focusing case ($\lambda > 0$), there exists a family of solitons,

$$u_\nu(t, x) = \alpha \sqrt{\frac{2}{\lambda}} \mathrm{sech}(\alpha(x - ct)) e^{i\left(\frac{c}{2}x + \left(\alpha^2 - \frac{c^2}{4}\right)t\right)} \begin{pmatrix} \cos\theta e^{i\gamma_1} \\ \sin\theta e^{i\gamma_2} \end{pmatrix}$$

that are solutions to (53) for all $\nu = (\alpha, c, \theta, \gamma_1, \gamma_2) \in \mathbb{R}^5$, with initial condition

$$u_\nu(x) = u_\nu(0, x) = \alpha \sqrt{\frac{2}{\lambda}} \mathrm{sech}(\alpha x) e^{i\left(\frac{c}{2}x\right)} \begin{pmatrix} \cos\theta e^{i\gamma_1} \\ \sin\theta e^{i\gamma_2} \end{pmatrix} \in E = H^1(\mathbb{R}, \mathbb{C}^2).$$

For each $\nu \in \mathbb{R}^5$, $u_\nu(x)$ is a G-relative equilibrium of (53). Indeed, the G-orbit of $u_\nu(x)$ is given by

$$\mathscr{O}_{u_\nu} = \{Su_\nu(x - a), (a, S) \in \mathbb{R} \times \mathrm{U}(2)\}.$$

Hence, it is clear that for all $t \in \mathbb{R}$, $u_\nu(t, x) \in \mathscr{O}_{u_\nu}$ and, by Definition 3, we can conclude that $u_\nu(x)$ is a G-relative equilibrium of (43).

3.4 The Nonlinear Wave Equation

Let us consider the nonlinear wave equation

$$\begin{cases} \partial_{tt}^2 u(t, x) - \Delta u(t, x) + \lambda |u(t, x)|^{\sigma - 1} u(t, x) = 0 \\ u(0, x) = u_0(x), \partial_t u(0, x) = u_1(x) \end{cases} \tag{57}$$

with $u(t,x) : \mathbb{R} \times \mathbb{R}^d \to \mathbb{R}$, and, for simplicity, let us take $d = 1, 2, 3$. Moreover, we restrict our attention to the defocusing case, that in our notation corresponds to $\lambda > 0$ (because of the minus sign in front of the Laplacian), and to the so-called algebraic nonlinearities, which means $\sigma \in \mathbb{N}$ is odd. As a consequence the function $f(u) = |u|^{\sigma-1}u$ is smooth.

Let H defined by

$$H(u, \partial_t u) = \frac{1}{2}\int_{\mathbb{R}^d} |\nabla u|^2 \, \mathrm{d}x + \frac{1}{2}\int_{\mathbb{R}^d} |\partial_t u|^2 \, \mathrm{d}x + \frac{\lambda}{\sigma+1}\int_{\mathbb{R}^d} |u|^{\sigma+1} \, \mathrm{d}x \tag{58}$$

be the Hamiltonian of the system. As for the Schrödinger equation, we will explain in Sect. 6 how the nonlinear wave equation defines an infinite dimensional Hamiltonian dynamical system.

In the defocusing case and whenever $1 \leq \sigma < +\infty$ for $d = 1$ or $1 \leq \sigma < 1 + \frac{4}{d-2}$ for $d = 2, 3$, we can define a global flow on $H^1(\mathbb{R}^d, \mathbb{R}) \times L^2(\mathbb{R}^d, \mathbb{R})$, i.e.

$$\begin{gathered} \Phi^X : \mathbb{R} \times (H^1(\mathbb{R}^d, \mathbb{R}) \times L^2(\mathbb{R}^d, \mathbb{R})) \to H^1(\mathbb{R}^d, \mathbb{R}) \times L^2(\mathbb{R}^d, \mathbb{R}) \\ (t, u(0), \partial_t u(0)) \to (t, u(t), \partial_t u(t)) \end{gathered} \tag{59}$$

with $u \in C(\mathbb{R}, H^1(\mathbb{R}^d)) \cap C^1(\mathbb{R}, L^2(\mathbb{R}^d))$ the unique solution to (57). Moreover the Hamiltonian energy (58) is conserved along the flow, i.e.

$$H(u(0), \partial_t u(0)) = H(u(t), \partial_t u(t))$$

for all $t \in \mathbb{R}$ (see [101] and references therein). Furthermore, it follows from the integral form of (57) (see [101, Ex. 2.18 and 2.22]) that $u \in C^2(\mathbb{R}, H^{-1}(\mathbb{R}^d))$.

In the algebraic case, thanks to the persistence of regularity, the flow can be restricted to $H^s(\mathbb{R}^d, \mathbb{R}) \times H^{s-1}(\mathbb{R}^d, \mathbb{R})$,

$$\Phi^X : \mathbb{R} \times (H^s(\mathbb{R}^d, \mathbb{R}) \times H^{s-1}(\mathbb{R}^d, \mathbb{R})) \to H^s(\mathbb{R}^d, \mathbb{R}) \times H^{s-1}(\mathbb{R}^d, \mathbb{R})$$

for all $s > \frac{d}{2}$. Hence, using the notation of Sect. 2.1, $E = H^1(\mathbb{R}^d, \mathbb{R}) \times L^2(\mathbb{R}^d, \mathbb{R})$ and the domain $\mathscr{D}$ of the vector field X can be chosen to be the Sobolev space $H^2(\mathbb{R}^d, \mathbb{R}) \times H^1(\mathbb{R}^d, \mathbb{R})$.

As for the nonlinear Schrödinger equation, by using the invariance of Eq. (57) under space rotations, space translations and phase rotations, we can show that the dynamics defined by Φ_t^X are invariant under the action of the group $G = \mathrm{SO}(d) \times \mathbb{R}^d$ on $E = H^1(\mathbb{R}^d, \mathbb{R}) \times L^2(\mathbb{R}^d, \mathbb{R})$ defined by

$$\Phi_{R,a}(u, \partial_t u) = (u(R^{-1}(x-a)), \partial_t u(R^{-1}(x-a))).$$

Moreover, $H \circ \Phi_{R,a,\gamma} = H$ and we will explain in Sect. 6.3 the consequences of this fact.

3.5 Generalized Symmetries

The nonlinear Schrödinger equation is often said to be invariant under Galilei transformations. This invariance is however of a slightly different nature than the one defined in Definition 2, as we now explain.[5]

Recall that Newtonian mechanics is known to be invariant under coordinate changes between inertial frames. These include space and time translations, rotations, and changes to a moving frame, often referred to as Galilei boosts. All together, they form a group, the Galilei group G_{Gal}, which is a Lie group that can be defined formally as

$$G_{\mathrm{Gal}} = \mathrm{SO}(d) \times \mathbb{R}^d \times \mathbb{R}^d \times \mathbb{R}$$

with composition law

$$(R', v', a', t')(R, v, a, t) = (R'R, R'v + v', R'a + a' + v't, t + t').$$

It acts naturally on space-time $(x, t) \in \mathbb{R}^d \times \mathbb{R}$ as follows:

$$(R', v', a', t')(x, t) = (R'x + a' + v't, t' + t).$$

Of course, the physical case corresponds to $d = 3$.

The statement that Newton's equations are invariant under boosts means for example that, if $t \to (q_1(t), q_2(t))$ is the solution of Newton's equations of motion for two particles moving in a spherically symmetric interaction potential V

$$m_1 \ddot{q}_1(t) = -\nabla_{q_1} V(\|q_1(t) - q_2(t)\|), \quad m_2 \ddot{q}_2(t) = -\nabla_{q_2} V(\|q_1(t) - q_2(t)\|),$$

with initial conditions

$$q_1(0) = q_1,\ q_2(0) = q_2,\ \dot{q}_1(0) = \frac{p_1}{m_1},\ \dot{q}_2(0) = \frac{p_2}{m_2},$$

then, for all $v \in \mathbb{R}^3$, $t \to (q_1(t) + vt, q_2(t) + vt)$ is also such a solution, with initial conditions

$$q_1(0) = q_1,\ q_2(0) = q_2,\ \dot{q}_1(0) = \frac{p_1}{m_1} + v,\ \dot{q}_2(0) = \frac{p_2}{m_2} + v.$$

[5] We will, in this section, make free use of the material of Appendix sections "Lie Algebras, Lie Groups and Their Actions" and "Hamiltonian Dynamical System with Symmetry in Finite Dimension".

In a Hamiltonian description,[6] the above equations of motion are associated to the Hamiltonian

$$H(q,p) = \frac{p_1^2}{2m_1} + \frac{p_2^2}{2m_2} + V(\|q_1 - q_2\|),$$

which generates a flow Φ_t^H that is clearly invariant under space translations and rotations. The situation for Galilei boosts, however, is different. Indeed, in this context they act on the phase space $E = \mathbb{R}^6 \times \mathbb{R}^6$ with symplectic transformations, as follows:

$$\forall v \in \mathbb{R}^3, \quad \Phi_v^K(q,p) = (q, p_1 - m_1 v, p_2 - m_2 v).$$

Here $K = m_1 q_1 + m_2 q_2$ and Φ_v^K is a shorthand notation for

$$\Phi_v^K = \Phi_{v_1}^{K_1} \circ \Phi_{v_2}^{K_2} \circ \cdots \circ \Phi_{v_n}^{K_n},$$

where each $\Phi_{v_i}^{K_i}$ is the hamiltonian flow of one component of K. But those do NOT commute with the dynamical flow Φ_t^H. Indeed, one easily checks that

$$\Phi_v^K \Phi_t^H \Phi_{-v}^K = \Phi_{vt}^P \Phi_t^H, \tag{60}$$

where $P = p_1 + p_2$ is the total momentum of the system, which generates translations: $\Phi_a^P(q_1, q_2, p_1, p_2) = (q_1 + a, q_2 + a, p_1, p_2)$. In that sense, the three dimensional commutative group of Galilei boosts is NOT an invariance group for the dynamical system according to Definition 2. To remedy this situation, one can proceed as follows. Define, on $E = \mathbb{R}^6 \times \mathbb{R}^6$, for each $g = (R, v, a, t) \in G_{\text{Gal}}$, the symplectic transformation

$$\Phi_g = \Phi_a^P \Phi_t^H \Phi_v^K \Phi_R,$$

where Φ_R is defined as in (22). It is then easily checked using (60) that the Φ_g define an action of G_{Gal} on E. It is clearly globally Hamiltonian (Definition 14).[7] It follows that the Galilei boosts are generalized symmetries for the dynamical system Φ_t^H, in the following sense:

Definition 4 Let G be a Lie group, and Φ an action of G on a Banach space E. Let Φ_t^X a dynamical system on E. We say G is a generalized symmetry group for Φ_t^X provided there exists $\xi \in \mathfrak{g}$ so that $\Phi_t^X = \Phi_{\exp(t\xi)}$.

For our purposes, an important difference between symmetries and generalized symmetries in Hamiltonian systems is that the latter do NOT give rise to constants of

[6] See Appendix section "Hamiltonian Dynamical System with Symmetry in Finite Dimension".

[7] It is however not Ad*-equivariant.

the motion. To illustrate this, remark that, although the Galilei boosts are generated by $K(q,p) = m_1 q_1 + m_2 q_2$, it is clear that K is not a constant of the motion of H:

$$\{K, H\} = P, \tag{61}$$

where $P = p_1 + p_2$ is the total momentum of the two-particle system. This is not a surprise: $K = MR$, where R is the center of mass of the two-particle system and $M = m_1 + m_2$ its mass. And of course, the center of mass moves: in fact, (61) implies it moves at constant velocity.

A similar situation occurs with the nonlinear Schrödinger equation. If $u(t,x)$ is a solution of (28) with a power law nonlinearity, then so is, for every $v \in \mathbb{R}^d$,

$$\tilde{u}(t,x) = \exp\big(-\tfrac{i}{2}(v\cdot x + \tfrac{v^2}{2}t)\big)\, u(t, x+vt), \tag{62}$$

as is readily checked. The function $\tilde{u}$ can be interpreted as the wave function in the moving frame, as can be seen from the shift $x \to x + vt$ in position and from the factor $\exp(-i\frac{v}{2}\cdot x)$, which corresponds to a translation by $\frac{1}{2}v$ in momentum, in the usual quantum mechanical interpretation of the Schrödinger equation. Adopting the framework of Sect. 3.2, one observes that the maps

$$\hat{\Psi}_v\, u(x) = \exp\big(-\tfrac{i}{2}(v\cdot x)\big)\; u(x),$$

defined for all $v \in \mathbb{R}^d$ on $E = H^1(\mathbb{R}^d)$ are not symmetries for the Schrödinger flow Φ^X defined in (41) but that

$$\hat{\Psi}_v \Phi^X_t \hat{\Psi}_{-v} = \Phi_{I, vt, -\frac{v^2}{4}t}\, \Phi^X_t, \tag{63}$$

where $\Phi_{I, vt, -\frac{v^2}{4}t}$ is defined in (42). This commutation relation is very similar to (60), except for the extra phase $\exp(-i\frac{v^2}{4}t)$. We note in passing that the boosts $\hat{\Psi}_v$ are unitary on L^2, but do not preserve the H^1 norm. They are nevertheless bounded operators on $E = H^1(\mathbb{R}^d)$.

As in classical mechanics, one can put together the above transformations with the representation of the Euclidean group in (42) to form a (projective) representation of the Galilei group showing that the Galilei boosts are generalized symmetries of the nonlinear Schrödinger equation with a power law nonlinearity. We will not work this out in detail here, but note for further use that

$$\Phi_{R,a,\gamma}\hat{\Psi}_v = \exp(i\tfrac{v\cdot a}{2})\hat{\Psi}_{Rv}\Phi_{R,a,\gamma}. \tag{64}$$

In particular $\Phi_{I,a,0}\hat{\Psi}_v = \exp(i\frac{v\cdot a}{2})\hat{\Psi}_v\Phi_{I,a,0}$ so that, in this setting, the boosts $\hat{\Psi}_v$ commute with translations only "up to a global phase" $\exp(i\frac{v\cdot a}{2})$, in the usual terminology of quantum mechanics. In contrast, in classical mechanics, Φ^K_v and Φ^P_a clearly commute.

Generalized symmetries do not provide constants of the motion via Noether's Theorem, and hence cannot quite play the same role as symmetries in the study of relative equilibria. We will now show how one may nevertheless use (63) in the analysis of the stability of the relative equilibria of the (non)linear Schrödinger equation.

We first remark that the $u_{\alpha,c}$, defined in (44), satisfy $u_{\alpha,c} = \hat{\Psi}_{-c}u_{\alpha,0}$. We will show that, thanks to (63), if $u_{\alpha,0}$ is orbitally stable, then so is $u_{\alpha,c}$, for any $c \in \mathbb{R}$. We will only sketch the argument, leaving the details to the reader. Note first that $u_{\alpha,0}$ is orbitally stable, if and only if, for all $\epsilon > 0$, there exists $\delta > 0$ so that, for all $w \in E$ with $\mathrm{d}(w, u_{\alpha,0}) \leq \delta$, there exists, for all $t \in \mathbb{R}$, $a(t) \in \mathbb{R}$, $\gamma(t) \in \mathbb{R}$ so that

$$\|\Delta_t\| \leq \epsilon, \quad \text{where} \quad \Delta_t := \Phi_t^X w - \Phi_{I,a(t),\gamma(t)}u_{\alpha,0}.$$

Now suppose $u \in E$ is sufficiently close to $u_{\alpha,c}$, for some $c \in \mathbb{R}$. Then, since $\hat{\Psi}_c$ is a bounded operator, $\hat{\Psi}_c u = w$ is close to $u_{\alpha,0}$. Then, using (63) and (64), one finds

$$\begin{aligned}
\Phi_t^X u &= \Phi_t^X \hat{\Psi}_{-c} w \\
&= \hat{\Psi}_{-c}\Phi_{I,ct,-\frac{c^2}{4}t}\Phi_t^X w \\
&= \hat{\Psi}_{-c}\Phi_{I,ct,-\frac{c^2}{4}t}\Phi_{I,a(t),\gamma(t)}u_{\alpha,0} + \hat{\Psi}_{-c}\Phi_{I,ct,-\frac{c^2}{4}t}\Delta_t \\
&= \hat{\Psi}_{-c}\Phi_{I,ct+a(t),-\frac{c^2}{4}t+\gamma(t)}u_{\alpha,0} + \hat{\Psi}_{-c}\Phi_{I,ct,-\frac{c^2}{4}t}\Delta_t \\
&= \Phi_{I,ct+a(t),-\frac{c^2}{4}t+\gamma(t)+\frac{c(ct+a(t))}{2}}\hat{\Psi}_{-c}u_{\alpha,0} + \hat{\Psi}_{-c}\Phi_{I,ct,-\frac{c^2}{4}t}\Delta_t.
\end{aligned}$$

Since $u_{\alpha,c} = \hat{\Psi}_{-c}u_{\alpha,0}$, and since $\hat{\Psi}_{-c}$ is bounded, it is now clear that $\Phi_t^X u$ is at all times close to $\mathscr{O}_{u_{\alpha,c}}$, defined in (45).

The above argument shows, more generally, that the relative equilibria of the homogeneous NLS for $G = \mathrm{SO}(d)\times\mathbb{R}^d\times\mathbb{R}$ [see (42)] come in families $\hat{\Psi}_{-c}u_0 = u_c$, indexed by $c \in \mathbb{R}^d$. Moreover, if u_0 is spherically symmetric and orbitally stable, then all u_c are orbitally stable.

4 Orbital Stability: A General Definition

We can now formulate the general definition of orbital stability that we shall study. In fact, several definitions appear naturally:

Definition 5 Let Φ_t^X be a dynamical system on a Banach space E and let G be a symmetry group for Φ_t^X.

(i) Let $u \in E$ and let $\mathscr{O}_u$ be the corresponding G-orbit. We say $u \in E$ is orbitally stable if

$$\forall \epsilon > 0, \exists \delta > 0, \forall v \in E, \left(\mathrm{d}(v,u) \leq \delta \Rightarrow \forall t \in \mathbb{R}, \inf_{t' \in \mathbb{R}} \mathrm{d}(v(t), \mathscr{O}_{u(t')}) \leq \epsilon \right).$$

(ii) Let $\mathscr{O}$ be a G-orbit in E. We say $\mathscr{O}$ is stable if each $u \in \mathscr{O}$ is orbitally stable in the sense of (i) above.

(iii) Let $\mathscr{O}$ be a G-orbit in E. We say $\mathscr{O}$ is uniformly stable if it is stable and δ in (i) does not depend on $u \in \mathscr{O}$. In other words, if $\forall \epsilon > 0$, there exists $\delta > 0$ so that, $\forall u \in \mathscr{O}$, $\forall v \in E$,

$$\mathrm{d}(v,u) \leq \delta \Rightarrow \forall t \in \mathbb{R}, \inf_{t' \in \mathbb{R}} \mathrm{d}(v(t), \mathscr{O}_{u(t')}) \leq \epsilon. \tag{65}$$

(iv) We say $\mathscr{O} \in E_G$ is Hausdorff orbitally stable if $\mathscr{O}$ satisfies: $\forall \epsilon > 0$, there exists $\delta > 0$ so that, $\forall \mathscr{O}' \in E_G$

$$\Delta(\mathscr{O}, \mathscr{O}') \leq \delta \Rightarrow \forall t \in \mathbb{R}, \inf_{t'} \Delta(\mathscr{O}'(t), \mathscr{O}(t')) \leq \epsilon. \tag{66}$$

The four definitions are subtly different.

Definition (i) requires that the dynamical orbit issued from the nearby initial condition v remains close to the orbit $\{\Phi_{t'}^X \Phi_g(u) \mid t' \in \mathbb{R}, g \in G\}$ of the larger group $\mathbb{R} \times G$. It is therefore a generalization of definition (4), which corresponds to the case $G = \{e\}$. This notion of orbital stability therefore depends on the choice of the group G and it is clear that, the larger G, the weaker it is. As we will see in the examples of Sects. 5 and 6.5, there are cases where definition (4) is not satisfied for some $u \in E$, but where the above definition holds for a suitable choice of G. As we will also see, the choice of G may depend on the point $u \in E$ considered and it is in particular not always necessary to use the largest symmetry group G available for Φ_t^X to obtain orbital stability.

The stability of the orbit $\mathscr{O}$ as defined in part (ii) simply requires the orbital stability of each point $u \in \mathscr{O}$, as defined in (i). Note that δ depends on u here. In part (iii) of the definition, uniformity is required.

Part (iv) requires that if two G-orbits $\mathscr{O}, \mathscr{O}' \subset E$ are initially close (in the sense of the Hausdorff metric) then, for all t, $\mathscr{O}'(t)$ is close to $\mathscr{O}(t')$ for some value of t'. It is the natural transcription of the definition of orbital stability in (4) from the original dynamical system on E to the reduced dynamics on E_G.

Parts (i), (ii) and (iii) are the most telling/interesting, since they give a statement directly on the phase space E, using the original distance d, rather than in the more abstract quotient space E_G. They do moreover not use the somewhat unpleasant Hausdorff metric. In applications, one really wants to prove (i), (ii) or (iii).

As shown in the lemma below, the four definitions in Definition 5 are equivalent when the group action is isometric. For many applications in infinite dimensional systems in particular, this is the case.

Lemma 1 *Let Φ_t^X be a dynamical system on E and let G be a symmetry group for Φ_t^X, acting isometrically. Let $u \in E$. Then the following statements are equivalent.*

(i) $u \in E$ *is orbitally stable.*
(ii) *Each* $v \in \mathcal{O}_u$ *is orbitally stable.*
(iii) $\mathcal{O}_u$ *is uniformly stable.*
(iv) $\mathcal{O}_u$ *is Hausdorff orbitally stable.*

In practice, one often proves (i) for a suitably chosen u on the orbit. This then automatically yields (iii). The statement in terms of the reduced dynamics in (iv) is intellectually satisfying but rarely encountered, it seems.

Proof We prove $(i) \Leftrightarrow (ii)$ and $(i) \Rightarrow (iii) \Rightarrow (iv) \Rightarrow (i)$.

$(i) \Rightarrow (iii)$ and $(i) \Rightarrow (ii)$: Let $v \in \mathcal{O}_u$ and $v' \in E$, $\mathrm{d}(v', v) \leq \delta$. Then there exists $g \in G$ so that $v = \Phi_g(u)$. Define $u' = \Phi_g^{-1}(v')$. Then, by the isometry of Φ_g, $\mathrm{d}(u', u) \leq \delta$ and hence, by hypothesis, for all t, there exists t' so that $\mathrm{d}(u'(t), \mathcal{O}_{u(t')}) < \epsilon$. Hence

$$\mathrm{d}(v'(t), \mathcal{O}_{v(t')}) = \mathrm{d}(\Phi_g(u'(t)), \mathcal{O}_{u(t')}) = \mathrm{d}(u'(t), \mathcal{O}_{u(t')}) \leq \epsilon.$$

This proves (iii) and, in particular, (ii). Since it is clear that $(ii) \Rightarrow (i)$, we obtain $(i) \Leftrightarrow (ii)$.

$(iii) \Rightarrow (iv)$: Suppose $\mathcal{O}_u$ is uniformly stable. Let $\mathcal{O}'$ be such that $\Delta(\mathcal{O}_u, \mathcal{O}') < \delta$. Let $u' \in \mathcal{O}'$ with $\mathrm{d}(u, u') \leq \delta$. Then (65), together with Proposition 1(ii), imply $\Delta(\mathcal{O}'(t), \mathcal{O}_{u(t')}) \leq \epsilon$.

$(iv) \Rightarrow (i)$: Suppose $\mathcal{O}_u$ is orbitally stable. Let $u' \in E$ so that $\mathrm{d}(u, u') \leq \delta$. Let $\mathcal{O}' = \mathcal{O}_{u'}$. Then, by Proposition 1$(iii)$, $\Delta(\mathcal{O}, \mathcal{O}') \leq \delta$. Hence, for all t, $\inf_{t'} \Delta(\mathcal{O}'(t), \mathcal{O}(t')) \leq \epsilon$. Proposition 1$(ii)$ then implies (i).

In many applications, especially in infinite dimensional problems, the Φ_g are both linear and norm-preserving: several examples were given in Sect. 2. In that case the action is of course isometric. In addition, all group orbits are then bounded. Note nevertheless that, if the Φ_g are norm-preserving, but not linear, the action is no longer isometric, while the group orbits are still bounded. Finally, isometric actions may have unbounded group orbits: think for example of translations on $E = \mathbb{R}^{2n}$.

5 Orbital Stability in Spherical Potentials

Before presenting the general Lyapunov approach to the proof of orbital stability in Sect. 8, we show here the orbital stability of the relative equilibria in spherical potentials that we identified in Sect. 3.1. This simple example is instructive for several reasons. First, it permits one to appreciate the group theoretic and symplectic mechanisms underlying the construction of a suitable candidate Lyapunov function. Second, it nicely illustrates the various methods available to use this Lyapunov

function in order to prove orbital stability via an appropriate "coercivity estimate" generalizing (2). We will present three such methods below.

5.1 Fixed Points

The proof of the uniform orbital stability of $\mathscr{O}_{\rho_*,0,0}$ in (26) is straightforward, and can be done with H itself as the Lyapunov function, in close analogy with the proof sketched in the introduction.

Proposition 2 *Let $V \in C^2(\mathbb{R}^3)$ be a spherical potential and $H(u) = \frac{1}{2}p^2 + V(q)$ the corresponding Hamiltonian. Let $\rho_* > 0$ with $V'(\rho_*) = 0$, $V''(\rho_*) > 0$. Let $\mathscr{O}_{\rho_*,0,0} = \{(q,p) \in \mathbb{R}^6 \mid \|q\| = \rho_*, p = 0\}$ be the corresponding $SO(3)$ orbit. Then $\mathscr{O}_{\rho_*,0,0}$ is uniformly orbitally stable.*

This result is intuitively clear. Under the assumptions stated, the Hamiltonian reaches a local minimum at each of the fixed points of the dynamics that make up the sphere $\mathscr{O}_{\rho_*,0,0}$, and it increases quadratically in directions perpendicular to that sphere. Any nearby initial condition must therefore give rise to an orbit that stays close to the sphere: the potential acts locally as a potential well trapping the particle close to $\mathscr{O}_{\rho_*,0,0}$.

Proof We know from Sect. 3.1 that the Hamiltonian H in (18) is an SO(3)-invariant constant of the motion, and that $D_u H = 0$ for all $u \in \mathscr{O}_{\rho_*,0,0}$, so that each such point is a fixed point of the dynamics. We will write $H_* = H(u), \forall u \in \mathscr{O}_{\rho_*,0,0}$. Moreover, for all $u = (q,0) \in \mathscr{O}_{\rho_*,0,0}$

$$D_u^2 H = \begin{pmatrix} V''(\rho_*)\hat{q}_i\hat{q}_j & 0 \\ 0 & \mathrm{I}_3 \end{pmatrix}.$$

Note that the Hessian is not positive definite. In fact, it vanishes on $w = (a,0)$, for $a \cdot q = 0$, which is the two-dimensional tangent space $T_u\mathscr{O}_{\rho_*,0,0}$ to the orbit. We can therefore not expect to obtain a coercive estimate as in (2). On the other hand, since $V''(\rho_*) > 0$, $D_u^2 H$ *is* positive definite on the four-dimensional orthogonal complement to the tangent space, given by

$$\left(T_u\mathscr{O}_{\rho_*,0,0}\right)^{\perp} = \{(\alpha\hat{q}, b) \in \mathbb{R}^6 \mid \alpha \in \mathbb{R}, b \in \mathbb{R}^3\}. \tag{67}$$

As a result, we can still show that there exist constants $c_*, \eta_* > 0$ with the property that

$$\forall u' \in E, \left(\mathrm{d}(u', \mathscr{O}_{\rho_*,0,0}) \leq \eta_* \Rightarrow H(u') - H_* \geq c_* \mathrm{d}(u', \mathscr{O}_{\rho_*,0,0})^2\right), \tag{68}$$

and this will suffice for the proof of orbital stability. To show (68), note first that setting $u' = (q', p')$ and taking $\eta_* < \rho_*/2$, one has $q' \neq 0$. Consider then

$u = (\rho_* \hat{q}', 0) \in \mathscr{O}_{\rho_*,0,0}$ and remark that $\mathrm{d}(u', \mathscr{O}_{\rho_*,0,0}) = \|u' - u\|$. Now compute

$$H(u') - H_* = H(u') - H(u) = D_v^2 H(u' - u, u' - u) + \mathrm{o}(\|u' - u\|^2)$$
$$\geq \min\{1, V''(\rho_*)\}\mathrm{d}(u', \mathscr{O}_{\rho_*,0,0})^2 + \mathrm{o}(\mathrm{d}(u', \mathscr{O}_{\rho_*,0,0})^2).$$

One can then conclude (68) holds by using that the term in $\mathrm{o}(\mathrm{d}(u', \mathscr{O}_{\rho_*,0,0})^2)$ is uniformly small in $u \in \mathscr{O}_{\rho_*,0,0}$ since H is SO(3)-invariant. We now prove that $\mathscr{O}_{\rho_*,0,0}$ is uniformly orbitally stable. Since the action of SO(3) is isometric, Lemma 1 shows it is enough to prove all $u \in \mathscr{O}_{\rho_*,0,0}$ are orbitally stable. Suppose that this is not true. Then there exists $u \in \mathscr{O}_{\rho_*,0,0}$ and $\epsilon > 0$, and for each $n \in \mathbb{N}_*$, $u_n' \in E$, $t_n \in \mathbb{R}$ so that $\mathrm{d}(u_n', u) \leq \frac{1}{n}$ and $\mathrm{d}(u_n'(t_n), \mathscr{O}_{\rho_*,0,0}) = \epsilon_0$. Since we can choose $\epsilon < \eta_*$, we can apply (68) to write

$$H(u_n') - H(u) = H(u_n'(t_n)) - H_* \geq c_* \mathrm{d}(u_n'(t_n), \mathscr{O}_{\rho_*,0,0})^2 = c_* \epsilon^2.$$

Taking $n \to +\infty$ leads to the desired contradiction.

5.2 Circular Orbits

Proving an appropriate notion of stability for the initial conditions in (25) giving rise to circular orbits of the dynamics turns out to be slightly less straightforward. Intuitively, as explained already in the introduction, one expects that, under a suitable condition on the potential, an initial condition close to a circular orbit will generate a dynamical orbit that stays close to this orbit. As a result, orbital stability is satisfied in the sense of (4). The following proposition gives a precise statement of this phenomenon.

Proposition 3 *Let $V \in C^2(\mathbb{R}^3)$ be a spherical potential and $H(u) = \frac{1}{2}p^2 + V(q)$ the corresponding Hamiltonian. Let $\rho_*, \sigma_* > 0$ with $V'(\rho_*)\rho_* = \sigma_*^2$. Consider $u_{\mu_*} = (q_*, p_*) = (\rho_* \hat{q}_*, \sigma_* \hat{p}_*)$, with $\hat{q}_* \cdot \hat{p}_* = 0$. Then u_{μ_*} is a relative equilibrium for the group SO(2) of rotations about $\mu_* = q_* \wedge p_*$. If in addition,*

$$V''(\rho_*) > -3\sigma_*^2 \rho_*^{-2}, \tag{69}$$

u_{μ_*} is orbitally stable in the sense of definition (4) and of Definition 5(i). In addition, u_{μ_*} is a local minimum of H_{μ_*}, the restriction of H to the level surface Σ_{μ_*}, defined in (24).

Note that the two definitions of orbital stability mentioned coincide in this particular case. Also, since the action of the rotation group is isometric, the result implies uniform orbital stability as well. Below, we will give three different arguments to prove the proposition, each of which can and has been used to treat various infinite dimensional problems.

The origin of the condition $V''(\rho_*) > -3\sigma_*^2\rho_*^{-2}$ can be understood as follows. In standard mechanics textbooks such as [50], motion in a spherical potential is treated by fixing the angular momentum $q \wedge p = \mu_*$, and then using for q, p polar coordinates $(r, \theta, p_r, p_\theta)$ in the plane perpendicular to the angular momentum. The Hamiltonian then reads, in these coordinates,

$$H(r, \theta, p_r, p_\theta) = \frac{p_r^2}{2} + \frac{p_\theta^2}{2r^2} + V(r).$$

The equation of motions are

$$\dot{r} = p_r, \quad \dot{\theta} = \frac{p_\theta}{r^2} \quad \dot{p}_r = \frac{p_\theta^2}{r^3} - V'(r), \quad \dot{p}_\theta = 0$$

and $|\mu_*| = p_\theta$. It follows that the radial motion is decoupled from the angular one, since $\ddot{r} = -V'_{\mu_*}(r)$ with $V_{\mu_*}(r) = V(r) + \frac{\mu_*^2}{2r^2}$. It is then clear that the circular orbits correspond to the critical points $r = \rho_*$ of the effective potential V_{μ_*} which are fixed points of the radial dynamics. By an argument as in the introduction, those are stable if the critical point is a local minimum of

$$H_{\mu_*}(r, p_r) = \frac{p_r^2}{2} + V_{\mu_*}(r),$$

and so in particular if $V''_{\mu_*}(\rho_*) > 0$, which is precisely condition (69). Note however that the preceding argument does not prove orbital stability of the circular orbits: it does not allow to consider initial conditions $u \in \mathbb{R}^6$ with $\mu \neq \mu_*$. This is actually the tricky part of the proof of the proposition.

Proof To mimic the previous proof, we would like to find a constant of the motion $\mathscr{L}$ which is SO(2) invariant and so that $D\mathscr{L}$ vanishes on the orbit under consideration. We cannot use H for this, since clearly $D_{u_{\mu_*}} H \neq 0$, as we are not dealing with a fixed point of the dynamics. On the other hand, as we pointed out after the definition of relative equilibrium, when u_{μ_*} is a relative equilibrium, then there exists an element ξ of the Lie-algebra of the invariance group so that $X_H(u_{\mu_*}) = X_\xi(u_{\mu_*})$ or, equivalently, so that

$$D_{u_{\mu_*}}(H - F_\xi) = 0.$$

In the present case, F_ξ is defined in (23), the invariance group is a one-dimensional rotation group and the statement becomes: there exists $\eta \in \mathbb{R}$ so that

$$D_{u_{\mu_*}}(H - \eta\mu_* \cdot L) = 0, \tag{70}$$

since, as we saw in Sect. 3.1, $\mu_* \cdot L$ generates rotations about the μ_*-axis. So here $\xi = \eta\mu_*$. Since, for all $u \in \mathbb{R}^6$

$$D_u H = (V'(\|q\|)\hat{q}, p), \qquad D_u(\mu_* \cdot L) = (p \wedge \mu_*, \mu_* \wedge q),$$

one easily checks that (70) is satisfied iff $\eta = \rho_*^{-2}$. This suggests to define

$$\mathscr{L}(u) = H(u) - \rho_*^{-2}\mu_* \cdot L(u)$$

and to try using it as a Lyapunov function. $\mathscr{L}$ is often referred to as the "augmented Hamiltonian". Note that the theory of Lagrange multipliers implies that (70) is equivalent to the statement that the restriction H_{μ_*} of H to Σ_{μ_*} has u_{μ_*} as a critical point. Hence the circular orbits can be characterized as the critical points of H_{μ_*}. This is a general feature of relative equilibria of Hamiltonian systems with symmetry, as shown in Theorem 7.

The main ingredient of the proof is the following statement:

$$\exists c > 0, \forall v \in \mathscr{O}_{u_{\mu_*}}, \forall w \in \left(T_v \mathscr{O}_{u_{\mu_*}}\right)^{\perp} \cap T_v \Sigma_{\mu_*}, \quad D_v^2 \mathscr{L}(w, w) \geq c\|w\|^2. \tag{71}$$

This is a lower bound on the Hessian of $\mathscr{L}$ restricted to the two-dimensional subspace of $\mathbb{R}^6$ spanned by the vectors tangent to Σ_{μ_*} [see (24)] and perpendicular to the dynamical orbit $\mathscr{O}_{u_{\mu_*}} \subset \Sigma_{\mu_*}$. It will allow us to show the following lower bound on the variation of the Lyapunov function, which is to be compared to (2):

$$\begin{aligned} &\exists \delta > 0,\ c > 0, \forall u' \in \Sigma_{\mu_*}, \\ &\left(\mathrm{d}(u', \mathscr{O}_{u_{\mu_*}}) \leq \delta \Rightarrow \mathscr{L}(u') - \mathscr{L}(u_{\mu_*}) \geq c\mathrm{d}^2(u', \mathscr{O}_{u_{\mu_*}})\right). \end{aligned} \tag{72}$$

Note that this immediately implies that H_{μ_*} attains a local minimum on $\mathscr{O}_{u_{\mu_*}}$.

To show (71), note that the three vectors

$$e_1 = \begin{pmatrix} p \\ -\left(\frac{\sigma^*}{\rho^*}\right)^2 q \end{pmatrix}, \quad e_2 = \begin{pmatrix} q \\ -p \end{pmatrix}, \quad e_3 = \begin{pmatrix} p \\ q \end{pmatrix}, \tag{73}$$

form an orthogonal basis of $T_v \Sigma_{\mu_*}$, for each point $v = (q, p) \in \mathscr{O}_{u_*}$; e_1 is easily seen to be tangent to $\mathscr{O}_{u_*}$, so that e_2 and e_3 span $(T_v \mathscr{O}_{u_*})^{\perp} \cap T_v \Sigma_{\mu_*}$. A simple but tedious computation then shows that the matrices of $D_v^2(\mu_* \cdot L)$ and of $D_v^2 H$ in this basis are

$$D_v^2(\mu_* \cdot L) = \begin{pmatrix} 2\sigma_*^4 & 0 & \mu_*^2\left[\left(\frac{\sigma_*}{\rho_*}\right)^2 - 1\right] \\ 0 & -2\mu_*^2 & 0 \\ \mu_*^2\left[\left(\frac{\sigma_*}{\rho_*}\right)^2 - 1\right] & 0 & -2\mu_*^2 \end{pmatrix}$$

and

$$D_v^2 H = \begin{pmatrix} V'(\rho_*)\rho_*^{-1}\sigma_*^2 & 0 & (V'(\rho_*)\rho_*^{-1}-1)\sigma_*^2 \\ 0 & V''(\rho_*)\rho_*^2+\sigma_*^2 & 0 \\ (V'(\rho_*)\rho_*^{-1}-1)\sigma_*^2 & 0 & V'(\rho_*)\rho_*^{-1}\sigma_*^2+\rho_*^2 \end{pmatrix}$$

The estimate (71) now follows immediately from the hypothesis that $V''(\rho_*)\rho_*^2 + 3\sigma_*^2 > 0$.

We now turn to the proof of (72). Let $u' \in \Sigma_{\mu_*}$. Then there exists $v' \in \mathscr{O}_{u_*}$ so that $\mathrm{d}(v', \mathscr{O}_{u_*}) = \|u'-v'\|$ and as a result, one has that $u'-v' \in (T_{v'}\mathscr{O}_{u_*})^\perp$. We can write

$$u' = u'-v'+v' = v' + (u'-v')_\parallel + (u'-v')_\perp.$$

Here $(u'-v')_\perp$ is perpendicular to $T_{v'}\Sigma_{\mu_*}$, and $(u'-v')_\parallel$ belongs to $T_{v'}\Sigma_{\mu_*}$ and is perpendicular to $T_{v'}\mathscr{O}_{u_*}$ since $u'-v'$ is. Now remark that, since $D_{v'}L((u'-v')_\parallel) = 0$, and since $u', v' \in \Sigma_{\mu_*}$,

$$0 = L(u') - L(v') = D_{v'}L((u'-v')_\perp) + \mathrm{O}(\|u'-v'\|^2). \tag{74}$$

It is easily checked that, for each $v' \in \mathscr{O}_{u_{\mu_*}}$, the restriction of $D_{v'}L$ to $(T_{v'}\Sigma_{\mu_*})^\perp$ is an isomorphism. It follows that there exists a constant C so that

$$\|(u'-v')_\perp\| \le C\|(u'-v')\|^2. \tag{75}$$

Note that this constant is independent of $v' \in \mathscr{O}_{\mu_*}$ since, for all $R \in \mathrm{SO}(3)$, and for all $u \in \mathbb{R}^6$,

$$\Phi_R \circ D_u L \circ \Phi_{R^{-1}} = D_{\Phi_R u} L,$$

where Φ_R, defined in (22), is an isometry. Returning to (74), and using this last remark, we conclude there exists a constant c_0 so that, for $\|u'-v'\|$ small enough, one has

$$\|(u'-v')_\parallel\| \ge \|u'-v'\| - \|(u'-v')_\perp\| \ge c_0\|u'-v'\|. \tag{76}$$

We can now conclude the proof of (72) as follows, using (75), (76) and (71):

$$\begin{aligned} \mathscr{L}(u') - \mathscr{L}(u_{\mu_*}) &= \mathscr{L}(u') - \mathscr{L}(v') \\ &= D_{v'}\mathscr{L}(u'-v') + \frac{1}{2}D^2_{v'}\mathscr{L}(u'-v', u'-v') + \mathrm{o}(\|u'-v'\|^2) \\ &= \frac{1}{2}D^2_{v'}\mathscr{L}((u'-v')_\parallel, (u'-v')_\parallel) + \mathrm{O}(\|u'-v'\|^3) + \mathrm{o}(\|u'-v'\|^2) \end{aligned}$$

$$
\begin{aligned}
&= \frac{1}{2} D^2_{v'} \mathscr{L}((u'-v')_{\|}, (u'-v')_{\|}) + \mathrm{o}(\|u'-v'\|^2) \\
&\geq \frac{1}{2} c \|(u'-v')_{\|}\|^2 + \mathrm{o}(\|u'-v'\|^2) \\
&\geq \tilde{c}\|u'-v'\|^2 = \tilde{c}\,\mathrm{d}^2(u', \mathscr{O}_{u_{\mu_*}}).
\end{aligned}
$$

Remark that as before, the constant c is independent of $v' \in \mathscr{O}_{\mu_*}$. This shows (72). Note that we used the boundedness of $D^2_{v'}\mathscr{L}$, uniformly in $v' \in \mathscr{O}_{u_{\mu_*}}$.

We can now prove orbital stability, namely:

$$
\forall \epsilon > 0, \exists \delta > 0, \forall u' \in \mathbb{R}^6, \quad \left(\mathrm{d}(u', \mathscr{O}_{u_{\mu_*}}) \leq \delta \Rightarrow \forall t \in \mathbb{R}, \mathrm{d}(u'(t), \mathscr{O}_{u_{\mu_*}}) \leq \epsilon\right). \tag{77}
$$

For that purpose, we propose three different arguments.

First Argument We proceed by contradiction, as before. Suppose there exists $\epsilon_0 > 0$ and for each $n \in \mathbb{N}$, $u'_n \in \mathbb{R}^6$ and $t_n \in \mathbb{R}$ such that $\mathrm{d}(u'_n, u_{\mu_*}) \leq \frac{1}{n}$ and $\mathrm{d}(u'_n(t_n), \mathscr{O}_{u_{\mu_*}}) = \epsilon_0$. We can suppose, without loss of generality, that $2\epsilon_0 < \delta$, where δ is given in (72). We know that $\mathscr{L}(u'_n(t_n)) = \mathscr{L}(u'_n)$, since $\mathscr{L}$ is a constant of the motion. Hence

$$
\lim_{n \to +\infty} \mathscr{L}(u'_n(t_n)) = \mathscr{L}(u_{\mu_*}) = \mu_*.
$$

Since the orbit $\mathscr{O}_{u_{\mu_*}}$ is bounded, and since $\mathrm{d}(u'_n(t_n), \mathscr{O}_{u_{\mu_*}}) = \epsilon_0$, it follows that the sequence $u'_n(t_n)$ is bounded; we can therefore conclude that $\lim_{n\to+\infty} \mathrm{d}(u'_n(t_n), \Sigma_{\mu_*}) = 0$. (In other words $\mathscr{L}$ satisfies Hypothesis F, see Lemma 5.) As a consequence, there exist $w_n \in \Sigma_{\mu_*}$ so that $\|w_n - u'_n(t_n)\| \to 0$. We can now conclude. Since, for n large enough, $\frac{\epsilon_0}{2} \leq \mathrm{d}(w_n, \mathscr{O}_{u_{\mu_*}}) \leq \frac{3}{2}\epsilon_0$, we have

$$
\begin{aligned}
\mathscr{L}(u'_n) - \mathscr{L}(u_{\mu_*}) &= \mathscr{L}(u'_n(t_n)) - \mathscr{L}(u_{\mu_*}) \\
&= \mathscr{L}(u'_n(t_n)) - \mathscr{L}(w_n) + \mathscr{L}(w_n) - \mathscr{L}(u_{\mu_*}) \\
&\geq \mathscr{L}(u'_n(t_n)) - \mathscr{L}(w_n) + c\,\mathrm{d}^2(w_n, \mathscr{O}_{u_{\mu_*}}).
\end{aligned}
$$

The sequences $u'_n(t_n)$ and w_n are bounded. This, combined with the uniform continuity of $\mathscr{L}$ on bounded sets, leads again to a contradiction upon taking $n \to +\infty$.

Second Argument The second proof uses the fact that the relative equilibrium u_{μ_*}, which gives rise to a circular orbit, belongs to a continuous family $\mu \to u_\mu$ of such equilibria, defined on a neighbourhood $I \subset \mathbb{R}^3$ of μ_*. We will only sketch the argument, the general case is treated in Theorem 10. One first observes that, for μ belonging to a suitably small neighbourhood of μ_*, both (71) and (72) hold, with μ_* replaced by μ, and with μ-independent c and δ. This allows one to prove that the equilibria u_μ are orbitally stable with respect to perturbations of the initial condition

within Σ_μ, that is:

$$\forall \epsilon > 0, \exists \delta > 0, \forall u' \in \Sigma_\mu, \quad \left(\mathrm{d}(u', \mathscr{O}_{u_\mu}) \leq \delta \Rightarrow \forall t \in \mathbb{R}, \mathrm{d}(u'(t), \mathscr{O}_{u_\mu}) \leq \epsilon\right). \tag{78}$$

Indeed, suppose that this is not true. Then there exists $\epsilon_0 > 0$, and for each $n \in \mathbb{N}^*$, $u'_n \in \Sigma_\mu, t_n \in \mathbb{R}$ so that $\mathrm{d}(u'_n, u_\mu) \leq \frac{1}{n}$ and $\mathrm{d}(u'_n(t_n), \mathscr{O}_{u_\mu}) = \epsilon_0$. Since we can choose $\epsilon_0 < \delta$, we can apply (72) to write

$$\mathscr{L}(u'_n) - \mathscr{L}(u_\mu) = \mathscr{L}(u'_n(t_n)) - \mathscr{L}(u_\mu) \geq c\mathrm{d}(u'_n(t_n), \mathscr{O}_{u_\mu})^2 = c_* \epsilon_0^2.$$

Taking $n \to +\infty$ leads to the desired contradiction. It remains to prove (78) with "$\forall u' \in \Sigma_\mu$" replaced by "$\forall u \in \mathbb{R}^6$." For that purpose, note that, if $u' \in \mathbb{R}^6$ is close to u_{μ_*}, then $\mu = L(u')$ is close to μ_* and hence u_μ close to u_{μ_*}. So u' is close to u_μ. Hence $u'(t)$ remains close at all times to $\mathscr{O}_{u_\mu}$ by (78). Now, since $\mathscr{O}_\mu$ is close to $\mathscr{O}_{\mu_*}$, the result follows.

Third Argument If (71) had been valid for all $w \in (T_v \mathscr{O}_{u_{\mu_*}})^\perp$, the first argument above would have been slightly easier, since we could then have mimicked the proof of Proposition 2 directly. As it stands, we were able to first show (72), which is valid only for $v' \in \Sigma_{\mu_*}$ and which shows $\mathscr{L}$, restricted to Σ_{μ_*}, attains a local minimum on the orbit. This immediately implies an orbital stability result for perturbations u' of the initial condition u_{μ_*} that stay within Σ_{μ_*}, as is readily seen. But to obtain a stability result for arbitrary perturbations $u' \in \mathbb{R}^6$ of the initial condition u_{μ_*}, we had to work a little harder and invoke Hypothesis F (see Sect. 8.3), which may fail in infinite dimensional problems, as we will see. It turns out that (71) is *not* valid[8] for all $w \in (T_v \mathscr{O}_{u_{\mu_*}})^\perp$. However, it is possible to adjust the Lyapunov function $\mathscr{L}$ so that this *is* the case. Consider, for all $K > 0$,

$$\mathscr{L}_K(u) = \mathscr{L}(u) + K(L(u) - \mu_*)^2. \tag{79}$$

Note that the additional term vanishes on Σ_{μ_*}, where $\mathscr{L}_K$ reaches an absolute minimum. We now show

$$\exists \hat{c} > 0, K > 0, \forall v \in \mathscr{O}_{u_{\mu_*}}, \forall w \in \left(T_v \mathscr{O}_{u_{\mu_*}}\right)^\perp, \quad D_v^2 \mathscr{L}_K(w, w) \geq \hat{c}\|w\|^2. \tag{80}$$

For that purpose, introduce, for each $v = (q, p) \in \mathscr{O}_{u_{\mu_*}}$,

$$e_4 = \begin{pmatrix} \hat{q} \wedge \hat{p} \\ 0 \end{pmatrix}, \quad e_5 = \begin{pmatrix} 0 \\ \hat{q} \wedge \hat{p} \end{pmatrix}, \quad e_6 = \frac{1}{\sqrt{\rho_*^2 + \sigma_*^2}} \begin{pmatrix} \sigma_* \hat{q} \\ \rho_* \hat{p} \end{pmatrix}, \tag{81}$$

[8] This can be seen from a straightforward computation, which is most readily made in the basis e_i introduced in (73) and (81).

which, together with e_1, e_2, e_3 in (73) form an orthonormal basis of $\mathbb{R}^6$. Clearly, $D_v(L-\mu_*)^2(w)=0$, for all $v\in\mathscr{O}_{u_{\mu_*}}$ and for all $w\in\mathbb{R}^6$. Moreover, if $\eta_1,\eta_2,\eta_3\in\mathbb{R}^3$ form an orthonormal basis, then

$$D_v^2(L-\mu_*)^2(w,w)=2\sum_{i=1}^{3}\left[D_v(\eta_i\cdot L)(w)\right]^2,$$

with

$$D_v(\eta_i\cdot L)(w)=w_1\cdot(p\wedge\eta_i)+w_2\cdot(\eta_i\wedge q),\quad w=(w_1,w_2)\in\mathbb{R}^6.$$

Now, writing $w=\sum_{j=2}^{6}\alpha_j e_j\in(T_v\mathscr{O}_{u_{\mu_*}})^{\perp}$ and using $\eta_1=\hat{q},\eta_2=\hat{p},\eta_3=\hat{q}\wedge\hat{p}$, we find

$$\begin{aligned}D_v^2(L-\mu_*)^2(w,w)&=2\left[\alpha_4^2\sigma_*^2+\alpha_5^2\rho_*^2+\alpha_6^2(\rho_*^2+\sigma_*^2)\right]\\&\geq 2\min\{\sigma_*^2,\rho_*^2\}\left[\alpha_4^2+\alpha_5^2+\alpha_6^2\right].\end{aligned}\tag{82}$$

We can now conclude the proof of (80) as follows. We write $w=w_A+w_B$ with $w_A=\alpha_2e_2+\alpha_3e_3$ and $w_B=\alpha_4e_4+\alpha_5e_5+\alpha_6e_6$. Then there exists a constant $C>0$, independent of $v\in\mathscr{O}_{u_{\mu_*}}$, so that

$$\begin{aligned}D_v^2\mathscr{L}_K(w,w)&\geq D_v^2\mathscr{L}(w,w)+2K\min\{\sigma_*^2,\rho_*^2\}\|w_B\|^2\\&\geq D_v^2\mathscr{L}(w_A,w_A)+2K\min\{\sigma_*^2,\rho_*^2\}\|w_B\|^2-C\left[\|w_A\|\|w_B\|+\|w_B\|^2\right].\end{aligned}$$

Using (71), one finds that, for all $m>0$,

$$D_v^2\mathscr{L}_K(w,w)\geq\left(c-\frac{Cm^2}{2}\right)\|w_A\|^2+\left(2K\min\{\sigma_*^2,\rho_*^2\}-C-\frac{C}{2m^2}\right)\|w_B\|^2,$$

where we have applied Young's inequality to the term $\|w_A\|\|w_B\|$. Choosing m small enough and K large enough, one finds (80). We can now prove the following statement, which is to be compared to (72): $\exists\delta,c>0$ so that, for all $u'\in\mathbb{R}^6$,

$$\mathrm{d}(u',\mathscr{O}_{u_{\mu_*}})\leq\delta\Rightarrow\mathscr{L}_K(u')-\mathscr{L}_K(u_{\mu_*})\geq c^2\mathrm{d}^2(u',\mathscr{O}_{u_{\mu_*}}).\tag{83}$$

Indeed, for all $u'\in\mathbb{R}^6$, there exists $v'\in\mathscr{O}_{u_{\mu_*}}$ so that $u'-v'\in(T_{v'}\mathscr{O}_{u_{\mu_*}})^{\perp}$. Hence

$$\mathscr{L}_K(u')-\mathscr{L}(u_{\mu_*})=\mathscr{L}(u')-\mathscr{L}_K(v')\geq\frac{\hat{c}}{2}\|u'-v'\|^2+\mathrm{O}(\|u'-v'\|^3).$$

This implies (83), from which orbital stability follows by the now familiar argument.

We point out that the core ingredient of all three arguments in the proof is estimate (71). Its proof constitutes the only truly model-dependent part of the proofs of orbital stability via the energy-momentum method. This will become clear in Sect. 8 where we will show how a suitably adapted version of this estimate implies orbital stability in a general infinite dimensional setting as well (Theorems 9–11).

As a second remark, note that (72) allows one to prove immediately the orbital stability for perturbations of the initial condition that preserve the angular momentum. The three strategies of the proof above therefore concern three different methods for extending this result to arbitrary perturbations of the initial condition. The same structure of the proof will be apparent in the general situation treated in Sect. 8.

The first argument in the above proof is the one used in [53, 54]. It has the disadvantage of using Hypothesis F, which, while obvious in finite dimensions, may not hold in infinite dimensional systems, notably when the group G_{μ_*} is not one-dimensional (as in [54]). We will illustrate this phenomenon in Sect. 8. It has the advantage—when Hypothesis F does work—of not using the fact that the relative equilibrium under consideration belongs to a continuous family.

The second argument seems to go back to Benjamin (see Sect. 11) and is used for example in [104], and in [40, 41]. For this argument the existence of a continuous family of relative equilibria is needed but not Hypothesis F.

The third argument is commonly used in the literature on finite dimensional Hamiltonian systems [84], and appears also in [99] in the infinite dimensional case. It is not universally useable, since it depends on the existence of a G_μ-invariant Euclidean structure on the dual of the Lie-algebra of G, as we will see in Sect. 8.

6 Hamiltonian Dynamics in Infinite Dimension

The modern formulation of Hamiltonian dynamics has been adapted to the framework of infinite dimensional Banach manifolds in [19, 74]. This approach is not well suited for our purposes for two reasons. First, we are interested in flows defined by the solutions to (nonlinear) partial differential equations that are defined on Banach (or even Hilbert) spaces, for which a general Banach manifold formulation is overly complex. In addition, the notions of "Hamiltonian vector field" and "Hamiltonian flow" introduced in [19] seem too general for the purpose of studying stability questions. We therefore present a simpler and more restricted framework that is well adapted to the analysis of the stability questions that are our main focus, including for nonlinear Schrödinger and wave equations.

Our main goal in this section is thus to give a workable and not too complex definition of "Hamiltonian dynamical system" or of "Hamiltonian flow" in the infinite dimensional Banach space setting (Sect. 6.2). The formalism allows us to easily obtain general results on the link between symmetries and conserved quantities for such systems, as in the finite dimensional case (Sect. 6.3). This link is indeed an essential ingredient for the identification of relative equilibria and the construction

of coercive Lyapunov functions in Hamiltonian systems with symmetry, as we shall explain in Sect. 7. Several examples of Hamiltonian PDE's that fit in our framework are given in Sect. 6.5. Although this section is self-contained, the reader unfamiliar with finite dimensional Hamiltonian dynamical systems and their symmetries may find it useful to consult Appendix section "Hamiltonian Dynamical System with Symmetry in Finite Dimension" for a concise and self-contained treatment of this case. We will make regular use of the notation and concepts introduced there.

6.1 Symplectors, Symplectic Banach Triples, Symplectic Transformations, Hamiltonian Vector Fields

We first generalize the notion of symplectic form to the infinite dimensional setting and introduce the equivalent notion of *symplector* (Definition 7). It turns out that, in the infinite dimensional setting, it is convenient to treat the latter as the central object of the theory, rather than the symplectic form itself, as is customary in finite dimensions. As we will see, the two approaches are perfectly equivalent.

We need some preliminary terminology. Let E be a Banach space and $B : E \times E \to \mathbb{R}$ a bilinear continuous form. We can then define, in the usual manner, for all $u \in E$, $\mathscr{J}_B u \in E^*$ via

$$\mathscr{J}_B u(v) = B(u, v).$$

It follows easily that $\mathscr{J}_B : u \in E \to \mathscr{J}_B u \in E^*$ is linear and continuous, with $\|\mathscr{J}_B\| = \|B\|$. We will write $\mathscr{R}_{\mathscr{J}_B} = \operatorname{Ran} \mathscr{J}_B$. Conversely, given a continuous linear map $\mathscr{J} : E \to E^*$, one can construct $B_{\mathscr{J}}(u, v) = (\mathscr{J} u)(v)$. We introduce the following terminology:

Definition 6 A bilinear continuous form B is non-degenerate (or weakly non-degenerate) if $\mathscr{J}_B$ is injective. It is strongly non-degenerate if $\mathscr{J}_B$ is both injective and surjective. Similarly, a linear map $\mathscr{J} : E \to E^*$ is said to be (weakly) non-degenerate if it is injective, and strongly non-degenerate if it is a bijection.

Definition 7 We now introduce the notion of symplector.[9]

(i) A symplector or weak symplector is a continuous linear map $\mathscr{J} : E \to E^*$ that is injective and anti-symmetric, in the sense that

$$(\mathscr{J} u)(v) = -(\mathscr{J} v)(u).$$

If in addition $\mathscr{J}$ is surjective, we say it is a strong symplector.

[9] This object does not seem to have been blessed with a name in the literature, so we took the liberty to baptize it.

(ii) A (strong) symplectic form ω is a (strongly) non-degenerate bilinear continuous form that is anti-symmetric.
(iii) When $\mathscr{J}$ is a (strong) symplector, we will say $(E, \mathscr{J})$ is a (strong) symplectic vector space, or simply that E is a (strong) symplectic vector space, when there is no ambiguity about the choice of $\mathscr{J}$.

There clearly is a one-to-one correspondence between (strong) symplectors and (strong) symplectic forms. Note that the definition implies that

$$\forall \alpha, \beta \in \mathscr{R}_{\mathscr{J}}, \quad \alpha(\mathscr{J}^{-1}\beta) = -\beta(\mathscr{J}^{-1}\alpha). \tag{84}$$

The following examples of (strong) symplectors cover all applications we have in mind in these notes. Let $\mathscr{K}$ be a real Hilbert space and set $E = \mathscr{K} \times \mathscr{K}$. Then

$$\mathscr{J} : (q, p) \in E \to (-p, q) \in E^*$$

is clearly a strong symplector. Here we wrote $u = (q, p) \in \mathscr{K} \times \mathscr{K}$ and used the Riesz identification of E with E^*. The corresponding strong symplectic form is

$$\omega_{\mathscr{J}}(u, u') = q \cdot p' - q' \cdot p,$$

where $\cdot$ denotes the inner product on $\mathscr{K}$. The analogy with (209) is self-evident: there $\mathscr{K} = \mathbb{R}^n$, where $\mathbb{R}^n$ is equipped with its standard Euclidean structure. Note that if Q is a bounded self-adjoint operator on $\mathscr{K}$ with $\mathrm{Ker} Q = \{0\}$, then

$$\mathscr{J} : (q, p) \in E \to (-Qp, Qq) \in E^*$$

is also a symplector with

$$\omega_{\mathscr{J}}(u, u') = q \cdot Qp' - p \cdot Qq'.$$

We will need the following straightforward generalization of the above construction. Let K^2 be a positive (possibly and typically unbounded) self-adjoint operator on $\mathscr{K}$, with domain $\mathscr{D}(K)$. Introduce, for all $s \in \mathbb{R}$, $\mathscr{K}_s = [\mathscr{D}(\langle K \rangle^s)]$, where $\langle K \rangle = \sqrt{1 + K^2}$ and where $\langle K \rangle^s$ is defined by the functional calculus of self-adjoint operators. Here $[\mathscr{D}(\langle K \rangle^s)]$ denotes the closure of $\mathscr{D}(\langle K \rangle^s)$ in the topology induced by the Hilbert norm

$$\|u\|_s := \|\langle K \rangle^s u\|.$$

Note that, since $\langle K \rangle^s : (\mathscr{D}(\langle K \rangle^s), \|\cdot\|_s) \to (\mathscr{D}(\langle K \rangle^{-s}), \|\cdot\|)$ is an isometric bijection, it extends to a unitary map from $\mathscr{K}_s$ to $\mathscr{K}$ for which we still write $\langle K \rangle^s$. With these conventions, we can then make the usual identification between $\mathscr{K}_s{}^*$ and $\mathscr{K}_{-s}$: $\forall v \in \mathscr{K}_{-s}$, we define

$$u \in \mathscr{K}_s \to v \cdot u \in \mathbb{R},$$

by setting $v \cdot u := \langle K\rangle^{-s} v \cdot \langle K\rangle^{s} u$. Note that

$$\forall s, s' \in \mathbb{R}, \quad s \leq s' \Rightarrow \mathscr{K}_{s'} \subset \mathscr{K}_s.$$

It is easy to see using the spectral theorem that this is an inclusion as sets, and we will therefore not introduce explicit identification operators to represent such inclusions which are moreover continuous for the respective Hilbert space topologies. The typical example of this construction to keep in mind is $K^2 = -\Delta$ on $\mathscr{K} = L^2(\mathbb{R}^d)$. We then have $\mathscr{K}_s = H^s(\mathbb{R}^d)$, the usual Sobolev spaces.

For $s = (s_1, s_2) \in \mathbb{R}^2$, we define $E_s = \mathscr{K}_{s_1} \times \mathscr{K}_{s_2}$. Defining a partial order relation by $s \preceq s'$ iff $s_1 \leq s_1'$ and $s_2 \leq s_2'$, we have

$$\forall s, s' \in \mathbb{R}^2, \quad s \preceq s' \Rightarrow E_{s'} \subset E_s.$$

Setting $\bar{s} = (s_2, s_1)$ we then define

$$\mathscr{J}_s : u = (q, p) \in E_s \to (-p, q) \in E_{\bar{s}}. \tag{85}$$

The following lemma is now immediate.

Lemma 2 *$\mathscr{J}_s$ is a weak symplector if and only if $s_1 \geq -s_2$. In that case*

$$\mathscr{J}_s : u = (q, p) \in E_s \to (-p, q) \in E_{\bar{s}} \subset E_{-s} = E_s^*.$$

We have $\mathscr{R}_s := \mathscr{R}_{\mathscr{J}_s} = E_{\bar{s}}$. And $\mathscr{J}_s^{-1} = \mathscr{J}_{-s|E_{\bar{s}}}$. If K^2 is unbounded, $\mathscr{J}_s$ is a strong symplector if and only if $s_1 = -s_2$.

Typical examples of this construction are the use of $E = E_{(1/2,-1/2)}$ or of $E = E_{(1,0)}$ with $\mathscr{K} = L^2(\mathbb{R}^d)$ and $K^2 = -\Delta$ to study the wave equation. For the Schrödinger equation, $E = E_{(1,1)}$ is a natural choice. We refer to Sect. 6.5 for the details of these examples. Note that of these three examples, only the first corresponds to a strong symplector and hence to a strong symplectic form. It is therefore clear that the use of weak symplectors is unavoidable in applications to PDE's.

We end our discussion of symplectors with a simple lemma that collects some of their essential properties.

Lemma 3 *Let E be a Banach space and $\mathscr{J} : E \to E^*$ be a bounded linear map. Then the following holds:*

(i) If $\mathscr{J}$ is a strong symplector, then $\mathscr{J}^{-1}$ is bounded.
(ii) If $\mathscr{J}$ is injective and (anti-)symmetric, and if E is reflexive, then $\mathscr{R}_{\mathscr{J}}$ is dense in E^*.
(iii) Suppose $\mathscr{J}$ is injective and (anti-)symmetric, and that its inverse is bounded on $\mathscr{R}_{\mathscr{J}}$. Suppose E is reflexive. Then $\mathscr{R}_{\mathscr{J}} = E^*$.

Proof

(i) This is a consequence of the open mapping theorem.

(ii) Suppose $v \in E$ satisfies $\mathscr{J}u(v) = 0$ for all $u \in E$. Then $\mathscr{J}v(u) = 0$ for all $u \in E$, by (anti-)symmetry. Hence $\mathscr{J}v = 0$ and hence, since $\mathscr{J}$ is injective, $v = 0$. Since E is reflexive, this means that, if $v \in E^{**}$ vanishes on $\mathscr{R}_{\mathscr{J}} \subset E^*$, then $v = 0$. This implies $\mathscr{R}_{\mathscr{J}}$ is dense (Hahn-Banach).
(iii) Since the inverse is bounded, $\mathscr{R}_{\mathscr{J}}$ is closed. The result then follows from (ii).

If E is not reflexive, a symplector may not have a dense range, as the following example[10] shows. Let

$$E = \{u \in L^1(\mathbb{R}, \mathrm{d}x) \mid \int_{\mathbb{R}} u(x)\mathrm{d}x = 0\} \subset L^1(\mathbb{R})$$

and define

$$\mathscr{J}u(x) = \int_{-\infty}^{x} u(y)\mathrm{d}y \in L^\infty(\mathbb{R}) \subset E^*.$$

This is clearly bounded, injective and antisymmetric. But it is clear that

$$\|\mathscr{J}u - 1\|_\infty \geq 1,$$

for all $u \in E$. So the range is not dense in $L^\infty(\mathbb{R})$ and a fortiori not dense in E^*.

We are now ready to define what we mean by a symplectic transformation and by a Hamiltonian vector field. First we recall a very basic definition: when $F : E_1 \to E_2$ is a function between two Banach spaces E_1 and E_2, and when $u \in E_1$, one says that F is (Fréchet) differentiable at u if there exists $D_uF \in \mathscr{L}(E_1, E_2)$ so that

$$\lim_{w \to 0} \frac{\|F(u+w) - F(u) - D_uF(w)\|_{E_2}}{\|w\|_{E_1}} = 0.$$

Also, one says that $F : E_1 \to E_2$ is differentiable on some subset of E_1 if for all u in that subset, F is differentiable in the above sense.

In particular, if $E_1 = E, E_2 = \mathbb{R}$, and if F is differentiable at $u \in E$, we have $D_uF \in E^*$. And if $\mathscr{D}$ is a domain in E, saying that $F : E \to \mathbb{R}$ *is differentiable on* $\mathscr{D}$ means that F is differentiable at each $u \in \mathscr{D}$. In that case, one can define

$$u \in \mathscr{D} \subset E \to D_uF \in E^*.$$

As a last comment, we stress that, in these definitions, the only topology used is the one on E. This is important to keep in mind in the applications, where the domain $\mathscr{D}$ often carries a natural topology, stronger than the one induced by the norm on E, and for which $\mathscr{D}$ is closed. One can think of $E = H^1(\mathbb{R})$ and $\mathscr{D} = H^3(\mathbb{R})$. Such a topology is NOT used in the above statements, nor in the

[10] Due to S. Keraani.

following general definition. We refer to the examples treated in Sects. 6.4 and 6.5 for several illustrations of this last comment.

Definition 8 Let E be a Banach space, $\mathscr{D}$ a domain in E (See Sect. 2.1) and $\mathscr{J}$ a symplector.

(i) We will refer to $\left(E, \mathscr{D}, \mathscr{J}\right)$ as a symplectic Banach triple.
(i) Let $\left(E, \mathscr{D}, \mathscr{J}\right)$ be a symplectic Banach triple and $\Phi \in C^0(E, E) \cap C^1(\mathscr{D}, E)$. We say Φ is a symplectic transformation if

$$\forall u \in \mathscr{D}, \forall v, w \in E, (\mathscr{J} D_u \Phi(v))(D_u \Phi(w)) = (\mathscr{J} v)(w). \tag{86}$$

(iii) We say that a function $F : E \to \mathbb{R}$ has a $\mathscr{J}$-compatible derivative if F is differentiable on $\mathscr{D}$ and if, for all $u \in \mathscr{D}$, $D_u F \in \mathscr{R}_{\mathscr{J}}$. In that case we write $F \in \mathrm{Dif}(\mathscr{D}, \mathscr{J})$.
(iv) For each $F \in \mathrm{Dif}(\mathscr{D}, \mathscr{J})$, the Hamiltonian vector field $X_F : \mathscr{D} \subset E \to E$ associated to F is defined by

$$X_F(u) = \mathscr{J}^{-1} D_u F, \quad \forall u \in \mathscr{D}. \tag{87}$$

The analogy between (86) and (225) as well as between (87) and (218) is evident. Note however that, when dealing with *weak* symplectors, as is often the case in applications, the vector field X_F does not inherit the continuity or smoothness properties that F may enjoy. In particular, even if

$$D.F : \mathscr{D} \subset E \to E^*$$

is continuous, the same may not hold for X_F. We shall for that reason avoid making use of the vector fields X_F where possible and state all our hypotheses in terms of F directly. We finally point out that, here and in what follows, and unless otherwise specified, all functions we consider are globally defined[11] on E.

6.2 *Hamiltonian Flows and Constants of the Motion*

Definition 9 Let $\left(E, \mathscr{D}, \mathscr{J}\right)$ be a symplectic Banach triple. Let $F \in \mathrm{Dif}(\mathscr{D}, \mathscr{J})$. A Hamiltonian flow for F is a separately continuous map $\Phi^F : \mathbb{R} \times E \to E$ with the following properties:

(i) For all $t, s \in \mathbb{R}$, $\Phi^F_{t+s} = \Phi^F_t \circ \Phi^F_s$, $\Phi^F_0 = \mathrm{Id}$;
(ii) For all $t \in \mathbb{R}$, $\Phi^F_t(\mathscr{D}) = \mathscr{D}$;

[11] This is a difference with [19], as we will explain in some detail in Sect. 6.4.

(iii) For all $u \in \mathscr{D}$, the curve $t \in \mathbb{R} \to u(t) := \Phi_t^F(u) \in \mathscr{D} \subset E$ is differentiable and is the unique solution of

$$\mathscr{J}\dot{u}(t) = D_{u(t)}F, \quad u(0) = u. \tag{88}$$

Local Hamiltonian flows are defined in the usual way. We refer to (88) as the Hamiltonian differential equation associated to F [Compare to (219) and (212)] and to its solutions as Hamiltonian flow lines. Note that in this setting separate continuity implies continuity (see [19], Sect. 3.2). We refer to Sect. 6.5 for examples of PDE's generating Hamiltonian flows.

To compare this definition to the ones of [53, 54, 99], we first observe that (88) implies that, for all $u \in \mathscr{D}$,

$$\forall \alpha \in \mathscr{R}_{\mathscr{J}}, \quad -\frac{\mathrm{d}}{\mathrm{d}t}\alpha(u(t)) = D_{u(t)}F(\mathscr{J}^{-1}\alpha), \tag{89}$$

which is a weak form of (88). With this in mind, one could think of changing Definition 9 by replacing (iii) by the following alternative statement[12]:

(iii') For all $u \in E$, the curve $t \in \mathbb{R} \to u(t) := \Phi_t^F(u) \in E$ belongs to $C(\mathbb{R}, E)$ and (89) holds.

This has the advantage of eliminating the introduction of the domain $\mathscr{D}$ [and therefore of condition (ii)] and is precisely the definition of "solution" to (88) used in [53, 54]. In [99], E is a Hilbert space and still a different formulation is adopted. Basically, the domain $\mathscr{D}$ is not introduced, the Eq. (88) is interpreted as an equation in E^* and the time derivative is understood as a strong derivative for E^*-valued functions. Those alternative formulations do not allow for a direct proof of the kind of natural "conservation theorems" such as Theorem 5 below, that are typical for Hamiltonian systems and that we need for the stability analysis. As a result, the conclusions of such conservation theorems are added as assumptions in the general setup of the cited works. It turns out that, in examples, the proof of such assumptions requires a stronger notion of "solution" than the ones used in [53, 54, 99], so we found it more efficient to adopt from the start the stronger notion of Hamiltonian flow found in Definition 9.

Let us finally point out that the formulation adopted in [99] puts further restrictions on $\mathscr{J}$, ruling out for example the treatment of the wave equation as a Hamiltonian system as in Sect. 6.5. Also, only one-dimensional invariance groups are considered there, and restrictions on their action rule out, for example, the consideration of the translation group as a symmetry group for the nonlinear homogeneous Schrödinger equation. The formalism does therefore not apply to the study of the orbital stability of the bright solitons in (44). On the other hand,

[12] Note that for this formulation one needs $F \in \mathrm{Dif}(E, \mathbb{R})$, but it is not necessary that it has a $\mathscr{J}$-compatible derivative.

it can and has been used to study the orbital stability of standing waves of the inhomogeneous nonlinear Schrödinger equation. We refer to Sect. 10 for more details.

Definition 10 Let $F, G \in \mathrm{Dif}(\mathscr{D}, \mathscr{J})$. Then the Poisson bracket of F and G is defined by

$$\{F, G\}(u) = D_u F(\mathscr{J}^{-1} D_u G), \qquad \forall u \in \mathscr{D}. \tag{90}$$

Equation (90) is the obvious transcription of (220) to the infinite dimensional setting. We now have the following crucial result, which is a simple form of Noether's Theorem in the Hamiltonian setting. A more complete form follows below (Theorem 6).

Theorem 5 *Let $(E, \mathscr{D}, \mathscr{J})$ be a symplectic Banach triple. Let $H, F \in C(E, \mathbb{R})$ and suppose they have a $\mathscr{J}$-compatible derivative, i.e. $H, F \in \mathrm{Dif}(\mathscr{D}, \mathscr{J})$. Suppose there exist Hamiltonian flows Φ_t^H, Φ_t^F for H and F. Then:*

(i) For all $u \in \mathscr{D}$, and for all $t \in \mathbb{R}$,

$$\frac{\mathrm{d}}{\mathrm{d}t} H(\Phi_t^F(u)) = \{H, F\}(\Phi_t^F(u)). \tag{91}$$

(ii) The following three statements are equivalent:

(a) For all $u \in \mathscr{D}$, $\{F, H\}(u) = 0$.
(b) For all $u \in E$, and for all $t \in \mathbb{R}$,

$$(H \circ \Phi_t^F)(u) = H(u). \tag{92}$$

(c) For all $u \in E$, and for all $t \in \mathbb{R}$,

$$(F \circ \Phi_t^H)(u) = F(u). \tag{93}$$

In this result, the roles of H and F are interchangeable. But in practice, one of the flows, say Φ_t^F, is simple, explicitly known, and often linear, whereas Φ_t^H is obtained by integrating a possibly nonlinear PDE of some complexity, such as the nonlinear Schrödinger or wave equations. It is then often very easy to check by a direct computation that $H \circ \Phi_t^F$ is constant in time for all $u \in E$: one says that H is invariant under the flow Φ_t^F, or that the Φ_t^F are symmetries of H. The important conclusion of the theorem is that this implies that F is a constant of the motion for Φ_t^H. This is a strong statement, since in applications, the flow Φ_t^H is complex and poorly known. So being able to assert that it leaves the level surfaces of F invariant is a non-trivial piece of information. Several examples are given in Sect. 6.5.

Proof

(i) Let $u \in \mathscr{D}$. Then $t \in \mathbb{R} \to H(\Phi_t^F(u)) \in \mathbb{R}$ is differentiable and the chain rule applies: writing $u(t) = \Phi_t^F(u)$, we have

$$\frac{\mathrm{d}}{\mathrm{d}t} H(\Phi_t^F(u)) = D_{\Phi_t^F(u)} H(\dot{u}(t)),$$

which yields the first equality in (91) since $\mathscr{J}\dot{u}(t) = D_{u(t)}F$.

(ii) That (92) or (93) imply $\{H, F\}(u) = 0$ for $u \in \mathscr{D}$ is immediate from (i). Conversely, it follows from (i) and the fact that $\{H, F\}(u) = 0$, for all $u \in \mathscr{D}$, that $(H \circ \Phi_t^F)(u) = H(u)$. Since $\mathscr{D}$ is dense in E, $H \in C(E, \mathbb{R})$ and $\Phi_t^F \in C(E, E)$, (b) now follows for all $u \in E$. Similarly for (c).

It should be noted that condition (ii) of Definition 9 is crucial here. We are assuming there is a common invariant domain for both flows. To obtain conservation theorems of the above type without such an assumption requires other technical conditions [19].

We end with some technical remarks. First, it follows from Theorem 18 in the Appendix, that Hamiltonian flows Φ_t^F are symplectic as soon as $F \in C^2(E, E)$ and $\Phi_t^F \in C^2(E, E)$. But these two assumptions (especially the latter) are generally too strong to be of use in infinite dimensional dynamical systems generated by PDE's, except possibly when they are linear. Of course, one can conceive of weaker conditions that imply the result. For efforts in that direction, we refer to [19]. In other words, proving that Hamiltonian flows, as defined above, are symplectic, can be painful. A second, related issue is the following. In finite dimensional systems, we know that, if $\{F_1, F_2\} = 0$, with $F_1, F_2 \in C^2(E)$, then the corresponding Hamiltonian flows commute: see (222) and Lemma 9. This is a very useful fact: indeed, computing a Poisson bracket is a routine matter of taking derivatives, and the information obtained about the flows is very strong. Again, this is not immediate in infinite dimensional systems under reasonable conditions. For our purposes, and in particular for the proof of Theorem 6, the following analog of Lemma 13 will suffice.

Lemma 4 *Let $(E, \mathscr{D}, \mathscr{J})$ be a symplectic Banach triple. Let Φ be a C^1-diffeomorphism on E and suppose that $\Phi(\mathscr{D}) = \mathscr{D}$ and that Φ is symplectic. Let $F \in \mathrm{Dif}(\mathscr{D}, \mathscr{J})$ and let X_F be its Hamiltonian vector field. [See Definition 8(iv).] Then, $F \circ \Phi \in \mathrm{Dif}(\mathscr{D}, \mathscr{J})$ and, for all $u \in \mathscr{D}$*

$$D_u \Phi(X_{F\circ\Phi}(u)) = X_F(\Phi(u)). \tag{94}$$

Moreover, for all $t \in \mathbb{R}$,

$$\Phi \circ \Phi_t^{F\circ\Phi} \circ \Phi^{-1} = \Phi_t^F. \tag{95}$$

In particular, if $F \circ \Phi = F$, then Φ commutes with Φ_t^F, for all $t \in \mathbb{R}$. Finally, if $F \in C^1(E, \mathbb{R})$ and if Φ commutes with Φ_t^F, for all $t \in \mathbb{R}$, then there exists $c \in \mathbb{R}$ so that $F \circ \Phi = F + c$.

Proof The proof is very close to the one of Lemma 13. It gives a good illustration of the technical difficulties associated with the domain $\mathscr{D}$. Since $F \in \mathrm{Dif}(\mathscr{D}, \mathscr{J})$ and since $\Phi \in C^1(E, E)$ and leaves $\mathscr{D}$ invariant, one can compute, for all $u \in \mathscr{D}$ and $v \in E$,

$$\begin{aligned} D_u(F \circ \Phi)(v) &= D_{\Phi(u)} F D_u \Phi(v) = \left[\mathscr{J} X_F(\Phi(u))\right] D_u \Phi(v) \\ &= -\left[\mathscr{J} D_u \Phi(v)\right](X_F(\Phi(u))). \end{aligned}$$

Since Φ is symplectic, this yields

$$D_u(F \circ \Phi)(v) = -\left[\mathscr{J} v\right]([D_u \Phi]^{-1}(X_F(\Phi(u)))) = \left[\mathscr{J}[D_u \Phi]^{-1}(X_F(\Phi(u))\right](v).$$

This shows $D_u(F \circ \Phi) \in \mathscr{R}_{\mathscr{J}}$ and that $X_{F\circ\Phi}(u) = [D_u\Phi]^{-1}(X_F(\Phi(u))$, for all $u \in \mathscr{D}$. Finally, considering for each $u \in \mathscr{D}$ the strongly differentiable curve $t \in \mathbb{R} \to \Phi^{-1} \circ \Phi_t^F \circ \Phi \in E$, one checks readily that it is the flowline of $X_{F\circ\Phi}$ with initial condition u, which concludes the proof.

The point here is that we suppose Φ to be a symplectic transformation. As we just saw, that is a strong assumption. In practice, to avoid the difficulties just mentioned, we will always *assume* that the symmetry group of the system under consideration acts with symplectic transformations. Since the latter are often linear, that they are symplectic can then be checked through a direct computation. We finally point out that, if one wanted to exploit the presence of a formal constant of the motion with a nonlinear flow, such as in completely integrable systems, it could in general be difficult to prove it acts symplectically and commutes with the dynamics. This, in turn, makes it difficult to exploit such formal constants of the motion in the stability analysis that is our main interest here.

6.3 Symmetries and Noether's Theorem

When dealing with a symplectic Banach triple, the appropriate type of group action to consider is the following.

Definition 11 Let $(E, \mathscr{D}, \mathscr{J})$ be a symplectic Banach triple. Let G be a Lie group and $\Phi : (g, x) \in G \times E \to \Phi_g(x) \in E$, an action of G on E. We will say Φ is a globally Hamiltonian action if the following conditions are satisfied:

(i) For all $g \in G$, $\Phi_g \in C^1(E, E)$ is symplectic.
(ii) For all $g \in G$, $\Phi_g(\mathscr{D}) = \mathscr{D}$.
(iii) For all $\xi \in \mathfrak{g}$, there exists $F_\xi \in C^1(E, \mathbb{R}) \cap \mathrm{Dif}(\mathscr{D}, \mathscr{J})$ such that $\Phi_{\exp(t\xi)} = \Phi_t^{F_\xi}$, and the map $\xi \to F_\xi$ is linear.

This definition reduces to Definition 14 in the Appendix, for finite dimensional spaces E: in that case $\mathscr{D} = E$ and the restriction that $F \in \mathrm{Dif}(\mathscr{D}, \mathscr{J})$ is superfluous.

We can now state the version of Noether's Theorem that we need. It links the invariance group of Hamiltonian dynamics to constants of the motion and is to be compared to the finite dimensional version given in the Appendix (Theorem 19). As in (230), we will identify $\mathfrak{g}$ and $\mathfrak{g}^*$ with $\mathbb{R}^m$ and view F as a map $F : E \to \mathbb{R}^m$ [See (232)]. This allows us to write

$$F_\xi = \xi \cdot F,$$

where $\cdot$ refers to the canonical inner product on $\mathbb{R}^m$.

Theorem 6 *Let $(E, \mathscr{D}, \mathscr{J})$ be a symplectic Banach triple. Let G be a Lie group and Φ a globally Hamiltonian action of G on E. Let $H \in C^1(E, \mathbb{R}) \cap \mathrm{Dif}(\mathscr{D}, \mathscr{J})$ and let Φ_t^H be the corresponding Hamiltonian flow. Suppose that*

$$\forall g \in G, \quad H \circ \Phi_g = H. \tag{96}$$

Then:

(i) For all $\xi \in \mathfrak{g}$, $\{H, F_\xi\} = 0$.
(ii) For all $t \in \mathbb{R}$, $F_\xi \circ \Phi_t^H = F_\xi$.
(iii) G is an invariance group[13] for Φ_t^H.

This is an immediate consequence of Theorem 5 and Lemma 4. In the applications, the result is used as follows. The action Φ of G is simple and well known. It is then easy to check (96) directly. One then concludes that (ii) and (iii) hold, which are the important pieces of information for the further analysis. In particular, the level surfaces Σ_μ, defined in (10) are invariant under the dynamics Φ_t^H. Examples are given in the next section. The result in [19] that is closest in spirit to our Theorem 6 is Theorem 2 of Sect. 6.2.

Remark 3 For the statements of this section, we could have taken $H, F \in C(E, \mathbb{R})$ rather than $H, F \in C^1(E, \mathbb{R})$, but in applications, it is more convenient to take them to be C^1, as we will see in the next section.

6.4 Linear Symplectic Flows

Since invariance groups often act linearly on the symplectic Banach space $(E, \mathscr{J})$, and since the nonlinear dynamical flows studied often are perturbations of linear ones, it is important to have a good understanding of linear symplectic flows. Their study also sheds some light on the various technical difficulties mentioned above, and in particular on the role of the domain $\mathscr{D}$, the definition of Hamiltonian flow we adopted, etc.

[13] See Definition 2.

Proposition 4 below (which corresponds to Theorem 2 in Sect. 2.3 of [19]) characterizes all strongly continuous linear symplectic one-parameter groups on a symplectic Banach space in terms of their generators. We adopt the following notation. Given a strongly continuous group of linear transformations on E, we denote its generator by A, with domain $\mathscr{D}(A)$. By the Hille-Yosida theorem, we then know that $t \in \mathbb{R} \to u(t) = \Phi_t u \in E$ satisfies

$$\dot{u}(t) = Y_A(u(t)), \tag{97}$$

provided $u \in \mathscr{D}(A)$, where we introduced the vector field

$$Y_A : u \in \mathscr{D}(A) \subset E \to Au \in E.$$

Note that Y_A is not continuous if A is an unbounded operator. Clearly, the Φ_t form a dynamical system as defined in Sect. 2. We introduce the function

$$H_A : u \in \mathscr{D}(A) \to H_A(u) = \tfrac{1}{2}\omega_{\mathscr{J}}(Au, u) \in \mathbb{R}.$$

Observe that H_A admits directional (or Gâteaux) derivatives $\delta_u H_A(v)$, for all $u, v \in \mathscr{D}(A)$:

$$\begin{aligned}\delta_u H_A(v) &= \lim_{t\to 0} \frac{1}{t}\left(H_A(u + tv) - H_A(u)\right) \\ &= \frac{1}{2}\left(\omega_{\mathscr{J}}(Av, u) + \omega_{\mathscr{J}}(Au, v)\right).\end{aligned}$$

Nevertheless, if A is an unbounded operator, H_A is not continuous since, for all $u, w \in \mathscr{D}(A)$

$$H_A(u + w) - H_A(u) = \omega_{\mathscr{J}}(Au, w) + \omega_{\mathscr{J}}(Aw, u) + \omega_{\mathscr{J}}(Aw, w)$$

and the last term in particular does not necessarily converge to 0 as $w \to 0$ in the topology of E. It follows that, a fortiori, H_A is not Fréchet differentiable.

Proposition 4 *Let $(E, \mathscr{J})$ be a symplectic vector space. Let Φ_t be a strongly continuous one-parameter group of bounded linear operators on E. Let $(A, \mathscr{D}(A))$ be the generator of Φ_t. Then the following are equivalent.*

(i) The Φ_t are symplectic, i.e. $\omega_{\mathscr{J}}(\Phi_t u, \Phi_t v) = \omega_{\mathscr{J}}(u, v)$ for all $u, v \in E$;
(ii) For all $u, v \in \mathscr{D}(A)$,

$$\omega_{\mathscr{J}}(Au, v) = -\omega_{\mathscr{J}}(u, Av);$$

(iii) For all $u \in \mathscr{D}(A)$, one has

$$\mathscr{J} Y_A(u) = \delta_u H_A \in E^*. \tag{98}$$

In this case, $\delta_u H_A(v) = \omega_{\mathscr{J}}(Au, v)$, $H_A(\Phi_t u) = H_A(u)$ *for all* $u \in \mathscr{D}(A)$ *and for all* $t \in \mathbb{R}$.

Proof The three equivalences are obvious. To prove H_A is a constant of the motion, it suffices to remember that the Hille-Yosida theorem implies $A\Phi_t u = \Phi_t A u$ provided $u \in \mathscr{D}(A)$.

In other words, when the Φ_t are symplectic, the equation of motion (97) can be rewritten

$$\mathscr{J}\dot{u}(t) = \delta_{u(t)} H_A, \tag{99}$$

which is to be compared to (88). Clearly, the symplectic linear flows considered here are NOT Hamiltonian in the sense of Definition 9. Still, (99) gives meaning to the idea that in infinite dimension as well, linear strongly continuous symplectic flows are of "Hamiltonian nature," with a quadratic Hamiltonian. Moreover, the Hamiltonian H_A is a constant of the motion for the flow Φ_t. But note that, whereas in (92), the conservation of energy holds for all $u \in E$, this makes no sense here, since H_A is only defined on $\mathscr{D}(A)$.

Generally, because of the appearance of the Gâteaux derivative rather than a Fréchet differential in the right hand side, it turns out that the above formulation is inadequate for various reasons. For example, the absence of a chain rule for Gâteaux derivatives prevents one from computing derivatives such as $\frac{\mathrm{d}}{\mathrm{d}t} H_A(u(t))$ directly to prove H_A is constant along the motion. In fact, in the proof above, this result is proven using the Hille-Yosida theorem, and without computing a derivative at all. This approach cannot work for nonlinear flows of course. Similar problems arise when dealing with other constants of the motion than the Hamiltonian himself, even in the linear case, due to various domain questions and the complications in defining commutators. Finally, for our purposes, we need to restrict the motion to the level sets of the constants of the motion, and to use their manifold structure. This requires sufficient smoothness, a property not guaranteed at all by Gâteaux differentiability alone. Again, as pointed out before, an approach to the resolution of these technical difficulties other than the one chosen here can be found in [19].

In applications to PDE's, the function spaces that occur naturally are often complex Hilbert spaces. To make the link with Hamiltonian dynamics, one then proceeds as follows. Let $\mathscr{H}$ be a complex Hilbert space and let us write $\langle \cdot, \cdot \rangle$ for its inner product. First, it is clear that $\mathscr{H}$ is a real Hilbert space for the real inner product defined by $\mathrm{Re}\langle \cdot, \cdot \rangle$, which induces the same topology on $\mathscr{H}$ as the original inner product since both inner products have the same associated norm. Let us write E for this real Hilbert space. We now identify E^* with E using the corresponding Riesz isomorphism. Note that this is not the same as identifying $\mathscr{H}^*$ with $\mathscr{H}$ through the Riesz isomorphism associated to $\langle \cdot, \cdot \rangle$ and that there is no natural identification between $\mathscr{H}^*$ and E^* as sets: each non-zero element of $\mathscr{H}^*$ necessarily takes complex values, whereas the elements of E^* take real values only.

On the real Hilbert space E, one checks readily that

$$\omega(u, v) = \mathrm{Im}\langle u, v\rangle \in \mathbb{R}$$

defines a strong symplectic form. Note in particular that ω is real bilinear, but not complex bilinear. To identify the corresponding symplector $\mathscr{J} : E \to E$ in a convenient manner,[14] one proceeds as follows:

$$\omega(u, v) = \mathrm{Re}\,\langle iu, v\rangle$$

so that $\mathscr{J}u = iu$. The reader should not let itself be confused by the fact that we write iu, while considering u as an element of the real vector space E. The way to see this is as follows: the real vector space E is, as a set, identical to $\mathscr{H}$. And on $\mathscr{H}$, multiplication by i is well defined and actually an isometric complex linear map. So multiplication by i is well defined on E as an isometric real linear map.

To sum up, we showed how to associate to a complex Hilbert space $(\mathscr{H}, \langle\cdot,\cdot\rangle)$ a real Hilbert space $(E, \langle\cdot,\cdot\rangle_E)$ with symplectic structure

$$\omega(u, v) = \langle \mathscr{J}u, v\rangle_E, \qquad \mathscr{J}u = iu.$$

Now let us return to the linear symplectic flows. Suppose B is a self-adjoint operator on $\mathscr{H}$, with domain $\mathscr{D}(B)$. Then $U_t = \exp(-iBt)$ is a strongly continuous one-parameter group of unitaries.[15] The corresponding Hille-Yosida generator is $A = -iB$, with $\mathscr{D}(A) = \mathscr{D}(B)$. Clearly, each U_t is a symplectic transformation on E with the symplectic form ω. We are therefore in the setting of Proposition 4 and

$$H_A(u) = \frac{1}{2}\langle u, Bu\rangle. \tag{100}$$

It turns out that in the applications we have in mind, the one parameter subgroups of the symmetry group G act with such unitary groups on the relevant Hilbert space $\mathscr{H}$. But within this framework, as we pointed out above, the U_t are NOT Hamiltonian flows. To remedy this situation, one can, and we will, proceed along the following lines. First remark that the function H_A above is C^1 if we view it as a function on the Banach space E_B obtained by considering on $\mathscr{D}(|B|^{1/2})$ the graph norm. And that the flow U_t is strongly differentiable on $\mathscr{D} := \mathscr{D}(|B|^{3/2})$, viewed as a subset of E_B. So now we are in the setting of Definition 9, and U_t is a Hamiltonian flow on E_B, on which $\mathscr{J}$ still defines a weak symplector. The trouble with this reformulation so far is that now the Banach space E_B and the domain $\mathscr{D}$ depend on B. If the symmetry group is multi-dimensional, it will have several generators, and we need a common

[14] We identified E^* with E, so the symplector can be seen as a map from E to E.

[15] By Stone's theorem, every strongly continuous one parameter group of unitaries is of this form.

domain and Banach space on which to realize them all as Hamiltonian flows. We will see several examples where this formalism is implemented.

In practice, very often, $\mathscr{H} = \mathscr{K}^{\mathbb{C}} = \mathscr{K} \oplus i\mathscr{K}$, where $\mathscr{K}$ is a real Hilbert space. One has $u = q + ip \in \mathscr{H}$ with $q, p \in \mathscr{K}$. Then, clearly $E = \mathscr{K} \times \mathscr{K}$ with its natural Hilbert space structure. Moreover, identifying $u \in \mathscr{H}$ with $(q, p) \in \mathscr{K} \times \mathscr{K}$, clearly $\mathscr{J}(q, p) = (-p, q)$ and we are back to the examples of symplectors given in Sect. 6.1.

6.5 Hamiltonian PDE's: Examples

In this section we give some examples of PDE's generating Hamiltonian flows in the sense of Definition 9.

Let $E = H^1(\mathbb{R}^d, \mathbb{C})$, $\mathscr{D} = H^3(\mathbb{R}^d, \mathbb{C})$ and consider the nonlinear Schrödinger equation

$$\begin{cases} i\partial_t u(t,x) + \Delta u(t,x) + \lambda |u(t,x)|^{\sigma-1} u(t,x) = 0 \\ u(0,x) = u_0(x) \end{cases} \tag{101}$$

introduced in Sect. 3.2, defined on $\mathbb{R}^d$, $d = 1, 2, 3$. For $d = 1$, suppose that $3 \leq \sigma < +\infty$ in the defocusing case and $3 \leq \sigma < 5$ in the focusing case. In dimension $d = 2, 3$, consider only the defocusing case and assume $3 \leq \sigma < 1 + \frac{4}{d-2}$. Let $\Phi_t^X : E \to E$ be the global flow defined in (41). Recall that the existence of Φ_t^X is ensured by Theorem 2 and, thanks to Theorem 3, $\Phi_t^X(\mathscr{D}) = \mathscr{D}$ for all $t \in \mathbb{R}$.

Our purpose is to show that Eq. (101) is the Hamiltonian differential equation associated to the function H defined by (38) and $\Phi_t^X = \Phi_t^H$ for all $t \in \mathbb{R}$.

As explained in the end of Sect. 6.4, we usually identify $u = q + ip \in H^s(\mathbb{R}^d, \mathbb{C})$ with $(q, p) \in H^s(\mathbb{R}^d, \mathbb{R}) \times H^s(\mathbb{R}^d, \mathbb{R})$ for all $s \in \mathbb{R}$. Hence, let $(E, \mathscr{D}, \mathscr{J})$ be the symplectic Banach triple given by

$$\begin{aligned} E &= H^1(\mathbb{R}^d, \mathbb{R}) \times H^1(\mathbb{R}^d, \mathbb{R}), \\ \mathscr{D} &= H^3(\mathbb{R}^d, \mathbb{R}) \times H^3(\mathbb{R}^d, \mathbb{R}), \\ \mathscr{J}(q, p) &= (-p, q), \ \forall (q, p) \in E. \end{aligned}$$

Clearly $\mathscr{J} u = iu$ and $\mathscr{R}_{\mathscr{J}} = E \subset E^*$. Now consider

$$H(q,p) = \frac{1}{2}\left(\|\nabla q\|_{L^2}^2 + \|\nabla p\|_{L^2}^2\right) - \frac{\lambda}{\sigma+1}\int_{\mathbb{R}^d} (|q|^2 + |p|^2)^{\frac{\sigma+1}{2}},$$

and remark that if we write $u = q + ip$ with $(q, p) \in E$, $H(u) = H(q, p)$ is exactly the energy defined in (38). A straightforward calculation, using the Sobolev embedding

theorem, shows that $H \in C^2(E, \mathbb{R})$. In particular,

$$D_{(q,p)}H = (-\Delta q, -\Delta p) - \lambda(|q|^2 + |p|^2)^{\frac{\sigma-1}{2}}(q,p) \in E^*$$

which can be written as

$$D_u H = -\Delta u - \lambda |u|^{\sigma-1} u$$

in terms of $u = q + ip$. Next, using the fact that the Sobolev space $H^3(\mathbb{R}^d)$ is an algebra for $d = 1, 2, 3$, we have $DH(\mathscr{D}) \subset \mathscr{R}_{\mathscr{J}}$ so that H has a $\mathscr{J}$-compatible derivative on $\mathscr{D}$.

Moreover, the curve $(q(t), p(t)) = \Phi_t^X(q,p)$ is the unique solution to

$$\mathscr{J}(\dot{q}(t), \dot{p}(t)) = (-\Delta q, -\Delta p) - \lambda(|q|^2 + |p|^2)^{\frac{\sigma-1}{2}}(q,p) = D_{(q(t),p(t))}H$$

that is Eq. (88). As a consequence, Φ^X is a Hamiltonian flow for H in the sense of Definition 9, $\Phi_t^X = \Phi_t^H$ and the nonlinear Schrödinger equation (101) is a Hamiltonian differential equation.

In Sect. 3.2, we prove directly from the equation that $G = \mathrm{SO}(d) \times \mathbb{R}^d \times \mathbb{R}$ with the action defined by (42) is an invariance group for the dynamics. In general, the action of this group is not globally Hamiltonian. Nevertheless, let us consider the subgroup $\tilde{G} = \mathbb{R}^d \times \mathbb{R}$ and the restricted action

$$\begin{aligned} \Phi : \tilde{G} \times E &\to E \\ (a, \gamma, u) &\to \Phi_{a,\gamma}(u) = e^{i\gamma} u(x - a). \end{aligned} \tag{102}$$

For all $g \in \tilde{G}$, $\Phi_g \in C^1(E, E)$ is symplectic, $\Phi_g(\mathscr{D}) = \mathscr{D}$ and for all

$$\xi = (\xi_1, \ldots, \xi_d, \xi_{d+1}) \in \mathfrak{g},$$

point (iii) of Definition 11 is satisfied by taking $F_{\xi_j} = \xi_j F_j$ with

$$F_j(u) = -\frac{i}{2} \int_{\mathbb{R}^d} \bar{u}(x) \partial_{x_j} u(x)\, \mathrm{d}x \ \forall j = 1, \ldots, d, \tag{103}$$

$$F_{d+1}(u) = -\frac{1}{2} \int_{\mathbb{R}^d} \bar{u}(x) u(x)\, \mathrm{d}x. \tag{104}$$

As a consequence the action Φ of $\tilde{G}$ on E is globally Hamiltonian. Moreover, in Sect. 3.2, we showed that $H \circ \Phi_g = H$, hence we may apply Theorem 6 and conclude that $F_{\xi_j} \circ \Phi_t^H = F_{\xi_j}$ that means that each F_j is a constant of the motion.

Finally we show that the action $\Phi : (R, u) \in G \times E \to \Phi_R(u) = u(R^{-1}x) \in E$ of $G = \mathrm{SO}(d)$ on E is not globally Hamiltonian. For simplicity, let us consider $d = 2$

and let us identify a matrix $\xi \in \mathrm{so}(2)$ with $\xi \in \mathbb{R}$

$$\xi = \begin{pmatrix} 0 & \xi \\ -\xi & 0 \end{pmatrix}.$$

Then for each $\xi \in \mathbb{R}$, $\Phi_{\exp(t\xi)} = \Phi_t^{F_\xi}$ with $F_\xi = \xi F$ and

$$F(u) = -\frac{i}{2} \int_{\mathbb{R}^d} (x_1 \partial_{x_2} - x_2 \partial_{x_1}) u(x) \bar{u}(x) \, \mathrm{d}x.$$

The issue is that F is not even well-defined on the Banach space $H^1(\mathbb{R}^2)$!

Finally, let us remark that if we choose $\mathscr{D} = H^2(\mathbb{R}^d) \times H^2(\mathbb{R}^d)$, then $DH(\mathscr{D}) \subset L^2(\mathbb{R}^d) \times L^2(\mathbb{R}^d) \not\subset \mathscr{R}_{\mathscr{J}} = H^1(\mathbb{R}^d) \times H^1(\mathbb{R}^d)$ and H does not have a $\mathscr{J}$-compatible derivative for this new choice of $\mathscr{D}$. In the same way, if we take $E = L^2(\mathbb{R}^d) \times L^2(\mathbb{R}^d)$ and $\mathscr{D} = H^1(\mathbb{R}^d) \times H^1(\mathbb{R}^d)$, the same function H is not even continuous.

We point out that the Manakov equation can be treated similarly. In that case, in addition to the momentum, there are four constants of the motion associated to the $U(2)$ symmetry.

Next, let $(E, \mathscr{D}, \mathscr{J})$ be the symplectic Banach triple given

$$\begin{aligned} E &= H^1(\mathbb{R}^d, \mathbb{R}) \times L^2(\mathbb{R}^d, \mathbb{R}), \\ \mathscr{D} &= H^2(\mathbb{R}^d, \mathbb{R}) \times H^1(\mathbb{R}^d, \mathbb{R}), \\ \mathscr{J}(q, p) &= (-p, q), \ \forall (q, p) \in E. \end{aligned}$$

and consider the nonlinear wave equation

$$\begin{cases} \partial_{tt}^2 u(t,x) - \Delta u(t,x) + \lambda |u(t,x)|^{\sigma-1} u(t,x) = 0 \\ u(0,x) = u_0(x), \partial_t u(0,x) = u_1(x) \end{cases} \tag{105}$$

introduced in Sect. 3.4, defined on $\mathbb{R}^d$, $d = 1, 2, 3$. Suppose $\lambda > 0$ and σ an odd integer such that $3 \leq \sigma < +\infty$ in dimension $d = 1$ and $3 \leq \sigma < 1 + \frac{4}{d-2}$ for $d = 2, 3$. Let $\Phi_t^X : E \to E$ the global flow defined in (59). Thanks to the persistence of regularity, we have $\Phi_t^X(\mathscr{D}) = \mathscr{D}$ for all $t \in \mathbb{R}$ (see Sect. 3.4).

As before, our purpose is to show that Eq. (105) is the Hamiltonian differential equation associated to the function H defined by (58) and $\Phi_t^X = \Phi_t^H$ for all $t \in \mathbb{R}$.

First of all, note that $\mathscr{R}_{\mathscr{J}} = L^2(\mathbb{R}^d) \times H^1(\mathbb{R}^d) \subset E^* = H^{-1}(\mathbb{R}^d) \times L^2(\mathbb{R}^d)$. Next, consider

$$H(q,p) = \frac{1}{2} \left(\|\nabla q\|_{L^2}^2 + \|p\|_{L^2}^2 \right) + \frac{\lambda}{\sigma + 1} \int_{\mathbb{R}^d} (|q|)^{\sigma+1},$$

and remark that if we write $q = u$ and $p = \partial_t u$ with $(q,p) \in E$, $H(u) = H(q,p)$ is exactly the energy defined in (58). As for the nonlinear Schrödinger equation,

a straightforward calculation, using the Sobolev embedding theorem, shows that $H \in C^2(E, \mathbb{R})$. In particular,

$$D_{(q,p)}H = (-\Delta q + \lambda |q|^{\sigma-1} q, p) \in E^*.$$

Next, using the fact that the Sobolev space $H^2(\mathbb{R}^d)$ is an algebra for $d = 1, 2, 3$, we have $DH(\mathscr{D}) \subset \mathscr{R}_{\mathscr{J}}$ so that H has a $\mathscr{J}$-compatible derivative on $\mathscr{D}$.

Moreover, the curve $(u(t), \partial_t u(t)) = \Phi_t^X(u(0), \partial_t u(0))$ is the unique solution to (105). As a consequence, using $u = q$ and $\partial_t u = p$, we have that $(q(t), p(t)) = \Phi_t^X(q, p)$ is the unique solution to

$$\mathscr{J}(\dot{q}(t), \dot{p}(t)) = (-\Delta q + \lambda |q|^{\sigma-1} q, p) = D_{(q(t),p(t))}H,$$

that is, Eq. (88). Finally, if $(q, p) \in \mathscr{D}$, the curve $t \to \Phi_t^H(q, p) \in C(\mathbb{R}, \mathscr{D}) \cap C^1(\mathbb{R}, E)$. As a consequence, Φ^X is a Hamiltonian flow for H in the sense of Definition 9, $\Phi_t^X = \Phi_t^H$ and the nonlinear wave equation (105) is a Hamiltonian differential equation.

7 Identifying Relative Equilibria

We now dispose of the necessary tools that will allow us to characterize the relative equilibria of Hamiltonian systems with symmetry and that will yield the candidate Lyapunov function to study their stability. Before stating the main result (Theorem 7), we recall some of the terminology used below, but refer to the Appendices for details. First, for $\mu \in \mathfrak{g}^*$, we have [see (203)],

$$G_\mu = \{g \in G \mid \mathrm{Ad}_g^* \mu = \mu\};$$

$\mathfrak{g}, \mathfrak{g}_\mu$ are the Lie algebras of G and G_μ respectively, and $\mathfrak{g}^*, \mathfrak{g}_\mu^*$ their duals. We always identify $\mathfrak{g}^*$ with $\mathbb{R}^m$ [see (204)]. Hence, if Φ is a globally Hamiltonian action, we think of its momentum map as a map $F : E \to \mathbb{R}^m$ and define, for all $\mu \in \mathbb{R}^m$,

$$\Sigma_\mu = \{u \in E \mid F(u) = \mu\}.$$

We then know from Proposition 10 that $G_\mu = G_{\Sigma_\mu}$ provided the momentum map is Ad*-equivariant.

Theorem 7 *Let $(E, \mathscr{D}, \mathscr{J})$ be a symplectic Banach triple. Let $H \in C^1(E, \mathbb{R}) \cap \mathrm{Dif}(\mathscr{D}, \mathscr{J})$ and suppose H has a Hamiltonian flow Φ_t^H. Let furthermore G be a Lie group, and Φ a globally Hamiltonian action on E with Ad*-equivariant momentum map F. Suppose that,*

$$\forall g \in G, \quad H \circ \Phi_g = H. \tag{106}$$

(i) Then G is an invariance group for Φ_t^H.
(ii) Let $u \in E$ and let $\mu = F(u) \in \mathbb{R}^m \simeq \mathfrak{g}^*$. Consider the following statements:

(1) u is a relative G-equilibrium.
(2) u is a relative G_μ-equilibrium.
(3) There exists $\xi \in \mathfrak{g}_\mu$ so that, for all $t \in \mathbb{R}$,

$$\Phi_t^H(u) = \Phi_{\exp(t\xi)}(u). \tag{107}$$

(4) There exists $\xi \in \mathfrak{g}_\mu$ so that

$$D_u H - \xi \cdot D_u F = 0. \tag{108}$$

(5) There exists $\xi \in \mathfrak{g}$ so that

$$D_u H - \xi \cdot D_u F = 0. \tag{109}$$

Then (1) $\Leftrightarrow$ (2) $\Leftarrow$ (3).
If $u \in \mathscr{D}$, then (1) $\Leftrightarrow$ (2) $\Leftarrow$ (3) $\Leftrightarrow$ (4) $\Leftrightarrow$ (5).
If in addition, μ is a regular value of F [See Definition 12], then
(1) $\Leftrightarrow$ (2) $\Leftarrow$ (3) $\Leftrightarrow$ (4) $\Leftrightarrow$ (5) $\Leftrightarrow$ (6), where (6) is the statement:

(6) u is a critical point of H_μ on Σ_μ, where $H_\mu = H|_{\Sigma_\mu}$.

In addition, ξ is then unique.

That (1) is equivalent to (2) is a particular feature of Hamiltonian systems. In fact, its statement makes no sense outside of the Hamiltonian setting. It implies that, if u is a G-relative equilibrium, it is automatically a relative equilibrium for the *smaller* group G_μ. So the relevant invariance group depends on the point u through the value $\mu = F(u)$ of the constants of the motion at u. This is important since, as we will see in Sect. 8, one then ends up showing u is G_μ-orbitally stable, which is a stronger result than G-orbital stability. We already saw examples of this mechanism in Sect. 5. The proof of the equivalence between (1) and (2), although very simple, uses the subtle relations between constants of the motion and symmetries for Hamiltonian systems explained in the previous section.

For our purposes, the most interesting information obtained in this result is the observation that if $u \in \mathscr{D}$ satisfies (108), sometimes referred to in the PDE literature as "the stationary equation", then it is a relative equilibrium. And that, if μ is a regular value of F, those solutions are precisely the critical values of H_μ. This means that, given a Hamiltonian system with symmetries, one can find relative equilibria by looking for critical points of the Hamiltonian H restricted to the surfaces Σ_μ. In practice, this can be done concretely by solving (109), which in applications to Hamiltonian PDE's often takes the form of a stationary PDE in which ξ is treated as a (vector valued) parameter. Examples are given in the following sections. See also Sect. 5 for examples in finite dimension.

One immediately suspects that the Lagrange theory of multipliers for the study of constrained extrema should be of relevance here. This is indeed the case: introducing, on E, the Lagrange function

$$\forall v \in E, \quad \mathscr{L}(v) = H(v) - \xi \cdot F(v), \tag{110}$$

one sees that (109) expresses the vanishing of its first variation at u: $D_u\mathscr{L} = 0$. Here, $\xi \in \mathfrak{g} \simeq \mathbb{R}^m$ plays the role of a Lagrange multiplier. From the experience gained with the examples given so far, one suspects that, to show u is a stable relative equilibrium, one could try proceeding in two steps. First, show u is not just a critical point, but actually a local minimum of H_μ by studying the second variation of the Lagrange function $\mathscr{L}$ on Σ_μ. Next, use the Lagrange function as Lyapunov function in the proof of stability. Indeed, $u \in \Sigma_\mu$ is a local minimum of H_μ if and only if

$$\exists \rho > 0, \forall v \in \Sigma_\mu, \quad \mathrm{d}(v,u) \leq \rho \Rightarrow H_\mu(v) - H_\mu(u) \geq 0,$$

which is equivalent to

$$\exists \rho > 0, \forall v \in \Sigma_\mu, \quad \mathrm{d}(v,u) \leq \rho \Rightarrow \mathscr{L}(v) - \mathscr{L}(u) \geq 0,$$

since F is constant on Σ_μ. This is clearly the strategy used in the proofs of Sect. 5. We will see in Sect. 8 how to implement it in a general setting and give examples from the nonlinear Schrödinger equation in Sects. 9 and 10. This is the approach that goes by the name of *energy-momentum method*.

Proof

(i) This is an immediate consequence of Theorem 6(iii).

(ii) (1) $\Leftrightarrow$ (2). If u is a relative G-equilibrium, then there exists, for each $t \in \mathbb{R}$, $g(t) \in G$ so that $\Phi_t^H(u) = \Phi_{g(t)}(u)$. Since $u \in \Sigma_\mu$, so is $\Phi_t^H(u)$, since F is a constant of the motion for H, by Theorem 6(ii). Hence

$$\mu = F(u) = F(\Phi_t^H(u)) = F(\Phi_{g(t)}(u)) = \mathrm{Ad}^*_{g(t)}\mu.$$

It follows that $g(t) \in G_\mu$, which concludes the argument. The reverse implication is obvious.
(3) $\Rightarrow$ (2). Obvious from the definition.
Now suppose $u \in \mathscr{D}$.
(3) $\Leftrightarrow$ (4). Suppose (3) holds. Since $u \in \mathscr{D}$, this implies that $\mathscr{J}^{-1}D_uH = \mathscr{J}^{-1}D_u(\xi \cdot F)$, which implies (4). Now suppose (4) holds. Since $u \in \mathscr{D}$ and since $H \circ \Phi_t^H = H$ and $F_\xi \circ \Phi_t^H = F_\xi$ by Theorem 6(ii), we have, for all $t \in \mathbb{R}$,

$$D_{\Phi_t^H(u)}HD_u\Phi_t^H = D_uH, \quad D_{\Phi_t^H(u)}(\xi \cdot F)D_u\Phi_t^H = D_u(\xi \cdot F).$$

Writing $u(t) = \Phi_t^H(u)$, this yields $D_{u(t)}H = D_{u(t)}(\xi \cdot F)$ so that $\mathscr{J}\dot{u}(t) = D_{u(t)}(\xi \cdot F)$, which shows $t \to u(t)$ is a flow line of the Hamiltonian $\xi \cdot F$, with

initial condition u. Since the latter is unique, we find $u(t) = \Phi_t^{\xi\cdot F}(u)$, which concludes the argument since $\Phi_t^{\xi\cdot F} = \Phi_{\exp(t\xi)}$ [See Definition 11(iii)].
(4) $\Leftrightarrow$ (5). We only need to establish that (5) implies (4). As above, (5) implies $u(t) = \Phi_{\exp(t\xi)}$. Hence

$$\mathrm{Ad}^*_{\exp(t\xi)}\mu = \mathrm{Ad}^*_{\exp(t\xi)}F(u) = (F \circ \Phi_{\exp(t\xi)})(u) = F(u(t)) = F(u) = \mu,$$

since $F_i \circ \Phi_t^H = F_i$. Hence $\xi \in \mathfrak{g}_\mu$.
Now suppose in addition μ is a regular value of F.
(4) $\Leftrightarrow$ (6). We remark that, since μ is a regular value of F, Σ_μ is a co-dimension m submanifold of E and [see (191)]

$$T_u\Sigma_\mu = \{v \in E \mid D_uF(v) = 0\}.$$

Hence clearly (4) implies (6). Conversely, suppose D_uH vanishes on $T_u\Sigma_\mu$. Since μ is a regular value of F, we know that D_uF is onto $\mathbb{R}^m$. Let W be a subspace of E complementary to $T_u\Sigma$, so that $E = T_u\Sigma \oplus W$. It follows $\dim W = m$ and that the m one-forms $D_uF_i \in W^*$, $i = 1, \ldots m$ form a basis of W^*. Consequently, the restriction of D_uH to W can be written uniquely as $D_uH = \sum_{i=1}^m \xi_i D_uF_i = D_u(\xi\cdot F)$. Since both sides vanish on $T_u\Sigma_\mu$, (4) follows.

We conclude this section with two technical remarks that can be skipped in a first reading.

Remark 4 We have seen that (3) implies (2). Under suitable technical conditions, the reverse is also true. This can be understood as follows. If $u \in \mathscr{D}$ is a G_μ-relative equilibrium then, for all $t \in \mathbb{R}$, there exists $g(t) \in G_\mu$ so that $u(t) = \Phi_t^H u = \Phi_{g(t)}u$. So the curve

$$t \in \mathbb{R} \to \Phi_t^H(u) \in G_\mu u := \{\Phi_g(u) \mid g \in G_\mu\} \subset E$$

is a smooth curve on the group orbit $G_\mu u$. Under appropriate topological conditions on G_μ and G_u [defined in (12)], and if the action Φ of the group G_μ is sufficiently smooth,[16] this orbit is an immersed submanifold of Σ_μ that can be identified with the homogeneous space G_μ/G_u, and its tangent space at u is therefore

$$T_u(G_\mu u) = \{X_{F_\xi}(u) \mid \xi \in \mathfrak{g}_\mu\}.$$

We recall that X_{F_ξ} is the Hamiltonian vector field associated to the function $F_\xi = \xi \cdot F$. Since $X_H(u) = \frac{\mathrm{d}}{\mathrm{d}t}\Phi_t^H(u)_{|t=0} \in T_u(G_\mu u)$, it follows that there exists $\xi \in \mathfrak{g}_\mu$ so that

$$X_H(u) = X_{\xi\cdot F}(u),$$

[16] See for example Sect. 4 of [2], and in particular Corollary 4.1.22.

which is equivalent to (108) and therefore implies (3). We refer to [2, 67] for the detailed argument, in the finite dimensional setting. We shall not have a need for the implication (2) $\Rightarrow$ (3), but will point out that, "morally", there is a one-one relationship between the critical points of H_μ and the relative equilibria of the Hamiltonian flow Φ_t^H.

Remark 5 What is the role of the condition that μ be a regular value of F? This has several consequences. First, it guarantees that Σ_μ is a co-dimension m submanifold of E and that $T_u\Sigma_\mu = \mathrm{Ker} D_u F$. This is convenient in the further stability analysis, as we will see. Second, if $u \in \mathscr{D}$ and $\mathrm{Rank}\, D_u F = m$, then $\xi \in \mathbb{R}^m \simeq \mathfrak{g} \to \Phi_1^{\xi \cdot F}(u) \in \mathscr{O}_u = Gu \subset E$ is a local immersion and the action is locally free, meaning that the isotropy group G_u of u is discrete. Hence $\xi \in \mathfrak{g}_\mu \to \Phi_1^{\xi \cdot F}(u) \in \mathscr{O}_u \cap \Sigma_\mu = G_\mu u \subset E$ is also a local immersion. This observation will be used in Lemma 7 in the next section. If μ is not regular, various additional technical difficulties arise in the stability analysis of the next section, even in finite dimensional settings, where they have been studied in [66, 81]. As an example of such a singular value μ, consider the action of SO(3) on $\mathbb{R}^6$ introduced in Sect. 3.1, on the level set $L(u) = \mu = 0$. The corresponding isotropy group G_μ is SO(3) itself in that case. Its action is not locally free, since G_u, for $u = (q, p)$, with q and p parallel, is the copy of SO(2) given by the rotations about the common axis of q and p. We will see another example of such a situation when treating the nonlinear Schrödinger equation on the torus in Sect. 9. In both these cases, the ensuing complication is easily dealt with on an ad hoc basis.

8 Orbital Stability: An Abstract Proof

8.1 Introduction: Strategy

We have seen that in many situations the relative equilibria of Hamiltonian systems with symmetry are precisely the critical points of the restriction H_μ of the Hamiltonian H to a level surface Σ_μ, for some $\mu \in \mathfrak{g}^*$, of the constants of the motion F associated to the symmetry group via the Noether Theorem. This at once explains why they tend to come in families u_μ, indexed by μ in some open subset of $\mathfrak{g}^* \simeq \mathbb{R}^m$. Indeed, considering equation (109), it is natural to think of it as an equation in which both ξ and u are unknown. And so, under suitable circumstances, one can hope to find a family of solutions u_ξ of (109) by letting ξ run through some neighbourhood inside $\mathfrak{g}$. Typically, as ξ changes, so does $\mu_\xi = F(u_\xi) \in \mathfrak{g}^*$. Depending on the situation, it may be more convenient to label the solutions by μ_ξ than by $\xi \in \mathfrak{g}$. In these notes, we use mostly μ as a parameter, except in Sect. 10 where ξ is used. The question of the existence of such families of relative equilibria—a problem related to bifurcation theory—is studied, in the finite dimensional setting, in [66, 80]. We already saw several examples of this phenomenon and more will be provided in Sects. 9 and 10.

It remains to see how one can prove the orbital stability of those relative equilibria. The basic intuition is that—modulo technical problems—they should be stable if they are not just critical points, but actually local minima of H_μ. To understand the origin of this intuition, recall that, if $u_\mu \in \Sigma_\mu$ is a relative equilibrium of the Hamiltonian dynamics Φ_t^H, then the orbit $G_\mu u_\mu = \{\Phi_g(u_\mu) \mid g \in G_\mu\}$ of G_μ, viewed as an element of the orbit space Σ_μ/G_μ, is a fixed point of the reduced dynamics. And, since H_μ is invariant under the action of G_μ, it can be viewed as a function on this orbit space. If H_μ has a local minimum at u_μ, it thus has a local minimum at the orbit $G_\mu u_\mu \in \Sigma_\mu/G_\mu$. Finally, since H_μ is a constant of the motion for the reduced dynamics, we are precisely in the situation described in the introduction: $G_\mu u_\mu$ is a fixed point of the reduced dynamics, and H_μ is a constant of the motion for which $G_\mu u_\mu$ is a minimum. We can therefore hope to use the Lyapunov method to prove the stability of $G_\mu u_\mu$. To do so, it would suffice to prove a coercive estimate of the type (2) for H_μ on Σ_μ/G_μ.

There are two obvious problems one has to face when trying to implement this strategy. First, even if one executes this program, one will have proven only that u_μ is orbitally stable with respect to perturbations v of u_μ with $v \in \Sigma_\mu$. But one would like to prove this is true for arbitrary perturbations $v \in E$. Second, it is difficult to work on the abstract quotient space Σ_μ/G_μ, which, even in finite dimensional systems, but particularly in infinite dimensional ones, may not have a nice topological or differentiable structure, so that analytical tools to prove estimates are not readily available. To deal with both these problems, the idea is to use the theory of constraint minimization and Lagrange multipliers. This has the obvious advantage that one can work in the ambient space E, which has the added redeeming feature of being linear. As already outlined in the discussion following Theorem 7, it turns out that it is the Lagrange function

$$\mathscr{L}_\mu = H - \xi_\mu \cdot F$$

associated to the relative equilibrium u_μ [see (110)] that plays the role of Lyapunov function in the proofs. In practice, one uses a Taylor expansion to second order of $\mathscr{L}_\mu$ about points on the orbit $G_\mu u_\mu$ and one controls the second derivative of $\mathscr{L}_\mu$ to prove it is a minimum; this in turn gives the necessary coercivity to conclude stability. The reader will have noticed that the above strategy was worked out in all detail in the simple example of motion in a spherical potential presented in Sect. 5.

In this section, we will provide a detailed implementation of the above strategy in the following general setup. We refer to Sect. 2 for the definitions of the objects used below.

Hypothesis A

(i) E is a Banach space and $\mathscr{D}$ a domain in E.
(ii) Φ_t^X is a dynamical system on E with a vector field $X : \mathscr{D} \to E$.
(iii) $F \in C^2(E, \mathbb{R}^m)$ is a vector of constants of the motion for Φ_t^X with level surfaces Σ_μ, $\mu \in \mathbb{R}^m$, as in (10).
(iv) Φ_t^X admits an invariance group G, with an action Φ of G on E.

Recall that if μ is a regular value for F then Σ_μ is a co-dimension m submanifold of E. In this setting, we consider relative equilibria of the following type.

Let $\mu \in \mathbb{R}^m$.

Hypothesis Bμ

(i) There exists $u_\mu \in \Sigma_\mu$ which is a relative equilibrium of the dynamics for the group $G_{\Sigma_\mu} = \{g \in G \mid \Phi_g \Sigma_\mu = \Sigma_\mu\}$.
(ii) There exists $\mathscr{L}_\mu \in C(E, \mathbb{R})$ which is a G_{Σ_μ}-invariant constant of the motion.
(iii) There exist $\eta > 0, c > 0$ so that

$$\forall u \in \mathscr{O}_{u_\mu}, \forall u' \in \Sigma_\mu, \quad \mathrm{d}(u, u') \leq \eta \Rightarrow \mathscr{L}_\mu(u') - \mathscr{L}_\mu(u) \geq c\mathrm{d}^2(u', \mathscr{O}_{u_\mu}) \tag{111}$$

where

$$\mathscr{O}_{u_\mu} = \Phi_{G_{\Sigma_\mu}}(u_\mu) = \{\Phi_g(u_\mu) \mid g \in G_{\Sigma_\mu}\}. \tag{112}$$

Under the above conditions, we say $\mathscr{L}_\mu$ is a coercive Lyapunov function on $\mathscr{O}_{u_\mu}$ *along* Σ_μ. If the G_{Σ_μ}-action is isometric then it is enough to check (111) holds at one single point $u \in \mathscr{O}_{u_\mu}$. It will then hold everywhere, with the same η, c, as a result of the G_{Σ_μ}-invariance of $\mathscr{L}_\mu$. Isometric actions are common in applications and this is one of the places where they provide a simplification. For what follows, the power 2 in the right hand side of (111) is of no consequence. One can generalize the definition by replacing the right hand side in (113) by $f(\mathrm{d}(u', \mathscr{O}_{u_\mu}))$, for some function $f : \mathbb{R}^+ \to \mathbb{R}^+, f(0) = 0, f(d) > 0$ if $d > 0$. In practice, as we will see below, one gets the lower bound in (111) from a Taylor expansion of $\mathscr{L}$, so that the square appears naturally. We point out that conditions (ii) and (iii) in Hypothesis Bμ imply (i). Indeed, if $u \in \mathscr{O}_{u_\mu}$ and $u' = u(t')$ for small enough t', then (ii) and (iii) imply that

$$0 = \mathscr{L}_\mu(u(t')) - \mathscr{L}_\mu(u) \geq c\mathrm{d}^2(u(t'), \mathscr{O}_{u_\mu}),$$

so that $u(t') \in \mathscr{O}_{u_\mu}$. Hence the flow Φ_t^X leaves $\mathscr{O}_{u_\mu}$ invariant and consequently each $u \in \mathscr{O}_{u_\mu}$ is a G_{Σ_μ} relative equilibrium. We have however found it convenient to keep this redundancy in the statement of the hypothesis.

We point out that Hypotheses A and Bμ are formulated without imposing the dynamical system to be Hamiltonian. Nor do they impose any link between the symmetry group G, the constants of the motion F and the Lyapunov function $\mathscr{L}_\mu$. The first goal of this section is to formulate and prove very general abstract theorems establishing orbital stability under the above general assumptions and some extra technical conditions. The first such result, Theorem 8, is a general version of Proposition 2: it imposes a strong coercivity condition, but is nevertheless sometimes of use, as we will see in Sect. 9. Theorems 9 and 10 correspond essentially to the first two arguments proposed in the proof of Proposition 3. The proofs of these results are quite simple, as we shall see. These three results show that

the essential ingredient in the proof of orbital stability is the coercivity condition in Hypothesis Bμ(iii).

It therefore remains to understand how to find a Lyapunov function satisfying in particular Hypothesis Bμ(iii). It is at this point that the Hamiltonian nature of the dynamical system plays an important role. We already saw in Sect. 7 that a candidate Lyapunov function arises naturally in that context. We will furthermore show in Proposition 5 how to obtain the coercivity condition Hypothesis Bμ(iii) from a lower bound on the Hessian of the Lyapunov function, in the case of Hamiltonian systems with symmetry. Combining this with Theorems 9 and 10 then yields a complete proof of orbital stability.

We will end this section with Theorem 11 which provides a slightly different proof of orbital stability of relative equilibria in Hamiltonian systems, and which is a generalization of the third argument proposed in the proof of Proposition 3. The argument uses Proposition 5 again, but combines it with the construction of an "augmented" Lyapunov function.

In applications of the theory developed in this section, the work is therefore reduced to solving (109) to identify the relative equilibria, and to proving a suitable lower bound on the Hessian of the corresponding Lyapunov function. This usually involves non-trivial (spectral) analysis, as one may expect. A first illustrative example—the orbital stability of plane waves for the nonlinear Schrödinger equation on the torus—is presented in Sect. 9. A widely applicable technique for obtaining the appropriate lower bound on the Hessian is described in [53, 54]. It is illustrated in Sect. 10 for standing wave solutions of the inhomogeneous nonlinear Schrödinger equation in one dimension.

In conclusion, the theorems of this section isolate the "soft analysis" part of the proof of orbital stability of relative equilibria from the more concrete and model dependent estimates needed to prove coercivity.

Remark 6 We point out that the domain $\mathscr{D}$ of the dynamical system Φ_t^X appears in Hypothesis A(i) and (ii). As already seen before, it is used in these notes when the system is Hamiltonian to identify the appropriate constants of the motion via Noether's theorem, to construct the Lyapunov function $\mathscr{L}$, and to identify the relative equilibria of the system. If this can be accomplished by some other means, $\mathscr{D}$ is not needed. In fact, for the results of Sects. 8.2, 8.3, and 8.4 the hypotheses involving $\mathscr{D}$ are not used. For the results of Sect. 8.5, and notably for Theorem 11, they are on the contrary essential.

8.2 A Simple Case

Before turning to the general results, we first formulate and prove a simple orbital stability result, under a stronger coercivity condition than (111).

Theorem 8 *Let Hypotheses A and Bμ_* (i)–(ii) for some $\mu_* \in \mathbb{R}^m$ be satisfied. Let $\mathcal{O}_{u_{\mu_*}}$ be as in (112). Suppose there exist $\eta > 0, c > 0$ so that*

$$\forall u \in \mathcal{O}_{u_{\mu_*}}, \forall v \in E, \quad \mathrm{d}(v,u) \leq \eta \Rightarrow \mathscr{L}_{\mu_*}(v) - \mathscr{L}_{\mu_*}(u) \geq c\mathrm{d}^2(v, \mathcal{O}_{u_{\mu_*}}). \tag{113}$$

Then, all $u \in \mathcal{O}_{u_{\mu_*}}$ are orbitally stable $G_{\Sigma_{\mu_*}}$-relative equilibria.

We refer to Definition 5 for the definition of orbital stability. Observe that in (113) the coercivity estimate is imposed for all perturbations v in E, rather than only in Σ_{μ_*}, as in (111). So here we are assuming that the Lyapunov function reaches a local minimum on $\mathcal{O}_{u_{\mu_*}}$, when viewed as a function on E, rather than only as a function on Σ_{μ_*}. This therefore constitutes a strengthening of Hypothesis Bμ_*(iii).The theorem can be used to prove orbital stability in some cases: for the fixed points in the spherical potentials treated in Sect. 5.1, for example, this is how we proceeded. Similarly, to establish the stability of the plane waves for the nonlinear defocusing Schrödinger equation on a one-dimensional torus, this theorem will also be sufficient, as we will see in Sect. 9. But we have already noticed in Sect. 5 that the coercivity imposed in (113) may be too strong a condition: we saw it is not satisfied for the natural choice of Lyapunov function for the circular orbits of Sect. 5.2, for example. It is too strong also in many situations involving the stability of solitons or standing waves. An example is treated in Sect. 10.

The proof is very simple, and based on the usual argument by contradiction.

Proof Suppose there exists a point $u \in \mathcal{O}_{u_{\mu_*}}$ that is not orbitally stable. Then there exists $\epsilon_0 > 0$ and for all $n \in \mathbb{N}^*$, there exists $v_n \in E$ so that $\mathrm{d}(v_n, u) \leq \frac{1}{n}$ and $\exists t_n \in \mathbb{R}$ so that $\mathrm{d}(v_n(t_n), \mathcal{O}_{u_{\mu_*}}) = \epsilon_0$. We can suppose $\epsilon_0 < \eta$. Then there exists $\tilde{v}_n \in \mathcal{O}_{u_{\mu_*}}$ so that $\mathrm{d}(v_n(t_n), \tilde{v}_n) \leq \eta$ and hence, since $\mathscr{L}_{\mu_*}$ is both a constant of the motion and constant on $\mathcal{O}_{u_{\mu_*}}$,

$$\mathscr{L}_{\mu_*}(v_n) - \mathscr{L}_{\mu_*}(u) = \mathscr{L}_{\mu_*}(v_n(t_n)) - \mathscr{L}_{\mu_*}(\tilde{v}_n) \geq c\mathrm{d}^2(v_n(t_n), \mathcal{O}_{u_{\mu_*}}) = c\epsilon_0^2.$$

Since $\mathscr{L}_{\mu_*}$ is continuous, the left hand side tends to zero when $n \to +\infty$, which is a contradiction.

8.3 Coercivity Implies Stability I

We now turn to the task of showing that Hypotheses A and Bμ_* imply the $G_{\Sigma_{\mu_*}}$-orbital stability of u_{μ_*}. For our first result, we need the following hypothesis.

Hypothesis F Let $F : E \to \mathbb{R}^m$. Let $\mu \in \mathbb{R}^m$. We say F satisfies Hypothesis F at μ if, for any bounded sequence u_n in E,

$$\lim_n F(u_n) = \mu \Rightarrow \mathrm{d}(u_n, \Sigma_\mu) \to 0. \tag{114}$$

The following lemma gives sufficient conditions for this to be satisfied.

Lemma 5

(a) Suppose $\dim E < +\infty$. *Let* $F \in C(E, \mathbb{R}^m)$. *Then F satisfies Hypothesis F for all* $\mu \in \mathbb{R}^m$.

(b) Suppose $F \in C(E, \mathbb{R}^m)$ *and that there exists* $C > 0$ *so that* $\{u \in E \mid F(u)^2 \leq C^2\}$ *is compact. Let* $\mu \in \mathbb{R}^m$ *with* $\mu^2 < C^2$. *Then F satisfies Hypothesis F at* μ.

(c) Let $F : E \to \mathbb{R}$. *Suppose that there exists* $k \in \mathbb{R}^*$ *so that,* $\forall u \in \mathscr{D}$, *for all* $\lambda \in \mathbb{R}^*$, $F(\lambda u) = \lambda^k F(u)$. *Suppose* $\mu \neq 0$. *Then F satisfies Hypothesis F at* μ.

Proof

(a) Suppose there exists $\epsilon_0 > 0$ and a bounded sequence u_n so that $F(u_n) \to \mu$, but $\mathrm{d}(u_n, \Sigma_\mu) \geq \epsilon_0$. Then the boundedness of the sequence implies the existence of a convergent subsequence $u_{n_k} \to v \in E$. By continuity of F, it follows that $F(v) = \mu$ so that $v \in \Sigma_\mu$. So $\mathrm{d}(u_{n_k}, \Sigma_\mu) \to 0$. This is a contradiction.

(b) The proof is similar to the one in (a).

(c) Let $(u_n)_n$ be a bounded sequence satisfying $F(u_n) \to \mu \neq 0$. Then, for large enough n one has $\mu/F(u_n) > 0$ and we can define $v_n = \left(\frac{\mu}{F(u_n)}\right)^{1/k} u_n$. Then $F(v_n) = \mu$. Clearly $\|v_n - u_n\| \to 0$ so that $\mathrm{d}(u_n, \Sigma_\mu) \to 0$.

Remark 7

(i) The boundedness of the sequence is important, even in finite dimension. Indeed, consider on $\mathbb{R}^2$ the function $F(x, y) = \frac{y^2}{1+x^4}$, $\mu = 0$ and remark that $F(x, x) \to 0$ as $x \to +\infty$.

(ii) Condition (c) can be used for constants of the motion arising from linear actions of one-parameter groups on a Hilbert space, as described in Sect. 6.4, and which have a quadratic hamiltonian of the type

$$F(u) = \frac{1}{2}\langle u, Bu\rangle,$$

such as in (103). An example of such application will be given in the proof of Proposition 6, at the end of Sect. 9.

(iii) The condition $\mu \neq 0$ is essential in part (c) of the Lemma. Indeed, consider $E = H^1(\mathbb{R}^d)$ and $F(u) = \|u\|^2_{L^2}$. Let $\mu = 0$. Then $\Sigma_\mu = \{0\}$. But $F(u_n) \to 0$ does not imply $u_n \to 0$ in $H^1(\mathbb{R}^d)$.

(iv) Condition (c) is no longer sufficient to ensure F satisfies Hypothesis F when $F : E \to \mathbb{R}^m$, with $m \geq 2$. To see this, we consider an example relevant to the treatment of the Manakov equation. Let $E = H^1(\mathbb{R}, \mathbb{C}^2)$ and consider $F_1(u) = \|v\|^2_{L^2}, F_2(u) = \|w\|^2_{L^2}$, where we wrote $u = (v, w) \in E$. Note that those are the two constants of the motion associated to the diagonal part of the $U(2)$ action on E (See Sect. 3.3). We choose $\mu = (1, 0) \neq 0 \in \mathbb{R}^2$. Then $\Sigma_\mu = \{u \in E \mid w = 0, \|v\|^2_{L^2} = 1\}$. Now let $a, b \in C_0^\infty(\mathbb{R})$, such that $\|a\|^2_{L^2} = 1 = \|b\|^2_{L^2}$ and consider $u_n(x) = (a(x), \frac{1}{\sqrt{n}} b(n(x - n))) =: (v_n, w_n) \in E$. Note

that this sequence is bounded. Moreover, clearly, $\lim_{n\to+\infty} F(u_n) = \mu$. Now, for $u = (v, 0) \in \Sigma_\mu$, one has

$$\|u_n - u\|^2 = \|a - v\|^2_{H^1(\mathbb{R},\mathbb{C})} + \|w_n\|^2_{H^1(\mathbb{R},\mathbb{C})}$$
$$\geq \|w_n\|^2_{H^1(\mathbb{R},\mathbb{C})} \geq \frac{n^2}{n}\int_{\mathbb{R}} |b'(n(x-n))|^2 \mathrm{d}x = \|b'\|^2_{L^2}.$$

It follows that $\mathrm{d}(u_n, \Sigma_\mu) = \inf_{u\in\Sigma_\mu} \|u_n - u\| \geq \|b'\|_{L^2}$, so that Hypothesis F is clearly not satisfied in this situation.

Theorem 9 *Suppose Hypotheses A and Bμ_* (Sect. 8.1) are satisfied for some $\mu_* \in \mathbb{R}^m$. Then*

$$\forall u \in \mathscr{O}_{u_{\mu_*}}, \forall \epsilon > 0, \exists \delta > 0, \ (\forall u' \in \Sigma_{\mu_*}, \mathrm{d}(u', u) \leq \delta \Rightarrow \sup_{t\in\mathbb{R}} \mathrm{d}(u'(t), \mathscr{O}_{u_{\mu_*}}) \leq \epsilon). \tag{115}$$

If in addition,

(i) $\mathscr{L}_{\mu_*}$ *is uniformly continuous on bounded sets,*
(ii) $\mathscr{O}_{u_{\mu_*}}$ *is bounded,*
(iii) $F : E \to \mathbb{R}^m$ *satisfies Hypothesis F,*

then all $u \in \mathscr{O}_{u_{\mu_*}}$ *are orbitally stable* $G_{\Sigma_{\mu_*}}$*-relative equilibria.*

We point out that (115) is already an orbital stability result for all $u \in \mathscr{O}_{u_{\mu_*}} = G_{\Sigma_{\mu_*}} u$, but only with respect to perturbations of the initial condition u *inside* Σ_{μ_*}. The theorem asserts that, with the extra conditions (i)–(ii)–(iii), orbital stability with respect to all perturbations within E is obtained. It is the observation that coercivity *along* Σ_{μ_*} [Hypothesis Bμ(iii)] suffices to establish orbital stability that explains, *in fine*, the advantage of Theorem 9 over Theorem 8. This is already illustrated in Sect. 5.2 on a simple example. Note furthermore that conditions (i) and (iii) of the theorem are automatically satisfied in finite dimension. The boundedness of $\mathscr{O}_{u_{\mu_*}}$ [condition (ii)] is guaranteed for example when the group is compact, or when E is a Hilbert space and the group acts with unitary transformations, which is often the case in infinite dimensional systems.

The argument in the proof of Theorem 9 is extracted from the proof of Theorem 5.3 in [53] and is used in [54] as well. We point out however, that conditions (i) and (iii) are not made explicit there. The first one is usually easy to check in examples, where the Lyapunov function tends at any rate to be uniformly Lipschitz on bounded sets. For the second one, we gave some sufficient conditions in Lemma 5. But, as pointed out in Remark 7, it may fail, in particular in the very general setting of [53, 54]. In that case, a different argument is needed; we will provide two below.

Proof We will prove (115) by contradiction, yet again. Let us therefore suppose there exists $u \in \mathscr{O}_{u_{\mu_*}}$ and $\epsilon_0 > 0$ so that for all $n \in \mathbb{N}_*$, there exists $u_n \in \Sigma_{\mu_*}$ so that

$$\mathrm{d}(u_n, u) \leq \frac{1}{n}, \quad \text{and} \quad \exists \tilde{t}_n \in \mathbb{R} \text{ so that } \mathrm{d}(u_n(\tilde{t}_n), \mathscr{O}_{u_{\mu_*}}) > \epsilon_0.$$

We can choose, without loss of generality, $\epsilon_0 < \eta$, where η is defined in (111) and choose t_n the smallest value of t so that

$$\mathrm{d}(u_n, u) \leq \frac{1}{n}, \quad \text{and} \quad \mathrm{d}(u_n(t_n), \mathscr{O}_{u_{\mu_*}}) = \epsilon_0 < \eta.$$

Consequently, there exists $y_n \in \mathscr{O}_{u_{\mu_*}}$ so that $\mathrm{d}(u_n(t_n), y_n) < \eta$. Note that $u_n(t_n) \in \Sigma_{\mu_*}$, since Σ_{μ_*} is invariant under the dynamical flow. Then, since $\mathscr{L}_{\mu_*}$ is a constant of the motion, and since it is constant and coercive on $\mathscr{O}_{u_{\mu_*}}$ along Σ_{μ_*},

$$\begin{aligned}\mathscr{L}_{\mu_*}(u_n) - \mathscr{L}_{\mu_*}(u) &= \mathscr{L}_{\mu_*}(u_n(t_n)) - \mathscr{L}_{\mu_*}(u) \\ &= \mathscr{L}_{\mu_*}(u_n(t_n)) - \mathscr{L}_{\mu_*}(y_n) \geq c\mathrm{d}^2(u_n(t_n), \mathscr{O}_{u_{\mu_*}}) = c\epsilon_0^2.\end{aligned}$$

Since $\mathscr{L}_{\mu_*}$ is continuous, one obtains a contradiction by taking $n \to +\infty$. This shows (115).

To prove the last statement, suppose $\mathscr{O}_{u_{\mu_*}}$ is bounded and $\mathscr{L}_{\mu_*}$ uniformly continuous on bounded sets. We need to show that

$$\forall u \in \mathscr{O}_{u_{\mu_*}}, \forall \epsilon > 0, \exists \delta > 0, \ (\forall u' \in E, \mathrm{d}(u', u) \leq \delta \Rightarrow \sup_{t \in \mathbb{R}} \mathrm{d}(u'(t), \mathscr{O}_{u_{\mu_*}}) \leq \epsilon). \tag{116}$$

We proceed again by contradiction. Suppose there exists $u \in \mathscr{O}_{u_{\mu_*}}$ and $0 < \epsilon_0 < \eta$ so that, for all $n \in \mathbb{N}$, there exists $u_n \in E$,

$$\mathrm{d}(u_n, u) \leq \frac{1}{n}, \quad \text{and} \quad \exists t_n \in \mathbb{R} \text{ so that } \mathrm{d}(u_n(t_n), \mathscr{O}_{u_{\mu_*}}) = \epsilon_0 < \eta.$$

Note that, this time, $u_n \in E$ and $u_n(t_n) \in E$, not in Σ_{μ_*}. So we can't use the coercivity of $\mathscr{L}_{\mu_*}$ along Σ_{μ_*} directly. We do know, however, that $F(u_n(t_n)) = F(u_n)$, since F is a constant of the motion. Hence

$$\lim_{n \to +\infty} F(u_n(t_n)) = \mu_*.$$

Since the orbit $\mathscr{O}_{u_{\mu_*}}$ is bounded, and since $\mathrm{d}(u_n(t_n), \mathscr{O}_{u_{\mu_*}}) = \epsilon_0$, it follows that the sequence $u_n(t_n)$ is bounded. Hypothesis F then implies there exist $z_n \in \Sigma_{\mu_*}$ so that $\|u_n(t_n) - z_n\| \to 0$.

We can now conclude. Since, for n large enough, $\frac{\epsilon_0}{2} \leq \mathrm{d}(z_n, \mathscr{O}_{u_{\mu_*}}) \leq \eta$, we have

$$\begin{aligned}\mathscr{L}_{\mu_*}(u_n) - \mathscr{L}(u) &= \mathscr{L}_{\mu_*}(u_n(t_n)) - \mathscr{L}_{\mu_*}(u) \\ &= \mathscr{L}_{\mu_*}(u_n(t_n)) - \mathscr{L}_{\mu_*}(z_n) + \mathscr{L}_{\mu_*}(z_n) - \mathscr{L}_{\mu_*}(u) \\ &\geq \mathscr{L}_{\mu_*}(u_n(t_n)) - \mathscr{L}_{\mu_*}(z_n) + c\mathrm{d}^2(z_n, \mathscr{O}_{u_{\mu_*}}).\end{aligned}$$

Since the orbit $\mathscr{O}_{u_{\mu_*}}$ is bounded, the sequences $u_n(t_n)$ and z_n are bounded. This, combined with the uniform continuity of $\mathscr{L}_{\mu_*}$ on bounded sets, leads again to a contradiction upon taking $n \to +\infty$.

We now give a third proof of orbital stability starting from a coercive Lyapunov function, along the lines of the second argument in the proof of Proposition 3. The point here is that we exploit the fact that the relative equilibria u_μ often come in families.

Theorem 10 *Suppose the following.*

(i) *Hypothesis A holds.*
(ii) *There exists a continuous map $\mu \in U \subset \mathbb{R}^m \to u_\mu \in \Sigma_\mu \subset E$ so that Hypothesis Bμ is satisfied for all $\mu \in U$, with η and c in (111) independent of μ.*
(iii) $\sup_{\mu \in U} \|u_\mu\| < +\infty$.
(iv) *There exists $C > 0$ so that*

$$\forall \mu \in U, \forall u' \in \Sigma_\mu, \quad \|u' - u_\mu\| \leq \eta \Rightarrow \mathscr{L}_\mu(u') - \mathscr{L}_\mu(u_\mu) \leq C\|u' - u_\mu\|. \tag{117}$$

(v) *$\forall g \in G$, Φ_g is an isometry on E: $\forall u, u' \in E$, $\mathrm{d}(\Phi_g(u), \Phi_g(u')) = \mathrm{d}(u, u')$.*

Then, any $u \in \mathscr{O}_{u_\mu}$ is an orbitally stable G_{Σ_μ}-relative equilibrium of the flow Φ_t^H.

Condition (iii) is not very restrictive. It is sufficient to take U bounded, for example. Condition (iv) follows if we know that $D_u\mathscr{L}_\mu$ is bounded for u in bounded sets. This is a reasonable condition. Condition (v) is commonly satisfied in PDE systems, but is quite restrictive, as we already explained. It implies we can use Proposition 1 and Lemma 1.

Proof Let $\mu_* \in U$. As a result of Lemma 1, it is enough to show the orbital stability of u_{μ_*}. So we need to show that, for all $\epsilon > 0$, there exists $\delta > 0$ so that, for all $u' \in E$, one has

$$\|u' - u_{\mu_*}\| \leq \delta \Rightarrow \forall t \in \mathbb{R}, \mathrm{d}(u'(t), \mathscr{O}_{u_{\mu_*}}) \leq \epsilon. \tag{118}$$

For that purpose, we need three preliminary estimates. We first show that $\forall \epsilon > 0$, there exists $\hat{\delta} > 0$ so that, for all $\mu \in U$, for all $u' \in \Sigma_\mu$,

$$\|u' - u_\mu\| \leq \hat{\delta} \Rightarrow \forall t \in \mathbb{R}, \mathrm{d}(u'(t), \mathscr{O}_{u_\mu}) \leq \epsilon/2. \tag{119}$$

In other words, we first show that the u_μ are all orbitally stable for perturbations *within* Σ_μ. The method of proof—by contradiction—is the same as several times before, but we need to make sure to obtain the necessary uniformity in μ. If the above is not true, then there exists $\epsilon_0 > 0$ so that for all $n \in \mathbb{N}^*$ there exist $\mu_n \in U$ and $u_n \in \Sigma_{\mu_n}$, $t_n \in \mathbb{R}$, so that

$$\|u_n - u_{\mu_n}\| \leq \frac{1}{n}, \quad \mathrm{d}(u_n(t_n), \mathscr{O}_{u_{\mu_n}}) = \frac{\epsilon_0}{2} < \eta.$$

Here η is given in Hypothesis Bμ(iii) and we recall that it is independent of μ_n. Hence

$$\mathscr{L}_{\mu_n}(u_n) - \mathscr{L}_{\mu_n}(u_{\mu_n}) = \mathscr{L}_{\mu_n}(u_n(t_n)) - \mathscr{L}_{\mu_n}(u_{\mu_n}) \geq c\mathrm{d}^2(u_n(t_n), \mathscr{O}_{\mu_n}) = c\frac{\epsilon_0^2}{4}.$$

Now, since the u_{μ_n} form a bounded set by hypothesis (iii) of the theorem, the same is true for the u_n. Hence, it follows from hypothesis (iv) of the theorem that

$$\mathscr{L}_{\mu_n}(u_n) - \mathscr{L}_{\mu_n}(u_{\mu_n}) \leq C\|u_n - u_{\mu_n}\|,$$

where C does not depend on n. Hence $C\|u_n - u_{\mu_n}\| \geq c\frac{\epsilon_0^2}{4}$, so that, taking $n \to +\infty$, we obtain a contradiction. This proves (119).

As a second step, we show the following estimate. Let $\mu_* \in U$. Then, for all $\epsilon > 0$, there exists $\hat{\rho} > 0$ so that,

$$\forall \mu \in U, \quad \left(\|\mu - \mu_*\| \leq \hat{\rho} \Rightarrow \forall v \in \mathscr{O}_{u_\mu}, \mathrm{d}(v, \mathscr{O}_{u_{\mu_*}}) \leq \frac{\epsilon}{2}\right). \tag{120}$$

To see, this, note that hypothesis (i) of the theorem implies that there exists $\hat{\rho} > 0$ so that $\|\mu - \mu_*\| \leq \hat{\rho}$ implies $\|u_\mu - u_{\mu_*}\| \leq \epsilon/2$. Hence $\mathrm{d}(u_\mu, \mathscr{O}_{u_{\mu_*}}) \leq \epsilon/2$. The result then follows from Proposition 1, since we suppose the action Φ of G is isometric.

The third ingredient for the proof of (118) is the following:

$$\begin{aligned} &\forall \hat{\delta} > 0, \forall \hat{\rho} > 0, \exists \delta > 0, \forall u' \in E, \\ &\quad \left(\|u' - u_{\mu_*}\| \leq \delta \Rightarrow \|\mu' - \mu_*\| \leq \hat{\rho}, \|u' - u_{\mu'}\| \leq \hat{\delta}\right), \end{aligned} \tag{121}$$

where $\mu' = F(u')$. This follows immediately from the continuity of F and of $\mu \to u_\mu$ at μ_*.

We can now conclude. Let $\mu_* \in U$ and $\epsilon > 0$. Choose $\hat{\delta}$ as in (119), $\hat{\rho}$ as in (120) and δ as in (121). Then, by (119) and (121), we find that

$$\forall u' \in E, \left(\|u' - u_{\mu_*}\| \leq \delta \Rightarrow \forall t \in \mathbb{R}, \mathrm{d}(u'(t), \mathscr{O}_{u_{\mu'}}) < \frac{\epsilon}{2}\right).$$

Hence, for all $t \in \mathbb{R}$, there exists $v(t) \in \mathscr{O}_{u_{\mu'}}$, so that $\mathrm{d}(u'(t), v(t)) < \epsilon/2$. Next, from (121) and (120), there exists $w(t) \in \mathscr{O}_{u_{\mu *}}$ so that $\mathrm{d}(v(t), w(t)) < \frac{\epsilon}{2}$. Hence $\mathrm{d}(u'(t), \mathscr{O}_{u_{\mu *}}) < \epsilon$. This proves (118).

8.4 *Sufficient Condition for Coercivity*

We now turn to the task of showing how one can obtain the coercivity Hypothesis Bμ(iii) from an estimate on the Hessian of $\mathscr{L}_\mu$ (Proposition 5). We work in the following setting.

As before, let E be a Banach space, G a Lie group and Φ a G-action on E. Let $F \in C^2(E, \mathbb{R}^m)$. We recall that, for $\mu \in \mathbb{R}^m$,

$$\Sigma_\mu = \{u \in E \mid F(u) = \mu\},$$

and that G_{Σ_μ} is the subgroup of G leaving Σ_μ invariant. We now introduce one extra ingredient to the theory. Let $\langle \cdot, \cdot \rangle$ be a scalar product on E, which is continuous in the sense that

$$\forall v, w \in E, \quad |\langle v, w \rangle| \leq \|v\| \|w\|,$$

where we recall that $\| \cdot \|$ is our notation for the Banach norm on E. This inner product induces a metric on E, that we shall denote by

$$\mathrm{d}_\mathrm{s}(v, w) = \langle v - w, v - w \rangle. \tag{122}$$

Clearly $\mathrm{d}_\mathrm{s}(v, w) \leq \mathrm{d}(v, w)$. We introduce this inner product since we need a notion of orthogonality for the statement of the main result of this section, Proposition 5: see in particular (126) and (127).

We point out that we are not supposing E is a Hilbert space for this inner product, and that the only topology we will be using in what follows is the one induced by the Banach norm on E. In addition, even if E *is* in fact a Hilbert space, the inner product $\langle \cdot, \cdot \rangle$ above is not necessarily the Hilbert space inner product. As an example, if $E = H^1(\mathbb{R}^d, \mathbb{C})$ and depending on the problem considered, one may want to use either the L^2 inner product or the H^1 inner product: in Sect. 9 the first choice is made and in Sect. 10 the second one. In the formalism developed in [53, 54, 99], E is always supposed to be a Hilbert space, and only the Hilbert space inner product is used in the analysis of the Hessian. But the introduction of a second inner product is a regularly used device in the literature on orbital stability for the Schrödinger in particular. Our approach here gives a systematic treatment in the general setting presented above.

Let $\mu \in \mathbb{R}^m$ and $u_\mu \in \Sigma_\mu$. We need the following hypothesis on the group action and on the function F.

Hypothesis Cμ

(i) Φ_g is linear and preserves both the structure $\langle\cdot,\cdot\rangle$ and the norm $\|\cdot\|$ for all $g \in G$;
(ii) $\mathrm{Ad}^*_g \in \mathrm{O}(m)$ for all $g \in G_{\Sigma_\mu}$;
(iii) μ is a regular value of F;
(iv) u_μ is a C^1-vector for Φ and the map

$$\xi \in \mathfrak{g}_{\Sigma_\mu} \to \Phi_{\exp(\xi)} u_\mu \in E \tag{123}$$

is one to one in a neighbourhood of $\xi = 0$.

Note that both Hypothesis Cμ above and Proposition 5 below involve G and its action on E, as well as F, but not the dynamics Φ_t^X itself.

Remark 8 (i) The meaning of condition (ii) of Hypothesis Cμ is explained in Remark 15.
(ii) We say $u \in E$ is a C^1-vector for the action Φ if the map $g \in G \to \Phi_g(u) \in E$ is C^1. Now, if $u' \in \mathscr{O}_u = \Phi_G(u)$, then u' is also a C^1-vector. Indeed, there exists $g' \in G$ so that $\Phi_{g'} u = u'$ and, since $g \to gg'$ is smooth, it follows that $g \to \Phi_{gg'} u$ is C^1.

To state the result, we need the following notation. Let $\tilde{G}$ be a subgroup of G; we can then define, for all $u' \in \mathscr{O}_u = \Phi_{\tilde{G}}(u)$,

$$T_{u'}\mathscr{O}_u := \{w \in E \mid \exists \xi \in \mathfrak{g}, w = X_\xi(u')\}, \tag{124}$$

where we recall from (206) that

$$X_\xi(u) = \frac{\mathrm{d}}{\mathrm{d}t} \Phi_{\exp(t\xi)}(u)_{|t=0}.$$

Proposition 5 *Let E be a Banach space and $\langle\cdot,\cdot\rangle$ be a continuous scalar product on E. Let G be a Lie group and Φ a G-action on E. Let $F \in C^2(E, \mathbb{R}^m)$. Let $\mu_* \in \mathbb{R}^m$ and $u_{\mu_*} \in \Sigma_{\mu_*}$. Let $\mathscr{L}_{\mu_*} \in C^2(E, \mathbb{R})$ be a $G_{\Sigma_{\mu_*}}$-invariant function. Suppose Hypothesis Cμ_* holds and that, for all $u \in \mathscr{O}_{u_{\mu_*}}$ [defined in (112)],*

$$\forall j = 1, \ldots, m \; \exists \nabla F_j(u) \in E \text{ such that } D_u F_j(w) = \langle \nabla F_j(u), w\rangle \; \forall w \in E. \tag{125}$$

Suppose $\mathscr{L}_{\mu_*}$ satisfies the following conditions:

(a) $D_u \mathscr{L}_{\mu_*}(w) = 0$ for all $u \in \mathscr{O}_{u_{\mu_*}}$ and $w \in E$;
(b) there exists $C > 0$ so that

$$\forall u \in \mathscr{O}_{u_{\mu_*}}, \forall w \in E, \; D^2_u \mathscr{L}_{\mu_*}(w, w) \le C\|w\|^2;$$

(c) there exists $c > 0$ so that

$$\forall u \in \mathscr{O}_{u_{\mu_*}}, \forall w \in T_u \Sigma_{\mu_*} \cap (T_u \mathscr{O}_{u_{\mu_*}})^{\perp},\ D_u^2 \mathscr{L}_{\mu_*}(w, w) \geq c\|w\|^2 \tag{126}$$

where

$$(T_w \mathscr{O}_u)^{\perp} = \{z \in E \mid \langle z, y\rangle = 0, \forall y \in T_w \mathscr{O}_u\}. \tag{127}$$

Then Hypothesis $B\mu_*$ (iii) holds.

Condition (125) is automatically satisfied when E is a Hilbert space and $\langle \cdot, \cdot \rangle$ the Hilbert space inner product. But not in general. For example, let $E = H^1(\mathbb{R}, \mathbb{C})$ and let $\langle u, v\rangle = \mathrm{Re} \int_{\mathbb{R}} \bar{u}(x) v(x) \mathrm{d}x$. Now, if $F_1(u) = \frac{1}{2i} \int \bar{u}(x) \partial_x u(x) \mathrm{d}x$, (125) is satisfied if $u \in H^2(\mathbb{R}, \mathbb{C})$ but not for arbitrary $u \in E$.

For the proof of this proposition, we need some simple technical results.

First, let V be a bounded open neighbourhood of e in a subgroup $\tilde{G}$ of G with the property that, for all $g \in \tilde{G}$, $gVg^{-1} = V$. Let us introduce

$$R_V(u) = \min\{\mathrm{d_s}(\Phi_g(u), u) \mid g \in \partial V\}.$$

It then follows that, for all $u' \in \mathscr{O}_u$, $R_V(u') = R_V(u)$. Indeed, there exists $g' \in \tilde{G}$ so that $\Phi_{g'}(u) = u'$. Hence

$$\begin{aligned} R_V(u') &= \min\{\mathrm{d_s}(\Phi_{gg'}(u), \Phi_{g'}(u)) \mid g \in \partial V\} \\ &= \min\{\mathrm{d_s}(\Phi_{g'^{-1}gg'}(u), u) \mid g \in \partial V\} = R_V(u), \end{aligned}$$

since $g'^{-1} \partial V g' = \partial V$.

We can now formulate the following simple but crucial technical result, which is a multi-dimensional version of Lemma 2.1 in [99].

Lemma 6 *Let E be a Banach space and $\langle \cdot, \cdot \rangle$ be a continuous scalar product on E. Let $\tilde{G}$ be a Lie subgroup of G and Φ a linear G-action on E which preserves the inner product $\langle \cdot, \cdot \rangle$. Suppose $u \in E$ is a C^1-vector for Φ and let V be a bounded open neighbourhood of $e \in \tilde{G}$ which is conjugation invariant (i.e. $gVg^{-1} = V$, for all $g \in \tilde{G}$). Suppose $R_V(u) > 0$. Then, for all $v \in E$,*

$$\mathrm{d}(v, \mathscr{O}_u) < \frac{1}{3} R_V(u) \Rightarrow \exists w \in \mathscr{O}_u = \Phi_{\tilde{G}}(u), w - v \in (T_w \mathscr{O}_u)^{\perp}. \tag{128}$$

The lemma states that if v is not too far from the orbit $\mathscr{O}_u$, then there exists a point w on the orbit so that the segment from v to w is orthogonal to the orbit at w. This point does *not* necessarily realize the distance between v and the orbit, which can vanish.

Proof Let $v \in E$ and $\mathrm{d}(v, \mathscr{O}_u) < \frac{1}{3}R_V(u)$. Then there exists $u' \in \mathscr{O}_u$ so that $\mathrm{d}(v, u') \leq \frac{1}{3}R_V(u) = \frac{1}{3}R_V(u')$ and hence $\mathrm{d_s}(v, u') \leq \frac{1}{3}R_V(u')$. Now consider

$$g \in \overline{V} \to \mathrm{d_s^2}(v, \Phi_g u') \in \mathbb{R}^+.$$

Since $\overline{V}$ is compact, this function reaches a minimum at some point $\tilde{g} \in \overline{V}$. We set $w = \Phi_{\tilde{g}} u' \in \mathscr{O}_u$ so that $\mathrm{d_s}(v, w) \leq \mathrm{d_s}(v, u') \leq \frac{1}{3}R_V(u')$. We now show that $\tilde{g}$ cannot belong to ∂V. Indeed, if $\tilde{g}$ were on the boundary of V, then, by the definition of $R_V(u')$, $\mathrm{d_s}(w, u') \geq R_V(u')$. But then

$$\mathrm{d_s}(w, v) \geq -\mathrm{d_s}(u', v) + \mathrm{d_s}(u', w) \geq R_V(u') - \frac{1}{3}R_V(u') = \frac{2}{3}R_V(u').$$

which is a contradiction because $\mathrm{d_s}(v, w) \leq \frac{1}{3}R_V(u')$. So $\tilde{g}$ belongs to V. Now choose $\xi \in \mathfrak{g}$ and consider

$$t \in \mathbb{R} \to \mathrm{d_s^2}(v, \Phi_{\exp(t\xi)\tilde{g}}(u')) \in \mathbb{R}^+,$$

which now reaches a local minimum at $t = 0$ since for small t, $\exp(t\xi)\tilde{g}$ belongs to V. Hence its derivative vanishes. So

$$\begin{aligned} 0 = \frac{\mathrm{d}}{\mathrm{d}t}\mathrm{d_s^2}(v, \Phi_{\exp(t\xi)\tilde{g}}(u'))_{|t=0} &= \frac{\mathrm{d}}{\mathrm{d}t}\langle v - \Phi_{\exp(t\xi)}(w), v - \Phi_{\exp(t\xi)}(w)\rangle_{|t=0} \\ &= -2\langle X_\xi(w), v - w\rangle, \end{aligned}$$

which proves the result in view of (124).

In the proof of Proposition 5, we will need to apply the previous lemma to the group $G_{\Sigma_{\mu_*}}$ for some $\mu_* \in \mathbb{R}^m$ and $u_{\mu_*} \in \Sigma_{\mu_*}$. The following lemma gives hypotheses for this to be possible. It appears in various guises in the literature, and can be referred to as a "modulation" argument.

Lemma 7 *Let E be a Banach space and $\langle \cdot, \cdot \rangle$ be a continuous scalar product on E. Let G be a Lie group and Φ a G-action on E. Let $F \in C^2(E, \mathbb{R}^m)$. Let $\mu_* \in \mathbb{R}^m$ and $u_{\mu_*} \in \Sigma_{\mu_*}$. Suppose Hypothesis $C\mu_*$ holds. Then, there exists $R > 0$ such that, for all $v \in E$,*

$$\mathrm{d}(v, \mathscr{O}_{u_{\mu_*}}) < R \Rightarrow \exists w \in \mathscr{O}_{u_{\mu_*}}, w - v \in \left(T_w \mathscr{O}_{u_{\mu_*}}\right)^\perp \tag{129}$$

where $\mathscr{O}_{u_{\mu_*}} = \Phi_{G_{\Sigma_{\mu_*}}} u_{\mu_*}$.

Proof Thanks to Lemma 6, it is enough to prove that there exists V a bounded open neighbourhood of $e \in G_{\Sigma_{\mu_*}}$, which is conjugation invariant (i.e. $gVg^{-1} = V$, for all $g \in G_{\Sigma_{\mu_*}}$) and such that $R_V(u_{\mu_*}) > 0$.

First of all, we recall that the exponential map

$$\exp : \xi \in \mathfrak{g}_{\mu *} \to \exp(\xi) \in G_{\Sigma_{\mu *}}$$

is a local diffeomorphism from some neighbourhood of $0 \in \mathfrak{g}_{\mu *}$ to a neighbourhood of $e \in G_{\Sigma_{\mu *}}$. In other words, there exists $\delta > 0$ such that

$$\exp : \xi \in B_\delta(0) \subset \mathfrak{g}_{\mu *} \to \exp(\xi) \in G_{\Sigma_{\mu *}}$$

is a local diffeomorphism onto a bounded open neighbourhood $V := \exp(B_\delta(0))$ of e in $G_{\mu *}$. In particular, note that $\partial V = \exp(\partial B_\delta(0))$.

Since, thanks to Hypothesis Cμ*(ii), $B_\delta(0)$ is Ad_g-invariant for all $g \in G_{\Sigma_{\mu *}}$, V is conjugation invariant. Indeed, for all $\xi \in B_\delta(0)$ and all $g \in G_{\Sigma_{\mu *}}$, we have that $g \exp(\xi) g^{-1} = \exp(\mathrm{Ad}_g \xi) \in V$.

Hence, it only remains to show that $R_V(u_{\mu *}) > 0$, which is equivalent to $G_{u_{\mu *}} \cap \partial V = \emptyset$. Thanks to Hypothesis C$\mu$*(iv), there exists $\delta_0 > 0$ such that

$$\xi \in B_{\delta_0}(0) \to \Phi_{\exp(\xi)} u_{\mu *} \in E$$

is one to one. As a conclusion, choosing $\delta < \delta_0$, we have $\partial V \subset \exp(B_{\delta_0}(0))$ which implies $\Phi_{\exp(\xi)} u_{\mu *} \neq u_{\mu *}$ for all $\exp(\xi) \in \partial V$. Hence, for all $\exp(\xi) \in \partial V$, $\exp(\xi) \notin G_{u_{\mu *}}$.

We can then conclude this section with the proof of Proposition 5.

Proof (of Proposition 5) Recall that we have to prove there exist $\eta > 0, \tilde{c} > 0$ so that

$$\forall u \in \mathscr{O}_{u_{\mu *}}, \forall u' \in \Sigma_{\mu *}, \quad \mathrm{d}(u, u') \leq \eta \Rightarrow \mathscr{L}_{\mu *}(u') - \mathscr{L}_{\mu *}(u) \geq \tilde{c} \mathrm{d}^2(u', \mathscr{O}_{u_{\mu *}}).$$

Let $u' \in \Sigma_{\mu *}$, $\mathrm{d}(u', \mathscr{O}_{u_{\mu *}}) < R$. Thanks to Lemma 7, there exists $v' \in \mathscr{O}_{u_{\mu *}}$ such that $u' - v' \in \left(T_{v'} \mathscr{O}_{u_{\mu *}}\right)^\perp$.

Next, let $W_{v'}$ be the subspace of E spanned by $\{\nabla F_j(v')\}_{j=1\ldots,m}$. It follows from (191) and hypothesis (125) that $T_{v'} \Sigma_{\mu *} = (W_{v'})^\perp$. As a consequence, we can write $E = T_{v'} \Sigma_{\mu *} \oplus W_{v'}$. Indeed, since $W_{v'}$ has finite dimension, it admits an orthonormal basis $\{e_1, \ldots, e_m\}$ w.r.t. $\langle \cdot, \cdot \rangle$. Hence, all $w \in E$ can be written as

$$w = \left(w - \sum_{j=1}^m \langle w, e_j \rangle e_j\right) + \sum_{j=1}^m \langle w, e_j \rangle e_j.$$

Clearly $w - \sum_{j=1}^m \langle w, e_j \rangle e_j \in (W_{v'})^\perp = T_{v'} \Sigma_{\mu *}$, $\sum_{j=1}^m \langle w, e_j \rangle e_j \in W_{v'}$ and $W_{v'} \cap (W_{v'})^\perp = \{0\}$. Then,

$$u' - v' = (u' - v')_1 + (u' - v')_2$$

where $(u'-v')_1 \in T_{v'}\Sigma_{\mu_*}$ and $(u'-v')_2 \in W_{v'}$. Moreover, since $u'-v' \in \left(T_{v'}\mathscr{O}_{u_{\mu_*}}\right)^{\perp}$, we can easily show $(u'-v')_1 \in T_{v'}\Sigma_{\mu_*} \cap \left(T_{v'}\mathscr{O}_{u_{\mu_*}}\right)^{\perp}$ and $(u'-v')_2 \in W_{v'} \cap \left(T_{v'}\mathscr{O}_{u_{\mu_*}}\right)^{\perp}$. Now, Lemma 10 ensures the existence of constants c_1, c_0 so that, for $\|u'-v'\|$ small enough, one has

$$\|(u'-v')_1\| \geq c_0\|u'-v'\| \text{ and } \|(u'-v')_2\| \leq c_1\|u'-v'\|^2. \tag{130}$$

Since the action Φ_g is linear and preserves both $\langle\cdot,\cdot\rangle$ and $\|\cdot\|$, the decomposition above is group invariant and the constant c_0 and c_1 do not depend on v'.

We can now conclude the proof as follows, using respectively conditions (a), (b) and (c), and (130):

$$\begin{aligned}
\mathscr{L}_{\mu_*}(u') - \mathscr{L}_{\mu_*}(u_{\mu_*}) &= \mathscr{L}_{\mu_*}(u') - \mathscr{L}_{\mu_*}(v') \\
&= D_{v'}\mathscr{L}_{\mu_*}(u'-v') + \frac{1}{2}D^2_{v'}\mathscr{L}_{\mu_*}(u'-v', u'-v') \\
&\quad + \mathrm{o}(\|u'-v'\|^2) \\
&= \frac{1}{2}D^2_{v'}\mathscr{L}_{\mu_*}((u'-v')_1, (u'-v')_1) + \mathrm{O}(\|u'-v'\|^3) \\
&\quad + \mathrm{o}(\|u'-v'\|^2) \\
&= \frac{1}{2}D^2_{v'}\mathscr{L}_{\mu_*}((u'-v')_1, (u'-v')_1) + \mathrm{o}(\|u'-v'\|^2) \\
&\geq \frac{c}{2}\|(u'-v')_1\|^2 + \mathrm{o}(\|u'-v'\|^2) \\
&\geq \tilde{c}\|u'-v'\|^2 \geq \tilde{c}\,\mathrm{d}^2(u', \mathscr{O}_{u_{\mu_*}}).
\end{aligned}$$

Remark that as before, the constant $\tilde{c}$ is independent of $v' \in \mathscr{O}_{\mu_*}$.

8.5 *Coercivity Implies Stability II*

We can now state and prove a fourth theorem yielding orbital stability under slightly different technical assumptions. We will work in the Hamiltonian setting and in particular use the characterization of relative equilibria given by Theorem 7. Recall that in this context, for each $\mu \in \mathfrak{g}^* \simeq \mathbb{R}^m$, $G_{\Sigma_\mu} = G_\mu$ (Proposition 10).

Theorem 11 *Let E be a Banach space and $\langle\cdot,\cdot\rangle$ be a continuous scalar product on E, $\mathscr{D}$ a domain in E and $\mathscr{J}$ a symplector. Let $H \in C^2(E,\mathbb{R}) \cap \mathrm{Dif}(\mathscr{D}, \mathscr{J})$. Let G be a Lie group, and Φ a globally Hamiltonian G-action on E with Ad^*-equivariant momentum map F. Let $\mu_* \in \mathbb{R}^m \simeq \mathfrak{g}^*$ and $u_{\mu_*} \in \mathscr{D} \cap \Sigma_{\mu_*}$. Suppose that Hypothesis $C\mu_*$(i)–(iii) is satisfied, and $H \circ \Phi_g = H$ for all $g \in G$. Let $\mathscr{L}_{\mu_*} = H - \xi_{\mu_*} \cdot F$ with $\xi_{\mu_*} \in \mathfrak{g}_{\mu_*}$ given by Theorem 7 and assume $D_{u_{\mu_*}}\mathscr{L}_{\mu_*} = 0$. Suppose*

in addition that

$$\forall j = 1, \ldots, m \; \exists \nabla F_j(u_{\mu_*}) \in E \text{ such that } D_{u_{\mu_*}} F_j(w) = \langle \nabla F_j(u_{\mu_*}), w \rangle \; \forall w \in E. \tag{131}$$

and

(a) G_{μ_*} is commutative;
(b) there exists $C > 0$ so that

$$\forall w \in E, \; D^2_{u_{\mu_*}} \mathscr{L}_{\mu_*}(w, w) \leq C \|w\|^2;$$

(c) there exists $c > 0$ so that

$$\forall w \in T_{u_{\mu_*}} \Sigma_{\mu_*} \cap (T_{u_{\mu_*}} \mathscr{O}_{u_{\mu_*}})^{\perp}, \; D^2_{u_{\mu_*}} \mathscr{L}_{\mu_*}(w, w) \geq c \|w\|^2.$$

Then all $u \in \mathscr{O}_{u_{\mu_*}}$ are orbitally stable G_{μ_*}-relative equilibria.

Hypothesis (a) in Theorem 11 is not very restrictive (see [31]).

Proof Let $K > 0$ and define

$$\mathscr{L}_K(u) = \mathscr{L}_{\mu_*}(u) + K(F(u) - \mu_*)^2.$$

Here $(F(u) - \mu_*)^2 = (F(u) - \mu_*) \cdot (F(u) - \mu_*)$ where, $\cdot$ is the G_{μ_*}-invariant inner product described in Remark 15. It follows that $\mathscr{L}_K$ is a G_{μ_*}-invariant constant of the motion. Indeed, for all $g \in G_{\mu_*}$ and for all $u \in E$,

$$\begin{aligned}
\mathscr{L}_K(\Phi_g u) &= H(\Phi_g u) - \xi_{\mu_*} \cdot F(\Phi_g u) + K(F(\Phi_g u) - \mu_*)^2 \\
&= H(u) - \xi_{\mu_*} \cdot \mathrm{Ad}^*_g F(u) + K(\mathrm{Ad}^*_g F(u) - \mathrm{Ad}^*_g \mu_*)^2 \\
&= H(u) - \mathrm{Ad}_g \xi_{\mu_*} \cdot F(u) + K(F(u) - \mu_*)^2 && \text{as } \mathrm{Ad}^*_g \in \mathrm{O}(m) \\
&= H(u) - \xi_{\mu_*} \cdot F(u) + K(F(u) - \mu_*)^2 && \text{as } G_{\mu_*} \\
& && \text{is commutative} \\
&= \mathscr{L}_K(u).
\end{aligned}$$

The main idea is to prove that the hypotheses of Proposition 5 are satisfied by $\mathscr{L}_K$ and then use its proof to conclude that all $u \in \mathscr{O}_{u_{\mu_*}}$ are orbitally stable G_{μ_*}-relative equilibria.

First, note that in this setting Hypothesis Cμ_*(iv) follows from Remark 5.

Next, we claim that $D_u \mathscr{L}_K(w) = 0$ for all $u \in \mathscr{O}_{u_{\mu_*}}$ and for all $w \in E$. Indeed, it is clear that $D_u(F(u) - \mu_*)^2 = 2(F(u) - \mu_*) \cdot D_u F = 0$ for all $u \in \mathscr{O}_{u_{\mu_*}}$ and, thanks to the fact that $D_{u_{\mu_*}} \mathscr{L}_{K_{\mu_*}}(w) = 0$, we obtain $D_{u_{\mu_*}} \mathscr{L}_K(w) = 0$ for all $w \in E$. Next, let $u \in \mathscr{O}_{u_{\mu_*}}$ and $g \in G_{\mu_*}$ such that $u = \Phi_g(u_{\mu_*})$, then

$$D_u \mathscr{L}_K(w) = [D_{\Phi_g(u_{\mu_*})} \mathscr{L}_K \circ \Phi_{g^{-1}}](w) = [D_{u_{\mu_*}} \mathscr{L}_K \circ D_{\Phi_g(u_{\mu_*})} \Phi_{g^{-1}}](w) = 0.$$

Using the fact that Φ_g is linear and preserves both $\langle\cdot,\cdot\rangle$ and $\|\cdot\|$, we can easily show, as a consequence of hypothesis (c), that

$$\forall u \in \mathscr{O}_{u_{\mu*}},\ D_u^2\mathscr{L}_{\mu*}(w,w) \geq c\|w\|^2, \tag{132}$$

for all $w \in T_u\Sigma_{\mu*} \cap (T_u\mathscr{O}_{u_{\mu*}})^\perp$. Indeed, for all $u \in \mathscr{O}_{u_{\mu*}}$ and $w \in T_u\Sigma_{\mu*} \cap (T_u\mathscr{O}_{u_{\mu*}})^\perp$,

$$\begin{aligned} D_u^2\mathscr{L}_{\mu*}(w,w) &= D^2_{\Phi_g u_{\mu*}}(\mathscr{L}_{\mu*}\circ\Phi_{g^{-1}})(w,w) \\ &= D^2_{u_{\mu*}}\mathscr{L}_{\mu*}(D_u\Phi_{g^{-1}}w, D_u\Phi_{g^{-1}}w) + D_{u_{\mu*}}\mathscr{L}_{\mu*}(D_u^2\Phi_{g^{-1}}(w,w)) \\ &= D^2_{u_{\mu*}}\mathscr{L}_{\mu*}(\Phi_{g^{-1}}w, \Phi_{g^{-1}}w) \geq c\|\Phi_{g^{-1}}w\|^2 = c\|w\|^2 \end{aligned}$$

because $\Phi_{g^{-1}}w \in T_{u_{\mu*}}\Sigma_{\mu*} \cap (T_{u_{\mu*}}\mathscr{O}_{u_{\mu*}})^\perp$.

Similarly, using hypothesis (b), we prove that

$$D_u^2\mathscr{L}_{\mu*}(w,w) \leq C\|w\|^2$$

for all $u \in \mathscr{O}_{u_{\mu*}}$ and $w \in E$.

Next, by a straightforward calculation, we obtain for all $u \in \mathscr{O}_{u_{\mu*}}$ and $w \in E$, $D_u^2(F-\mu_*)^2(w,w) = 2D_uF(w)\cdot D_uF(w)$, and

$$\begin{aligned} D_uF(w) &= [D_{\Phi_g u_{\mu*}}F\circ\Phi_g\circ\Phi_{g^{-1}}](w) = [D_{u_{\mu*}}F\circ\Phi_g](D_u\Phi_{g^{-1}}w) \\ &= [D_{u_{\mu*}}\mathrm{Ad}_g^*\circ F](\Phi_{g^{-1}}w) = \mathrm{Ad}_g^*(D_{u_{\mu*}}F(\Phi_{g^{-1}}w)). \end{aligned} \tag{133}$$

As a consequence, since $\mathrm{Ad}_g^* \in \mathrm{O}(m)$,

$$D_u^2(F-\mu_*)^2(w,w) = 2D_{u_{\mu*}}F(\Phi_{g^{-1}}w)\cdot D_{u_{\mu*}}F(\Phi_{g^{-1}}w). \tag{134}$$

It is then clear that $D_u^2(F-\mu_*)^2(w,w) \leq C_{\mu*}\|w\|^2$ for all $u \in \mathscr{O}_{u_{\mu*}}$ and $w \in E$, and hypothesis (b) of Proposition 5 is satisfied by $\mathscr{L}_K$. In addition (133) together with the fact that the Φ_g preserve the inner product $\langle\cdot,\cdot\rangle$ shows that (131) implies (125).

Now let $w \in (T_u\mathscr{O}_{u_{\mu*}})^\perp$ and write $w = w_1 + w_2$ with $w_1 \in T_u\Sigma_{\mu*} \cap (T_u\mathscr{O}_{u_{\mu*}})^\perp$ and $w_2 \in W_u \cap (T_u\mathscr{O}_{u_{\mu*}})^\perp$. Then

$$\begin{aligned} D_u^2\mathscr{L}_K(w,w) &= D_u^2\mathscr{L}_{\mu*}(w,w) + 2KD_{u_{\mu*}}F(\Phi_{g^{-1}}w_2)\cdot D_{u_{\mu*}}F(\Phi_{g^{-1}}w_2) \\ &\geq D_u^2\mathscr{L}_{\mu*}(w_1,w_1) - C(\|w_1\|\|w_2\| + \|w_2\|^2) \\ &\quad + 2KD_{u_{\mu*}}F(\Phi_{g^{-1}}w_2)\cdot D_{u_{\mu*}}F(\Phi_{g^{-1}}w_2) \\ &\geq c\|w_1\|^2 - C(\|w_1\|\|w_2\| + \|w_2\|^2) + Kc_{\mu*}\|w_2\|^2, \end{aligned}$$

where in the last line we use the fact that $\dim W_{u_{\mu_*}} = m$ and $D_{u_{\mu_*}} F_{|W_{u_{\mu_*}}} : W_{u_{\mu_*}} \to \mathbb{R}^m$ is an isomorphism. Finally, thanks to Young's inequality, there exists $\varepsilon > 0$ so that

$$D^2_u \mathscr{L}_K(w,w) \geq \left(c - \frac{C\varepsilon}{2}\right) \|w_1\|^2 + \left(Kc_{\mu_*} - C - \frac{C}{2\varepsilon}\right) \|w_2\|^2 \geq \tilde{c}\|w\|^2$$

with $\tilde{c} > 0$ provided that $K > 0$ is chosen large enough. As a consequence, using the same arguments as in the proof of Proposition 5, we conclude that there exist $\eta > 0, c > 0$ so that

$$\forall u \in \mathscr{O}_{u_{\mu_*}}, \forall v \in E, \quad \mathrm{d}(u,v) \leq \eta \Rightarrow \mathscr{L}_K(v) - \mathscr{L}_K(u) \geq c\mathrm{d}^2(v, \mathscr{O}_{u_\mu})$$

which implies, thanks to Theorem 8, that all $u \in \mathscr{O}_{u_{\mu_*}}$ are orbitally stable G_{μ_*}-relative equilibria.

9 Plane Wave Stability on the Torus for NLS

In this section we will illustrate the general theory described above on a simple example, that is the orbital stability of plane waves of the cubic focusing and defocusing nonlinear Schrödinger equation on the one-dimensional torus. More precisely, let us consider the cubic Schrödinger equation

$$i\partial_t u(t,x) + \beta \partial^2_{xx} u(t,x) + \lambda |u(t,x)|^2 u(t,x) = 0 \tag{135}$$

in the space periodic setting $\mathbb{T}_L$, the one-dimensional torus of length $L > 0$, and with $u(t,x) \in \mathbb{C}$. The constants β and λ are parameters of the model; $\beta\lambda < 0$ corresponds to the defocusing case and $\beta\lambda > 0$ to the focusing one. In what follows, we fix $\beta > 0$.

Using the same arguments as in Sect. 6.5, we can show that Eq. (135) is the Hamiltonian differential equation associated to the function H defined by

$$H(u) = \frac{1}{2}\left(\beta \int_0^L |\partial_x u(x)|^2 \,\mathrm{d}x - \frac{\lambda}{2} \int_0^L |u(x)|^4 \,\mathrm{d}x\right). \tag{136}$$

As before the symplectic Banach triple is given by $(E, \mathscr{D}, \mathscr{J})$ with $E = H^1(\mathbb{T}_L, \mathbb{C})$, $\mathscr{D} = H^3(\mathbb{T}_L, \mathbb{C})$, both viewed as real Hilbert spaces, and $\mathscr{J} u = iu$ (see Sect. 6.4 to understand how a complex Hilbert space can be viewed as a real Hilbert space with symplectic structure). We recall that the scalar product on $E = H^1(\mathbb{T}_L, \mathbb{C})$ is

$$(u,v)_E = \mathrm{Re} \int_0^L (\partial_x u(x) \partial_x \bar{v}(x) + u(x)\bar{v}(x)) \,\mathrm{d}x \quad u, v \in E, \tag{137}$$

and the dual space E^* can be identified with $H^{-1}(\mathbb{T}_L, \mathbb{C})$ through the pairing

$$\langle u, v\rangle = \mathrm{Re}\int_0^L u(x)\bar{v}(x)\,\mathrm{d}x, \quad u \in E^*,\ v \in E. \tag{138}$$

Moreover, since the action Φ of the group $G = \mathbb{R}\times\mathbb{R}$ defined by $\Phi_{a,\gamma}(u) = e^{i\gamma}u(x-a)$ is globally Hamiltonian (see Sect. 6.5) and $H\circ\Phi_g = H$ (see Sect. 3.2), the quantities

$$F_1(u) = -\frac{i}{2}\int_0^L \bar{u}(x)\partial_x u(x)\,\mathrm{d}x, \tag{139}$$

$$F_2(u) = -\frac{1}{2}\int_0^L |u(x)|^2\,\mathrm{d}x = -\frac{1}{2}\langle u, u\rangle \tag{140}$$

are constants of the motion.

As pointed out in Sect. 3.2, the two-parameter family of plane waves

$$u_{\alpha,k}(t,x) = \alpha e^{-ikx}e^{i\xi t} \tag{141}$$

with $\xi \in \mathbb{R}$, $k \in \frac{2\pi}{L}\mathbb{Z}$ and $\alpha \in \mathbb{R}$ are G-relative equilibria of (135) whenever ξ, k and α satisfy the dispersion relation

$$\xi + \beta k^2 = \lambda|\alpha|^2. \tag{142}$$

In the notation of the previous sections, $u_{\alpha,k} = u_{\mu_{\alpha,k}}$ with $\mu_{\alpha,k} \in \mathbb{R}^2$ given by

$$\mu_{\alpha,k} = \begin{pmatrix} F_1(u_{\alpha,k}) \\ F_2(u_{\alpha,k}) \end{pmatrix} = -\frac{\alpha^2}{2}L\begin{pmatrix} k \\ 1 \end{pmatrix}.$$

Remark that in this case $\mu_{\alpha,k}$ is not a regular value of $F = (F_1, F_2)$, as is readily checked (see Definition 12).

The G-orbit of the initial condition $u_{\mu_{\alpha,k}}(x) = \alpha e^{-ikx}$ is given by

$$\mathcal{O}_{u_{\mu_{\alpha,k}}} = \left\{\alpha e^{i\gamma}e^{-ik(x-a)}, (a,\gamma) \in G\right\}. \tag{143}$$

Our goal is to investigate the orbital stability of these particular solutions by applying the general arguments presented above. Our main result is the following theorem showing the orbital stability of plane waves in the defocusing case ($\lambda < 0$) as well as in the focusing case provided $0 < 2\lambda|\alpha|^2 < \beta\left(\frac{2\pi}{L}\right)^2$.

Theorem 12 *If $\beta\left(\frac{2\pi}{L}\right)^2 - 2\lambda|\alpha|^2 > 0$, then all $u \in \mathcal{O}_{u_{\mu_{\alpha,k}}}$ are orbitally stable relative equilibria.*

Furthermore, in the case $\beta\left(\frac{2\pi}{L}\right)^2 - 2\lambda|\alpha|^2 < 0$, we can investigate the linear stability of the plane waves and we obtain the following theorem.

Theorem 13 *Let the plane wave $u_{\alpha,k}(t,x) = \alpha e^{i(\xi t - kx)}$ be a solution to (135) and $\beta\left(\frac{2\pi}{L}\right)^2 - 2\lambda|\alpha|^2 < 0$. Then the spectrum of the linearization of (135) around $u_{\alpha,k}$ in $L^2(\mathbb{T}_L)$ has eigenvalues with strictly positive real part. Consequently, this wave is spectrally unstable in $L^2(\mathbb{T}_L)$.*

This second result follows from a rather straightforward computation that we do not reproduce here.

As discussed in the introduction, the nonlinear (in)stability of plane waves for the cubic focusing and defocusing nonlinear Schrödinger equation in a one-dimensional space is a result known to the experts in the field (see the introduction of [40, 41], for example). We did not however find a complete proof of it in the literature, so we furnish one here as an illustration of the general theory presented in the previous sections.

In [106], a related but slightly different analysis is proposed. The cubic nonlinear Schrödinger equation is defined on the entire line $\mathbb{R}$ and not on the one-dimensional torus $\mathbb{T}_L$. Using the Galilean invariance of the equation (see Sect. 3.5), the stability of any plane wave is equivalent to that of $u(t,x) = \alpha e^{i\lambda|\alpha|^2 t}$. The main result on stability of plane waves of [106] is given in Theorem III.3.1. It states that, in the defocusing case ($\lambda < 0$), the plane wave $u(t,x) = \alpha e^{i\lambda|\alpha|^2 t}$ is orbitally stable under small perturbations in $H^1(\mathbb{R})$.

Our approach is different: we focus on the Schrödinger equation on a one-dimensional torus. Our functions live on a torus and the perturbations too. In other words, our definition of stability is with respect to perturbations within $H^1(\mathbb{T}_L) = H^1_{\text{per}}([0,L])$. Moreover in Zhidkov's book nothing is said about the (in)stability of plane waves in the focusing case, a situation we cover partially.

Finally, the analysis of orbital stability of plane waves of the cubic nonlinear Schrödinger equation on a torus of dimension $1 < d \leq 3$ is more involved and it will be done in a forthcoming paper together with the periodic Manakov equation [29].

9.1 Orbital Stability

To study the stability of $u_{\mu_{\alpha,k}}(x)$, it is useful to write the solutions of (135) in the form

$$u(t,x) = e^{-ikx}U(t,x) \tag{144}$$

where $U(t,x)$ is a function which satisfies the evolution equation

$$i\partial_t U + \beta\partial_{xx}^2 U - 2i\beta k\partial_x U + \lambda|U|^2 U - \beta k^2 U = 0. \tag{145}$$

Equation (145) is the Hamiltonian differential equation associated to the function $\tilde{H}$ defined by

$$\tilde{H}(U) = H(U) - 2\beta k F_1(U) - \beta k^2 F_2(U). \tag{146}$$

As before, the action Φ of the group $G = \mathbb{R} \times \mathbb{R}$ defined by $\Phi_{a,\gamma}(u) = e^{i\gamma} u(x-a)$ is globally Hamiltonian, $\tilde{H} \circ \Phi_g = \tilde{H}$ and the quantities F_1, F_2 defined by (139) and (140) are constants of the motion.

If ξ, k and α satisfy the dispersion relation (142), $U_{\mu_\alpha}(t,x) = \alpha e^{i\xi t}$ is a solution to (145). Moreover, $U_{\mu_\alpha}(x) = U_{\mu_\alpha}(0,x) = \alpha$ is a one-parameter family of G-relative equilibria and our goal is to study their stability. Here $\mu_\alpha = -\frac{\alpha^2}{2} L \begin{pmatrix} 0 \\ 1 \end{pmatrix}$ and, as above, μ_α is not a regular value of $F = (F_1, F_2)$.

Recall that the G-orbit of $U_{\mu_\alpha}(x) = \alpha$ is

$$\mathcal{O}_{U_{\mu_\alpha}} = \left\{ e^{i\gamma}\alpha, \gamma \in [0, 2\pi) \right\}. \tag{147}$$

and, by definition, $U \in \mathcal{O}_{U_{\mu_\alpha}}$ is orbitally stable if

$$\forall \epsilon, \exists \delta, \forall W \in E, \ \left(\mathrm{d}(W, U) \leq \delta \Rightarrow \forall t \in \mathbb{R}, \ \mathrm{d}(W(t,\cdot), \mathcal{O}_{U_{\mu_\alpha}}) \leq \epsilon \right)$$

(see Definition 5).

Proposition 6 *Let $\beta \left(\frac{2\pi}{L}\right)^2 - 2\lambda|\alpha|^2 > 0$. Then every $U \in \mathcal{O}_{U_{\mu_\alpha}}$ is orbitally stable.*

Our stability result in Theorem 12 is an immediate consequence of the previous statement since the change of variables $u \to U$ is bounded in E.

Now, to prove this proposition, we would like to apply the general results given in the previous section and more precisely Theorem 8 or Theorem 9. The idea is to construct a Lyapunov function $\mathscr{L}_{\mu_\alpha}$ which is a group invariant constant of the motion and such that $D\mathscr{L}_{\mu_\alpha}$ vanishes on $\mathcal{O}_{U_{\mu_\alpha}}$. Since U_{μ_α} is a G-relative equilibrium, Theorem 7 ensures that it satisfies

$$D_{U_{\mu_\alpha}} \tilde{H} - \tilde{\xi} \cdot D_{U_{\mu_\alpha}} F = 0$$

for some $\tilde{\xi} \in \mathbb{R}^2$. As a consequence, $\tilde{H} - \tilde{\xi} \cdot F$ is a good candidate to be a Lyapunov function. Nevertheless, since $D_{U_{\mu_\alpha}} F_1 = 0$, μ_α is not a regular value of F, and the choice of $\tilde{\xi} \in \mathbb{R}^2$ is not unique. Hence, working in the spirit of Sect. 8.1, we will consider only F_2 as constant of motion and we define

$$\Sigma_\alpha = \left\{ W \in E \mid F_2(W) = -\frac{\alpha^2}{2} L \right\}. \tag{148}$$

With this definition, Σ_α is a co-dimension 1 submanifold of E.

Moreover, we need $\mathscr{L}_{\mu_\alpha}$ to be coercive on $\mathscr{O}_{U_{\mu_\alpha}}$, which means here that there exist $\delta > 0$ and $c > 0$, depending only on β, L, λ and $|\alpha|^2$, such that, for all $W \in E$ [as in (113)] or $W \in \Sigma_\alpha$ [as in (111)],

$$\mathrm{d}(W, \mathscr{O}_{U_{\mu_\alpha}}) \leq \delta \Rightarrow \mathscr{L}_{\mu_\alpha}(W) - \mathscr{L}_{\mu_\alpha}(U_{\mu_\alpha}) \geq c\mathrm{d}(W, \mathscr{O}_{U_{\mu_\alpha}})^2. \tag{149}$$

A convenient choice for $\mathscr{L}_{\mu_\alpha}$ turn out to be

$$\mathscr{L}_{\mu_\alpha}(U) = H(U) - (\xi + \beta k^2)F_2(U), \tag{150}$$

which corresponds to $\tilde{\xi} = \begin{pmatrix} -2\beta k \\ \xi \end{pmatrix}$. By construction, $D_U\mathscr{L}_{\mu_\alpha}$ vanishes for $U \in \mathscr{O}_{U_{\mu_\alpha}}$. Indeed, since $D_U\mathscr{L}_{\mu_\alpha} \in E^*$, $D_U\mathscr{L}_{\mu_\alpha}(V) = \langle D_U\mathscr{L}_{\mu_\alpha}, V\rangle$ with

$$D_U\mathscr{L}_{\mu_\alpha} = -\beta\partial_{xx}^2 U - \lambda|U|^2U + (\xi + \beta k^2)U \in H^{-1}(\mathbb{T}_L, \mathbb{C}), \tag{151}$$

so clearly $D_U\mathscr{L}_{\mu_\alpha} = 0$ if $U \in \mathscr{O}_{U_{\mu_\alpha}}$. Furthermore, the bilinear form $D_U^2\mathscr{L}_{\mu_\alpha} : E \times E \to \mathbb{R}$ is given by $D_U^2\mathscr{L}(V, V) = \langle \nabla^2\mathscr{L}_{\mu_\alpha}(U)V, V\rangle$ with

$$\nabla^2\mathscr{L}_{\mu_\alpha}(U)V = -\beta\partial_{xx}^2 V - \lambda|U|^2V - \lambda(|U|^2V + \bar{V}U^2) + (\xi + \beta k^2)V \in H^{-1}(\mathbb{T}_L; \mathbb{C}); \tag{152}$$

in particular, for all $U \in E$, $\nabla^2\mathscr{L}_{\mu_\alpha}(U)$ is a bounded linear operator from E to E^* and the expression above makes sense.

Now to prove (149), the main ingredient is the property:

$$\exists c > 0, \forall V \in \left(T_{U_{\mu_\alpha}}\mathscr{O}_{U_{\mu_\alpha}}\right)^\perp,\ D_{U_{\mu_\alpha}}^2\mathscr{L}_{\mu_\alpha}(V, V) \geq c\|V\|^2,$$

or

$$\exists c > 0, \forall V \in T_{U_{\mu_\alpha}}\Sigma_\alpha \cap \left(T_{U_{\mu_\alpha}}\mathscr{O}_{U_{\mu_\alpha}}\right)^\perp,\ D_{U_{\mu_\alpha}}^2\mathscr{L}_{\mu_\alpha}(V, V) \geq c\|V\|^2,$$

where

$$T_{U_{\mu_\alpha}}\Sigma_\alpha = \{W \in E, \langle \alpha, W\rangle = 0\},$$
$$\left(T_{U_{\mu_\alpha}}\mathscr{O}_{U_{\mu_\alpha}}\right)^\perp = \{W \in E, \langle i, W\rangle = 0\}.$$

This is proven in the following proposition, from which coercivity is deduced in Proposition 8.

Proposition 7 *Let* $\beta\left(\frac{2\pi}{L}\right)^2 - 2\lambda\alpha^2 > 0$ *and* $\alpha \neq 0$.

(a) If $\lambda < 0$ *then*

$$D_{U_{\mu_\alpha}}^2\mathscr{L}_{\mu_\alpha}(V, V) = \langle \nabla^2\mathscr{L}_{\mu_\alpha}(U_{\mu_\alpha})V, V\rangle \geq c_\lambda\|V\|^2 \tag{153}$$

for all $V \in \left(T_{U_{\mu_\alpha}} \mathscr{O}_{U_{\mu_\alpha}}\right)^\perp$ *and* $c_\lambda = \min\left\{ \frac{\beta\left(\frac{2\pi}{L}\right)^2}{1+\left(\frac{2\pi}{L}\right)^2}, -2\lambda\alpha^2 \right\}$.

(b) If $0 < 2\lambda\alpha^2 < \beta\left(\frac{2\pi}{L}\right)^2$ *then,*

$$D^2_{U_{\mu_\alpha}} \mathscr{L}_{\mu_\alpha}(V,V) = \langle \nabla^2 \mathscr{L}_{\mu_\alpha}(U_{\mu_\alpha})V, V\rangle \geq c_\lambda \|V\|^2 \tag{154}$$

for all $V \in T_{U_{\mu_\alpha}} \Sigma_\alpha \cap \left(T_{U_{\mu_\alpha}} \mathscr{O}_{U_{\mu_\alpha}}\right)^\perp$ *and* $c_\lambda = \frac{\beta\left(\frac{2\pi}{L}\right)^2 - 2\lambda\alpha^2}{1+\left(\frac{2\pi}{L}\right)^2}$.

Proof Let $V = v_1 + iv_2 = (v_1, v_2) \in E$. A straightforward calculation gives

$$\begin{aligned} D^2_{U_{\mu_\alpha}} \mathscr{L}_{\mu_\alpha}(V,V) &= \mathrm{Re} \int_0^L \left(-\beta\partial_{xx}^2 V - \lambda\alpha^2(V+\bar{V})\right)\bar{V} \\ &= \int_0^L \beta(|\nabla v_1|^2 + |\nabla v_2|^2) - 2\lambda\alpha^2 |v_1|^2. \end{aligned}$$

Now, since v_1 and v_2 are real functions on the torus, we can write them in Fourier representation, namely,

$$\begin{aligned} v_1(x) &= \frac{a_0(v_1)}{2} + \sum_{n=1}^\infty a_n(v_1)\cos\left(\frac{2\pi}{L}nx\right) + b_n(v_1)\sin\left(\frac{2\pi}{L}nx\right), \\ v_2(x) &= \frac{a_0(v_2)}{2} + \sum_{n=1}^\infty a_n(v_2)\cos\left(\frac{2\pi}{L}nx\right) + b_n(v_2)\sin\left(\frac{2\pi}{L}nx\right), \end{aligned}$$

and recall that

$$\begin{aligned} \|V\|^2 = \frac{L}{2}&\left(\frac{a_0^2(v_1)}{2} + \sum_{n=1}^\infty \left(\left(\frac{2\pi}{L}n\right)^2 + 1\right)(a_n^2(v_1) + b_n^2(v_1))\right) \\ &+ \frac{L}{2}\left(\frac{a_0^2(v_2)}{2} + \sum_{n=1}^\infty \left(\left(\frac{2\pi}{L}n\right)^2 + 1\right)(a_n^2(v_2) + b_n^2(v_2))\right). \end{aligned}$$

Next,

$$\begin{aligned} D^2_{U_{\mu_\alpha}} \mathscr{L}_{\mu_\alpha}(V,V) = \frac{L}{2}&\left(-2\lambda\alpha^2\frac{a_0^2(v_1)}{2} + \sum_{n=1}^\infty \left(\beta\left(\frac{2\pi}{L}n\right)^2 - 2\lambda\alpha^2\right)(a_n^2(v_1) + b_n^2(v_1))\right) \\ &+ \frac{L}{2}\left(\sum_{n=1}^\infty \beta\left(\frac{2\pi}{L}n\right)^2 (a_n^2(v_2) + b_n^2(v_2))\right). \end{aligned}$$

(a) If $\lambda < 0$, it is clear that $D^2_{U_{\mu_\alpha}} \mathscr{L}_{\mu_\alpha}(V,V) \geq 0$ for all $V \in E$. Moreover, if $V \in \left(T_{U_{\mu_\alpha}} \mathscr{O}_{U_{\mu_\alpha}}\right)^\perp$, then $\langle i, V\rangle = 0$, that is $a_0(v_2) = 0$. Hence, the coercivity property of $D^2_{U_{\mu_\alpha}} \mathscr{L}_{\mu_\alpha}(\cdot,\cdot)$ on $\left(T_{U_{\mu_\alpha}} \mathscr{O}_{U_{\mu_\alpha}}\right)^\perp$ follows easily.

(b) Now, let $0 < 2\lambda\alpha^2 < \beta\left(\frac{2\pi}{L}\right)^2$ and $V \in T_{U_{\mu_\alpha}} \Sigma_\alpha \cap \left(T_{U_{\mu_\alpha}} \mathscr{O}_{U_{\mu_\alpha}}\right)^\perp$. As a consequence, $\langle i, V\rangle = 0 = \langle \alpha, V\rangle$ which implies $a_0(v_1) = 0 = a_0(v_2)$. As before, the coercivity property of $D^2_{U_{\mu_\alpha}} \mathscr{L}_{\mu_\alpha}(\cdot,\cdot)$ on $T_{U_{\mu_\alpha}} \Sigma_\alpha \cap \left(T_{U_{\mu_\alpha}} \mathscr{O}_{U_{\mu_\alpha}}\right)^\perp$ follows.

The following lemma gives a representation of the elements of E which are close to the G-orbit $\mathscr{O}_{U_{\mu_\alpha}}$. It is used in the proof of Proposition 8 and is a special case of Lemma 6. We give a direct proof in the current simple setting.

Lemma 8 *There exists $\delta > 0$ such that any $W \in E$ with $\mathrm{d}(W, \mathscr{O}_{U_{\mu_\alpha}}) \leq \delta$ can be represented as*

$$e^{i\gamma} W = U_{\mu_\alpha} + V \tag{155}$$

with $\gamma = \gamma(W) \in [0, 2\pi)$ and $V \in \left(T_{U_{\mu_\alpha}} \mathscr{O}_{U_{\mu_\alpha}}\right)^\perp$. Moreover, there exists a positive constant C such that

$$\mathrm{d}(W, \mathscr{O}_{U_{\mu_\alpha}}) \leq \|V\| \leq C\mathrm{d}(W, \mathscr{O}_{U_{\mu_\alpha}}). \tag{156}$$

Proof Let $W \in E$ such that $\mathrm{d}(W, \mathscr{O}_{U_{\mu_\alpha}}) < \delta$ with $\delta > 0$ sufficiently small. Hence there exists $\tilde{\gamma}$, which depends on W, such that

$$\|e^{i\tilde{\gamma}} W - \alpha\| \leq 2 \inf_{\lambda \in [0,2\pi)} \|W - e^{i\lambda}\alpha\| \leq 2\delta$$

Next, consider the functional

$$\begin{aligned} &\mathscr{F} : E \times \mathbb{R} \to \mathbb{R} \\ &(v, \phi) \to \langle e^{i\phi} v, i\rangle = -\mathrm{Re} \int_0^L i e^{i\phi} v(x)\, \mathrm{d}x. \end{aligned}$$

Since $\mathscr{F}(\alpha, 0) = 0$ and $\partial_\phi \mathscr{F}(\alpha, 0) = \alpha L \neq 0$, by means of the implicit function theorem, we can conclude that there exists $\Lambda : \mathscr{V} \to (-\varepsilon, \varepsilon)$ with $\mathscr{V}$ a neighbourhood of α in E and $\varepsilon > 0$ sufficiently small, such that if $v \in \mathscr{V}$ then there exists a unique $\phi = \Lambda(v) \in (-\varepsilon, \varepsilon)$ for which we have $\langle e^{i\phi} v, i\rangle = 0$.

As a consequence, since $\|e^{i\tilde{\gamma}} W - \alpha\| < 2\delta$, if we choose $\delta > 0$ sufficiently small then there exists $\phi \in \mathbb{R}$ such that $\langle e^{i(\phi+\tilde{\gamma})} W, i\rangle = 0$. By taking $\gamma = \tilde{\gamma} + \phi$ modulo 2π, we obtain (155). Indeed, $E = T_{U_{\mu_\alpha}} \mathscr{O}_{U_{\mu_\alpha}} \oplus \left(T_{U_{\mu_\alpha}} \mathscr{O}_{U_{\mu_\alpha}}\right)^\perp$ and $T_{U_{\mu_\alpha}} \mathscr{O}_{U_{\mu_\alpha}} = \mathrm{span}_{\mathbb{R}} \{i\}$. Hence,

$$e^{i\gamma} W - \alpha = ai + V$$

with $a \in \mathbb{R}$ and $V \in \left(T_{U_{\mu_\alpha}} \mathscr{O}_{U_{\mu_\alpha}}\right)^\perp$. As a consequence,

$$0 = \langle e^{i\gamma} W - \alpha, i\rangle = a\langle i, i\rangle$$

and a has to be equal to 0.

Estimate (156) follows directly from the definition of V.

Finally, the following proposition, in the same spirit of Proposition 5, proves the coercivity of $\mathscr{L}_{\mu_\alpha}$ on $\mathscr{O}_{U_\alpha}$.

Proposition 8 *Let $\beta\left(\frac{2\pi}{L}\right)^2 - 2\lambda|\alpha|^2 > 0$, $\alpha \neq 0$ and $\mathscr{L}_{\mu_\alpha}$ be defined as in (150).*

(a) If $\lambda < 0$, let $c_\lambda = \min\left\{\frac{\beta\left(\frac{2\pi}{L}\right)^2}{1+\left(\frac{2\pi}{L}\right)^2}, -2\lambda\alpha^2\right\}$. Then there exists $\delta > 0$ such that

$$\mathscr{L}_{\mu_\alpha}(W) - \mathscr{L}_{\mu_\alpha}(U_{\mu_\alpha}) \geq \frac{c_\lambda}{4} \mathrm{d}(W, \mathscr{O}_{U_{\mu_\alpha}})^2 \tag{157}$$

for all $W \in E$, such that $\mathrm{d}(W, \mathscr{O}_{U_{\mu_\alpha}}) \leq \delta$.

(b) If $0 < 2\lambda\alpha^2 < \beta\left(\frac{2\pi}{L}\right)^2$, let $c_\lambda = \frac{\beta\left(\frac{2\pi}{L}\right)^2 - 2\lambda\alpha^2}{1+\left(\frac{2\pi}{L}\right)^2}$. Then there exists $\delta > 0$ such that

$$\mathscr{L}_{\mu_\alpha}(W) - \mathscr{L}_{\mu_\alpha}(U_{\mu_\alpha}) \geq \frac{c_\lambda}{16} \mathrm{d}(W, \mathscr{O}_{U_{\mu_\alpha}})^2 \tag{158}$$

for all $W \in \Sigma_\alpha$, such that $\mathrm{d}(W, \mathscr{O}_{U_{\mu_\alpha}}) \leq \delta$.

Proof Let $W \in E$ such that $\mathrm{d}(W, \mathscr{O}_{U_{\mu_\alpha}}) \leq \delta$ with $\delta > 0$ sufficiently small. By Lemma 8, there exists $\gamma \in [0, 2\pi]$ such that $e^{i\gamma} W - U_{\mu_\alpha} = V$ with $V \in \left(T_{U_{\mu_\alpha}} \mathscr{O}_{U_{\mu_\alpha}}\right)^\perp$ and $\|V\| \leq C\mathrm{d}(W, \mathscr{O}_{U_{\mu_\alpha}})$. As a consequence, since $D_{U_{\mu_\alpha}} \mathscr{L}_{\mu_\alpha} = 0$,

$$\begin{aligned}
\mathscr{L}_{\mu_\alpha}(W) - \mathscr{L}_{\mu_\alpha}(U_{\mu_\alpha}) &= \mathscr{L}_{\mu_\alpha}(e^{i\gamma} W) - \mathscr{L}_{\mu_\alpha}(U_{\mu_\alpha}) \\
&= \frac{1}{2} D^2_{U_{\mu_\alpha}} \mathscr{L}_{\mu_\alpha}(e^{i\gamma} W - U_{\mu_\alpha}, e^{i\gamma} W - U_{\mu_\alpha}) + \mathrm{o}(\|e^{i\gamma} W - U_{\mu_\alpha}\|^2) \\
&= \frac{1}{2} D^2_{U_{\mu_\alpha}} \mathscr{L}_{\mu_\alpha}(V, V) + \mathrm{o}(\|V\|^2).
\end{aligned}$$

If $\lambda < 0$, we can apply (153), and for all $W \in E$ with $\mathrm{d}(W, \mathscr{O}_{U_{\mu_\alpha}})$ small, we obtain

$$\mathscr{L}_{\mu_\alpha}(W) - \mathscr{L}_{\mu_\alpha}(U_{\mu_\alpha}) \geq \frac{c_\lambda}{4} \mathrm{d}(W, \mathscr{O}_{U_{\mu_\alpha}})^2.$$

If $0 < 2\lambda\alpha^2 < \beta\left(\frac{2\pi}{L}\right)^2$, we proceed as follows. Let $W \in \Sigma_\alpha$ such that $\mathrm{d}(W, \mathscr{O}_{U_{\mu_\alpha}}) \leq \delta$ with $\delta > 0$ sufficiently small. As before, thanks to Lemma 8, there exists $\gamma \in [0, 2\pi]$ such that $e^{i\gamma} W - U_{\mu_\alpha} = V$ with $V \in \left(T_{U_{\mu_\alpha}} \mathscr{O}_{U_{\mu_\alpha}}\right)^\perp$

and $\|V\| \leq C\mathrm{d}(W, \mathscr{O}_{U_{\mu_\alpha}})$. Next, it is clear that $E = T_{U_{\mu_\alpha}}\Sigma_\alpha \oplus \mathrm{span}\{U_{\mu_\alpha}\}$. Hence, $V = V_1 + V_2$ with $V_1 \in T_{U_{\mu_\alpha}}\Sigma_\alpha \cap \left(T_{U_{\mu_\alpha}}\mathscr{O}_{U_{\mu_\alpha}}\right)^\perp$ and $V_2 \in \mathrm{span}\{U_{\mu_\alpha}\} \cap \left(T_{U_{\mu_\alpha}}\mathscr{O}_{U_{\mu_\alpha}}\right)^\perp$. Moreover, using the same arguments as in Lemma 10, for $\|V\|$ small enough, one has

$$\|V_2\| \leq \frac{1}{2\sqrt{\alpha^2 L}}\|V\|^2 \text{ and } \|V_1\| \geq \frac{1}{2}\|V\|.$$

As a consequence,

$$\begin{aligned}\mathscr{L}_{\mu_\alpha}(W) - \mathscr{L}_{\mu_\alpha}(U_{\mu_\alpha}) &= \frac{1}{2}D^2_{U_{\mu_\alpha}}\mathscr{L}_{\mu_\alpha}(V,V) + \mathrm{o}(\|V\|^2)\\ &= \frac{1}{2}D^2_{U_{\mu_\alpha}}\mathscr{L}_{\mu_\alpha}(V_1,V_1) + \mathrm{o}(\|V\|^2)\\ &\geq \frac{c_\lambda}{2}\|V_1\|^2 + \mathrm{o}(\|V\|^2) \geq \frac{c_\lambda}{8}\|V\|^2 + \mathrm{o}(\|V\|^2).\end{aligned}$$

Finally, if $0 < 2\lambda\alpha^2 < \beta\left(\frac{2\pi}{L}\right)^2$, and for all $W \in \Sigma_\alpha$ with $\mathrm{d}(W, \mathscr{O}_{U_{\mu_\alpha}})$ small, we obtain

$$\mathscr{L}_{\mu_\alpha}(W) - \mathscr{L}_{\mu_\alpha}(\alpha) \geq \frac{c_\lambda}{16}\mathrm{d}(W, \mathscr{O}_{U_{\mu_\alpha}})^2.$$

Now, whenever $\lambda|\alpha|^2 < 0$, a straightforward application of the proof of Theorem 8 with $\mathscr{L}_{\mu_\alpha}$ as Lyapunov function allows us to conclude that $\mathscr{O}_{U_{\mu_\alpha}}$ is orbitally stable under small perturbations in E.

To conclude in the case $0 < 2\lambda\alpha^2 < \beta\left(\frac{2\pi}{L}\right)^2$, we can apply Theorem 9. Indeed, Hypotheses A and Bμ_α (Sect. 8.1) are fulfilled and the function F_2 satisfies Hypothesis F thanks to Lemma 5.

10 Orbital Stability for Inhomogeneous NLS

This section is concerned with an NLS equation of the form

$$i\partial_t u + \Delta u + f(x, |u|^2)u = 0, \quad u = u(t,x) : \mathbb{R}\times\mathbb{R}^d \to \mathbb{C}. \tag{159}$$

We consider standing wave solutions $u(t,x) = e^{i\xi t}w(x)$, where $w : \mathbb{R}^d \to \mathbb{R}$ is localized[17]—typically $w \in H^1(\mathbb{R}^d)$ and $w(x) \to 0$ exponentially as $|x| \to \infty$. Such a solution exists if and only if

$$\Delta w - \xi w + f(x, w^2)w = 0, \tag{160}$$

[17]Note that we focus here on situations where the wave profile $w(x)$ is real-valued.

which is precisely the "stationary equation" (108). Note that the notation for the nonlinearity in (159) is slightly different than in Sect. 3.2, and automatically ensures that (32) holds, for all $u \in \mathbb{C} \setminus \{0\}$.

The existence of solutions of (160) can be obtained under various hypotheses on f, the easiest case being the pure power nonlinearity, $f(x, w^2) = |w|^{\sigma-1}$, $\sigma > 1$. Note that, unlike in the case of periodic boundary conditions studied in the previous section, it is crucial here that the nonlinearity be focusing for standing waves to exist. The stationary equation (160) has no solutions if, for instance, $f(x, w^2) = -|w|^{\sigma-1}$. In the sequel, we will indeed suppose that the nonlinearity is focusing, which in the context of (159) means that $f(x, s)$ is positive and increasing in $s > 0$.

The purpose of this section is to further illustrate the general stability theory developed in Sect. 8. Orbital stability results for standing waves of (159) have been obtained in [44, 45, 48, 49] and will be summarized here. The stability analysis in these papers benefits from having solution curves $\xi \to w_\xi$. In the setting of Sect. 8, they can be seen as an application of Theorem 10. The approach used in [44, 45, 48, 49] was to apply the celebrated Theorem 2 of Grillakis, Shatah, Strauss [53]. This result essentially relies on the set of spectral conditions (S1)–(S3), formulated below in the context of (159), together with a convexity condition, which here takes the form (172). In the framework developed in these notes, the role of Theorem 2 of [53] can be interpreted as follows. It will be shown in Proposition 9 that the conditions (S1)–(S3) and (172) ensure that the coercivity property (126) required by Proposition 5 is satisfied at the relative equilibrium w_ξ. Theorem 10 can then be applied. As already mentioned in the introduction to Sect. 8, and explained in more detail after the proof of Proposition 9, the relative equilibria of (159) can be parametrized equivalently by the parameter ξ appearing in (160), or by the corresponding value $\mu = \frac{1}{2}\|w_\xi\|_{L^2}^2$ of the constant of the motion. It turns out that using ξ is more convenient here. Note that, since this constant of the motion satisfies Hypothesis F, one could also apply Theorem 9 instead of Theorem 10.

The notion of orbital stability we shall be concerned with here is that corresponding to the group action (102) of Sect. 6.5. Note however that the explicit spatial dependence in (159) breaks the invariance under translations, and one rather needs to consider the restricted action Φ_γ on the phase space $E = H^1(\mathbb{R}^d, \mathbb{C})$,

$$\Phi_\gamma(u) = e^{i\gamma}u(x), \quad u \in E, \ \gamma \in \mathbb{R}. \tag{161}$$

The standing waves corresponding to solutions w_ξ of the stationary equation (160) are then relative equilibria for the dynamics of (159), with respect to the action Φ_γ.

Remark 9 If f does not depend on x then the full group action (102) is to be considered, and the standing waves of (159) are in general not orbitally stable in the sense of (161). Orbital stability in the sense of the full group action (102) was proved by Cazenave and Lions [18] by variational arguments.

We will only consider here situations where the coefficient f explicitly depends on the space variable $x \in \mathbb{R}^d$—(159) is then often referred to as an *inhomogeneous NLS*—and decays as $|x| \to \infty$, in a sense that will be made more precise below.

We shall also suppose that $f(x, w^2) \sim V(x)|w|^{\sigma-1}$ as $w \to 0$. Conditions relating the function V and the power $\sigma > 1$ will be given for stability of standing waves to hold. In particular our assumptions will imply $\sigma < 1 + \frac{4}{d-2}$, so that local existence in $H^1(\mathbb{R}^d)$ for the Cauchy problem associated with (159) is ensured by the results of Sect. 3.2. Two cases will be considered:

(PT) the power-type nonlinearity $f(x, w^2) = V(x)|w|^{\sigma-1}$;
(AL) the asymptotically linear case $f(x, w^2) \to V(x)$ as $|w| \to \infty$

[e.g. with $f(x, w^2) = V(x)\frac{|w|^{\sigma-1}}{1+|w|^{\sigma-1}}$].

We will give a short account of the main arguments used in [44, 45, 48, 49] to establish the stability of standing waves along a global solution curve. We will also briefly sketch the bifurcation analysis yielding a smooth branch of non-trivial solutions of (160) emerging from the trivial solution $w = 0$. This part of the argument is crucial since, in the approach originally developed in [49], the spectral properties and the condition (172) required to obtain the coercivity of an appropriate Lyapunov functional are derived by continuation from the limit $w_\xi \to 0$. It is worth emphasizing here that the verification of these hypotheses is precisely that part of the stability analysis which strongly relies on the model considered. Once the required coercivity properties are established, the orbital stability can be deduced from the abstract results of Sect. 8.

10.1 Hamiltonian Setting

Similarly to Sect. 9, we work here with

$$E = H^1(\mathbb{R}^d, \mathbb{C}), \quad (u, v)_E = \mathrm{Re} \int_{\mathbb{R}^d} \nabla u(x) \cdot \nabla \bar{v}(x) + u(x)\bar{v}(x)\, \mathrm{d}x.$$

The Hamiltonian and the charge are respectively defined by $H, Q : E \to \mathbb{R}$,

$$H(u) = \frac{1}{2}\int_{\mathbb{R}^d} |\nabla u|^2\, \mathrm{d}x - \frac{1}{2}\int_{\mathbb{R}^d}\int_0^{|u|^2} f(x, s)\, \mathrm{d}s\, \mathrm{d}x, \quad Q(u) = \frac{1}{2}\int_{\mathbb{R}^d} |u|^2\, \mathrm{d}x, \quad u \in E. \tag{162}$$

In the notation of Sect. 6.5, $Q(u) \equiv -F_{d+1}(u)$, but we will keep the customary notation Q here. Under our assumptions, $H, Q \in C^2(E, \mathbb{R})$.

Now (159) can precisely be written in the form

$$\mathscr{J}\dot{u}_t = D_{u_t} H \tag{163}$$

considered in Sect. 6, with $E = H^1(\mathbb{R}^d, \mathbb{C}) \simeq H^1(\mathbb{R}^d, \mathbb{R}) \times H^1(\mathbb{R}^d, \mathbb{R})$ and

$$\mathscr{J} = \begin{pmatrix} 0 & -I \\ I & 0 \end{pmatrix}$$

with $I : H^1 \hookrightarrow H^{-1}$ the (dense) injection. That is, $\mathscr{J}(q,p) = (-p,q) \in E^*$, for all $(q,p) \in E$, as in Sect. 6.5. Note that we use the identification

$$H^1(\mathbb{R}^d,\mathbb{R}) \subset L^2(\mathbb{R}^d,\mathbb{R}) = L^2(\mathbb{R}^d,\mathbb{R})^* \subset H^{-1}(\mathbb{R}^d,\mathbb{R}).$$

In this setting a solution of (159) is a function $u \in C^1((-T_{\min},T_{\max}),E)$, for some $T_{\min},T_{\max} > 0$ [depending on $u(0)$], satisfying (163) for all $t \in (-T_{\min},T_{\max})$. Standing waves are particular solutions of the form $u(t) = \Phi_{(\xi t)}w$, $w \in E$, and the stationary equation (160) now reads

$$D_w H + \xi D_w Q = 0. \tag{164}$$

Hence, the discussion in Sects. 7 and 8 indicates that

$$\mathscr{L}_\xi = H + \xi Q \tag{165}$$

is the natural candidate for the Lyapunov function. Furthermore, the invariance of H and Q under the action of Φ_γ implies that

$$D_{\Phi_\gamma(w)}H + \xi D_{\Phi_\gamma(w)}Q = 0, \quad \gamma \in \mathbb{R}. \tag{166}$$

Finally, note that the isometric action (161) can equivalently be expressed as

$$\Phi_\gamma \begin{pmatrix} \operatorname{Re} u \\ \operatorname{Im} u \end{pmatrix} = \begin{pmatrix} \cos\gamma & -\sin\gamma \\ \sin\gamma & \cos\gamma \end{pmatrix} \begin{pmatrix} \operatorname{Re} u \\ \operatorname{Im} u \end{pmatrix}, \quad u \in E,\ \gamma \in \mathbb{R}.$$

10.2 Bifurcation Results

In this section we present bifurcation results ensuring the existence of smooth curves of solutions of (160). From a bifurcation-theoretic viewpoint the peculiarity of these results is that, in both the (PT) and (AL) cases, bifurcation occurs from the essential spectrum of the linearization of (160), namely

$$\Delta w = \xi w,$$

this linear problem set on $\mathbb{R}^d$ having no eigenvalues.

We start with the power-type case (PT), that is, we first consider the problem

$$\Delta w(x) + V(x)|w(x)|^{\sigma-1}w(x) = \xi w(x), \quad w \in H^1(\mathbb{R}^d,\mathbb{R}), \tag{167}$$

where $d \geq 1$ and $V : \mathbb{R}^d \to \mathbb{R}$ satisfies:

(V1) $V \in C^1(\mathbb{R}^d)$;

(V2) there exists $b \in (0,2)$ [$b \in (0,1)$ if $d = 1$] such that

$$1 < \sigma < \tfrac{4-2b}{d-2} \quad \text{if } d \geq 3, \quad 1 < \sigma < \infty \quad \text{for } d = 1,2,$$
$$\lim_{|x|\to\infty} |x|^b V(x) = 1 \quad \text{and} \quad \lim_{|x|\to\infty} |x|^b [x \cdot \nabla V(x) + bV(x)] = 0;$$

(V3) V is radial with $V(r) > 0$ and $V'(r) < 0$ for $r > 0$;

(V4) $r\dfrac{V'(r)}{V(r)}$ is decreasing in $r > 0$ [and so $\to -b$ by (V2)].

Note that $V(x) = (1 + |x|^2)^{-b/2}$ satisfies all of the above assumptions.

Theorem 14 *Suppose that the hypotheses (V1) to (V4) hold. Then there exists a curve $w \in C^1\big((0,\infty), H^1(\mathbb{R}^d)\big)$ such that, for all $\xi \in (0,\infty)$, $w_\xi \equiv w(\xi)$ is the unique positive radial solution of (167), $w_\xi \in C^2(\mathbb{R}^d) \cap L^\infty(\mathbb{R}^d)$, and w_ξ is strictly radially decreasing, with $w_\xi(x), |\nabla w_\xi(x)| \to 0$ exponentially as $|x| \to \infty$. Furthermore, the asymptotic behaviour of the curve reads*

$$\lim_{\xi\to 0} \|w_\xi\|_{H^1} = \begin{cases} 0 & \text{if} \quad 1 < \sigma < 1 + \frac{4-2b}{d}, \\ \infty & \text{if} \quad 1 + \frac{4-2b}{d} < \sigma < 1 + \frac{4-2b}{d-2}, \end{cases}$$

and

$$\lim_{\xi\to\infty} \|w_\xi\|_{H^1} = \infty \quad \text{for all} \quad 1 < \sigma < 1 + \tfrac{4-2b}{d-2}.$$

This theorem has been proved in [46] by a combination of variational and analytical arguments. It provides a global continuation, in the radial case, of the local curve of solutions of (167) obtained in [49] [parametrized by $\xi \in (0, \xi_0)$, with $\xi_0 > 0$ small] under the much weaker assumptions (V1) and (V2). Note in particular that (V2) only requires the problem to be focusing at infinity, no further sign restrictions being imposed on V. The orbital stability of the solutions w_ξ, $\xi \in (0, \xi_0)$, is also discussed in [49], and it is found that they are stable provided

$$1 < \sigma < 1 + \tfrac{4-2b}{d}, \tag{168}$$

and unstable if $1 + \frac{4-2b}{d} < \sigma < 1 + \frac{4-2b}{d-2}$.

Remark 10 In fact, more information about the asymptotic behaviour as $\xi \to 0$ is obtained in [49]. In particular,

$$\lim_{\xi\to 0} \|w_\xi\|_{L^2} = \begin{cases} 0 & \text{if} \quad 1 < \sigma < 1 + \frac{4-2b}{d}, \\ \infty & \text{if} \quad 1 + \frac{4-2b}{d} < \sigma < 1 + \frac{4-2b}{d-2}, \end{cases}$$

whereas

$$\lim_{\xi\to 0} \|\nabla w_\xi\|_{L^2} = 0 \quad \text{for all } 1 < \sigma < 1 + \tfrac{4-2b}{d-2}.$$

We now state a global bifurcation result similar to Theorem 14, for (160) in dimension $d = 1$, in the asymptotically linear case (AL). That is, we consider

$$w''(x) + f(x, w(x)^2)w(x) = \xi w(x), \quad w \in H^1(\mathbb{R}, \mathbb{R}), \tag{169}$$

where, to fix the ideas,[18] we let

$$f(x, w^2) = V(x)\frac{|w|^{\sigma-1}}{1 + |w|^{\sigma-1}}. \tag{170}$$

In the asymptotically linear case, one cannot expect to find positive solutions of (169)–(170) for large values of $\xi > 0$. Heuristically, letting $u \to \infty$ in (169)–(170) leads to the so-called asymptotic linearization

$$w''(x) + V(x)w(x) = \xi w(x), \tag{171}$$

having a ray of positive eigenfunctions $\{\mu w_\infty : \mu > 0\}$ corresponding to a principal eigenvalue $\xi_\infty > 0$. This has been put on rigorous grounds in [47], where it is shown that positive even solutions of (169)–(170) only exist for $\xi < \xi_\infty$, and satisfy $\|w_\xi\|_{H^1} \to \infty$ as $\xi \to \xi_\infty$.

Theorem 15 *Suppose (V1) to (V3) and $1 < \sigma < 5 - 2b$. Then there exists a curve $w \in C^1\big((0, \xi_\infty), H^1(\mathbb{R})\big)$ such that, for all $\xi \in (0, \xi_\infty)$, w_ξ is the unique positive even solution of (169)–(170), $w_\xi \in C^2(\mathbb{R}) \cap H^2(\mathbb{R})$ with $w_\xi'(x) < 0$ for $x > 0$, and $w_\xi(x), w_\xi(x)' \to 0$ exponentially as $|x| \to \infty$. Furthermore, there holds*

$$\lim_{\xi\to 0} \|w_\xi\|_{H^1(\mathbb{R})} = 0 \quad \textit{and} \quad \lim_{\xi\to\xi_\infty} \|w_\xi\|_{H^1(\mathbb{R})} = \infty.$$

Remark 11 The reader might wonder why (V4) is not needed for Theorem 15. It turns out that this assumption is essential in the proof of Theorem 14, where it ensures uniqueness of positive radial solutions of (167), for any fixed $\xi > 0$. In the one-dimensional problem (169)–(170), uniqueness can be proved without invoking (V4).[19] However, we will see in the next section that this hypothesis is crucial to the stability analysis, in both the (PT) and (AL) cases.

[18] More general assumptions on the coefficient f in (AL) can be given, under which the bifurcation and stability results presented here still hold, see [48].

[19] Note that the main reason for restricting the discussion to $d = 1$ in Theorem 15 is the lack of uniqueness results in higher dimensions for the (AL) case.

Remark 12 Thanks to the form of the nonlinearity in (170) the global branch of Theorem 15, bifurcating from the trivial solution $u = 0$ at $\xi = 0$, is obtained by perturbation from the (PT) nonlinearity dealt with in Theorem 14. In fact, the case where asymptotic bifurcation occurs at $\xi = 0$, corresponding in dimension $d = 1$ to $5 - 2b < \sigma < \infty$, could also be extended to the (AL) case, where instability could be inferred, in the limit $\xi \to 0$. We refrain from going in this direction here since we were only able so far to extend the discussion to a global branch in the stable case. We shall therefore assume (168) from now on, both for (PT) and (AL).

10.3 Stability

In dimension $d = 1$, assuming that $1 < \sigma < 5 - 2b$, the global curves of standing wave solutions given by Theorems 14 and 15 are stable. This has been proved in [45] for the (PT) case and in [48] for the (AL) case. The proofs rely on the theory of orbital stability in [53] and we will now outline the main arguments.

We shall start by convincing the reader that, in the context of (159), one cannot hope for stability in the usual sense (1). Indeed, suppose $\xi_n \to \xi$ and consider

$$u_\xi(t,x) = e^{i\xi t} w_\xi(x) \quad \text{and} \quad u_n(t,x) = e^{i\xi_n t} w_{\xi_n}(x).$$

Then

$$\forall \delta > 0 \; \exists N_\delta \in \mathbb{N}, \; n \geq N_\delta \Rightarrow \|u_n(0,\cdot) - u_\xi(0,\cdot)\|_{H^1} = \|w_{\xi_n} - w_\xi\|_{H^1} \leq \delta.$$

However,

$$\begin{aligned} \|u_n(t,\cdot) - u_\xi(t,\cdot)\|_{H^1} &\geq \left| |e^{i\xi t} - e^{i\xi_n t}| \|w_\xi\|_{H^1} - \|w_{\xi_n} - w_\xi\|_{H^1} \right| \\ \Rightarrow \sup_{t \geq 0} \|u_n(t) - u_\xi(t)\|_{H^1} &\geq 2\|w_\xi\|_{H^1} - \delta, \; n \geq N_\delta. \end{aligned}$$

Therefore, for n large enough, the initial datum $u_n(0)$ may be chosen δ-close to $u_\xi(0)$, $u_n(t)$ will nevertheless drift at least $2\|w_\xi\|_{H^1} - \delta$ far away from $u_\xi(t)$.

Theorem 16 *Suppose that $d = 1$ and the hypotheses (V1)–(V4) are satisfied. Then the standing waves $u_\xi(t,x) = e^{i\xi t} w_\xi(x)$ of (159) given by either Theorem 14 or Theorem 15 are orbitally stable.*

The proofs of Theorem 16 given in [45, 48] used Theorem 2 of [53], and so relied upon verifying Assumptions 1–3 of [53], as well as the condition

$$\|w_\xi\|_{L^2} \text{ is strictly increasing in } \xi > 0. \tag{172}$$

The latter is often referred to as *the slope condition* or the *Vakhitov-Kolokolov condition*. It seems to have indeed first appeared in the paper [103] of Vakhitov and Kolokolov (1968), in the context of nonlinear optical waveguides.[20]

Assumption 1 of [53] is about the well-posedness of the Cauchy problem for (159) which, under our hypotheses, follows from Sect. 3.2. Assumption 2 pertains to the existence of smooth solution curves and is ensured by Theorem 14/15. It is this property which allows us to apply Theorem 10 of Sect. 8.

We will see that Assumption 3 of [53], together with the slope condition (172), ensure the required coercivity property of the Lyapunov function $\mathscr{L}_\xi$ introduced in (165). In order to formulate Assumption 3 in the present context, consider the bounded linear operator $D^2_{w_\xi}\mathscr{L}_\xi : E \to E^*$,

$$D^2_{w_\xi}\mathscr{L}_\xi = D^2_{w_\xi}H + \xi D^2_{w_\xi}Q, \quad \xi > 0. \tag{173}$$

We define the *spectrum* of $D^2_{w_\xi}\mathscr{L}_\xi$ as the following subset of $\mathbb{R}$:

$$\sigma(D^2_{w_\xi}\mathscr{L}_\xi) = \left\{\lambda \in \mathbb{R} : D^2_{w_\xi}\mathscr{L}_\xi - \lambda\tilde{R} : E \to E^* \text{ is not an isomorphism}\right\}, \tag{174}$$

where $\tilde{R} = \mathrm{diag}(R, R)$ and $R = -\frac{\mathrm{d}^2}{\mathrm{d}x^2} + 1 : H^1(\mathbb{R}, \mathbb{R}) \to H^{-1}(\mathbb{R}, \mathbb{R})$ is the Riesz isomorphism. Under the hypotheses of Theorem 14/15, $\tilde{R}^{-1}D^2_{w_\xi}\mathscr{L}_\xi : E \to E$ is a bounded self-adjoint Schrödinger operator, and its spectrum coincides with $\sigma(D^2_{w_\xi}\mathscr{L}_\xi)$. The motivation for this definition of the spectrum of $D^2_{w_\xi}\mathscr{L}_\xi$ will be discussed in Remark 13.

A straightforward calculation shows that $D^2_{w_\xi}\mathscr{L}_\xi$ is explicitly given by

$$D^2_{w_\xi}\mathscr{L}_\xi = \begin{pmatrix} -\dfrac{\mathrm{d}^2}{\mathrm{d}x^2} + \xi - [f(x, w_\xi^2) + 2\partial_2 f(x, w_\xi^2)w_\xi^2] & 0 \\ 0 & -\dfrac{\mathrm{d}^2}{\mathrm{d}x^2} + \xi - f(x, w_\xi^2) \end{pmatrix}, \tag{175}$$

and the spectral conditions formulated in Assumption 3 of [53] are:

(S1) $\exists \alpha_\xi \in \mathbb{R}$ such that $\sigma(D^2_{w_\xi}\mathscr{L}_\xi) \cap (-\infty, 0) = \{-\alpha_\xi^2\}$ and $\ker(D^2_{w_\xi}\mathscr{L}_\xi + \alpha_\xi^2\tilde{R})$ is one-dimensional;

(S2) $\ker D^2_{w_\xi}\mathscr{L}_\xi = \mathrm{span}\{iw_\xi\}$;

(S3) $\sigma(D^2_{w_\xi}\mathscr{L}_\xi) \setminus \{-\alpha_\xi^2, 0\}$ is bounded away from zero.

The fact that $iw_\xi \in \ker D^2_{w_\xi}\mathscr{L}_\xi$ directly follows by differentiating (166) with respect to γ at $\gamma = 0$. So (S2) really only states that $\ker D^2_{w_\xi}\mathscr{L}_\xi$ is one-dimensional.

[20] The mathematical theory of NLS has been intimately connected to nonlinear optics from its early days. See [45] for additional references on this.

We now explain how hypotheses (S1)–(S3), together with (172), imply the coercivity property (126) in Proposition 5. In order to explicitly write down condition (126), let us first observe that we parametrized the standing waves by the "frequency" ξ here, whereas in Sect. 8 the relative equilibria are rather labelled using the value μ of the constraint. In the present context, $\mu = \mu(\xi) = Q(w_\xi)$, and we only deal with situations where μ is a smooth, strictly increasing function of ξ, so both parametrizations are equivalent. Now the level surface

$$\Sigma_{Q(w_\xi)} = \{u \in E \mid Q(u) = Q(w_\xi)\}$$

and, given a standing wave $u_\xi(t) = \Phi_{(\xi t)} w_\xi$ we have, for any $u = e^{-i\gamma(u)} w_\xi \in \mathscr{O}_{u_\xi}$,

$$T_u \Sigma_{Q(w_\xi)} = \{v \in E \mid \langle e^{-i\gamma(u)} D_{w_\xi} Q, v\rangle = 0\}.$$

On the other hand, $T_u \mathscr{O}_{u_\xi} = \operatorname{span}\{e^{-i\gamma(u)} i w_\xi\}$, so that

$$T_u \Sigma_{Q(w_\xi)} \cap (T_u \mathscr{O}_{u_\xi})^\perp = \{v \in E \mid \langle e^{-i\gamma(u)} D_{w_\xi} Q, v\rangle = (e^{-i\gamma(u)} i w, v)_E = 0\}.$$

Next, differentiating

$$D_{w_\xi} H + \xi D_{w_\xi} Q = 0$$

with respect to ξ yields

$$D^2_{w_\xi} \mathscr{L}_\xi \chi_\xi = -D_{w_\xi} Q, \quad \text{where} \quad \chi_\xi := \frac{\mathrm{d} w_\xi}{\mathrm{d}\xi}, \tag{176}$$

so that

$$\langle D^2_{w_\xi} \mathscr{L}_\xi \chi_\xi, \chi_\xi\rangle = -\langle D_{w_\xi} Q, \chi_\xi\rangle = -\frac{\mathrm{d}}{\mathrm{d}\xi} Q(w_\xi) < 0 \tag{177}$$

by (172).

Proposition 9 *Suppose that (S1) to (S3) hold, as well as (172). Then there exists $c > 0$ such that*

$$\forall u \in \mathscr{O}_{u_\xi}, \forall v \in T_u \Sigma_{Q(w_\xi)} \cap (T_u \mathscr{O}_{u_\xi})^\perp,\ D^2_u \mathscr{L}_\xi(v, v) \geq c \|v\|^2_E.$$

Proof Let $u = e^{-i\gamma(u)} w_\xi \in \mathscr{O}_{u_\xi}$. First remark that, by the invariance of $\mathscr{L}$ on the orbit $\{\Phi_\gamma w_\xi \mid \gamma \in \mathbb{R}\}$, we have

$$D^2_u \mathscr{L}_\xi = D^2_{\Phi_{\gamma(u)} w_\xi} \mathscr{L}_\xi = D^2_{w_\xi}(\mathscr{L}_\xi \circ \Phi_{-\gamma(u)}) = D^2_{w_\xi} \mathscr{L}_\xi.$$

Therefore, we need only prove the result at $u = w_\xi$, i.e. that there exists $c > 0$ such that

$$\forall v \in E,\ \langle D_{w_\xi} Q, v\rangle = (iw_\xi, v)_E = 0 \Rightarrow D^2_{w_\xi} \mathscr{L}_\xi(v, v) \geq c\|v\|^2_E.$$

Introducing the bounded self-adjoint operator $S_\xi := \tilde{R}^{-1} D^2_{w_\xi} \mathscr{L}_\xi : E \to E$, this is equivalent to

$$\forall v \in E,\ (S_\xi \chi_\xi, v)_E = (iw_\xi, v)_E = 0 \Rightarrow (S_\xi v, v)_E \geq c\|v\|^2_E.$$

Now by (177) we see that $(S_\xi \chi_\xi, \chi_\xi)_E < 0$, and the result readily follows from Lemma 5.3 in [99].

The verification of properties (S1)–(S3) and of the slope condition (172) in [45, 48] is intimately connected with the behaviour as $\xi \to 0$ of the solutions given by Theorems 14 and 15. The main idea is to show that the required properties hold true for a limiting problem obtained by letting $\xi \to 0$ in the stationary equation (160) (in suitably rescaled variables), and then to deduce them for the original problem by perturbation and continuation along the global curve given by Theorem 14/15. In other words, it is first shown that (S1)–(S3) and (172) hold for small values of $\xi > 0$, and then that these properties cannot change along the global curve. It is worth noting here that, in both Theorems 14 and 15, it can be shown that $\|w_\xi\|_{L^\infty} \to 0$ as $\xi \to 0$ (see Sect. 10.3.1 below). Therefore, case (AL) can be seen as a perturbation of (PT), in the limit of small ξ, and the stability properties of standing waves are the same in both cases for small $\xi > 0$.

The remainder of this section is devoted to the proof of Theorem 16. We will sketch the arguments yielding the local stability results close to $\xi = 0$, and the continuation procedure extending these to the whole curves of solutions in Theorems 14 and 15. For the local results, we shall only consider case (PT), the details of the perturbation argument one has to go through to deal with (AL) being cumbersome and not very enlightening (see [44] for more details). We will however present the global continuation procedure for both cases in a unified manner. For this we will use the general notation of (159)–(160) rather than the particular form of f in each case, and we will merely write $\xi > 0$ throughout, of course really meaning $0 < \xi < \xi_\infty$ in the (AL) case.

10.3.1 Local Stability by Bifurcation

We consider here (160) in dimension $d = 1$, and with $f(x, s^2) = V(x)|s|^{\sigma-1}$. The scaling

$$\xi = k^2, \quad u(x) = k^{\frac{2-b}{\sigma-1}} v(y), \quad y := kx, \quad k > 0, \tag{178}$$

yields

$$v'' - v + k^{-b}V(y/k)|v|^{\sigma-1}v = 0, \quad k > 0. \tag{179}$$

Then, by (V2),

$$\lim_{k\to 0} k^{-b}V(y/k) = |y|^{-b}|y/k|^b V(y/k) = |y|^{-b} \quad \forall y \neq 0,$$

which suggests considering the limit problem

$$v'' - v + |y|^{-b}|v|^{\sigma-1}v = 0. \tag{180}$$

It turns out [45] that (180) has a unique positive radial solution $v_0 \in H^1(\mathbb{R})$. This solution can be shown to have a variational characterization, from which it bears the name *ground state* of (180).

The advantage of the scaling is that, in the new variables (k, v), one can now obtain solutions by perturbation of (180), which is non-degenerate. More precisely, one can apply a version of the implicit function theorem to the function $F : \mathbb{R} \times H^1(\mathbb{R}) \to H^{-1}(\mathbb{R})$ defined by

$$F(k,v) = \begin{cases} v'' - v + |k|^{-b}V(y/|k|)|v|^{\sigma-1}v, & k \neq 0, \\ v'' - v + |y|^{-b}|v|^{\sigma-1}v, & k = 0, \end{cases}$$

at the point $(k, v) = (0, v_0) \in \mathbb{R} \times H^1(\mathbb{R})$, where $D_2F(0, v_0) : H^1(\mathbb{R}) \to H^{-1}(\mathbb{R})$ is an isomorphism (see [45, Proposition 2.1]). This provides a small $k_0 > 0$ and a local C^1 curve of solutions $\{(k, v_k) : |k| < k_0\} \subset \mathbb{R} \times H^1(\mathbb{R})$ of $F(k, v) = 0$. The local bifurcation in Theorem 14 can then be obtained by going back to the original variables using (178), which yields a local C^1 curve of solutions

$$\left\{(\xi, w_\xi) : 0 < \xi < k_0^2\right\} \subset \mathbb{R} \times H^1(\mathbb{R})$$

of (160). The various solution norms in the two sets of variables are related by

$$\|w_\xi\|_{L^2}^2 = \xi^{\alpha-1}\|v_{\xi^{1/2}}\|_{L^2}^2, \quad \|\nabla w_\xi\|_{L^2}^2 = \xi^{\alpha}\|\nabla v_{\xi^{1/2}}\|_{L^2}^2,$$
$$\|w_\xi\|_{L^\infty} = \xi^{\frac{2-b}{2(\sigma-1)}}\|v_{\xi^{1/2}}\|_{L^\infty}, \quad \text{where } \alpha = \tfrac{4-2b+(\sigma-1)}{2(\sigma-1)}.$$

The behaviour of w_ξ as $\xi \to 0$ follows readily from these relations and the fact that $v_k \to v_0$ both in $H^1(\mathbb{R})$ and in $L^\infty(\mathbb{R})$ (see [45, Proposition 3.1]).

The Slope Condition Let us now explain how the slope condition (172) can be derived from this analysis, for small $\xi > 0$. We show that $\frac{\mathrm{d}}{\mathrm{d}\xi}\|w_\xi\|_{L^2}^2 > 0$ for $\xi > 0$ small enough. Observe that

$$\frac{\mathrm{d}}{\mathrm{d}\xi}\|w_\xi\|_{L^2}^2 = \frac{1}{2k}\frac{\mathrm{d}}{\mathrm{d}k}\|w_{k^2}\|_{L^2}^2 = \frac{1}{2k}\frac{\mathrm{d}}{\mathrm{d}k}\{k^\beta\|v_k\|_{L^2}^2\}$$

where

$$\beta = \frac{4 - 2b - (\sigma - 1)}{\sigma - 1} = 2(\alpha - 1). \tag{181}$$

Now

$$\frac{\mathrm{d}}{\mathrm{d}k}\{k^\beta \|v_k\|_{L^2}^2\} = \beta k^{\beta-1}\|v_k\|_{L^2}^2 + k^\beta 2\langle v_k, \frac{\mathrm{d}}{\mathrm{d}k}v_k\rangle_{L^2}$$

$$= k^{\beta-1}\{\beta\|v_k\|_{L^2}^2 + 2k\langle v_k, \frac{\mathrm{d}}{\mathrm{d}k}v_k\rangle_{L^2}\}.$$

Since $\|v_k\|_{L^2}^2 \to \|v_0\|_{L^2}^2 > 0$ as $k \to 0$, we have that

$$\mathrm{sgn}\{\frac{\mathrm{d}}{\mathrm{d}\xi}\|w_\xi\|_{L^2}^2\} = \mathrm{sgn}\{\alpha - 1\} \text{ for } \xi = k^2 \text{ small}, \tag{182}$$

provided

$$k\langle v_k, \frac{\mathrm{d}}{\mathrm{d}k}v_k\rangle_{L^2} \to 0 \text{ as } k \to 0. \tag{183}$$

On the other hand,

$$\begin{aligned} F(k, v_k) = 0 &\Rightarrow D_k F(k, v_k) + D_v F(k, v_k)\frac{\mathrm{d}}{\mathrm{d}k}v_k = 0 \\ &\Rightarrow k\frac{\mathrm{d}}{\mathrm{d}k}v_k = -D_v F(k, v_k)^{-1} k D_k F(k, v_k) \\ &= -D_v F(k, v_k)^{-1} k^{-b} W(y/k) v_k^\sigma, \end{aligned}$$

where $W(x) := x \cdot V'(x) + bV(x)$ appears in hypothesis (V2). Then, using (V2), it is not difficult to show that

$$k^{-b} W(y/k) v_k^\sigma \to 0 \text{ in } H^{-1} \text{ as } k \to 0.$$

Finally, it follows from the open mapping theorem that

$$D_v F(k, v_k)^{-1} \to D_v F(0, v_0)^{-1} \text{ in } B(H^{-1}, H^1) \text{ as } k \to 0,$$

and we conclude that $k\frac{\mathrm{d}}{\mathrm{d}k}v_k \to 0$ in H^1 as $k \to 0$, from which (183) follows. Recalling our assumption that $1 < \sigma < 5 - 2b$, the slope condition (172) now readily follows from (181) and (182).

The Spectral Assumptions Regarding the verification of (S1)–(S3), we shall not give as much detail as for the slope condition. That the solutions w_ξ indeed give rise to a Hessian $D^2_{w_\xi}\mathscr{L}_\xi : E \to E^*$ with the appropriate spectral structure also follows from the properties of the limit problem (180) through the perturbation procedure outlined above. The crucial point is the variational characterization of the ground state v_0, which can be shown to minimize the functional

$$\tilde{\mathscr{L}}_0(v) = \frac{1}{2}\int_{\mathbb{R}} (v')^2 + v^2\,\mathrm{d}x - \frac{1}{\sigma+1}\int_{\mathbb{R}} |x|^{-b}|v|^{\sigma+1}\,\mathrm{d}x$$

on an appropriate codimension 1 submanifold N of $H^1(\mathbb{R})$. Note that the direct method of the calculus of variations cannot be applied to the functional $\tilde{\mathscr{L}}_0$ since it is not coercive. In fact it turns out that v_0 is a saddle-point of $\tilde{\mathscr{L}}_0$. More precisely, v_0 is a critical point of $\tilde{\mathscr{L}}_0$ (i.e. $D_{v_0}\tilde{\mathscr{L}}_0 = 0$), and the quadratic form $D^2_{v_0}\tilde{\mathscr{L}}_0 : H^1 \times H^1 \to \mathbb{R}$ is positive definite tangentially to N, and negative along the ray spanned by v_0, transverse to N. This information—together with some Schrödinger operator theory—precisely implies that $D^2_{v_0}\tilde{\mathscr{L}}_0$ enjoys the properties (S1)–(S3). Furthermore, if w_ξ and v_k are related by the change of variables (178), a straightforward calculation shows that

$$\mathscr{L}_\xi(w_\xi) = k^{\frac{3-2b+\sigma}{(\sigma-1)}}\tilde{\mathscr{L}}_0(v_k),$$

where $\mathscr{L}_\xi$ is the Lyapunov function defined in (165). However, it is by no means trivial to verify that the spectral properties of $D^2_{v_0}\tilde{\mathscr{L}}_0$ are carried through to $D^2_{w_\xi}\mathscr{L}_\xi$, for $\xi > 0$ small, in the perturbation procedure. This was shown in [49] in arbitrary dimension.

Note that, if the solutions w_ξ are themselves saddle-points of $\mathscr{L}_\xi$, the perturbation procedure can be dispensed of, and the spectral properties of the Hessian $D^2_{w_\xi}\mathscr{L}_\xi$ derived directly from this variational characterization. This is in fact the case for the solutions obtained in Theorem 14, but it is not known in the (AL) case, where the variational structure is much less transparent.

Remark 13 When verifying assumptions (S1)–(S3) in the context of (159)–(160) (which are set on the whole of $\mathbb{R}^d$) one has to deal with the continuous spectrum of $D^2_{w_\xi}\mathscr{L}_\xi$ in addition to the negative eigenvalue lying at the bottom of the spectrum. The standard approach to tackle this is *via* the theory of Schrödinger operators applied to the self-adjoint operator $\tilde{R}^{-1}D^2_{w_\xi}\mathscr{L}_\xi : E \to E$. This motivates the definition of $\sigma(D^2_{w_\xi}\mathscr{L}_\xi)$ given in (174). On the other hand, the problem considered in Sect. 9 (set on a compact manifold) only gives rise to discrete spectrum in the linearization, and so can be handled with a more elementary spectral analysis, not requiring to introduce the Riesz isomorphism $\tilde{R} : E \to E^*$ explicitly.

10.3.2 Global Continuation

In this section we show how both the slope condition (172) and the spectral properties (S1)–(S3) extend from the previous local analysis to the global curve given by either Theorem 14 or Theorem 15. We will handle the two cases in a unified approach, using the general notation $f(x, w^2)w$ for the nonlinearity. As earlier, we will often merely write $\xi > 0$, really meaning $\xi \in (0, \infty)$ in the (PT) case and $\xi \in (0, \xi_\infty)$ in the (AL) case. Again, we only consider here the case $d = 1$.

The Slope Condition From the previous analysis, (172) holds for $\xi > 0$ small enough. Hence we need only verify that

$$\frac{\mathrm{d}}{\mathrm{d}\xi} \int_{\mathbb{R}} w_\xi^2 \, \mathrm{d}x \neq 0 \quad \forall \xi > 0.$$

First notice that, since the solutions w_ξ are even,

$$\frac{\mathrm{d}}{\mathrm{d}\xi} \int_{\mathbb{R}} w_\xi^2 \, \mathrm{d}x = 2 \int_{\mathbb{R}} w_\xi \frac{\mathrm{d}}{\mathrm{d}\xi} w_\xi \, \mathrm{d}x = 4 \int_0^\infty w_\xi \chi_\xi,$$

where $\chi_\xi = \frac{\mathrm{d}w_\xi}{\mathrm{d}\xi}$ satisfies

$$\chi_\xi'' + \{f(x, w_\xi^2) + 2\partial_2 f(x, w_\xi^2) w_\xi^2\} \chi_\xi = \xi \chi_\xi + w_\xi.$$

To simplify the notation, we will drop the subscript ξ in the remainder of the argument. It can be shown [45, 48] that

$$\int_0^\infty \{2f(x, w^2) + x\partial_1 f(x, w^2) - \partial_2 f(x, w^2) w^2\} w\chi \, \mathrm{d}x = 2\xi \int_0^\infty w\chi \, \mathrm{d}x \tag{184}$$

and that there exists $x_0 > 0$ such that

$$\chi > 0 \text{ on } (0, x_0), \quad \chi(x_0) = 0, \quad \chi < 0 \text{ for } x > x_0.$$

Supposing by contradiction that $\int_0^\infty w\,\chi \, \mathrm{d}x = 0$, we can write (184) as

$$\int_0^\infty \left\{ \frac{2f(x, w^2) + x\partial_1 f(x, w^2)}{\partial_2 f(x, w^2) w^2} - 1 \right\} \partial_2 f(x, w^2) w^3 \chi \, \mathrm{d}x = 0.$$

Denoting by $\zeta(x)$ the function in the curly brackets, this becomes

$$\int_0^\infty \zeta(x) \partial_2 f(x, w^2) w^3 \chi \, \mathrm{d}x = 0.$$

Now using the unique zero x_0 of χ, we can rewrite this identity as

$$\int_0^\infty \{\zeta(x)-\zeta(x_0)\}\partial_2 f(x,w^2)w^3\chi\,\mathrm{d}x+\zeta(x_0)\int_0^\infty \partial_2 f(x,w^2)w^3\chi\,\mathrm{d}x=0.$$

Moreover, multiplying the equation for w by χ, the equation for χ by w, subtracting and integrating, yields

$$\int_0^\infty w^2\,\mathrm{d}x=2\int_0^\infty \partial_2 f(x,w^2)w^3\chi\,\mathrm{d}x,$$

and so

$$\int_0^\infty \partial_2 f(x,w^2)w^3\{\zeta(x)-\zeta(x_0)\}\chi\,\mathrm{d}x+\frac{\zeta(x_0)}{2}\int_0^\infty w^2\,\mathrm{d}x=0. \tag{185}$$

Now,

$$\partial_2 f(x,w^2)w^3=\begin{cases}\frac{\sigma-1}{2}V(x)w^\sigma & \text{in the (PT) case,}\\ \frac{\sigma-1}{2}V(x)\frac{w^\sigma}{(1+w^{\sigma-1})^2} & \text{in the (AL) case,}\end{cases}$$

hence $\partial_2 f(x,w^2)w^3>0$ on $(0,\infty)$ in any case. On the other hand,

$$\zeta(x)=\begin{cases}\frac{2}{\sigma-1}[x\frac{V'(x)}{V(x)}+\frac{5-\sigma}{2}] & \text{(PT)}\\ \frac{2}{\sigma-1}[x\frac{V'(x)}{V(x)}+\frac{5-\sigma}{2}]+\frac{2}{\sigma-1}[x\frac{V'(x)}{V(x)}+2]w^{\sigma-1} & \text{(AL)}\end{cases}$$

and we claim that ζ is positive and decreasing in any case, which immediately leads to a contradiction with (185). To conclude, the claim follows from our hypotheses since

$$x\to x\frac{V'(x)}{V(x)}\ \text{decreasing},\quad x\frac{V'(x)}{V(x)}\geq -b\quad\text{and}\quad \sigma<5-2b$$
$$\Rightarrow x\frac{V'(x)}{V(x)}+\frac{5-\sigma}{2}>0\ \text{and decreasing}$$

[note that hypothesis (V4) is crucial here]. Furthermore,

$$w>0\ \text{and decreasing}\ \Rightarrow \Big[\underbrace{x\frac{V'(x)}{V(x)}+2}_{\geq -b+2>0}\Big]w^{\sigma-1}>0\ \text{and decreasing},$$

so that ζ is indeed positive and decreasing in any case.

The Spectral Conditions The spectral conditions (S1)–(S3) can be reformulated in terms of the self-adjoint operators $L_\xi^+, L_\xi^- : H^2(\mathbb{R}) \subset L^2(\mathbb{R}) \to L^2(\mathbb{R})$ defined by

$$L_\xi^+ v = -v'' + \xi v - [f(x, w_\xi^2) + 2\partial_2 f(x, w_\xi^2) w_\xi^2] v,$$
$$L_\xi^- v = -v'' + \xi v - f(x, w_\xi^2) v.$$

Then (S1)–(S3) are equivalent to

(C1) $\inf \sigma_{\text{ess}}(L_\xi^+) > 0, \quad M(L_\xi^+) = 1, \quad \ker L_\xi^+ = \{0\},$
(C2) $\inf \sigma_{\text{ess}}(L_\xi^-) > 0, \quad 0 = \inf \sigma(L_\xi^-), \quad \ker L_\xi^- = \text{vect}\{w_\xi\},$

where $\sigma_{\text{ess}}(A)$ denotes the *essential spectrum* of a self-adjoint operator A, and $M(A)$ its *Morse index*, i.e. the dimension of the larger subspace where A is negative definite.

A first step toward verifying that (C1) and (C2) hold for all $\xi > 0$ is to show that all eigenvalues of L_ξ^+, L_ξ^- are simple, which follows by standard ODE arguments. Then, since

$$\lim_{|x|\to\infty} f(x, w_\xi(x)^2) = \lim_{|x|\to\infty} 2\partial_2 f(x, w_\xi(x)^2) w_\xi(x)^2 = 0,$$

it follows from the spectral theory of Schrödinger operators (see e.g. [98]) that

$$\inf \sigma_{\text{ess}}(L_\xi^+) = \inf \sigma_{\text{ess}}(L_\xi^-) = \xi > 0.$$

Furthermore, applying ODE comparison arguments to the equations $L_\xi^+ v = 0$ and (160), it can be seen that $\ker L_\xi^+ = \{0\}$. On the other hand, since $w_\xi > 0$ is a solution of (160), it follows again from standard spectral theory that

$$\ker L_\xi^- = \text{span}\{w_\xi\} \text{ and } 0 = \inf \sigma(L_\xi^-).$$

It remains to show that L_ξ^+ has exactly one negative eigenvalue. As discussed earlier, the local bifurcation analysis close to $\xi = 0$ shows that $M(L_\xi^+) = 1$ for $\xi > 0$ small enough. By perturbation theory, the eigenvalues of L_ξ^+ depend continuously on $\xi > 0$. Since $\ker L_\xi^+ = \{0\}$ for all $\xi > 0$, the eigenvalues cannot cross zero as ξ varies. Therefore, $M(L_\xi^+) = 1$ for all $\xi > 0$, which completes the proof of conditions (C1) and (C2).

11 A Brief History of Orbital Stability

The stability theory of infinite dimensional nonlinear evolution equations has been the object of intense study in the past four decades. It originated in the mathematical analysis of nonlinear waves propagating in dispersive media, such as waves on a

water surface, or electromagnetic waves in dielectric media. Giving an exhaustive review of the subject would take us far outside the scope of these notes. We shall only aim to guide the reader through a choice of references which appear important to us, providing possible directions for further investigation of the literature on orbital stability.

Let us first remark that the notion of *orbital stability* defined in (4) is a classical one in the study of periodic solutions of finite dimensional dynamical systems, which originated in the pioneering works of Floquet [37], Poincaré [87] and Lyapunov [69]. The rigorous mathematical analysis of orbital stability for *nonlinear dispersive PDE's* has been initiated in 1972 by Benjamin [8], who considered solitary waves of the Korteweg–de Vries (KdV) equation. This equation was first written down by Boussinesq in 1877 [13] and then rediscovered independently by Korteweg and de Vries in 1895 [61], as a model for water wave motions. It describes long waves in shallow water (i.e. with water depth small compared to wavelength) propagating in one space direction.[21] The terminology of "orbital stability" is not employed by Benjamin, who rather speaks of the stability of the shape of the solitary waves: "A device entailing the definition of a certain quotient space is used to discriminate the stability of solitary waves in respect of shape—which is a more reasonable property to investigate than absolute stability" ([8, p. 155]). The quotient referred to by Benjamin is with respect to space translations in $\mathbb{R}$, which is a group of symmetry for the KdV equation. Benjamin's proof of stability makes use of a Lyapunov functional constructed by means of the constants of motion, i.e. the energy-momentum method studied in these notes. It is worth observing here that, before proving stability for arbitrary perturbations of the initial data, he starts by proving stability for perturbations having same L^2 norm as the solitary wave, and then uses the fact that solitary waves come as continuous families parametrized by the wave speed. This idea was later used by Weinstein [104] for general NLS equations and a generalized KdV equation. We use it to prove our Theorem 10. Benjamin motivates his approach heuristically by discussing some early remarks of Boussinesq [13] suggesting the use of a Lyapunov function to prove stability.

An abundant literature on the stability theory of solitary waves for equations modelling water waves has followed Benjamin's paper. Just to mention a few, the interested reader may consult the following papers and references therein: [10, 11, 23, 24, 32, 33, 104] for waves in shallow water, including the KdV and Camassa-Holm equations; [14, 15, 25] for the full water wave problem, governed by the Euler equation.

A couple of years after Benjamin's seminal work, Bona [10] made a substantial contribution to the theory, by grounding it into the Sobolev space setting. Indeed, in the absence of a general well-posedness theory, Benjamin had assumed that solutions were global in time and smooth. Bona proved global well-posedness in appropriate Sobolev spaces and rephrased Benjamin's arguments in this natural

[21] The KdV equation also appears in other physical contexts [105].

framework. This was an important step for subsequent work on stability for nonlinear dispersive equations.

Two remarkable contributions to the stability theory of KdV-like equations were given about a decade later by Weinstein [104] and by Bona, Souganidis and Strauss [11], who applied the energy-momentum method to generalized versions of the KdV equation. Weinstein [104] also proves the orbital stability of standing wave solutions to a general class of nonlinear Schrödinger equation. His proof, based on the energy-momentum method, provides the first alternative, in the NLS context, to the proof of orbital stability given a few years earlier by Cazenave and Lions [18] for the NLS with a power-law nonlinearity (see also [16]), which is purely variational, based on Lions' concentration-compactness principle [68].

In the same spirit, taking advantage of general existence results for nonlinear waves that were obtained in the early 1980s (see e.g. [9, 97]), an important body of work including [51, 52, 57, 58, 90, 91] made use of linear stability analysis and the energy-momentum method to study stability properties of standing/solitary waves for Hamiltonian systems including the NLS and nonlinear Klein-Gordon equations. This line of research culminated in the general theory of orbital stability of Grillakis, Shatah and Strauss [53, 54], who derived sufficient and necessary conditions for the stability of standing/solitary waves of infinite-dimensional Hamiltonian systems with symmetry, *via* a combination of spectral properties and a general convexity condition. In the NLS context, this convexity condition takes the form of the condition (172) of Sect. 10. This stability condition seems to have first appeared in 1968 in a paper of Vakhitov and Kolokolov [103], where stability of trapped modes in a cylindrical nonlinear optical waveguide is discussed by formal arguments. In fact, the NLS equation is a standard model for slowly modulated waves in nonlinear media, for instance in nonlinear optics, see [72, 100].

Following the seminal contributions of the 1980s, the amount of work on stability for the NLS and other nonlinear dispersive equations has increased tremendously. Important results have been obtained for instance in [3, 4, 21, 22, 30, 36, 38–41, 48, 49, 55, 56, 63–65, 70, 71, 82], and many other references can be found in these papers.

In addition to orbital stability, the stronger property of asymptotic (orbital) stability[22] has also been investigated, see e.g. [75–78, 86] for KdV and [26–28, 59, 79, 93, 94] for NLS. Roughly speaking, a relative equilibria U is (orbitally) *asymptotically stable* if it is orbitally stable and any solution starting close to its orbit eventually resolves into a "modulation" of the original wave U and a purely dispersive part, solution of the linear version of the governing equation. An important related conjecture, known as the *soliton resolution conjecture* stipulates that, generically, any reasonable initial data should give rise to a solution which eventually resolves into a sum of solitary waves (solitons) and a purely dispersive part (radiation). More details and references on these topics can be found in [92, 102]. Let us just conclude by remarking that the term "soliton" (which was

[22] This notion is well known in the finite dimension context, see e.g. [20].

coined in [105]) comes from the literature on integrable systems, originating in [35, 42, 62, 73, 89, 105]. Loosely speaking, solitons are (stable) solitary waves of integrable systems, that can be obtained by exact solution methods,[23] such as the *inverse scattering transform* [62]. However, the term soliton is now used in a more flexible manner throughout the nonlinear dispersive PDE's community, whenever referring to a persistent localized wave resulting from a balance of dispersion and nonlinear effects. The inverse scattering transform provides detailed information about the asymptotic behaviour (e.g. soliton resolution) of general solutions *in the integrable cases*—see [60, 102] and references therein for recent accounts comparing the inverse scattering to other PDE methods.

Further discussion and more references about nonlinear dispersive PDE's can be found in the monographs [1, 5, 17, 101].

Appendix

The goal of this Appendix is to present those very basic notions from differential geometry, Lie group theory and Hamiltonian mechanics that are indispensable to follow the treatment of the main text and that are not necessarily familiar to all. The only prerequisites for this part are a good grasp of differential calculus on finite dimensional normed vector spaces not going much beyond a fluent mastery of the chain rule for differentiation and an intuitive grasp of what a submanifold of such spaces is.

Differential Geometry: The Basics

We first recall some elementary notions of differential geometry and dynamical systems on a normed vector space E. For the general theory on differentiable manifolds, one may for example consult [2, 67, 96].

By a vector field on E we will mean a smooth map $X : E \to E$. Given $u \in E$, one should think of $X(u)$ as a "tangent vector to E at u". With this idea in mind, a vector field naturally determines a differential equation

$$\dot{u}(t) = X(u(t)), \quad u_0 = u,$$

the solutions of which induce a flow on E defined as $\Phi_t^X(u) = u(t)$. For ease of discussion, we will suppose throughout the Appendix that all solutions are global

[23] These methods are somewhat reminiscent of the Fourier transform approach to solve linear PDE's, though the formulas are much more involved for nonlinear waves.

and hence all flows complete. Most results carry over even if the flow exists only locally in time.

The diffeomorphisms[24] Φ of E act naturally on vector fields as follows. First note that, when Φ is a diffeomorphism, and $\gamma : t \in (a,b) \to E$ a curve with $\gamma(0) = u, \dot\gamma(0) = v$, then we can consider the curve $\tilde\gamma : t \in (a,b) \to E$ defined by $\tilde\gamma(t) = \Phi(\gamma(t))$. This is the curve γ, "pushed forward" by Φ: we invite the reader to draw a picture. This new curve satisfies $\tilde\gamma(0) = \Phi(u)$, so it passes through $\Phi(u)$. What is its tangent vector at that point? The chain rule yields immediately

$$\dot{\tilde\gamma}(0) = D_u\Phi(v),$$

where $D_y\Phi$ is our notation for the Fréchet derivative of Φ at $y \in E$, which is a continuous linear map from E to E. This equality gives a geometric interpretation to the purely analytical object $D_u\Phi(v)$: it is the tangent vector at $\Phi(u)$ to the curve $\tilde\gamma$ at $t = 0$. With this in mind, given a vector field X, we can now define a new vector field Φ_*X, the *push forward* of the vector field X by the diffeomorphism Φ, as follows:

$$\Phi_*X(\Phi(u)) := D_u\Phi(X(u)).$$

Note that, with the above interpretation of the "push forward" of a vector at u, $D_u\Phi(X(u))$ is a vector "at $\Phi(u)$", which explains why $\Phi(u)$ appears in the argument in the left hand side. Of course, we can write

$$\Phi_*X(u) = D_{\Phi^{-1}(u)}\Phi(X(\Phi^{-1}(u))). \tag{186}$$

We will make little use of this notation from differential geometry, preferring to write out the explicit expression $D_u\Phi(X(u))$ whenever needed.

Diffeomorphisms also act naturally on flows, as follows. Given a diffeomorphism $\Phi : E \to E$, one has, for all $u \in E$,

$$\frac{\mathrm{d}}{\mathrm{d}t}(\Phi \circ \Phi_t^X)(u) = D_{\Phi_t(u)}\Phi(X(\Phi_t(u))).$$

From this and (186), one concludes

$$\begin{aligned}\frac{\mathrm{d}}{\mathrm{d}t}(\Phi \circ \Phi_t^X \circ \Phi^{-1})(u) &= D_{\Phi_t^X(\Phi^{-1}(u))}\Phi(X(\Phi_t^X(\Phi^{-1}(u))))\\ &= \Phi_*X(\Phi \circ \Phi_t^X \circ \Phi^{-1}(u)).\end{aligned}$$

In other words, the flow $\Phi \circ \Phi_t^X \circ \Phi^{-1}$ is generated by the pushed forward vector field Φ_*X.

[24] We mean $\Phi \in C^1(E,E)$ with a $C^1(E,E)$ inverse.

It follows from the above and an application of the chain rule that, if X, Y are two vector fields on E, then, for all $u \in E$,

$$\begin{aligned}\frac{\partial^2}{\partial s \partial t} \Phi_s^Y \circ \Phi_t^X \circ \Phi_{-s}^Y(u)_{|s=0=t} &= \frac{\mathrm{d}}{\mathrm{d}s} D_{\Phi_{-s}^Y(u)} \Phi_s^Y(X(\Phi_{-s}^Y(u)))_{s=0} \\ &= \frac{\mathrm{d}}{\mathrm{d}s} X(\Phi_{-s}^Y(u))_{s=0} + \frac{\mathrm{d}}{\mathrm{d}s} D_x \Phi_s^Y(X(u))_{s=0} \\ &= [X, Y](u), \end{aligned} \tag{187}$$

where the commutator $[X, Y]$ of two vector fields is defined as follows:

$$[X, Y](u) = D_u Y(X(u)) - D_u X(Y(u)).$$

This definition is justified by the following observation. Given a vector field X and a C^1 function $F : E \to \mathbb{R}$, one can define a differential operator

$$\hat{X}(F)(u) = D_u F(X(u)), \tag{188}$$

which is—geometrically—nothing but the directional derivative of F at u in the direction $X(u)$. A simple computation shows readily that

$$[\hat{X}, \hat{Y}] = \widehat{[X, Y]}. \tag{189}$$

The following is then well known:

Lemma 9 *The following are equivalent:*

(i) For all $s, t \in \mathbb{R}$, $\Phi_t^X \circ \Phi_s^Y = \Phi_s^Y \circ \Phi_t^X$;
(ii) $[X, Y] = 0$.

Proof That (i) implies (ii) follows immediately from the preceding computation. The proof of the converse is slightly more involved, for a simple argument we refer to [96].

Remark 14 Note that, if $X(u) = Au, Y(u) = Bu$, where $A, B : E \to E$ are linear, then, with our convention, $[X, Y](u) = -[A, B]u$. Here $[A, B] = AB - BA$ is the standard commutator of linear maps.

Definition 12 Let $F \in C^k(E, \mathbb{R}^m)$ for some $k \geq 1$. For each $\mu \in \mathbb{R}^m$ we define a level set of F by

$$\Sigma_\mu = \{u \in E \mid F(u) = \mu\}. \tag{190}$$

We will say $u \in E$ is a regular point of F if $D_u F : E \to \mathbb{R}^m$ is surjective. We will say μ is a regular value of F, if $\Sigma_\mu \neq \emptyset$ and all $u \in \Sigma_\mu$ are regular points of F.

If μ is a regular value of F, then Σ_μ is a co-dimension m submanifold of E [7, Theorem 6.3.34]. In that case, the tangent space to Σ_μ at u is defined as follows:

$$T_u\Sigma_\mu = \{w \in E \mid D_uF(w) = 0\} = \mathrm{Ker}(D_uF). \tag{191}$$

We point out that if $r = \mathrm{Rank}(D_uF)$ is constant on Σ_μ, then Σ_μ is a co-dimension r submanifold. We will need the following simple result in Sect. 8.4.

Lemma 10 *Let $F \in C^k(E, \mathbb{R}^m)$ for some $k \geq 2$. Let $\mu \in \mathbb{R}^m$ be a regular value of F. Let $u \in \Sigma_\mu$ and let W_u be a subspace of E so that $E = T_u\Sigma_\mu \oplus W_u$. Then, for all $v \in \Sigma_\mu$,*

$$\|(v-u)_2\| \leq \mathrm{O}(\|v-u\|^2),$$

and there exist $\delta, C > 0$ such that

$$\|v-u\| \leq \delta \Rightarrow \|(v-u)_1\| \geq C\|v-u\|,$$

where $(v-u) = (v-u)_1 + (v-u)_2 \in T_u\Sigma_\mu \oplus W_u$.

Note that both δ and C depend on u and on the decomposition of E chosen.

Proof Write $u - v = w_1 + w_2$, with $w_1 \in T_u\Sigma_\mu$ and $w_2 \in W_u$. Then, using that $D_uF(w_1) = 0$, we have

$$0 = F(v) - F(u) = D_uF(w_2) + \mathrm{O}(\|v-u\|^2).$$

Now, since D_uF is a diffeomorphism from W_u to $\mathbb{R}^m$, there exists $c > 0$ so that

$$\|D_uF(w_2)\| \geq c\|w_2\|, \quad \text{hence} \quad \mathrm{O}(\|v-u\|^2) \geq c\|w_2\|.$$

Finally

$$\|w_1\| = \|u - v - w_2\| \geq \|u-v\| - \|w_2\| \geq \|u-v\| - \mathrm{O}(\|v-u\|^2),$$

from which the result follows.

Lie Algebras, Lie Groups and Their Actions

In general, a Lie algebra is a vector space V equipped with a bilinear composition law $(u, v) \in V \times V \to [u, v] \in V$, called a Lie bracket, which is anti-symmetric and satisfies the Jacobi identity, meaning that for all $u, v, w \in V$:

$$[[u, v], w] + [[v, w], u] + [[w, u], v] = 0. \tag{192}$$

The basic example of this structure is given by spaces of matrices or, more generally, of linear operators on vector spaces, where the Lie bracket is given by the usual commutator. Two other examples play an important role in these notes, namely the space of vector fields on a normed vector space with the commutator defined in (187) and the space of all smooth functions on a symplectic vector space, where the Lie bracket is given by the Poisson bracket, as explained in Sect. 11 "Hamiltonian Dynamical System with Symmetry in Finite Dimension" below. The validity of the Jacobi identity follows in all these examples from a direct computation, whereas the bilinearity and the anti-symmetry are obvious. Lie algebras are intimately linked to Lie groups, as the terminology strongly suggests, and as we now further explain.

In general, a Lie group is a group equipped with a compatible manifold structure. For our purposes, it is however enough to define a Lie group G to be a subgroup of $\mathrm{GL}(\mathbb{R}^N)$, such that G is also a submanifold of $\mathbb{R}^{N^2}$ (i.e. for our purposes, typically the level surface of a vector-valued function). As such, $\mathrm{GL}(\mathbb{R}^N)$ itself, which is an open subset of $\mathbb{R}^{N^2}$, is a Lie group. So are the rotation group

$$\mathrm{SO}(N) = \{R \in \mathrm{GL}(N, \mathbb{R}) \mid R^T R = \mathrm{I}_N\}$$

and the symplectic group

$$\mathrm{Sp}(2N) = \{S \in \mathrm{GL}(2N, \mathbb{R}) \mid S^T J S = J\}, \quad \text{with} \quad J = \begin{pmatrix} 0 & \mathrm{I}_N \\ -\mathrm{I}_N & 0 \end{pmatrix}. \tag{193}$$

A simple verification shows that $\mathrm{Sp}(2) = \mathrm{SL}(2, \mathbb{R})$, the space of two by two matrices of determinant one. The dimension of a Lie group is by definition its dimension as a manifold. For $\mathrm{SO}(N)$, it is $N(N-1)/2$, and for $\mathrm{Sp}(2N)$, it is $N(2N+1)$, as is readily checked. The group $\mathbb{R}^n$ is also a Lie group in this sense. Indeed, putting $N = n + 1$, and defining, for each $a \in \mathbb{R}^n$,

$$A(a) = \begin{pmatrix} \mathrm{I}_n & a \\ 0 & 1 \end{pmatrix}$$

one readily sees that $A(a)A(b) = A(a + b)$, so that one can view $\mathbb{R}^n$ as a subgroup of $\mathrm{GL}(n + 1, \mathbb{R})$.

We recall that, in general, an action of a group G on a set Σ is a map $\Phi : (g, x) \in G \times \Sigma \to \Phi_g(x) \in \Sigma$ which satisfies $\Phi_e(x) = x$, for all $x \in \Sigma$, and $\Phi_{g_1} \circ \Phi_{g_2} = \Phi_{g_1 g_2}$. In these notes, we consider actions that are defined on a normed vector space E. If the Φ_g are linear, one says Φ is a representation of the group. This will *not* always be the case in these notes: actions may be nonlinear. Furthermore, all actions considered will be at least continuous, and very often they will have additional smoothness properties. In this Appendix, where we deal with finite dimensional systems only, the actions are supposed to be separately C^1 in each

of their two variables $g \in G$ and $u \in E$. Appropriate technical conditions to deal with infinite dimensional spaces E are given in the main part of the text as needed.

By definition, *the* Lie algebra $\mathfrak{g}$ of a Lie group G is the tangent space to the manifold G at the unit element $e \in G$:

$$\mathfrak{g} = T_e G.$$

In other words, for each $\xi \in \mathfrak{g}$, there exists $\gamma : t \in \mathbb{R} \to G$, a smooth curve with $\gamma(0) = e = \mathrm{I}_N$, and $\dot{\gamma}(0) = \xi$. Note that one should think of ξ as a matrix, since for each t, $\gamma(t)$ is one. In addition, it turns out that, given $\xi \in \mathfrak{g}$,

$$\exp(t\xi) \in G,$$

for all $t \in \mathbb{R}$ where $\exp(t\xi)$ is to be understood as the exponential of the matrix $t\xi$. Indeed, given ξ and γ as above, for all $n \in \mathbb{N}$, $\gamma(\frac{t}{n}) \in G$ and so $\gamma(\frac{t}{n})^n \in G$. Taking $n \to +\infty$, the result follows. A one-parameter subgroup of G is, by definition, a smooth curve $\gamma : t \in \mathbb{R} \to \gamma(t) \in G$, which is also a group diffeomorphism: $\gamma(t + s) = \gamma(t)\gamma(s)$. What precedes shows that any such one-parameter group is of the form $t \to \exp(t\xi)$. So there is a one-to-one correspondence between the one-parameter subgroups of G and its Lie-algebra, which starts to explain the importance of this latter notion. In addition, it turns out that, if $\xi, \eta \in T_e G$, then so is their commutator (seen as matrices)

$$[\xi, \eta] = \xi\eta - \eta\xi,$$

which justifies calling $T_e G$ a Lie algebra. Indeed, consider, for each $s \in \mathbb{R}$, the curve

$$\gamma : t \in \mathbb{R} \to \exp(s\eta) \exp(t\xi) \exp(-s\eta) \in G.$$

Clearly $\gamma(0) = \mathrm{I}_N$ and $\dot{\gamma}(0) = \exp(s\eta)\xi \exp(-s\eta) \in T_e G$. So we have a curve

$$s \in \mathbb{R} \to \exp(s\eta)\xi \exp(-s\eta) \in T_e G.$$

Taking the derivative with respect to s yields $[\eta, \xi] \in T_e G$:

$$\frac{\mathrm{d}}{\mathrm{d}s} \exp(s\eta)\xi \exp(-s\eta)_{|s=0} = [\eta, \xi]. \tag{194}$$

As an example, the Lie algebra of $\mathrm{SO}(N)$, denoted by $\mathrm{so}(N)$, is given by

$$\mathrm{so}(N) = \{A \in \mathscr{M}(N, \mathbb{R}) \mid A^T + A = 0\},$$

which is the space of all anti-symmetric $N \times N$ matrices. This is easily established by writing $\exp(tA^T) \exp(tA) = \mathrm{I}_N$ and taking a t-derivative at $t = 0$. And it is obvious

that the commutator of two anti-symmetric matrices is anti-symmetric. A basis for so(3) is

$$e_1 = \begin{pmatrix} 0 & 0 & 0 \\ 0 & 0 & -1 \\ 0 & 1 & 0 \end{pmatrix}, \; e_2 = \begin{pmatrix} 0 & 0 & 1 \\ 0 & 0 & 0 \\ -1 & 0 & 0 \end{pmatrix}, \; e_3 = \begin{pmatrix} 0 & -1 & 0 \\ 1 & 0 & 0 \\ 0 & 0 & 0 \end{pmatrix}, \tag{195}$$

and one readily checks that

$$[e_1, e_2] = e_3, \quad [e_2, e_3] = e_1, \quad [e_3, e_1] = e_2. \tag{196}$$

One then identifies $\xi \in \mathrm{so}(3)$ with $\xi \in \mathbb{R}^3$ via

$$\xi = \sum_{i=1}^{3} \xi_i e_i = \begin{pmatrix} 0 & -\xi_3 & \xi_2 \\ \xi_3 & 0 & -\xi_1 \\ -\xi_2 & \xi_1 & 0 \end{pmatrix}. \tag{197}$$

Similarly, a basis for $\mathrm{sl}(2, \mathbb{R})$, the Lie algebra of $\mathrm{SL}(2, \mathbb{R})$, is

$$e_0 = \begin{pmatrix} 1 & 0 \\ 0 & -1 \end{pmatrix}, \; e_+ = \begin{pmatrix} 0 & 1 \\ 0 & 0 \end{pmatrix}, \; e_- = \begin{pmatrix} 0 & 0 \\ 1 & 0 \end{pmatrix}, \tag{198}$$

and one has

$$[e_0, e_+] = 2e_+, \quad [e_0, e_-] = -2e_-, \quad [e_-, e_+] = -e_0. \tag{199}$$

In general, if e_i, $i = 1, \ldots, m$ is a basis of $\mathfrak{g}$, there exists constants c_{ij}^k so that

$$[e_i, e_j] = c_{ij}^k e_k, \tag{200}$$

where the summation over k is understood; the c_{ij}^k are called the structure constants of $\mathfrak{g}$.

There exists a natural *linear* action of G on its Lie algebra, called the *adjoint action* or *adjoint representation*, defined as follows, for all $g \in G, \xi \in T_e G$:

$$\mathrm{Ad}_g \xi = g \xi g^{-1}.$$

Clearly $\mathrm{Ad}_{g_1 g_2} = \mathrm{Ad}_{g_1} \mathrm{Ad}_{g_2}$. Note that for a commutative Lie group G, such as $\mathbb{R}^n$, it is trivial: $\mathrm{Ad}_g \xi = \xi$. It is instructive to compute some non-trivial adjoint actions explicitly. For SO(3), one finds, with the above (somewhat abusive) notation

$$\mathrm{Ad}_R \xi = \begin{pmatrix} 0 & -(R\xi)_3 & (R\xi)_2 \\ (R\xi)_3 & 0 & -(R\xi)_1 \\ -(R\xi)_2 & (R\xi)_1 & 0 \end{pmatrix} = R\xi. \tag{201}$$

We invite the reader to do the analogous computation for $\mathrm{sl}(2,\mathbb{R})$, determining the matrix of Ad_g in the basis given above.

The dual of the Lie algebra $\mathfrak{g}$ (as a vector space) is denoted by $\mathfrak{g}^*$. It appears very naturally in the study of symplectic group actions arising in the study of Hamiltonian systems with symmetry, as we will see in section "Symmetries and Constants of the Motion" below. Given a basis e_i of $\mathfrak{g}$, we denote by e_i^* the dual basis defined by $e_i^*(e_j) = \delta_{ij}$.

Moreover, there is a natural action of G on $\mathfrak{g}^*$, obtained by dualization as follows. For all $\mu \in \mathfrak{g}^*$, for all $\xi \in \mathfrak{g}$, we define

$$\mathrm{Ad}_g^* \mu(\xi) = \mu(\mathrm{Ad}_{g^{-1}} \xi). \tag{202}$$

This is called the co-adjoint action of G. For later purposes, we define, for all $\mu \in \mathfrak{g}^*$,

$$G_\mu = \{g \in G \mid \mathrm{Ad}_g^* \mu = \mu\}, \tag{203}$$

the so-called *stabilizer* or *isotropy group* of $\mu \in \mathfrak{g}^*$.

As above, given a basis e_i of $\mathfrak{g}$, one identifies $\mu \in \mathfrak{g}^*$ with $\mu = (\mu_1, \ldots, \mu_m) \in \mathbb{R}^m$ by writing

$$\mu = \sum_{i=1}^{m} \mu_i e_i^* \text{ so that } \mu(\xi) = \sum_{i=1}^{m} \mu_i \xi_i. \tag{204}$$

Let $\mu \in \mathrm{so}(3)^*$; we write $\mu(\xi) = \sum_{i=1}^{3} \mu_i \xi_i$ and identify $\mu \in \mathrm{so}(3)^*$ with $\mu = (\mu_1, \mu_2, \mu_3) \in \mathbb{R}^3$. Again, one readily checks that

$$\mathrm{Ad}_R{}^* \mu = R\mu. \tag{205}$$

Remark 15 It is often useful to suppose there exists an Euclidian structure on $\mathfrak{g}$ that is preserved by Ad_g for all $g \in G$. This is equivalent to supposing that there exists a basis e_i of $\mathfrak{g}$ so that the matrix of Ad_g in e_i belongs to $\mathrm{O}(m)$. We will simply write $\mathrm{Ad}_g \in \mathrm{O}(m)$ in this case. It follows that the matrix of Ad_g^* in the dual basis e_i^* belongs to $\mathrm{O}(m)$ as well. This implies that the natural Euclidian structure induced on $\mathfrak{g}^*$ by the one on $\mathfrak{g}$ is preserved by Ad_g^* for all $g \in G$. Such a structure always exists if the group G is compact.

Suppose now we have a C^1-action $\Phi : (g, u) \in G \times E \to \Phi_g(u) \in E$ of a Lie group G on a normed vector space E. Then, for all $\xi \in T_eG$, one can define the vector field X_ξ on E, called *generator*, via

$$X_\xi(u) = \frac{\mathrm{d}}{\mathrm{d}t} \Phi_{\exp(t\xi)}(u)_{|t=0}. \tag{206}$$

Lemma 11 *If Φ is a C^2-action, then for all $g \in G$, $\xi, \eta \in \mathfrak{g}$, for all $u \in E$, one has*

$$[X_\xi, X_\eta] = -X_{[\xi,\eta]}, \tag{207}$$

$$X_{\mathrm{Ad}_g \xi}(\Phi_g(u)) = D_u \Phi_g(X_\xi(u)). \tag{208}$$

Proof It follows from (187) that

$$\frac{\partial^2}{\partial s \partial t} \Phi_{\exp(s\eta)\, \exp(t\xi) \exp(-s\eta)\,|s=0=t} = \left[X_\xi, X_\eta\right].$$

Now, by definition,

$$X_{\exp(s\eta)\xi \exp(-s\eta)} = \frac{\mathrm{d}}{\mathrm{d}t} \Phi_{\exp(s\eta) \exp(t\xi) \exp(-s\eta)\,|t=0}$$

and furthermore

$$\frac{\mathrm{d}}{\mathrm{d}s} X_{\exp(s\eta)\xi \exp(-s\eta)\,|s=0} = X_{[\eta,\xi]}.$$

This proves (207). For (208), note that the chain rule implies

$$\frac{\mathrm{d}}{\mathrm{d}t} \Phi_g(\Phi_{\exp(t\xi)}(u))_{|t=0} = D_u \Phi_g(X_\xi(u)).$$

On the other hand, $\Phi_{g \exp(t\xi)}(u) = \Phi_{g \exp(t\xi)\ g^{-1}}(\Phi_g(u))$. Hence

$$\frac{\mathrm{d}}{\mathrm{d}t} \Phi_g(\Phi_{\exp(t\xi)}(u))_{|t=0} = X_{\mathrm{Ad}_g \xi}.$$

Lemma 11 shows that the map $\xi \in \mathfrak{g} \to X_\xi$ is a Lie algebra anti-homomorphism.

Hamiltonian Dynamical System with Symmetry in Finite Dimension

We now turn to a very short description of Hamiltonian dynamical systems and their symmetries on a finite dimensional normed vector space E. We present the theory in a simple but slightly abstract formalism that is well-suited for the generalization to the infinite dimensional situation needed for the main body of the text and presented in Sect. 6. The modern theory of finite dimensional Hamiltonian dynamical systems finds its natural setting in the theory of (finite dimensional) symplectic geometry [2, 6, 67, 95]. We shall however have no need for this more general formulation in these notes.

Hamiltonian Dynamical Systems

The central object of the theory in its usual formulation is a symplectic form, that we now define. Let $\omega : E \times E \to \mathbb{R}$ be a bilinear form which is anti-symmetric, meaning

$$\forall u, u' \in E,\ \omega(u, u') = -\omega(u', u),$$

and non-degenerate, meaning that, for all $u \in E$,

$$\big(\forall u' \in E,\ \omega(u, u') = 0\big) \Rightarrow u = 0.$$

Such a form is called a symplectic form. The standard example is $E = \mathbb{R}^n \times \mathbb{R}^n$ with $u = (q, p)$ and

$$\omega(u, u') = q \cdot p' - q' \cdot p, \tag{209}$$

where $\cdot$ indicates the standard inner product on $\mathbb{R}^n$. Given a C^1-function $F : E \to \mathbb{R}$, one defines the *Hamiltonian vector field X_F associated to F* as follows: for all $u \in E$,

$$\omega(X_F(u), u') = D_u F(u'), \quad \forall u' \in E. \tag{210}$$

We recall that $D_u F \in E^*$ is our notation for the Frechet derivative of F at u. Observe that one can think of the map $u \in E \to D_u F \in E^*$ as a differential one-form on E. The vector field X_F is well-defined and unique, thanks to the non-degeneracy of the symplectic form. If ω were symmetric, rather than anti-symmetric, it would define an inner product on E, rather than a symplectic form, and (210) would actually define the gradient of F; in analogy, one sometimes refers to X_F as the symplectic gradient of F. We will see it has radically different features from the gradient.

For later reference, we point out that

$$X_F = 0 \Rightarrow \exists c \in \mathbb{R},\ \forall u \in E,\ F(u) = c. \tag{211}$$

The flow of the Hamiltonian vector field X_F, for which we shall write Φ_t^F, is obtained by integrating the differential equation

$$\dot{u}(t) = X_F(u(t)), \quad u_0 = u, \tag{212}$$

referred to as the Hamiltonian equation of motion. One writes $\Phi_t^F(u) = u(t)$. In this section we suppose that (212) admits a unique and global solution and that, for all $t \in \mathbb{R}$, $\Phi_t \in C(E, E)$.

As a typical example from elementary mechanics, let $V \in C^1(\mathbb{R}^3; \mathbb{R})$ and define the function

$$H(q, p) = \tfrac{1}{2} p^2 + V(q) \tag{213}$$

on $E = \mathbb{R}^6$, with the symplectic form as above. The equations of motion corresponding to H are then

$$\dot{q}(t) = p(t), \quad \dot{p}(t) = -\nabla V(q(t)). \tag{214}$$

Note that they lead to Newton's force law in the form $\ddot{q}(t) = -\nabla V(q(t))$. More generally, in the example above, with $E = \mathbb{R}^{2n}$, one finds

$$X_F(q,p) = \begin{pmatrix} \partial_p F(q,p) \\ -\partial_q F(q,p) \end{pmatrix},$$

which leads to the familiar Hamiltonian equations of motion:

$$\dot{q}(t) = \partial_p F(q(t), p(t)), \qquad \dot{p}(t) = -\partial_q F(q(t), p(t)).$$

We give several other explicit examples of such flows in the main part of these notes.

Let us return to the general situation. Given two functions $F_1, F_2 : E \to \mathbb{R}$, one defines their Poisson bracket $\{F_1, F_2\}$ via

$$\{F_1, F_2\} = \omega(X_{F_1}, X_{F_2}) = -\{F_2, F_1\}. \tag{215}$$

Observe that, with the notation from (188), we have

$$\hat{X}_{F_1}(F_2) = DF_2(X_{F_1}) = \omega(X_{F_2}, X_{F_1}) = \{F_2, F_1\}, \tag{216}$$

i.e. for all $u \in E$,

$$\hat{X}_{F_1}(F_2)(u) = D_u F_2(X_{F_1}(u)) = \omega(X_{F_2}(u), X_{F_1}(u)) = \{F_2, F_1\}(u).$$

It is then immediate from what precedes that, for all $u \in E$,

$$\begin{aligned} \frac{\mathrm{d}}{\mathrm{d}t}(F_2 \circ \Phi_t^{F_1})(u) &= D_{\Phi_t^{F_1}(u)} F_2(X_{F_1}(\Phi_t^{F_1}(u))) \\ &= \{F_2, F_1\}(\Phi_t^{F_1}(u)) \end{aligned}$$

which in turn yields:

Theorem 17 *Let $F_1, F_2 \in C^1(E, \mathbb{R})$. Then $F_1 \circ \Phi_t^{F_2} = F_1$ for all t iff $F_2 \circ \Phi_t^{F_1} = F_2$ for all t, iff $\{F_1, F_2\} = 0$.*

When $F_1 \circ \Phi_t^{F_2} = F_1$ for all t, one says either that the $\Phi_t^{F_2}$ form a symmetry group[25] for F_1 or that F_1 is a constant of the motion[26] for the flow $\Phi_t^{F_2}$. The theorem, which is a Hamiltonian version of Noether's theorem (See [2, 6, 67, 95] for a general treatment), can therefore be paraphrased by saying that F_2 is a constant of the motion for the flow $\Phi_t^{F_1}$ iff the flow $\Phi_t^{F_2}$ of F_2 forms a group of symmetries for F_1. Several instances and applications of this result appear in the main body of the text. It is typically used in the following manner. One wishes to study the dynamical flow $\Phi_t^{F_1}$. One has a simple and well-known one parameter group $\Phi_t^{F_2}$ for which one readily establishes with an explicit computation that $F_1 \circ \Phi_t^{F_2} = F_1$. From this, one can then conclude that F_2 is a constant of the motion for the dynamical group $\Phi_t^{F_1}$. We will elaborate on this point in section "Symmetries and Constants of the Motion" below.

The radical difference between the properties of the symplectic gradient and the "usual" gradient is now apparent. The anti-symmetry of the Poisson bracket implies $\hat{X}_F(F) = 0$, that is, the symplectic gradient is *tangent* to the level surfaces of F [see (191)], rather than orthogonal. Hence its flow Φ_t^F preserves these surfaces rather than moving points to increasing values of F as does the usual gradient. These features, together with the Jacobi identity, are at the origin of all special properties of Hamiltonian systems.

To prepare for the treatment of Hamiltonian dynamical systems in infinite dimension (see Sect. 6), we reformulate the above as follows. Given a symplectic form ω on a finite dimensional normed vector space E, one can define a bijective linear map

$$\mathscr{J} : u \in E \to \mathscr{J}u \in E^*$$

by $\mathscr{J}u(v) = \omega(u, v)$. It is clear that

$$\mathscr{J}u(v) = -\mathscr{J}v(u). \tag{217}$$

With this notation, we find that

$$X_F = \mathscr{J}^{-1}DF, \quad \text{or} \quad \mathscr{J}X_F = DF \tag{218}$$

so that the Hamiltonian equations of motion (212) can be equivalently rewritten as

$$\mathscr{J}\dot{u}(t) = D_{u(t)}F. \tag{219}$$

This formulation is the one that we carry over to the infinite dimensional setting in the main body of these notes. Note that the Poisson bracket of two functions can

[25] See Definition 2.

[26] Defined in (9).

now be written as

$$\{F, G\} = DF(\mathscr{J}^{-1}DG). \tag{220}$$

The point to make is that all objects of the theory can be expressed in terms of $\mathscr{J}$. This is illustrated in the proof of the following result.

Lemma 12 *If $F_1, F_2, F_3 \in C^2(E, \mathbb{R})$, then the Jacobi identity holds:*

$$\{\{F_1, F_2\}, F_3\} + \{\{F_2, F_3\}, F_1\} + \{\{F_3, F_1\}, F_2\} = 0 \tag{221}$$

If $F_1, F_2 \in C^2(E, \mathbb{R})$, then

$$X_{\{F_1,F_2\}} = -[X_{F_1}, X_{F_2}]. \tag{222}$$

Proof To prove (221), one first easily checks that

$$\begin{aligned}
&\{\{F_1, F_2\}, F_3\}(u) \\
&\quad = D_u^2 F_1(\mathscr{J}^{-1}D_u F_2, \mathscr{J}^{-1}D_u F_3) + D_u F_1(\mathscr{J}^{-1}D_u^2 F_2(\cdot, \mathscr{J}^{-1}D_u F_3)) \\
&\quad = D_u^2 F_1(\mathscr{J}^{-1}D_u F_2, \mathscr{J}^{-1}D_u F_3) - D_u^2 F_2(\mathscr{J}^{-1}D_u F_1, \mathscr{J}^{-1}D_u F_3),
\end{aligned}$$

where we used (217). The result is then immediate. To prove (222) we use (188)–(189) to write

$$\begin{aligned}
\widehat{[X_{F_1}, X_{F_2}]}(F_3) &= \hat{X}_{F_1}(\hat{X}_{F_2}(F_3)) - \hat{X}_{F_2}(\hat{X}_{F_1}(F_3)) \\
&= \hat{X}_{F_1}(\{F_3, F_2\}) - \hat{X}_{F_2}(\{F_3, F_1\})) \\
&= \{\{F_3, F_2\}, F_1\} - \{\{F_3, F_1\}, F_2\} \\
&= \{\{F_1, F_2\}, F_3\} = -\hat{X}_{\{F_1,F_2\}}(F_3),
\end{aligned}$$

where we used the Jacobi identity in the last line.

For the case where $E = \mathbb{R}^{2n}$ with the standard symplectic structure, one readily finds

$$\{F_1, F_2\} = \partial_q F_1 \cdot \partial_p F_2 - \partial_p F_1 \cdot \partial_q F_2. \tag{223}$$

The above lemma then follows from a direct computation.

The lemma implies that the vector space $C^\infty(E, \mathbb{R})$, equipped with the Poisson bracket, is a Lie algebra. In addition, it follows that the constants of the motion of a given function $F \in C^\infty(E, \mathbb{R})$ form a Lie subalgebra. Indeed, introducing the space of constants of the motion of F,

$$\mathscr{C}_F = \{G \in C^\infty(E, \mathbb{R}) \mid G \circ \Phi_t^F = G, \forall t \in \mathbb{R}\}, \tag{224}$$

which is clearly a vector space, it follows immediately from (221) that

$$G_1, G_2 \in \mathscr{C}_F \Rightarrow \{G_1, G_2\} \in \mathscr{C}_F,$$

so that $\mathscr{C}_F$ is a Lie subalgebra of $C^\infty(E, E)$.

We finally need to introduce symplectic transformations.

Definition 13 A symplectic transformation on a symplectic space (E, ω) is a C^1 diffeomorphism $\Phi : E \to E$ so that, for all $u, v, w \in E$

$$\omega(D_u\Phi(v), D_u\Phi(w)) = \omega(v, w). \tag{225}$$

This is often paraphrased by the statement that "Φ preserves the symplectic structure." To understand what this means, one should recall the interpretation of $D_u\Phi(v)$ as the "push forward" of v by Φ, explained in section "Differential Geometry: The Basics" below. Equation (225) states that a diffeomorphism is symplectic if the symplectic form is left invariant by the "push forward" operation of its arguments. Note that, if Φ is linear, (225) reduces to $\omega(\Phi(v), \Phi(w)) = \omega(v, w)$. And if $E = \mathbb{R}^{2n}$ with its standard symplectic structure, this then means that $\Phi \in \mathrm{Sp}(2n)$, defined in (193).

Lemma 13 *Let $F \in C^1(E, \mathbb{R})$ and let $\Phi \in C^1(E, E)$ be a symplectic transformation. Then, for all $u \in E$,*

$$D_u\Phi(X_{F\circ\Phi}(u)) = X_F(\Phi(u)). \tag{226}$$

Moreover, for all $t \in \mathbb{R}$,

$$\Phi \circ \Phi_t^{F\circ\Phi} \circ \Phi^{-1} = \Phi_t^F. \tag{227}$$

In particular, if $F \circ \Phi = F$, then Φ commutes with Φ_t^F, for all $t \in \mathbb{R}$. And if Φ commutes with Φ_t^F, for all $t \in \mathbb{R}$, then there exists $c \in \mathbb{R}$ so that $F \circ \Phi = F + c$.

Equation (226) asserts that the push forward of the vector field $X_{F\circ\Phi}$ by Φ is X_F.

Proof For all $u, v \in E$, one has

$$\begin{aligned}\omega(X_{F\circ\Phi}(u), v) &= D_u(F \circ \Phi)(v) = D_{\Phi(u)}F(D_u\Phi(v)) \\ &= \omega(X_F(\Phi(u)), D_u\Phi(v)).\end{aligned}$$

Hence, since Φ is symplectic and since $D_{\Phi(u)}\Phi^{-1}D_u\Phi = \mathrm{Id}_E = D_u\Phi D_{\Phi(u)}\Phi^{-1}$,

$$\omega(D_u\Phi(X_{F\circ\Phi}(u)), v) = \omega(X_{F\circ\Phi}(u), D_{\Phi(u)}\Phi^{-1}(v)) = \omega(X_F(\Phi(u)), v)$$

which yields (226). Next, for all $u \in E$, one finds from the chain rule and (226)

$$\begin{aligned}\frac{\mathrm{d}}{\mathrm{d}t}\Phi(\Phi_t^{F\circ\Phi}(\Phi^{-1}(u))) &= D_{\Phi_t^{F\circ\Phi}(\Phi^{-1}(u))}\Phi\left(X_{F\circ\Phi}(\Phi_t^{F\circ\Phi}(\Phi^{-1}(u))\right)\\ &= X_F((\Phi\circ\Phi_t^{F\circ\Phi}\circ\Phi^{-1})(u)).\end{aligned}$$

This shows $t \in \mathbb{R} \to (\Phi \circ \Phi_t^{F\circ\Phi} \circ \Phi^{-1})(u) \in E$ is a flow line of X_F. Since the latter are unique, (227) follows.

We end with a proof of a basic fact about Hamiltonian flows: if they are smooth, they are symplectic.

Theorem 18 *Let $F \in C^2(E,\mathbb{R})$. Suppose that the corresponding Hamiltonian flow $\Phi^F : \mathbb{R}\times E \to E$ is of class C^2. Then, for all $t \in \mathbb{R}$, Φ_t^F is a symplectic transformation.*

Proof It will be sufficient to show that, for all $u, v, w \in E$, and for all $t \in \mathbb{R}$,

$$\frac{\mathrm{d}}{\mathrm{d}t}(\mathscr{J}D_u\Phi_t^F v)(D_u\Phi_t^F w) = 0.$$

Using the group property of the flow, one sees it is enough to show this at $t = 0$. Then

$$\frac{\mathrm{d}}{\mathrm{d}t}(\mathscr{J}D_u\Phi_t^F v)(D_u\Phi_t^F w)_{|t=0} = \mathscr{J}(\mathscr{J}^{-1}D_u^2F(v,\cdot))(w) + (\mathscr{J}v)(\mathscr{J}^{-1}D_u^2F(w,\cdot)).$$

where we used the continuity of $\mathscr{J}$, the Schwarz Lemma (exchange of partial derivatives) and the observation that

$$\mathscr{J}\frac{\partial\Phi^F}{\partial t}(u) = D_{u(t)}F \in E^*,$$

and hence, at $t = 0$,

$$\mathscr{J}D_u\left(\frac{\partial\Phi^F}{\partial t}\right)(u) = \left(D_u^2F\right),$$

which means that, for all $v \in E$,

$$\mathscr{J}D_u\left(\frac{\partial\Phi^F}{\partial t}\right)(u)v = \left(D_u^2F\right)(v,\cdot).$$

Note that both sides are elements of E^* since $u \in E \to \frac{\partial\Phi^F}{\partial t} \in E$ so that $D_u\left(\frac{\partial\Phi^F}{\partial t}\right)(u) \in \mathscr{B}(E,E)$. Using the anti-symmetry of $\mathscr{J}$, one then finds

$$\frac{\mathrm{d}}{\mathrm{d}t}(\mathscr{J}D_u\Phi_t^F v)(D_u\Phi_t^F w)_{|t=0} = D_u^2F(v,w) - D_u^2F(w,v) = 0.$$

Remark 16 We point out that the proof, as it stands, is valid in infinite dimensional systems. Remark however that the conditions imposed on the flow Φ_t^F are very strong for systems in infinite dimension. Too strong actually to be of much use in that context. We use/need those conditions to apply the Schwarz Lemma at several points in the proof. Also, it is known that Hamiltonian flows in infinite dimension need not always be symplectic. In the framework of Sect. 6 it is possible to give sufficient smoothness conditions on the restriction of the flow to $\mathscr{D}$ that will guarantee the result, but we shall not need this. For a different set of technical conditions guaranteeing the symplecticity of the flow, we refer to [19].

Symmetries and Constants of the Motion

Hamiltonian dynamical systems have many special features, but the one important to us here is that there exists for them a special link between the symmetries of the dynamics and the constants of the motion. This link takes the form of a Hamiltonian version of Noether's Theorem, of which we already gave a simple version in Theorem 17, and has far-reaching consequences, some of which we further explore in this section. Again, a general treatment can for example be found in [2, 67]; we give just those few elements needed in these notes.

We start with some notions on Hamiltonian Lie group actions on a symplectic vector space.

Definition 14 Let G be a Lie group and $\Phi : (g, x) \in G \times E \to \Phi_g(x) \in E$, an action of G on E with $\Phi_g \in C^1(E, E)$. We will say Φ is globally Hamiltonian if Φ_g is symplectic for all $g \in G$ and if, for all $\xi \in \mathfrak{g}$, there exists $F_\xi \in C^2(E, \mathbb{R})$ so that $\Phi_{\exp(t\xi)} = \Phi_t^{F_\xi}$.

In other words, an action is globally Hamiltonian if all Φ_g are symplectic and if all one parameter groups are realized by Hamiltonian flows. In the notation of the previous sections this means that

$$X_\xi = X_{F_\xi}.$$

Here, the left hand side is the generator of the action, defined in (206) and the right hand side is the Hamiltonian vector field associated to F_ξ.

Remark 17 In view of Theorem 18, if $g = \exp(\xi)$ for some $\xi \in \mathfrak{g}$ and Φ_g can be written as $\Phi_{\exp(\xi)} = \Phi_1^{F_\xi}$ for some $F_\xi \in C^2(E, \mathbb{R})$ such that $\Phi_1^{F_\xi}$ is C^2, then Φ_g is symplectic. This will obviously hold as well for all g that can be written as a finite product of elements of the form $\exp(\xi)$, which is the case for all g in the connected component of G containing $e \in G$ (see [67, page 145, Proposition 2.10]). So the assumption that Φ_g is symplectic is only needed for elements g that are not connected to $e \in G$. In infinite dimensional systems, as indicated in Remark 16 at the end of the previous section, the condition that all Φ_g must be symplectic is more

restrictive. In practice, one often works with linear actions of the symmetry group, for which the symplectic property can be checked directly.

The above definition is a special case of the more general definition of *globally Hamiltonian action* for infinite dimensional systems that we introduced in Definition 11. It suffices to take $\mathscr{D} = E$ in the latter to obtain the definition here.

We shall now continue with the abstract theory where, in particular, we will see through a version of Noether's Theorem that, if the Hamiltonian is invariant under a globally Hamiltonian action Φ as above, then the functions $F_\xi \in C^2(E, \mathbb{R})$ are constants of the motion. The theory will be illustrated in Example 2 at the end of the section, in the simple case where $E = \mathbb{R}^6$ and $G = \mathrm{SO}(3)$.

Theorem 19 *Let G be a Lie group and Φ a globally Hamiltonian action of G on a symplectic vector space E. Let $H \in C^1(E, \mathbb{R})$ and let Φ_t^H be the corresponding Hamiltonian flow. Suppose that*

$$\forall g \in G, \quad H \circ \Phi_g = H. \tag{228}$$

Then the following statements hold.

(i) For all $\xi \in \mathfrak{g}$, $\{H, F_\xi\} = 0$.
(ii) For all $t \in \mathbb{R}$, $F_\xi \circ \Phi_t^H = F_\xi$.
(iii) G is an invariance group[27] for Φ_t^H.

Proof This is an immediate consequence of Theorem 17 and of Lemma 13.

This result is useful because it is often easy to check (228), whereas the conclusions (ii) and (iii) are statements about the flow Φ_t^H, which is usually not explicitly known, and are therefore hard to check directly. In particular, (iii) says that if the Hamiltonian H is G-invariant as a function, then G is an invariance group of the dynamics.[28] And (ii) ascertains that the group generators F_ξ are then constants of the motion for Φ_t^H.

Let us point out that (iii) implies neither (i), (ii) or (228) (see Lemma 13).

So the hypothesis that the Hamiltonian is invariant under the group action is strictly stronger than the statement that the Hamiltonian flow is invariant under G. The map

$$\xi \in \mathfrak{g} \to F_\xi \in C^2(E, \mathbb{R}) \tag{229}$$

can be chosen to be linear. Indeed, if e_i, $i = 1, \ldots, d$ is a basis of $\mathfrak{g}$, if we choose $F_i = F_{e_i}$, and if we write $\xi = \sum_i \xi_i e_i$, we can define

$$F_\xi = \sum_i \xi_i F_i, \tag{230}$$

[27] See Definition 2.

[28] This is the point in the proof where the symplectic nature of the Φ_g is used, via Lemma 13.

by linearity. This allows one to define the *momentum map* for the action Φ, as follows:

$$\mathscr{F} : u \in E \to \mathscr{F}(u) \in \mathfrak{g}^*, \quad \mathscr{F}(u)(\xi) = F_\xi(u). \tag{231}$$

This, of course, is just a rewriting of (229). In the main body of the text we shall always assume a basis has been chosen for $\mathfrak{g}$, as above, so that we can identify $\mathfrak{g} \simeq \mathbb{R}^m$. And we shall simply write

$$F : u \in E \to (F_1(u), \cdots, F_m(u)) \in \mathbb{R}^m \simeq \mathfrak{g}^*. \tag{232}$$

We shall refer to $\mathscr{F}$ or to F as a momentum map for the action, indifferently.

Definition 15 Let Φ be a globally Hamiltonian action of G on E, with momentum map F. One says the momentum map is Ad^*-equivariant if, for all $g \in G$, for all $\xi \in \mathfrak{g}$,

$$F_\xi \circ \Phi_g = F_{\mathrm{Ad}_{g^{-1}}\xi}. \tag{233}$$

The terminology comes from the following observation. If (233) holds, then it follows from (231) and (202) that

$$\mathscr{F} \circ \Phi_g = \mathrm{Ad}^*_g \circ \mathscr{F}. \tag{234}$$

Since we identify $\mathfrak{g}^* \simeq \mathbb{R}^m$, this can be written

$$F \circ \Phi_g = \mathrm{Ad}^*_g F. \tag{235}$$

We can now formulate the final result from the theory of invariant Hamiltonian systems that we need. It is an immediate consequence of (235) or, for the reader weary of duals, of (233).

Proposition 10 *Let Φ be a globally Hamiltonian, Ad^*-equivariant action of a Lie group G on a symplectic vector space E. Let $\mu \in \mathfrak{g}^* \simeq \mathbb{R}^m$ and define*

$$\Sigma_\mu = \{u \in E \mid F(u) = \mu\} \tag{236}$$

Then $G_\mu = G_{\Sigma_\mu}$, where G_μ is the stabilizer of μ, defined in (203) and G_{Σ_μ} is defined in (16).

The situation we have in mind is the one where G is such that $H \circ \Phi_g = H$, for all $g \in G$. By Theorem 19, the functions F_i are then constants of the motion for the flow Φ^H_t and hence the surfaces Σ_μ are Φ^H_t invariant. We can therefore consider the dynamical system (Σ_μ, Φ^H_t), which has G_μ as an invariance group (G_μ leaves invariant both Σ_μ and the flow Φ^H_t). This viewpoint will prove useful in the study of orbital stability in several situations.

Definition 16 Let Φ be a globally Hamiltonian action of a Lie group G on a symplectic vector space E. Let $\mu \in \mathfrak{g}^*$. We say μ is a regular point of the momentum map F if, for all $u \in \Sigma_\mu$, $D_u F$ is surjective.

This definition simply guarantees that Σ_μ is a co-dimension m submanifold of E, where m is the dimension of $\mathfrak{g}$.

Example 2 For the simple Hamiltonian system with spherical potentials considered in Sects. 3.1 and 5, one has $E = \mathbb{R}^6$, $G = \mathrm{SO}(3)$, and it is not difficult to check that, for all $u(q,p) \in \mathbb{R}^6$, $F(u) = L(q,p) \in \mathbb{R}^3 \simeq \mathrm{so}(3)^*$ and $F_\xi(q,p) = \xi \cdot L(q,p)$, where we use the identifications (197) and (204). Furthermore, for all $R \in \mathrm{SO}(3)$,

$$L(Rq, Rp) = RL(q,p),$$

which shows the action is Ad^*-invariant, in view of (205).

We end this section with some comments on the Poisson brackets of the components of the momentum map. Remark first that the momentum map of a globally Hamiltonian action is not unique since, for any choice of $\lambda \in \mathfrak{g}^*$, $\tilde{F}_\xi = F_\xi + \lambda(\xi)$ also satisfies $X_\xi = X_{\tilde{F}_\xi}$. Note furthermore that, in view of (207) and (222), the momentum map satisfies, for all $\xi, \eta \in \mathfrak{g}$,

$$X_{F_{[\xi,\eta]}} = X_{[\xi,\eta]} = X_{\{F_\xi, F_\eta\}}.$$

It then follows from (211) that, for all $\xi, \eta \in \mathfrak{g}$, there exists a constant $c(\xi,\eta)$ so that

$$F_{[\xi,\eta]} = \{F_\xi, F_\eta\} + c(\xi,\eta).$$

The following lemma is useful and an easy consequence of (235):

Lemma 14 *Let Φ be a globally Hamiltonian action of G on E, with momentum map F. If F is Ad^*-equivariant, then, for all $\xi, \eta \in \mathfrak{g}$,*

$$F_{[\xi,\eta]} = \{F_\xi, F_\eta\}. \tag{237}$$

Conversely, if (237) holds, then (233) holds for all $g \in G$ of the form $g = \exp(\eta)$, for some $\eta \in \mathfrak{g}$ and then for all g in the connected component of e.

What one has to remember here is this. In applications, we often wish to assure (233) holds. The preceding lemma states this is essentially guaranteed by (237), at least for all $g = \exp \eta$, which, for many Lie groups, means all of G. Finally, (237) is guaranteed by

$$\{F_i, F_j\} = c_{ij}^k F_k, \tag{238}$$

where we used the notation introduced in (200) and (230). As an example, one may remark that the components of the angular momentum vector L satisfy the

commutation relations of the Lie algebra of SO(3), namely

$$\{L_i, L_j\} = \epsilon_{ijk} L_k, \quad i, j, k = 1, 2, 3.$$

One may therefore show that an action is Ad*-equivariant by showing (238) holds. However, in infinite dimension, this is not immediate since the necessary smoothness properties of the F_i's and even of the corresponding Hamiltonian vector fields are not readily verified.

Finally, an Ad^*-equivariant moment map may not exist. An easy example is $E = \mathbb{R}^2$, $G = \mathbb{R}^2$ and $\Phi : \mathbb{R}^2 \times \mathbb{R}^2 \to \mathbb{R}^2$ given by $\Phi_{(a,b)}(q, p) = (q + a, p - b)$. Identifying $\mathfrak{g} \simeq \mathbb{R}^2$ in the obvious way, this action has a moment map $F_1(q, p) = p, F_2(q, p) = q$ and $\{F_1, F_2\} = -1$. Since the group is commutative, it is clearly not Ad^*-equivariant. Ways to handle such situations exist, but we shall not deal with such complications in the main part of the text. We refer to [2, 67, 95] for details.

References

1. M.J. Ablowitz, P.A. Clarkson, *Solitons, Nonlinear Evolution Equations and Inverse Scattering*. London Mathematical Society Lecture Note Series, vol. 149 (Cambridge University Press, Cambridge, 1991). doi:10.1017/CBO9780511623998. http://dx.doi.org/10.1017/CBO9780511623998
2. R. Abraham, J.E. Marsden, *Foundations of Mechanics*, 2nd edn. (Benjamin/Cummings Publishing Co. Inc. Advanced Book Program, Reading, 1978) [Revised and enlarged, With the assistance of Tudor Rațiu and Richard Cushman]
3. R. Adami, D. Noja, Stability and symmetry-breaking bifurcation for the ground states of a NLS with a δ' interaction. Commun. Math. Phys. **318**(1), 247–289 (2013). doi:10.1007/s00220-012-1597-6. http://dx.doi.org/10.1007/s00220-012-1597-6
4. R. Adami, C. Cacciapuoti, D. Finco, D. Noja, Variational properties and orbital stability of standing waves for NLS equation on a star graph. J. Differ. Equ. **257**(10), 3738–3777 (2014). doi:10.1016/j.jde.2014.07.008. http://dx.doi.org/10.1016/j.jde.2014.07.008
5. J. Angulo Pava, *Nonlinear Dispersive Equations*. Mathematical Surveys and Monographs, vol. 156 (American Mathematical Society, Providence, 2009). doi:10.1090/surv/156. http://dx.doi.org/10.1090/surv/156 [Existence and stability of solitary and periodic travelling wave solutions]
6. V.I. Arnold, Mathematical methods of classical mechanics, in *Graduate Texts in Mathematics*, vol. 60 (Springer, New York, 1978) [Translated from the 1974 Russian original by K. Vogtmann and A. Weinstein, Corrected reprint of the second (1989) edition]
7. M.S. Baouendi, P. Ebenfelt, L.P. Rothschild, *Real Submanifolds in Complex Space and Their Mappings*. Princeton Mathematical Series (Princeton University Press, Princeton, 1999)
8. T.B. Benjamin, The stability of solitary waves. Proc. R. Soc. Lond. Ser. A **328**, 153–183 (1972)
9. H. Berestycki, P.L. Lions, Nonlinear scalar field equations. I. Existence of a ground state. Arch. Ration. Mech. Anal. **82**(4), 313–345 (1983). doi:10.1007/BF00250555. http://dx.doi.org/10.1007/BF00250555
10. J. Bona, On the stability theory of solitary waves. Proc. R. Soc. Lond. Ser. A **344**(1638), 363–374 (1975)
11. J.L. Bona, P.E. Souganidis, W.A. Strauss, Stability and instability of solitary waves of Korteweg-de Vries type. Proc. R. Soc. Lond. Ser. A **411**(1841), 395–412 (1987)

12. J. Bourgain, Fourier transform restriction phenomena for certain lattice subsets and application to nonlinear evolution equations. Geom. Funct. Anal. **3**(2), 107–156 (1993)
13. J. Boussinesq, *Essai sur la Théorie des Eaux Courantes* (Imprimerie National, Paris, 1877)
14. B. Buffoni, Existence and conditional energetic stability of capillary-gravity solitary water waves by minimisation. Arch. Ration. Mech. Anal. **173**(1), 25–68 (2004). doi:10.1007/s00205-004-0310-0. http://dx.doi.org/10.1007/s00205-004-0310-0
15. B. Buffoni, M.D. Groves, S.M. Sun, E. Wahlén, Existence and conditional energetic stability of three-dimensional fully localised solitary gravity-capillary water waves. J. Differ. Equ. **254**(3), 1006–1096 (2013). doi:10.1016/j.jde.2012.10.007. http://dx.doi.org/10.1016/j.jde.2012.10.007
16. T. Cazenave, Stable solutions of the logarithmic Schrödinger equation. Nonlinear Anal. **7**(10), 1127–1140 (1983). doi:10.1016/0362-546X(83)90022-6. http://dx.doi.org/10.1016/0362-546X(83)90022-6
17. T. Cazenave, *Semilinear Schrödinger Equations*. Courant Lecture Notes (American Mathematical Society, Providence, 2003)
18. T. Cazenave, P.L. Lions, Orbital stability of standing waves for some nonlinear Schrödinger equations. Commun. Math. Phys. **85**, 549–561 (1982)
19. P.R. Chernoff, J.E. Marsden, *Properties of Infinite Dimensional Hamiltonian Systems*. Lecture Notes in Mathematics, vol. 425 (Springer, Berlin, 1974)
20. E.A. Coddington, N. Levinson, *Theory of Ordinary Differential Equations* (McGraw-Hill, New York, 1955)
21. M. Colin, L. Jeanjean, M. Squassina, Stability and instability results for standing waves of quasi-linear Schrödinger equations. Nonlinearity **23**(6), 1353–1385 (2010). doi:10.1088/0951-7715/23/6/006. http://dx.doi.org/10.1088/0951-7715/23/6/006
22. A. Comech, D. Pelinovsky, Purely nonlinear instability of standing waves with minimal energy. Commun. Pure Appl. Math. **56**(11), 1565–1607 (2003). doi:10.1002/cpa.10104. http://dx.doi.org/10.1002/cpa.10104
23. A. Constantin, L. Molinet, Orbital stability of solitary waves for a shallow water equation. Phys. D **157**(1–2), 75–89 (2001). doi:10.1016/S0167-2789(01)00298-6. http://dx.doi.org/10.1016/S0167-2789(01)00298-6
24. A. Constantin, W.A. Strauss, Stability of peakons. Commun. Pure Appl. Math. **53**(5), 603–610 (2000). doi:10.1002/(SICI)1097-0312(200005)53:5<603::AID-CPA3>3.3.CO;2-C. http://dx.doi.org/10.1002/(SICI)1097-0312(200005)53:5<603::AID-CPA3>3.3.CO;2-C
25. A. Constantin, W.A. Strauss, Stability properties of steady water waves with vorticity. Commun. Pure Appl. Math. **60**(6), 911–950 (2007). doi:10.1002/cpa.20165. http://dx.doi.org/10.1002/cpa.20165
26. S. Cuccagna, A survey on asymptotic stability of ground states of nonlinear Schrödinger equations, in *Dispersive Nonlinear Problems in Mathematical Physics*. Quad. Mat., vol. 15 (Seconda Univ. Napoli, Caserta, 2004), pp. 21–57
27. S. Cuccagna, The Hamiltonian structure of the nonlinear Schrödinger equation and the asymptotic stability of its ground states. Commun. Math. Phys. **305**(2), 279–331 (2011). doi:10.1007/s00220-011-1265-2. http://dx.doi.org/10.1007/s00220-011-1265-2
28. S. Cuccagna, D.E. Pelinovsky, The asymptotic stability of solitons in the cubic NLS equation on the line. Appl. Anal. **93**(4), 791–822 (2014). doi:10.1080/00036811.2013.866227. http://dx.doi.org/10.1080/00036811.2013.866227
29. S. De Bièvre, S. Rota Nodari, Orbital stability of plane wave solutions of periodic nonlinear Schrödinger and Manakov equations (in preparation)
30. A. De Bouard, R. Fukuizumi, Stability of standing waves for nonlinear Schrödinger equations with inhomogeneous nonlinearities. Ann. Henri Poincaré **6**(6), 1157–1177 (2005). doi:10.1007/s00023-005-0236-6. http://dx.doi.org/10.1007/s00023-005-0236-6
31. M. Duflo, M. Vergne, Une propriété de la représentation coadjointe d'une algèbre de Lie. C. R. Acad. Sci. Paris **268**(A), 583–585 (1969)

32. N. Duruk Mutlubaş, A. Geyer, Orbital stability of solitary waves of moderate amplitude in shallow water. J. Differ. Equ. **255**(2), 254–263 (2013). doi:10.1016/j.jde.2013.04.010. http://dx.doi.org/10.1016/j.jde.2013.04.010
33. M. Ehrnström, M.D. Groves, E. Wahlén, On the existence and stability of solitary-wave solutions to a class of evolution equations of Whitham type. Nonlinearity **25**(10), 2903–2936 (2012). doi:10.1088/0951-7715/25/10/2903. http://dx.doi.org/10.1088/0951-7715/25/10/2903
34. E. Faou, L. Gauckler, C. Lubich, Sobolev stability of plane wave solutions to the cubic nonlinear Schrödinger equation on a torus. Commun. Partial Differ. Equ. **38**(7), 1123–1140 (2013)
35. E. Fermi, J. Pasta, S. Ulam, Studies of nonlinear problems. Los Alamos Scientific Laboratory Report No. LA-1940 (1955)
36. G. Fibich, X.P. Wang, Stability of solitary waves for nonlinear Schrödinger equations with inhomogeneous nonlinearities. Phys. D **175**(1–2), 96–108 (2003). doi:10.1016/S0167-2789(02)00626-7. http://dx.doi.org/10.1016/S0167-2789(02)00626-7
37. G. Floquet, Sur les équations différentielles linéaires à coefficients périodiques. Ann. Sci. École Norm. Sup. [2] **12**, 47–88 (1883)
38. R. Fukuizumi, Stability of standing waves for nonlinear Schrödinger equations with critical power nonlinearity and potentials. Adv. Differ. Equ. **10**(3), 259–276 (2005)
39. R. Fukuizumi, M. Ohta, Stability of standing waves for nonlinear Schrödinger equations with potentials. Differ. Integr. Equ. **16**(1), 111–128 (2003)
40. T. Gallay, M. Hărăgus, Orbital stability of periodic waves for the nonlinear Schrödinger equation. J. Dyn. Differ. Equ. **19**(4), 825–865 (2007)
41. T. Gallay, M. Hărăgus, Stability of small periodic waves for the nonlinear Schrödinger equation. J. Differ. Equ. **234**(2), 544–581 (2007)
42. C.S. Gardner, J.M. Greene, M.D. Kruskal, R.M. Miura, Method for solving the Korteweg-de Vries equation. Phys. Rev. Lett. **19**(19), 1095 (1967)
43. M. Gazeau, Analyse de modèles mathématiques pour la propagation de la lumière dans les fibres optiques en présence de biréfringence aléatoire. Ph.D. thesis, École Polytechnique (2012)
44. F. Genoud, Existence and orbital stability of standing waves for some nonlinear Schrödinger equations, perturbation of a model case. J. Differ. Equ. **246**, 1921–1943 (2009)
45. F. Genoud, Bifurcation and stability of travelling waves in self-focusing planar waveguides. Adv. Nonlinear Stud. **10**, 357–400 (2010)
46. F. Genoud, A smooth global branch of solutions for a semilinear elliptic equation on $\mathbb{R}^n$. Calc. Var. Partial Differ. Equ. **38**, 207–232 (2010)
47. F. Genoud, Bifurcation from infinity for an asymptotically linear problem on the half-line. Nonlinear Anal. **74**, 4533–4543 (2011)
48. F. Genoud, Orbitally stable standing waves for the asymptotically linear one-dimensional NLS. Evol. Equ. Control Theory **2**, 81–100 (2013)
49. F. Genoud, C.A. Stuart, Schrödinger equations with a spatially decaying nonlinearity: existence and stability of standing waves. Discrete Contin. Dyn. Syst. **21**, 137–186 (2008)
50. H. Goldstein, *Classical Mechanics*. Addison-Wesley Series in Physics, 2nd edn. (Addison-Wesley, Reading, 1980)
51. M. Grillakis, Linearized instability for nonlinear Schrödinger and Klein-Gordon equations. Commun. Pure Appl. Math. **41**(6), 747–774 (1988). doi:10.1002/cpa.3160410602. http://dx.doi.org/10.1002/cpa.3160410602
52. M. Grillakis, Analysis of the linearization around a critical point of an infinite-dimensional Hamiltonian system. Commun. Pure Appl. Math. **43**(3), 299–333 (1990). doi:10.1002/cpa.3160430302. http://dx.doi.org/10.1002/cpa.3160430302
53. M. Grillakis, J. Shatah, W. Strauss, Stability theory of solitary waves in the presence of symmetry. I. J. Funct. Anal. **74**(1), 160–197 (1987). doi:10.1016/0022-1236(87)90044-9. http://dx.doi.org/10.1016/0022-1236(87)90044-9

54. M. Grillakis, J. Shatah, W. Strauss, Stability theory of solitary waves in the presence of symmetry. II. J. Funct. Anal. **94**(2), 308–348 (1990). doi:10.1016/0022-1236(90)90016-E. http://dx.doi.org/10.1016/0022-1236(90)90016-E
55. H. Hajaiej, C.A. Stuart, On the variational approach to the stability of standing waves for the nonlinear Schrödinger equation. Adv. Nonlinear Stud. **4**, 469–501 (2004)
56. L. Jeanjean, S. Le Coz, An existence and stability result for standing waves of nonlinear Schrödinger equations. Adv. Differ. Equ. **11**(7), 813–840 (2006)
57. C.K.R.T. Jones, Instability of standing waves for nonlinear Schrödinger-type equations. Ergodic Theory Dyn. Syst. **8***(Charles Conley Memorial Issue), 119–138 (1988). doi:10.1017/S014338570000938X. http://dx.doi.org/10.1017/S014338570000938X
58. C.K.R.T. Jones, J.V. Moloney, Instability of standing waves in nonlinear optical waveguides. Phys. Lett. A **117**(4), 175–180 (1986). doi:http://dx.doi.org/10.1016/0375-9601(86)90734-6. http://www.sciencedirect.com/science/article/pii/0375960186907346
59. E. Kirr, A. Zarnescu, Asymptotic stability of ground states in 2D nonlinear Schrödinger equation including subcritical cases. J. Differ. Equ. **247**(3), 710–735 (2009). doi:10.1016/j.jde.2009.04.015. http://dx.doi.org/10.1016/j.jde.2009.04.015
60. C. Klein, J.C. Saut, IST versus PDE, a comparative study (2014). http://arxiv.org/abs/1409.2020
61. D.J. Korteweg, G. de Vries, On the change of form of long waves advancing in a rectangular canal, and on a new type of long stationary waves. Philos. Mag. **39**, 422–443 (1895)
62. P.D. Lax, Integrals of nonlinear equations of evolution and solitary waves. Commun. Pure Appl. Math. **21**(5), 467–490 (1968)
63. S. Le Coz, Standing waves in nonlinear Schrödinger equations, in *Analytical and Numerical Aspects of Partial Differential Equations* (Walter de Gruyter, Berlin, 2009), pp. 151–192
64. S. Le Coz, R. Fukuizumi, G. Fibich, B. Ksherim, Y. Sivan, Instability of bound states of a nonlinear Schrödinger equation with a Dirac potential. Phys. D **237**(8), 1103–1128 (2008). doi:10.1016/j.physd.2007.12.004. http://dx.doi.org/10.1016/j.physd.2007.12.004
65. M. Lemou, F. Méhats, P. Raphaël, Orbital stability of spherical galactic models. Invent. Math. **187**(1), 145–194 (2012). doi:10.1007/s00222-011-0332-9. http://dx.doi.org/10.1007/s00222-011-0332-9
66. E.M. Lerman, S.F. Singer, Stability and persistence of relative equilibria at singular values of the moment map. Nonlinearity **11**(6), 1637–1649 (1998). doi:10.1088/0951-7715/11/6/012. http://dx.doi.org/10.1088/0951-7715/11/6/012
67. P. Libermann, C.M. Marle, *Symplectic Geometry and Analytical Mechanics*. Mathematics and Its Applications, vol. 35 (D. Reidel Publishing Co., Dordrecht, 1987). doi:10.1007/978-94-009-3807-6. http://dx.doi.org/10.1007/978-94-009-3807-6 [Translated from the French by Bertram Eugene Schwarzbach]
68. P.L. Lions, The concentration-compactness principle in the calculus of variations. The locally compact case. I. Ann. Inst. H. Poincaré Anal. Non Linéaire **1**(2), 109–145 (1984). http://www.numdam.org/item?id=AIHPC_1984__1_2_109_0
69. A.M. Lyapunov, *Problème Général de la Stabilité du Mouvement* (Princeton University Press, Princeton, 1952) [French translation of the original manuscript published in Russian by the Mathematical Society of Kharkov in 1892]
70. M. Maeda, Stability and instability of standing waves for 1-dimensional nonlinear Schrödinger equation with multiple-power nonlinearity. Kodai Math. J. **31**(2), 263–271 (2008). doi:10.2996/kmj/1214442798. http://dx.doi.org/10.2996/kmj/1214442798
71. M. Maeda, Stability of bound states of Hamiltonian PDEs in the degenerate cases. J. Funct. Anal. **263**(2), 511–528 (2012). doi:10.1016/j.jfa.2012.04.006. http://dx.doi.org/10.1016/j.jfa.2012.04.006
72. A.I. Maimistov, Solitons in nonlinear optics. Quantum Electron. **40**(9), 756–781 (2010)
73. S.V. Manakov, On the theory of two-dimensional stationary self-focusing of electromagnetic waves. Sov. Phys. JETP **38**(2), 248–253 (1974)

74. J.E. Marsden, T.S. Ratiu, *Introduction to Mechanics and Symmetry*. Texts in Applied Mathematics, vol. 17 (Springer, New York, 1994). doi:10.1007/978-1-4612-2682-6. http://dx.doi.org/10.1007/978-1-4612-2682-6 [A basic exposition of classical mechanical systems]
75. Y. Martel, F. Merle, Asymptotic stability of solitons for subcritical generalized KdV equations. Arch. Ration. Mech. Anal. **157**(3), 219–254 (2001). doi:10.1007/s002050100138. http://dx.doi.org/10.1007/s002050100138
76. Y. Martel, F. Merle, Asymptotic stability of solitons of the subcritical gKdV equations revisited. Nonlinearity **18**(1), 55–80 (2005). doi:10.1088/0951-7715/18/1/004. http://dx.doi.org/10.1088/0951-7715/18/1/004
77. Y. Martel, F. Merle, Asymptotic stability of solitons of the gKdV equations with general nonlinearity. Math. Ann. **341**(2), 391–427 (2008). doi:10.1007/s00208-007-0194-z. http://dx.doi.org/10.1007/s00208-007-0194-z
78. Y. Martel, F. Merle, T.P. Tsai, Stability and asymptotic stability in the energy space of the sum of N solitons for subcritical gKdV equations. Commun. Math. Phys. **231**(2), 347–373 (2002). doi:10.1007/s00220-002-0723-2. http://dx.doi.org/10.1007/s00220-002-0723-2
79. Y. Martel, F. Merle, T.P. Tsai, Stability in H^1 of the sum of K solitary waves for some nonlinear Schrödinger equations. Duke Math. J. **133**(3), 405–466 (2006). doi:10.1215/S0012-7094-06-13331-8. http://dx.doi.org/10.1215/S0012-7094-06-13331-8
80. J. Montaldi, Persistence and stability of relative equilibria. Nonlinearity **10**(2), 449–466 (1997). doi:10.1088/0951-7715/10/2/009. http://dx.doi.org/10.1088/0951-7715/10/2/009
81. J. Montaldi, M. Rodríguez-Olmos, On the stability of Hamiltonian relative equilibria with non-trivial isotropy. Nonlinearity **24**(10), 2777–2783 (2011). doi:10.1088/0951-7715/24/10/007. http://dx.doi.org/10.1088/0951-7715/24/10/007
82. M. Ohta, Stability and instability of standing waves for one-dimensional nonlinear Schrödinger equations with double power nonlinearity. Kodai Math. J. **18**(1), 68–74 (1995). doi:10.2996/kmj/1138043354. http://dx.doi.org/10.2996/kmj/1138043354
83. J.P. Ortega, T.S. Ratiu, Stability of Hamiltonian relative equilibria. Nonlinearity **12**(3), 693–720 (1999). doi:10.1088/0951-7715/12/3/315. http://dx.doi.org/10.1088/0951-7715/12/3/315
84. G.W. Patrick, Relative equilibria in Hamiltonian systems: the dynamic interpretation of nonlinear stability on a reduced phase space. J. Geom. Phys. **9**(2), 111–119 (1992). doi:10.1016/0393-0440(92)90015-S. http://dx.doi.org/10.1016/0393-0440(92)90015-S
85. G.W. Patrick, M. Roberts, C. Wulff, Stability of Poisson equilibria and Hamiltonian relative equilibria by energy methods. Arch. Ration. Mech. Anal. **174**(3), 301–344 (2004). doi:10.1007/s00205-004-0322-9. http://dx.doi.org/10.1007/s00205-004-0322-9
86. R.L. Pego, M.I. Weinstein, Asymptotic stability of solitary waves. Commun. Math. Phys. **164**(2), 305–349 (1994). http://projecteuclid.org/euclid.cmp/1104270835
87. H. Poincaré, *Les Méthodes Nouvelles de la Mécanique Céleste, Tome I* (Gauthier-Villars et Fils, Paris, 1892)
88. M. Roberts, T. Schmah, C. Stoica, Relative equilibria in systems with configuration space isotropy. J. Geom. Phys. **56**(5), 762–779 (2006). doi:10.1016/j.geomphys.2005.04.017. http://dx.doi.org/10.1016/j.geomphys.2005.04.017
89. A. Shabat, V. Zakharov, Exact theory of two-dimensional self-focusing and one-dimensional self-modulation of waves in nonlinear media. Sov. Phys. JETP **34**, 62–69 (1972)
90. J. Shatah, Stable standing waves of nonlinear Klein-Gordon equations. Commun. Math. Phys. **91**(3), 313–327 (1983). http://projecteuclid.org/euclid.cmp/1103940612
91. J. Shatah, W. Strauss, Instability of nonlinear bound states. Commun. Math. Phys. **100**(2), 173–190 (1985). http://projecteuclid.org/euclid.cmp/1103943442
92. A. Soffer, Soliton dynamics and scattering, in *International Congress of Mathematicians*, vol. 3 (Eur. Math. Soc., Zürich, 2006), pp. 459–471
93. A. Soffer, M.I. Weinstein, Multichannel nonlinear scattering for nonintegrable equations. Commun. Math. Phys. **133**(1), 119–146 (1990). http://projecteuclid.org/euclid.cmp/1104201318

94. A. Soffer, M.I. Weinstein, Multichannel nonlinear scattering for nonintegrable equations. II. The case of anisotropic potentials and data. J. Differ. Equ. **98**(2), 376–390 (1992). doi:10.1016/0022-0396(92)90098-8. http://dx.doi.org/10.1016/0022-0396(92)90098-8
95. J.M. Souriau, *Structure of Dynamical Systems: A Symplectic View of Physics*. Progress in Mathematics, vol. 149 (Springer, New York, 1997)
96. M. Spivak, *A Comprehensive Introduction to Differential Geometry*, vol. 1, 2nd edn. (Publish or Perish Inc., Wilmington, 1979)
97. W.A. Strauss, Existence of solitary waves in higher dimensions. Commun. Math. Phys. **55**(2), 149–162 (1977)
98. C.A. Stuart, An introduction to elliptic equations on $\mathbb{R}^n$, in *Nonlinear Functional Analysis and Applications to Differential Equations (Trieste, 1997)* (World Science, River Edge, 1998), pp. 237–285
99. C.A. Stuart, Lectures on the orbital stability of standing waves and application to the nonlinear Schrödinger equation. Milan J. Math. **76**, 329–399 (2008)
100. C. Sulem, P.L. Sulem, *The Nonlinear Schrödinger Equation. Self-Focusing and Wave Collapse*. (Springer, New York, 1999)
101. T. Tao, *Nonlinear Dispersive Equations. Local and Global Analysis*. CBMS Regional Conf. Ser. Math. (American Mathematical Society, Providence, 2006)
102. T. Tao, Why are solitons stable? Bull. Am. Math. Soc. **46**(1), 1–33 (2009)
103. N. Vakhitov, A.A. Kolokolov, Stationary solutions of the wave equation in a medium with nonlinearity saturation. Radiophys. Quantum Electron. **16** (1973)
104. M.I. Weinstein, Lyapunov stability of ground states of nonlinear dispersive evolution equations. Commun. Pure Appl. Math. **39**(1), 51–67 (1986)
105. N.J. Zabusky, M.D. Kruskal, Interaction of solitons in a collisionless plasma and the recurrence of initial states. Phys. Rev. Lett. **15**(6), 240–243 (1965)
106. P.E. Zhidkov, *Korteweg-de Vries and Nonlinear Schrödinger Equations: Qualitative Theory*. Lecture Notes in Mathematics (Springer, Heidelberg, 2001)

High-Frequency Dynamics for the Schrödinger Equation, with Applications to Dispersion and Observability

Fabricio Macià

1 Introduction

1.1 The Schrödinger Equation

The dynamics of a quantum particle of mass $m = 1$ propagating under the influence of a real potential V is described by its *wave function* $\psi(t,x)$, which solves *Schrödinger's equation*:

$$i\hbar\partial_t\psi(t,x) + \frac{\hbar^2}{2}\Delta_x\psi(t,x) - V(x)\psi(t,x) = 0, \tag{1}$$

where $\hbar > 0$ is the normalized Planck's constant and Δ_x stands for the Laplace-Beltrami operator. On Euclidean space $\mathbb{R}^d$ this is:

$$\Delta_x = \sum_{j=1}^{d} \partial_{x_j}^2,$$

and, more generally, on a smooth Riemannian manifold (M,g), one has $\Delta_x = \operatorname{div}\left(\nabla_g \cdot\right)$ where the gradient and the divergence are taken with respect to the Riemannian metric g. In a local chart:

$$\Delta_x = \frac{1}{\sqrt{\det g}} \sum_{k,j=1}^{d} \partial_{x_j}\left(\sqrt{\det g}\, g^{kj}\partial_{x_k}\cdot\right),$$

F. Macià (✉)
Universidad Politécnica de Madrid, DCAIN, ETSI Navales, Avda. Arco de la Victoria, s/n. 28040 Madrid, Spain
e-mail: Fabricio.Macia@upm.es

C. Besse, J.-C. Garreau (eds.), *Nonlinear Optical and Atomic Systems*,
Lecture Notes in Mathematics 2146, DOI 10.1007/978-3-319-19015-0_4

where, following standard conventions, g stands for the matrix defining the Riemannian metric and $\left(g^{kj}\right) := g^{-1}$. This more general framework is the one we shall adopt here.

The wave function allows to construct a probability density $|\psi\,(t,x)|^2$ describing the probability of finding the quantum particle in an infinitesimal neighborhood of x at time t. In other words, the probability of finding the quantum particle in a region $U \subset M$ at time t is simply:

$$\int_U |\psi\,(t,x)|^2\,dx,$$

where dx stands for the Riemannian measure.

This problem is the quantum analog (or the *quantization*) of the classical Hamiltonian system corresponding to the Hamiltonian function

$$H : T^*M \longrightarrow \mathbb{R}, \qquad H\,(x,\xi) = \frac{1}{2}\,\|\xi\|_x^2 + V\,(x)\,, \tag{2}$$

defined on the cotangent bundle of M. This system is given by the Hamiltonian vector field, whose local expression is $X_H := \partial_\xi H \partial_x - \partial_x H \partial_\xi$ and whose trajectories are given by:

$$\begin{cases} \dot{x}\,(t) = \partial_\xi H\,(x\,(t)\,,\xi\,(t))\,, \\ \dot{\xi}\,(t) = -\partial_x H\,(x\,(t)\,,\xi\,(t))\,. \end{cases} \tag{3}$$

Under suitable assumptions on (M,g) and V (for instance, if (M,g) is geodesically complete and $V \in C^{1,1}\,(M;\mathbb{R})$ is bounded from below), system (3) defines a global flow on T^*M:

$$\phi_t^H : T^*M \longrightarrow T^*M, \qquad t \in \mathbb{R} \tag{4}$$

called the *Hamiltonian flow* of H. For any $(x_0,\xi_0) \in T^*M$, $\phi_t^H\,(x_0,\xi_0)$ is the unique solution to (3) with initial datum (x_0,ξ_0). When ϕ_t^H is globally defined in $t \in \mathbb{R}$, ϕ_t^H is called (*classically*) *complete*. When $V \equiv 0$, the classical flow is denoted by $\phi_t \equiv \phi_t^0$ and coincides with the geodesic flow of (M,g).

The rescaling $(t,x) \longmapsto (t/\hbar, x/\hbar)$ transforms equation (1) in the adimensional problem:

$$i\partial_t u\,(t,x) + \frac{1}{2}\Delta_x u\,(t,x) - V\,(x)\,u\,(t,x) = 0, \tag{5}$$

where, with a slight abuse of notation, V denotes again the rescaled potential. When the operator

$$\hat{H} := -\frac{1}{2}\Delta_x + V,$$

is essentially self-adjoint over $C_c^\infty(M)$, Stone's theorem (see for instance, [101]) ensures that $\hat{H}$ generates a group of unitary operators on $L^2(M)$, the *Schrödinger flow* associated to (M, g) and V, that we denote by:

$$e^{-it\hat{H}} : L^2(M) \longrightarrow L^2(M), \quad t \in \mathbb{R}. \tag{6}$$

In that case, given any initial datum $u_0 \in L^2(M)$, there exists a unique solution $u(t,\cdot) = e^{-it\hat{H}}u_0$ to (5) satisfying $u(0,\cdot) = u_0$. Moreover, the L^2-norm is conserved by the dynamics of the Schrödinger flow: for any $t \in \mathbb{R}$,

$$\|u(t,\cdot)\|_{L^2(M)} = \|u_0\|_{L^2(M)} := \left(\int_M |u_0(x)|^2\, dx\right)^{1/2}.$$

Therefore, as soon as $\|u_0\|_{L^2(M)} = 1$, the density $|u(t,\cdot)|^2$ defines a probability measure on M.

When $\hat{H}$ is not essentially self-adjoint, there is not a unique way to extend the dynamics from $C_c^\infty(M)$ to $L^2(M)$. Consequently, (5) is not well-posed (the reader can consult [100, 105] for a comprehensive account on the conditions on (M, g) and V that ensure that $\hat{H}$ is essentially self-adjoint). When $\hat{H}$ is essentially self-adjoint then $e^{-it\hat{H}}$ is said to be *quantum complete*. Quantum completeness is achieved, for instance, as soon as (M, g) is geodesically complete and $V \in L^\infty_{\mathrm{loc}}(M)$ is essentially bounded from below. The article [99] gives examples of systems for which ϕ_t^H is complete but $e^{it\hat{H}}$ is not, and viceversa. Therefore, classical and quantum completeness are independent notions.

In contrast to what happens in the classical setting (3), the linear, conservative character of problem (5) restricts considerably the class of dynamics that $e^{-it\hat{H}}$ can develop. The spectral theorem for self-adjoint operators establishes the existence of a Borel measure σ on $\mathbb{R}$ supported on the spectrum $\mathrm{sp}(\hat{H})$ of $\hat{H}$, as well as the existence of a unitary operator:

$$U : L^2(M) \longrightarrow L^2(\mathbb{R}, \sigma)$$

such that $e^{-it\hat{H}}$ is conjugated to a multiplication operator on $L^2(\mathbb{R}, \sigma)$:

$$Ue^{-it\hat{H}}U^* = e^{-its}. \tag{7}$$

Nonetheless, these objects are hard to compute explicitly, and even when this is possible, it is not always simple to extract from the spectral representation a useful description of the structure of the solutions to (5).

When $\mathrm{sp}(\hat{H})$ consists only of eigenvalues of $\hat{H}$, formula (7) takes a very simple form. This is the case, for instance, when M is compact. In the non compact case this issue is related to the growth of the potential at infinity (more precisely, with the fact that the resolvent $(\hat{H} - \lambda)^{-1}$ is a compact operator in $L^2(M)$ for some $\lambda \in \mathbb{R}$).

In that case, there exists an orthonormal basis $(\psi_n)_{n\in\mathbb{N}}$ of $L^2(M)$ consisting of eigenfunctions:

$$\hat{H}\psi_n = \lambda_n \psi_n.$$

In that case, $\sigma = \sum_{n\in\mathbb{N}} \delta_{\lambda_n}$ and

$$U : u \longmapsto (\hat{u}(\lambda_n))_{n\in\mathbb{N}},$$

where:

$$\hat{u}(\lambda_n) = (u|\psi_n)_{L^2(M)} := \int_M u(x)\,\overline{\psi_n(x)}dx.$$

Formula (7) takes the form:

$$e^{-it\hat{H}}u = \sum_{n\in\mathbb{N}} e^{-it\lambda_n}\hat{u}(\lambda_n)\,\psi_n. \tag{8}$$

This shows that any solution $e^{-it\hat{H}}u$ can be written as a superposition of plane waves $e^{-it\lambda_n}\psi_n$ of frequency λ_n. The dynamics of $e^{-it\hat{H}}$ are therefore quasi-periodic.

1.2 Some (More or Less) Explicit Examples

We next present some examples for which these objects can be computed to some extent.

- **The free Hamiltonian on** $\mathbb{R}^d$ ($(M, g) = (\mathbb{R}^d, \text{can})$ and $V \equiv 0$). In this case, one has:

$$e^{-it\hat{H}}u_0(x) = e^{it\Delta_x/2}u_0(x) = \frac{e^{-i\frac{\pi}{4}d\,\operatorname{sgn} t}}{(2\pi|t|)^{d/2}}\int_{\mathbb{R}^d} e^{i\frac{|x-y|^2}{2t}}u_0(y)\,dy. \tag{9}$$

  This formula is obtained by inverting the identity:

$$\hat{u}(t,\xi) = e^{-it|\xi|^2/2}\widehat{u_0}(\xi) \tag{10}$$

  for the Fourier transform of a solutions u:

$$\hat{u}(t,\xi) = \int_{\mathbb{R}^d} u(t,x)\,e^{-i\xi\cdot x}dx.$$

- **The harmonic oscillator** ($(M,g) = (\mathbb{R}^d,\text{can})$ and $V \equiv |x|^2$). The quantum Hamiltonian $\hat{H} = -\frac{1}{2}\Delta_x + |x|^2$ has purely discrete spectrum:

$$\lambda_n = \sqrt{2}\left(n + \frac{d}{2}\right), \quad n \in \mathbb{N},$$

its eigenfunctions are expressed in terms of Hermite polynomials and decay exponentially at infinity. It is clear from (8) that $e^{-it\hat{H}}$ is periodic in t, as happens for its classical counterpart ϕ_t^H.

- **The free Hamiltonian on the torus** $\mathbb{T}^d = \mathbb{R}^d/2\pi\mathbb{Z}^d$ ($(M,g) = (\mathbb{T}^d,\text{can})$ and $V \equiv 0$). The spectrum of $-\frac{1}{2}\Delta_x$ is explicit:

$$\lambda_k = \frac{|k|^2}{2}, \quad k \in \mathbb{Z}^d,$$

as well as the corresponding eigenfunctions:

$$\psi_k(x) := \frac{e^{ik\cdot x}}{(2\pi)^{d/2}}.$$

The representation formula (8) shows that $e^{it\Delta_x/2}$ is periodic in t. Note that this is not the case for its classical counterpart, the geodesic flow ϕ_t, when $d \geq 2$.

- **The free Hamiltonian on the sphere** $\mathbb{S}^d$ ($(M,g) = (\mathbb{S}^d, \text{can})$ and $V \equiv 0$). The spectrum of the Laplacian in this case is:

$$\lambda_n = n(n+d-1), \quad n \in \mathbb{N},$$

and its eigenfunctions, called *spherical harmonics*, are obtained by restricting to the sphere the harmonic polynomials in $\mathbb{R}^{d+1}$. In this case, both $e^{it\Delta_x/2}$ and ϕ_t are periodic.

- **The free Hamiltonian on a Zoll manifold.** A *Zoll manifold* is a manifold (M,g) all of whose geodesics are closed (see [18] for a comprehensive treatment of this type of geometry). The spectrum of the Laplacian is a union of clusters of the form:

$$C_n := \left\{ \left(\frac{2\pi}{L}\right)^2 \left(n + \frac{\beta}{4}\right)^2 + \rho_{n,j} : j = 1, \ldots, r_n \right\}, \tag{11}$$

with $r_n \in \mathbb{N}$, $|\rho_{n,j}| \leq K$ for every $n \in \mathbb{N}$ and some fixed values $\beta, K, L > 0$ depending on the geometry of (M,g). This expression is not as explicit as the previous ones. However, Precise asymptotic formulae for r_n for the statistical distribution of eigenvalues on each cluster C_n for $n \to \infty$ are known. The interested reader can consult [40, 48, 115, 117, 121, 122] for additional

information. Generically, $e^{it\Delta_x/2}$ is quasiperiodic, even though the geodesic flow is always periodic.

1.3 A First Approach to the Study of the Dynamics: The Correspondence Principle and the Semiclassical Regime

The correspondence principle states that the laws of quantum mechanics, valid at atomic scales, should tend to their classical counterparts in the high-frequency limit. For instance, if the characteristic length scale over which the potential V and the metric g vary significantly are much larger than the characteristic wave length of a solution $u(t,\cdot) = e^{-it\hat{H}}u_0$ to (5) then the probability density $|u(t,\cdot)|^2$ should follow a propagation law based on classical mechanics (i.e. the propagation should be related to the dynamics of the Hamiltonian flow ϕ_t^H).

Let us suppose that $M = \mathbb{R}^d$ and that we have normalized the problem in order to have that the characteristic wave length of the solution under consideration is equal to one. The potential varies at a macroscopic scale much larger than the wave length; suppose this scale is of order $1/h$ with $h \ll 1$. Therefore, if the microscopic variable for the position is x, the potential can be written in those variables as $V(hx)$. The corresponding Schrödinger equation is:

$$i\partial_t u(t,x) + \frac{1}{2}\Delta_x u(t,x) - V(hx)\,u(t,x) = 0.$$

If a change to macroscopic variables is performed:

$$t \longmapsto T = ht, \quad x \longmapsto X = hx, \quad u_h(T,X) = \frac{1}{h^{d/2}} u\left(\frac{T}{h}, \frac{X}{h}\right),$$

then the *semiclassical* Schrödinger equation is obtained:

$$ih\partial_T u_h(T,X) + \frac{h^2}{2}\Delta_X u_h(T,X) - V(X)\,u_h(T,X) = 0. \tag{12}$$

One expects that in the limit $h \longrightarrow 0^+$ the position density $|u_h(T,\cdot)|^2$ can be described in terms of ϕ_T^H. The reader should be aware of the fact that the parameter h cannot be identified to Planck's constant; this notation for the characteristic frequency may be unfortunate, but we maintain it as it is widely used in the literature.

Consider now the operator:

$$\hat{H}_h := -\frac{h^2}{2}\Delta_x + V(x)\,; \tag{13}$$

the propagator $e^{-i\frac{t}{h}\hat{H}_h}$ associated to (12) will be referred to as the *semiclassical Schrödinger flow*.

Among the first results obtained on the dynamics of the Schrödinger flow, we find those of Wentzel, Kramers and Brillouin in 1926, that dealt with the study of stationary solutions of the semiclassical Schrödinger equation:

$$\hat{H}_h \psi_h = E_h \psi_h,$$

and were aimed at describing the spectrum of $\hat{H}_h$. To that effect, they introduce the nowadays known as *WKB Ansatz*:

$$\psi_h(x) = a(x)\, e^{i\frac{S(x)}{h}},$$

where the amplitude a is obtained as a power series in h.

The time-dependent version of this ansatz that we next describe is due to Van Vleck [116]. The goal is to construct an approximate solution to the semiclassical Schrödinger (12) having the initial datum:

$$u_h^0(x) = a_0(x)\, e^{i\frac{S_0(x)}{h}}, \tag{14}$$

where, for instance, $a_0, S_0 \in C_c^\infty(M)$. One makes the following *Ansatz* on the form of the solution:

$$u_h(t,x) = e^{-i\frac{t}{h}\hat{H}_h} u_h^0(x) \sim a(t,x)\, e^{i\frac{S(t,x)}{h}} =: v_h(t,x).$$

The first step of the construction consists in introducing the expression for v_h in Eq. (12), and then grouping together those terms having the same power of h. One next imposes that each of the terms thus obtained must vanish. The nullity of the lowest order term implies that S must solve the *Hamilton-Jacobi* equation:

$$\partial_t S(t,x) + H(x, \nabla_x S(t,x)) = 0, \qquad S|_{t=0} = S_0; \tag{15}$$

and the nullity of the next term amounts to the fact that a is a solution to the transport equation:

$$\partial_t a + \nabla_x S \cdot \nabla_x a + \frac{1}{2} a \Delta_x S = 0, \qquad a|_{t=0} = a_0. \tag{16}$$

The Hamilton-Jacobi (15) does not have in general solutions that are globally defined in t. Therefore, $S(t,x)$ can be constructed for $|t| \leq T$; Duhamel's formula ensures then that the exact and approximate solutions are close to each other:

$$\lim_{h \to 0^+} \|u_h(t,\cdot) - v_h(t,\cdot)\|_{L^2(M)} = 0., \qquad |t| \leq T.$$

The position densities must satisfy, for $|t| \leq T$:

$$\lim_{h\to 0^+} |u_h(t,x)|^2 = \lim_{h\to 0^+} |v_h(t,x)|^2 = |a(t,x)|^2 .$$

One easily checks from (16) that $|a|^2$ solves the following transport equation:

$$\partial_t |a|^2 + \operatorname{div}\left(|a|^2 \nabla_x S\right) = 0, \qquad |a|^2|_{t=0} = |a_0|^2 .$$

If S solves (15) then the integral curves $x(t)$ of the gradient vector field $\nabla_x S(t,\cdot)$ with $x(0) = x_0$ are:

$$x(t) = \pi \circ \phi_t^H (x_0, \nabla_x S_0(x_0)) ,$$

where $\pi : T^*M \longrightarrow M$ is the projection onto the base. Define

$$\varphi_t(x) := \pi \circ \phi_t^H (x, \nabla_x S_0(x)) ,$$

then the following explicit formula for the limiting position density is obtained:

$$\lim_{h\to 0^+} |u_h(t,x)|^2 = |a(t,x)|^2 = \frac{\left|a_0\left(\varphi_t^{-1}(x)\right)\right|^2}{\left|\det d\varphi_t\left(\varphi_t^{-1}(x)\right)\right|}, \qquad |t| \leq T.$$

This makes precise the claim that, in the limit $h \to 0^+$ the dynamics of $|u_h(t,x)|^2$ is described by means of the classical Hamiltonian flow ϕ_t^H.

1.4 Semiclassical Analysis of the Non-semiclassical Problem

These notes are devoted to presenting an approach to the study of the high-frequency propagation of the position densities $|e^{-it\hat{H}} u_h^0|^2$ associated to solutions of the non-semiclassical Schrödinger equation (5) using tools arising from the study of the semiclassical propagator. The key observation in our analysis is the following.

Remark 1 The non-semiclassical propagator $e^{-it\hat{H}}$ can be expressed in terms of a certain semiclassical propagator as follows:

$$e^{-it\hat{H}} = e^{-i\frac{t}{h^2}\mathscr{H}_h}, \qquad \text{with } \mathscr{H}_h := -\frac{h^2}{2}\Delta_x + h^2 V.$$

Therefore, looking at $e^{-it\hat{H}}$ amounts to looking at a semiclassical equation at times of the order of $1/h$ with a potential of size h^2.

A precise statement of the problem we are interested in is given in Sect. 2, as well as its relevance to the study of other aspects of the dynamics of the Schrödinger flow, such as dispersive effects and unique continuation properties. In this regards, the reader can also consult the survey articles [8, 87].

Section 3 is devoted to introducing the main tools from semiclassical analysis that we shall need: semiclassical pseudodifferential operators, semiclassical measures, Egorov's theorem, etc.; these objects are used to prove our first results on high-frequency dynamics of Schrödinger flows in Sect. 4 and relate it to the dynamics of the Hamiltonian flow ϕ_t^H.

Finally, Sect. 5 presents the main ideas of the proof of the more advanced results of [9] based on two-microlocal analysis in the model case of the two-dimensional torus.

Acknowledgements These notes are an expanded version of the lectures given by the author at the Laboratoire Paul Painlevé of Université de Lille 1 during October 2013 in the framework of the CEMPI program. The author wishes to thank that institution for its warm hospitality and support.

2 The Compactness Approach to the Study of the Dynamics of the Schrödinger Flow

2.1 Description of the Problem

Instead of looking at the dynamics of a specific solution, we shall consider a sequence of solutions associated to some sequence of initial data:

$$(u_n^0), \qquad ||u_n^0||_{L^2(M)} = 1. \tag{17}$$

This approach is similar in spirit to the WKB method (14), except that no assumptions are made a priori on the form of the sequence of initial data. The corresponding solutions $u_n(t,\cdot) := e^{-it\hat{H}}u_n^0$ define a sequence of one-parameter probability densities:

$$\mathbb{R} \ni t \longmapsto |u_n(t,\cdot)|^2 \in \mathscr{P}(M),$$

where $\mathscr{P}(M)$ denotes the set of probability measures on M. Therefore, $|u_n|^2$ can be identified with an element of $L^\infty(\mathbb{R};\mathscr{P}(M))$, or more generally, to an element of $L^\infty(\mathbb{R};\mathscr{M}_+(M))$, where now $\mathscr{M}_+(M)$ stands for the cone of positive Radon measures on M.

The space $L^\infty(\mathbb{R}; \mathscr{M}_+(M))$ is compact for the weak $*$-topology[1]; hence there exist a subsequence $(u_{n'})$ and an element measure $\nu \in L^\infty(\mathbb{R}; \mathscr{M}_+(M))$ such that, for every $\varphi \in C_c(M)$ and every couple of real numbers $a < b$ one has:

$$\lim_{n' \to \infty} \int_a^b \int_M \varphi(x) |u_{n'}(t,x)|^2 dx dt = \int_a^b \int_M \varphi(x) \nu(t, dx) dt. \tag{18}$$

We shall denote by $\mathscr{M}$ the set of all measures $\nu \in L^\infty(\mathbb{R}; \mathscr{M}_+(M))$ obtained as a limit (18) as the sequence of initial data (u_n^0) varies among sequences satisfying (17). Note that, when M is compact since no mass can escape to infinity one has $\mathscr{M} \subseteq L^\infty(\mathbb{R}; \mathscr{P}(M))$.

Our goal will be to characterize the elements in $\mathscr{M}$. More precisely, we are interested in questions such as:

- How can an element of $\mathscr{M}$ be computed in terms of the sequence of initial data?
- Do the elements of $\mathscr{M}$ satisfy some kind of propagation law?
- Are the elements in $\mathscr{M}$ more regular than one would expect a priori?
- Are there any restrictions on the sets that are the support of an element of $\mathscr{M}$?

The last two questions are related to dynamical properties of the Schrödinger flow such as dispersive effects and unique continuation, respectively. The rest of this section will be devoted to elaborating on those connections.

Before doing that, let us anticipate that the answer to those questions is closely related to the global dynamics of the geodesic flow ϕ_t. In fact, the natural approach to this problem consists in lifting the measures $|u_n(t,\cdot)|^2$ to the cotangent bundle T^*M. This is done by using the theory of pseudodifferential operators and is described in Sect. 3.

Let us also mention that this problem is related to the study of concentration effects of high-frequency eigenfunctions (in the physics literature this is known as *scarring* phenomena). Denote by $\mathscr{M}_\infty$ the subset of $\mathscr{M}$ consisting of those ν that are obtained as a weak-$*$ limit (18) for some sequence of initial data (u_n^0) consisting of eigenfunctions of $\hat{H}$ with eigenfrequencies tending to infinity. In other words: $u_n^0 = \psi_n$ where:

$$\hat{H}\psi_n = \lambda_n \psi_n, \qquad \|\psi_n\|^2_{L^2(M)} = 1, \qquad \lim_{n \to \infty} \lambda_n = \infty.$$

Of course, $\mathscr{M}_\infty$ can be empty when M is non-compact. Note that every $\nu \in \mathscr{M}_\infty$ is constant in t, since:

$$|e^{-it\hat{H}}\psi_n|^2 = |e^{-it\lambda_n}\psi_n|^2 = |\psi_n|^2.$$

[1] Riesz's theorem implies that $L^\infty(\mathbb{R}; \mathscr{M}_+(M))$ can be identified to the dual of $L^1(\mathbb{R}; C_c(M))$; the weak-$*$ topology is induced by this duality.

The study of $\mathscr{M}_\infty$ on a compact manifold has been the object of a considerable effort in the last forty years. Clearly, as $\mathscr{M}_\infty \subseteq \mathscr{M}$, any result on the characterization of $\mathscr{M}$ will also be a result on $\mathscr{M}_\infty$. We shall come back to this problem in Sect. 4.4.

2.2 Dispersive Effects

The Schrödinger equation is a dispersive equation. This means that its solutions can be written as a superposition of waves that propagate at different speeds, that depend on the characteristic oscillation frequencies of the initial data. This can be readily seen, for instance, in the representation formula (8) that was obtained when M is compact. For $M = \mathbb{R}^d$ it is straightforward to obtain, from (10), the identity:

$$e^{it\Delta_x/2}u^0(x) = \int_{\mathbb{R}^d} \widehat{u^0}(\xi)\, e^{i\xi\cdot\left(x-t\frac{\xi}{2}\right)} \frac{d\xi}{(2\pi)^d}.$$

Above, $e^{it\Delta_x/2}u^0$ is written as a superposition of plane waves $e^{i\xi\cdot(x-t\xi/2)}$, propagating at velocity $\xi/2$. From the equivalent representation (9) on deduces the *dispersion estimate*:

$$\left\| e^{it\Delta_x/2}u^0 \right\|_{L^\infty\left(\mathbb{R}^d\right)} \leq \frac{C}{|t|^{d/2}} \left\| u^0 \right\|_{L^1\left(\mathbb{R}^d\right)}, \tag{19}$$

that quantifies the decay of solutions to the Schrödinger equation due to dispersive effects. Combining this estimate with the conservation of the $L^2(\mathbb{R}^d)$-norm, and applying the TT^* argument (see for instance [108]) one obtains the following estimate, known as a *Strichartz estimate*:

$$\left\| e^{it\Delta_x/2}u^0 \right\|_{L^p\left(\mathbb{R}_t\times\mathbb{R}^d_x\right)} \leq C \left\| u^0 \right\|_{L^2\left(\mathbb{R}^d\right)}, \tag{20}$$

where

$$p = p_d := 2\left(1+\frac{2}{d}\right). \tag{21}$$

This estimate shows that the singularities that any solution can develop (quantified through a L^p-norm) are "better" than one could expect using only the fact that $u^0 \in L^2\left(\mathbb{R}^d\right)$. These estimates play a key role in the well-posedness theory for semilinear Schrödinger equations, see for instance [30, 38, 59, 60, 108] .

It is very natural to try to understand the circumstances under which an estimate such as (20) remains valid when $\mathbb{R}^d$ is replaced by a more general Riemannian manifold (M, g). One must clarify how the geometry of M affects the dispersive character of the Schrödinger flow. When M is compact, a first difficulty arises: since

the dynamics of $e^{it\Delta_x/2}$ are quasiperiodic, it is not possible to obtain an estimate that is global in time, nor a decay estimate such as (19).

Even if (20) is replaced by an estimate that is local in time, there are situations in which the estimate fails for every $p > 2$, as is the case for the sphere $\mathbb{S}^2$, see [21].

In fact, the validity of a Strichartz estimate:

$$\left\| e^{it\Delta_x/2} u^0 \right\|_{L^p([a,b]\times M)} \leq C \left\| u^0 \right\|_{L^2(M)}, \tag{22}$$

on a compact manifold M is closely related to the regularity of the elements in $\mathscr{M}$. To see this, suppose that (22) holds for some $p > 2$, and let $\nu \in \mathscr{M}$ be obtained from a sequence of initial data (u_n^0) of norm one. Then (22) implies that the corresponding solutions (u_n) satisfy:

$$(|u_n|^2) \quad \text{is bounded in } L^{p/2}([a,b]\times M).$$

Therefore, the accumulation point ν must also belong to $L^{p/2}([a,b]\times M)$.

Proposition 1 *If the Strichartz estimate (22) holds for some $p > 2$ then, for every $\nu_t dt \in \mathscr{M}$ we have $\nu|_{t\in[a,b]} \in L^{p/2}([a,b]\times M)$. In particular, the projection onto M of the measures in $\mathscr{M}$ are absolutely continuous with respect to the Riemannian measure.*

As a consequence of this, if one is able to construct a sequence of initial data (u_n^0) that produce a measure $\nu \in \mathscr{M}$ that has a non trivial singular component, it automatically follows that the Strichartz estimate (22) fails for every $p > 2$.

Let us review some well-studied situations.

- **Zoll manifolds.** If (M, g) is a Zoll manifold then we shall see that $\delta_\gamma \in \mathscr{M}$ for every geodesic γ of M. This automatically proves that Strichartz estimates are always false in this case (see [87]). However, some frequency-dependent analogues of (22) still hold in this setting: i.e., when the $L^2(M)$-norm in the right hand side of (22) is replaced by a Sobolev norm $H^s(M)$) with $0 < s < 2^*$, where 2^* is the exponent given by the Sobolev injection. The interested reader should consult the series of articles [22–24].
- **The torus.** The situation is completely different for the torus $\mathbb{T}^d$ equipped with the flat metric. When $d = 1$, a classical argument by Zygmund [125] shows that (22) holds for $p = 4$. This is no longer the case if $d = 1$, $p = p_1 = 6$ or $d = 2$, $p = p_2 = 4$ which are the exponents corresponding to Euclidean space. Estimate (22) fails in those cases [28, 31] (see also [23]). We shall see later on that $\mathscr{M} \subseteq L^\infty\left(\mathbb{R}; L^1(M)\right)$ (see [9, 29]), which does not exclude in principle the validity of a Strichartz estimate in this case.
- **Negatively curved manifolds.** In the case of manifolds with negative curvature, the dispersive effect is stronger than in Euclidean space. The reader can find more details in [15, 19, 32].

2.3 Unique Continuation and Observability

Another aspect of the dynamics of the Schrödinger flow that is related to the structure of the elements of $\mathscr{M}$, is the validity of the *observability* property, a quantitative version of the unique continuation property that is of great importance in Control Theory [82], and Inverse Problems [70].

Let $T > 0$ and $U \subset M$ a non-empty open set; the Schrödinger flow $e^{it(\Delta_x/2-V)}$ on (M, g) satisfies the observability property for T and U if a constant $C = C(T, U) > 0$ exists such that the following estimate holds:

$$\left\|u^0\right\|^2_{L^2(M)} \leq C \int_0^T \int_U |e^{it(\Delta_x/2-V)} u^0(x)|^2 dxdt \tag{23}$$

for every initial datum $u^0 \in L^2(M)$. The Unique Continuation Property:

$$e^{it(\Delta_x/2-V)} u_0|_{(0,T)\times U} \equiv 0, u^0 \in L^2(M) \Longrightarrow u^0 = 0$$

follows immediately from (23). Notice, however, that (23) also implies a stronger stability result: two solutions that are close to each other in $(0, T) \times U$ (with respect to the norm $L^2((0, T) \times U)$) are close to each other globally.

A sufficient condition on U for the observability property to hold for every $T > 0$ is the *Geometric Control Condition*:

$$\begin{gathered} \text{There exists } L_U > 0 \text{ such that} \\ \text{every geodesic } (M, g) \text{ of length greater than } L_U \text{ intersects } \overline{U}. \end{gathered} \tag{24}$$

This result is due to Lebeau [78] (see also [49, 103]).

The validity of the observability estimate (23) is related to the structure of $\mathscr{M}$. The fact that (23) fails for some T and U is clearly equivalent to the existence of a sequence of initial data (u_n^0) such that:

$$||u_n^0||_{L^2(M)} = 1, \qquad \lim_{n\to\infty} \int_0^T \int_U |e^{it(\Delta_x/2-V)} u_n^0(x)|^2 dxdt = 0.$$

This in turn is equivalent to the existence of a $\nu \in \mathscr{M}$ such that:

$$\int_0^T \nu(t, U)\, dt = 0.$$

Therefore, the following must hold.

Proposition 2 *The observability estimate (23) holds for U and T if and only if for every $\nu \in \mathscr{M}$ one has*

$$\int_0^T \nu(t, U)\, dt \neq 0.$$

Taking this into account, it is easy to prove that (24) is necessary when (M, g) is a Zoll manifold (see [87]). This is again due to the fact that, for these geometries, one has $\delta_\gamma \in \mathscr{M}$ for every γ geodesic of (M, g). A proof of this fact will be given in Sect. 5.

However, this is a rather uncommon situation. For instance, if (M, g) is the flat torus $\mathbb{T}^d$, Jaffard has shown [71] (see also [36]), when $V \equiv 0$, that (23) holds for every open set U. This was further extended to the case $d = 2$, $V \in C(\mathbb{T}^2)$, see [37], the case V continuous except for a set of null measure and d arbitrary, see [9], and very recently to $d = 2$, $V \in L^{2+\varepsilon}(\mathbb{T}^2)$, see [17].

Analogously, in [12] it is shown that the observability property holds under conditions weaker than (24) for manifolds with negative curvature.

3 Pseudodifferential Operators and Semiclassical Measures

3.1 *Basic Notions from the Theory of Pseudodifferential Operators*

The theory of pseudodifferential operators has its origins in the works by Calderón and Zygmund [46] on singular integrals that appear, for instance, as resolvents of elliptic operators. The theory was shaped by Kohn-Nirenberg [75] and Hörmander [68]. Many books present a comprehensive introduction to the theory; the reader may consult for instance [2, 63, 69, 107, 110, 114]. We shall briefly review the aspects of the theory that will be useful in the sequel.

As it is customary in this context we shall use the notation:

$$D_{x_k} := \frac{1}{i}\partial_{x_k};$$

the Fourier transform of $D_{x_k} u$ is then:

$$\widehat{D_{x_k} u}\,(\xi) = \int_{\mathbb{R}^d} D_{x_k} u\,(x)\, e^{-i\xi\cdot x} dx = \xi_k \hat{u}\,(\xi)\,.$$

If $P\,(D_x)$ is a constant-coefficient differential operator of order N:

$$P\,(D_x)\,u\,(x) = \sum_{\alpha\in\mathbb{N}^d, |\alpha|\leq N} a_\alpha D_x^\alpha u\,(x)\,,$$

one clearly has:

$$\widehat{P\,(D_x)\,u}\,(\xi) = p\,(\xi)\,\hat{u}\,(\xi)\,, \quad \text{where } p\,(\xi) := \sum_{\alpha\in\mathbb{N}^d, |\alpha|\leq N} a_\alpha \xi^\alpha;$$

and applying the inverse Fourier transform, one obtains:

$$P(D_x)\,u(x) = \int_{\mathbb{R}^d}\int_{\mathbb{R}^d} p(\xi)\,u(y)\,e^{i\xi\cdot(x-y)}dy\frac{d\xi}{(2\pi)^d}.$$

This formula shows how to define an operator $a(x, D_x)$ for a function $a(x, \xi)$ that is not necessarily polynomial in ξ. One defines $a(x, D_x)$ as an *oscillatory integral*:

$$a(x, D_x)\,u(x) := \int_{\mathbb{R}^d}\int_{\mathbb{R}^d} a(x,\xi)\,u(y)\,e^{i\xi\cdot(x-y)}dy\frac{d\xi}{(2\pi)^d};$$

this expression is in principle only defined for $u \in C_c^\infty(\mathbb{R}^d)$; it can be extended to more general functions or distributions provided the integrals are interpreted in distributional sense.

Operators of the form $a(x, D_x)$ are called *pseudodifferential operators (ΨDO)*; the function $a(x, \xi)$ is the *symbol* of the operator $a(x, D_x)$. It is easy to check that if $a(x)$ does not depend on ξ the corresponding pseudodifferential operator coincides with the operator acting by multiplication by $a(x)$. When $a(\xi)$ does not depend on x, the corresponding pseudodifferential operator is usually called a *Fourier Multiplier*. The Calderón-Vaillancourt theorem [45] establishes that, for any $a \in C^\infty(\mathbb{R}^d \times \mathbb{R}^d)$ that is bounded, as well as its derivatives up to a certain order $K_d > 0$, the operator $a(x, D_x)$ is bounded on $L^2(\mathbb{R}^d)$ and

$$\|a(x, D_x)\|_{\mathscr{L}(L^2(\mathbb{R}^d))} \leq \sum_{\alpha\in\mathbb{N}^{2d},|\alpha|\leq K_d} \left\|D^\alpha_{x,\xi}a\right\|_{L^\infty(\mathbb{R}^d\times\mathbb{R}^d)}. \tag{25}$$

Moreover, as we shall see below, the composition of two ΨDO is again a ΨDO as well as the adjoint of any ΨDO.

3.2 Symbolic Calculus for Semiclassical Pseudodifferential Operators

Pseudodifferential operators can be viewed as quantizations of classical observables. A *quantization* procedure is a rule that associates to each classical observable $a(x, \xi)$ an operator $\mathrm{Op}(a)$ acting on $L^2(\mathbb{R}^d)$ (i.e. a quantum observable) in such a way that algebraic properties of the functions a (boundedness, positivity, Lie algebra structure, etc.) are reflected somehow in the operators $\mathrm{Op}(a)$. From this point of view, $\mathrm{Op}(a) = a(x, D_x)$ is a quantization rule, usually called the Kohn-Nirenberg or classical quantization rule. However, historically the first quantization procedure is slightly different from that; it is due to Weyl [118] and called the Weyl quantization rule. In some aspects, it is more satisfactory than the Kohn-Nirenberg quantization rule. A good introduction to the theory of pseudodifferential operators from the point of view of quantization rules is the book [54].

The form of the semiclassical Hamiltonian (13) suggests to introduce a class of pseudodifferential operators that involve a small parameter h. For instance, we could introduce operators of the form $a(x, hD_x)$. Instead of this, we shall work with Weyl quantization rule. Let $a \in \mathscr{S}'(\mathbb{R}^d \times \mathbb{R}^d)$ be a tempered distribution; the *semiclassical pseudodifferential operator* of symbol a, obtained by Weyl's quantization rule, acts on a function $u \in C_c^\infty(\mathbb{R}^d)$ as:

$$\begin{aligned} \mathrm{Op}_h(a)\, u(x) &= a^w(x, hD_x)\, u(x) \\ &:= \int_{\mathbb{R}^d} \int_{\mathbb{R}^d} a\left(\frac{x+y}{2}, h\xi\right) u(y)\, e^{i\xi\cdot(x-y)} dy \frac{d\xi}{(2\pi)^d}. \end{aligned}$$

This definition differs from the classical quantization $a(x, hD_x)$ in the symmetric role that x and y play in the oscillatory integral defining $a^w(x, hD_x)$. For instance, if $a(x, \xi) = b(x)\, \xi_j$ then:

$$a^w(x, hD_x) = \frac{1}{2}\left[b(x)\, hD_{x_j} + hD_{x_j} b(x)\right], \quad \text{but } a(x, hD_x) = b(x)\, hD_{x_j}.$$

The quantum semiclassical Hamiltonian (13) and the classical Hamiltonian (2) are related through:

$$\hat{H}_h = -\frac{h^2}{2}\Delta_x + V = \mathrm{Op}_h\left(\frac{1}{2}|\xi|^2 + V(x)\right) = \mathrm{Op}_h(H).$$

The theory of semiclassical pseudodifferential operators was developed in the seventies; many textbooks present this theory in a comprehensive way. Among others, we cite [50, 65, 88, 98, 124].

Many properties of the operators $\mathrm{Op}_h(a)$ rely on the particular smoothness properties of the symbol a. In many cases, the problem one is interested to solve determines the symbols class to be used. The following classes of symbols will suffice to our purposes:

$$\begin{aligned} S^k := \Big\{ & a \in C^\infty(\mathbb{R}^{2d} \times [0, h_0]) : \forall \alpha \in \mathbb{N}^{2d}, \exists C_\alpha > 0 \text{ t.q. } \left|\partial_z^\alpha a(z, h)\right| \\ & \leq C_\alpha \left(1 + |z|^2\right)^{k/2} \Big\}. \end{aligned}$$

Clearly, S^k contains all symbols of differential operators of order k with bounded, smooth coefficients. It should be noted from the very beginning that the class of operators under consideration does not depend on the choice of the quantization we have made. If $a \in S^k$ then there exists $b \in S^k$ such that:

$$a^w(x, hD_x, h) = b(x, hD_x, h),$$

and conversely.

In what follows we will not make explicit the dependence of the symbols on the small parameter h.

We next state some properties of semiclassical pseudodifferential operators.

1. $L^2(\mathbb{R}^d)$-*boundedness*. If $a \in S^0$ then $\mathrm{Op}_h(a)$ is a bounded operator on $L^2(\mathbb{R}^d)$ and

$$\|\mathrm{Op}_h(a)\|_{\mathscr{L}(L^2(\mathbb{R}^d))} \leq C \sum_{|\alpha| \leq M_d} \sup_{z \in \mathbb{R}^{2d}} \left|\partial_z^\alpha a(z)\right|, \tag{26}$$

   where M_d only depends on the dimension d.
2. *Regularizing operators*. If $a \in \mathscr{S}(\mathbb{R}^{2d})$ then

$$\mathrm{Op}_h(a) : L^2(\mathbb{R}^d) \longrightarrow H^s(\mathbb{R}^d)$$

   is bounded for every $s \in \mathbb{R}$.
3. *Adjoints*. Let $a \in S^k$ be real-valued. Then $\mathrm{Op}_h(a)$ is a self-adjoint operator on $L^2(\mathbb{R}^d)$:

$$\mathrm{Op}_h(a) = \mathrm{Op}_h(a)^*.$$

4. *Composition*. Let $a \in S^{k_1}$ and $b \in S^{k_2}$, then there exists $c \in S^{k_1+k_2}$ depending on a, b such that:

$$\mathrm{Op}_h(a)\,\mathrm{Op}_h(b) = \mathrm{Op}_h(c).$$

   If at least one of the symbols belongs to the Schwartz class $\mathscr{S}(\mathbb{R}^{2d})$ then[2]:

$$\mathrm{Op}_h(a)\,\mathrm{Op}_h(b) = \mathrm{Op}_h(ab) + \mathscr{O}_{\mathscr{L}(L^2(\mathbb{R}^d))}(h).$$

   The nontrivial proof of this fact is based on the *Stationary Phase principle* (see for instance [124]).
5. *Commutators*. Let a and b be as above, suppose that at least one of a or b belongs to $\mathscr{S}(\mathbb{R}^{2d})$; then the commutator $[\mathrm{Op}_h(a), \mathrm{Op}_h(b)] = \mathrm{Op}_h(a)\,\mathrm{Op}_h(b) - \mathrm{Op}_h(b)\,\mathrm{Op}_h(a)$ satisfies:

$$[\mathrm{Op}_h(a), \mathrm{Op}_h(b)] = \frac{h}{i}\,\mathrm{Op}_h(\{a, b\}) + \mathscr{O}_{\mathscr{L}(L^2(\mathbb{R}^d))}\left(h^3\right). \tag{27}$$

[2]Here and in what follows we shall use the notation $\mathscr{O}_{\mathscr{L}(L^2(\mathbb{R}^d))}(g(h))$ to denote a family of bounded operators on $L^2(\mathbb{R}^d)$ depending on the parameter h such that their operator norm is bounded by a uniform constant times $g(h)$.

The order h^3 of the remainder term is specific to the fact that we are using the Weyl quantizations procedure. It can be also shown that this formula is exact (i.e. the remainder $\mathcal{O}_{\mathscr{L}\left(L^2(\mathbb{R}^d)\right)}(h^3)$ is identically equal to zero) when either a or b is a polynomial of degree at most two.

These last three statements are part of what is usually known as the *symbolic calculus* of semiclassical ΨDO.

3.3 Operators on a Manifold

It is possible to define semiclassical ΨDO on a smooth manifold M. First note that it is straightforward to generalize the definition of the class of symbols S^k to functions that are defined on T^*M. To define $\mathrm{Op}_h(a)$ it suffices to take a partition of unity $(\chi_i)_{i\in I}$ subordinated to a locally finite covering of M by charts such that $\sum \chi_j^2 \equiv 1$ and define, for $a \in S^k$:

$$\mathrm{Op}_h(a)\, u = \sum_{j\in I} \mathrm{Op}_h\left(\chi_j a\right) \chi_j u;$$

each summand $\mathrm{Op}_h\left(\chi_j a\right)\chi_j u$ is defined through the formula on $\mathbb{R}^d$ in each chart. This definition is by no means intrinsic, it depends on the systems of charts used to define $\mathrm{Op}_h(a)$ as well as on the partition of unity. However, the difference between any two operators defined by this procedure from the same symbol a is a regularizing operator (see [124]).

The Laplacian on a Riemannian manifold (M, g) can be written in terms of pseudodifferential operators:

$$-h^2\Delta_x = \mathrm{Op}_h(H_0) + ih\,\mathrm{Op}_h(r) + h^2\,\mathrm{Op}_h(m), \tag{28}$$

where $m \in C^\infty(M)$ is a function of x alone, that only depends on the derivatives up to order to of the metric g. In a coordinate patch, the functions H_0 and r are given by:

$$H_0(x,\xi) := \sum_{i,j=1}^{d} g^{ij}(x)\,\xi_i\xi_j, \tag{29}$$

$$r(x,\xi) := \frac{1}{\sqrt{\det g(x)}} \sum_{i,j=1}^{d} g^{ij}(x)\,\partial_{x_i}\sqrt{\det g(x)}\xi_j. \tag{30}$$

Finally, let us recall that ΨDO are well-behaved regarding the functional calculus of self-adjoint operators. Given $\sigma \in C_c^\infty(\mathbf{R})$, the operator $\sigma\left(-h^2\Delta_x\right)$ defined using the spectral theorem can be written as:

$$\sigma\left(-h^2\Delta_x\right) = \mathrm{Op}_h(\sigma\circ H_0) + \mathcal{O}_{\mathscr{L}\left(L^2(M)\right)}(h). \tag{31}$$

When M is compact, a proof of this result can be found in [22]; the Euclidean version of this result can be found in [98], whereas [33] deals with some classes of non-compact manifolds.

3.4 Semiclassical Measures: Motivations

It is time to come back to the dynamics of the Schrödinger equation. Recall the definition of the semiclassical propagator and the WKB method presented in Sect. 1.3. Motivated by that, we are going to try to generalize that analysis to more general classes of initial data. More precisely, we are interested in understanding the propagation law obeyed by the weak-$*$ limits $\nu(t,\cdot)$ of a sequence of probability densities:

$$\nu_n(t,\cdot) := |e^{-i\frac{t}{h_n}\hat{H}_{h_n}} u_n^0|^2$$

corresponding to a sequence of initial data $\left(u_n^0\right)$ with $\left\|u_n^0\right\|_{L^2(M)} = 1$, and a sequence (h_n) of positive real numbers tending to zero. This problem is different than the one presented in Sect. 2.1; in the one we are considering here, t is the order of one, whereas in the one described in Sect. 2.1, t is taken of the order of $1/h_n$ (recall the discussion in Sect. 1.4).

The major drawback in trying to analyze $\nu_n(t,\cdot)$ directly comes from the fact that the accumulation points of (ν_n) do not obey a closed propagation law. In other words, the limiting measure $\nu(t,\cdot)$ is not going to be, in general, completely determined by the measure $\nu(0,\cdot)$ corresponding to the sequence of initial data. This can be easily verified for $M = \mathbb{R}^d$ and $V = 0$.

Let $(x_0,\xi_0) \in \mathbb{R}^d \times \mathbb{R}^d$ and consider the sequence of initial data:

$$u_h^0(x) = \frac{1}{(\pi h)^{d/4}} e^{-\frac{|x-x_0|^2}{2h}} e^{i\frac{\xi_0}{h}\cdot x}. \tag{32}$$

This type of sequence is usually known as a *wave-packet* or a *coherent state* centered at (x_0,ξ_0). As $h \longrightarrow 0^+$ the sequence (u_h^0) concentrates near x_0 and oscillates rapidly in the direction of ξ_0. It is straightforward to check that:

$$\left|u_h^0(x)\right|^2 = \frac{1}{(\pi h)^{d/2}} e^{-\frac{|x-x_0|^2}{h}} \rightharpoonup \delta_{x_0}(x), \quad \text{as } h \longrightarrow 0^+,$$

where δ_{x_0} is the Dirac mass centered at x_0. Notice that this result is independent of the choice of the direction of oscillation ξ_0.

Using the representation formula (9) one gets:

$$|e^{-i\frac{t}{h}\hat{H}_h}u_h^0|^2 = |e^{iht\Delta_x/2}u_h^0|^2$$
$$= \frac{1}{(\pi h\,(1+t^2))^{d/2}}e^{-\frac{|x-x_0-t\xi_0|^2}{h(1+t^2)}} \rightharpoonup \delta_{x_0+t\xi_0}(x)\,, \quad \text{as } h \longrightarrow 0^+, \tag{33}$$

which indeed does depend on ξ_0. Therefore, there is no hope to find a propagation law for $\nu(t,\cdot) = \delta_{x_0+t\xi_0}$ solely in terms of $\nu(0,\cdot) = \delta_{x_0}$.

3.5 Semiclassical Measures, Definition

The preceding discussion shows the need of finding an object that detects, in addition to the asymptotic behavior of the sequence in physical space, the characteristic frequencies of oscillations developed by the sequence. This leads to the definition of *semiclassical* or *Wigner measures*.

In order to properly motivate the definition that follows, it is convenient to shift a little bit our point of view. Given a function $u \in L^2\left(\mathbb{R}^d\right)$, the action of the measure $|u|^2$ on a test function $\varphi \in C_c(\mathbb{R}^d)$ can be written as follows:

$$\int_{\mathbb{R}^d} \varphi(x)\,|u(x)|^2\,dx = \left(m_\varphi u|u\right)_{L^2\left(\mathbb{R}^d\right)}, \tag{34}$$

where m_φ denotes the operator acting on $L^2(\mathbb{R}^d)$ by multiplication by φ, and $(\cdot|\cdot)_{L^2\left(\mathbb{R}^d\right)}$ is the scalar product in $L^2(\mathbb{R}^d)$. The operator m_φ somewhat localizes a function u in the x-variable, but the expected value $\left(m_\varphi u|u\right)_{L^2\left(\mathbb{R}^d\right)}$ destroys the structure of the oscillations developed by u. In order to keep track of this structure, one should replace m_φ by an operator that localizes simultaneously in x and ξ (in other words, by an operator that localizes in phase-space $T^*\mathbb{R}^d = \mathbb{R}^d \times \mathbb{R}^d$). This is precisely what a pseudodifferential operator $\mathrm{Op}_h(a)$ achieves when $a \in C_c^\infty(\mathbb{R}^d \times \mathbb{R}^d)$.

Therefore, this leads to replacing (34) by:

$$\left(\mathrm{Op}_h(a)\,u|u\right)_{L^2\left(\mathbb{R}^d\right)}. \tag{35}$$

Using the boundedness of $\mathrm{Op}_h(a)$, Eq. (26), it follows that the mapping:

$$w_u^h : C_c^\infty(\mathbb{R}^d \times \mathbb{R}^d) \ni a \longmapsto \left(\mathrm{Op}_h(a)\,u|u\right)_{L^2\left(\mathbb{R}^d\right)} \in \mathbb{C}$$

is a distribution $w_u^h \in \mathscr{D}'(\mathbb{R}^d \times \mathbb{R}^d)$. This object was introduced by Wigner in [119] and is known as the *Wigner distribution of* u (although the terms Wigner function

or Wigner transform are also used). One easily checks that w_u^h has the following expression:

$$w_u^h(x,\xi) = \int_{\mathbb{R}^d} u\left(x - \frac{h}{2}v\right)\overline{u\left(x + \frac{h}{2}v\right)}e^{i\xi\cdot v}\frac{dv}{(2\pi)^d}.$$

Notice that:

$$\int_{\mathbb{R}^d} w_u^h(x,\xi)\,d\xi = |u(x)|^2, \quad \int_{\mathbb{R}^d} w_u^h(x,\xi)\,dx = \frac{1}{(2\pi h)^d}\left|\hat{u}\left(\frac{\xi}{h}\right)\right|^2,$$

hence, w_u^h contains more information than $|u|^2$ does; in particular, it keeps track of the oscillations of u via the modulus square of the semiclassical Fourier transform:

$$\mathscr{F}_h u(\xi) = \frac{1}{(2\pi h)^{d/2}}\hat{u}\left(\frac{\xi}{h}\right).$$

However, w_u^h is not positive in general.[3]

It follows from (26) that for a sequence (u_n) bounded in $L^2\left(\mathbb{R}^d\right)$ and a *scale* (h_n), i.e. a positive sequence of real numbers tending to zero,

$$(w_{u_n}^{h_n}) \text{ is a bounded sequence in } \mathscr{D}'(\mathbb{R}^d\times\mathbb{R}^d).$$

Therefore, the sequence $(w_{u_n}^{h_n})$ has at least an accumulation point $\mu \in \mathscr{D}'(\mathbb{R}^d\times\mathbb{R}^d)$ as $n \longrightarrow \infty$ (with respect to the inductive limit weak topology in $\mathscr{D}'$). In spite of the fact that the distributions $w_{u_n}^{h_n}$ are not, in general, positive, the accumulation points μ always are.

Theorem 1 ([55, 57, 83]) *Let μ be an accumulation point of $(w_{u_n}^{h_n})$ in $\mathscr{D}'(\mathbb{R}^d\times\mathbb{R}^d)$. Then μ is a finite, positive, Radon measure on $\mathbb{R}^d\times\mathbb{R}^d$.*

In that case, one says that μ is a *semiclassical measure* or *Wigner measure* of the sequence (u_n). This definition extends in a natural way to sequences in $L^2(M)$, where M is a smooth manifold equipped with a Riemannian metric. It suffices to replace $\mathrm{Op}_h(a)$ in (35) by the pseudodifferential operator associated to a tes symbols $a \in C_c^\infty(T^*M)$. Note that, although the operators $\mathrm{Op}_h(a)$ are not intrinsically defined on M, the difference between any two different realizations of $\mathrm{Op}_{h_n}(a)$ is a term that tends to zero as $n \longrightarrow \infty$ in operator norm. This shows that the accumulation points of $(w_{u_n}^{h_n})$ are intrinsically defined on T^*M.

It is possible to define similar objects using non-semiclassical ΨDO of the form $\mathrm{Op}_1(a)$ with $a(x,\xi)$ zero-homogeneous at infinity in the variable ξ. Historically,

[3]The Wigner distribution of u is positive if and only if $u(x) = ce^{ib\cdot x}e^{-(Ax\cdot x)}$ for some matrix A symmetric and positive definite, see [54].

that construction precedes the one presented here, and was performed independently by Gérard [56] and Tartar [109], and the corresponding limiting measures were respectively called *Microlocal Defect Measures* and *H-measures*. Those authors were originally motivated by problems arising from the study of the defect of compactness of bounded sequences in L^2 due to oscillation and concentration phenomena that appear in numerous problems in the Calculus of Variations and the theory of P.D.E., see for instance [80, 81].

3.6 Semiclassical Measures, Properties and Examples

We next describe some relevant properties of semiclassical measures. The reader may consult [61] for a systematic presentation of the theory, as well as the survey article [35]. We start by describing to what extent semiclassical measures are able to describe the limit of the position densities $|u_n|^2$.

In this section, (h_n) will denote a sequence of positive real numbers that tends to zero as $n \longrightarrow \infty$. In what follows, we shall use the term *scale* to refer to a sequence with those properties.

Let (u_n) be a bounded sequence in $L^2(M)$ and suppose that:

$$|u_n|^2 \rightharpoonup \nu, \quad \text{as } n \longrightarrow \infty, \tag{36}$$

in the weak$*$ topology of Radon measures. Suppose moreover that μ is a semiclassical measure of (u_n), that is:

$$w_{u_n}^{h_n} \rightharpoonup \mu, \quad \text{as } n \longrightarrow \infty, \tag{37}$$

weakly in $\mathscr{D}'(T^*M)$. The measures μ and ν are related by:

$$\int_{T^*M} a(x)\, \mu(dx, d\xi) \leq \int_M a(x)\, \nu(dx), \tag{38}$$

for every non-negative $a \in C_c(M)$. In general, equality in (38) may not hold. This is due to the non-compactness of T^*M which allows some loss of mass of $(w_{u_n}^{h_n})$ at infinity as $|\xi| \longrightarrow \infty$.

The following definition characterizes precisely those sequences for which this loss of mass does not occur. A sequence (u_n) bounded in $L^2(M)$ is h_n-oscillating provided that, for every $\varphi \in C_c^\infty(M)$ the following holds:

$$\limsup_{n\longrightarrow\infty} \left\| \mathbb{1}_{[R,\infty)}(-h_n^2\Delta_x)\varphi u_n \right\|_{L^2(M)} \longrightarrow 0, \quad \text{as } R \longrightarrow \infty. \tag{39}$$

Here, $\mathbb{1}_{[R,\infty)}(s)$ denotes the characteristic function of the interval $[R,\infty)$; the operator $\mathbb{1}_{[R,\infty)}(-h_n^2\Delta_x)$ is the one given by the spectral theorem.

The meaning of condition (39) when $M = \mathbb{R}^d$ is simply:

$$\limsup_{n\longrightarrow\infty} \int_{|\xi|\geq R/h_n} \left|\widehat{\varphi u_n}\left(\xi\right)\right|^2 d\xi \longrightarrow 0, \quad \text{as } R \longrightarrow \infty;$$

whereas, if M is compact and $\left(\lambda_j\right)$ are the eigenvalues of $-\Delta_x$ indexed in increasing order, (39) simply states that:

$$\limsup_{n\longrightarrow\infty} \sum_{\lambda_j\geq R/h_n^2} \left|\widehat{u_n}\left(\lambda_j\right)\right|^2 \longrightarrow 0, \quad \text{as } R \longrightarrow \infty.$$

Intuitively, this condition prevents that a fraction of the L^2-norm of (u_n) may concentrate on frequencies of order greater than $1/h_n^2$. One should notice that any sequence (u_n) bounded in $L^2\left(M\right)$ is h_n-oscillating for a suitable choice of the scale (h_n).

On the other hand, we shall say that (u_n) is *compact at infinity* provided that:

$$\limsup_{n\longrightarrow\infty} \int_{M\setminus K_n} \left|u_n\left(x\right)\right|^2 dx \longrightarrow 0, \quad \text{as } n \longrightarrow \infty,$$

where (K_n) is a sequence of compact sets whose union is the whole M.

Theorem 2 *Suppose that (u_n) satisfies (36) and (37). Then the following statements hold:*

(i) *(u_n) is h_n-oscillating if and only if:*

$$\nu\left(x\right) = \int_{T_x^*M} \mu\left(x, d\xi\right).$$

(ii) *If (u_n) is h_n-oscillating and compact at infinity then:*

$$\lim_{n\to\infty} \left\|u_n\right\|_{L^2(M)}^2 = \mu\left(T^*M\right).$$

(iii) *If (u_n) is h_n-oscillating and compact at infinity then:*

$$\mu = 0 \Longleftrightarrow (u_n) \text{ converges strongly to } 0 \text{ in } L^2\left(M\right).$$

(iv) *If $u_n \rightharpoonup u$ as $n \longrightarrow \infty$ in $L^2\left(M\right)$ then:*

$$\mu\left(x,\xi\right) \geq \left|u\left(x\right)\right|^2 \delta_0\left(\xi\right).$$

(v) *If (v_n) is a sequence in $L^2\left(M\right)$ with a semiclassical measure μ' satisfying $\mu \perp \mu'$ then:*

$$u_n v_n \rightharpoonup 0, \quad \text{as } n \longrightarrow \infty \text{ in } \mathscr{D}'\left(M\right). \tag{40}$$

We refer the reader to [55, 61, 62, 83] for a proof. We next present some explicit computations of semiclassical measures in $M = \mathbb{R}^d$. In the examples that follow, $a \in L^2(\mathbb{R}^d)$ and (ε_n) is a scale.

1. *Convergent sequence*. Suppose $u_n \longrightarrow u$ strongly in $L^2(M)$. Then,

$$\mu(x,\xi) = |u(x)|^2 \delta_0(\xi).$$

2. *Oscillating sequence*. Let

$$u_n(x) := a(x) e^{ix\cdot\xi_0/\varepsilon_n}.$$

Then[4]

$$\mu(x,\xi) = \begin{cases} |a(x)|^2 dx\delta_0(\xi) \text{ if } h_n \ll \varepsilon_n, \\ |a(x)|^2 dx\delta_{\xi_0}(\xi) \text{ if } h_n = \varepsilon_n, \\ 0 \text{ if } h_n \gg \varepsilon_n. \end{cases}$$

3. *Concentrating sequence*. Let

$$u_n(x) := \frac{1}{(\varepsilon_n)^{d/2}} a\left(\frac{x-x_0}{\varepsilon_n}\right).$$

Then

$$\mu(x,\xi) = \begin{cases} \|a\|^2_{L^2(\mathbb{R}^d)} \delta_{x_0}(x)\delta_0(\xi) \text{ if } h_n \ll \varepsilon_n, \\ \delta_{x_0}(x)|\hat{a}(\xi)|^2 \dfrac{d\xi}{(2\pi)^d} \text{ if } h_n = \varepsilon_n, \\ 0 \text{ if } h_n \gg \varepsilon_n. \end{cases}$$

4. *Wave-packet or Coherent state*. Let

$$u_n(x) := \frac{1}{(\varepsilon_n)^{d/2}} a\left(\frac{x-x_0}{\varepsilon_n}\right) e^{ix\cdot\xi_0/h_n}, \tag{41}$$

with $h_n \ll \varepsilon_h$. Then:

$$\mu(x,\xi) = \|a\|^2_{L^2(\mathbb{R}^d)} \delta_{x_0}(x)\delta_{\xi_0}(\xi).$$

5. *W.K.B. state*. Let

$$u_n(x) = a(x) e^{i\frac{S(x)}{h_n}}.$$

[4]Here we use the notation $h_n \ll \varepsilon_n$ (resp. $h_n \gg \varepsilon_n$) do express that $\lim_{n\to\infty} h_n/\varepsilon_n = 0$ (resp. $\lim_{n\to\infty} h_n/\varepsilon_n = \infty$).

Then:

$$\mu(x,\xi) = |a(x)|^2 \, dx \delta_{\nabla_x S(x)}(\xi),$$

meaning that

$$\int_{\mathbb{R}^d \times \mathbb{R}^d} b(x,\xi) \, \mu(dx, d\xi) = \int_{\mathbb{R}^d} b(x, \nabla_x S(x)) \, |a(x)|^2 \, dx.$$

Notice that, as soon as $h_n \ll \varepsilon_n$ or $h_n = \varepsilon_n$, all the above sequences are h_n-oscillating. All these examples illustrate how the semiclassical measure is able to capture simultaneously oscillation and concentration effects developed by a sequence (u_n). This key property makes semiclassical measures a suitable object to study the semiclassical approximation.

4 Semiclassical Measures and the Schrödinger Flow

4.1 Semiclassical Propagation and Egorov's Theorem

We now return to the study of the dynamics of the semiclassical Schrödinger flow. Recall that the semiclassical Schrödinger equation reads:

$$ih\partial_t u_h + \hat{H}_h u_h = 0, \tag{42}$$

where $\hat{H}_h = -\frac{h^2}{2}\Delta_x + V$.

Let (u_n^0) be a sequence of initial data such that $\left\|u_n^0\right\|_{L^2(M)} = 1$ which is h_n-oscillating. Recall that one of the central questions in the semiclassical approximation and the correspondence principle (see Sect. 1.3) is to compute the weak-$*$ limit $\nu(t,\cdot)$ of the sequence of probability densities associated to the corresponding solutions to the semiclassical Schrödinger equation:

$$|e^{-i\frac{t}{h_n}\hat{H}_{h_n}} u_n^0|^2. \tag{43}$$

It is not difficult to check that for any $t \in \mathbb{R}$, the sequence $(e^{-i\frac{t}{h_n}\hat{H}_{h_n}} u_n^0)$ is also h_n-oscillating. Therefore, because of Theorem 2, in order to obtain $\nu(t,\cdot)$ it suffices to compute the semiclassical measures associated to $e^{-i\frac{t}{h_n}\hat{H}_{h_n}} u_n^0$. Denote by $w_n(t)$ the Wigner distribution of $e^{-i\frac{t}{h_n}\hat{H}_{h_n}} u_n^0$. It turns out that the weak-$*$ accumulation points of $w_n(t)$ satisfy a propagation law that involves the classical Hamiltonian $H(x,\xi) = \frac{1}{2}\|\xi\|_x^2 + V(x)$.

Theorem 3 ([55, 62, 83]) *Suppose that $(w_n(0) = w^{h_n}_{u_n})$ converges to the semiclassical measure $\mu_0 \in \mathscr{M}_+(T^*M)$. Then, for every $t \in \mathbb{R}$, $(w_n(t))$ converges to a semiclassical measure $m(t,\cdot)$ that solves the transport equation:*

$$\frac{d}{dt}\int_{T^*M} a(x,\xi)\, m(t,dx,d\xi) = \int_{T^*M} \{H,a\}(x,\xi)\, m(t,dx,d\xi)\,. \tag{44}$$

Therefore, $m(t,\cdot)$ is described by the formula:

$$\int_{T^*M} a(x,\xi)\, m(t,dx,d\xi) = \int_{T^*M} a\left(\phi^H_t(x,\xi)\right)\mu_0(dx,d\xi)\,. \tag{45}$$

The propagation law (44) simply states that $m(t,\cdot)$ is a weak solution (in the sense of distribution) of Liouville's equation:

$$\partial_t m + \{H,m\} = 0.$$

Note also that identity (45) is equivalent to the fact that $m(t,\cdot)$ is obtained as the push-forward of μ_0 along ϕ^H_t; this is usually written as:

$$m(t,\cdot) = \left(\phi^H_t\right)_* \mu_0.$$

Using the h_n-oscillation property of the solutions and Theorem 2, (i) we deduce that $m(t,\cdot)$ is given by the following Corollary.

Corollary 1 *Suppose the hypotheses of Theorem 3 hold. Then one has, for every $t \in \mathbb{R}$ and $\varphi \in C_c(M)$:*

$$\lim_{n\to\infty}\int_M \varphi(x)\,|e^{-i\frac{t}{h_n}\hat{H}_{h_n}}u^0_n|^2 dx = \int_{T^*M}\varphi\left(\pi\left(\phi^H_t(x,\xi)\right)\right)\mu_0(dx,d\xi)\,,$$

where $\pi : T^*M \longrightarrow M$ is the canonical projection.

With this result in mind, we can generalize the computation made in (3.4) for $M = \mathbb{R}^d$ and $V \equiv 0$ to the general case. Let $(x_0,\xi_0) \in T^*M$ and define, locally on a chart,

$$u^0_n(x) := \frac{1}{(h_n)^{d/4}} a\left(\frac{x-x_0}{\sqrt{h_n}}\right) e^{ix\cdot\xi_0/h_n},$$

where $\|a\|_{L^2(M)} = 1$. Then (41) implies that

$$\mu_0(x,\xi) = \delta_{x_0}(x)\,\delta_{\xi_0}(\xi)\,.$$

As a direct consequence of (45) we deduce:

$$m(t,\cdot) = \left(\phi^H_t\right)_*\mu_0 = \delta_{\phi^H_t(x_0,\xi_0)},$$

and, by Corollary 1, for every $t \in \mathbb{R}$:

$$\lim_{n\to\infty} |e^{-i\frac{t}{h_n}\hat{H}_{h_n}} u_n^0|^2 = \delta_{x(t)},$$

where $x(t) = \pi\left(\phi_t^H(x_0, \xi_0)\right)$.

We next sketch the main ideas of the proof of Theorem 3, as they lie on the basis of further developments.

A straightforward computation shows that $w_n(t)$ solves *Wigner's equation*:

$$\frac{d}{dt}\langle w_n(t), a\rangle_{\mathscr{D}'\times C_c^\infty} = \frac{i}{h_n}([\hat{H}_{h_n}, \mathrm{Op}_{h_n}(a)]e^{-i\frac{t}{h_n}\hat{H}_{h_n}} u_n^0 | e^{-i\frac{t}{h_n}\hat{H}_{h_n}} u_n^0)_{L^2(M)}, \tag{46}$$

for every $a \in C_c^\infty(T^*M)$. When $M = \mathbb{R}^d$ this equation admits a simpler, closed expression, on w_n:

$$\partial_t w_n + \xi \cdot \nabla_x w_n - \mathscr{L}_V^{h_n} w_n = 0,$$

where $\mathscr{L}_V^h$ is the integral operator acting on functions $f \in C_c^\infty(\mathbb{R}^d \times \mathbb{R}^d)$ by:

$$\mathscr{L}_V^h f(x,\xi) := i\int_{\mathbb{R}^d}\int_{\mathbb{R}^d}\left[V\left(x - \frac{hv}{2}\right) - V\left(x + \frac{hv}{2}\right)\right] f(x,\eta)\, e^{i(\xi-\eta)\cdot v} dv \frac{dv}{(2\pi)^d};$$

Using the commutator identity (27) in the symbolic calculus we conclude that:

$$\frac{d}{dt}\langle w_n(t), a\rangle_{\mathscr{D}'\times C_c^\infty} = \langle w_n(t), \{H, a\}\rangle_{\mathscr{D}'\times C_c^\infty} + \mathscr{O}(h_n),$$

where the remainder is $\mathscr{O}(h_n)$ locally uniformly bounded in t. This identity shows that the distributions $(w_n(t))$ form an equilipschitz family with respect to t. Hence, it is possible to apply a diagonal extraction argument and conclude that $(w_n(t))$ converges for every t along some subsequence, showing (44).

Equivalently, one can obtain (44) as a consequence of Egorov's theorem (see, for instance, [124] for a proof). This result shows that conjugation of $\mathrm{Op}_{h_n}(a)$ by the semiclassical propagator amounts to transporting the symbol a along the classical flow ϕ_t^H.

Theorem 4 (Egorov) *For every $a \in C_c^\infty(T^*M)$ there exists a family $R_h(t)$ of bounded operators on $L^2(M)$ such that:*

$$e^{i\frac{t}{h}\hat{H}_h}\,\mathrm{Op}_h(a)\, e^{-i\frac{t}{h}\hat{H}_h} = \mathrm{Op}_h\left(a \circ \phi_t^H\right) + R_h(t), \tag{47}$$

where $\|R_h(t)\|_{\mathscr{L}(L^2(M))} \leq \rho(|t|)\, h$ *for some continuous function* $\rho : \mathbb{R}_+ \longrightarrow \mathbb{R}_+$. *If* $M = \mathbb{R}^d$ *and* H *is a polynomial in* (x, ξ) *of degree at most two, then* $R_h \equiv 0$.

At this point, the reader should remember the problem that was the main object of these notes, as described in Sect. 2.1, namely the study of those probability measures that arise as accumulation points of sequences of position densities associated to solutions to the non-semiclassical Schrödinger equation (5). As already noticed in Remark 1, the non-semiclassical Schrödinger equation can be rewritten as a semiclassical problem provided the time scaling $t \rightsquigarrow t/h$ is performed.

Remark 2 For an initial datum $u^0 \in L^2(M)$, the corresponding solution u to (5) can be written as:

$$u(t,\cdot) = e^{-it\hat{H}}u^0 = e^{i\frac{t}{h^2}\left(\frac{h^2}{2}\Delta - h^2 V\right)}u^0 =: v_h(t/h,\cdot),$$

where v_h is a solution to the semiclassical problem:

$$ih\partial_t v_h + \frac{h^2}{2}\Delta v_h - h^2 V v_h = 0.$$

The corresponding Wigner distributions are related by:

$$w_u^h(t) = w_{v_h}^h(t/h).$$

Therefore, Egorov's theorem implies that understanding the dynamics of $w_u^h(t)$ requires:

1. understanding the long-time dynamics of ϕ_t^H;
2. controlling the time behavior of the remainder term $R_h(t)$ for $t \sim 1/h$ in (47).

4.2 The Ehrenfest Time

We shall now address the issue of understanding the influence of the long-time dynamics of ϕ_t^H in the behavior of the Wigner distributions $w_n(t)$. Let us come back to the explicit computation that was performed in Sect. 3.4 for $M = \mathbb{R}^d$ and $V \equiv 0$. We showed that the position densities associated to a Gaussian wave-packet (32) followed the explicit propagation law (33). That formula showed, in particular, that the propagated object is again a Gaussian wave-packet of width $\sqrt{h(1+t^2)}$. Therefore, for times $t \sim h^{-1/2}$ the width of the wave-packet is of order one, and there is no hope that for $t \gg h^{-1/2}$ the position densities converge to a Dirac mass.

This behavior is better seen at the level of the Wigner distributions $w_h(t)$. In this setting, Egorov's theorem is exact and,

$$w_h(t,x,\xi) = w_h(0, x - t\xi, \xi);$$

one can compute $w_h(0,\cdot)$ explicitly in this case [assuming that (u_h^0) is a gaussian wave-packet centered at (x_0,ξ_0) of the form (32)]:

$$w_h(t,x,\xi) = \frac{1}{(\pi h)^d} e^{-\frac{|x-x_0-t\xi|^2}{h}} e^{-\frac{|\xi-\xi_0|^2}{h}}.$$

For $a \in C_c^\infty\left(\mathbb{R}^d \times \mathbb{R}^d\right)$ a Taylor expansion shows the following:

$$\begin{aligned}\langle w_h(t,\cdot), a\rangle &= \frac{1}{\pi^d}\int_{\mathbb{R}^{2d}} a\left(x_0 + t\xi_0 + \sqrt{h}(x+t\xi), \xi_0 + \sqrt{h}\xi_0\right) e^{-|x|^2-|\xi|^2} dx d\xi \\ &= a\left(\phi_t^{H_0}(x_0,\xi_0)\right) + \mathcal{O}\left(\sqrt{h}(1+|t|)\right),\end{aligned}$$

where $\phi_t^{H_0}$ is the classical flow corresponding to the free Hamiltonian. Therefore, the convergence $w_h(t,\cdot) \rightharpoonup \delta_{\phi_t^{H_0}(x_0,\xi_0)}$ takes place uniformly on intervals of the form $|t| \leq h^{-1/2+\varepsilon}$ for every $\varepsilon > 0$. A larger time intervals, the dispersive nature of the classical flow enters into play and it is no longer possible to describe the dynamics of $w_h(t,\cdot)$ solely in terms of $\phi_t^{H_0}$.

Let us assume now that V is not identically zero; the preceding computation gives in this setting:

$$\int_{\mathbb{R}^{2d}} a(z)\, w_h\left(0, \phi_{-t}^H(z)\right) dz = \int_{\mathbb{R}^{2d}} a\left(\phi_t^H(z)\right) \frac{1}{(\pi h)^d} e^{-\frac{|z-z_0|^2}{h}} dz$$

where $z_0 = (x_0,\xi_0)$. As expected, this converges to $\delta_{\phi_t^H(z_0)}$ locally uniformly in t. In order to find the size (in terms of h) of the time intervals for which the convergence is uniform, we must estimate:

$$D_H(t,a) := \int_{\mathbb{R}^{2d}} \left(a\left(\phi_t^H(z)\right) - a\left(\phi_t^H(z_0)\right)\right) \frac{1}{(\pi h)^d} e^{-\frac{|z-z_0|^2}{h}} dz \tag{48}$$

A standard computation shows:

$$|D_H(t,a)| \leq h^{1/2} \int_{\mathbb{R}^{2d}} \sup_{w\in\mathbb{R}^{2d}} \left\|d_w a\left(\phi_t^H(w)\right)\right\| \frac{|z-z_0|}{h^{1/2}} e^{-\frac{|z-z_0|^2}{h}} \frac{dz}{(\pi h)^d},$$

and

$$h^{1/2} \int_{\mathbb{R}^{2d}} \sup_{w\in\mathbb{R}^{2d}} \left\|d_w a\left(\phi_t^H(w)\right)\right\| |z| \frac{1}{\pi^d} e^{-|z|^2} dz \leq C h^{1/2} e^{|t|\Gamma},$$

as soon as

$$\left\|d_w \phi_t^H(w)\right\| \leq M e^{|t|\Gamma}.$$

The coefficient $\Gamma \geq 0$ is the Liapunov exponent of ϕ_t^H; it measures the maximal expansion rate of the flow ϕ_t^H a along the unitary unstable directions of the dynamics (see [74] for additional details).

This leads to introducing the following distinguished time-scale:

$$T_{\mathrm{E}}^h := \frac{1}{2\Gamma} \log\left(\frac{1}{h}\right). \tag{49}$$

At times $t \sim T_{\mathrm{E}}^h$ the difference (48) is of order one; whereas for $|t| \leq (1-\varepsilon)\, T_{\mathrm{E}}^h$ the difference (48) is of the order of h^ε and tends to zero as $h \longrightarrow 0^+$. The smallest time scale that enjoys the property is known as the *Ehrenfest time*; when $\Gamma > 0$ the Ehrenfest time is precisely T_{E}^h; for the free Hamiltonian, it is $h^{-1/2}$.

Note that, in the previous computation, the remainder term $R_h(t)$ given by Ergorov's theorem (Theorem 4) has been ignored. However, a careful analysis shows, [20, 34, 44, 66, 67] that $w_h(t,\cdot)$ converges to $\delta_{\phi_t^H(x_0,\xi_0)}$ in intervals of the form $|t| \leq (1-\varepsilon)\, T_{\mathrm{E}}^h$.

As seen in the case of the free Hamiltonian, the logarithmic scale T_{E}^h does not always coincide with the Ehrenfest time. The articles [47, 76] show that this scale is indeed optimal for some hyperbolic systems, in the sense that for time-scales greater than T_{E}^h, the Wigner distributions $w_h(t,\cdot)$ associated to a coherent state do not converge to the Dirac mass centered at the corresponding classical trajectory.

4.3 Beyond the Eherenfest Time

We now turn to the problem of describing the global in time dynamics of the Wigner distributions $w_n(t,\cdot)$, corresponding to a sequence $(e^{-i\frac{t}{h_n}\hat{H}_{h_n}} u_n^0)$ of solutions to the semiclassical Schrödinger equation (12). This issue is intimately related to the problem proposed in Sect. 2.1, as explained in Remark 2.

Let us fix a time scale $\tau = (\tau_n)$ with $\lim_{n\to\infty} \tau_n = \infty$ (we will be particularly interested in the case $\tau_n = 1/h_n$, see Remark 2). One may ask in general whether or not it is possible to describe the dynamics of $w_n(t,\cdot)$ uniformly in intervals of the form $|t| \leq \tau_n$. The answer to this question is affirmative as soon as τ_n is asymptotically smaller or comparable to $(1-\varepsilon)\, T_{\mathrm{E}}^{h_n}$; however, this problem can be very complicated as soon as $\tau_n \gg T_{\mathrm{E}}^{h_n}$. An example of this is given by the flat torus: Wigner distributions are explicit, although very complicated oscillating sums whose pointwise behavior is hard to study, due to interferences caused by superposition of different terms. The case of negatively curved compact surfaces provides also examples of explicit constructions. In this setting, it is possible to construct coherent states whose evolution is explicit up to times $\tau_n \sim h_n^{-2}$ [94], Schubert (2007, Semiclassical wave propagation for large times, http://www.maths.bris.ac.uk/~marcvs/publications.html, unpublished), whose Wigner distributions have a very complicated structure. Moreover, as we shall immediately see, Wigner

distributions do not converge to a limiting object on general intervals of the form $[-\tau_n, \tau_n]$, for τ_n big enough.

However, this question becomes more tractable if we perform an average with respect to t. Instead of considering the pointwise behavior of $w_n(t,\cdot)$ we can analyze the behavior of the means:

$$\frac{1}{2\tau_n}\int_{-\tau_n}^{\tau_n} w_n(t,\cdot)\,dt = \frac{1}{2}\int_{-1}^{1} w_n(\tau_n s,\cdot)\,ds. \tag{50}$$

At this point notice that $w_n(\tau_n s,\cdot)$ is nothing but the Wigner distribution associated to the time-rescaled solution to the Schrödinger equation:

$$e^{-i\frac{\tau_n}{h_n}s\hat{H}_{h_n}}u_n^0.$$

Therefore, computing the accumulation points of the time averages (50) amounts to performing the semiclassical limit $h_n \longrightarrow 0^+$ and simultaneously letting time go to infinity as $t = \tau_n s \longrightarrow \infty$.

Set $w_n^{\tau_n}(t,\cdot) := w_n(\tau_n t,\cdot)$; the convergence of $(w_n^{\tau_n}(t,\cdot))$ in average sense is easy to establish. In fact, $(w_n^{\tau_n})$ is bounded in $L^\infty(\mathbb{R};\mathscr{D}'(T^*M))$ since

$$||e^{-i\frac{\tau_n}{h_n}s\hat{H}_{h_n}}u_n^0||_{L^2(M)} = ||u_n^0||_{L^2(M)} = 1,$$

and, for any compact set $K \subset T^*M$ and every $a \in L^1(\mathbb{R};C_c^\infty(T^*M))$ such that $\operatorname{supp} a(t,\cdot) \subset K$ for a.e. $t \in \mathbb{R}$, one has:

$$\begin{aligned}\left|\int_{\mathbb{R}}\left\langle w_n^{\tau_n}(t,\cdot),a(t,\cdot)\right\rangle dt\right| &\leq C_K\sup_{t\in\mathbb{R}}||e^{-i\frac{\tau_n}{h_n}t\hat{H}_{h_n}}u_n^0||_{L^2(M)}^2\int_{\mathbb{R}}\|a(t,\cdot)\|_{C^{d+1}(T^*M)}\,dt\\ &\leq C_K\,\|a\|_{L^1(\mathbb{R};C^{d+1}(T^*M))},\end{aligned}$$

for some constant $C_K > 0$ depending only of d and K. At this point one can invoke the Banach-Alaoglu theorem to conclude that $(w_n^{\tau_n})$ is a relatively compact set in $L^\infty(\mathbb{R};\mathscr{D}'(T^*M))$ when equipped with the weak-$*$ topology. In particular, we can extract a subsequence from $(w_n^{\tau_n})$, which we shall not relabel and a distribution $\mu \in L^\infty(\mathbb{R};\mathscr{D}'(T^*M))$ such that:

$$\begin{aligned}&\lim_{n\to\infty}\int_{\mathbb{R}}\int_{T^*M}a(t,x,\xi)\,w_n^{\tau_n}(t,dx,d\xi)\,dt\\ &\quad=\int_{\mathbb{R}}\int_{T^*M}a(t,x,\xi)\,\mu(t,dx,d\xi)\,dt,\ \ \forall a\in L^1\left(\mathbb{R};C_c^\infty\left(T^*M\right)\right).\end{aligned} \tag{51}$$

Similarly as we did in Sect. 2.1, we denote by $\tilde{\mathscr{M}}(\tau)$ the set consisting in all distributions $\mu \in L^\infty(\mathbb{R};\mathscr{D}'(T^*M))$ that are obtained as an accumulation point, for the weak-$*$ topology in $L^\infty(\mathbb{R};\mathscr{D}'(T^*M))$, of some sequence of Wigner

distributions of the form $(w_n^{\tau_n})$ associated to a sequence of initial data (u_n^0) that is normalized in $L^2(M)$ and is h_n-oscillating in the sense of (39).

Theorem 5 ([85]) *Let τ be a time scale. Then the set $\tilde{\mathscr{M}}(\tau)$ is contained $L^\infty(\mathbb{R}; \mathscr{M}_+(T^*M))$. Moreover, every $\mu \in \tilde{\mathscr{M}}(\tau)$ is invariant by the classical flow: for a.e. $t \in \mathbb{R}$ and every $s \in \mathbb{R}$,*

$$\mu(t,\cdot) = \left(\phi_s^H\right)_* \mu(t,\cdot).$$

If, in addition, μ is obtained from a sequence of initial data (u_n^0) then:

$$\lim_{n\to\infty} \int_a^b \int_M \varphi(x) \left|e^{i\frac{\tau_n}{h_n} t\hat{H}_{h_n}} u_n^0\right|^2(x)\, dxdt = \int_a^b \int_{T^*M} \varphi(x)\, \mu(t, dx, d\xi)\, dt, \tag{52}$$

for every $a < b$ and $\varphi \in C_c(M)$.

If M is compact, then property (52) automatically implies that $\mu(t,\cdot)$ is a probability measure for a.e. $t \in \mathbb{R}$. Therefore, in this case $\tilde{\mathscr{M}}(\tau) \subset L^\infty(\mathbb{R}; \mathscr{P}(T^*M))$.

When $\hat{H}_h = \frac{h^2}{2}\Delta - h^2 V$ and $\tau_h = 1/h$ (which corresponds to study the non-semiclassical case, see Remark 2), the set $\tilde{\mathscr{M}}(1/h)$ determines the set $\mathscr{M}$ introduced in Sect. 2.1. To see this, simply note that given any sequence (u_n^0) that is normalized in $L^2(M)$, it is always possible to find a sequence (h_n) of positive real numbers that tends to zero such that

$$\lim_{n\longrightarrow\infty} \left\| \mathbb{1}_{[1,\infty)}(-h_n^2\Delta_x) u_n \right\|_{L^2(M)} = 0;$$

in other words, it is always possible to find (h_n) such that (u_n^0) is h_n-oscillating. Then, identity (52) implies that the elements of $\mathscr{M}$ are obtained by projecting those of $\tilde{\mathscr{M}}(1/h_n)$ onto M.

The following result, whose proof can be found in [1], deals with the dependence of $\tilde{\mathscr{M}}(\tau)$ on the time scale (τ_n).

Proposition 3 *Let (τ_n) and (σ_n) be time scales tending to infinity as $n \longrightarrow \infty$ such that $\lim_{n\to\infty} \sigma_n/\tau_n = 0$. Then for every $\mu \in \tilde{\mathscr{M}}(\tau)$ and almost every $t \in \mathbb{R}$ there exist $\mu^t \in \operatorname{Conv} \tilde{\mathscr{M}}(\sigma)$ such that*

$$\mu(t,\cdot) = \int_0^1 \mu^t(s,\cdot)\, ds. \tag{53}$$

Above, $\operatorname{Conv} \tilde{\mathscr{M}}(\sigma)$ denotes the convex hull of $\tilde{\mathscr{M}}(\sigma)$. As a consequence of this result, we see that if $\sigma_n \ll \tau_n$, then the measures in $\tilde{\mathscr{M}}(\tau)$ can be constructed using those in $\tilde{\mathscr{M}}(\sigma)$. Therefore, $\tilde{\mathscr{M}}(\tau)$ is somewhat decreasing with respect to the scale τ.

The problem of characterizing $\tilde{\mathscr{M}}(\tau)$ when $\tau_n \gg T_{\mathrm{E}}^{h_n}$ on an arbitrary Riemannian manifold can be very complex. In order to get some insight in it, let

us first assume that the convergence of the Wigner distributions $w_n(t,\cdot)$ to their corresponding semiclassical measures $m(t,\cdot) = \left(\phi_t^H\right)_* \mu_0$, as given by Theorem 3, is uniform in the interval $t \in [-\tau_n, \tau_n]$. Then, necessarily, for any $a \in C_c^\infty(T^*M)$ we would have:

$$\begin{aligned}\lim_{n\to\infty} \int_{-1}^{-1} \int_{T^*M} a(x,\xi)\, w_n^{\tau_n}(t, dx, d\xi)\, dt \\ = \lim_{n\to\infty} \frac{1}{\tau_n} \int_{-\tau_n}^{\tau_n} \int_{T^*M} a(x,\xi)\, w_n(t, dx, d\xi)\, dt \\ = \lim_{n\to\infty} \int_{T^*M} \langle a \rangle_{\tau_n}(x,\xi)\, \mu_0(dx, d\xi),\end{aligned}$$

where, recall, $\mu_0 = \mu(0,\cdot)$ stands for the semiclassical measure of the sequence of initial data and:

$$\langle a \rangle_T(x,\xi) := \frac{1}{T} \int_{-T}^{T} a\left(\phi_s^H(x,\xi)\right) ds.$$

Therefore, under the assumption that the convergence of $w_n(t,\cdot)$ to $m(t,\cdot)$ is uniform for $t \in [-\tau_n, \tau_n]$, the time averages (50) converge to:

$$\int_{-1}^{-1} \int_{T^*M} a(x,\xi)\, \mu(t, dx, d\xi)\, dt = \lim_{n\to\infty} \int_{T^*M} \langle a \rangle_{\tau_n}(x,\xi)\, \mu_0(dx, d\xi), \tag{54}$$

where μ is a weak-$*$ accumulation point of $w_n^{\tau_n}$.

If

$$\langle a \rangle(x,\xi) := \lim_{T\to\infty} \langle a \rangle_T(x,\xi) \quad \text{exists } \mu_0\text{-almost everywhere}, \tag{55}$$

then (54) implies:

$$\int_{-1}^{-1} \int_{T^*M} a(x,\xi)\, \mu(t, dx, d\xi)\, dt = \int_{T^*M} \langle a \rangle(x,\xi)\, \mu_0(dx, d\xi). \tag{56}$$

To summarize, we have showed that under the assumption that $w_n(t,\cdot)$ converges uniformly in $t \in [-\tau_n, \tau_n]$, the measure μ satisfies (56) provided one of the two following statements holds.

1. $\lim_{T\to\infty} \langle a \rangle_T(x,\xi)$ exists for every $(x,\xi) \in T^*M$ (for instance, when H is completely integrable in the sense of Liouville). Condition (55) is trivially satisfied in this case.
2. The measure μ_0 is ϕ_t^H-invariant. Then (55) is the well-known result on convergence of Birkhoff averages.

This is the situation when (u_n^0) is a *quasi-mode*; that is, when

$$\hat{H}_{h_n} u_n^0 = \lambda_{h_n} u_n^0 + r_{h_n},$$

where $\lambda_{h_n} \to \lambda \in \mathbb{R}$ and $\|r_{h_n}\|_{L^2(M)} \to 0$ as $n \to \infty$. In this case, it is easy to check that:

$$\left\| e^{-i\frac{t}{h_n}\hat{H}_{h_n}} u_n^0 - e^{-i\frac{t}{h}\lambda_{h_n}} u_n^0 \right\|_{L^2(M)} = t\mathscr{O}\left(\frac{\|r_{h_n}\|_{L^2(M)}}{h_n} \right),$$

which in turn implies:

$$w_n(t,\cdot) - w_n(0,\cdot) = t^2 \mathscr{O}\left(\frac{\|r_{h_n}\|^2_{L^2(M)}}{h_n^2} \right).$$

In this case, $w_n(t,\cdot)$ converges to μ_0 uniformly in time intervals $[-\tau_n, \tau_n]$ provided $\tau_n \ll h_n \|r_{h_n}\|^{-1}_{L^2(M)}$. The problem of constructing quasi-modes in a Riemannian manifold has been the object of numerous studies, see for instance [13, 16, 39, 95, 96].

4.4 Concentration of Laplacian Eigenfunctions

Another instance in which the convergence of Wigner distributions towards their limiting semiclassical measures is uniform in time corresponds to the case in which the sequence of initial data consists of eigenfunctions of the Laplacian.

In this section we shall assume that (M, g) is a compact Riemannian manifold; this ensures that the Laplace-Beltrami operator $-\Delta_x$ has discrete spectrum, consisting of an non-decreasing sequence of eigenvalues:

$$0 = \lambda_0 < \lambda_1 \leq \lambda_2 \leq \ldots \leq \lambda_n \nearrow \infty, \quad \text{as } n \longrightarrow \infty.$$

The corresponding normalized eigenfunctions satisfy:

$$-\frac{1}{2}\Delta_x \psi_n = \lambda_n \psi_n, \qquad \|\psi_n\|_{L^2(M)} = 1, \tag{57}$$

and it is possible to construct an orthonormal basis of $L^2(M)$ formed exclusively by eigenfunctions.

A sequence (ψ_n) formed by eigenfunctions corresponding to an increasing sequence of eigenvalues is clearly h_n-oscillating if $h_n = \lambda_n^{-1/2}$ (or h_n tends to zero faster than $\lambda_n^{-1/2}$) since (57) can be written in this case as:

$$-\frac{h_n^2}{2}\Delta_x \psi_n = \psi_n. \tag{58}$$

The corresponding solutions to the semiclassical Schrödinger equation can be written, in view of (8), as:

$$e^{-i\frac{t}{h_n}\widehat{H_0},h_n}\psi_n = e^{ith_n\Delta_x/2}\psi_n = e^{-it\sqrt{\lambda_n}/2}\psi_n.$$

Therefore, for every $t \in \mathbb{R}$:

$$\left|e^{ith_n\Delta_x/2}\psi_n\right|^2 = |\psi_n|^2,$$

and, for any time scale (τ_n), the corresponding time-rescaled Wigner distributions satisfy:

$$w_n^{\tau_n}(t,\cdot) = w_n^{\tau_n}(0,\cdot) = w_{\psi_n}^{h_n},$$

Hence, the convergence of $\left|e^{ith_n\Delta_x/2}\psi_n\right|^2$ or $w_n(t,\cdot)$ towards its limit is (trivially) *uniform* in $t \in \mathbb{R}$.

Any weak-$*$ limit μ of $w_n(t,\cdot) = w_{\psi_n}^{h_n}$ is necessarily independent of t. Moreover, (44) can be rewritten as:

$$\int_{T^*M} a(x,\xi)\,\mu(dx,d\xi) = \int_{T^*M} a(\phi_t(x,\xi))\,\mu(dx,d\xi),$$

for every $a \in C_c^\infty(T^*M)$, $t \in \mathbb{R}$. In other words, μ is *invariant by the geodesic flow* ϕ_t, which is the classical flow associated to the classical Hamiltonian $\widehat{H_0}$.

An application of the symbolic calculus developed in Sect. 3.2 to the semiclassical problem (58) for eigenfunctions gives:

$$\begin{aligned} 0 &= \left(\mathrm{Op}_{h_n}(a)\left(-h_n^2\Delta_x - 1\right)\psi_n|\psi_n\right)_{L^2(M)} \\ &= \left(\mathrm{Op}_{h_n}\left((H_0-1)\,a\right)\psi_n|\psi_n\right)_{L^2(M)} + \mathscr{O}(h_n). \end{aligned}$$

Therefore, taking limits as $n \to \infty$ shows:

$$\int_{T^*M} a(x,\xi)\left(\frac{1}{2}\|\xi\|_x^2 - 1\right)\mu(dx,d\xi) = 0,$$

which in turn implies that μ is supported on the sphere bundle S^*M:

$$\mathrm{supp}\,\mu \subseteq S^*M := \left\{(x,\xi) \in T^*M : \frac{1}{2}\|\xi\|_x^2 = 1\right\},$$

which is the energy level $E = 1$ for the classical Hamiltonian H_0.

Let us introduce some notation: we shall denote by $\mathscr{M}_{\mathrm{inv}}(T^*M)$ (resp. $\mathscr{M}_{\mathrm{inv}}(S^*M)$) the set of all probability measures on T^*M (resp. supported on S^*M) that are invariant by the geodesic flow. We shall also denote by $\tilde{\mathscr{M}}_\infty$ the set of those

measures that arise as semiclassical measures of a sequence of eigenfunctions of the Laplacian. The following chain of inclusions trivially takes place for any time scale (τ_n):

$$\tilde{\mathscr{M}}_\infty \subset \tilde{\mathscr{M}}(\tau) \subset L^\infty\left(\mathbb{R}; \mathscr{M}_{\text{inv}}\left(T^*M\right)\right).$$

Naturally, the set $\mathscr{M}_\infty$ introduced in Sect. 2.1 is obtained by projecting the elements of $\tilde{\mathscr{M}}_\infty$ onto the base.

The question of characterizing the set $\tilde{\mathscr{M}}_\infty$ is an extremely difficult one; its answer relies on fine aspects of the global dynamics of ϕ_t (the reader can consult the recent survey [123]). A complete answer is known in very few cases, in some others partial results are available. We next describe some examples.

- *The Spheres* ($\mathbb{S}^d$, can). In this case $\tilde{\mathscr{M}}_\infty = \mathscr{M}_{\text{inv}}(S^*M)$, i.e. every invariant measure on S^*M can be realized as a semiclassical measure for some sequence of eigenfunctions. This was first proved by Jakobson and Zelditch [73]. The proof relies on three ingredients. The first one is an explicit computation. The sequence:

$$\psi_k(x) := \sqrt{\frac{\Gamma\left(k+\frac{d+1}{2}\right)}{2\pi^{\frac{d+1}{2}}\Gamma(k+1)}}(x_1+ix_2)^k$$

of eigenfunctions corresponds to the eigenvalues $k(k+d-1)$ and concentrates onto the equator γ_0 given by $x_3 = \ldots = x_{d+1} = 0$. More precisely,

$$|\psi_k|^2 \rightharpoonup \delta_{\gamma_0}, \quad w^{h_k}_{\psi_k} \rightharpoonup \delta_{\tilde{\gamma}_0} \quad \text{as } k \longrightarrow \infty;$$

where $\tilde{\gamma}_0$ denotes the lift of γ_0 to S^*M.[5] The second ingredient is that the isometries of the sphere act transitively on the space of geodesics: if γ is a geodesic then there exists an isometry $\Phi \in \text{Isom}(\mathbb{S}^d,\text{can})$ such that $\Phi(\gamma) = \gamma_0$. Since $\psi_k \circ \Phi$ is again a normalized eigenfunction of the Laplacian, this shows that $\delta_{\tilde{\gamma}} \in \tilde{\mathscr{M}}_\infty$ for every orbit $\tilde{\gamma}$ of the geodesic flow; finally, the third step consists in noticing that convex combinations of orbit measures $\delta_{\tilde{\gamma}}$ are dense in $\mathscr{M}_{\text{inv}}(S^*M)$. One concludes by applying a diagonal extraction argument combined with the quasi-orthogonality property (40) of semiclassical measures. It should be noted, nonetheless, that this phenomenon is not very robust. It has been recently proved in [90] that if one considers sequences of eigenfunctions

[5] The orbit measure $\delta_{\tilde{\gamma}}$ corresponding to an orbit $\tilde{\gamma}$ of the classical flow ϕ_t^H is defined as

$$\int_{T^*M} a(x,\xi)\,\delta_{\tilde{\gamma}}(dx,d\xi) := \lim_{T\to\infty}\frac{1}{T}\int_0^T a\left(\phi_t^H(x_0,\xi_0)\right)dt$$

where $(x_0,\xi_0) \in \tilde{\gamma}$.

for the operator $-\frac{1}{2}\Delta + V$, for V generic, only a finite number of orbit measures $\delta_{\tilde{\gamma}}$ can be realized as semiclassical measures.

- *Zoll manifolds*. For manifolds with periodic geodesic flow, the situation is not so clear. However, if one assume additional structure on the manifold one has again that $\tilde{\mathscr{M}}_\infty = \mathscr{M}_{\rm inv}(S^*M)$. This is the case for all rank-one compact symmetric spaces, as proved in [84] (in fact, it only suffices to assume a spectral separation property for $-\Delta_x$). In [7] it is showed that $\tilde{\mathscr{M}}_\infty = \mathscr{M}_{\rm inv}(S^*M)$ holds as soon as (M, g) has constant positive sectional curvature (in that case, M is a quotient of the sphere by a group of isometries).
- *Flat tori* $(\mathbb{T}^d, {\rm can})$. In spite that the geodesic flow is completely integrable (as was the case in the sphere and Zoll manifolds), in this case $\tilde{\mathscr{M}}_\infty$ is strictly contained in $\mathscr{M}_{\rm inv}(S^*M)$. A result by Bourgain (see Jakobson's article [72]) shows that the set $\mathscr{M}_\infty$ of projections onto $\mathbb{T}^d$ of the elements of $\tilde{\mathscr{M}}_\infty$ are measures that are absolutely continuous with respect to the Lebesgue measure. In particular $\delta_{\tilde{\gamma}} \notin \tilde{\mathscr{M}}_\infty$ whenever $\tilde{\gamma}$ is periodic. Jakobson [72] refined this result for $d = 2$: any element of $\mathscr{M}_\infty$ is of the form $\sum_{|k|\in\{n_1,n_2\}} a_k e^{ik\cdot x}$ for certain $n_1, n_2 \in \mathbb{R}_+$. In higher dimensions, see [3, 72, 93], it can be proved that the Fourier coefficients of the elements in $\mathscr{M}_\infty$ satisfy an estimate of the form $\sum_{k\in\mathbb{Z}^d} |a_k|^{d-2} \leq C_d$. The proofs of these results are based on fine results on the distribution of points of $\mathbb{Z}^d$ on spheres and on deep results on the structure of solutions to Pell's type equations. In [9], Bourgain's result is generalized to sequences of eigenfunctions of more general operators of the form $-\frac{1}{2}\Delta_x + V(x)$; this proof is very different, of microlocal nature, and follows from the analysis presented in the next section.
- *General completely integrable geodesic flow and KAM type situations*. For completely integrable geodesic flows it is possible to show the existence of sequences of eigenfunctions that concentrate on unstable periodic orbits of the geodesic flow [42, 111–113]. It is possible to show the existence of sequences of eigenfunctions or quasi-modes that concentrate on invariant Lagrangian tori in some KAM situations [43, 77, 95]. Bourgain's result also generalizes to quantum completely integrable systems [1].
- *Ergodic geodesic flow.* When the geodesic flow of (M, g) is ergodic, i.e. every invariant subset of S^*M has either full or zero measure, the situation is rather different. Shnirelman's theorem (whose proof can be found in [41, 106, 120]) states the following. Suppose that (ψ_n) is an orthonormal basis of $L^2(M)$ consisting of eigenfunctions of the Laplacian. Then there exists a subset $\mathscr{S} \subset \mathbb{N}$, of *density* 1, such that $(w^{h_n}_{\psi_n})_{n\in\mathscr{S}}$ converges to the Liouville measure on S^*M. This fact can be interpreted as stating that a "generic" sequence of eigenfunctions asymptotically equidistributes on S^*M (both in physical and frequency space). It has been proved by Hassell that there exists plane domains whose billiard flow is ergodic for which measures different from Liouville can be realized as semiclassical measure for eigenfunctions, see [64]. The *Quantum Unique Ergodicity* conjecture of Rudnick and Sarnak [102, 104] states that in a compact manifold with negative curvature (and therefore, whose geodesic flow is ergodic) the set $\tilde{\mathscr{M}}_\infty$ reduces to the Liouville measure. This conjecture has been partially solved in the case of

arithmetic congruence surfaces by Lindenstrauss [26, 79]. On general manifolds of negative sectional curvature, Anantharaman and Nonnenmacher have proved [10, 11] a lower bound for the *Kolmogorov-Sinai Entropy* of elements in $\tilde{\mathscr{M}}_\infty$. This was further refined by Rivière [97] in the case of surfaces.

5 Results in Completely Integrable Geometries

5.1 Averaging and Zoll Manifolds

In this last section we shall focus on manifolds with completely integrable geodesic flows. We shall mainly focus on Zoll manifolds and flat tori. We shall restrict ourselves to compact M and will consider the non-semiclassical Hamiltonian case. For the rest of these notes, let:

$$\hat{H} = -\frac{1}{2}\Delta + V,$$

where $V \in C^\infty(M)$.[6] As we did before, we introduce the associated semiclassical operator:

$$\hat{\mathscr{H}}_h := -\frac{h^2}{2}\Delta + h^2 V,$$

that satisfies:

$$e^{-it\hat{H}} = e^{-i\frac{\tau_h t}{h}\hat{\mathscr{H}}_h}, \quad \text{with } \tau_h = \frac{1}{h}.$$

We shall use semiclassical notation and denote generically by $w_h^{\tau_h}(t,\cdot)$ the Wigner distribution associated to a solution $e^{-i\frac{\tau_h t}{h}\hat{\mathscr{H}}_h}u_h^0$:

$$w_h^{\tau_h}(t,\cdot) := w^h_{e^{-i\frac{\tau_h t}{h}\hat{\mathscr{H}}_h}u_h^0}.$$

Theorem 5 gives that all accumulation points of $(w_h^{\tau_h})$ are elements of $L^\infty(\mathbb{R}; \mathscr{M}_{\text{inv}}(T^*M))$, where $\mathscr{M}_{\text{inv}}(T^*M)$ is the set of probability measures on T^*M that are invariant by the geodesic flow of (M,g). A proof of this fact is sketched in the proof of Proposition 4 below. When we write $h \to 0^+$ it should be understood that convergence takes place along a subsequence. Again, we shall denote by ϕ_t the geodesic flow of (M,g) acting on T^*M.

[6] Most of the results presented here hold for potentials satisfying lower regularity requirements.

We start by presenting a result that exploits the existence of completely integrable structure in the geodesic flow. It can be interpreted as a weak version of Egorov's theorem for very long times.

Proposition 4 ([85]) *Let (u_h^0) an h-oscillating sequence that is normalized in $L^2(M)$, and suppose that $\tau_h \ll h^{-2}$. Assume that $\left(w_h^{\tau_h}\right)$, the sequence of Wigner distributions corresponding to $e^{-i\frac{\tau_h t}{h}\hat{\mathscr{H}_h}}u_h$, converges to $\mu \in \tilde{\mathscr{M}}(\tau)$ and that $(w_h^{\tau_h}(0) = w^h_{u_h^0})$ converges to $\mu_0 \in \mathscr{M}_+(T^*M)$. Then, if $a \in C_c^\infty(T^*M)$ is ϕ_t-invariant one has, for every $t \in \mathbb{R}$:*

$$\lim_{h\to 0^+} \left\langle w_h^{\tau_h}(t,\cdot), a\right\rangle = \int_{T^*M} a(x,\xi)\,\mu_0(dx,d\xi). \tag{59}$$

In particular, for every such a and for a.e. $t \in \mathbb{R}$, the following holds:

$$\int_{T^*M} a(x,\xi)\,\mu(t,dx,d\xi) = \int_{T^*M} a(x,\xi)\,\mu_0(dx,d\xi). \tag{60}$$

Proof Recall that $w_n^{\tau_n}$ solves the Wigner equation (46), which after taking into account the change of time scale reads:

$$\frac{d}{dt}\left\langle w_h^{\tau_h}(t), a\right\rangle_{\mathscr{D}'\times C_c^\infty} = \frac{i\tau_h}{h}([\hat{\mathscr{H}_h}, \mathrm{Op}_h(a)]e^{-i\frac{\tau_h t}{h}\hat{\mathscr{H}_h}}u_h^0 | e^{-i\frac{\tau_h t}{h}\hat{\mathscr{H}_h}}u_h^0)_{L^2(M)}. \tag{61}$$

Let us analyze the structure of the above commutator. First notice that, applying the commutator rule (27) to the term involving the potential V we obtain:

$$[\hat{\mathscr{H}_h}, \mathrm{Op}_h(a)] = \frac{1}{2}[-h^2\Delta_x, \mathrm{Op}_h(a)] + \mathscr{O}\left(h^3\right).$$

Now recall that the Laplace-Beltrami operator (28) can be expressed in terms of Weyl pseudodifferential operators as:

$$-h^2\Delta_x = \mathrm{Op}_h(H_0) + ih\,\mathrm{Op}_h(r) + h^2\,\mathrm{Op}_h(m),$$

where $H_0(x,\xi) = \|\xi\|_x^2$, $m \in C^\infty(M)$ and r can be written as (30), which is equivalent to:

$$r(x,\xi) = \frac{1}{2}\{H_0, \log\rho\},$$

where $\rho = \sqrt{\det g}$. The commutator rule implies in this case:

$$[-h^2\Delta_x, \mathrm{Op}_h(a)] = \frac{h}{i}\,\mathrm{Op}_h(\{H_0, a\}) + h^2\,\mathrm{Op}_h(\{r, a\}) + \mathscr{O}\left(h^3\right). \tag{62}$$

Since $a \circ \phi_s = a$ for every $s \in \mathbb{R}$, necessarily $\{H_0, a\} = 0$ and therefore:

$$[\hat{\mathscr{H}}_h, \mathrm{Op}_h(a)] = \frac{h^2}{2} \mathrm{Op}_h(\{r, a\}) + \mathscr{O}\left(h^3\right).$$

Introducing this into the Wigner equation (61) gives:

$$\frac{d}{dt} \left\langle w_h^{\tau_h}(t), a \right\rangle_{\mathscr{D}' \times C_c^\infty} = \frac{i}{2} \tau_h h \left\langle w_h^{\tau_h}(t), \{r, a\} \right\rangle_{\mathscr{D}' \times C_c^\infty} + \mathscr{O}\left(\tau_h h^2\right).$$

Integrating with respect to time, we obtain:

$$\begin{aligned} &\left\langle w_h^{\tau_h}(t), a \right\rangle_{\mathscr{D}' \times C_c^\infty} - \left\langle w_h^{\tau_h}(0), a \right\rangle_{\mathscr{D}' \times C_c^\infty} \\ &\quad = \frac{i}{2} \tau_h h \int_0^t \left\langle w_h^{\tau_h}(s), \{r, a\} \right\rangle_{\mathscr{D}' \times C_c^\infty} ds + \mathscr{O}\left(\tau_h h^2\right). \end{aligned}$$

Now notice that $\tau_h h^2 \to 0^+$ by hypothesis and that using Jacobi's identity for the Poisson bracket:

$$\{r, a\} = \frac{1}{2} \{H_0, \{\log \rho, a\}\}.$$

Now, it is an easy exercise to prove, using (61) and (62), that, for any $b \in C_c^\infty(T^*M)$ and any $\varphi \in L^1(\mathbb{R})$ one has:

$$\int_{\mathbb{R}} \varphi(t) \left\langle w_h^{\tau_h}(t), \{H_0, b\} \right\rangle_{\mathscr{D}' \times C_c^\infty} dt = o\left(\frac{1}{\tau_h h}\right).$$

This, in particular, shows that $\mu(t, \cdot)$ is invariant by the geodesic flow for almost every $t \in \mathbb{R}$. We therefore conclude that:

$$\lim_{h \to 0^+} \left\langle w_h^{\tau_h}(t), a \right\rangle_{\mathscr{D}' \times C_c^\infty} = \lim_{h \to 0^+} \left\langle w_h^{\tau_h}(0), a \right\rangle_{\mathscr{D}' \times C_c^\infty},$$

which is (59). Identity (60) now follows from the fact that (59) implies that, for $a \in C_c^\infty(T^*M)$ that is ϕ_t-invariant:

$$\begin{aligned} &\int_{\mathbb{R}} \int_{T^*M} \varphi(t)\, a(x, \xi)\, \mu(t, dx, d\xi)\, dt \\ &\quad = \left(\int_{\mathbb{R}} \varphi(t)\, dt \right) \int_{T^*M} a(x, \xi)\, \mu_0(dx, d\xi), \end{aligned}$$

for every $\varphi \in L^1(\mathbb{R})$.

Surprisingly, in some situations Proposition 4 suffices to characterize the set $\tilde{\mathscr{M}}(\tau)$. In order to simplify our presentation, we shall restrict the class of initial

data we shall be interested in. In what follows, we shall assume that the sequence $\left(u_h^0\right)$ of initial data is normalized in $L^2(M)$ and satisfies the stronger assumption of *strict h*-oscillation:

$$\lim_{R\to\infty} \limsup_{h\longrightarrow 0^+} \sum_{\lambda_j \geq R/h^2} |\widehat{u_h^0}(\lambda_j)|^2 = \lim_{\delta\to 0^+} \limsup_{h\longrightarrow 0^+} \sum_{\lambda_j \leq \delta/h^2} |\widehat{u_h^0}(\lambda_j)|^2 = 0; \tag{63}$$

this condition expresses that no oscillations take place at scales asymptotically higher or lower than $1/h$. It should be pointed out that it is not always possible to find a scale for which both sides of (63) are satisfied simultaneously,[7] see [58] for an example. If $\left(u_h^0\right)$ satisfies (63) and the Wigner distributions $(w^h_{u_h^0})$ converge to a probability measure $\mu_0 \in \mathscr{P}(T^*M)$ then:

$$\mu_0(\{\xi = 0\}) = 0.$$

In fact this condition is equivalent to the right hand side of (63).

We now turn to the case of Zoll manifolds. Recall that (M, g) is a Zoll manifold provided all its geodesics are closed. In this case, the geodesic flow ϕ_t is periodic on each level set $\|\xi\|_x = E$ (see [18] for a proof). We shall denote by L the period on ϕ_t for $E = 1$. Then, on $\|\xi\|_x = E$ the period of the geodesic flow is $L/\|\xi\|_x$.

The book [18] provides a detailed exposition of this type of geometries. Note that Zoll's contribution was to show the existence of a Riemannian structure on $\mathbb{S}^2$ that is not isometric to the canonical one with the property that all its geodesics are closed. Examples of Zoll manifolds are Compact Rank-One Symmetric Spaces (CROSS) and their quotients. Note also that the topology of a Zoll manifold (under the additional hypothesis that all geodesics have the same length) is close to that of a CROSS: the cohomology ring of such a Zoll manifold must be that of a CROSS.

The following holds.

Theorem 6 ([85]) *Let (M, g) be a Zoll manifold. Suppose $\tau_h \ll h^{-2}$ and that (u_h^0) satisfies (63) and is normalized in $L^2(M)$. If $\left(w_h^{\tau_h}\right)$ and $(w_h^{\tau_h}(0))$ converge respectively to μ and μ_0 then $\mu \in \mathscr{M}_{inv}(T^*M)$ does not depend on t and is given by:*

$$\int_{T^*M} a(x,\xi)\,\mu(dx,d\xi) = \int_{T^*M} \langle a\rangle(x,\xi)\,\mu_0(dx,d\xi). \tag{64}$$

Remark 3 Recall that:

$$\langle a\rangle(x,\xi) = \lim_{T\to\infty} \frac{1}{T}\int_0^T a(\phi_s(x,\xi))\,ds. \tag{65}$$

[7] Note, however, that it is always possible to find a scale such that the left hand side of (63) holds. The right hand side is equivalent to the fact that (u_h^0) converges weakly to zero in $L^2(M)$.

Our periodicity assumption implies that if $a \in C_c^\infty(T^*M)$ vanishes close to $\xi = 0$ then $\langle a \rangle \in C_c^\infty(T^*M)$. In fact:

$$\langle a \rangle(x,\xi) = \frac{\|\xi\|_x}{L} \int_0^{L/\|\xi\|_x} a(\phi_s(x,\xi))\, ds.$$

Proof (Proof of Theorem 6) Let $a \in C_c^\infty(T^*M)$ vanish close to $\xi = 0$. Identity (60) combined with the preceding remark show that:

$$\int_{T^*M} \langle a \rangle(x,\xi)\, \mu(t, dx, d\xi) = \int_{T^*M} \langle a \rangle(x,\xi)\, \mu_0(dx, d\xi). \tag{66}$$

Since the convergence in (65) takes places for every $(x,\xi) \in T^*M$ we conclude, using the invariance of $\mu(t,\cdot)$:

$$\begin{aligned}\int_{T^*M} \langle a \rangle(x,\xi)\, \mu(t, dx, d\xi) &= \lim_{T\to\infty} \frac{1}{T} \int_0^T \int_{T^*M} a(\phi_s(x,\xi))\, \mu(t, dx, d\xi)\, ds \\ &= \int_{T^*M} a(x,\xi)\, \mu(t, dx, d\xi).\end{aligned}$$

Note also that (66) implies that $\mu(t, T^*M \setminus \{0\}) = \mu_0(T^*M \setminus \{0\}) = 1$ and therefore, $\mu(t,\cdot)$ cannot charge $\{\xi = 0\}$. We conclude that (64) holds for every a and therefore characterizes μ.

Formula (64) should be interpreted as that μ is obtained by averaging μ_0 along the geodesic flow. Note in particular that as soon as $\mu_0 \in \mathscr{M}_{\mathrm{inv}}(T^*M)$ one has:

$$\mu = \mu_0.$$

As a consequence, the following holds.

Corollary 2 *Let (M,g) be a Zoll manifold and suppose that $\tau_h \ll h^{-2}$. Then $\mathscr{M}_{inv}(T^*M) \subset \tilde{\mathscr{M}}(\tau)$.*

A complete characterization of the structure of μ close to the zero section requires preforming a second microlocalization close to $\xi = 0$ (second microlocalizations will be described for the case of the torus in Sect. 5.3). The following formula holds when one does not assume (63):

$$\begin{aligned}\int_{T^*M} a(x,\xi)\, \mu(t, dx, d\xi) = &\int_{T^*M\setminus\{0\}} \langle a \rangle(x,\xi)\, \mu_0(dx, d\xi) \\ &+ \int_M \langle a \rangle(x,0)\, \nu_0(dx) \\ &+ \int_M a(x,0)\, |e^{-it\hat{H}} u^0|^2(x)\, dx,\end{aligned}$$

with $\nu_0 \in \mathscr{M}_+(M)$ only depending on $\left(u_h^0\right)$ and u^0 being the weak limit of $\left(u_h^0\right)$ in $L^2(M)$.

We stress the fact that the effect of V cannot be detected on these time scales. This is no longer true if $\tau_h \sim h^{-2}$ as has been recently proved in [90].

Another interesting corollary of Theorem 6 refers to the propagation of wave-packets (41) at the scale $\tau_h = 1/h$ [which is equivalent to consider the non-semiclassical propagation (5)]. Suppose u_h^0 is supported on a coordinate chart and locally of the form:

$$u_h^0(x) = \frac{1}{h^{d/4}} \rho\left(\frac{x - x_0}{\sqrt{h}}\right) e^{i\xi_0/h \cdot x}, \tag{67}$$

where $\rho \in L^2(M)$ with $\|\rho\|_{L^2(M)} = 1$ and $(x_0, \xi_0) \in T^*M \setminus \{0\}$. Then, as we saw in Sect. 3.6, the Wigner distributions of u_h^0 converge towards:

$$\mu_0 = \delta_{x_0} \otimes \delta_{\xi_0}.$$

Let $\tilde{\gamma}$ be the orbit of the geodesic flow issued from (x_0, ξ_0) and let γ be the corresponding geodesic in M. Theorems 5 and 6 imply the following.

Corollary 3 *Let (M, g) be a Zoll manifold and u_h^0 be given by (67). Then, for every $a < b$ and every $\varphi \in C(M)$:*

$$\lim_{h \to 0+} \int_a^b \int_M \varphi(x) \left|e^{it\left(\frac{1}{2}\Delta - V\right)} u_h^0\right|^2 (x)\, dxdt = (b-a) \int_M \varphi(x)\, \delta_\gamma(dx).$$

As a consequence of this, no Strichartz estimate can hold on a Zoll manifold, as explained in Sect. 2.2. Moreover, it also shows that the Geometric Control Condition is necessary in order to have an observability estimate (see Sect. 2.3).

5.2 Flat Tori

The periodicity assumption on the dynamics of ϕ_t is deceptively simple. One may ask whether or not an averaging formula as (64) still holds under more complicated dynamical hypotheses.

The simplest setting to consider is perhaps flat tori. Suppose that $M = \mathbb{T}^d = \mathbb{R}^d/2\pi\mathbb{Z}^d$ is equipped with the canonical flat metric. The geodesic flow on $T^*\mathbb{T}^d$ is explicit:

$$\phi_s(x, \xi) = (x + s\xi, \xi).$$

The the flow ϕ_s is the prototype of a completely integrable Hamiltonian flow (see, for instance, [14, 91]). The orbits of ϕ_s are quasi-periodic. In fact, they are dense in

tori of dimension less or equal to d. In order to describe them precisely, define the submodule:

$$\Lambda_\xi := \left\{k \in \mathbb{Z}^d \ : \ k \cdot \xi = 0\right\}.$$

Kronecker's lemma states that the orbit corresponding to $(x, \xi) \in T^*\mathbb{T}^d$ is dense in a torus of dimension $d - \operatorname{rk} \Lambda_\xi$. Therefore, if $\Lambda_\xi = \{0\}$ then the corresponding orbits are dense in $\mathbb{T}^d$, whereas if $\operatorname{rk} \Lambda_\xi = d - 1$, they are periodic. A $\xi \in \mathbb{R}^d$ is said to be resonant if $\operatorname{rk} \Lambda_\xi > 0$; we shall denote by $\Omega \subset \mathbb{R}^d$ the set of resonant frequencies.

Note that the average $\langle a \rangle (x, \xi)$ of a smooth function $a \in C_c^\infty(T^*\mathbb{T}^d)$, as defined in (65), exists for every $(x, \xi) \in T^*\mathbb{T}^d$; but is not a smooth function in general. In fact, for $\xi \in \mathbb{R}^d \setminus \Omega$ one has:

$$\langle a \rangle (x, \xi) = \frac{1}{(2\pi)^d} \int_{\mathbb{T}^d} a(y, \xi)\, dy.$$

This is clearly not generally the case if the orbit corresponding to (x, ξ) is periodic. Therefore, it is not possible to apply the same strategy we used to prove Theorem 6.

In fact, the only smooth functions $a \in C_c^\infty(T^*\mathbb{T}^d)$ that are invariant under the geodesic flow are of the form $a(\xi)$, i.e. they do not depend on x. In this context, Proposition 4 gives the following result.

Proposition 5 *Let $(M, g) = (\mathbb{T}^d, can)$ and suppose $\tau_h \ll h^{-2}$ and that (u_h^0) is normalized in $L^2(\mathbb{T}^d)$. Assume again that $\left(w_h^{\tau_h}\right)$ and $(w_h^{\tau_h}(0))$ converge respectively to μ and μ_0. Let $\overline{\mu}$ and $\overline{\mu_0}$ denote the respective images of μ and μ_0 by the projection $(x, \xi) \longmapsto \xi$. Then $\overline{\mu} \in \mathscr{M}_+(\mathbb{R}^d)$ does not depend on t and is given by:*

$$\overline{\mu} = \overline{\mu_0}.$$

Proof Proposition 4 ensures that for every $a \in C_c^\infty(\mathbb{R}^d_\xi)$ one has:

$$\int_{T^*\mathbb{T}^d} a(\xi)\, \mu(t, dx, d\xi) = \int_{T^*\mathbb{T}^d} a(\xi)\, \mu_0(dx, d\xi),$$

which is equivalent to the claim.

An immediate consequence of this is the following.

Corollary 4 *Suppose the hypotheses of Proposition 5 hold. If $\mu_0(\mathbb{T}^d \times \Omega) = 0$ then for almost every $t \in \mathbb{R}$,*

$$\mu(t, \cdot) = \frac{1}{(2\pi)^d} dx \otimes \overline{\mu_0}.$$

Proof The hypothesis and Proposition 5 imply that $\mu(t, \mathbb{T}^d \times \Omega) = 0$,

$$\frac{1}{(2\pi)^d} \int_{\mathbb{T}^d} a(y, \xi)\, dy = \langle a \rangle (x, \xi), \quad \text{for } \mu(t, \cdot)\text{-a.e. } (x, \xi) \in T^*\mathbb{T}^d,$$

and the convergence (65) of the Birkhoff mean to the average takes place $\mu(t, \cdot)$-almost everywhere. Therefore, since $\mu(t, \cdot)$ is invariant by the geodesic flow:

$$\begin{aligned}
\int_{T^*\mathbb{T}^d} a(x, \xi)\, \mu(t, dx, d\xi) &= \frac{1}{T} \int_0^T \int_{T^*\mathbb{T}^d} a(\phi_s(x, \xi))\, \mu(t, dx, d\xi)\, ds \\
&= \int_{T^*\mathbb{T}^d} \langle a \rangle (x, \xi)\, \mu(t, dx, d\xi) \\
&= \int_{T^*\mathbb{T}^d} \left(\frac{1}{(2\pi)^d} \int_{\mathbb{T}^d} a(y, \xi)\, dy \right) \mu(t, dx, d\xi) \\
&= \int_{\mathbb{R}^d} \left(\frac{1}{(2\pi)^d} \int_{\mathbb{T}^d} a(y, \xi)\, dy \right) \overline{\mu}(d\xi),
\end{aligned}$$

and we conclude using Proposition 5.

Corollary 4 shows that in order to get a complete characterization of $\mu(t, \cdot)$ it only remains to understand the structure of $\mu(t, \cdot)\rceil_{\mathbb{T}^d \times \Omega}$. It turns out that this is more difficult than one would a priori think. In the following example, $V = 0$ and $\tau_h = 1/h$.

Example 1 ([85], Proposition 11) Let $\rho \in L^2(\mathbb{T}^2)$ with $\|\rho\|_{L^2(\mathbb{T}^2)} = 1$. Define:

$$u_h^0(x) = \rho(x)\, e^{ix_1/h}, \quad v_h^0(x) = \rho(x)\, e^{i\left(x_1 + k_1^h\right)/h} e^{i\varepsilon_h k_2^h/h},$$

where $k^h := \left(k_1^h, k_2^h\right) \in \mathbb{Z}^2$ and $h \ll \varepsilon_h \to 0$. It is possible to choose (h_n), (ε_{h_n}) and $\left(k^h\right)$ in such a way that: both $\left(u_h^0\right)$ and $\left(v_h^0\right)$ belong to $L^2(\mathbb{T}^2)$ and have the same semiclassical measure:

$$|\rho(x)|^2\, dx \delta_{(1,0)}(\xi),$$

but their time-dependent Wigner distributions $w^h_{e^{it\Delta}u_h^0}$ and $w^h_{e^{it\Delta}v_h^0}$ converge respectively to:

$$\left(\int_{\mathbb{T}} \left| e^{it\Delta} \rho(y_1, x_2) \right|^2 \frac{dy_1}{2\pi} \right) dx \delta_{(1,0)}(\xi),$$

and

$$\frac{1}{(2\pi)^2} dx \delta_{(1,0)}(\xi).$$

In fact $\left(k^h / \left|k^h\right|\right)$ converges to an element of $\mathbb{R}^2 \setminus \Omega$.

This example shows that if $\mu_0(\mathbb{T}^d \times \Omega) > 0$ the measure $\mu(t,\cdot)$ may depend on t in a non trivial way and, most importantly, that μ_0 does not determine $\mu(t,\cdot)$ anymore. Two sequences of initial data may have the same semiclassical measure but the semiclassical measures associated to the evolution at $\tau_h = 1/h$ may differ. In particular, there is no hope of obtaining a simple averaging formula as (65).

This problem was solved in [86] for $d = 2$ and $V = 0$ and in its full generality in [9], in 2010, in any dimension and allowing for time dependent potentials that are continuous except in at most a set of zero measure. In those articles it is proved that any $\mu \in \tilde{\mathscr{M}}(1/h)$ enjoys the following properties:

1. $\mu \in C(\mathbb{R}; \mathbb{P}(T^*M))$ and the image of μ under the projection $(x,\xi) \longmapsto x$ is absolutely continuous with respect to the Lebesgue measure.
2. μ can be decomposed as a sum of measures whose propagation is described by a Schrödinger type equation in lower dimensional tori.
3. $\int_0^T \mu(t, \omega \times \mathbb{R}^d)dt > 0$ for every open subset $\omega \subset \mathbb{T}^d$.

Here we shall not present this result in its full generality. Instead, we shall restrict us to the case $d = 2$, $V \in C^\infty(\mathbb{T}^2)$ and to sequences of initial data satisfying (63).

In order to state our result, we need some notation. Denote by $\mathscr{L}_1$ the set of all primitive submodules of $\mathbb{Z}^2$ of rank one.[8] An element $\Lambda \in \mathscr{L}_1$ is a one dimensional lattice of $\mathbb{Z}^2$ generated by a $k \in \mathbb{Z}^2$ whose components are relatively prime. Denote by $L^2_\Lambda(\mathbb{T}^2)$ the subspace of $L^2(\mathbb{T}^2)$ consisting of those functions u such that:

$$u(x+v) = u(x), \quad \forall v \in \Lambda^\perp.$$

Above, $\Lambda^\perp$ denotes the subspace of the vectors of $\mathbb{R}^2$ that are orthogonal to Λ. Note that every $u \in L^2_\Lambda(\mathbb{T}^2)$ has a Fourier expansion of the form:

$$u(x) = \sum_{k \in \Lambda} b_k e^{ik\cdot x}.$$

Given $a \in C_c^\infty(T^*\mathbb{T}^2)$, $a(x,\xi) = \sum_{k\in\mathbb{Z}^2} a_k(\xi)\, e^{ik\cdot x}$ denote:

$$\langle a \rangle_\Lambda (x,\xi) := \sum_{k\in\Lambda} a_k(\xi)\, e^{ik\cdot x}.$$

Note at this point that $\langle a \rangle_\Lambda$ can also be obtained as a Birkhoff average along a periodic flow. If $v \in \Lambda^\perp \setminus \{0\}$ then:

$$\langle a \rangle_\Lambda (x,\xi) = \lim_{T\to\infty} \frac{1}{T} \int_0^T a(x+tv,\xi)\, dt.$$

[8] A submodule Λ of $\mathbb{Z}^d$ is *primitive* provided the intersection of its linear span over reals with $\mathbb{Z}^d$ is Λ itself.

That limit exists everywhere and

$$\|\langle a\rangle_{\Lambda}\|_{L^{\infty}(\mathbb{T}^2)} \leq \|a\|_{L^{\infty}(\mathbb{T}^2)}\,. \tag{68}$$

Let $m_{\langle a\rangle_{\Lambda}}(\xi)$ be the operator acting on $L^2_{\Lambda}(\mathbb{T}^2)$ by multiplication by $\langle a\rangle_{\Lambda}(\cdot,\xi)$. Denote by $U_{\Lambda}(t)$ the propagator on $L^2_{\Lambda}(\mathbb{T}^2)$ associated to the Schrödinger equation:

$$i\partial_t u(t,x) + \frac{1}{2}\Delta_{\Lambda} u(t,x) - \langle V\rangle_{\Lambda}(x)\, u(t,x) = 0. \tag{69}$$

where Δ_{Λ} is the restriction of Δ to $L^2_{\Lambda}(\mathbb{T}^2)$; note that (69) is a one-dimensional Schrödinger equation.

Define:

$$R_{\Lambda} := \Lambda^{\perp} \setminus \{0\}\,,$$

and note that

$$\bigsqcup\nolimits_{\Lambda\in\mathscr{L}_1} R_{\Lambda} \sqcup \left(\mathbb{R}^2 \setminus \Omega\right) = T^*\mathbb{T}^2 \setminus \{0\}\,.$$

Finally, given a Hilbert space H, recall that $\mathscr{L}^1_+(H)$ denotes the set of positive, hermitian, trace-class operators on H.

Theorem 7 ([9]) *Let $\left(u^0_h\right)$ be normalized in $L^2(\mathbb{T}^2)$ and satisfy (63). Let $\mu \in L^{\infty}(\mathbb{R};\mathscr{P}(T^*\mathbb{T}^2))$ be a weak-$*$ accumulation point of $\left(w^h_{u_h}\right)$. Then for every $\Lambda\in\mathscr{L}_1$ there exists a $\overline{\mu}$-integrable family of operators:*

$$R_{\Lambda} \ni \xi \longmapsto \rho_{\Lambda}(\xi) \in \mathscr{L}^1_+(L^2_{\Lambda}(\mathbb{T}^2))$$

that only depends on the sequence of initial data such that:

$$\int_{T^*\mathbb{T}^2} a(x,\xi)\,\mu(t,dx,d\xi) = \sum_{\Lambda\in\mathscr{L}_1}\int_{R_{\Lambda}} \mathrm{Tr}\left(m_{\langle a\rangle_{\Lambda}}(\xi)\, U_{\Lambda}(t)\,\rho_{\Lambda}(\xi)\, U^*_{\Lambda}(t)\right)\overline{\mu}(d\xi) + \int_{\mathbb{T}^2}\int_{\mathbb{R}^2\setminus\Omega} \langle a\rangle(x,\xi)\,\overline{\mu}(d\xi)\,dx.$$

Before giving some ideas of the proof of this result, let us present some consequences.

Corollary 5 *Let μ be as in Theorem 7. Then the image of μ under the projection $(x,\xi)\longmapsto x$ is absolutely continuous. In particular, any weak-$*$ accumulation point of $|e^{it\left(\frac{1}{2}\Delta - V\right)}u^0_h|^2 dxdt$ is of the form $\rho(t,x)\,dxdt$ with $\rho\in C(\mathbb{R};L^1_+(\mathbb{T}^2))$.*

Proof The image measure $\nu \in \mathscr{P}(\mathbb{T}^2)$ is given by:

$$\int_{\mathbb{T}^2} b(x)\, \nu(t, dx) = \sum_{\Lambda \in \mathscr{L}_1} \mathrm{Tr}\left(m_{\langle b \rangle_\Lambda} M_\Lambda(t)\right) + \overline{\mu}(\mathbb{R}^2 \setminus \Omega) \int_{\mathbb{T}^2} b(x) \frac{dx}{(2\pi)^2}, \tag{70}$$

where $M_\Lambda(t) \in \mathscr{L}^1_+(L^2_\Lambda(\mathbb{T}^2))$. Note that any measure of the form:

$$C_c(\mathbb{T}^2) \ni b \longmapsto \mathrm{Tr}(m_{\langle b \rangle_\Lambda} K),$$

where $K \in \mathscr{L}^1_+(L^2_\Lambda(\mathbb{T}^2))$, extends to a bounded form on $L^\infty(\mathbb{T}^2)$ because of (68), and therefore can be represented by a positive element of $L^1(\mathbb{T}^2)$. Since both sides of the identity (70) define a probability measure, the sum of the densities corresponding to each summand must converge to an element $\rho \in C(\mathbb{R}; L^1_+(\mathbb{T}^2))$, by the monotone convergence theorem.

Remark 4 The result of Corollary 5 can be improved. It is showed in [4] that, in fact, the density ρ is in $C(\mathbb{R}; L^2(\mathbb{T}^2))$, and similar results hold in any dimension. This is the result predicted by the Strichartz estimate corresponding to the *two dimensional* Euclidean exponent, which is known to be false since the work of Bourgain [28] (see also Sect. 2.2). The failure of this estimate is thus a very subtle phenomenon.

Corollary 6 *Let μ be as in Theorem 7. Then, for every $T > 0$ and every open, non-empty subset $\omega \subset \mathbb{T}^2$ the following holds:*

$$\int_0^T \mu(t, \omega \times \mathbb{R}^2) dt > 0.$$

Proof Suppose that, on the contrary

$$\int_0^T \mu(t, \omega \times \mathbb{R}^2) dt = 0,$$

for some $T > 0$ and non-empty $\omega \subset \mathbb{T}^2$. We are going to show that μ must vanish identically, and therefore, it is not a probability measure. Using formula (70), one deduces the identity:

$$\int_0^T \sum_{\Lambda \in \mathscr{L}_1} \mathrm{Tr}\left(m_{\langle \mathbb{1}_\omega \rangle_\Lambda} M_\Lambda(t)\right) dt + \overline{\mu}(\mathbb{R}^2 \setminus \Omega) \frac{T\,|\omega|}{(2\pi)^2} = 0.$$

Since all the terms in the above sum are positive, we infer that:

$$\overline{\mu}(\mathbb{R}^2 \setminus \Omega) = 0,$$
$$\int_0^T \mathrm{Tr}\left(m_{\langle \mathbb{1}_\omega \rangle_\Lambda} M_\Lambda(t)\right) dt = 0. \tag{71}$$

Theorem 7 ensures:

$$M_\Lambda(t) = U_\Lambda(t)\, M_\Lambda(0)\, U_\Lambda^*(t).$$

Since $M_\Lambda(0)$ is self-adjoint and trace class, it possesses an orthonormal basis of $L^2_\Lambda(\mathbb{T}^2)$ consisting of eigenfunctions. Write this basis as $\left(\psi_n^\Lambda\right)$; clearly:

$$M_\Lambda(0)\,\psi_n^\Lambda = \lambda_n^\Lambda \psi_n^\Lambda, \quad \lambda_n^\Lambda \geq 0, \quad \sum_{n\in\mathbb{N}} \lambda_n^\Lambda \leq 1.$$

Now, $M_\Lambda(t)$ can be written in terms of this expansion as a superposition of orthogonal projections:

$$M_\Lambda(t) = \sum_{n\in\mathbb{N}} \lambda_n^\Lambda \left|U_\Lambda(t)\,\psi_n^\Lambda\right\rangle\left\langle U_\Lambda(t)\,\psi_n^\Lambda\right|.$$

Identity (71) becomes, since again all the terms involved in the sums are non-negative:

$$\lambda_n^\Lambda \int_0^T \int_{\mathbb{T}^2} \langle \mathbb{1}_\omega \rangle_\Lambda(x)\, |U_\Lambda(t)\,\psi_n^\Lambda|^2(x)\, dx = 0,$$

for every $n \in \mathbb{N}$. If $\lambda_n^\Lambda \neq 0$ then $|U_\Lambda(t)\,\psi_n^\Lambda|^2(x) = 0$ for a.e. $t \in (0,T)$ and a.e. $x \in \omega_\Lambda := \bigcup_{v\in\Lambda^\perp} (\omega + v)$. Since $|U_\Lambda(t)\,\psi_n^\Lambda|^2$ can be viewed as defined on a one-dimensional torus (more precisely, $U_\Lambda(t)$ can be unitarily conjugated to a propagator acting on $L^2(\mathbb{T}_\Lambda)$ for some one-dimensional torus $\mathbb{T}_\Lambda$, see [9]), and ω_Λ projects onto an open set of that torus, one concludes $U_\Lambda(t)\,\psi_n^\Lambda = 0$ by a standard unique continuation result for the one-dimensional Schrödinger equation. This proves that μ vanishes identically.

It turns out that Corollary 6 is essentially equivalent to the validity of the observability estimate (23) on the torus. See Sect. 2.3 and [9, 87] for more details.

5.3 Some Ideas from the Proof of Theorem 7

The proof of Theorem 7, even in our relatively simple setting is quite lengthy and technical. Here we present the main ideas.

Our starting point is a geometric remark that motivates the introduction of the sets R_Λ.

Proposition 6 *Let $\mu \in \mathscr{M}_{inv}\left(T^*\mathbb{T}^2\right)$. Then $\mu\rceil_{\mathbb{T}^2\times R_\Lambda}$, $\Lambda \in \mathscr{L}_1$, and $\mu\rceil_{\mathbb{T}^2\times(\mathbb{R}^2\setminus\Omega)}$ are invariant measures that possesses additional regularity properties.*

(i) $\mu\rceil_{\mathbb{T}^2\times(\mathbb{R}^2\setminus\Omega)}$ is constant with respect to x;
(ii) each $\mu\rceil_{\mathbb{T}^2\times R_\Lambda}$ is invariant with respect to the translations:

$$x \longmapsto x + v, \quad v \in \Lambda^\perp. \tag{72}$$

As a consequence of statement (ii) of Proposition 6 we conclude that $\mu\rceil_{\mathbb{T}^2\times R_\Lambda}$ is completely determined by its action on functions $a \in C_c(T^*\mathbb{T}^2)$ that are invariant by translations of the form (72). Those functions admit a Fourier series development of the form:

$$a(x,\xi) = \sum_{k\in\Lambda} a_k(\xi)\, e^{ik\cdot x}. \tag{73}$$

We say that such a function has only frequencies in Λ. This remark translates into the problem under consideration by concluding that, if μ is now a time-dependent measure as in the statement of Theorem 7, then, in order to compute $\mu(t,\cdot)\rceil_{\mathbb{T}^2\times R_\Lambda}$ it suffices to test Wigner distributions against symbols that have only frequencies in Λ.

On the other hand, Example 1 suggests that in order to compute $\mu(t,\cdot)\rceil_{\mathbb{T}^2\times R_\Lambda}$ one must take into account the specific way in which energy concentrates onto R_Λ. This vague statement can be made precise using ideas from two-microlocal analysis [25, 27] and, more precisely, two-microlocal semiclassical measures. Those objects were introduced independently by Nier and Fermanian-Kammerer and further developed in the following articles [51–53, 89, 92].

To simplify matters a little bit, let us just consider the case

$$\Lambda = \{(n,0) : n \in \mathbb{Z}\}.$$

We introduce the class of symbols $\mathscr{S}^1_\Lambda$ that are defined on $T^*\mathbb{T}^2_{(x,\xi)} \times \mathbb{R}_\eta$ and have the following properties.

1. they are compactly supported in $(x,\xi) \in T^*\mathbb{T}^2$, and only have frequencies in Λ;
2. they are homogeneous of degree zero at infinity in $\eta \in \mathbb{R}$. This means that there exists a function $a_{\hom} \in C^\infty_c(T^*\mathbb{T}^2 \times \{-1,1\})$ and $R_0 > 0$ such that:

$$a(x,\xi,\eta) = a_{\hom}\left(x,\xi,\frac{\eta}{|\eta|}\right), \quad \text{for } |\eta| > R_0 \text{ and } (x,\xi) \in T^*\mathbb{T}^2.$$

Note that the requirement of only having frequencies in Λ (see (73)) translates into the fact that a does not depend on the variable x_2. Hence, symbols in $\mathscr{S}^1_\Lambda$ can be canonically identified to functions defined on $\mathbb{T}_{x_1}\times\mathbb{R}^2_\xi\times\mathbb{R}_\eta$.

From now on, we shall suppose that (u_h^0) satisfies the hypotheses of the theorem and we denote by $w_h(t,\cdot)$ the Wigner distribution of the solution $e^{it\left(\frac{1}{2}\Delta-V\right)}u_h^0$. We are going to decompose (two-microlocalize) $w_h(t,\cdot)$ around

$$R_\Lambda\subset\Lambda^\perp=\{(0,\xi_2):\xi_2\in\mathbb{R}\}.$$

To this aim, we use the symbols of the class $a\in\mathscr{S}^1_\Lambda$ as follows. Take $\chi\in C_c^\infty(\mathbb{R})$ to be a nonnegative cut-off function that is identically equal to one near the origin. For every $R>0$ and $a\in\mathscr{S}^1_\Lambda$, we define

$$\left\langle w^\Lambda_{h,R}(t),a\right\rangle:=\int_{T^*\mathbb{T}^2}\left(1-\chi\left(\frac{\xi_1}{Rh}\right)\right)a\left(x,\xi,\frac{\xi_1}{h}\right)w_h(t,dx,d\xi),$$

and

$$\langle w_{\Lambda,h,R}(t),a\rangle:=\int_{T^*\mathbb{T}^2}\chi\left(\frac{\xi_1}{Rh}\right)a\left(x,\xi,\frac{\xi_1}{h}\right)w_h(t,dx,d\xi). \tag{74}$$

Clearly,

$$\left\langle w_h(t),a\left(x,\xi,\frac{\xi_1}{h}\right)\right\rangle=\left\langle w^\Lambda_{h,R}(t),a\right\rangle+\langle w_{\Lambda,h,R}(t),a\rangle.$$

One readily sees that $w^\Lambda_{h,R}(t)$ is concentrated on the region $\{|\xi_1|\gtrsim Rh\}$, whereas $w_{\Lambda,h,R}(t)$ lives in $\{|\xi_1|\lesssim Rh\}$. The distribution $w_{\Lambda,h,R}(t)$ is intended to capture the fraction of the "energy" of $e^{it\left(\frac{1}{2}\Delta-V\right)}u_h^0$ that stays at a distance of order h to $\Lambda^\perp$, while $w^\Lambda_{h,R}(t)$ captures the energy that concentrates on $\Lambda^\perp$ at a slower speed.

One then defines $\tilde\mu^\Lambda,\tilde\mu_\Lambda\in(\mathscr{S}^1_\Lambda)'$ by taking limits (whose existence follows from the Calderón-Vaillancourt theorem, identity (25), adapted to the present setting):

$$\int_{\mathbb{R}}\varphi(t)\left\langle\tilde\mu^\Lambda(t,\cdot),a\right\rangle dt:=\lim_{R\to\infty}\lim_{h\to0^+}\int_{\mathbb{R}}\varphi(t)\left\langle w^\Lambda_{h,R}(t),a\right\rangle dt,$$

and

$$\int_{\mathbb{R}}\varphi(t)\left\langle\tilde\mu_\Lambda(t,\cdot),a\right\rangle dt:=\lim_{R\to\infty}\lim_{h\to0^+}\int_{\mathbb{R}}\varphi(t)\left\langle w_{\Lambda,h,R}(t),a\right\rangle dt. \tag{75}$$

Let us start by analyzing $\tilde\mu^\Lambda$. Clearly, $\int_{\mathbb{R}}\varphi(t)\left\langle\tilde\mu^\Lambda(t,\cdot),a\right\rangle dt$ only depends on $a_{\hom}$. One can prove, following for instance the arguments in [56], that $\tilde\mu^\Lambda$ is positive and it is supported in $\left\{\xi\in\Lambda^\perp\right\}\simeq\mathbb{R}_{\xi_2}$. It can be therefore identified to a positive

measure on $T^*\mathbb{T}^2 \times \{-1,1\}$ (or on $\mathbb{T}_{x_1} \times \mathbb{R}_{\xi_2} \times \{-1,1\}$, since it has only frequencies in Λ).

Using Egorov's theorem (which is exact for $-\Delta$ in this case) one can prove that $\tilde{\mu}^{\Lambda}(t,\cdot)$ is invariant by the geodesic flow and that it satisfies, in addition:

$$\omega \partial_{x_1} \tilde{\mu}^{\Lambda}(t,x,\xi,\omega) = 0, \quad (x,\xi,\omega) \in T^*\mathbb{T}^2 \times \mathbb{R}^2 \times \{-1,1\}.$$

This clearly implies that $\tilde{\mu}^{\Lambda}$ does not depend on x_1.

Let us postpone our discussion on $\tilde{\mu}_{\Lambda}$ and focus on how $\mu(t,\cdot)\rceil_{\mathbb{T}^2 \times R_{\Lambda}}$ is related to $\tilde{\mu}^{\Lambda}$ and $\tilde{\mu}_{\Lambda}$. Let

$$\mu^{\Lambda}(t,\cdot) := \int_{\{-1,1\}} \tilde{\mu}^{\Lambda}(t,\cdot,d\eta)\rceil_{\mathbb{T}^2 \times R_{\Lambda}}, \quad \mu_{\Lambda}(t,\cdot) := \int_{\mathbb{R}} \tilde{\mu}_{\Lambda}(t,\cdot,d\eta)\rceil_{\mathbb{T}^2 \times R_{\Lambda}}.$$

We shall show later on that $\int_{\mathbb{R}} \tilde{\mu}_{\Lambda}(t,\cdot,d\eta)$ is a positive measure, so that the preceding definition makes sense. In that case:

$$\mu(t,\cdot)\rceil_{\mathbb{T}^2 \times R_{\Lambda}} = \mu^{\Lambda}(t,\cdot) + \mu_{\Lambda}(t,\cdot). \tag{76}$$

Note that, since $\mu^{\Lambda}(t,\cdot)$ does not depend on x_1, is concentrated in $\{\xi \in R_{\Lambda}\}$, and is invariant by the geodesic flow, necessarily it does not depend at all on x, by Proposition 6.

Now it only remains to compute $\tilde{\mu}_{\Lambda}(t,\cdot)$. Clearly, writting $u_h(t) := e^{it\left(\frac{1}{2}\Delta - V\right)} u_h^0$, one has:

$$\begin{aligned}
\langle w_{\Lambda,h,R}(t), a\rangle =& \left(\mathrm{Op}_h\left(\chi\left(\frac{\xi_1}{Rh}\right) a\left(x_1,\xi,\frac{\xi_1}{h}\right)\right) u_h(t) \,|\, u_h(t)\right)_{L^2(\mathbb{T}^2)} \\
=& \left(\mathrm{Op}_1^{(x_1,\xi_1)}\left(\chi\left(\frac{\xi_1}{R}\right) a(x_1,0,hD_{x_2},\xi_1)\right) u_h(t) \,|\, u_h(t)\right)_{L^2(\mathbb{T}^2)} \\
&+ \mathscr{O}(h)
\end{aligned}$$

Note that

$$\mathrm{Op}_1^{(x_1,\xi_1)}\left(\chi\left(\frac{\xi_1}{R}\right) a(x_1,0,hD_{x_2},\xi_1)\right)$$

can be viewed as a semiclassical operator in the variables (x_2,ξ_2) taking values into the space $\mathscr{K}\left(L^2(\mathbb{T}_{x_1})\right)$ of compact operators on $L^2(\mathbb{T}_{x_1})$. This motivates the following definition. For $K \in C_c^{\infty}\left(T^*\mathbb{T}_{x_2}; \mathscr{K}\left(L^2(\mathbb{T}_{x_1})\right)\right)$ denote:

$$\left\langle n_h^{\Lambda}(t), K\right\rangle := \left(K(x_2,hD_{x_2})\, u_h(t) \,|\, u_h(t)\right)_{L^2\left(\mathbb{T}_{x_2}; L^2\left(\mathbb{T}_{x_1}\right)\right)}. \tag{77}$$

Above, we have made the natural identification $L^2(\mathbb{T}^2) \simeq L^2\left(\mathbb{T}_{x_2}; L^2\left(\mathbb{T}_{x_1}\right)\right)$.

Proposition 7 *Modulo a subsequence, one has the following:*

$$\lim_{h\to 0^+}\int_{\mathbb{R}}\varphi(t)\left\langle n_h^{\Lambda}(t),K\right\rangle dt=\int_{\mathbb{R}}\varphi(t)\,\mathrm{Tr}\int_{T^*\mathbb{T}_{x_2}}K(x_2,\xi_2)\,\tilde{\rho}_{\Lambda}(t,dx_2,d\xi_2)\,dt, \tag{78}$$

for every $K\in C_c^{\infty}\left(T^*\mathbb{T}_{x_2};\mathscr{K}\left(L^2(\mathbb{T}_{x_1})\right)\right)$ *and every* $\varphi\in L^1(\mathbb{R})$. *Therefore,* $\tilde{\rho}_{\Lambda}$ *is a weak-∗ accumulation point in the space of operator-valued distributions:*

$$L^{\infty}\left(\mathbb{R};\mathscr{D}'\left(T^*(\mathbb{T}_{x_2});\mathscr{L}^1\left(L^2(\mathbb{T}_{x_1})\right)\right)\right).$$

Moreover, for a.e. $t\in\mathbb{R}$, $\tilde{\rho}_{\Lambda}(t,\cdot)$ *is a positive* $\mathscr{L}^1\left(L^2(\mathbb{T}_{x_1})\right)$*-valued measure on* $T^*\mathbb{T}_{x_2}$ *and it is invariant by the geodesic flow* $\phi_s|_{T^*\mathbb{T}_{x_2}}$.

In general,

$$\int_{\mathbb{R}}\varphi(t)\left\langle w_{\Lambda,h,R}(t),a\right\rangle dt=\int_{\mathbb{R}}\varphi(t)\left\langle n_h^{\Lambda}(t),K_{a,R}\right\rangle dt+\mathscr{O}(h), \tag{79}$$

where

$$K_{a,R}(\xi_2):=\mathrm{Op}_1^{(x_1,\xi_1)}\left(\chi\left(\frac{\xi_1}{R}\right)a(x_1,0,\xi_2,\xi_1)\right);$$

note that when $a(x,\xi)$ does not depend on η this is merely:

$$K_{a,R}(\xi_2):=a(x_1,0,\xi_2)\,\chi\left(\frac{D_{x_1}}{R}\right).$$

Identity (79) shows in particular that:

$$\int_{\mathbb{R}}\varphi(t)\left\langle\tilde{\mu}_{\Lambda}(t,\cdot),a\right\rangle dt=\int_{\mathbb{R}}\varphi(t)\,\mathrm{Tr}\int_{T^*\mathbb{T}_{x_2}}K_a(\xi_2)\,\tilde{\rho}_{\Lambda}(t,dx_2,d\xi_2)\,dt,$$

where

$$K_a(\xi_2):=\mathrm{Op}_1^{(x_1,\xi_1)}\left(a(x_1,0,\xi_2,\xi_1)\right),$$

and, for $a\in\mathscr{S}^1_{\Lambda}$ not depending on η,

$$\int_{\mathbb{R}}\varphi(t)\left\langle\mu_{\Lambda}(t,\cdot),a\right\rangle dt=\int_{\mathbb{R}}\varphi(t)\,\mathrm{Tr}\int_{\mathbb{T}_{x_2}\times\left(\mathbb{R}_{\xi_2}\setminus\{0\}\right)}m_a(\xi_2)\,\tilde{\rho}_{\Lambda}(t,dx_2,d\xi_2)\,dt.$$

Finally, using the Radon-Nikodym theorem for operator-valued measures, as described for instance in the Appendix of [56], and the fact that $\int_{\mathbb{T}^2} \mu_\Lambda(t, dx, \cdot)$ does not depend on t, we obtain:

$$\int_{\mathbb{T}_{x_2}} \tilde{\rho}_\Lambda(t, dx_2, \xi_2) = \rho_\Lambda(t, \xi_2)\, \lambda_\Lambda(\xi_2),$$

for some positive measure λ_Λ on $\{\xi \in \Lambda^\perp\} \simeq \mathbb{R}_{\xi_2}$ and some λ_Λ-integrable family $\rho(t, \xi_2) \in \mathscr{L}^1\left(L^2(\mathbb{T}_{x_1})\right)$.

Let us now deduce the propagation law for $\rho_\Lambda(t, \xi_2)$. Start with:

$$\begin{aligned}&\frac{d}{dt}\left\langle n_h^\Lambda(t), K_{a,R}\right\rangle \\ &\quad = i\left(\left[-\frac{1}{2}\Delta + V, \mathrm{Op}_1^{(x_1,\xi_1)}\left(\chi\left(\frac{\xi_1}{R}\right) a(x_1, 0, hD_{x_2}, \xi_1)\right)\right] u_h(t) \,|\, u_h(t)\right)_{L^2(\mathbb{T}^2)}.\end{aligned}$$

Clearly,

$$\begin{aligned}&\left[-\frac{1}{2}\Delta, \mathrm{Op}_1^{(x_1,\xi_1)}\left(\chi\left(\frac{\xi_1}{R}\right) a(x_1, 0, hD_{x_2}, \xi_1)\right)\right] \\ &\quad = \left[-\frac{1}{2}\partial_{x_1}^2, \mathrm{Op}_1^{(x_1,\xi_1)}\left(\chi\left(\frac{\xi_1}{R}\right) a(x_1, 0, hD_{x_2}, \xi_1)\right)\right] \\ &\quad = \left[-\frac{1}{2}\partial_{x_1}^2, K_{a,R}(hD_{x_2})\right].\end{aligned}$$

Therefore,

$$\frac{d}{dt}\left\langle n_h^\Lambda(t), K_{a,R}\right\rangle = i\left\langle n_h^\Lambda(t), \left[-\frac{1}{2}\partial_{x_1}^2 + V, K_{a,R}\right]\right\rangle,$$

Taking limits and using the fact $\tilde{\rho}_\Lambda(t, \cdot)$ is invariant by the geodesic flow, we can average V:

$$\begin{aligned}&\frac{d}{dt}\,\mathrm{Tr}\int_{\mathbb{T}_{x_2}\times(\mathbb{R}_{\xi_2}\setminus\{0\})} K_a(\xi_2)\, \tilde{\rho}_\Lambda(t, dx_2, d\xi_2) \\ &\quad = i\,\mathrm{Tr}\int_{\mathbb{T}_{x_2}\times(\mathbb{R}_{\xi_2}\setminus\{0\})}\left[-\frac{1}{2}\partial_{x_1}^2 + \langle V\rangle_\Lambda, K_a(\xi_2)\right]\tilde{\rho}_\Lambda(t, dx_2, d\xi_2),\end{aligned}$$

where

$$\langle V\rangle_\Lambda(x_1) := \frac{1}{2\pi}\int_{\mathbb{T}} V(x_1, x_2)\, dx_2$$

which allows us to conclude.

For an arbitrary $\Lambda \in \mathscr{L}_1$ one has to perform a change of coordinates to reduce to problem to the one studied above. In higher dimensions or when $\mu_0(\{\xi = 0\}) \neq 0$ one has to iterate the two-microlocal scheme in a recursive manner. Additional work is also required to lower the regularity requirements of the potential, see [9].

5.4 Other Results in Other Geometries

Let us briefly comment on recent developments on the subject. The results in [9] can be used to obtain sharp decay rates for the damped wave equation on $\mathbb{T}^2$, see [5].

Moreover, the results of [9] have been extended in [1] to encompass semiclassical completely integrable systems of the form:

$$ih\partial_t u(t,x) - H(hD_x)\,u(t,x) - h^2 V(x, hD_x)\,u(t,x) = 0, \quad (t,x) \in \mathbb{R} \times \mathbb{T}^d, \tag{80}$$

at different time scales under convexity assumptions on $H(\xi)$, that turn to be necessary. Let us simply mention that the scale $\tau_h = h^{-1}$ is critical for this type of problem in the following sense. If $\tau_h \ll h^{-1}$ then $\tilde{\mathscr{M}}(\tau)$ contains all orbit measures associated to the classical flow. If $\tau_h \sim h^{-1}$ one can show that $\mathscr{M}(\tau) \subseteq C\left(\mathbb{R}; L^1\left(\mathbb{T}^d\right)\right)$ and it is possible to prove a microlocal propagation law, much more complicated than the one presented here, that involves superpositions of Schrödinger propagators of the form $e^{it\left(d^2H(\xi)D_x \cdot D_x - \langle V\rangle_\Lambda(\xi)\right)}$. Finally, if $\tau_h \gg h^{-1}$ and under certain separation assumptions on the spectrum of $H(hD_x)$ (that are satisfied, for instance, when $H(\xi) = |\xi|^2$ and $V = 0$) it is proved that $\tilde{\mathscr{M}}(\tau) = \mathrm{Conv}\,\tilde{\mathscr{M}}_\infty$.

The strategy of proof of Theorem 7 also adapts to boundary value problems. In [6] analogous results are proved for the disk in $\mathbb{R}^2$, whose billiard flow is completely integrable.

Let us note that in the case of negative curvature, [12] proves lower bounds for the Kolmogorov-Sinai entropy of the elements $\tilde{\mathscr{M}}\left(h^{-1}\right)$ and establishes observability results for the corresponding Schrödinger equations under conditions much weaker than the Geometric Control Condition.

Acknowledgements The author takes part into the visiting faculty program of ICMAT and is partially supported by grants ERC Starting Grant 277778 and MTM2013-41780-P (MEC).

References

1. N. Anantharaman, C. Fermanian-Kammerer, F. Macià, Semiclassical completely integrable systems: long-time dynamics and observability via two-microlocal Wigner measures. Amer. J. Math. **137**(3), 577–638 (2015)
2. S. Alinhac, P. Gérard, *Pseudo-Differential Operators and the Nash-Moser Theorem*. Graduate Studies in Mathematics, vol. 82 (American Mathematical Society, Providence, RI, 2007) [Translated from the 1991 French original by Stephen S. Wilson]

3. T. Aïssiou, Semiclassical limits of eigenfunctions on flat n-dimensional tori. Can. Math. Bull. **56**(1), 3–12 (2013)
4. T. Aïssiou, D. Jakobson, F. Macià, Uniform estimates for the solutions of the Schrödinger equation on the torus and regularity of semiclassical measures. Math. Res. Lett. **19**(3), 589–599 (2012)
5. N. Anantharaman, M. Léautaud, Sharp polynomial decay rates for the damped wave equation on the torus. Anal. PDE **7**(1), 159–214 (2014)
6. N. Anantharaman, M. Léautaud, F. Macià, Wigner measures and observability for the Schrödinger equation on the disk. Preprint arXiv:1406.0681 (2014)
7. D. Azagra, F. Macià, Concentration of symmetric eigenfunctions. Nonlinear Anal. **73**(3), 683–688 (2010)
8. N. Anantharaman, F. Macià, The dynamics of the Schrödinger flow from the point of view of semiclassical measures, in *Spectral Geometry*, ed. by A.H. Barnett, C.S. Gordan, P.A. Perry, A. Uribe. Proceedings of Symposium on Pure Mathematics, vol. 84 (American Mathematical Society, Providence, RI, 2012), pp. 93–116
9. N. Anantharaman, F. Macià, Semiclassical measures for the Schrödinger equation on the torus. J. Eur. Math. Soc. (JEMS) **16**(6), 1253–1288 (2014)
10. N. Anantharaman, S. Nonnenmacher, Half-delocalization of eigenfunctions for the Laplacian on an Anosov manifold. Ann. Inst. Fourier (Grenoble) **57**(7), 2465–2523 (2007) [Festival Yves Colin de Verdière]
11. N. Anantharaman, Entropy and the localization of eigenfunctions. Ann. Math. (2) **168**(2), 435–475 (2008)
12. N. Anantharaman, G. Rivière, Dispersion and controllability for the Schrödinger equation on negatively curved manifolds. Anal. PDE **5**(2), 313–338 (2012)
13. V.I. Arnol′d, Modes and quasimodes. Funkcional. Anal. Priložen. **6**(2), 12–20 (1972)
14. V.I. Arnol′d, Mathematical Methods of Classical Mechanics. Graduate Texts in Mathematics, vol. 60 (Springer, New York, 1989)
15. V. Banica, The nonlinear Schrödinger equation on hyperbolic space. Commun. Partial Differ. Equat. **32**(10–12), 1643–1677 (2007)
16. V.M. Babič, V.S. Buldyrev, *Short-Wavelength Diffraction Theory*. Springer Series on Wave Phenomena, vol. 4 (Springer, Berlin, 1991) [Asymptotic methods, Translated from the 1972 Russian original by E.F. Kuester]
17. J. Bourgain, N. Burq, M. Zworski, Control for Schrödinger operators on 2-tori: rough potentials. J. Eur. Math. Soc. (JEMS) **15**(5), 1597–1628 (2013)
18. A.L. Besse, *Manifolds All of Whose Geodesics Are Closed*. Ergebnisse der Mathematik und ihrer Grenzgebiete, vol. 93 (Springer, Berlin, 1978)
19. N. Burq, C. Guillarmou, A. Hassell, Strichartz estimates without loss on manifolds with hyperbolic trapped geodesics. Geom. Funct. Anal. **20**(3), 627–656 (2010)
20. D. Bambusi, S. Graffi, T. Paul, Long time semiclassical approximation of quantum flows: a proof of the Ehrenfest time. Asymptot. Anal. **21**(2), 149–160 (1999)
21. N. Burq, P. Gérard, N. Tzvetkov, An instability property of the nonlinear Schrödinger equation on S^d. Math. Res. Lett. **9**(2–3), 323–335 (2002)
22. N. Burq, P. Gérard, N. Tzvetkov, Strichartz inequalities and the nonlinear Schrödinger equation on compact manifolds. Am. J. Math. **126**(3), 569–605 (2004)
23. N. Burq, P. Gérard, N. Tzvetkov, Bilinear eigenfunction estimates and the nonlinear Schrödinger equation on surfaces. Invent. Math. **159**(1), 187–223 (2005)
24. N. Burq, P. Gérard, N. Tzvetkov, Multilinear eigenfunction estimates and global existence for the three dimensional nonlinear Schrödinger equations. Ann. Sci. École Norm. Sup. (4) **38**(2), 255–301 (2005)
25. J.-M. Bony, N. Lerner, Quantification asymptotique et microlocalisations d'ordre supérieur I. Ann. Sci. École Norm. Sup. (4) **22**(3), 377–433 (1989)
26. J. Bourgain, E. Lindenstrauss, Entropy of quantum limits. Commun. Math. Phys. **233**(1), 153–171 (2003)

27. J.-M. Bony, Second microlocalization and propagation of singularities for semilinear hyperbolic equations, in *Hyperbolic Equations and Related Topics (Katata/Kyoto, 1984)*, ed. by S. Mizohata (Academic, Boston, 1986), pp. 11–49
28. J. Bourgain, Fourier transform restriction phenomena for certain lattice subsets and applications to nonlinear evolution equations, I. Schrödinger equations. Geom. Funct. Anal. **3**(2), 107–156 (1993)
29. J. Bourgain, Analysis results and problems related to lattice points on surfaces, in *Harmonic Analysis and Nonlinear Differential Equations (Riverside, CA, 1995)*, ed. by V.L. Shapiro, M.L. Lapidus, L.H. Harper, A.J. Rumbos. Contemporary Mathematics, vol. 208 (American Mathematical Society, Providence, 1997), pp. 85–109
30. J. Bourgain, *Global Solutions of Nonlinear Schrödinger Equations*. American Mathematical Society Colloquium Publications, vol. 46 (American Mathematical Society, Providence, 1999)
31. J. Bourgain, On Strichartz's inequalities and the nonlinear Schrödinger equation on irrational tori, in *Mathematical Aspects of Nonlinear Dispersive Equations*, ed. by J. Bourgain, C.E. Kenig, S. Klainerman. Annals of Mathematics Studies, vol. 163 (Princeton University Press, Princeton, 2007), pp. 1–20
32. J.-M. Bouclet, Strichartz estimates on asymptotically hyperbolic manifolds. Anal. PDE **4**(1), 1–84 (2011)
33. J.-M. Bouclet, Semi-classical functional calculus on manifolds with ends and weighted Lp estimates. Ann. Inst. Fourier (Grenoble) **61**(3), 1181–1223 (2011)
34. A. Bouzouina, D. Robert, Uniform semiclassical estimates for the propagation of quantum observables. Duke Math. J. **111**(2), 223–252 (2002)
35. N. Burq, Mesures semi-classiques et mesures de défaut. Séminaire Bourbaki, vol. 1996/1997. Astérisque (245); Exp. No. 826, **4**, 167–195 (1997)
36. N. Burq, M. Zworski, Geometric control in the presence of a black box. J. Am. Math. Soc. **17**(2), 443–471 (2004) (electronic)
37. N. Burq, M. Zworski, Control for Schrödinger operators on tori. Math. Res. Lett. **19**(2), 309–324 (2012)
38. T. Cazenave, *Semilinear Schrödinger Equations*. Courant Lecture Notes in Mathematics, vol. 10 (New York University Courant Institute of Mathematical Sciences, New York, 2003)
39. Y. Colin de Verdière, Quasi-modes sur les variétés Riemanniennes. Invent. Math. **43**(1), 15–52 (1977)
40. Y. Colin de Verdière, Sur le spectre des opérateurs elliptiques à bicaractéristiques toutes périodiques. Comment. Math. Helv. **54**(3), 508–522 (1979)
41. Y. Colin de Verdière, Ergodicité et fonctions propres du laplacien. Commun. Math. Phys. **102**(3), 497–502 (1985)
42. Y. Colin de Verdière, B. Parisse, Équilibre instable en régime semi-classique, I. Concentration microlocale. Commun. Partial Differ. Equat. **19**(9–10), 1535–1563 (1994)
43. H. Christianson, Quantum monodromy and nonconcentration near a closed semi-hyperbolic orbit. Trans. Am. Math. Soc. **363**(7), 3373–3438 (2011)
44. M. Combescure, D. Robert, Semiclassical spreading of quantum wave packets and applications near unstable fixed points of the classical flow. Asymptot. Anal. **14**(4), 377–404 (1997)
45. A.-P. Calderón, R. Vaillancourt, On the boundedness of pseudo-differential operators. J. Math. Soc. Jpn. **23**, 374–378 (1971)
46. A.-P. Calderón, A. Zygmund, Singular integral operators and differential equations. Am. J. Math. **79**, 901–921 (1957)
47. S. de Bièvre, D. Robert, Semiclassical propagation on $|\log h|$ time scales. Int. Math. Res. Not. (12), 667–696 (2003)
48. J.J. Duistermaat, V.W. Guillemin, The spectrum of positive elliptic operators and periodic bicharacteristics. Invent. Math. **29**(1), 39–79 (1975)
49. B. Dehman, P. Gérard, G. Lebeau, Stabilization and control for the nonlinear Schrödinger equation on a compact surface. Math. Z. **254**(4), 729–749 (2006)

50. M. Dimassi, J. Sjöstrand, *Spectral Asymptotics in the Semi-classical Limit*. London Mathematical Society Lecture Note Series, vol. 268 (Cambridge University Press, Cambridge, 1999)
51. C. Fermanian-Kammerer, Mesures semi-classiques 2-microlocales. C. R. Acad. Sci. Paris Sér. I Math. **331**(7), 515–518 (2000)
52. C. Fermanian Kammerer, Propagation and absorption of concentration effects near shock hypersurfaces for the heat equation. Asymptot. Anal. **24**(2), 107–141 (2000)
53. C. Fermanian-Kammerer, P. Gérard, Mesures semi-classiques et croisement de modes. Bull. Soc. Math. France **130**(1), 123–168 (2002)
54. G.B. Folland, *Harmonic Analysis in Phase Space*. Annals of Mathematics Studies, vol. 122 (Princeton University Press, Princeton, 1989)
55. P. Gérard, Mesures semi-classiques et ondes de Bloch, in *Séminaire sur les Équations aux Dérivées Partielles, 1990–1991*, pp. Exp. No. XVI, 19 (École Polytechnique, Palaiseau, 1991)
56. P. Gérard, Microlocal defect measures. Commun. Partial Differ. Equat. **16**(11), 1761–1794 (1991)
57. P. Gérard, Oscillations and concentration effects in semilinear dispersive wave equations. J. Funct. Anal. **141**(1), 60–98 (1996)
58. P. Gérard, Description du défaut de compacité de l'injection de Sobolev. ESAIM Control Optim. Calc. Var. **3**, 213–233 (1998) (electronic)
59. P. Gérard, Nonlinear Schrödinger equations in inhomogeneous media: wellposedness and illposedness of the Cauchy problem, in *International Congress of Mathematicians*, vol. III (European Mathematical Society, Zürich, 2006), pp. 157–182
60. J. Ginibre, Le problème de Cauchy pour des EDP semi-linéaires périodiques en variables d'espace (d'après Bourgain). Séminaire Bourbaki, vol. 1994/1995. Astérisque (237), Exp. No. 796, **4**, 163–187 (1996)
61. P. Gérard, É. Leichtnam, Ergodic properties of eigenfunctions for the Dirichlet problem. Duke Math. J. **71**(2), 559–607 (1993)
62. P. Gérard, P.A. Markowich, N.J. Mauser, F. Poupaud, Homogenization limits and Wigner transforms. Commun. Pure Appl. Math. **50**(4), 323–379 (1997)
63. A. Grigis, J. Sjöstrand, *Microlocal Analysis for Differential Operators: An Introduction*. London Mathematical Society Lecture Note Series, vol. 196 (Cambridge University Press, Cambridge, 1994)
64. A. Hassell, Ergodic billiards that are not quantum unique ergodic. Ann. Math. (2) **171**(1), 605–619 (2010) [With an appendix by the author and Luc Hillairet]
65. B. Helffer, *Semi-classical Analysis for the Schrödinger Operator and Applications*. Lecture Notes in Mathematics, vol. 1336 (Springer, Berlin, 1988)
66. G.A. Hagedorn, A. Joye, Semiclassical dynamics with exponentially small error estimates. Commun. Math. Phys. **207**(2), 439–465 (1999)
67. G.A. Hagedorn, A. Joye, Exponentially accurate semiclassical dynamics: propagation, localization, Ehrenfest times, scattering, and more general states. Ann. Henri Poincaré **1**(5), 837–883 (2000)
68. L. Hörmander, Pseudo-differential operators. Commun. Pure Appl. Math. **18**, 501–517 (1965)
69. L. Hörmander, *The Analysis of Linear Partial Differential Operators. III Pseudo-Differential Operators*. Classics in Mathematics (Springer, Berlin, 2007) [Reprint of the 1994 edition]
70. V. Isakov, *Inverse Problems for Partial Differential Equations*, 2nd edn. Applied Mathematical Sciences, vol. 127 (Springer, New York, 2006)
71. S. Jaffard, Contrôle interne exact des vibrations d'une plaque rectangulaire. Port. Math. **47**(4), 423–429 (1990)
72. D. Jakobson, Quantum limits on flat tori. Ann. Math. (2) **145**(2), 235–266 (1997)
73. D. Jakobson, S. Zelditch, Classical limits of eigenfunctions for some completely integrable systems, in *Emerging Applications of Number Theory (Minneapolis, MN, 1996)*, ed. by D.A. Hejhal, J. Friedman, M.C. Gutzwiller, A.M. Odlyzko. IMA Volumes in Mathematics and Its Applications, vol. 109 (Springer, New York, 1999), pp. 329–354

74. A. Katok, B. Hasselblatt, *Introduction to the Modern Theory of Dynamical Systems*. Encyclopedia of Mathematics and Its Applications, vol. 54 (Cambridge University Press, Cambridge, 1995) [With a supplementary chapter by Katok and Leonardo Mendoza]
75. J.J. Kohn, L. Nirenberg, An algebra of pseudo-differential operators. Commun. Pure Appl. Math. **18**, 269–305 (1965)
76. O. Lablée, Semi-classical behaviour of Schrödinger's dynamics: revivals of wave packets on hyperbolic trajectory. Asymptot. Anal. **71**(1–2), 59–99 (2011)
77. V.F. Lazutkin, *KAM Theory and Semiclassical Approximations to Eigenfunctions*. Ergebnisse der Mathematik und ihrer Grenzgebiete (3) [Results in Mathematics and Related Areas (3)], vol. 24 (Springer, Berlin, 1993) [With an addendum by A.I. Shnirel′man]
78. G. Lebeau, Contrôle de l'équation de Schrödinger. J. Math. Pures Appl. (9) **71**(3), 267–291 (1992)
79. E. Lindenstrauss, Invariant measures and arithmetic quantum unique ergodicity. Ann. Math. (2), **163**(1), 165–219 (2006)
80. P.-L. Lions, The concentration-compactness principle in the calculus of variations. The limit case, I. Rev. Mat. Iberoam. **1**(1), 145–201 (1985)
81. P.-L. Lions, The concentration-compactness principle in the calculus of variations. The limit case, II. Rev. Mat. Iberoam. **1**(2), 45–121 (1985)
82. J.-L. Lions, Exact controllability, stabilization and perturbations for distributed systems. SIAM Rev. **30**(1), 1–68 (1988)
83. P.-L. Lions, T. Paul, Sur les mesures de Wigner. Rev. Mat. Iberoam. **9**(3), 553–618 (1993)
84. F. Macià, Some remarks on quantum limits on Zoll manifolds. Commun. Partial Differ. Equat. **33**(4–6), 1137–1146 (2008)
85. F. Macià, Semiclassical measures and the Schrödinger flow on Riemannian manifolds. Nonlinearity **22**(5), 1003–1020 (2009)
86. F. Macià, High-frequency propagation for the Schrödinger equation on the torus. J. Funct. Anal. **258**(3), 933–955 (2010)
87. F. Macià, The Schrödinger flow in a compact manifold: high-frequency dynamics and dispersion, in *Modern Aspects of the Theory of Partial Differential Equations*, ed. by M. Ruzhansky, J. Wirth. Operator Theory: Advances and Applications, vol. 216 (Birkhäuser/Springer, Basel, 2011), pp. 275–289
88. A. Martinez, *An Introduction to Semiclassical and Microlocal Analysis*. Universitext (Springer, New York, 2002)
89. L. Miller, Propagation d'ondes semi-classiques à travers une interface et mesures 2-microlocales. Ph.D. thesis, École Polythecnique, Palaiseau, 1996
90. F. Macià, G. Rivière, Concentration and non-concentration for the Schrödinger evolution on Zoll manifolds. Preprint arXiv:1505.04945 (2015)
91. J. Moser, E.J. Zehnder, *Notes on Dynamical Systems*. Courant Lecture Notes in Mathematics, vol. 12 (New York University Courant Institute of Mathematical Sciences, New York, 2005)
92. F. Nier, A semi-classical picture of quantum scattering. Ann. Sci. École Norm. Sup. (4) **29**(2), 149–183 (1996)
93. N. Nadirashvili, J. Toth, D. Jakobson, Geometric properties of eigenfunctions. Russ. Math. Surv. **56**(6), 1085–1105 (2001)
94. T. Paul, Semiclassical approximation and noncommutative geometry. Preprint (2011), http://www.math.polytechnique.fr/~paul/
95. J.V. Ralston. On the construction of quasimodes associated with stable periodic orbits. Commun. Math. Phys. **51**(3), 219–242 (1976)
96. J.V. Ralston, Approximate eigenfunctions of the Laplacian. J. Differ. Geom. **12**(1), 87–100 (1977)
97. G. Rivière, Entropy of semiclassical measures in dimension 2. Duke. Math. J. **155**(2), 271–335 (2010)
98. D. Robert, *Autour de l'Approximation Semi-classique*. Progress in Mathematics, vol. 68 (Birkhäuser, Boston, 1987)

99. J. Rauch, M. Reed, Two examples illustrating the differences between classical and quantum mechanics. Commun. Math. Phys. **29**, 105–111 (1973)
100. M. Reed, B. Simon, *Methods of Modern Mathematical Physics, II. Fourier Analysis, Self-adjointness* (Academic [Harcourt Brace Jovanovich Publishers], New York, 1975)
101. M. Reed, B. Simon, *Methods of Modern Mathematical Physics, I. Functional Analysis*, 2nd edn. (Academic [Harcourt Brace Jovanovich Publishers], New York, 1980)
102. Z. Rudnick, P. Sarnak. The behaviour of eigenstates of arithmetic hyperbolic manifolds. Commun. Math. Phys. **161**(1), 195–213 (1994)
103. J. Rauch, M. Taylor, Exponential decay of solutions to hyperbolic equations in bounded domains. Indiana Univ. Math. J. **24**, 79–86 (1974)
104. P. Sarnak, Arithmetic quantum chaos, in *The Schur Lectures (1992) (Tel Aviv)*. Israel Mathematical Conference Proceedings, vol. 8 (Bar-Ilan University, Ramat Gan, 1995), pp. 183–236
105. M. Shubin, Classical and quantum completeness for the Schrödinger operators on non-compact manifolds, in *Geometric Aspects of Partial Differential Equations (Roskilde, 1998)*, ed. by B. Booss-Bavnbek, K. Wojciechowski. Contemporary Mathematics, vol. 242 (American Mathematical Society, Providence, 1999), pp. 257–269
106. A.I. Šnirel′man, Ergodic properties of eigenfunctions. Uspehi Mat. Nauk **29**(6(180)), 181–182 (1974)
107. E.M. Stein, *Harmonic Analysis: Real-Variable Methods, Orthogonality, and Oscillatory Integrals*. Princeton Mathematical Series, vol. 43. (Princeton University Press, Princeton, 1993) [With the assistance of Timothy S. Murphy, Monographs in Harmonic Analysis, III]
108. T. Tao, *Nonlinear Dispersive Equations: Local and Global Analysis*. CBMS Regional Conference Series in Mathematics, vol. 106 (Published for the Conference Board of the Mathematical Sciences, Washington, DC, 2006)
109. L. Tartar, *H*-measures, a new approach for studying homogenisation, oscillations and concentration effects in partial differential equations. Proc. R. Soc. Edinb. Sect. A **115**(3–4), 193–230 (1990)
110. M.E. Taylor, *Pseudodifferential Operators*. Princeton Mathematical Series, vol. 34 (Princeton University Press, Princeton, 1981)
111. J.A. Toth, Eigenfunction localization in the quantized rigid body. J. Differ. Geom. **43**(4), 844–858 (1996)
112. J.A. Toth, On the quantum expected values of integrable metric forms. J. Differ. Geom. **52**(2), 327–374 (1999)
113. J.A. Toth, On the small-scale mass concentration of modes. Commun. Math. Phys. **206**(2), 409–428 (1999)
114. F. Trèves, *Introduction to Pseudodifferential and Fourier Integral Operators. Pseudodifferential Operators*. The University Series in Mathematics, vol. 1 (Plenum Press, New York, 1980)
115. A. Uribe, S. Zelditch, Spectral statistics on Zoll surfaces. Commun. Math. Phys. **154**(2), 313–346 (1993)
116. J.M. Van Vleck, The correspondence principle in the statistical interpretation of quantum mechanics. Proc. Natl. Acad. Sci. USA **14**(2), 178–188 (1928)
117. A. Weinstein, Asymptotics of eigenvalue clusters for the Laplacian plus a potential. Duke Math. J. **44**(4), 883–892 (1977)
118. H. Weyl, *The Theory of Groups and Quantum Mechanics* (Methuen, London, 1931) [Reprinted by Dover, New York, 1950]
119. E.P. Wigner, On the quantum correction for thermodynamic equilibrium. Phys. Rev. **40**, 749–759 (1932)
120. S. Zelditch, Uniform distribution of eigenfunctions on compact hyperbolic surfaces. Duke Math. J. **55**(4), 919–941 (1987)
121. S. Zelditch, Maximally degenerate Laplacians. Ann. Inst. Fourier (Grenoble) **46**(2), 547–587 (1996)
122. S. Zelditch, Fine structure of Zoll spectra. J. Funct. Anal. **143**(2), 415–460 (1997)

123. S. Zelditch, Local and global analysis of eigenfunctions on Riemannian manifolds, in *Handbook of Geometric Analysis, No. 1*, ed. by L. Ji, P. Li, R. Schoen, L. Simon. Advanced Lectures in Mathematics (ALM), vol. 7 (International Press, Somerville, 2008), pp. 545–658
124. M. Zworski, *Semiclassical Analysis*. Graduate Studies in Mathematics, vol. 138 (American Mathematical Society, Providence, 2012)
125. A. Zygmund, On Fourier coefficients and transforms of functions of two variables. Stud. Math. **50**, 189–201 (1974)

Index

C. Besse, J.-C. Garreau (eds.), *Nonlinear Optical and Atomic Systems*,
Lecture Notes in Mathematics 2146, DOI 10.1007/978-3-319-19015-0

LECTURE NOTES IN MATHEMATICS

Springer

Edited by J.-M. Morel, B. Teissier; P.K. Maini

Editorial Policy (for Multi-Author Publications: Summer Schools / Intensive Courses)

1. Lecture Notes aim to report new developments in all areas of mathematics and their applications - quickly, informally and at a high level. Mathematical texts analysing new developments in modelling and numerical simulation are welcome. Manuscripts should be reasonably selfcontained and rounded off. Thus they may, and often will, present not only results of the author but also related work by other people. They should provide sufficient motivation, examples and applications. There should also be an introduction making the text comprehensible to a wider audience. This clearly distinguishes Lecture Notes from journal articles or technical reports which normally are very concise. Articles intended for a journal but too long to be accepted by most journals, usually do not have this "lecture notes" character.

2. In general SUMMER SCHOOLS and other similar INTENSIVE COURSES are held to present mathematical topics that are close to the frontiers of recent research to an audience at the beginning or intermediate graduate level, who may want to continue with this area of work, for a thesis or later. This makes demands on the didactic aspects of the presentation. Because the subjects of such schools are advanced, there often exists no textbook, and so ideally, the publication resulting from such a school could be a first approximation to such a textbook. Usually several authors are involved in the writing, so it is not always simple to obtain a unified approach to the presentation.
   For prospective publication in LNM, the resulting manuscript should not be just a collection of course notes, each of which has been developed by an individual author with little or no coordination with the others, and with little or no common concept. The subject matter should dictate the structure of the book, and the authorship of each part or chapter should take secondary importance. Of course the choice of authors is crucial to the quality of the material at the school and in the book, and the intention here is not to belittle their impact, but simply to say that the book should be planned to be written by these authors jointly, and not just assembled as a result of what these authors happen to submit.
   This represents considerable preparatory work (as it is imperative to ensure that the authors know these criteria before they invest work on a manuscript), and also considerable editing work afterwards, to get the book into final shape. Still it is the form that holds the most promise of a successful book that will be used by its intended audience, rather than yet another volume of proceedings for the library shelf.

3. Manuscripts should be submitted either online at www.editorialmanager.com/lnm/ to Springer's mathematics editorial, or to one of the series editors. Volume editors are expected to arrange for the refereeing, to the usual scientific standards, of the individual contributions. If the resulting reports can be forwarded to us (series editors or Springer) this is very helpful. If no reports are forwarded or if other questions remain unclear in respect of homogeneity etc, the series editors may wish to consult external referees for an overall evaluation of the volume. A final decision to publish can be made only on the basis of the complete manuscript; however a preliminary decision can be based on a pre-final or incomplete manuscript. The strict minimum amount of material that will be considered should include a detailed outline describing the planned contents of each chapter.
   Volume editors and authors should be aware that incomplete or insufficiently close to final manuscripts almost always result in longer evaluation times. They should also be aware that parallel submission of their manuscript to another publisher while under consideration for LNM will in general lead to immediate rejection.

4. Manuscripts should in general be submitted in English. Final manuscripts should contain at least 100 pages of mathematical text and should always include

   – a general table of contents;
   – an informative introduction, with adequate motivation and perhaps some historical remarks: it should be accessible to a reader not intimately familiar with the topic treated;
   – a global subject index: as a rule this is genuinely helpful for the reader.

   Lecture Notes volumes are, as a rule, printed digitally from the authors' files. We strongly recommend that all contributions in a volume be written in the same LaTeX version, preferably LaTeX2e. To ensure best results, authors are asked to use the LaTeX2e style files available from Springer's web-server at
   ftp://ftp.springer.de/pub/tex/latex/svmonot1/ (for monographs) and
   ftp://ftp.springer.de/pub/tex/latex/svmultt1/ (for summer schools/tutorials).
   Additional technical instructions, if necessary, are available on request from:
   lnm@springer.com.

5. Careful preparation of the manuscripts will help keep production time short besides ensuring satisfactory appearance of the finished book in print and online. After acceptance of the manuscript authors will be asked to prepare the final LaTeX source files and also the corresponding dvi-, pdf- or zipped ps-file. The LaTeX source files are essential for producing the full-text online version of the book. For the existing online volumes of LNM see:
   http://www.springerlink.com/openurl.asp?genre=journal&issn=0075-8434.
   The actual production of a Lecture Notes volume takes approximately 12 weeks.

6. Volume editors receive a total of 50 free copies of their volume to be shared with the authors, but no royalties. They and the authors are entitled to a discount of 33.3 % on the price of Springer books purchased for their personal use, if ordering directly from Springer.

7. Commitment to publish is made by letter of intent rather than by signing a formal contract. Springer-Verlag secures the copyright for each volume. Authors are free to reuse material contained in their LNM volumes in later publications: a brief written (or e-mail) request for formal permission is sufficient.

Addresses:

Professor J.-M. Morel, CMLA,
École Normale Supérieure de Cachan,
61 Avenue du Président Wilson, 94235 Cachan Cedex, France
E-mail: morel@cmla.ens-cachan.fr

Professor B. Teissier, Institut Mathématique de Jussieu,
UMR 7586 du CNRS, Équipe "Géométrie et Dynamique",
175 rue du Chevaleret,
75013 Paris, France
E-mail: teissier@math.jussieu.fr

For the "Mathematical Biosciences Subseries" of LNM:

Professor P. K. Maini, Center for Mathematical Biology,
Mathematical Institute, 24-29 St Giles,
Oxford OX1 3LP, UK
E-mail: maini@maths.ox.ac.uk

Springer, Mathematics Editorial I,
Tiergartenstr. 17,
69121 Heidelberg, Germany,
Tel.: +49 (6221) 4876-8259
Fax: +49 (6221) 4876-8259
E-mail: lnm@springer.com